REDARS 2 Methodology and Software for Seismic Risk Analysis of Highway Systems

By

Stuart D. Werner, Craig E. Taylor, Sungbin Cho, Jean-Paul Lavoie, Charles Huyck, Chip Eitzel, Howard Chung and Ronald T. Eguchi

This publication was produced by MCEER for the Federal Highway Administration under contract number DTFH61-98-C-00094

MCEER is a national center of excellence dedicated to establishing disaster-resilient communities through the application of multidisciplinary, multi-hazard research. Headquartered at the University at Buffalo, State University of New York, the Center was originally established by the National Science Foundation (NSF) in 1986, as the National Center for Earthquake Engineering Research (NCEER).

Comprising a consortium of researchers from numerous disciplines and institutions throughout the United States, the Center's mission has expanded from its original focus on earthquake engineering to address a variety of other hazards, both natural and man-made, and their impact on critical infrastructure and facilities. The Center's goal is to reduce losses through research and the application of advanced technologies that improve engineering, pre-event planning and post-event recovery strategies. Toward this end, the Center coordinates a nationwide program of multidisciplinary team research, education and outreach activities.

Funded principally by NSF, the State of New York and the Federal Highway Administration (FHWA), the Center derives additional support from the Department of Homeland Security (DHS)/Federal Emergency Management Agency (FEMA), other state governments, academic institutions, foreign governments and private industry.

MCEER
EARTHQUAKE ENGINEERING TO EXTREME EVENTS

U.S. Department of Transportation
Federal Highway Administration

REDARS 2 Methodology and Software for Seismic Risk Analysis of Highway Systems

by

Stuart D. Werner (Coordinating Author),[1] Craig E. Taylor,[2] Sungbin Cho,[3]
Jean-Paul Lavoie,[4] Charles Huyck,[3] Chip Eitzel,[4]
Howard Chung[3] and Ronald T. Eguchi[3]

Publication Date: August 31, 2006

Special Report MCEER-06-SP08

Task Number 094-B-2

FHWA Contract Number DTFH61-98-C-00094
Contract Officer's Technical Representative: W. Phillip Yen, Ph.D., P.E. HRDI-7
Senior Research Structural Engineer/Seismic Research Program Manager
Federal Highway Administration

1 Seismic Systems & Engineering Consultants, Oakland, California
2 Natural Hazards Management Inc., Torrance, California
3 ImageCat, Inc., Long Beach, California
4 Geodesy, 8 California Street, Suite 650, San Francisco, California

MCEER
University at Buffalo, The State University of New York
Red Jacket Quadrangle, Buffalo, NY 14261
Phone: (716) 645-3391; Fax (716) 645-3399
E-mail: *mceer@buffalo.edu*; WWW Site: *http://mceer.buffalo.edu*

EXECUTIVE SUMMARY

Earthquake damage to components in a highway system (e.g., bridges, tunnels, roadways, etc.) can cause major traffic disruption which, in turn, can adversely impact the region's economic recovery and emergency response. These impacts will depend not only on the seismic performance of the components in the system, but also on the properties of the system itself such as its network configuration and roadway characteristics (e.g., locations, redundancies, and traffic-carrying capacities). Unfortunately, such traffic impacts are usually not considered in seismic risk reduction activities at state transportation agencies. One reason for this has been the lack of a technically-sound and practical method for estimating these impacts.

To address this deficiency, a new methodology for seismic risk analysis (SRA) of highway systems nationwide has been developed as part of the two six-year seismic research projects that have been carried out at MCEER under the sponsorship of the Federal Highway Administration. During the first project, the methodology was initially developed and demonstrated in an application to the highway system in Shelby County, Tennessee. Under the second (current) multi-year project, the methodology was validated, its models were updated, and it was programmed into a public-domain software package named REDARS™ 2 (Risks from Earthquake DAmage to Roadway Systems). A demonstration application of the software to the Los Angeles, California highway system was also conducted.

For any given earthquake, REDARS™ 2 uses state-of-knowledge models to estimate: (a) seismic hazards (ground motions, liquefaction, and surface fault rupture) throughout the highway system; (b) the resulting damage states for each component in the system; and (c) how each component's damage will be repaired, including its repair costs, downtimes, and time-dependent traffic states (i.e., its ability to carry traffic as the repairs proceed over time after the earthquake). Next, REDARS™ 2 includes these traffic states into a highway-network link-node model, in order to form a set of system-states that reflect the extent and spatial distribution of link closures at various times after the earthquake. Then, REDARS™ 2 applies network analysis procedures to each system-state, in order to estimate how these closures affect system-wide travel times and traffic flows. Finally, REDARS™ 2 estimates corresponding economic losses and increases in travel times to/from key locations or along key lifeline routes. These steps can be applied for single earthquakes and no uncertainties (deterministic analysis), or for multiple earthquakes and simulations in which uncertainties in earthquake occurrence and in estimates of seismic hazards and component damage are considered (probabilistic analysis).

REDARS™ 2 can serve as a pre- or post-earthquake decision-guidance tool. As a pre-earthquake planning tool, it can be used to: (a) estimate the effectiveness of various seismic-upgrade options in reducing earthquake losses; (b) compare costs and benefits (e.g., reduction in traffic-related losses/risks) for each option; and (c) enable decision-makers to use these results in order to make a more informed selection of a preferred option to implement. As a post-earthquake emergency-response tool in real time, REDARS™ 2 can incorporate actual damage data from the field, and can then develop results to enable officials to assess the relative abilities of various repair options and traffic-management options to facilitate traffic flows.

This report contains eight chapters and eleven appendices, whose contents are summarized below:

Chapter 1. Introduction. Chapter 1 includes a statement of the problem addressed by this research, and a discussion of the research benefits and the anticipated users of the research.

Chapter 2. Seismic Risk Analysis Methodology. Chapter 2 describes the main features of the REDARS™ 2 SRA methodology, including its analysis modules and procedures, and how its results can be used to guide seismic-improvement decision making. Appendix A describes the REDARS™ 2 probabilistic framework, and Appendix C summarizes a REDARS™ 2 Import Wizard that was developed under this research program to greatly simplify the development of input data for a SRA application. Appendix J describes a new statistical-analysis procedure that was developed under this project to estimate confidence limits in probabilistic SRA results.

Chapter 3. Earthquake Modeling and Hazards Module. Chapter 3 summarizes: (a) the "walkthrough" process that is used in REDARS™ 2 for probabilistic SRA applications; (b) the development of scenario-earthquake walkthrough tables for this process; and (c) the models that are currently used in REDARS™ 2 to estimate ground-motion, liquefaction, and surface-fault-rupture hazards. Appendix B describes the development of earthquake walkthrough tables for coastal California and the central United States under this project, and Appendices D, E, and F further describe the above ground-motion, liquefaction, and surface-fault-rupture hazard models.

Chapter 4. Component Module. Chapter 4 describes how REDARS™ 2 uses either default or user-specified models to estimate component damage and repair requirements, and how such models are developed for deterministic and probabilistic SRA applications. In addition, the chapter summarizes the default models that are now included in REDARS™ 2 to estimate damage states and repair requirements for bridges, approach fills, roadways, and tunnels. Appendices G and H provide further detail on the default modeling methods for these component types, and Appendix K describes how the model for estimating bridge damage due to ground shaking was calibrated against Northridge Earthquake bridge-damage observations.

Chapter 5. Transportation Network Analysis. Chapter 5 summarizes the features of the REDARS™ 2 transportation network analysis procedure, including its variable-demand model, its minimum-path algorithm for reducing run times, and its approach for considering multiple trip types. Appendix I provides further details on this network analysis procedure.

Chapter 6. Economic Module. Chapter 6 describes the approach used in REDARS™ 2 to develop default estimates of economic losses due to repair costs, travel-time delays, and trips foregone, and how user-specified parameters can be used to override these default estimates.

Chapter 7. Demonstration Application. Chapter 7 describes a demonstration application of the REDARS™ 2 software to carry out deterministic and probabilistic SRA of a large segment of the Los Angeles highway-roadway system. The chapter also includes a "hindsight" probabilistic economic analysis of a prior bridge retrofit program within this system, in order to illustrate one way that REDARS™ 2 results can be used to guide seismic-risk-reduction decision making.

Chapter 8. Conclusion. Chapter 8 contains concluding comments and recommended directions for continued development and application of the REDARS™ 2 methodology and software

ACKNOWLEDGEMENTS

This REDARS™ 2 technical manual describes seismic risk analysis (SRA) research performed under Tasks B1-2 and B1-4 of the project titled "Seismic Vulnerability of the Highway System." This project was directed by the Multidisciplinary Center for Earthquake Engineering Research (MCEER) under Federal Highway Administration (FHWA) sponsorship.

This SRA research was performed by a REDARS™ Development Team comprised of Stuart D. Werner (earthquake engineering, and principal investigator for development of REDARS™ 2 and for Task B1-2), Craig E. Taylor of Natural Hazards Management Inc. (risk analysis, earthquake modeling, and hazard modeling), Sungbin Cho of ImageCat Inc. (network analysis, Import Wizard development, and seismic modeling and analysis support), Jean Paul Lavoie of Geodesy (lead programmer for REDARS™ 2 SRA software, with support from his co-worker at Geodesy, Chip Eitzel), Charles Huyck of ImageCat Inc. (Import Wizard development and programming support), Howard Chung of ImageCat Inc. (seismic modeling and analysis support), and Ronald T. Eguchi of ImageCat Inc. (principal investigator for Task B1-4 and internal project review). In addition, the following major contributors are acknowledged:

- Dr. Ian Buckle, Dr. George Lee and Mr. Jerry O'Connor for their leadership of this overall FHWA-MCEER research project on behalf of MCEER, and their encouragement and helpful suggestions throughout this research.
- Dr. Phillip Yen of FHWA for his leadership of this overall project on behalf of FHWA, and his foresight and support of this SRA research.
- Prof. Masanobu Shinozuka of the University of California at Irvine CA for his excellent contributions and support of this SRA research.
- Prof. James E. Moore II of the University of Southern California in Los Angeles CA for his helpful guidance and support of the network-analysis research throughout this project.
- The helpful and thoughtful comments and questions from the Highway Seismic Research Council and its Research Advisory Subcommittee (which included Charles Kircher, Keith Porter, Edgar Small, and Steve Leung).

Over the past 2½ years, the California Department of Transportation (Caltrans) has also supported this work through a "REDARS Demonstration Project." The objective of this project has been to assess the applicability of the REDARS™ SRA methodology and software to Caltrans' seismic risk reduction programs. During the course of this project, their staff beta tested the REDARS™ 2 software, facilitated the development of the default component repair models presented in this manual that were largely based on the experience and background of their technical staff, and provided helpful suggestions throughout the project. The support of the following Caltrans project staff is particularly acknowledged: Mandy Chu (Caltrans' project manager); Zhongren Wang, Brian Chiou, Loren Turner, and Mike Jenkinson (beta testers and technical reviewers); and the following members of their technical staff who interacted with REDARS Development Team members during this project: Dan Adams, Randy Anderson, Matt Bailey, Bill Farnback, Minh Ha, Tom Harrington, Leo Mahserelli, Ray Mailhot, Tinu Mishra, Ganapathy Murugesh, Steve Sahs, Tom Shantz, Kirsten Stahl, Kevin Thompson, Brian Weber, Mark Yashinsky, and Foued Zayati.

CONTENTS

SECTION	TITLE	PAGE
1	**INTRODUCTION**	**1**
1.1	Statement of the Problem	1
1.2	Prior FHWA-MCEER Development Efforts	1
1.3	Current Project	2
1.4	Benefits	2
1.4.1	Applications	3
1.4.2	Decision-Guidance Tool	3
1.5	Users	4
1.6	Report Outline	5
2	**SEISMIC RISK ANALYSIS METHODOLOGY**	**7**
2.1	Overview	7
2.2	Features	7
2.3	Seismic Analysis Modules	10
2.3.1	System Module	10
2.3.1.1	Input Data	10
2.3.1.2	Transportation Network Analysis Procedure	11
2.3.2	Hazards Module	11
2.3.2.1	Input Data	11
2.3.2.2	Hazards Estimation Models	12
2.3.3	Component Module	13
2.3.3.1	Overview	13
2.3.3.2	Default and User-Specified Models	13
2.3.3.3	Input Data for Default Bridge Models	14
2.3.3.4	Bridge Overpasses	14
2.3.3.5	Retrofitted Bridges	15
2.3.3.6	Use of Component Traffic States to Develop System States	15
2.3.4	Economic Module	15
2.4	Analysis Procedures	15
2.4.1	Step 1. Initialization	15
2.4.1.1	Data from Import Wizard	16
2.4.1.2	Walkthrough Table Data	16
2.4.1.3	Other User-Provided Data	16
2.4.1.4	“Lambda” Calculations	16
2.4.2	Step 2. System Analysis	17
2.4.3	Step 3. Check Need for Additional System Analysis	17
2.4.4	Step 4. Aggregate Results	18
2.5	Use of SRA Results for Seismic Risk Reduction Decision Making	18
2.5.1	Step 1. Identify Seismic Decision Alternatives	18
2.5.2	Step 2. Establish Seismic Performance Requirements	20

CONTENTS (Continued)

SECTION	TITLE	PAGE
2.5.3	Step 3. Apply SRA for Baseline Condition and for Each Seismic Decision Alternative	22
2.5.3.1	Baseline System Performance	22
2.5.3.2	Post-Earthquake System Performance for Each Decision Alternative	23
2.5.4	Step 4. Evaluate Seismic Design Alternatives and Select Preferred Alternative	23
3	**EARTHQUAKE MODELING AND HAZARDS MODULE**	**25**
3.1	Objective	25
3.2	Scenario Earthquakes	25
3.2.1	Overview	25
3.2.2	Regional Earthquake Source Models	25
3.2.3	Walkthrough Analysis Procedure	26
3.2.3.1	Step 1. Total Duration of Walkthrough Table	26
3.2.3.2	Step 2. Scenario Earthquakes during Each Year of Walkthrough	26
3.3	Ground Motion Hazards	27
3.3.1	Hazard Description	27
3.3.2	Hazard Evaluation Procedure	27
3.3.2.1	Model Overview	27
3.3.2.2	Model Differences	27
3.3.2.3	Model Output	28
3.3.3	Input Data	29
3.3.4	Current REDARS 2 Ground Motion Models	29
3.3.4.1	Abrahamson-Silva (1997) Model	30
3.3.4.2	Silva et al. (2002 and 2003) Model	30
3.3.4.3	Future Direction	31
3.4	Liquefaction Hazards	31
3.4.1	Hazard Description	31
3.4.2	Hazard Evaluation Procedure	31
3.4.2.1	Step 1. Initial Screening	31
3.4.2.2	Step 2. Lateral Spread Displacement Hazards	32
3.4.2.3	Step 3. Vertical Settlement	32
3.5	Surface Fault Rupture Hazards	33
3.5.1	Hazard Description	33
3.5.2	Hazard Evaluation Procedure	34
3.5.2.1	Step 1. Initial Screening	34
3.5.2.2	Step 2. Permanent Ground Displacement Hazards	34
4	**COMPONENT MODULE**	**37**
4.1	Introduction	37
4.1.1	Performance Metrics	37
4.1.2	Modeling Procedure	37
4.1.3	Default and User-Specified Models	38

CONTENTS (Continued)

SECTION	TITLE	PAGE
4.1.4	Deterministic and Probabilistic Models	38
4.2	Default Models for Bridges	39
4.2.1	Input Data	39
4.2.1.1	Data Needs	39
4.2.1.2	Current Databases and Bridge Management Systems	39
4.2.1.3	Further Developments	40
4.2.1.4	Bridge Database for REDARS™ 2	41
4.2.2	Model for Estimating Bridge Damage due to Ground Shaking	41
4.2.2.1	General Evaluation Procedure	41
4.2.2.2	Damage States	42
4.2.2.3	Development of HAZUS99-SR2 Model	42
4.2.2.4	Modification of HAZUS99-SR2 Structural Capacities	44
4.2.2.5	Implementation of Modified HAZUS99-SR2 Model	46
4.2.3	Model for Estimating Bridge Damage due to Ground Displacement	46
4.2.4	Bridge Repair Model	47
4.3	Default Model for Approach Fills	48
4.3.1	Approach Fill Settlement	48
4.3.2	Repair Model	49
4.4	Default Model for Roadway Pavements	49
4.5	Tunnel Models	49
5	**SYSTEM MODULE**	**53**
5.1	Overview	53
5.2	Variable-Demand Model	53
5.2.1	Statement of the Problem	53
5.2.2	Modeling Issues	54
5.2.3	Model Development	54
5.2.4	Loss Estimation Challenges	56
5.2.5	Calibrating the Demand Function	57
5.2.6	Performance of Variable-Demand Model	58
5.3	Update of Minimum Path Algorithm	60
5.3.1	Background	60
5.3.2	Moore-Pape Minimum-Path Algorithm	60
5.3.3	Dual-Simplex Minimum-Path Algorithm	61
5.4	Multiple Trip Types	62
6	**ECONOMIC MODULE**	**63**
6.1	Background	63
6.2	Objective	63
6.3	General Approach for Developing Default Loss Estimates	64
6.4	Loss Sources	64
6.4.1	Repair Costs	64

CONTENTS (Continued)

SECTION	TITLE	PAGE
6.4.2	Losses due to Travel-Time Delays and Trips Foregone	64
6.5	Unit Losses	65
7	**DEMONSTRATION APPLICATION**	**67**
7.1	Objective and Scope	67
7.2	Models	68
7.2.1	Highway System	68
7.2.2	Bridges	68
7.2.3	Soil Conditions	70
7.2.4	Traffic Analysis Zones	70
7.2.5	Routes	71
7.2.6	Earthquake Scenarios	73
7.3	Deterministic Analysis	76
7.3.1	Earthquake Scenario	76
7.3.2	Seismic Hazards	76
7.3.2.1	Ground Shaking	76
7.3.2.2	Surface Fault Rupture	78
7.3.2.3	Approach Fill Settlement	78
7.3.3	Component Performance	78
7.3.4	System States	83
7.3.5	Traffic and Trip-Demand Impacts	83
7.3.6	Economic Losses	92
7.4	Probabilistic Analysis	94
7.4.1	Probabilistic Output	94
7.4.1.1	Characterization of Seismic Performance of Overall Highway System	94
7.4.1.2	Characterization of Seismic Performance of Individual Components of Highway System	99
7.4.1.3	Characterization of Uncertainties in Ground Motions	102
7.4.2	Convergence Checks	102
7.4.2.1	Background	102
7.4.2.2	Results	103
7.5	Example Economic Analysis of a Bridge Retrofit Program	105
7.5.1	Background	105
7.5.2	Suppositions	107
7.5.3	Analysis Approach	107
7.5.3.1	Estimation of Retrofit Costs	107
7.5.3.2	Estimation of Reduction of Losses due to Bridge Retrofits	107
7.5.3.3	Computation of Benefit-Cost Ratio	108
7.5.3.4	Computation of Standard Deviation of Losses	108
7.5.4	Results	108
7.5.4.1	Benefit-Cost Ratio	108
7.5.4.2	Standard Deviation of Losses	109

CONTENTS (Continued)

SECTION	TITLE	PAGE
7.6	Closing Comments	110
8	**CONCLUSION**	**111**
8.1	Summary	111
8.2	Comments	112
8.3	Future Directions	113
9	**REFERENCES**	115

LIST OF ILLUSTRATIONS

FIGURE	TITLE	PAGE
2-1	REDARS™ 2 Methodology for Seismic Risk Analysis of Highway Systems	8
2-2	REDARS™ 2 Seismic Analysis Modules	9
2-3	Development of REDARS™ 2 Input Data from Publicly Available Databases	10
2-4	Use of SRA Results for Seismic Risk Reduction Decision Making	19
2-5	Selection of Design Acceleration for a Wharf Structure	21
2-6	Illustrative Results for Evaluation of Alternative Bridge Retrofit Priorities	22
4-1	HAZUS99-SR2 Tunnel Fragility Models: Ground Shaking	50
4-2	HAZUS99-SR2 Tunnel Fragility Models: Permanent Ground Displacement	51
5-1	Fixed Demand Model for an Earthquake-Damaged Network	55
5-2	Variable-Demand Model for an Earthquake-Damaged Network	55
5-3	Real Trip Rate and Estimated Demand Function	58
5-4	Trip Demand and Travel Time	59
5-5	Reduced Trips and Travel Time	59
5-6	Comparison of Minimum Paths from Neighboring Origins	61
6-1	Variable-Demand Model for Earthquake-Damaged Highway System	65
7-1	LA-Testbed Highway System	68
7-2	REDARS™ 2 Model of LA-Testbed Highway System	69
7-3	Locations of Bridges in LA-Testbed Highway System	69
7-4	Soil Conditions (in terms of NEHRP Site Classifications) Throughout LA-Testbed Highway System	70
7-5	Traffic Analysis Zones whose Travel-Times and Trips to/from These Zones are Displayed as Output from this Demonstration Application	71
7-6	Routes Whose Travel Times are Displayed as Output from This Demonstration Analysis	72
7-7	Epicenters of Earthquake Scenarios in 10,000-Year Walkthrough Table	73
7-8	Ground Motions	77
7-9	Permanent Ground Displacement from Surface Fault Rupture and Approach-Fill Settlement	79
7-10	Component Damage States	80
7-11	Post-Earthquake System States	84
7-12	Post-Earthquake Traffic Volumes	86
7-13	Post-Earthquake Travel-Time Increases for Automobile Trips	87

LIST OF ILLUSTRATIONS (Continued)

FIGURE	TITLE	PAGE
7-14	Post-Earthquake Reductions in Automobile Trips	89
7-15	Economic Losses	95
7-16	Percent Increase in Access Times to UCLA Medical Center	96
7-17	Percent Increase in Travel Time along I-405 between I-10 and I-105 (Key Route to LA International Airport)	97
7-18	Percent Reduction in Trips to Downtown LA	98
7-19	LA-Area Highway System Map showing Those Bridges with the Highest Probability of Collapse	100
7-20	Probability Bar Charts for Bridges with Different Degrees of Vulnerability	101
7-21	Probability Bar Charts for Unretrofitted and Retrofitted Bridge 53 1984L	101
7-22	REDARS™ 2 Probabilistic Ground Motion Estimates at Bridge 53 1318 in LA-Testbed Highway System	102
7-23	Confidence Intervals for Results of Probabilistic SRA of LA-Testbed System	104
7-24	Column-Jacketed Bridges in LA Testbed Highway System	105
7-25	Maps showing Probabilities of Collapse of Bridges throughout LA Testbed Highway System	106

LIST OF TABLES

TABLE	TITLE	PAGE
2-1	Uses of Highway System SRA for Seismic Risk Reduction Decision Making	19
4-1	Supplementary Bridge Database under Development at Caltrans	40
4-2	Jernigan et al. (1998) Database for Bridges in Shelby County, Tennessee	41
4-3	Fields in NBI Database used in HAZUS99-SR2 Bridge Model to Infer Bridge Attributes Relevant to Seismic Performance	42
4-4	Damage States considered in HAZUS99-SR2 Bridge Model	43
4-5	Example Repair Model for Drilled Tunnel in California	51
7-1	Component Damage Summary	81
7-2	Collapsed Bridges and Nearby Uncollapsed Bridges from Scenario Earthquake along Santa Monica Fault	82
7-3	Summary of Estimated Earthquake Impacts on System-Wide Traffic	85
7-4	Post-Earthquake Travels Time Increases for Traffic Analysis Zones shown in Figure 7-5	90
7-5	Post-Earthquake Trips to/from Traffic Analysis Zones shown in Figure 7-5	91
7-6	Post-Earthquake Travel Times along Key Routes shown in Figure 7-6	92
7-7	Economic Losses due to Travel-Time Delays and Trips Foregone	93
7-8	Estimated Total Economic Loss due to This Scenario Earthquake	93
7-9	Benefit-Cost Ratios for Evaluation of Economic Viability of Program to Retrofit 231 Bridges in LA-Testbed System between 1994 and 2004	109
7-10	Standard Deviations of Losses for use in Evaluation of Economic Viability of Program to Retrofit 231 Bridges in LA-Testbed System between 1994 and 2004	109

APPENDICES

****NOTE: Appendices A – K are provided at the end of this report.**

APPENDIX	TITLE
A	PROBABILISTIC FRAMEWORK**
B	EARTHQUAKE SCENARIOS AND WALKTHROUGH FILES**
C	IMPORT WIZARD**
D	SOURCE-SITE DISTANCES AND GROUND-MOTION HAZARDS**
E	LIQUEFACTION HAZARDS**
F	SURFACE FAULT RUPTURE HAZARDS**
G	DEFAULT BRIDGE MODELING PROCEDURES**
H	DEFAULT MODELS FOR APPROACH FILLS AND ROADWAY PAVEMENTS**
I	POST-EARTHQUAKE TRIP REDUCTION AND UPDATED MINIMUM PATH ALGORITHM IN NETWORK ANALYSIS PROCEDURE**
J	CONFIDENCE LIMITS FOR PROBABILISTIC SEISMIC RISK ANALYSIS RESULTS**
K	CALIBRATION OF DEFAULT BRIDGE-DAMAGE MODEL**
	Post-Sampling Variance Reduction for Seismic Risk Analysis of Spatially Distributed Lifeline Networks

LIST OF ACRONYMS

AAL	Average Annualized Loss
AC	Asphalt Concrete
ADOX	Active Data Object Extension
CALTRANS	California Department of Transportation
CERI	Center for Earthquake Research and Information
CGS	California Geological Survey
CI	Confidence Interval
CUS	Central United States
ER&R	Earthquake Response and Recovery
FDM	Fixed-Demand Model
FEMA	Federal Emergency Management Agency
FHWA	Federal Highway Administration
GIS	Geographic Information Systems
GUI	Graphical User Interface
HPMS	Highway Performance Monitoring System
LA	Los Angeles
LRS	Linear Referencing System
MDB	Microsoft Access Database
MPO	Metropolitan Planning Organization
NBI	National Bridge Inventory
NCEDC	Northern California Earthquake Data Center
NEHRP	National Earthquake Hazards Reduction Program
NHPN	National Highway Planning Network
OD	Origin-Destination
PGA	Peak Ground Acceleration
PGD	Permanent Ground Displacement
PSHA	Probabilistic Seismic Hazard Analysis
RCR	Repair Cost Ratio
RDF	REDARS Data File
REDARS	Risk from Earthquake Damage to Roadway Systems

RPR	REDARS Probabilistic Analysis
RVB	REDARS Visual Basic for Application
SCAG	Southern California Area of Governments
SCEC	Southern California Earthquake Center
SRA	Seismic Risk Analysis
TAZ	Traffic Analysis Zone
TCW	Tri-Center Workshops
USGS	United Stated Geological Survey
VDM	Variable-Demand Model
ZOD	Zone of Deformation

CHAPTER 1: INTRODUCTION

1.1 STATEMENT OF THE PROBLEM

Past experience has shown that earthquake damage to highway components (e.g., bridges, roadways, tunnels, retaining walls, etc.) can go well beyond life safety risks and the costs to repair the component itself. Rather, such damage can also severely disrupt traffic flows and this, in turn, can impact the economy of the region as well as post-earthquake emergency response, repair, and reconstruction operations. Furthermore, the extent of these impacts depends not only on the seismic performance characteristics of the individual components, but also on the characteristics of the highway system that contains these components. System characteristics that will affect post-earthquake traffic flows include: (a) the highway system network configuration; (b) locations, redundancies, and traffic capacities and volumes of the system's roadway links; and (c) component locations within these links (Basoz and Kiremidjian, 1996; Shinozuka et al., 1999, Wakabashi 1999; Werner et al., 2004).

From this, it is evident that earthquake damage to certain components (e.g., those along important and non-redundant links within the system) will have a greater impact on the system performance (e.g., post-earthquake traffic flows) than will other components. Unfortunately, such system issues are typically ignored when specifying seismic retrofit priorities, performance requirements, and design/strengthening criteria for new and existing components; i.e., each component is usually treated as an individual entity only, without regard to how the extent of its damage from earthquakes may impact highway system performance. For example, current criteria for prioritizing bridges for seismic retrofit represent the importance of the bridge as a traffic-carrying entity only by using average daily traffic count, detour length, and route type as parameters in the prioritization process. These criteria do not account for the systemic effects associated with the loss of a given bridge, or for combinatorial effects associated with the loss of other bridges in the highway system. However, consideration of these systemic and combinatorial effects can provide a much more rational basis for establishing seismic retrofit priorities and performance requirements for bridges and other highway components.

1.2 PRIOR FHWA-MCEER DEVELOPMENT EFFORTS

During the period extending from 1993-2000, the Federal Highway Administration (FHWA) sponsored a seismic research project that was directed and conducted by the Multidisciplinary Center for Earthquake Engineering Research (MCEER). The purpose of this program was to develop: (a) seismic retrofit and evaluation methodologies for existing highway systems and structures (including bridges and also tunnels, retaining structures, slopes, culverts, and pavements); and (b) improved seismic design criteria and procedures for these structures.

One of the tasks from this project was to develop a new methodology for seismic risk analysis (SRA) of highway systems that addresses the issues summarized in Section 1.1. This methodology is named REDARS™ (Risks from Earthquake DAmage to Roadway Systems). It uses data and models from the geosciences (seismology and geology), engineering (structural, geotechnical, and transportation), repair and reconstruction, system evaluation (for roadway

transportation network analysis), and economics, in order to develop deterministic and probabilistic estimates of the seismic performance of highway systems. In this, seismic performance of these systems is measured in terms of potential for earthquake-induced disruptions of system-wide travel times and traffic flows, and the economic impacts and other losses due to these disruptions. The methodology was successfully used to estimate seismic risks and potential earthquake-induced losses to the highway in Shelby County, Tennessee (Werner et al., 2000).

1.3 CURRENT PROJECT

After the above research was completed, a second multi-year FHWA-MCEER seismic research project has been carried out to perform various structural, geotechnical, and SRA tasks that focused on the seismic performance of the highway system. This report is a one of the final deliverables that is the combined effort of two of these tasks -- Tasks B1-2 and B1-4. These tasks focused on validation of the REDARS™ methodology that was developed under the prior FHWA-MCEER project, updating of the REDARS™ modules and models from the prior project, and development of the REDARS™ methodology into a public-domain software package that can be used to assess the seismic performance of highway systems nationwide.

This task resulted in the development of two software packages -- REDARS™ 1, which was interim demonstration software and REDARS™ 2 which is the end product of this public-domain software development effort. REDARS™ 1 performs simplified deterministic SRA of the Los Angeles area highway system for which SHAKEMAP ground-motion data are available (http://earthquake.usgs.gov/shakemap). Development of this interim software was motivated by the interest of several state highway transportation agencies, and the need to: (a) provide a simple tool to familiarize these agencies with basic SRA concepts, while the more extensive public-domain software REDARS™ 2 was being developed; and (b) enable the agencies to provide early feedback regarding desirable features to include in REDARS™ 2 (Werner et al., 2003).

Development of the REDARS™ 2 software package is now complete. This report describes the various models and modules that are included in this software, together with results of a demonstration application of the software to the northern Los Angeles area highway system. It is intended to familiarize users of REDARS™ 2 with the technical features of the software, and how it can be used to guide decision makers from government, transportation agencies, and consulting firms in their establishment of rational pre-earthquake risk-reduction strategies and post-earthquake risk reduction measures. In this, the unique feature of REDARS™ 2 is its ability to include traffic flow and travel time impacts in the assessment of alternative strategies that may be under consideration.

1.4 BENEFITS

This section summarizes the main benefits of REDARS™ 2 in terms of its capabilities to: (a) perform multiple levels and types of SRA applications that will accommodate the needs of a wide variety of users; and (b) serve as a pre- and post-earthquake decision guidance tool.

1.4.1 APPLICATIONS

REDARS™ 2 can implement a wide variety of deterministic and probabilistic analyses that will facilitate its application as a tool for pre-earthquake planning and for post-earthquake emergency response. It was specifically developed for use in the following types of applications by transportation agencies and/or their consultants:

- ***Pre-Earthquake Planning***. REDARS™ 2 can be used to evaluate and assess alternative pre-earthquake planning strategies and priorities for strengthening of existing highway components, establishing appropriate design criteria for new highway components, expanding the highway system, etc.

- ***Post-Earthquake Emergency Response.*** REDARS™ 2 can be used in real time after an actual earthquake to assist with emergency response activities in areas where SHAKEMAP-type ground-motion data have been recorded and transmitted back to a regional response-coordination center. For example, immediately after an earthquake (and before field inspectors have identified actual damage), REDARS™ 2 may be used to estimate potential "hot spots" within the highway system that may be likely to experience earthquake damage. In addition, after actual damage data for bridges and other components are obtained from field surveys, REDARS™ 2 can carry out analyses that incorporate these field damage data in order to: (a) estimate potential earthquake-damage consequences for the highway system (e.g., traffic flow bottlenecks, difficulties in accessing key medical or other emergency response facilities, etc.); and (b) help to assess various emergency response strategies for reducing these consequences (e.g., which damaged bridges to repair first, traffic rerouting around damaged areas, etc.).

1.4.2 DECISION GUIDANCE TOOL

The REDARS™ 2 SRA methodology can be applied to the existing system as well as to modified systems in which various seismic-risk-reduction options are modeled. In this way, the SRA methodology can indicate the effectiveness of these options in reducing system-wide economic and traffic flow impacts of system damage due to earthquakes. For example, options associated with each of the following types of seismic risk reduction can be evaluated:

- ***How should the System be Improved?*** The SRA methodology can evaluate relative effects of various system enhancement options for improving post-earthquake seismic performance. System enhancements that could be evaluated include: (a) strengthening of individual components; (b) construction of additional roadways to expand system redundancy; and (c) alternative post-earthquake traffic-management strategies.

- ***What Components should be Retrofitted First?*** REDARS™ 2 can be used when establishing priorities for retrofit of bridges and other roadway components, by enabling users to consider how various prioritization options could impact post-earthquake system performance. This can be accomplished by using the methodology to assess the how much the seismic performance of the overall highway system (i.e., how losses due to system-wide travel time delays) are improved when different sequences of component retrofits are followed.

- ***How should the Components be Retrofitted?*** The SRA methodology can also evaluate alternative retrofit strategies for the individual components and their relative impacts on post-earthquake traffic flows, travel times, and trip demands. For example, for those components selected for retrofit, SRA can assess the relative effectiveness of alternative levels and types of seismic strengthening in reducing system-wide traffic disruptions and economic losses, as well as overall repair costs. When assessing these options, these relative benefits should be weighed against the relative cost of each level and type of retrofit.

- ***What Post-Earthquake Response and Recovery (ER&R) Strategies should be Carried Out?*** Results from the SRA methodology can guide the planning of ER&R strategies that would be most effective in the presence of actual damage to the highway system. Such results can also guide the prioritization of highway-system risk-reduction options that would optimize the effectiveness of ER&R operations after an earthquake.

- ***How can Traffic best be Managed after an Earthquake?*** The effectiveness of various post-earthquake traffic-management strategies for reducing congestion can be tested by applying the SRA methodology.

- ***What Funding Level is Appropriate for Improving the System's Seismic Performance?*** Because SRA can estimate economic impacts of highway-system damage, it can help to justify government funding levels for system-wide seismic strengthening programs.

Section 2.5 of Chapter 2 provides further discussion of how the REDARS™ 2 SRA methodology can guide seismic risk reduction decision making.

1.5 USERS

REDARS™ 2 can be used by decision makers, technical staff, and researchers, as described below.

Decision makers are senior members of a transportation-agency staff, who have the ultimate responsibility and authority for: (a) identifying options for pre-earthquake seismic-risk-reduction or post-earthquake emergency response that are to be considered for the highway system; and for (b) selecting a preferred option that best meets highway-system-user needs and agency cost and acceptable-risk constraints. It is anticipated that these decision makers would direct technical staff, who would carry out the actual running and implementation of the REDARS™ 2 SRA for each option and then provide the analysis results to the decision maker for his/her review. To facilitate use of REDARS™ 2 by such decision makers, the software has been designed to provide a variety of deterministic and probabilistic output in clear and concise tabular, graphical, and GIS formats.

Technical staff consists of those users of REDARS™ 2 with the technical background for developing the appropriate input data, understanding the various models and modules that are included in REDARS™ 2, overriding REDARS™ 2 default models/data with user-specified models/data where appropriate, running the software, and interpreting its results.

Since the REDARS™ 2 SRA methodology is multidisciplinary, it is anticipated that, for a given application, the above tasks could be carried out by a team of multiple technical staff members (rather than a single staff member) who together encompass the range of engineering and scientific disciplines embodied in REDARS™ 2. It is further anticipated that this technical staff would work closely with the decision makers to support their planning of the SRA cases and options to be considered and their interpretation of the analysis results.

Researchers are representatives of university staffs or consulting firms who are experts in one or more of the technical disciplines embodied in the REDARS™ 2 methodology. Accordingly, they may use REDARS™ 2 in various research and development applications. For example, such applications could include improvement of REDARS™ 2 models/modules, investigation of consequences of various seismic-improvement or emergency-response options that may be considered for a particular scenario, and identification/evaluation of other types of output and results that may be developed by REDARS™ 2.

1.6 REPORT OUTLINE

The remainder of this report is organized into eight main chapters and eleven appendices. The eight chapters provide the basic framework and a demonstration application of the SRA methodology and its modules. Chapter 2 provides a summary of the main elements of the REDARS™ 2 SRA methodology. Chapters 3 through 6 summarize the main elements of the hazards, component, system, and economic modules of the methodology. A demonstration application of the SRA methodology to the northern Los Angeles, California highway system is provided in Chapter 7. Chapter 8 provides concluding comments and recommended directions for future maintenance, support, and upgrading of the REDARS™ 2 SRA methodology and software.

The eleven appendices of this report provide additional technical detail on the material contained in the main chapters. In particular, they address the probabilistic framework for the REDARS™ 2 SRA methodology (Appendix A), development of the earthquake walkthrough tables now included in REDARS™ 2 (Appendix B), the REDARS™ 2 Import Wizard which has been programmed to automate development of much of the input data needed for SRA of an actual highway system (Appendix C), the seismic hazard models for estimating seismic hazards from ground shaking, liquefaction, and surface fault rupture that are now built into REDARS™ 2 (Appendices D through F), the default procedures used to estimate damage states and repair costs, downtimes, and traffic states for bridges, approach fills, pavements, and tunnels (Appendices G and H), the network analysis procedure (Appendix I), a variance reduction procedure that has been developed under this project to assess confidence levels and limits in probabilistic loss results as increasing numbers of simulations are included (Appendix J), and advanced statistical analysis procedures for modifying the original default bridge model to enable its damage-state predictions for the Northridge earthquake to be more consistent with earthquake damage observations (Appendix K).

CHAPTER 2: SEISMIC RISK ANALYSIS METHODOLOGY

2.1 OVERVIEW

REDARS™ 2 enables users to carry out deterministic or probabilistic SRA for any user-specified highway system within the United States. The methodology for accomplishing this is shown in Figure 2-1. For probabilistic SRA, results are developed for multiple simulations, in which a "simulation" is defined as a complete set of system SRA results for one particular set of randomly selected input parameters and model parameters. The model and input parameters for one simulation may differ from those for other simulations because of random and systematic uncertainties. For deterministic SRA, one set of results is developed either for median input and model parameters or for one set of randomly-selected parameters.

For each simulation of a probabilistic SRA or for the single set of input parameters for a deterministic SRA, this multidisciplinary procedure uses geoseismic, geotechnical and structural engineering, repair/construction, transportation network, and economic models to estimate:

- ***Hazards.*** Seismic hazards at the site of each component in the highway system.

- ***Component Performance.*** Each component's damage state and traffic state due to these site-specific seismic hazards, in which the traffic state reflects the component's ability to carry traffic at various times after the earthquake as the damage is being repaired.

- ***System Performance.*** System-wide traffic flows (e.g., travel times, paths, and distances) throughout the system, also at various times after the earthquake, that are dependent on each component's traffic state, the redundancies and traffic-carrying capacities of the various roadways that comprise the system, and the trip demands (i.e., the number, type, origin, and destination for all trips that use the highway system).

- ***Losses.*** Consequences of earthquake-induced damage to the highway system, including: (a) economic impacts (repair costs and losses due to travel time delays); increases in travel times to/from key locations in the region (e.g., medical facilities, airports, centers of commerce, etc.); and (c) increases in travel times along "lifeline" routes within the system, which are previously designated routes that are essential for emergency response or national defense.

2.2 FEATURES

This REDARS™ 2 SRA methodology has the following features.

- ***Modular.*** The methodology includes a series of seismic-analysis modules (Fig. 2-2) that contain the input data and analytical models needed to characterize the highway system and its seismic performance, the seismic hazards, the seismic performance of the components, and the economic losses due to repair costs and traffic disruption. This modular structure will facilitate the inclusion of improved REDARS™ hazards, component, and network models, as they are developed from future research. It is further described in Section 2.3.

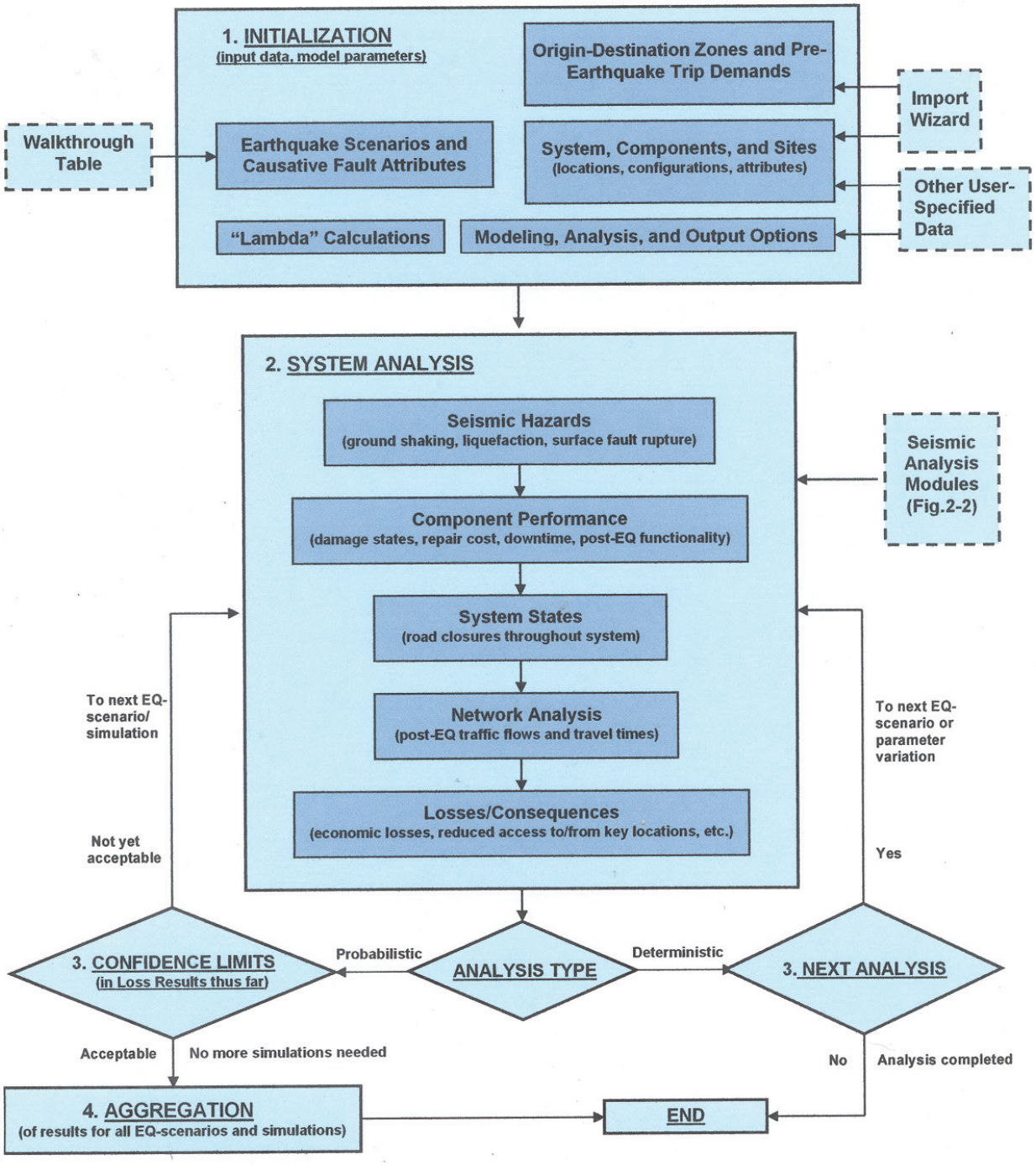

Figure 2-1. REDARS™ 2 Methodology for Seismic Risk Analysis of Highway Systems

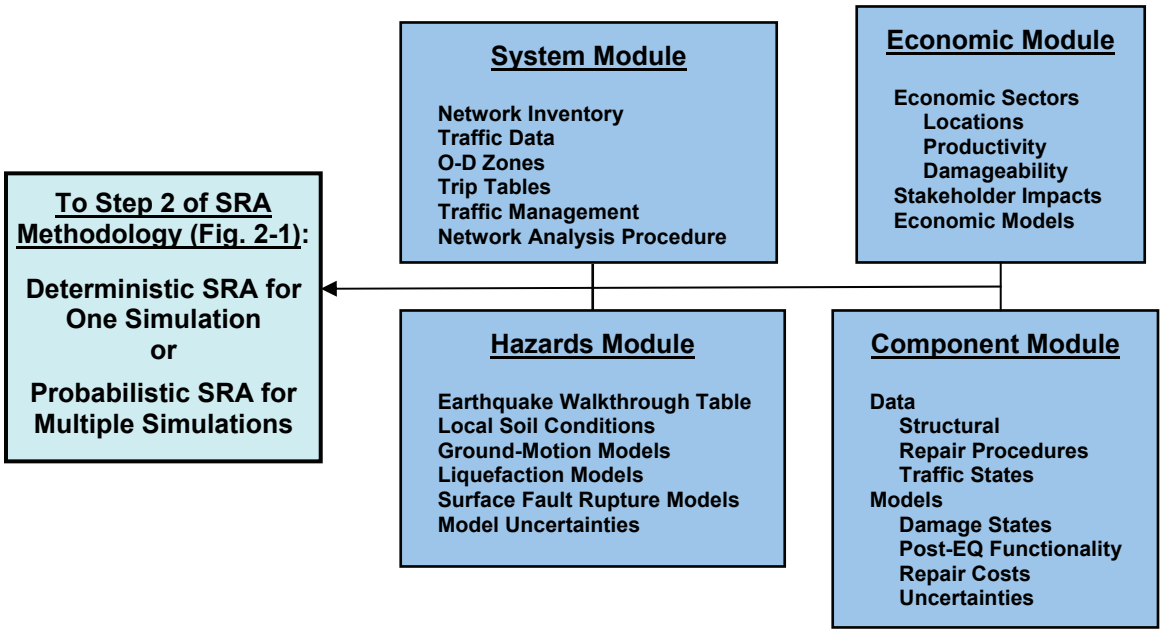

Figure 2-2. REDARS™ 2 Seismic Analysis Modules

- ***Multidisciplinary.*** The SRA methodology is a synthesis of models developed by earth scientists, geotechnical and structural earthquake engineers, transportation engineers and planners, and economists.

- ***Wide Range of Results.*** The methodology can develop multiple types/forms of results from deterministic or probabilistic SRA, in order to meet needs of a wide range of possible future users. Such results can be developed for use in pre-earthquake assessment of various options for seismic risk reduction, in which the effectiveness of each option in reducing losses due to highway-system disruption is evaluated. Results can also be developed for use in real time after an actual earthquake, in order to enable responders to assess the effectiveness of various options for reducing traffic congestion after an actual earthquake.

- ***Confidence Intervals (or Confidence Limits) for Probabilistic Loss Results.*** As loss results are developed from each multiple simulation in a probabilistic SRA, running displays of confidence intervals (CIs) in the loss results are displayed. Since the CIs improve as additional simulations are considered, these CI displays enable users to assess whether a sufficient number of simulations have been considered and the analysis can be terminated. This feature can substantially reduce analysis times for probabilistic SRA applications.

- ***Import Wizard.*** To carry out SRA of highway systems, publicly available databases must be used to define: (a) roadway topology and attributes; (b) bridge locations and attributes; (c) origin-destination (O-D) zones and pre-earthquake trip tables; and (d) site-specific NEHRP soil conditions (Figure 2-3). However, experience has shown that use of these databases can be time consuming due to various data inconsistency, connectivity, and continuity issues that often arise. Therefore, REDARS™ 2 includes an "Import Wizard" that facilitates the use of these publicly available databases by: (a) accessing the publicly available databases; (b)

guiding the user though the application of these databases to develop input data for REDARS™ 2; (c) resolving any inconsistencies between data from the various databases; and (d) checking the resulting highway-network model and the connectivity and continuity of the O-D zones. The Wizard is further described in Appendix C of this Manual and in Cho et al. (2006b).

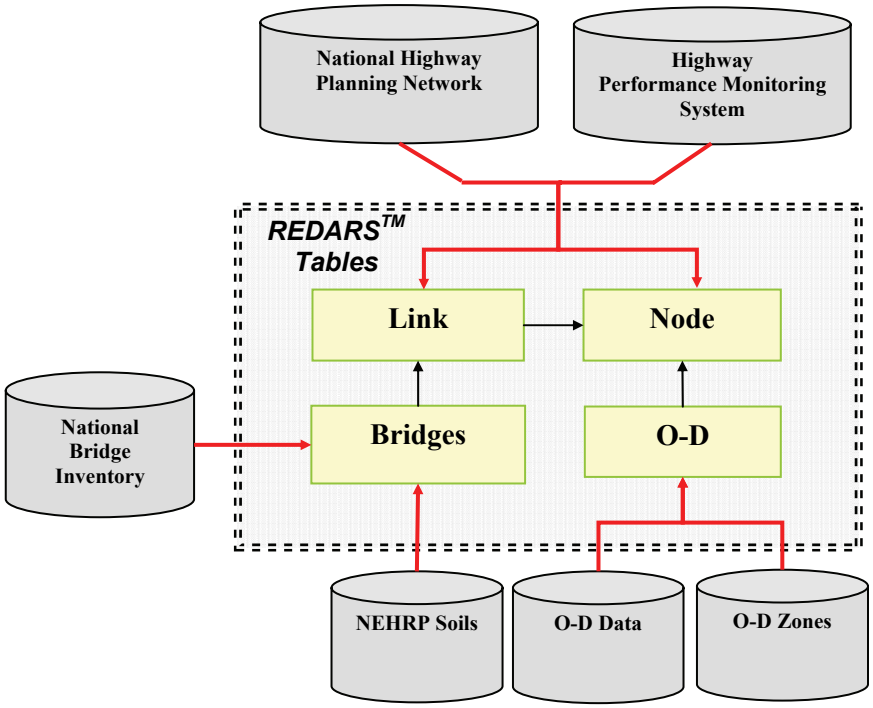

Figure 2-3. Development of REDARS™ 2 Input Data from Publicly Available Databases

2.3 SEISMIC ANALYSIS MODULES

The four REDARS™ 2 seismic analysis modules that are shown in Figure 2-2 are described in the following paragraphs.

2.3.1 SYSTEM MODULE

The system module contains input data and models for characterizing the highway system and its seismic performance (traffic flows, travel times, etc.) at various times after an earthquake.

2.3.1.1 Input Data

The input data contained in the System Module includes: (a) system network configuration linkages, and component types and locations; (b) numbers of lanes, traffic flows, capacities, and congestion functions for each highway link; (c) origin-destination (O-D) zones, the various trip types to be considered in the SRA (i.e., auto various types of freight, etc.) and, for each trip type,

the pre-earthquake trip tables; (d) any in-place traffic-management measures for modifying the system to ease post-earthquake traffic congestion (e.g., detour routes, changing roadways from two-way to one-way traffic, etc.); and (e) any special system characteristics, such as certain highways being critical for emergency response or national defense.

In order to develop the above data listed under Items (a), (b), and (c) above, the REDARS™ 2 user must first contact the Metropolitan Planning Organization (MPO) for the region being investigated, in order to obtain data that define the region's O-D zones and its trip tables for the various types of trips that are to be considered. Then, these O-D data are input into the Import Wizard, which also accesses various federal databases (i.e., the National Highway Planning Network, Highway Performance Monitoring System, and National Bridge Inventory databases, as shown in Figure 2-3) and then processes all of these data in order to provide them in a form that can be directly input into the REDARS™ 2 SRA.

The input data that describe post-earthquake traffic-management measures and special system characteristics (Items (d) and (e) above), are obtained by contacting the state, county, or local transportation departments for the region being evaluated.

2.3.1.2 Transportation Network Analysis Procedure

The transportation network analysis procedure contained in the System Module estimates post-earthquake traffic flows throughout the highway system, for each simulation and scenario earthquake. The procedure has the following features: (a) it represents the latest well-developed technology for providing rapid and dependable estimates of flows in congested networks, for given changes in network configuration due to earthquake damage; (b) it includes a "variable demand" feature that accounts for reductions in trip demands that would occur due to increased traffic congestion after an earthquake; (c) it accommodates various types of trips along the highway system (i.e., via automobile, via trucking for various types of freight, etc.) by enabling the user to specify separate trip tables for each trip type; and (d) it uses a numerically efficient minimum-path algorithm to significantly reduce computer times for estimating post-earthquake traffic flows. This procedure is further described in Chapter 5, and Appendix I of this report.

2.3.2 HAZARDS MODULE

The Hazards Module contains input data and models for characterizing system-wide seismic hazards for each scenario earthquake and simulation considered in the SRA of the highway system. The seismic hazards evaluated in the current Hazards Module are ground motion, liquefaction, and surface fault rupture. Earthquake-induced landslide hazards are not included at this time, but will be added into the next version of REDARS™.

2.3.2.1 Input Data

Input data used in the Hazards Module to evaluate seismic hazards for a probabilistic SRA consist of: (a) multiple earthquake scenarios, provided as a "walkthrough table" that specifies earthquake occurrences (magnitudes and locations) over time in accordance with established earthquake models for the region (see Section 2.4.1 and Appendix B); (b) local soil conditions

throughout the system, for use in estimating local geologic effects on ground shaking and the potential for liquefaction; and (c) locations and characteristics of any faults within the system that can produce surface rupture. Charter 3 provides a further description of these input data.

Deterministic SRA in REDARS™ 2 can be based on one of the following options: (a) a single earthquake from the walkthrough table, or any other earthquake with a user-specified magnitude and location; or (b) ShakeMap input data, which consist of near real-time maps of ground motion and shaking intensity following significant earthquakes (http://earthquake.usgs.gov/shakemap)[1]. For the first option, the input data are identical to that described above for probabilistic SRA applications, except that a single earthquake is considered instead of a walkthrough table of multiple earthquake scenarios. For ShakeMap applications, REDARS™ 2 downloads ground-motion maps directly from the above website.

2.3.2.2 Hazards Estimation Models

The main features of the hazards models currently included in REDARS™ 2 are summarized below, and are further described in Chapter 3 and Appendices D, E, and F of this report.

2.3.2.2(a) Ground-Motion Hazards

For each scenario earthquake and simulation, ground-motion hazards for a given scenario earthquake are estimated at the site of each component in the highway system. In most applications, these estimates are developed from ground-motion models built into REDARS™ 2 that consider: (a) site-specific rock motions, and their rate of attenuation over the distance from the seismic source to the site; (b) effects of local soil conditions in modifying the ground surface motions in the vicinity of the bridge or other highway component, relative to the underlying rock motions; (c) effects of faulting/directivity; and (d) uncertainties in these various estimates (if probabilistic SRA is being carried out. These ground-motion hazards are provided as peak accelerations or spectral accelerations at various natural periods, depending on the requirements of the component damage-state model[2].

2.3.2.2(b) Liquefaction Hazards

When the ground-motion hazards are estimated at each potentially liquefiable site in the highway system, liquefaction hazards are then estimated. In this, the potentially liquefiable sites within the system must be identified beforehand by the REDARS™ 2 user, through an initial geologic screening that is based on the REDARS™ 2 user's review of site soil conditions and topography. Then, for each potentially liquefiable site, permanent ground displacement (PGD) hazards (lateral spreading and vertical settlement) are evaluated for each scenario earthquake, using

[1] ShakeMap is a product of the United States Geologic Survey's Earthquake Hazards Program in conjunction with seismic network operators. At this time (June 2006), ShakeMap real-time ground motion maps can be generated in Northern California, Southern California, the Pacific Northwest, Nevada, Utah, and Alaska. In addition, ShakeMap estimates of ground motions from various hypothetical earthquakes or prior actual earthquakes are available.

[2] Of course, if deterministic SRA using a ShakeMap ground-motion map is instead being carried out, site-specific ground-motion hazards are estimated directly from these maps.

models that account for effects of uncertainties and the site's subsurface soil conditions, water table depth, ground shaking due to that earthquake, and topography.

2.3.2.2(c) Surface Fault Rupture Hazards

For each scenario earthquake that is caused by rupture along a fault of finite length that extends up to or very near the ground surface, PGD hazards are estimated at those sites within the highway system that fall in the fault rupture's zone of deformation. These estimates use input data that define the fault rupture attributes (location, orientation, type, rupture plane dip and directions) and the earthquakes magnitude and location within the rupture plane. From this, each component near the fault rupture is assessed to estimate whether it actually falls with the rupture's zone of deformation. For sites within this zone, PGDs are then estimated. Effects of uncertainties are included in these various estimates.

2.3.3 COMPONENT MODULE

2.3.3.1 Overview

The Component Module contains input data and models for estimating: (a) each component's seismic response to site-specific ground shaking and PGD hazards that are estimated by the models in the Hazards Module; (b) the component's "damage state," (i.e., the degree, types, and locations of any earthquake damage to the component); (c) how the damage will be repaired; (d) the costs and time duration of these repairs; and (e) the component's "traffic state" (i.e., whether it will need to be fully or partially closed to traffic during the repairs, and the durations of these closures). These traffic states will vary with time after the earthquake, to reflect the rate of traffic restoration over time as the repairs proceed.

2.3.3.2 Default and User-Specified Models

REDARS™ 2 contains first-order default models for estimating earthquake-induced damage states and associated repair requirements for bridges, pavements, and approach fills. The end results of these estimates are component repair costs and time-dependent traffic states, as a function of the level of site-specific ground motion and PGD. For bridges, these default models are probabilistic (in the form of fragility curves) whereas, for pavements and approach fills, they provide deterministic estimates of repair costs and traffic states as a function of PGD only. The models are further described in Chapter 4 and Appendices G and H of this report.

REDARS™ 2 also enables users to override any component's default model with a user-specified model. For bridges or tunnels, these user-specified models are typically based on detailed seismic analyses that are carried out by the user prior to the start of the REDARS™ 2 SRA. They take the form of fragility curves that prescribe the probability of occurrence of various damage states (and associated repair costs and traffic states) as a function of the level of ground shaking and PGD. For pavements and approach fills, the user-specified models consist of modifications to the default models. For tunnels, REDARS™ 2 requires that user-specified models must always be provided, in view of the variations in structural and site conditions and that will virtually always be present between various tunnels.

User-specified models for bridges will provide more refined seismic-performance estimates than will the default models. Therefore, they are most appropriate for modeling of bridges that: (a) have unique geometries and/or structural attributes; (b) are located along routes that are either non-redundant or are critical to post-earthquake response; or (c) will have a large impact on traffic flows over a significant portion of the highway system, if they are severely damaged. For example, in a past application of an early version of REDARS™ to the Shelby County (Memphis), Tennessee roadway system, user-specified models were developed for two major crossings of the Mississippi River (along Interstate Highways 40 and 55) whose seismic performance is vital to the region and to interstate-trucking traffic (Werner and Taylor, 2002).

However, the development of user-specified models for an individual bridge can be time consuming. Therefore, it is impractical to develop such models for most of the large number of more "typical" bridges that comprise a highway system. For such bridges, the default models are much more feasible to implement. Development of improvements to current default bridge modeling procedures is an area of active research (TCW 2003 and 2005).

For pavements and approach fills, the current REDARS™ 2 default models are based on California construction and repair practices. Therefore, they will not adequately characterize the seismic performance of pavements and approach fills for other states whose construction or repair practices will differ from those in California. Under such conditions, user-specified models that reflect these differing practices should be used.

2.3.3.3 Input Data for Default Bridge Models

The National Bridge Inventory (NBI) database is the only electronic database of attributes that is available for bridges nationwide (FHWA 2003). For this reason, the default bridge models currently included in REDARS™ 2 are based on the NBI database. In REDARS™ 2, the NBI data needed for analysis of the bridges in the particular system being analyzed are obtained through the Import Wizard.

The NBI database was developed primarily for bridge-maintenance applications. Therefore, it does not include much of the bridge-attribute data that would ordinarily be needed for seismic analysis. This was a constraint during the prior development of the default bridge models that are currently included in REDARS™ 2.

2.3.3.4 Bridge Overpasses

REDARS™ 2 estimates effects of bridge damage on traffic flows, not only along the roadway that the bridge is on, but also along any underlying roadway(s). However, the federal databases that are accessed by the Import Wizard do not specify whether a bridge crosses over a roadway, nor do they identify the underlying roadway(s). Therefore, REDARS™ 2 users must specify which bridges cross over an underlying roadway, together with the link numbers for the portion of each underlying roadway that is beneath the bridge.

2.3.3.5 Retrofitted Bridges

In many earthquake-prone regions of the United States, programs are underway to improve the seismic performance of vulnerable bridges by means of column-jacket retrofits. REDARS™ 2 can represents the beneficial effects of column jacketing by modifying the default bridge model as described in Chapter 4. However, the NBI database does not identify those bridges that have been column-jacketed. Therefore, the user must identify each retrofitted bridge in the highway system, as input to REDARS™ 2.

2.3.3.6 Use of Component Traffic States to Develop System States

After each component's traffic states at various post-earthquake times are obtained, they are incorporated into the highway system's network model in order to develop overall post-earthquake "system states" at each of these times. The system states consist of modified highway systems (relative to the pre-earthquake system) that now incorporate reduced traffic states of the various links in the system that have been damaged during the earthquake. These system states must also include the effect of each component's damage state on adjacent and underlying roadways. This, in turn, will depend on the level of damage to the component, and also on the component's location within the system. These system states are used by the REDARS™ 2 network-analysis procedure described in Chapter 5 and Appendix I, in order to estimate system-wide travel times and trip demands at each post-earthquake time.

2.3.4 ECONOMIC MODULE

The Economic Module contains a first-order model for estimating repair costs and economic losses due to increased travel times and reduced trip demands. Broader economic impacts of earthquake-induced travel-time increases and reduced trip-demands (i.e., their effects on businesses, stakeholders, and the regional/national economy) are not included. This module is further described in Chapter 6.

2.4 ANALYSIS PROCEDURE

This section summarizes the various analysis steps shown in Figure 2-1.

2.4.1 STEP 1. INITIALIZATION

Step 1 involves the development of input data that defines: (a) the highway system to be analyzed; (b) the attributes and locations of the various components that comprise this system, together with the soil conditions at the site of each component; (c) origin-destination zones and pre-earthquake trip demands; and (d) various modeling, analysis, and output options. These data are obtained from the Import Wizard, an earthquake walkthrough table, or user-specified input. In addition, calculation of a parameter named lambda -- which establishes the frequency of occurrence of damaging earthquakes within the full duration of the walkthrough table -- is computed. This parameter is needed for subsequent REDARS™ 2 calculation of confidence intervals for the loss results, under Step 3 of this analysis procedure.

2.4.1.1 Data from Import Wizard

The input data that defines the highway system, the bridge attributes, site-specific soil conditions needed to estimate ground-motion hazards, and origin-destination zones and pre-earthquake trip tables developed through the REDARS™ 2 Import Wizard, as summarized earlier in this chapter and further described in Appendix C and in Cho et al. (2006b).

2.4.1.2 Walkthrough Table Data

Earthquake scenarios are provided in terms of a walkthrough table. For each year within a total walkthrough duration that can be on the order of thousands or tens-of-thousands of years, this table prescribes the number of earthquakes occurring during that year, the location of each earthquake and whether it is caused by rupture along a known fault or an unknown (i.e., randomly-defined) fault, the moment magnitude of each earthquake, and the location and relevant attributes of the causative fault. This table is developed prior to the REDARS™ 2 analysis, using established regional earthquake models that account for the region's seismologic and geologic characteristics. Thus far, walkthrough tables have been developed for coastal California and for the region of the Central United States region that surrounds the New Madrid seismic zone. These walkthrough tables are described in Appendix B.

2.4.1.3 Other User-Provided Data

Other input data to be provided by the user during this initialization step are: (a) identification of potentially liquefiable sites within the highway system, and input soils data needed for the REDARS™ 2 analyses of earthquake-induced liquefaction hazards at these sites; (b) identification of column-jacketed bridges; (c) identification of bridges that cross over other roadways, along with the link number for the underlying bridge; (d) unit cost data, in units of dollars per unit travel-time-delay; and (e) modeling, analysis, and output options. These latter options include: (f) whether the analysis is to be deterministic or probabilistic; (g) user-specified models to be used for any components in the network; (h) identification of bridges and other components for which seismic-hazard and/or component-damage probabilities are to be monitored; (i) identification of origin-destination zones for which access and egress times and/or trip attraction and production are to be monitored; and (j) identification of lifeline routes along which travel times are to be monitored.

2.4.1.4 "Lambda" Calculations

After the highway-system model, bridge-attribute data, soils data, and earthquake walkthrough table are provided, and if the SRA is to be probabilistic, REDARS™ 2 initially performs an analysis that identifies those years within the walkthrough table during which at least some bridge damage occurs. Then, a parameter named "lambda" is calculated as the ratio of this number of years during which such damage occurs to the total number of years in the walkthrough table. This "lambda" parameter is used in the subsequent estimation of confidence intervals for the loss results (under Step 3 of the REDARS™ 2 methodology). Only those years during which some bridge damage occurs are further analyzed in the later steps of the SRA.

.

2.4.2 STEP 2. SYSTEM ANALYSIS

Step 2 consists of a full system analysis for one particular scenario earthquake and one set of site, component, and system parameters. If the SRA is to be deterministic, these input parameters can consist of either median values or one set of randomly selected values of parameters whose uncertainties have been modeled. For probabilistic SRA applications, this single analysis represents one simulation -- which is one set of loss results corresponding to one earthquake in the walkthrough table and one set of randomly selected parameters whose uncertainties have been modeled.

For the earthquake considered in Step 2, the system analysis consists of the following evaluations:

- *Hazard Evaluation.* First, the data and models contained in the Hazards Module are used to estimate the earthquake ground motion and PGD hazards throughout the system.

- *Direct Loss and System State Evaluation.* Once the ground motion and PGD hazards are estimated, the data and models from the Component Module are used to evaluate direct losses and system states (defined at various times after the earthquake).

- *Transportation Network Analysis.* The data and transportation network-analysis procedure from the System Module are applied to each post-earthquake system state, in order to estimate (a) system-wide travel times and trip demands; (b) access/egress times to/from key locations identified under Step 1; and (c) travel times along key lifeline routes also identified in Step 1. Differences between these post-earthquake results and pre-earthquake travel times measure how earthquake damage to the system affects its ability to carry traffic.

- *Economic Impact Evaluation.* The data and models from the Economic Module are applied to the above post-earthquake travel-time delays and trip demands, in order to estimate repair costs and losses due to travel time delays and trips foregone.

2.4.3 STEP 3. CHECK NEED FOR ADDITIONAL SYSTEM ANALYSIS

The operations under Step 3 will depend on whether the SRA is deterministic or probabilistic. If the SRA is deterministic, another analysis is carried out only if the user wishes to consider another scenario earthquake or input parameter variation (e.g., if deterministic sensitivity studies are being carried out). Otherwise, the deterministic analysis is ended.

If the SRA is probabilistic, Step 3 uses procedures described in Appendix J of this report to estimate confidence intervals (CIs) for the results from all simulations developed thus far. These CIs are then displayed for consideration by the user. If the user decides that these CIs are not yet acceptable, the SRA then develops another simulation by repeating the system analysis under Step 2 for a new earthquake scenario and a new set of randomly selected values of the uncertain parameters. When the CIs are judged to be acceptable, the SRA then proceeds to the final aggregation of all probabilistic results under Step 4 (as summarized in Section 2.4.4).

2.4.4 STEP 4. AGGREGATE RESULTS

Step 4 is carried out only if the SRA is probabilistic. If so, the results from all simulations are compiled and probabilistic aggregations of these results are developed. Such probabilistic results can be developed for: (a) economic losses due to highway-system damage; (b) ground-motion hazards at any component site previously identified under Step 1; (c) damage states for any component previously identified under Step 1; (d) increases in access/egress time and/or reductions in trip attraction/production for any key location previously identified under Step 1; and (e) travel time increases along any key lifeline route previously identified under Step 1.

When these aggregations are completed, the probabilistic SRA is terminated. These aggregations and the overall probabilistic SRA process are illustrated in a demonstration application of REDARS™ 2 to an actual highway system that is documented in Chapter 7.

2.5 USE OF SRA RESULTS FOR SEISMIC RISK REDUCTION DECISION MAKING

This development of the REDARS™ 2 software has been largely motivated by the need for a tool that can bring system-wide seismic risk issues into the decision-making process for establishing appropriate pre- and post-earthquake seismic risk reduction programs for a highway system. This important type of REDARS™ 2 application was first addressed in Section 1.4.2 and is further discussed here.

Table 2-1 summarizes the types of seismic-risk-reduction decisions that can be guided by REDARS™ 2 applications. One approach for using REDARS™ 2 in this way is through an acceptable-risk decision-guidance process. The process is based on the recognition that it is not possible to achieve a "zero seismic risk;" i.e., regardless of what degree of seismic risk reduction is implemented, there will always be some residual risk of unacceptable seismic performance of the highway system. An "acceptable" level of seismic risk is that level for which the costs to further reduce these residual risks are no longer acceptable.

The steps that comprise this process are shown in Figure 2-4 and are described in the remainder of this section. The demonstration application of REDARS™ 2 to an actual highway system that is described in Chapter 7 provides an example of the use of REDARS™ 2 results in this way.

2.5.1 STEP 1. IDENTIFY SEISMIC DECISION ALTERNATIVES

Under Step 1, the various options that are available to decision-makers as possible strategies for reducing seismic risks to the highway system are identified. In addition to the various measures listed in Table 2-1, other measures could include (a) financial planning to ensure adequate funds for emergency response and recovery operations, and to establish appropriate funding levels for seismic risk reduction; and (b) coordination with FEMA and other federal agencies to streamline the post-earthquake procurement of funds for highway-system repair and recovery.

Table 2-1. Uses of Highway System SRA for Seismic Risk Reduction Decision Making

Strategy	Description
Prioritization of Bridges for Seismic Retrofit	Evaluation of what retrofit sequence should be adopted for various bridges in the region, in order to optimize the benefits of the retrofit to the seismic performance of the highway system. SRA would be applied for different retrofit sequences, and would assess which sequence leads to the optimum seismic performance of the system.
Establishment of Design Acceleration Level for Bridge Design or Retrofit	Selection of alternative design acceleration levels should be considered for design of a new bridge or retrofit of an existing bridge. This should consider the initial construction costs associated with each design acceleration level, the potential for bridge damage, and its impact on the seismic performance of the highway system.
Emergency Response Planning	Evaluation of effects of various seismic decision options on access/egress times to or from key locations (e.g., hospitals, fire stations, airports, emergency command centers, centers of commerce). This could guide establishment of seismic retrofit priorities and design acceleration levels for components along emergency response routes. SRA can also be used in real-time assessment of seismic performance of a highway system after an actual earthquake, to guide real-time emergency response decision making.
Assessment of Available Repair Resources	Roadway downtimes due to earthquake damage will depend on available equipment, material, and labor for repair. SRA can assess how losses due to travel time delays are affected by these downtimes, and optimal repair resources for reducing these losses, by considering relative costs and benefits of various repair resource options.
System Enhancement	Assessment of how construction of new roadways that are being planned could improve the seismic performance of the highway system, as well as the effectiveness of possible short term traffic management strategies (e.g., conversion of selected roadways from one-way to two-way traffic) in improving system performance.

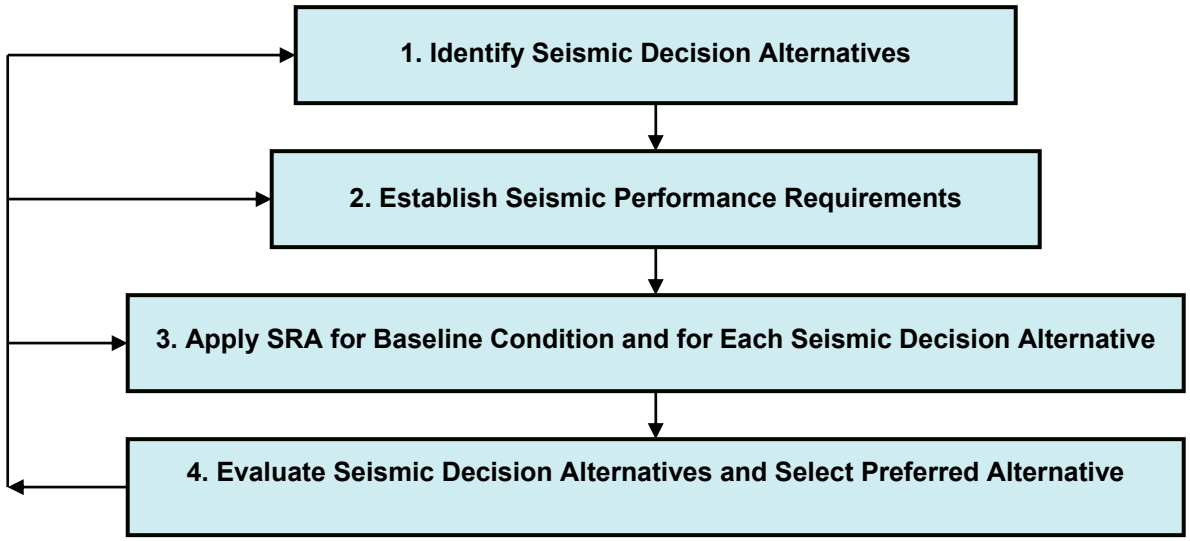

Figure 2-4. Use of SRA Results for Seismic Risk Reduction Decision Making

2.5.2 STEP 2. ESTABLISH SEISMIC PERFORMANCE REQUIREMENTS

Under Step 2, decision makers would tentatively select types and forms of SRA results that will be used to evaluate the seismic decision alternatives. This selection can consider input from stakeholders in the seismic performance of the highway system, such as: (a) federal, state, and local transportation officials -- who may wish to focus on performance requirements that minimize repair costs and downtimes of the highway system; (b) emergency response planners -- who may wish to include performance requirements that address acceptable levels of travel time delays to/from critical facilities; and (c) business and civic leaders -- who may wish to include performance requirements based on accessibility to/from regional commercial centers, etc.

The performance requirements may be either deterministic or probabilistic. For example, deterministic requirements could consist of acceptable levels of loss for a designated Level 1 earthquake (a moderate and frequently occurring event), and for a Level 2 earthquake (a severe and infrequently occurring event). Probabilistic requirements may consist of acceptable probabilities of exceedance for designated levels of loss due to highway system damage, or acceptable means and variances of total losses. In this, the losses should be computed as the present value of the initial cost for implementing the seismic decision alternative (e.g., the initial construction cost associated with a given design acceleration level), the post-earthquake repair costs, and the post-earthquake losses due to increased travel times and reduced accessibility to key locations in the region.

When establishing acceptable-risk levels and corresponding seismic-performance requirements, one must consider the initial costs needed to meet such requirements (e.g., initial costs of construction for alternative levels of design acceleration for retrofit of an existing bridge) as well as potential losses due to earthquake-induced damage of the highway system.

A systematic approach for obtaining an acceptable level of seismic risk uses evaluation of means and variances of total life-cycle costs for various seismic decision options (Werner et al. 1997; Ferritto et al., 1999; Werner et al., 2002). Features of the approach are:

- It estimates total life-cycle cost for each seismic-decision alternative which, as previously noted is computed as the present value of: (a) the initial cost for implementing the alternative (e.g., cost of construction associated with different design acceleration levels for a bridge); (b) post-earthquake repair costs; and (c) post-earthquake losses due to increases in travel time reductions in trip demands, or reduced access to key locations. Where higher-order economic losses can be estimated, they can also be included in this total cost computation.

- Mean values and variances of these life-cycle costs are computed through statistical analysis of the life-cycle costs associated with a given seismic decision alternative, as obtained from probabilistic SRA of that alternative for each scenario earthquake and simulation.

- Seismic decision alternatives are treated as “investments” in seismic risk reduction. One basis for evaluating an investment is in terms of its financial yield. In this SRA application, a higher “yield” of an investment in seismic risk reduction is viewed being analogous to minimizing the mean value of the total life cycle cost. In addition, a prudent investor

evaluates his/her investments not only in terms of their yield but in also in terms of their safety. In this, the safety (or reduction in volatility) of an investment in seismic risk reduction can be viewed in terms of lowering the variance (or standard deviation) of the life-cycle costs to an acceptable level.

- Figure 2-5 shows how this approach was used to establish a design acceleration level for a wharf structure at a major seaport in California. In this case, the decision-makers opted to use a design acceleration level of about 0.45 g, which is higher than the design acceleration at the minimum value of the life-cycle cost (which is about 0.25 g). This was based on their desire for reduced volatility in the seismic performance of this wharf. (Werner et al., 1997).

- Figure 2-6 shows how SRA results can be used to guide the establishment of priorities for retrofit of a several bridges within a highway system. In this, alternative priorities are evaluated in terms of the means and standard deviations of the resulting total costs. The dashed line in this figure shows those prioritization plans with the most favorable combinations of mean and variance (i.e., the lowest values of these quantities).

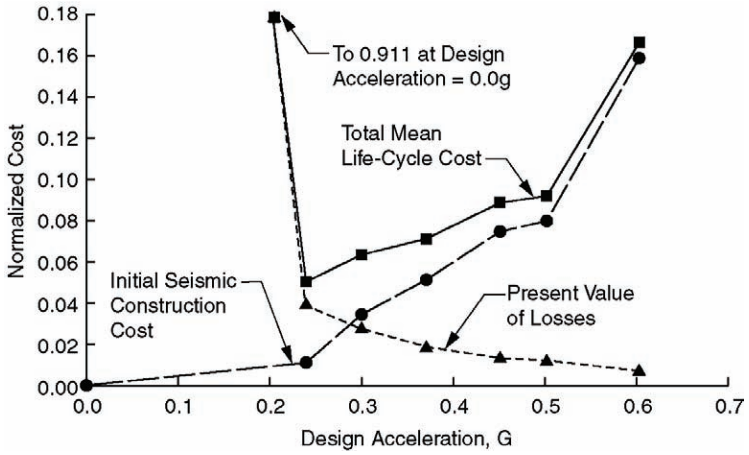

a) Mean Value of Total Life-Cycle Cost

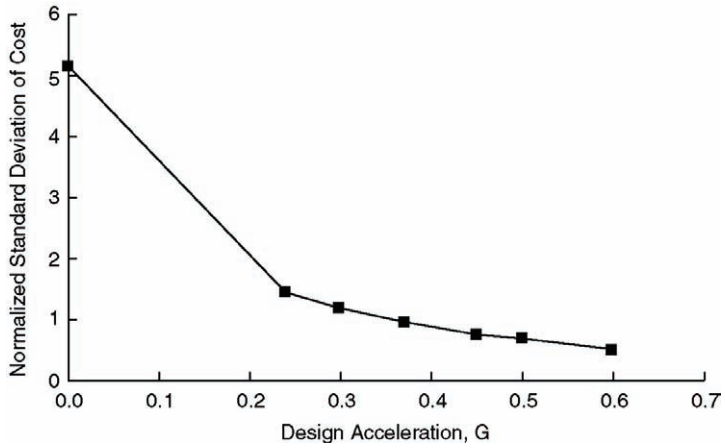

b) Volatility (Standard Deviation) of Total Life Cycle Cost

Figure 2-5. Selection of Design Acceleration for a Wharf Structure (Werner et al., 1999)

2.5.3 STEP 3. APPLY SRA FOR BASELINE CONDITION AND FOR EACH SEISMIC DECISION ALTERNATIVE

Under Step 3, SRA of the highway system is carried out for each earthquake event and simulation identified for consideration under the seismic performance requirements for the system (from Step 2).

2.5.3.1 Baseline System Performance

The SRA application starts with the development of a set of baseline system performance results. These baseline results should consist of:

- *Pre-Earthquake Performance of Existing Highway system.* The REDARS™ 2 transportation network analysis procedure is used in the Import Wizard to assess the pre-earthquake traffic flows, travel times, and costs of travel for the existing (undamaged) highway system.

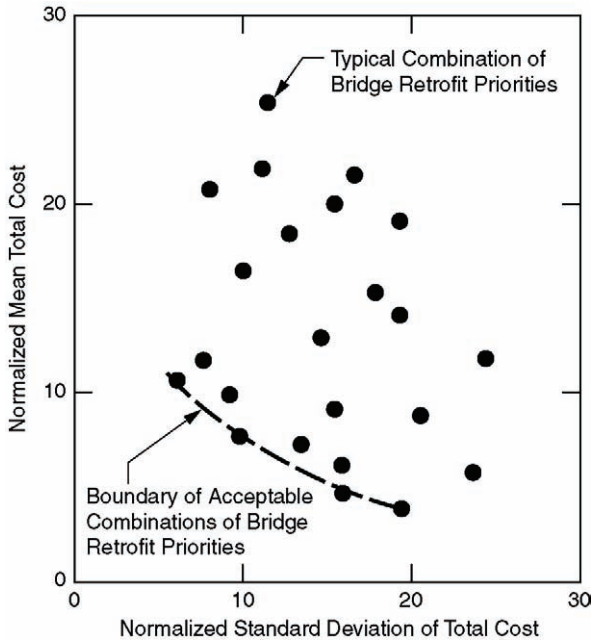

Figure 2-6. Illustrative Results for Evaluation of Alternative Bridge Retrofit Priorities

- *Post-Earthquake Performance of Existing Highway system.* Scenario earthquakes are applied to the existing highway system (before any seismic decision alternatives are considered), and SRA is carried out to evaluate post-earthquake traffic flows, travel times, and travel costs.

- *Baseline Results.* The pre- and post-earthquake performance of the existing highway system is compared in order to indicate the potential risks and losses that could occur in the absence of seismic risk reduction.

2.5.3.2 Post-Earthquake System Performance for Each Decision Alternative

Once the baseline system performance results are developed, it remains to carry out SRA of the highway system after each seismic decision alternative is implemented. To illustrate this process, suppose that the objective of the SRA is to establish appropriate levels of design acceleration for the upgrade of a major bridge for which seismic retrofit is planned. Also, suppose that five different levels of design acceleration have been identified as seismic decision alternatives in Step 1. Then, SRA of the highway system is carried out for cases in which the bridge is retrofitted to correspond to each of the alternative design acceleration levels. The resulting losses due to damage to the highway system after the bridge is retrofitted to each design acceleration level (due to repair costs, travel time delays, etc.), and the initial cost of construction for that design acceleration level, are used in Step 4 to evaluate the various design acceleration levels being considered.

2.5.4 STEP 4. EVALUATE SEISMIC DESIGN ALTERNATIVES AND SELECT PREFERRED ALTERNATIVE

Under Step 4, the SRA results for the baseline (existing) condition and for each seismic decision alternative are evaluated and compared. From this, a preferred alternative is selected. Stakeholder interaction in evaluating system performance goals relative to this overall decision-making process should be an important element of this step. On the basis of this interaction, it is possible that additional seismic decision alternatives may be identified, the seismic performance requirements for the highway system may need to modified, and/or additional SRAs may need to be implemented for additional cases or decision alternatives. If this occurs, one or more of the previous steps of the procedure may need to be repeated (see Figure 2-4).

CHAPTER 3: EARTHQUAKE MODELING AND HAZARDS MODULE

3.1 OBJECTIVE

The seismic hazards imposed on a highway system will depend on the magnitudes, locations, and frequencies of occurrence of earthquakes in the region, and on the local geology and soil conditions throughout the system. This chapter summarizes how earthquake scenarios are modeled in REDARS™ 2. It also describes the main elements of the REDARS™ 2 Hazards Module, which contains the data and models necessary to characterize the seismic and geologic hazards throughout the highway system due to each scenario earthquake and simulation. The hazards now included in this module are ground motions, liquefaction, and surface fault rupture. For each hazard, this chapter summarizes: (a) the hazard and its possible effects on highway systems; (b) methods for evaluating the hazard at each component site; and (c) the input data needed to implement the hazard evaluation procedure.

3.2 SCENARIO EARTHQUAKES

3.2.1 OVERVIEW

In a SRA of any lifeline system with spatially dispersed components, individual scenarios are needed to evaluate correlation effects of earthquakes -- i.e., the simultaneous effects (including systemic consequences of damage) of individual earthquakes on components at diverse locations. REDARS™ 2 enables users to specify earthquake scenarios in three ways: (a) as a walkthrough table of earthquake occurrences over time that are based on established regional earthquake models; (b) as an earthquake with an arbitrary user-specified moment magnitude and epicentral location; and (c) as an earthquake with ShakeMap estimates of regional ground motions. Section 3.2 addresses one of these earthquake designations -- the earthquake walkthrough-table.

An earthquake walkthrough table is developed during the initialization of the SRA methodology (Section 2.4.1). It is based on the use of random sampling of an established regional earthquake model to estimate earthquake occurrences during each year of a multi-year walkthrough duration. Each earthquake occurrence during each year of the walkthrough table is represented in terms of its moment magnitude, location, and causative fault attributes, and the table's earthquake occurrences over time represent the regional model's estimation of frequencies of earthquake occurrence. The table is used in a walkthrough analysis procedure for probabilistic SRA in REDARS™ 2 (Daykin et al., 1994). This procedure facilitates development of loss distributions from the SRA, estimation of confidence intervals for the loss results, and display of their variability over time.

3.2.2 REGIONAL EARTHQUAKE SOURCE MODELS

The REDARS™ 2 SRA methodology incorporates regional earthquake source models that have been adapted from models used by the United States Geological Survey (USGS) during their development of seismic hazard maps for the conterminous United States (Frankel et al., 2002). The USGS models have been selected because of their development by recognized earth

scientists and because of their subsequent extensive external review process. These models incorporate: (a) smoothed historical seismicity as one component of the hazard calculation; (b) a weighted combination of alternative models with different reference magnitudes, as well as large background zones based on broad geologic criteria; and (c) the use of geologic slip rates to estimate earthquake recurrence times for faults in the Western United States.

Thus far, earthquake walkthough tables have been developed for Coastal California and the Central United States (CUS), as described in Appendix B. The Coastal California walkthrough table is used in the demonstration SRA of the northern Los Angeles, California highway system that is described in Chapter 7. Future work will adapt the USGS models to other regions of the United States, so that REDARS™ will contain an extensive, consistent, and technically-robust set of walkthrough tables for earthquake-prone regions throughout the country.

3.2.3 WALKTHROUGH ANALYSIS PROCEDURE

The following paragraphs summarize the REDARS™ 2 walkthrough analysis procedure for probabilistic SRA applications. This procedure is further described in Appendix A.

3.2.3.1 Step 1. Total Duration of Walkthrough Table

In Step 1, the user selects the total time duration of the earthquake walkthrough table. This duration will typically be in the thousands of years. As noted in Chapter 2, the number of years actually considered in the walkthrough table may include only a segment of this total time duration if, for this segment, it turns out that the confidence intervals for the loss results are acceptable to the REDARS™ 2 user.

3.2.3.2 Step 2. Scenario Earthquakes during Each Year of Walkthrough

Step 2 generates the earthquake walkthrough table with the above duration. This is done first for Year 1, and then for each succeeding year of the walkthrough. For each year, a series of uniform random numbers is generated and used with various earthquake probability distributions developed from regional earthquake models (Sec. 3.2.2), in order to establish: (a) the number of potentially damaging earthquakes -- i.e., earthquakes with moment magnitude (M_w) ≥ 5.0 -- that have occurred somewhere in the region during the year; and (b) the location and the magnitude of each of these earthquakes. The table also includes the attributes of the causative fault for each earthquake (see Sec. 3.5.2.2). For earthquakes caused by rupture along known active faults, these attributes are estimated from regional fault-specific data. For earthquakes in the walkthrough table whose source is designated as “random” (i.e., the causative fault is unknown), fault attributes are estimated from regional seismologic and tectonic data (see App. B).

Note that, for the demonstration SRA of the northern Los Angeles, California highway system that is described in Chapter 7, the analysis allows for the possibility that more than one potentially damaging earthquake can occur during a single year. For other regions of the United States that are less seismically active, this possibility is more remote.

3.3 GROUND MOTION HAZARDS

3.3.1 HAZARD DESCRIPTION

Past earthquakes have shown that highway components can be susceptible to damage from strong ground shaking. The extent of this damage depends not only on the geometry and structural characteristics of the component, but also on the amplitude, frequency content, and duration of the ground shaking. Past earthquakes have also shown that the spatial distribution of ground shaking throughout a system will depend on the nature of the fault-rupture process, the travel paths followed by the seismic waves as they propagate from the earthquake source and throughout the highway system, and the local soil conditions within the system. Furthermore, empirical studies of recorded ground motions have shown that this distribution of ground shaking is not random; rather, it tends to attenuate with increasing distance from the seismic source and is usually most severe in soft soil deposits. In addition, for a given source-site distance and site conditions, the ground motions tend to increase with increasing earthquake magnitude, except for large magnitude earthquakes where saturation of the ground-motion amplitudes tends to occur. The estimation of ground shaking hazards is essential not only to evaluate the potential for system and component damage from these hazards, but also to assess other collateral hazards such as liquefaction.

3.3.2 HAZARD EVALUATION PROCEDURE

The procedure used to estimate earthquake ground motions for SRA of a highway system must account for the seismologic, geologic, and tectonic characteristics of the region and the local conditions at each component site throughout the system. Documentation of various approaches for considering these factors in the estimation of site-specific ground motions is readily available in the technical literature (e.g., Housner and Jennings, 1982; Seed and Idriss, 1982; Kramer 1996; Campbell 2003).

3.3.2.1 Model Overview

REDARS™ 2 uses ground-motion attenuation models to estimate ground motions at each component site due to each earthquake in the walkthrough table. This is because such models are plentiful and are the most practical approach available for rapid estimation of ground motions for the large number of sites and the many earthquakes that will need to be considered in a probabilistic SRA of a highway system.

Ground-motion attenuation models estimate site-specific ground motion by using an equation that includes terms to account for the earthquake's magnitude and distance from the site, local site conditions and, in many cases, hanging-wall, foot-wall, and directivity effects. Terms for representing uncertainties in the ground-motion predictions are also included in these equations.

3.3.2.2 Model Differences

Many different attenuation models are used in current practice (e.g., Campbell 2003 summarizes several of these models). Different models are used for different regions of the country, in order

to account for regional differences in tectonic characteristics. For example, because the Eastern and Central United States is more tectonically stable than the West, earthquakes in the East and Midwest are usually associated with higher stress drops and lower attenuation rates. This results in larger ground-motion amplitudes at short periods and large distances for earthquakes in the eastern and central regions of the country.

There are also differences between ground-motion models for a given region, due to differences in assumptions, data, and analysis procedures used to develop the various models. For example, the various ground-motion models developed for California earthquakes, where strong motion recordings are most plentiful, model differences arise because of: (a) different databases of the strong motion recordings used to develop the models; (b) different procedures for statistically analyzing the records from these databases; (c) different definitions of magnitude, distance, and site conditions; and /or (d) different definitions of ground-motion output from the model (i.e., some models may be based on statistical analysis of the largest component of horizontal motion recorded at a given station, whereas other models may be based on the average of the two horizontal components). In general, for comparable definitions of ground-motion output, most ground-motion models for California earthquakes provide reasonably similar ground-motion estimates when applied for ranges of magnitudes, distances, and site conditions where recorded motions are most plentiful. However, for other ranges of these parameters where ground-motion records are sparse, the ground-motion predictions by the various models can differ substantially.

Models for predicting ground motions in the central and eastern United States do not have the benefit of strong motion recordings that can provide a statistical basis for these models. Instead, the models have been developed from a variety of other methods such as: (a) statistical analysis of seismologically-based estimates of strong ground motion (e.g., Atkinson and Boore, 1995; Toro et al., 1997); (b) modifications of attenuation relationships from the western United States that were based on seismological estimates of ground motions from the western and eastern United States (e.g., Campbell 2003); and/or (c) consideration of qualitative effects of historical earthquakes that have been documented. Because of the lack of recorded strong motions on which to base these models, uncertainties in predicting ground motions in the Central and Eastern United States are much greater than for western United States.

3.3.2.3 Model Output

Output from the ground-motion attenuation models is provided as spectral accelerations for a range of natural periods (including the zero-period spectral acceleration which is equal to the peak acceleration). However, it is necessary to save spectral accelerations only for those periods that are used in the various geologic-hazard and component damage-state models that require ground-motion input data. In REDARS™ 2, spectral accelerations at periods of 0.3 sec. and 1.0 sec. are used in the default bridge damage-state model, and the peak ground acceleration is used in the liquefaction hazard model. If user-specified bridge models are used that require spectral accelerations at other natural periods, these spectral accelerations will also need to be saved.

It is, of course, important that the spectral acceleration output from the ground-motion attenuation model be consistent with the ground-motion input needed for the component damage-state and geologic-hazard models that are to be applied in REDARS™ 2. That is, if the

ground-motion model provides output as the average of the two components of recorded horizontal motion (instead of the maximum value), the damage state or geologic hazard models that use this data should be based on the same definition. Most current ground-motion models provide output as the average of the two horizontal components. Unfortunately, current bridge damage models often do not make this distinction (Baker and Cornell, 2006).

3.3.3 INPUT DATA

Input data for modeling earthquake ground-motion hazards at a given site in the highway system consist of: (a) the earthquake's moment magnitude; (b) the distance from the site to earthquake source; (c) the local soil conditions at the site; and possibly (d) other data, such as hanging-wall and foot-wall locations, and directivity parameters.

In REDARS™ 2, the moment magnitude for each scenario earthquake is specified in the earthquake walkthrough table, along with various parameters needed to compute source-site distances. These parameters include: (a) epicenter location; (b) depth to hypocenter and to seismogenic zone; (c) latitude, longitude, and depth of center of energy release; (d) fault type; (e) length, width, azimuth, and dip of each segment of the fault rupture plane; (f) direction of rupture along fault plane; and (g) zone of deformation due to fault rupture (if specified by the user). These quantities enable REDARS™ 2 to compute a wide variety of source-site distances, thereby enabling it to accommodate not only the ground-motion models that are currently included in REDARS™ 2, but also a wide variety of other models that may be added in the future. These source-site distance calculations are further described in Section D.2 of Appendix D.

The various ground-motion attenuation models typically characterize effects of local soil conditions by a single term in the ground-motion equation. In these models, local site conditions are represented either as NEHRP soil categories or as other categories that can be converted to the NEHRP categories. As described in Appendix C, the Import Wizard can accommodate digital NEHRP soils data, if such data are available for the region being analyzed and if: (a) the data are based on local geology and shear wave velocity and are provided in ESRI Shapefile format; (b) the data are in a geographic coordinate system; and (c) the datum matches that of the National Highway Planning Network (NHPN) base data, which are currently in NAD 1927. If such digital data are not available, the user must provide the NEHRP soil-category input data for all component sites in the highway system. For this situation, these estimates should be based on: (a) available topographic maps, quaternary-geologic maps, and maps with depth-to-bedrock contours throughout the system area; (b) available soil test data obtained along or near the highway system; and (c) correlation of the geologic units from the geologic maps with the various soil categories indicated by the soil test data.

3.3.4 CURRENT REDARS™ 2 GROUND MOTION MODELS

REDARS™ 2 now includes two ground-motion models. These models are briefly summarized below and are further described in Sections D.3 and D.4 of Appendix D.

3.3.4.1 Abrahamson-Silva (1997) Model

The Abrahamson-Silva (1997) ground-motion model applies to shallow crustal earthquakes in active tectonic regions of the western United States. Its main features are summarized below:

- It expresses the ground motion as a function of the earthquake magnitude, source-site distance, local soil conditions, type of faulting, whether the site is along the hanging wall of footwall of the ruptured fault plane, and inter-event and intra-event uncertainties.

- It computes spectral accelerations of horizontal and vertical ground motions at 28 periods that range from 0.01 sec. to 5.0 sec. The horizontal spectral acceleration represents the average of the two components of horizontal motion recorded during the various earthquake events cited in the Abrahamson-Silva (1997) paper.

- It uses moment magnitude to represent earthquake magnitude, and defines the source-site distance as the closest distance from the site to the rupture plane. Local soil conditions are characterized using two site classifications: (a) rock site, which has a soil thickness of less than 20 m that overlies rock; and (b) deep soil site, with soils whose thickness exceeds 20 m.

- It also includes: (a) a "style-of-faulting factor that accounts for whether the causative fault is reverse or strike-slip; and (b) a "hanging wall" factor that models differences between ground motions recorded on the hanging wall or foot wall of a dipping fault.

3.3.4.2 Silva et al. (2002 and 2003) Model

The Silva et al. (2002 and 2003) model applies to stable tectonic regions of the central and eastern United States. It has the following main features:

- The computation of ground motions involve the following steps: (a) computation of earthquake motions in hard rock (NEHRP Type A sites) as a function of earthquake magnitude and source-site distance; (b) conversion of these hard rock motions to corresponding motions in firm rock (NEHRP Type B sites); (c) development of a soil amplification factor relative to firm-rock motions; and (d) use of this factor, together with the firm-rock motions from Step b, in order to estimate site-specific ground motions including effects of local soil conditions and uncertainties.

- It uses moment magnitude to represent earthquake magnitude, and defines the source-site distance as the closest distance from the site to the surface projection of the rupture surface. Soil amplification factors are tabulated for different NEHRP site classifications and, for each classification, are provided as a function of the peak acceleration in firm rock.

- Hard rock motions are estimated from numerical simulations using a stochastic point-source model. The hard rock motions are computed in terms of medians and standard deviations that are estimating by weighting results from a single-corner model with variable stress drop and a double-corner model with saturation.

3.3.4.3 Future Direction

Future versions of REDARS™ will include a library of ground-motion models for various regions of the United States, to provide users with a choice when selecting a model that they view as being most appropriate for their particular application. Furthermore, in addition to using a single model, users will also be able to estimate site-specific ground motions as a weighted average of estimates from multiple models built into REDARS™ for a given region.

3.4 LIQUEFACTION HAZARDS

3.4.1 HAZARD DESCRIPTION

Liquefaction is a process that occurs in loose, saturated, granular soil materials subjected to earthquake ground shaking. If this shaking is of sufficient strength and duration, the soils tend to decrease in volume due to a collapse of the soil "skeleton." This volume change is restricted by the rate at which the pore water can flow out of the soil, thereby resulting in a dramatic increase in pore-water pressure and a temporary loss of soil stiffness and shear strength when the pore water pressure approaches the in-situ vertical effective stress. Liquefaction-induced soil failure can result in lateral spread displacement and vertical settlement, reduced bearing strength, increased lateral pressures against retaining structures (e.g., abutment walls), and a loss of frictional resistance of pile elements at their interface with liquefied soils layers.

3.4.2 HAZARD EVALUATION PROCEDURE

The REDARS™ 2 procedure for estimating liquefaction hazards was chosen with two objectives in mind. First, the procedure was to be technically sound and based on well-established liquefaction hazard evaluation methods. The second objective addressed the absence of electronic databases of soil attributes that would facilitate the development of input data for liquefaction hazard analysis. Therefore, these input data will need to be compiled by the REDARS™ 2 user. The effort to compile these input data could be formidable, if the highway system includes many potentially liquefiable sites. In view of this, it was determined that technically sound liquefaction hazard analysis method that uses a minimum number of input soil parameters would be most desirable for incorporation into REDARS™ 2.

With this as background, the procedure currently used in REDARS™ 2 to estimate liquefaction hazards is summarized below. The procedure is further described in Appendix E.

3.4.2.1 Step 1. Initial Screening

Step 1 consists of initial screening of soil sites throughout the highway system to identify those sites within the system that are potentially liquefiable. This screening step is performed by the user prior to the start of the REDARS™ 2 application. It is based on the user's assessment of soil properties, water table depths, and site topography, as described in Section E.3. In REDARS™ 2, liquefaction hazards are computed only at those sites within the highway system that are identified as being potentially liquefiable in this initial screening step.

3.4.2.2 Step 2. Lateral Spread Displacement Hazards

Under Step 2, the Bardet et al. (2002) four-parameter model is used to estimate lateral spread displacements at each site in the highway system that was designated as potentially liquefiable in Step 1. An attractive feature of this model for application to large numbers of sites is that it is less input-data intensive than other models that were considered for inclusion in REDARS™ 2.

3.4.2.2(a) Input Data

Input data to the Bardet et al. models consists of

- *Earthquake-Dependent Data,* which are the moment magnitude of the earthquake and the horizontal distance from the site to the earthquake's center of energy release. For sites east of the Rocky Mountains, an equivalent distance for use in the lateral spread calculations is estimated as a function of the moment magnitude and the peak ground acceleration

.

- *Site Topography Data*, which are either the ground slope or, for sites with a free face, the ratio of the height of the free face to the distance from the face to the site (which is termed a "free-face ratio").

- *Site Soils Data*, which is an effective thickness (T_{15}) that is computed as the sum of the thicknesses of all saturated sand layers at the site whose effective blow-count is less than 15.

3.4.2.2(b) Median Value of Lateral Spread Displacement

After these input data are compiled, the Bardet et al. model computes the median value of the natural logarithm of the lateral spread displacement, as a function of the above input parameters.

3.4.2.2(c) Treatment of Uncertainty

The Bardet et al. model includes effects of uncertainties by computing the standard deviation of the natural logarithm of the median displacement, as a function of all of the above input parameters. Then, a normally distributed random number is generated and used with the standard deviation to obtain an uncertainty factor in log space. The above median displacement and the uncertainty factor are added, and the anti-log of this sum represents the lateral-spread displacement including uncertainties, for this particular scenario earthquake and simulation.

3.4.2.3 Step 3. Vertical Settlement

In addition to lateral spread displacements, REDARS™ 2 computes liquefaction-induced vertical settlements at each potentially liquefiable site. The Tokimatsu-Seed (1987) model is used to perform this computation.

3.4.2.3(a) Input Data

The input data for the Tokimatsu-Seed estimate of vertical settlement consist of:

- *Ground Motions.* The site-specific peak ground acceleration computed using the selected ground-motion model from the library of models contained in REDARS™ 2.

- *Soils Data.* For all layers at the site (regardless of whether they are potentially liquefiable), the layer's thickness, depth below the ground surface, total overburden pressure, and effective overburden pressure must be provided. In addition, for layers that are potentially liquefiable, the corrected standard penetration test (SPT) blow-counts must also be specified.

3.4.2.3(b) Vertical Settlement Computation

The Tokimatsu-Seed model consists of a series of curves of cyclic stress ratio vs. corrected SPT blow-count, in which each curve corresponds to a different fixed value of volumetric strain. The REDARS™ 2 adaptation of this model consisted of fitting equations to these curves and then programming the equations into the software. After this was done, the following procedure was used to estimate site-specific vertical settlement for a given earthquake scenario and simulation:

- For a given saturated sandy layer at the site, compute the cyclic stress ratio. Enter the programmed version of the Tokimatsu-Seed curves with this cyclic stress ratio and the layer's corrected SPT blow-count to obtain the layer's median volumetric strain. Then, multiply this volumetric strain by the thickness of the layer to obtain the layer's change in thickness.

- Repeat the above step for all saturated sand layers at the site. After this, compute the vertical settlement for this scenario earthquake and simulation as the sum of the changes in thickness for all of the saturated sand layers.

3.5 SURFACE FAULT RUPTURE HAZARDS

3.5.1 HAZARD DESCRIPTION

Roadway components can be damaged by permanent displacement of the ground surface due to fault rupture. Such displacements may be vertical and/or horizontal, with associated tension fissures or compression bulging. The direction and amount of ground movement will depend on the type of faulting, the magnitude and depth of the earthquake, and the complexity of the fault zone. For strike-slip faults, the zone of deformation often includes one or more primary fault strands that contain most of the ground displacement. For thrust or reverse faults, the width of the deformation zone may vary from a single fault strand to a broad zone of primary/secondary deformation on the hanging wall (i.e., the rock and soil above the fault) in excess of 300 ft.

The surface fault rupture hazard will be limited to locations where the rupture approaches and reaches the ground surface and, as a result, this hazard will be much more localized than will ground shaking hazards. Also, surface fault rupture is most likely to occur in regions whose earthquakes typically have a shallow focal depth, such as California and the Wasatch Fault zone in Utah. Surface fault rupture is unlikely in regions of the Eastern and Central United States where the major faults are typically deeply buried.

3.5.2 HAZARD EVALUATION PROCEDURE

For highway systems that are located in regions where surface fault rupture is possible, fault rupture hazards are evaluated by applying the following steps. In REDARS™ 2, surface fault rupture hazards are estimated only for earthquakes included in the walkthrough table. Fault rupture hazards are not estimated for earthquakes that are defined by a user-specified magnitude and point-source location, or by ShakeMap ground-motion maps.

3.5.2.1 Step 1. Initial Screening

Step 1 is carried out by the REDARS™ 2 user before initiating the REDARS™ 2 analysis. It consists of a geologic screening of the region around the highway system to be analyzed, in order to identify active faults in the region that are within or close to the system.

3.5.2.2 Step 2. Permanent Ground Displacement Hazards

For each earthquake in the walkthrough table, REDARS™ 2 uses causative fault attribute and rupture data also contained in the table to identify the extent of the ruptured segment of the fault for this earthquake scenario. Then, each component in the highway system is checked to determine whether it is on or near this fault rupture segment. Permanent ground displacement (PGD) hazards are then computed only for those components found to be on or near the ruptured segment of the fault.

REDARS™ 2 uses the Youngs et al. (2003) model to estimate surface fault rupture hazards. Input data and the REDARS™ 2 procedure for applying this model are briefly summarized below. Further description of this procedure is provided in Appendix F.

3.5.2.2(a) Input Data

All data needed to characterize the causative fault in order to estimate surface fault rupture hazards are provided in the earthquake walkthrough table. As noted in Section 3.3.3, these data consist of: (a) the moment magnitude of the earthquake; (b) the location of the epicenter; (c) the depth to the hypocenter and to the seismogenic zone; (d) the latitude, longitude, and depth of the center of energy release; (e) the fault type; (f) the length, width, azimuth, and dip angle of each segment of fault rupture plane; (g) the direction of rupture along fault plane; and (h) the zone of deformation due to fault rupture (if specified by the user).

3.5.2.2(b) Check whether Component can Undergo PGD due to Fault Rupture (for Probabilistic SRA Application)

REDARS™ 2 generates a series of parameters to determine whether each component may undergo surface fault rupture hazards from this scenario earthquake. These parameters check if any of the following conditions occur:

- The probability of displacement at the site, as computed for this earthquake, exceeds a threshold value (0.004) and a line normal to the fault rupture can be drawn that also extends through the site;

- The site is in a user-specified zone of deformation, if such a zone is defined by the user and input into REDARS™ 2;

- Any line normal to the fault extends through the site, and the site is within 100 m of the fault rupture

- Any line normal to the fault extends through the site, and the site is within 500 m of the hanging wall of the fault; or

- The probability of slip at the site, as computed for this earthquake, exceeds a threshold value of 0.004.

3.5.2.2(c) Calculation of PGD (for Probabilistic SRA Application)

If any of the above conditions occur for any site in the highway system, PGD hazards due to surface fault rupture are calculated for that site. The Youngs et al. (2003) methodology for computing these PGDs relates the occurrence of fault displacement at or near the ground surface to the occurrence of earthquakes (fault slip at depth) in the site region, in much the same manner as is done in a probabilistic seismic hazard analysis (PSHA) for ground shaking. The methodology for this model is taken from PSHA methodology, with the ground-motion attenuation function replaced by a fault displacement attenuation function. In this, the probability of a given level of fault displacement is assumed to follow a beta distribution that depends on the position of the site along the length of the ruptured fault segment. From this, a cumulative probability distribution for fault displacement value is construction for different values of the site's position along the fault. This distribution is then entered with a random number, and the site's PGD for this particular scenario earthquake and simulation is obtained.

3.5.2.2(d) Calculation of PGD (for Deterministic SRA Application)

In REDARS™ 2, surface fault rupture hazards can be estimated for deterministic as well as probabilistic SRA applications. In this, the above cumulative probability curves are simply entered with a probability value of 0.5 (median case), and the corresponding PGD for the site is then estimated.

CHAPTER 4: COMPONENT MODULE

4.1 INTRODUCTION

4.1.1 PERFORMANCE METRICS

This chapter describes the process for characterizing the seismic performance of components for a given earthquake scenario and simulation. In this, two seismic performance metrics are required for use in SRA of highway systems. The first and most important metric is the component's traffic state at various times after the earthquake which, as noted in Chapter 2, represents the component's traffic-carrying capacity at that post-earthquake time. This is most often represented in terms of number of lanes open to traffic although other measures, such as allowable vehicle speed and/or vehicle speed, may also be used.

A second performance metric is the cost for repair of earthquake damage to the components. These costs are estimated separately for each component, and therefore can be obtained without performing a full highway system SRA using REDARS™ 2. They are added to the losses due to system-wide travel-time delays and trips-foregone due to increased post-earthquake congestion, in order to estimate the total economic loss due to earthquake damage to the highway system.

4.1.2 MODELING PROCEDURE

The general procedure for estimating component traffic states and repair costs for a given earthquake scenario and simulation consists of the following general steps:

- ***Damage States.*** After the site-specific ground motion and PGD hazards are computed, the component's damage state is estimated. As noted in Chapter 2, the damage state refers to the extent, location, and type of damage to the component due to the above seismic hazards. These damage-state estimates are typically developed from seismic analysis of a model of the physical component, from statistical analysis of empirical data of component performance during past earthquakes, and/or from expert opinion (or some combination thereof). Ideally, the damage estimates should be provided in terms of metrics that facilitate the subsequent estimation of repair requirements, although this is often not achieved.

- ***Repair Estimates.*** With the component's damage state now established, the next step is to assess how this damage will be repaired, how much it will cost, how long it will take, and whether the component can carry at least partial traffic at any time while the repairs are proceeding. These repair estimates are generally best obtained from engineering and construction personnel with extensive experience in post-earthquake component repair. However, these estimates will depend on the component construction, maintenance, and design practices, as well as available repair resources and experience. These factors can differ substantially from region to region. Therefore, it is typically inappropriate to apply repair estimates for one region of the country to some other region.

- ***Traffic States and Repair Costs.*** With the above repair estimates in place, the component's repair costs and traffic states at various times after the earthquake can be obtained. The traffic state estimates will vary with time after an earthquake, in accordance with the estimated rate of repair of the earthquake damage. As noted in Chapter 2, once the traffic states are obtained for all components in the system, a time-dependent system state (which corresponds to the degree of closure and traffic carrying capacity for all components in the system) is obtained. The transportation network analysis procedure described in Chapter 5 is then used to estimate travel-time delays and trips-foregone for each system state. This information, in turn, is used with the economic model described in Chapter 6 to estimate economic losses due to earthquake damage to the highway system.

4.1.3 DEFAULT AND USER-SPECIFIED MODELS

The damage and repair models summarized in Section 5.1.2 can either be default or user-specified models. The default models use simplified methods to develop first-order estimates of component damage states and time-dependent traffic states, as a function of the level of ground shaking and PGD at the site. They are based on various generic groupings of component types rather than component-specific attributes, and can develop rapid estimates of the performance of the components that are included in each grouping. However, default models do not account for differences in attributes among the various components in each grouping, nor do they account for all of the various component response characteristics that can affect damage-state predictions. They are most appropriate for modeling of components in the highway system which have more-or-less "typical" configurations and structural attributes that are represented by the above groupings. Because this typically constitutes most of the many components in a typical highway system, use of default models will greatly increase the efficiency of the highway system SRA.

As a second modeling option, REDARS™ 2 enables users to provide their own user-specified model as an override to the default model for any component(s) in the highway system. For bridges and tunnels, such models are typically based on detailed seismic analysis that provide a much more refined representation of a component's actual configuration and attributes than do default models. Therefore, user-specified models are particularly appropriate for modeling of those components that have unusual configurations or whose seismic performance is vital to the performance of the overall highway system (e.g., long-span bridges along a major non-redundant highway). However, since such models are usually time consuming to develop, their application to large numbers of components is impractical.

4.1.4 DETERMINISTIC AND PROBABILISTIC MODELS

Models for estimation of component performance can be deterministic or probabilistic. Probabilistic models estimate the cumulative probability of various levels of damage as a function of the applied seismic hazards. They are intended to account for uncertainties in analysis procedure, material properties, and other factors related to seismic performance estimation whose characterization is not certain. Deterministic models do not account for these various uncertainties.

REDARS™ 2 provides default models for three types of components -- bridges, approach fills, and pavements. The default models for bridges are probabilistic, and the default model for approach fills and pavements are deterministic. The remainder of this chapter summarizes these default models, as well as basic principles for development of user-specified models.

4.2 DEFAULT MODELS FOR BRIDGES

This section summarizes the input data and default procedures used in REDARS™ 2 to model the seismic performance of bridges subjected to ground shaking and PGD hazards.

4.2.1 INPUT DATA

4.2.1.1 Data Needs

Ideally, input data for analysis of the seismic response of a bridge should include information on: (a) bridge geometry, including lengths, widths, overall heights, relative heights of various bents along the length of the bridge, and skew; (b) materials of construction; (c) member sizes, reinforcement, and detailing; (c) bearings, joints, and seat widths; (d) foundations and soil conditions; and (e) abutments. Although this information can be obtained from as-built drawings for individual bridges, this can be a laborious task when many bridges are involved (e.g., for SRA of a highway system). Furthermore, such data are usually not available in a computerized database that can be rapidly accessed for seismic evaluation of large numbers of bridges.

4.2.1.2 Current Databases and Bridge Management Systems

The only available nationwide computerized database for bridges is the National Bridge Inventory (NBI) database that is required by the National Bridge Inspection Standards established by the Federal Highway Administration. This database serves to facilitate inspection, to provide information for aggregation into a report to Congress on the number and state of the nation's highway bridges, and to identify and classify the Strategic Highway Corridor Network and its connectors for defense purposes (FHWA 2003). The database has not been developed to provide information for evaluation of bridge performance during earthquakes or other natural or man-made hazards. Therefore, although the NBI database includes some relevant bridge attributes, it does not include sufficient data for detailed seismic vulnerability evaluation.

In addition to the NBI database, bridge management systems -- which include PONTIS (initiated by the FHWA) and BRIDGIT (initiated through the National Cooperative Highway Research Program) -- are being used by a number of states. These systems provide analytical methods that facilitate efficient and cost-effective allocation of resources for maintenance, repair, and upgrading of the nation's highway bridges. They do not currently address seismic risk issues and, as a result, the data fields contained in these systems do not include most of the attributes that would be needed for seismic vulnerability assessment of a bridge. In recognition of this need, the feasibility of including seismic vulnerability evaluation in the PONTIS bridge management system has been assessed (Small 1997 and 1999).

4.2.1.3 Further Developments

4.2.1.3(a) California Department of Transportation Database

In some states whose highway systems have been subjected to damaging earthquakes, expanded bridge databases have been developed that supplement the data contained in the NBI database by providing additional bridge attributes that are relevant to seismic response. For example, the California Department of Transportation (Caltrans) is in the process of developing a supplementary database for bridges statewide. Some of the data fields that have been developed thus far are listed in Table 4-1 (Yashinsky 2005).

Table 4-1. Supplementary Bridge Database under Development at Caltrans

Type	Description
Relevant Dates	Dates of initial construction and any improvement (rebuilding, widening, etc.)
Seismic Retrofit	Whether bridge has undergone Phase 1 retrofit (joint restrainers) or Phase 2 retrofit (column jacketing), or whether it has been rebuilt.
Route Type	Whether bridge is along lifeline route (route critical to emergency response) and whether there are nearby detour routes.
Seismic Hazards	Design earthquake magnitude, distance to causative fault, and ground (rock) acceleration. Whether prone to damage from vertical acceleration, liquefaction, fault rupture, or tsunami, and whether on hanging wall of a dipping fault.
Superstructure	Number of spans, number of hinges, material of construction; Whether large skew angles, ,slab bridge with hinges, concrete bridge with restrainers.
Substructure	Whether substructure includes outriggers (including type of outrigger), flared columns (and whether flares are not retrofitted), pier walls,
Foundations	Types of piles, whether piles are battered, whether pile extensions, whether footings have top mat steel but no ties, whether footings are cantilevered and have long length-to-depth ratio
Joints/Seats	Whether joints have restrainers with threaded lock, grouted restrainers, short seat widths with no restrainers

Yashinsky 2005

4.2.1.3(b) Expanded Bridge Database for Shelby County, Tennessee (Jernigan 1998)

As part of his Ph.D. dissertation work, Jernigan (1998) performed research with the following objectives: (a) to develop structural attribute data for bridges in Shelby County that can be used in demonstration SRAs of the county's highway system; (b) to develop a framework for guiding the future development of structural attribute databases for SRA of highway systems nationwide; and (c) to provide data that can be used by state, county, and city government agencies for seismic risk evaluation and risk reduction planning. To accomplish this, Jernigan compiled extensive spatial and structural data from the NBI database, engineering drawings, inspection

reports, and visual observations of 452 bridges and culverts in Shelby County. These data were incorporated into a GIS database developed at the Center for Earthquake Research and Information at the University of Memphis (see Table 4-2).

Table 4-2. Jernigan et al. (1998) Database for Bridges in Shelby County, Tennessee

File Number	Description	Structural Attributes
B-1	Relevant Information from NBI Database	Bridge ID number, route, location (log mile), feature crossed by bridge, maximum span length, total length, roadway width, bridge width, average daily traffic, year built, skew angle, superstructure types (main span and approach span), number of main spans, and number of approach spans.
B-2	Abutment Attributes	Bridge ID number, abutment type (material, type, and fixity), abutment bearing and expansion type, seat width, foundation type, and whether seismic retrofit was implemented.
B-3	Bent File No. 1	Bridge ID number, bent type and material, superstructure to substructure connectivity, bent bearing and expansion type, seat width, number of columns per bent, maximum column height, and minimum column height.
B-4	Bent File No. 2	Bridge ID number, column fixity (to bent cap and to pile cap or footing), column size (at top and bottom), column shape, vertical reinforcement, transverse reinforcement, and foundation type.

4.2.1.4 Bridge Database for REDARS™ 2

In view of the lack of other computerized bridge data, the REDARS™ 2 Import Wizard is using the NBI database as the source of bridge data for use in SRA applications (Appendix C). However, the limitations of the use of this database for seismic analysis applications are well known, and initial discussions among various researchers and transportation agencies have addressed the needed for expanding this database (TCW 2003 and 2005).

4.2.2 MODEL FOR ESTIMATING BRIDGE DAMAGE STATES DUE TO GROUND SHAKING

4.2.2.1 General Evaluation Procedure

REDARS™ 2 uses a default model for estimating bridge damage due to ground motions that corresponds to the HAZUS99-SR2 model (FEMA 2002). This model uses input-data fields extracted from the NBI database for bridges nationwide. Table 4-3 shows how data relevant to seismic performance evaluation were inferred from these NBI data. This model is summarized in the following subsections, and is further described in Section G.2 of Appendix G.

Table 4-3. Fields in NBI Database used in HAZUS99-SR2 Bridge Model to Infer Bridge Attributes Relevant to Seismic Performance

NBI Data Item	Definition	Skew Factor	3-D Response Factor	Use in Inferring Bridge Fragility
1	State		X	To infer seismic design code used.
8	Structure Number			General ID Number.
27	Year Built		X	Infer whether seismic or conventional design
34	Skew	X		
42	Service Type			To select highway bridges.
43	Structure Type		X	To infer which type of "standard" bridge to use as basis for fragility curve development.
45	Number of Spans in Main Unit		X	To infer whether single- or multiple-span bridge.
46	Number of Approach Spans			To infer if bridge is a major bridge (as defined in FEMA, 2002).
48	Length of Maximum Span		X	To also infer if bridge is a major bridge (as defined in FEMA, 2002)
49	Structure Length		X	To infer average span length. To compute replacement value.
52	Deck Width			To compute replacement value.

Mander and Basoz 1999

4.2.2.2 Damage States

Table 4-4 defines the qualitative damage state descriptors used by the HAZUS99-SR2 bridge model. Five different damage descriptors are used. These descriptors provide only partial information needed for the repair estimates that are subsequently discussed in Section 4.5.

4.2.2.3 Development of HAZUS99-SR2 Model

The HAZUS99-SR2 estimation of bridge damage states is based on development of an equivalent pushover capacity spectrum, use of this capacity spectrum along with the bridge attributes listed in Table 4-3 in order to develop spectral acceleration capacities for each damage state, and comparisons of the earthquake's demand spectral acceleration to these various spectral acceleration capacities in order to obtain the bridge damage state.

Table 4-4. Damage States considered in HAZUS99-SR2 Bridge Model

Damage State Designation		Description
Number	Level	
1	None	First yield.
2	Slight	Minor cracking and spalling of the abutment, cracks in shear keys at abutment, minor spalling and cracking at hinges, minor spalling of column requiring no more than cosmetic repair, or minor cracking of deck.
3	Moderate	Any column experiencing moderate shear cracking and spalling (with columns still structurally sound), moderate movement of abutment (< 5.1 cm) (< 2 inches), extensive cracking and spalling of shear keys, connection with cracked shear keys or bent bolts, keeper bar failure without unseating, rocker bearing failure, or moderate settlement of approach.
4	Extensive	Any column degrading without collapse (e.g., shear failure) but with column structurally unsafe, significant residual movement of connections, major settlement of approach fills, vertical offset or shear key failure at abutments, or differential settlement.
5	Complete	Collapse of any column, or unseating of deck span leading to collapse of deck. Tilting of substructure due to foundation failure.

FEMA 2002

4.2.2.3(a) Pushover Capacity Spectrum

The pushover capacity spectrum is a plot of equivalent five percent damped spectral acceleration vs. spectral displacement (which is related to drift). Spectral displacements (drifts) that represent the onset of each damage state are also defined. In their original development of an early version of this HAZUS99-SR2 model, Mander and his colleagues established capacity spectra and drift limits for each damage state for each of each of six "standard" bridges, defined as long, un-skewed bridges that represent six different commonly occurring bridge types. Each capacity spectrum (which includes effects of strength degradation and hysteretic energy dissipation) was obtained as the sum of the capacity contributions of the piers and the three-dimensional arching action of the deck (Dutta and Mander, 1998; Mander and Basoz, 1999).

- ***Pier Contribution to Bridge Capacity.*** The strength capacity of a bridge pier will usually decay as the earthquake shaking proceeds. The magnitude and rate of this decay will depend on the design details at potential plastic hinge zones -- particularly connection details such as lap splices and anchorage zones -- and on the shear capacity of the columns and the column-to-cap connections. Although sophisticated energy-based procedures are available to evaluate these sources of strength decay, a simplified displacement-based analysis method is used here, to increase the speed of the evaluation. The method uses a simplified strength-degradation model for the bridge pier, where the total pier capacity consists of: (a) diagonal strut (or arch) action to represent the concrete resistance; and (b) resistance contributions of

the longitudinal and transverse reinforcing steel. These contributions to the pier capacity are expressed in terms of geometric factors obtained or inferred from the NBI database.

- ***Deck Contribution to Bridge Capacity.*** The deck's contribution to the bridge's total base shear capacity has been systematically overlooked in most capacity analyses. This contribution is due to the resistance of the deck resulting from plastic moments that are mobilized by the bearings working as a group. This action occurs because, as the deck rotates, the resulting lateral displacements are resisted by frictional forces in each bearing and by arching action of the deck. These effects are evaluated for bridges with multiple simply-supported spans and with continuous spans, by using a plastic mechanism analysis to establish the deck capacity as the lowest capacity of all possible postulated failure mechanisms. These failure mechanisms depend on the geometry of the deck spans, the relative flexibility of the pier bents, and the resistance and capacities of the bearings.

4.2.2.3(b) Median Spectral Acceleration Capacity for each Damage State – Standard Bridges

With this capacity spectrum as a starting point, Mander et al. used the following steps to establish median acceleration capacities for each standard bridge type and each damage state:

- The capacity spectrum is overlaid onto a smoothed five percent damped spectrum shape, whose spectral accelerations at a period of 1.0 sec. and 0.3 sec. are assumed to be equal to the peak ground acceleration (PGA, or zero-period spectral acceleration) and 2.5 x PGA, respectively. This assumption is also a basis for the ground motion spectrum shape developed under the National Earthquake Hazard Reduction Program (NEHRP).

- This smoothed spectrum shape is scaled by alternative PGA values until it intersects the capacity spectrum at the drift (spectral displacement) level that corresponds to the onset of a given damage state. The PGA level at which this occurs is defined as the median PGA for the onset of the given damage state.

- Using the above relationships between spectral acceleration and PGA for the smoothed spectrum shape, the above median PGA capacities are converted to corresponding spectral acceleration capacities at periods of 1.0 sec. and 0.3 sec.

4.2.2.3(c) Median Acceleration Capacities for each Damage State – Actual Bridge

The acceleration capacities for each damage state at the actual bridge being evaluated are obtained by multiplying the corresponding acceleration capacities for the appropriate standard bridge (see Section 4.3.3.2) by factors that correct for the effects of skew and three-dimensional arching action of the actual bridge.

4.2.2.4 Modification of HAZUS99-SR2 Structural Capacities

During the development and testing of the REDARS™ 2 software, the software was used to predict bridge damage during the 1994 Northridge Earthquake, and these predictions were then compared to bridge damage observations after the earthquake. These comparisons showed that

the HAZUS99-SR2 model substantially over-predicted the number of bridge collapses from the earthquake. This will have a particularly important effect on the REDARS™ 2 travel time estimates, since the default bridge repair model that is described in Section G.4 shows that by far, the most reductions in bridge traffic states occur when the bridge has collapsed.

For this reason, it was necessary to adjust the HAZUS99-SR2 model to improve these bridge collapse predictions. This adjustment consisted of determining a modification factor, named "α," that is applied to the HAZUS99-SR2 median bridge capacity, in which the bridge damage probability distribution was assumed to be lognormal with a standard deviation of 0.35. The process that was used to develop α is described in detail in Appendix K. It involved carrying out multiple sets of 4,000 simulations of bridge damage estimates for the Northridge Earthquake, in which uncertainties in the ground-motion estimates and the bridge damage predictions were considered. For each set of simulations, different α factors were assumed, and bridge damage throughout the northern Los Angeles area due to the Northridge Earthquake was estimated. Then, the average number of bridge collapses was estimated, and those bridges with the highest probability of collapse were identified in order to check whether these bridges corresponded to the bridges that actually collapsed during the Northridge Earthquake. In these analyses, retrofit enhancement factors developed by Shinozuka (2004) were used in the modeling of the relatively few bridges in the system that had been column jacketed at the time of the Northridge Earthquake.

These results for each different α factor were then compared to the Northridge Earthquake bridge damage observations. This comparison was the basis for selecting an α factor whose probabilistic predictions of bridge collapse (in terms of average number of collapses and locations of bridge collapses) were consistent with Northridge Earthquake observations.

In addition to determination of α factors for probabilistic SRA, the above process was repeated assuming median values of all uncertain parameters and carrying out deterministic estimates of bridge damage. The α factors for use in deterministic applications of REDARS™ 2 were thereby obtained. Results from the development of α factors for probabilistic and deterministic applications of REDARS™ 2 are provided in Appendix K.

It is noted that this adjustment of the HAZUS99-SR2 structural capacities was based on damage observations from one earthquake only. Additional investigations of bridge damage should be made for other earthquakes in the United States where bridge damage observations are well documented, and electronic databases of bridge attributes at the time of these earthquakes are available. Unfortunately, the Northridge Earthquake is the only known major earthquake that has occurred in the United States where these criteria are met.[3]

[3] During this project, development of alpha factors based on calibrations against observed bridge damage during the 1989 Loma Prieta, California Earthquake was also attempted. However, it was found that data describing bridge attributes in the San Francisco Bay Area at the time of that earthquake were not available. This was important because the attributes of many of the Bay Area's bridges at the time of the earthquake (particularly for the bridges that were severely damaged during the earthquake) were very different than the current attributes of these bridges

4.2.2.5 Implementation of Modified HAZUS99-SR2 Model

The step-by-step procedure for applying the modified HAZUS99-SR2 bridge model in REDARS™ 2 is described in Appendix G. This procedure contains the following main steps for each earthquake scenario and simulation:

- *Demand Spectral Acceleration.* Use the models described in Section 3.3 to estimate the demand spectral acceleration at the site of the bridge.

- *Spectral Acceleration Capacity.* Use the procedures described in Section G.2. to estimate the spectral acceleration capacity for each damage state of the bridge. In this, include the structural capacity modification factors (α factors) listed in Table G-6 to obtain an adjusted capacity for each damage state.

- *Bridge Damage State.* Compare the demand spectral acceleration to the spectral acceleration capacity for each damage state, in order to identify the damage state of the bridge for this earthquake scenario and simulation.

4.2.3 MODEL FOR ESTIMATING BRIDGE DAMAGE STATES DUE TO GROUND DISPLACEMENT

In addition to ground shaking, bridges can be damaged by permanent ground displacement (PGD) from earthquake-induced liquefaction, landslide, or rupture of a fault located beneath the bridge. The REDARS™ 2 default model for estimating bridge damage states due to PGD is the simplified HAZUS99-SR2 model (FEMA 2002). This model only considers effects of PGD on incipient unseating and collapse, and on bearings. It does not consider the possibly significant effects of PGD on abutments and foundations (probably because bridge abutment and foundation attributes are not included in the NBI database). In this, it is noted that only limited research has been carried out to estimate potential bridge damage states due to PGD. Future research to develop improved models is recommended.

The main steps in applying the HAZUS99-SR2 model for estimation of bridge damage due to PGD are summarized below. The model is further described in Section G.3.

Step 1. Estimate Demand PGD

For a given earthquake scenario and simulation, use the procedures outlined in Section 3.4 or 3.5 to estimate the bridge's site-specific PGD due to liquefaction or fault rupture hazards.

Step 2. Develop PGD Capacity for "Standard" Bridge

The HAZUS99-SR2 model includes a table of PGD capacities that correspond to the onset of each damage state for various types of "standard" bridges as defined in Section 4.2.2.3(a). (This table is reproduced as Table G-8 in Section G.3). This table is used to obtain the PGD capacity for the standard bridge type that best corresponds to the actual bridge.

Step 3. Develop PGD Capacity for Actual Bridge

The above standard bridge PGD capacities are multiplied by a factor that depends of the actual bridge's length, width, skew angle, and number of spans, in order to obtain PGD capacities for each damage state that correspond to the actual bridge.

Step 4. Estimate Bridge Damage State

The demand PGD from Step 1 is compared to the actual bridge's PGD capacity for each damage state to estimate the bridge's damage state for this earthquake scenario and simulation.

4.2.4 BRIDGE REPAIR MODEL

After a bridge's damage state is estimated for a given earthquake scenario and simulation, the next step is to use an appropriate repair model to estimate how the damage will be repaired, how much the repairs will cost, how long they will take, and how traffic along the bridge will be affected during repair. As previously noted, these repair estimates will depend on the transportation department's experience and resources for post-earthquake bridge repair and on the construction, maintenance, and design practices for bridges within the region.

Because these factors will invariably differ from one region of the country to the next, it is not possible to provide a default repair model that applies to all regions. Instead, REDARS™ 2 provides a default model developed in close collaboration with senior bridge engineers from Caltrans. Because these models incorporate the extensive Caltrans experience in post-earthquake bridge repairs, they represent a reasonable starting point for establishing a REDARS™ 2 bridge repair model for other regions of the country. However, because of the factors listed in the previous paragraph, it will be necessary for REDARS™ 2 users from other states/regions to adjust/override this default repair model to better represent their particular operating conditions, repair resources, and construction practices.

The default bridge repair model developed in collaboration with Caltrans staff is described in detail in Section G.4. In this, bridge traffic states are provided as a percentage of the bridge's pre-earthquake traffic-carrying capacity for each of the HAZUS99-SR2 damage states listed in Table 4-3. For each damage state, these traffic capacities will vary with time after the earthquake in order to reflect estimated rates of repair. They also vary with the number of bridge spans. In this model, it is assumed that a bridge will be either fully closed or fully open at any time during the repairs; i.e., reopening of the bridge to partial traffic at any time prior to completion of repairs is not included in this model.

The default bridge repair model also includes repair cost estimates for each damage state. These are provided as repair cost ratios, which is the ratio of the repair cost for that damage state to the replacement cost. The replacement cost is estimated as the product of a unit replacement cost (assumed to be $\$150/ft^2$) and the bridge deck's surface area. These repair cost ratios and unit replacement costs can be overridden by the REDARS™ 2 user.

4.3 DEFAULT MODEL FOR APPROACH FILLS

If approach fills alongside bridge abutments have not been adequately compacted during construction, they are vulnerable to damage from earthquake-induced differential settlement. These differential settlements are often localized due to the rigidity of the abutment wall, and the difficulty in manipulating large compactors near walls. This increases their potential for damage. It is noted that approach-fill settlement was the most common type of highway-system damage due to the 1994 Northridge Earthquake.

The REDARS™ 2 default approach-fill model is described in detail in Section H.1 of Appendix H and is briefly summarized here. It contains two main parts: (a) estimation of approach fill settlement; and (b) estimation of corresponding damage states, repair costs, and traffic states.

4.3.1 APPROACH FILL SETTLEMENT

The REDARS™ 2 approach for estimating earthquake-induced settlement of bridge approach fills is based on the Youd (2002) model for dry soils. The settlement is computed separately for each earthquake scenario and simulation, once the magnitude and location of the earthquake are specified and the level of ground shaking is estimated throughout the highway system.

The Youd (2002) model for estimating approach fill settlement (Section H.1.1) requires input data that characterizes the bridge (bridge number and location, relative compaction of approach-fill soils, and maximum thickness of the soils) and the earthquake scenario/simulation (the earthquake's moment magnitude and the bridge's peak ground acceleration). These data are used in a table developed by Youd that estimates volumetric strain (percent) for loose, moderately-dense, and dense fills as a function of: (a) moment magnitude; and (b) for each moment magnitude, the peak ground acceleration. After the volumetric strain is obtained from this table, it is multiplied by the approach-fill thickness to estimate the earthquake-induced settlement.

The REDARS™ 2 model uses a default approach-fill thickness of 12 ft and a default relative compaction of 95 percent. In addition, the following algorithm is used in REDARS™ 2 to estimate a default number of approach fills for each bridge (which can be overridden by the user):

- If the REDARS™ 2 bridge model shows the bridge location to be on a link with no other bridges nearby, the bridge is assumed to have two approach fills -- one at each end of the bridge.

- The NBI database often represents an elevated viaduct of extended length as a series of very closely spaced bridges. Therefore, an individual bridge within this series that is immediately adjacent to another bridge on each side is considered to be within the elevated viaduct and therefore is assumed to have no abutments, and no approach fills. An individual bridge that is located at one end of this series of bridges is considered to represent the start/end of the elevated viaduct. Therefore, it is assumed to have one abutment and one approach fill.

4.3.2 REPAIR MODEL

As for the bridges, the default model for repair of earthquake damage to approach fills was developed in close collaboration with senior members of Caltrans' engineering/maintenance staff who have extensive experience in approach-fill design, construction, maintenance, and repair. Therefore, it is directly applicable to repair of approach fills in California only. REDARS™ 2 users from other regions of the country whose approach-fill configurations, soil conditions, and maintenance, design, construction, and repair practices differ from those in California should override these default repair estimates.

The REDARS™ 2 default repair model is described in detail in Section H.1.2 and is briefly summarized here. It defines three ranges of approach-fill settlement that will entail different levels and types of repair. For each range, the model prescribes the approach fill's traffic state at various times after the earthquake as well as its repair cost (expressed as a percentage of the replacement cost). In this, a default replacement cost of $14,500/lane is assumed. These default traffic states, repair costs, and replacement cost can be overridden by the user.

4.4 DEFAULT MODEL FOR ROADWAY PAVEMENTS

Flexible or rigid roadway pavements are susceptible to damage/closure due to earthquake-induced ground displacement hazards. These hazards include differential settlement of dry or moist soils, lateral spreading and settlement of liquefiable soils, sliding of embankments or slopes due to instability of embankments or underlying soil materials, and surface fault rupture.

The default model for roadway pavements is described in detail in Section H.2 and is briefly summarized here. The process for developing the model and the form of the model are similar to those summarized above for approach fills. As with the approach fill model, the roadway pavement model takes the form of a table that, for different ranges of earthquake induced PGD, provides default repair procedures and associated traffic states at various times after the earthquake as well as repair costs per lane mile.

This roadway-pavement model was developed in close collaboration with Caltrans' senior staff members who have extensive experience in pavement design, construction, maintenance, and repair. Therefore, the model is directly applicable to roadway pavements in California only. REDARS™ 2 users from other regions of the country should override the model as needed to more appropriately represent roadway-pavement practices in their region.

4.5 TUNNEL MODELS

The seismic performance of tunnel structures will depend on many factors such as: (a) whether they are constructed as drilled or cut-and-cover structures; (b) their length, cross section, depth below the ground surface, and materials of construction; and (c) the characteristics of the surrounding subsurface soil or rock materials in the vicinity of the tunnel, including their material properties, layering, and susceptibility to major ground movement due to liquefaction or fault rupture. In view of this, and also because the tunnels are often important to the seismic

performance of the overall highway system, it was decided that such structures can best be represented by user-specified fragility models that are based on special analysis of these key facilities, rather than by default models.

However, if no such analysis results are available or if time and budget constraints preclude the development of such results for REDARS™ 2 applications, the user can fall back on existing fragility models that have been developed for broad classes of tunnel structures. For example, HAZUS99-SR2 models that may be implemented as user-specified models under these circumstances are shown in Figures 4-1 and 4-2. An example repair model that was recently developed for a drilled tunnel in California is shown in Table 4-5.

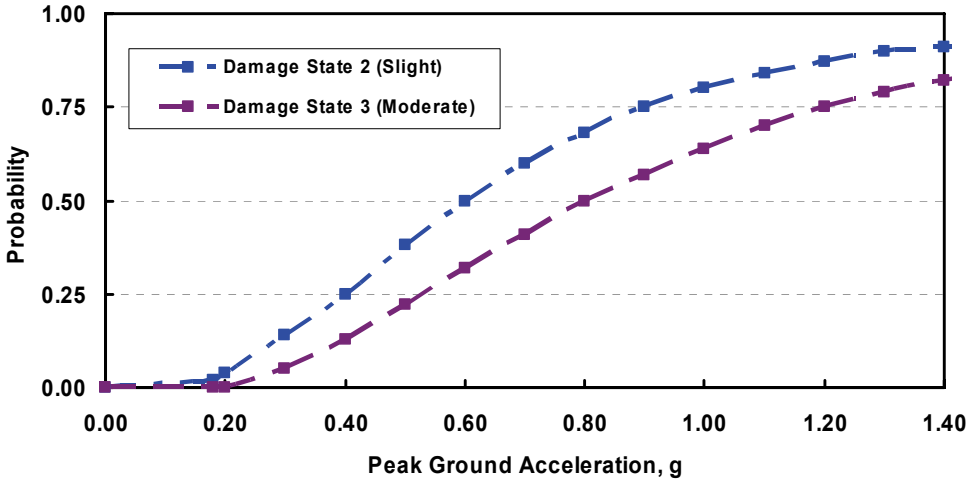

a) Drilled Tunnels

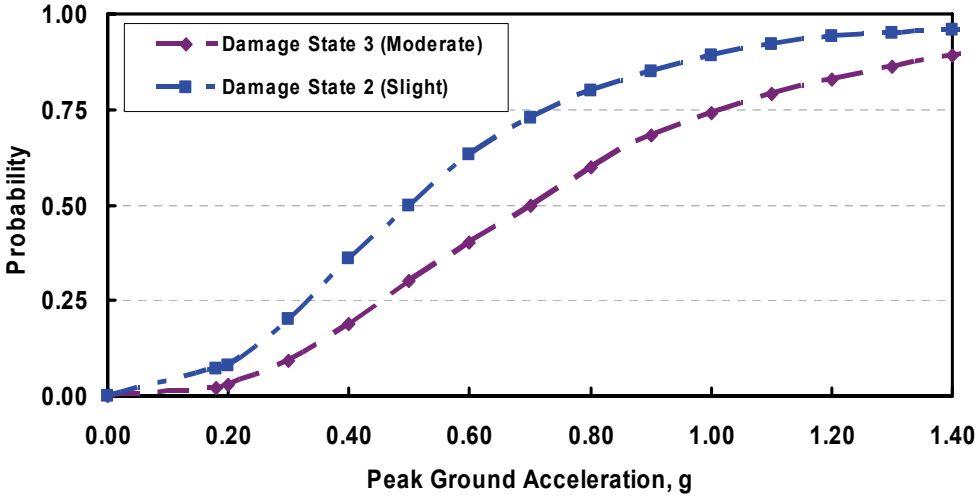

b) Cut-and-Cover Tunnels

Figure 4-1. HAZUS99-SR2 Tunnel Fragility Models: Ground Shaking (FEMA 2002)

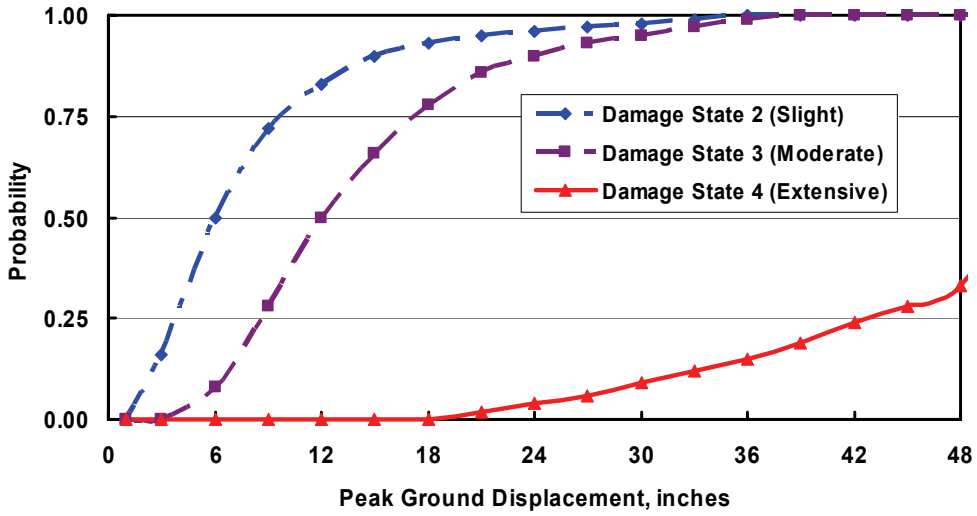

Figure 4-2. HAZUS99-SR2 Tunnel Fragility Models: Permanent Ground Displacement (NIBS 2002)

Table 4-5. Example Repair Model for Drilled Tunnel in California[1,2]

Damage State[3]		Seismic Hazard that can Cause this Damage State	Traffic State		Repair Cost (percent of Replacement Cost)[5]
No.	Description		Days after EQ[4]	Percentage of Pre-EQ Lanes Available	
2	*Slight.* Minor cracking of tunnel liner (requiring only cosmetic repair). Some rock falling or slight ground settlement at tunnel portal.	Ground Shaking (GS) or Permanent Ground Displacement (PGD)	0 days	0%	10%
			4 days	100%	
3	*Moderate*. Moderate structural cracking of tunnel liner and/or moderate rock falling	GS or PGD	0 days	0%	25%
			11 days	100%	
4	*Major.* Major structural cracking of tunnel liner and/or major settlement at tunnel portal	PGD only	0 days	0%	75%
			30 days	100%	

Assumptions:

1. Tunnel is about 4,000 ft-long and each bore contains two 12-ft lanes.
2. Tunnel is located along designated lifeline route (i.e., route must remain open to emergency vehicles after an earthquake). Therefore, repair materials, equipment, and crews will be rapidly mobilized to repair the tunnel after an earthquake.
3. Various damage states extend through up to half of the length of the tunnel bores.
4. Downtimes = times needed to reopen tunnel to traffic. It includes time for mobilization of repair/construction resources to tunnel site. Times to complete repair may extend beyond above downtimes; i.e., it is assumed that repairs can be completed after tunnel is reopened to traffic (by construction crews working during off hours, etc.).
5. Replacement cost = \$75/ (ft^2 of area), where area = damaged length along tunnel x width of roadway with two 12-ft lanes.

CHAPTER 5: SYSTEM MODULE

5.1 OVERVIEW

The first SRA applications using a forerunner of the current REDARS™ 2 software (termed REDARS™ beta) used a network-analysis process that was based on the following assumptions:

- ***User-Equilibrium Model.*** For a given trip, a user will choose a route between an origin and destination that will minimize the travel time required for that trip.

- ***Fixed Trip Demands.*** The conventional user-equilibrium model assumes that the network's post-earthquake trip demand is equal to the pre-earthquake trip demand. Under these conditions, even though earthquake-induced damage may result in road closures and a corresponding increase in traffic congestion, the trip demand on the highway-roadway system would not be affected by this increased congestion.

- ***One Trip Type.*** All traffic is represented by a single OD matrix, and every trip is represented by the same economic value whether it is taken by car or truck.

- ***Moore-Pape Minimum-Path Algorithm.*** Route choice in accordance with the above user-equilibrium model is estimated by the Moore-Pape algorithm, which attributes nodes according to the travel time from an origin (Moore 1957; Pape 1974).

The REDARS™ 2 network-analysis procedure has been significantly improved. These improvements are listed below and are summarized in the remainder of this chapter.

- ***Variable-Trip Demands.*** The user-equilibrium model with fixed trip demand has been replaced by a variable-demand model that accounts for the effects of traffic congestion.

- ***Dual-Simplex Minimum-Path Algorithm.*** The Moore-Pape algorithm has been replaced by the less computationally intensive dual-simplex algorithm, detailed by Florian et al. (1981).

- ***Multiple Trip Types.*** REDARS™ 2 enables users to define multiple types of trips to be carried by the highway-roadway system and to input separate trip tables and economic loss calculation parameters for each different trip type.

5.2 VARIABLE-DEMAND MODEL

5.2.1 STATEMENT OF THE PROBLEM

The user-equilibrium model with fixed trip demands that was included in the beta version of REDARS™, is widely used in transportation network analysis. However, initial results from a recent validation of this model against observed traffic flows after the Northridge Earthquake indicate that, although the model is adequate for region-wide modeling of traffic flows, it does not provide adequate estimates of traffic along specific highways or links (App. I). For example,

according to local traffic reports obtained one day after the earthquake (Caltrans 1995), observed traffic volumes doubled on roads near collapsed bridge sites (i.e., near the bridge collapses at I-10/La Cienega, SR-118/Gothic, and I-5/SR-14). Under these conditions, the observed travel-times along these roads increased by only 15 minutes per trip relative to pre-earthquake travel times. However, when the user-equilibrium model with fixed trip demand was used to predict post-earthquake travel time along these same roads, the model over-estimated travel time by as much as a factor of 10.

One reason for this result is that this model assumes inelastic (i.e., fixed) trip demands. However, this assumption is not plausible under conditions of substantially reduced network capacity and corresponding increased traffic congestion. Under this situation, observed data has shown that many travelers are unwilling to endure such travel time delays and will instead forego their trip. To account for this, major efforts under this project have focused on the development of a variable-demand model (VDM) for network analysis that replaces the fixed-demand model (FDM). This model is summarized below, and is further described in Section I.1 of Appendix I.

5.2.2 MODELING ISSUES

Implementation of the VDM in REDARS™ 2 was complicated by the two issues listed below. Section 5.2.3 describes how these modeling issues have been addressed.

- The VDM presumes that less network traffic capacity will reduce trip demand and increase travel times. However, in an actual highway-roadway system, the available capacity for some zone-pairs may actually increase after an earthquake due to unique rerouting conditions.

- Initial VDM results indicate that the predicted equilibrium for zone-to-zone travel times will not always fall on the demand curve. Therefore, to address this complication, REDARS™ uses a rules-based approach to address zone-pair demand on a case-by-case basis.

5.2.3 MODEL DEVELOPMENT

This section summarizes the REDARS™ methodology for calculating the social cost of earthquake-induced traffic disruption using: a) zone-to-zone trip demands; and b) the corresponding change in travel time estimated by the VDM. Social cost includes the value of time due to increased traveler time on the roadway and the value of trips foregone.

As noted above, the FDM assumes that trip demand associated with zone-to-zone travel is inelastic; i.e., it does not vary with travel time. Under these conditions, all drivers continue to attempt travel, even if a trip takes several hours and has an unreasonable social cost. Figure 5-1 illustrates the social cost of a hypothetical earthquake under this situation. If the traffic-carrying capacity is reduced due to earthquake damage, the congestion will increase. The network capacity (or supply) is reduced from S_1 to S_2, and the fixed trip demand is represented by D_1.[4] The corresponding travel costs are P_1 and P_2 respectively, and the social cost is $(P_2 - P_1) * D_1$.

[4] Note that, in Figure 5-1, the axes are reversed for consistency with subsequent examples.

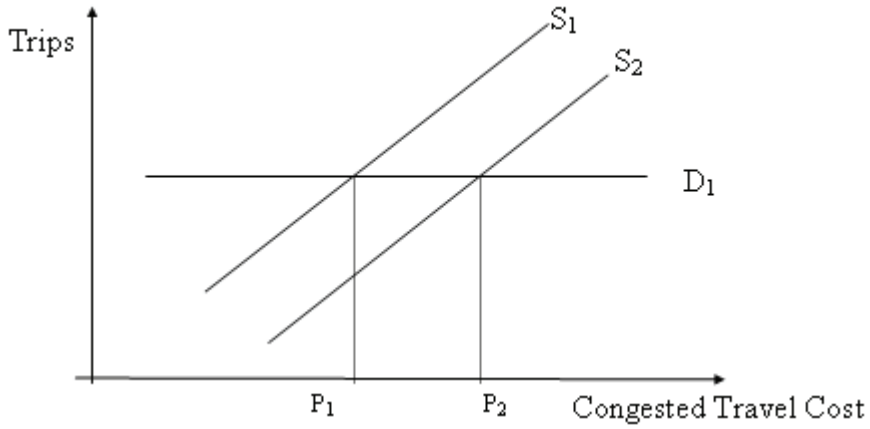

Figure 5-1. Fixed Demand Model for an Earthquake-Damaged Network

The assumption that travel demand remains constant is not appropriate for the analysis of a highway network where traffic-carrying capacity is drastically changing. Under these conditions, many drivers would be unwilling to endure very large increases in travel time, and would instead forego the trip or change their mode of travel. Thus, travel demand would be elastic; i.e., the travel time for trips taken would depend on the available capacity.

Figure 5-2 illustrates the resulting effects of elastic trip demand, as characterized by the VDM. This figure shows that before an earthquake, the highway system would provide a capacity of S_1, and the travel demand (D_1) on this network would result in an equilibrium travel time of P_1. After an earthquake, the capacity would be reduced to S_2, and the travel demand D_2 would results in a travel time of P_2'. The resulting social cost of this reduction in network capacity is given by the expression $[(P_2'-P_1)*D_2]+[(P_2'-P_1)*(D_1-D_2)/2]$, and will be much lower than the cost predicted by the FDM.

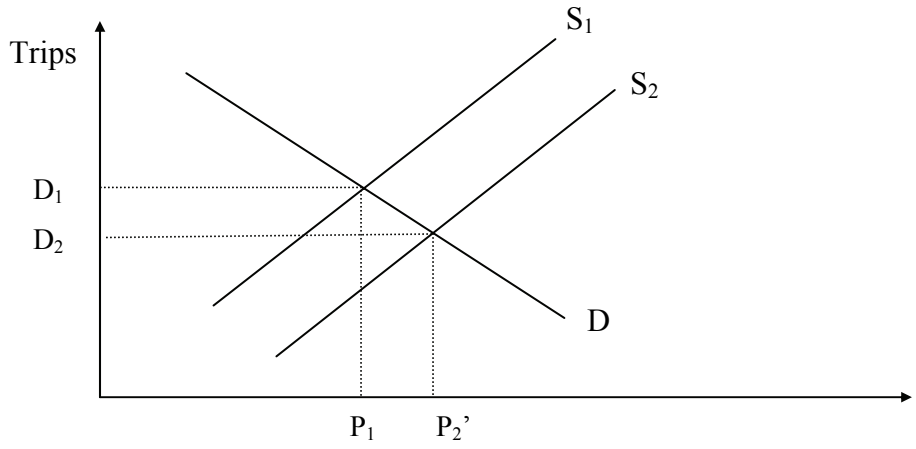

Figure 5-2. Variable-Demand Model for an Earthquake-Damaged Network

5.2.4 LOSS ESTIMATION CHALLENGES

Use of the VDM to estimate economic losses due to a reduction in network capacity presents several computational challenges. For example, the slope of the aggregate trip-demand curve must be estimated from minimal information. This process is discussed in this section, and its specific functional forms are provided in Section I.4 of Appendix I.

The mathematical form to the model is as follows:

$$\min\ z(\mathbf{x},\mathbf{q}) = \sum_a \int_0^{x_a} t_a(w)\ \ dw - \sum_{rs} \int_0^{q_{rs}} D_{rs}^{-1}(w)\ \ dw \tag{5-1}$$

subject to

$$\sum_k f_k^{rs} = q_{rs} \qquad \forall r,s \tag{5-2}$$

$$f_k^{rs} \geq 0 \qquad \forall k, r, s \tag{5-3}$$

$$q_{rs} \geq 0 \qquad \forall r,s \tag{5-4}$$

$$q_{rs} = D_{rs}(u_{rs}) \qquad \forall r,s \tag{5-5}$$

$$x_a = \sum_{rs}\sum_k f_k^{rs} \cdot \delta_{a,k}^{rs} \qquad \forall a \tag{5-6}$$

where

t_a : link performance function of link a.
D : demand function.
D^{-1}: inverse of demand function.
f_k^{rs} : flow on path k connecting OD pair r-s.
q_{rs}: trip rate between OD pair r-s.
u_{rs}: travel time between OD pair r-s.
x_a : flow on link a.
$\delta_{a,k}^{rs}$: = 1 if link a is on path k between OD pair r-s, otherwise = 0.

For some origin-destination zones with a minimal number of trips, the demand curve for specific zone-pairs may not match the elasticity and demand over time parameters established for the entire data set; therefore, the demand curve must be adjusted. In REDARS™ 2, individual zone-pairs with problematic results are identified and adjusted through a series of rules-based statements. The VDM adjusts trips and travel time by a constant value in each iteration. Each iteration seeks the optimal total travel time and the travel time associated with trip generation that minimizes the object function value given by Equation 5-1. In practice, the solution to this equation is dominated by zone-pairs with heavier demand in the first few iterations. For zone-pairs with light demand, VDM can not guarantee the equilibrium conditions. The details of these parameters are explained in Section I.4 of Appendix I.

There are additional cases where the VDM conditions are not solvable, due to a conflict with the demand curve. However, the demand curve is not established from survey data, and it cannot be

assumed that the curve characterizes the actual activity system. Some possible relationships between pre- and post-earthquake trips, travel times, and demand where the VDM is not solvable are listed below, along with a description of how each relationship is handled in REDARS™ 2.

d_1 : Pre-earthquake trips
d_2 : Post-earthquake trips
t_1 : Pre-earthquake travel time
t_2 : Post-earthquake travel time
D : Demand function
C_1 : Additional travel time spent by drivers remaining in the system
C_2 : The value of forgone trips

***Case 1*: $d_1 = D(t_1)$, $d_2 = D(t_2)$, $d_1 > d_2$, and $t_1 < t_2$**

In this case, the earthquake reduces trip demand and causes higher travel time. This is the expected behavior, and occurred in more than 95 percent of all trips. If a zone is isolated from the network, d_2=0, and t_2= ∞. In this case the earthquake calculations are as follows.

$$C_1 = d_2 \cdot (t_2 - t_1) \tag{5-7}$$

$$C_2 = \int_{t_1}^{t_2} D(w)\, dw \; - C_1 \tag{5-8}$$

***Case 2*: $d_1 = D(t_1)$, $d_2 = D(t_2)$, $d_1 < d_2$, and $t_1 > t_2$**

This suggests that traffic conditions are improved by earthquake damage. This situation is unlikely. REDARS™ 2 assumes $d_1 = d_2$, and $t_1 = t_2$.

***Case 3*: $d_1 \neq D(t_1)$ and/or $d_2 \neq D(t_2)$**

Where the global solution from the VDM does not correspond to the given input demand function, the demand curve is shifted so that $d_1 = D(t_1)$ or $d_2 = D(t_2)$. Then, Equations 5-7 and 5-8 are applied.

When drivers forego travel, they can pursue other activities. The value of these forgone trips depends on differences between pre- and post-earthquake travel times and number of trips.

5.2.5 CALIBRATING THE DEMAND FUNCTION

A demand function should include origin-destination-specific parameters that reflect population size, income distribution, and vehicle ownership by origin zone, as well as employment statistics and retail-activity variables by destination zone. However, the only parameter in the demand function between origin-destination-zone pairs, is the travel time between zones. Therefore, the demand function must be calibrated against the estimated travel time. This calibration is summarized below.

In the VDM, a demand function must reflect a decrease in the percentage of trips as the travel time between zone-pairs increases. As travel time increases, trip rate decreases. In reality, however, the distribution of trip-rate as a function of travel time shows that the trip rate is largest at a certain travel time not equal to 0 (an anomaly of the model is an infinite demand calculate at T=0). For example, in the SRA of the Shelby County, Tennessee highway system that is described in Werner et al. (2000), this peak was estimated to be about 8 minutes. Although the actual trip rate is not a monotonic function of travel time, the VDM assumes that the relationship between trip rate and travel time follows the simple form shown in Figure 5-3. Based on this assumption, the demand curve is calibrated through a statistical regression between the trip rate and travel time. This process is included in the REDARS™ 2 Import Wizard.

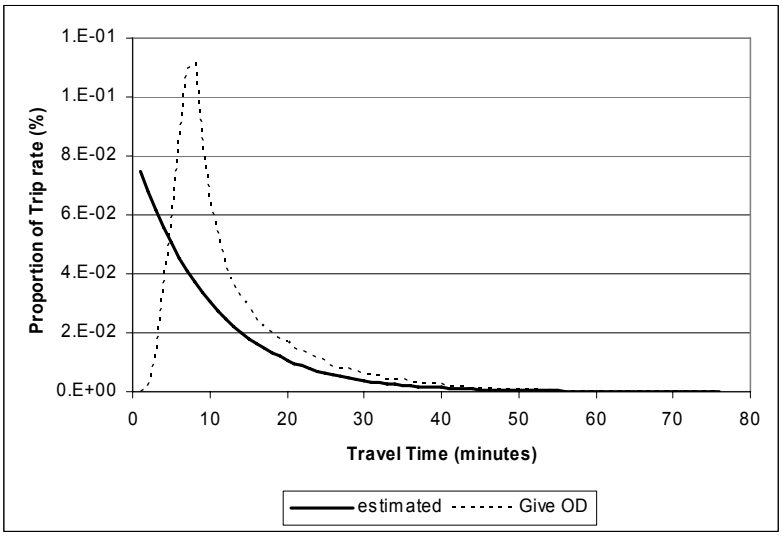

Figure 5-3. Real Trip Rate and Estimated Demand Function

5.2.6 PERFORMANCE OF VARIABLE-DEMAND MODEL

The VDM adjusts the trip rate according to the difference in level-of-service or increment of travel time. Figure 5-4 shows that most of the reduction in trip rate occurs for travel-time increases in the range of 10 ~30 minutes; and that this reduction tends to even out as the travel time increases beyond this range. This shows that the absolute value of the travel time is not directly associated with trip rate reduction. However, as shown in Figure 5-5, the reduction rate of travel demand has negative correlation to the rate of travel time. Travel times range from 0.85 to more than 2 times the baseline travel time. Over this range, more demand is reduced as travel time increases. For example, Figure 5-5, shows that when the travel time increases by 20-percent, the trip rate is about 80-percent of the baseline value. From this it can be concluded that the VDM is working as expected for cases where travel time is increased by a factor of ≤ 2 due to earthquake damage to the highway-roadway system.

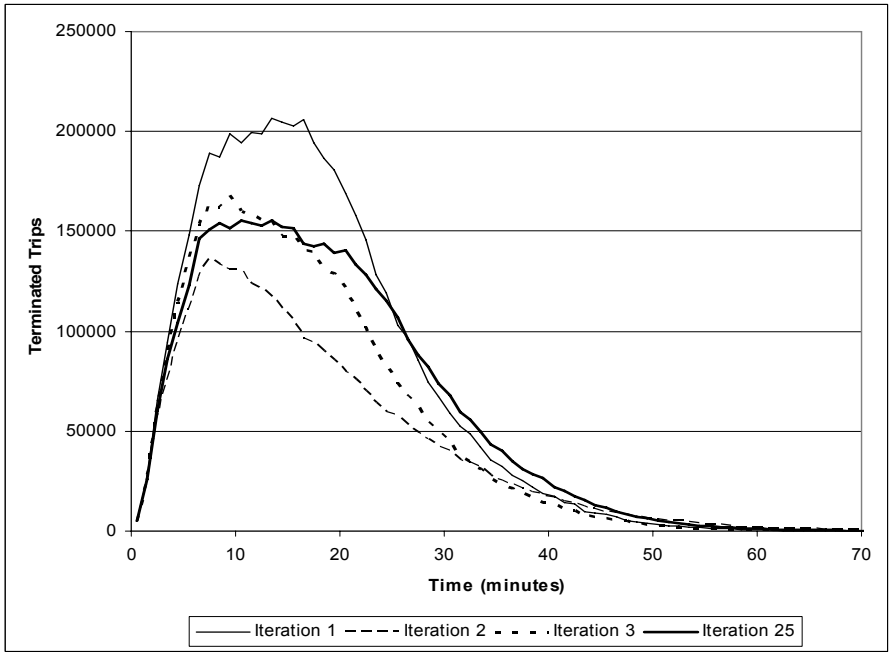

Figure 5-4. Trip Demand and Travel Time

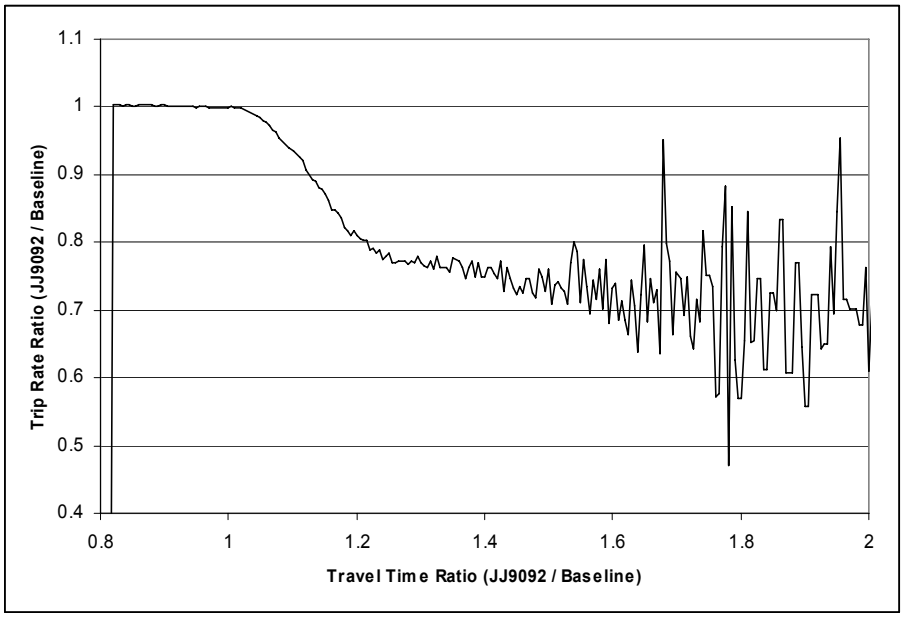

Figure 5-5. Reduced Trips and Travel Time

Results from REDARS™ 2 indicate that the VDM accounts for a reduction in trip rate and an increase in travel time according to the post-earthquake changes in network capacity. Analyzing the economic impact of an earthquake must consider the difference in system cost calculated by congestion. The difference in trip rate must be considered as another type of social cost, along with the value of foregone trips. REDARS™ 2 results using the VDM show that the model is useful for evaluating trip reduction as travel time increases. This indicates that the VDM is more appropriate for estimating post-earthquake traffic congestion than is the FDM.

5.3 UPDATE OF MINIMUM-PATH ALGORITHM

5.3.1 BACKGROUND

The network analysis procedure that was incorporated into the prior version of REDARS™ (see Werner et al., 2000) used the Moore-Pape minimum-path algorithm, which is an improved version of a label-correcting algorithm by Sheffi (1985). This algorithm establishes the path from a single "root" transportation zone to all zones in the system, and assigns travel demand from this zone to all other zones along the established path. The model repeats this process for all zones.

The efficiency of this model was increased through the discovery that two paths built from two adjacent root zones often share common links (Florian et. al., 1981). Through complex data structures implemented in the Dual-Simplex algorithm, the path information from one root is reusable for adjacent zones. Recycling the path information reduces computer running times significantly. In REDARS™ 2, run times for analyses that use this Dual-Simplex algorithm have been found to be about 30-percent lower than run times for the same analysis using the Moore-Pape algorithm. See Appendix I.6 for reduction rates for various size network configurations.

This section describes the minimum-path algorithm that recycles path information which, in REDARS™ 2, leads to reduced network-analysis run times. The role of the minimum-path algorithm in network analysis is summarized, and the more efficient Dual-Simplex algorithm, is described. In addition, the internal-memory structure of the network is included, and comparisons of results from the Moore-Pape and Dual-Simplex algorithms are cited.

5.3.2 MOORE-PAPE MINIMUM-PATH ALGORITHM

Previous versions of REDARS™ used the Moore-Pape path search algorithm adapted for transportation networks. This algorithm is particularly effective in cases where the number of nodes is much less than number of links, such as in power or communication networks. A communications switching-station, for example, typically manages thousands of telephone lines. When the number of nodes outnumbers the number of links, finding nodes on a path is more efficient than tracing links.

The Moore-Pape algorithm attributes nodes according to travel time from an origin. The transportation network analysis procedure repeats the algorithm iteratively in order to identify paths from all origins to all destinations in the network. After each path is calculated, the specific path, defined by a series of links, is discarded.

5.3.3 DUAL-SIMPLEX MINIMUM-PATH ALGORITHM

This process of discarding a minimum path after a calculation, as described above, is valid, since the minimum path from each origin is mathematically independent of that from other origins. However, independence does not imply that minimum paths from distinct origins do not share collections of links in a particular sequence. For example, in an urban transportation network, freeways accommodate a significant percentage of vehicle trips. For these networks, trips usually require shorter travel times when using freeways rather than local roads, and the proportional congestion due to the additional vehicles that use the freeway is less than that of local streets. Therefore, freeways are typically included in the minimum path between multiple zone-pairs, which indicates that a collection of links can be included in many travel paths.

Figure 5-6 illustrates how a collection of links can be shared by neighboring nodes. For example, the minimum path from Node 5 is seen to share many of the links included in the path to that node from Node 1. Links within the dashed box are common in paths from Node 1 to Node 5. For this situation, the minimum-path information, and the travel time to each node through the minimum path attained in a previous iteration of the algorithm may be reusable, which would reduce the overall network-analysis run times. The numbers in parenthesis in Figure 5-6 indicate travel time to reach the node from origin. The Dual-Simplex algorithm recycles the collection of links that are calculated in each iteration. When a set of links defines the shortest path between two nodes calculated in a previous iteration, these values are taken from these prior iterations, and are not recalculated. Section I.6 of Appendix I provides results from a simple test, which reveals that, use of the Dual-Simplex algorithm within REDARS™ 2 leads to computer-run times that are lower than run-times from the Moore-Pape algorithm, by factors ranging from 24-percent to 57-percent, depending on network redundancy.

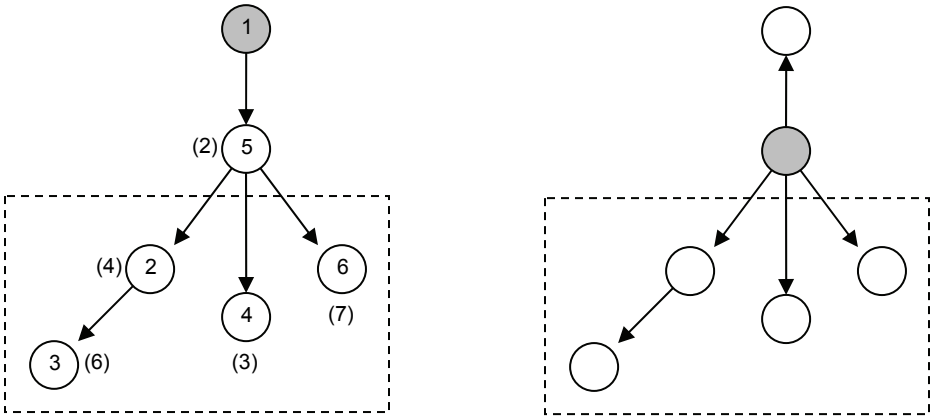

(a) Path from Root-Node 1 **(b) Path from Root-Node 5**

Figure 5-6. Comparison of Minimum Paths from Neighboring Origins

5.4 MULTIPLE TRIP TYPES

Prior versions of REDARS™ used a single origin-destination trip table and set of economic loss parameters for computing losses due to travel-time delays. However, a highway-roadway system will invariably accommodate many different types of trips (e.g., automobile trips and various types of freight trips). In addition, these various types of trips will often have different origins and destinations within the region served by the highway-roadway system. Furthermore, these various types of trips will have different economic values.

In recognition of this, REDARS™ 2 now can consider any number of different types of trips. For each trip type, REDARS™ 2 enables users to input separate origin-destination trip tables that would reflect the uniqueness of its region-wide travel patterns.

This new feature of REDARS™ 2 also enables users to estimate separate economic losses for each trip type, and then aggregate the losses from all of the trip types in order to estimate total region-wide economic losses due to earthquake damage to a highway-roadway system. The process used in REDARS™ 2 for estimating these separate losses for each trip type consists of the following steps:

- ***Losses due to Travel-Time Delays***. Chapter 6, describes how, for different post-earthquake times, REDARS™ 2 estimates the total loss per day as the product of an economic-loss factor and the travel-time delays incurred at those times. As noted above, prior versions of REDARS™ accommodated only one economic-loss factor for all trip type, and multiplied that factor by a single set of system-wide travel-time delays, also for all trip types, in order to estimate a loss per day at each user-specified post-earthquake time. However, for each trip type, REDARS™ 2 now enables users to input different economic-loss factors for each trip type. In addition, REDARS™ 2 now separately tracks the travel-time delays for each trip and then uses these results to estimate separate overall system-wide travel-time delays for each trip type at each post-earthquake time. From this, for each separate trip type, the loss per day at a given post-earthquake time is computed as the product of the economic loss factor and the system-wide travel-time delay for that trip type. These loss results for each trip type can, of course, be summed over all trip types to obtain an aggregated total economic loss due to earthquake damage to the highway-roadway system.

- ***Losses due to Trips Foregone.*** As noted earlier in this chapter, the variable-demand model enables REDARS™ 2 to estimate economic losses from trips foregone due to increased traffic congestion caused by earthquake damage to the highway-roadway system. With the addition of this new capability for considering multiple trip types, REDARS™ 2 can now: (a) separately track each pre-earthquake trip for each trip type, along with its pre-earthquake travel time; (b) separately track each post-earthquake trip for each trip type at each post-earthquake time; (c) compare the pre-earthquake trips to the post-earthquake trips for each trip type, and thereby identify those trips not taken for each trip type at each post-earthquake time; and (d) from this, estimate the total losses due to trips foregone for each trip type, as described earlier in this chapter.

CHAPTER 6: ECONOMIC MODULE

6.1 BACKGROUND

One set of important end results from SRA of highway systems is the estimation of economic impacts of earthquake damage to the system. These effects can be conceptualized by considering that, in addition to damaging the highway system, earthquakes can also damage buildings, contents, and lifeline infrastructure. Building, content, and infrastructure damage will reduce the region's industrial capacity to produce goods and services. This will affect the traffic demands placed on the highway system after the earthquake. At the same time, the highway system damage will reduce the system's capacity to transport materials, equipment, employees, and other personnel essential to the productivity of firms and households in the region.

These factors together will affect the stricken region's economic productivity and capacity. Estimation of these effects requires the coupling of system, hazards, and component models, with regional economic models, which is a formidable task. Although progress has been made in this area (e.g., Cho et al. 2001; Shinozuka 2004), this is still an area of extensive research and development. This is because most regional economic models are aspatial. These models may treat interactions between economic sectors in considerable detail, but not in a spatially dis-aggregate way. Spatial dis-aggregation is needed to make the link between economic performance and access to lifeline services, including transportation. Furthermore, since access to transportation facilities is un-priced, the value of transportation services is not adequately represented in most regional economic models. Even if a spatially dis-aggregate model of the regional economy is available, it is still necessary to model economic responses to highway-system damage. These responses include changes in the propensity to travel, choice of destination, and choice of route.

Another important factor when using economic loss results for decision-making is evaluation of impacts of the highway-system damage on stakeholders. Future development of economic models should include assessment of who gains (e.g., construction industry) and who loses (e.g., business sectors heavily dependent on trucking to distribute goods) in the event of such damage.

6.2 OBJECTIVE

The objective of the Economic Module is to provide the input data and models necessary to estimate economic losses due to highway-system damage. REDARS™ 2 considers the following sources of economic loss: (a) repair costs; (b) losses due to earthquake-induced travel-time delays; and (c) losses from trips foregone due to earthquake-induced increases in traffic congestion. Section 6.3 summarizes the general approach used in REDARS™ 2 to develop default estimates of these loss sources, and Section 6.4 further discusses each of the sources. . The estimation of unit losses for calculating economic losses due to travel-time delays and trips foregone is discussed in Section 6.5.

6.3 GENERAL APPROACH FOR DEVELOPING DEFAULT LOSS ESTIMATES

REDARS™ 2 provides default parameters for estimating repair costs and losses due to travel-time delays and trips foregone. Any of these default parameters can be overridden by the REDARS™ 2 user.

REDARS™ 2 default repair-model parameters for bridges and for approach fills and roadway parameters are described in Appendices G and H respectively. These parameters are based on construction practices, repair resources (i.e., materials, equipment, and labor), and earthquake-repair experience in California. Their selection as the REDARS™ 2 default repair model was motivated by the extensive post-earthquake repair experience of the California Department of Transportation, which was viewed as a reasonable starting point for developing repair models for highway systems in other parts of the country. Of course, since construction procedures and repair resources and experience will differ from region to region, REDARS™ 2 users from other regions should override the current default repair-model parameters as needed to best represent repair procedures, resources, and experience for their particular region.

6.4 LOSS SOURCES

6.4.1 Repair Costs

REDARS™ 2 expresses default repair costs as percentages of the estimated total replacement cost for the component. These percentages will depend on the component's earthquake-induced damage state. The replacement cost is computed as the product of a unit cost and an effective area of the component. The effective area, in turn, is represented as the product of the component's length and its effective width, which will depend on the component type.

6.4.2 LOSSES DUE TO TRAVEL-TIME DELAYS AND TRIPS FOREGONE

The REDARS™ 2 variable-demand network-analysis procedure that is described in Chapter 5 represents how increased traffic congestion due to earthquake damage affects travel times throughout the system as well as trip demands on the system. That is, it accounts for possible increases in travel times and reductions in trip demands relative to the pre-earthquake conditions, as the level of traffic congestion increases. It also recognizes that different types of trips throughout the system (i.e., automobile trips and various types of freight trips) will have different economic values, and therefore estimates separate travel-time delays and trips foregone for each trip type. These new features are significant extensions of the prior network analysis procedure used in the initial version of REDARS™ 2 that is described in Werner et al. (2000). In that procedure, post-earthquake trip demands were assumed to be equal to pre-earthquake demands, and no distinction was made between different types of trips.

Figure 6-1, which is identical to Figure 5-2 shows how these losses are computed. In this figure, the highway system's pre-earthquake traffic-carrying capacity is represented by the parameter S_1, and the corresponding system-wide travel times and trip demands are represented by the parameters P_1, and D_1 respectively. After the earthquake occurs, the system's traffic carrying capacity reduces to S_2, its travel times increase to P_2', and its trip demands reduce to D_2.

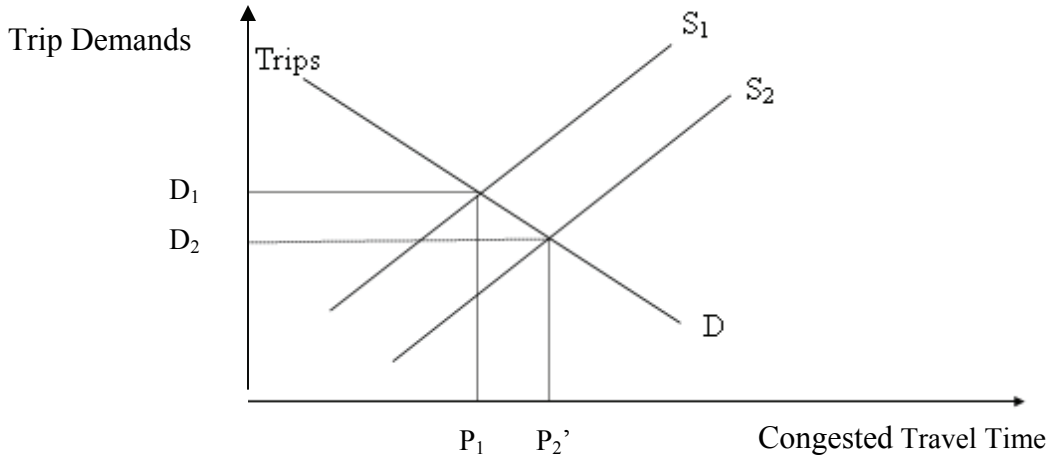

Figure 6-1. Variable-Demand Model for Earthquake-Damaged Highway System

The economic losses due to travel-time increases and trip reductions are computed as the product of a unit loss and the area of the trapezoid in Figure 6-1 that is defined by P_1 and P_2' and D_1 and D_2. Within this trapezoid, the losses due to travel-time increases are represented by the area of the rectangle that is defined by P_1, P_2', and D_2. The corresponding losses due to trips foregone are represented by the area of the triangle defined by P_1 and P_2' and D_1 and D_2 multiplied by the unit loss. These concepts are discussed more fully in the description of the REDARS™ 2 variable-demand network-analysis procedure that is provided in Chapter 5 and Appendix I.

6.5 UNIT LOSSES

In the above approach, the unit loss represents the cost (in dollars per hour per passenger-car-unit) of the travel-time delays and trips foregone. These unit losses will depend on the type of trip (i.e., automobile vs. freight type 1, freight type 2, etc.) and will also vary for different regions of the United States. Werner et al. (2000) used a unit-cost estimation procedure that Caltrans applied to estimate economic losses due to disruption of the Los-Angeles area highway system by the 1994 Northridge Earthquake. This procedure applies user-specified estimates of such factors as vehicle occupancy rates, truck-trip dollar value, cost of excess fuel, etc. to develop these unit costs.

The default unit costs that are currently used in REDARS™ 2 are based on data for the greater Los Angeles area that were based on traffic-congestion statistics developed by the Rand Corporation of California (and obtained from their website, which is http://ca.rand.org). Based on these studies, REDARS™ 2 uses default unit losses of $13.45/(pcu-hour) for automobile trips and $71.05/(pcu-hour) for commercial-vehicle (freight-transport) trips. These unit losses were used in the demonstration application of REDARS™ 2 to the Los Angeles area highway system that is described in Chapter 7.

As noted above, these unit costs will vary for different regions of the United States. Therefore, REDARS™ 2 users from regions outside of the greater Los Angeles area should not use the unit-cost values that are given above. Instead, it is important that these users obtain unit-cost values from data sources that are most appropriate for their particular region.

CHAPTER 7: DEMONSTRATION APPLICATION

7.1 OBJECTIVE AND SCOPE

This chapter describes a demonstration application of the REDARS™ 2 SRA methodology and software to a highway system that extends through a significant section of the greater Los Angeles (LA), California area, and is hereafter referred to as the LA-testbed highway system (see Section 7.2). This analysis will show how REDARS™ 2 can be applied to a major highway system and, in addition, will illustrate how REDARS™ 2 can be used to guide seismic-risk-reduction decision-making by estimating how each candidate risk-reduction-option affects losses due to traffic-flow and travel-time disruptions.

The demonstration SRA consists of three applications of REDARS™ 2 to this highway system, all of which are based on earthquake events contained in a new Coastal California walkthrough table that specifies earthquake occurrences over a 10,000-year time period (App. B). The first application, which is described in Section 7.3, consists of a deterministic analysis of the highway system (without uncertainties) subjected to a single earthquake in the walkthrough table. It illustrates the variety of results that REDARS™ 2 can provide for a system subjected to a single earthquake, in terms of: (a) the distribution and intensity of the earthquake-induced ground-motion and permanent ground displacement (PGD) hazards throughout the highway network; (b) the extent of the damage to the various highway components (bridges, approach fills, pavements, and tunnels) caused by these hazards; (c) how this damage affects post-earthquake travel times and trip demands; and (d) losses due to any travel-time disruptions and trip-demand increases that may occur. As noted earlier, these losses can be represented as economic losses, reduced access to key locations in the region, and/or reduced travel times along key routes that may be important to the emergency response and recovery of the region.

The remaining two applications of REDARS™ 2 within this demonstration application are probabilistic. The first of these applications (described in Section 7.4), is based on the same highway-system and component attributes as considered in the deterministic analysis, and provides the same types of results. However, now, the analysis accounts for how these results are affected by uncertainties in earthquake occurrence and in the estimation of seismic hazards and component damage states. This involves the development of multiple simulations for multiple earthquake scenarios listed in the Coastal California walkthrough table (Chapter 2).

The last application (Section 7.5) involves use of REDARS™ 2 results to assess the economic viability of bridge retrofits within the LA-testbed system. It is based on results from two REDARS™ 2 probabilistic analyses of this system, in which one includes the small number of bridge column-jacketing retrofits that were in place at the time of the 1994 Northridge Earthquake, and the second includes the additional bridge retrofits that were constructed through 2004. The efficacy of these additional retrofits is assessed by computing their benefit-cost ratio (where the benefits include reduction of future losses due to estimated repair costs, travel-time delays, and trips foregone), and also by comparing the variances of the loss results for these two cases (which are a measure of how the uncertainties in the estimates of these losses are reduced by the additional retrofits).

7.2 MODELS

7.2.1 HIGHWAY SYSTEM

Figure 7-1 shows the LA-testbed highway system that is considered in this analysis. This system extends from the town of Santa Clarita to the north to beyond the Century Freeway (I-105) to the south, and from the Pacific coast east to just beyond downtown LA.

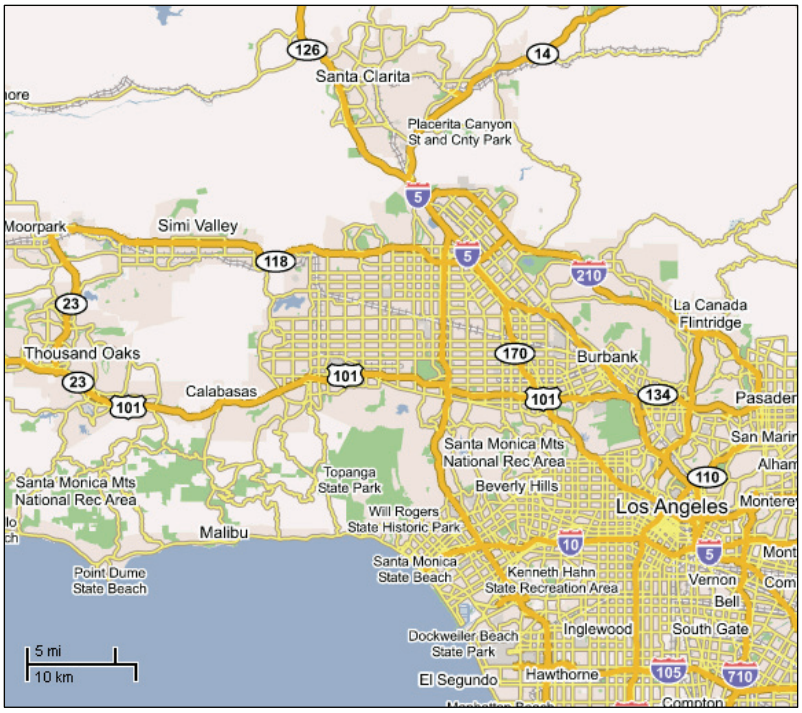

Source: http://maps.google.com

Figure 7-1. LA-Testbed Highway System

The REDARS™ 2 model of this system (Fig. 7-2) includes all of the system's freeways and major arterials. It contains 1,694 nodes and 5,100 links, whose locations and traffic capacities are obtained from the Highway Performance Monitoring System (HPMS) and the National Highway Planning Network (NHPN), as accessed by the REDARS™ 2 Import Wizard (App. C).

7.2.2 BRIDGES

This highway system contains 944 bridges, of which 288 have been retrofitted by column jacketing (see Fig. 7-3), as well as 1,709 pavement links and 5 tunnels. The attributes of the various bridges are based on data from the National Bridge Inventory (NBI) database, as accessed by the REDARS™ 2 Import Wizard. Those bridges that have been column jacketed as of the end of 2004 have been identified from the California Department of Transportation (Caltrans) statewide bridge database (Yashinsky 2005). The structural capacities of these column-jacketed bridges were estimated by multiplying the un-retrofitted-bridge capacities by damage-state-dependent enhancement factors that were developed by Shinozuka (2004).

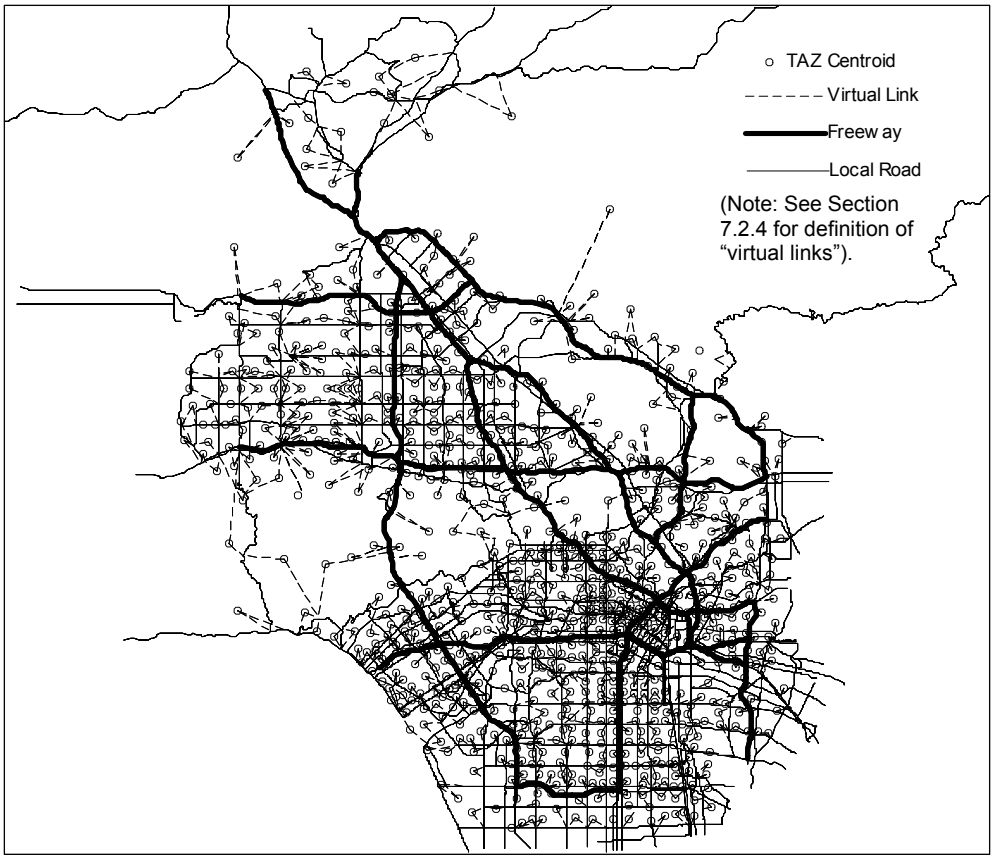

Figure 7-2. REDARS™ 2 Model of LA-Testbed Highway System

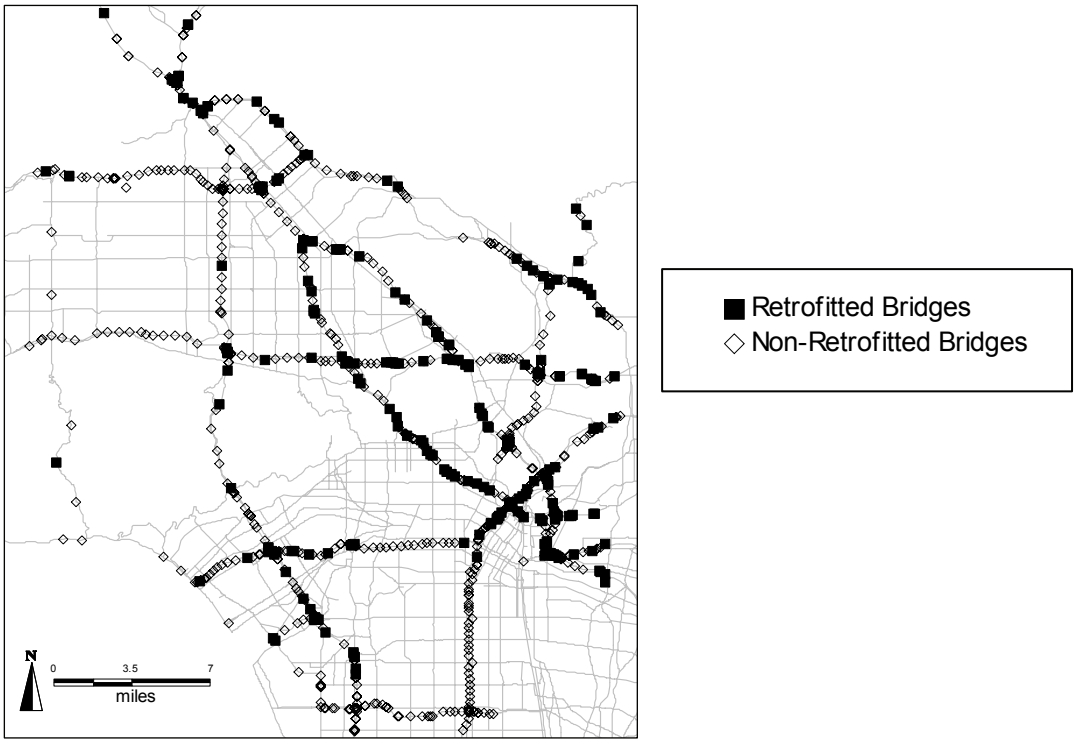

Figure 7-3. Locations of Bridges in LA-Testbed Highway System

7.2.3 SOIL CONDITIONS

The soils along the roadways in this system consist of soft rock and firm soils, which are represented in REDARS™ 2 primarily as NEHRP site classifications C and D (see Fig. 7-4). None of the soils within the system are considered to be prone to liquefaction hazards.

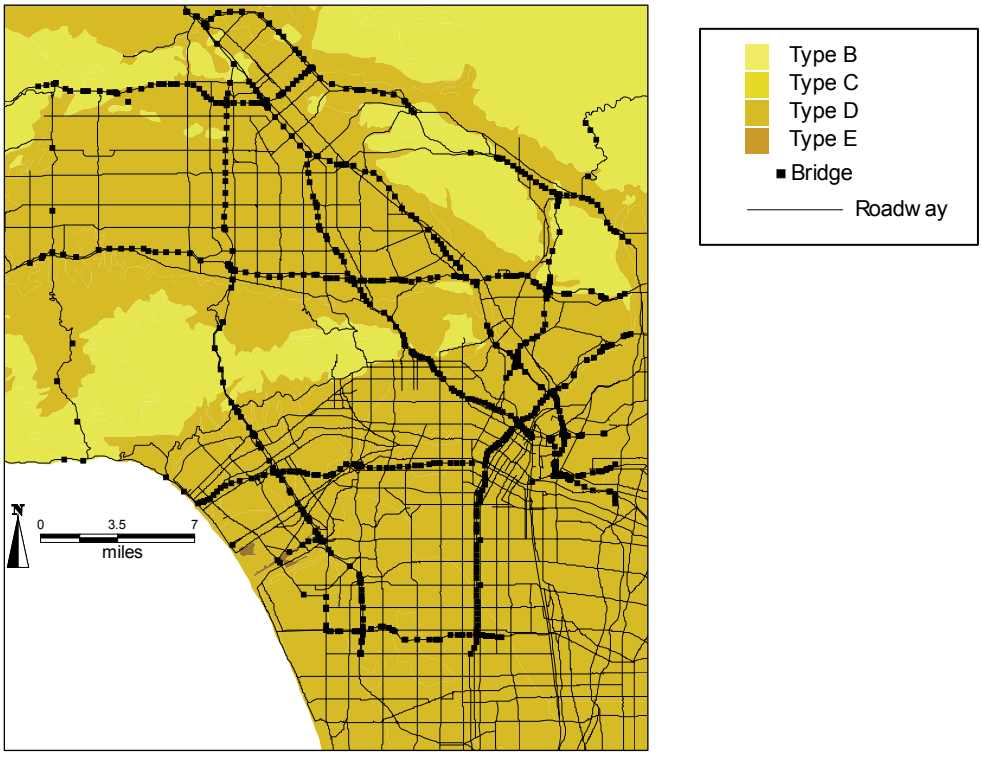

Figure 7-4. Soil Conditions (in terms of NEHRP Site Classifications) Throughout LA-Testbed Highway System

7.2.4 TRAFFIC ANALYSIS ZONES

Figure 7-5 shows the section of the greater LA area within which this highway system is located. This area is modeled using 977 traffic analysis zones (TAZs) whose locations and trips to all other zones are based on data obtained from the Southern California Area of Governments (SCAG). In addition, 59 external TAZs are included that represent aggregations of trips into and out of the region from locations beyond the region are included in this model. In this REDARS™ 2 model, 3,908 virtual links are used to connect the centroid of each TAZ to the actual highway system (see Fig. 7-2).

Several of these TAZs are highlighted in Figure 7-5. These TAZs represent those particular zones for which earthquake-effects on trips and travel times to-and-from the zones at different times after each earthquake scenario are displayed as output from this analysis. They were selected because they represent centers of commerce, locations of major medical centers, and locations of airports and other facilities that could be important for post-earthquake emergency response and recovery.

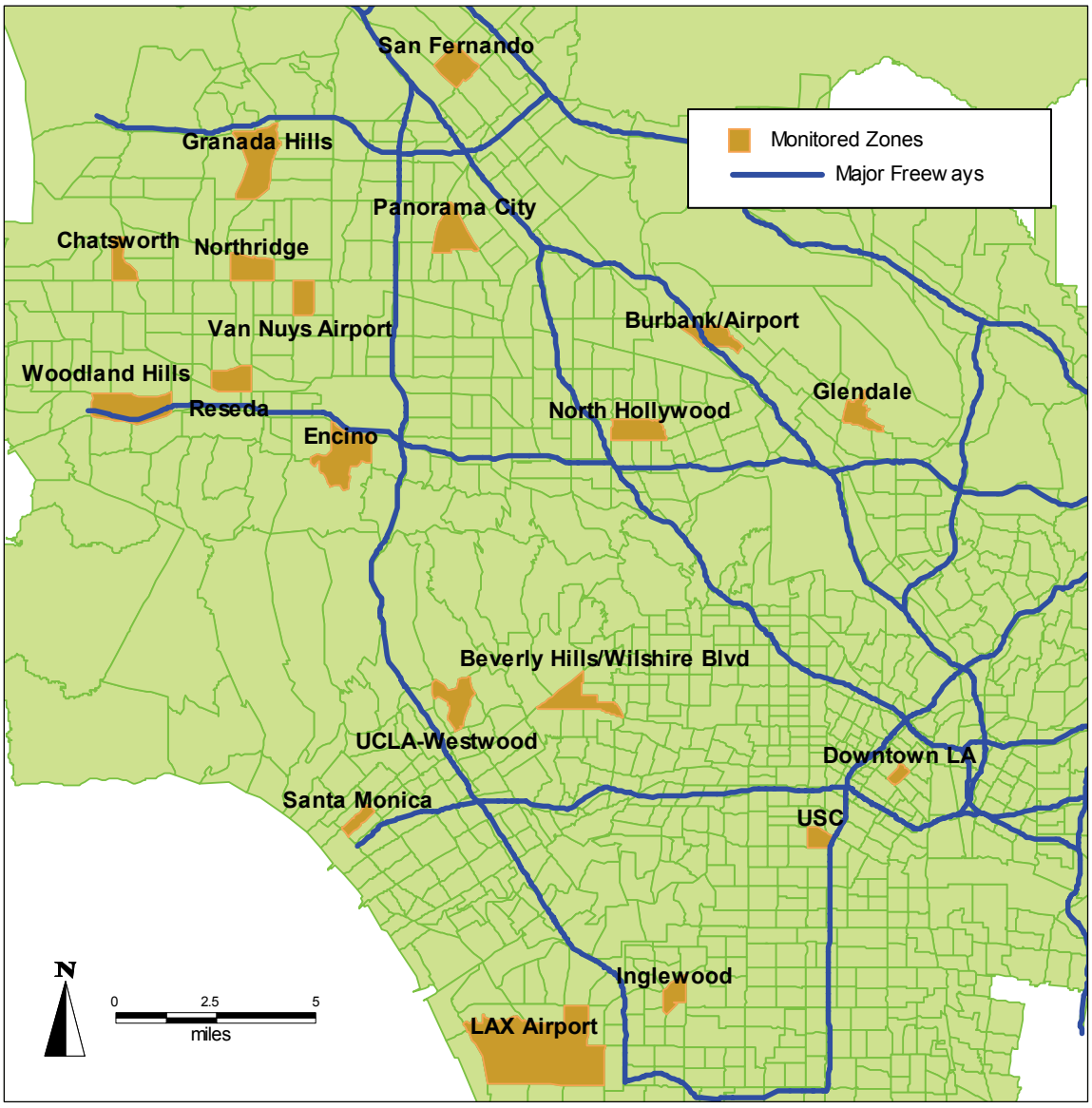

Figure 7-5. Traffic Analysis Zones whose Travel-Times and Trips to/from These Zones are Displayed as Output from this Demonstration Application

7.2.5 ROUTES

Figure 7-6 shows selected routes within this LA-testbed highway system whose post-earthquake travel times have been displayed as output from this demonstration application. Of course, any number of additional or alternative routes within this system could also have been selected for travel-time display.

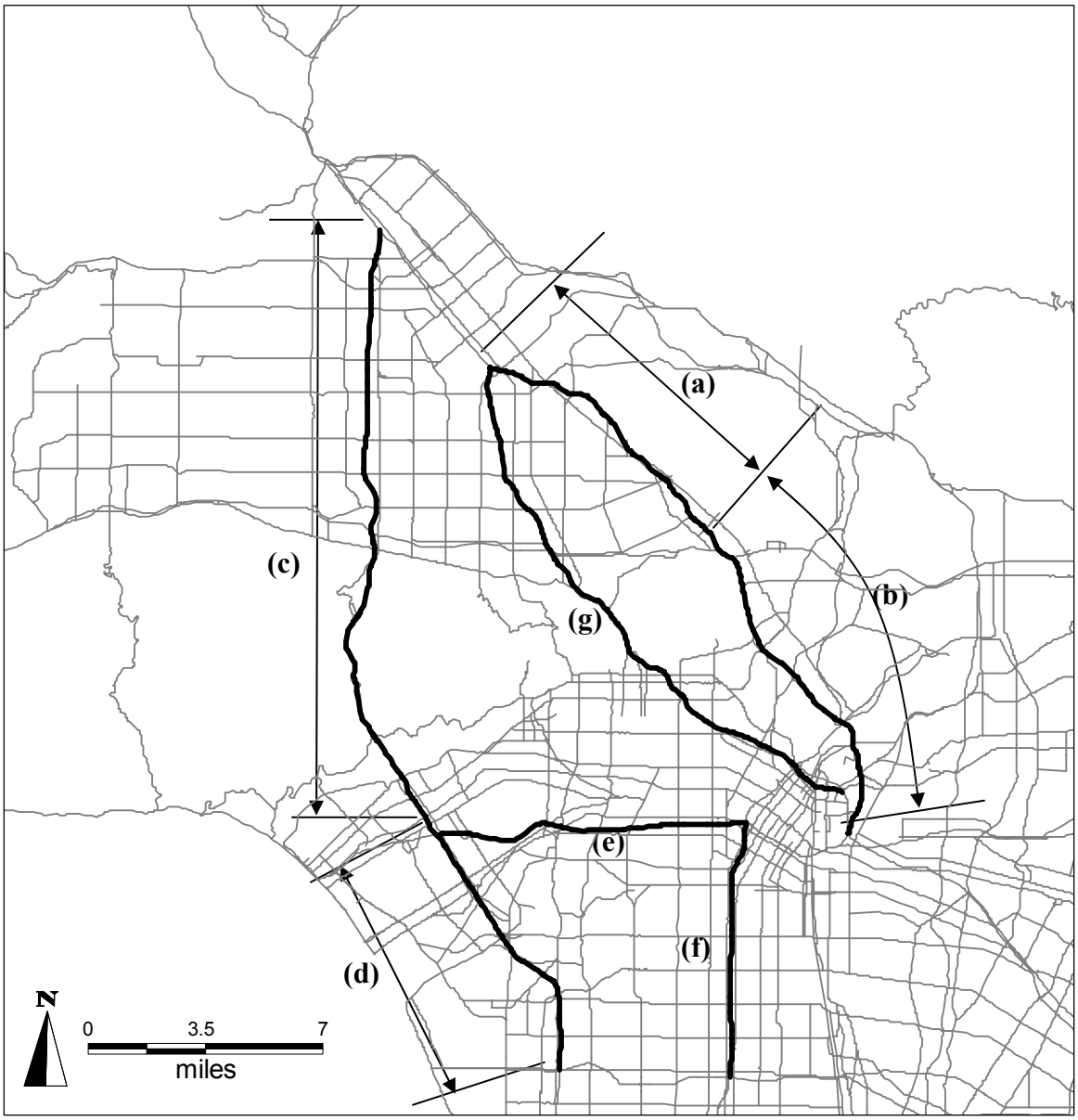

(a) I-5 from San Fernando to Burbank
(b) I-5 from Burbank to downtown LA
(c) I-405 from I-5 to I-10 interchange
(d) I-405 from I-405/I-10 interchange to LAX
(e) I-10 from Santa Monica to downtown LA
(f) I-110 from I-105 to downtown LA
(g) I-101 from I-405 interchange to downtown LA

Figure 7-6. Routes whose Travel Times are Displayed as Output from This Demonstration Analysis

7.2.6 EARTHQUAKE SCENARIOS

The earthquake scenarios for this analysis are those events from the overall 10,000-year Coastal-California walkthrough table (App. B) that are located within about two-hundred miles of this LA-testbed highway system. They consist of 7,035 earthquakes with $M_w \geq 5.0$, whose breakdown by moment magnitude is shown in Figure 7-7. Of these, it turns out that 2,645 of these events actually caused damage to this system (see Sec. 2.4.1.4 of Chap. 2). Only these damaging events were considered in the probabilistic SRAs described in Sections 7.4 and 7.5.

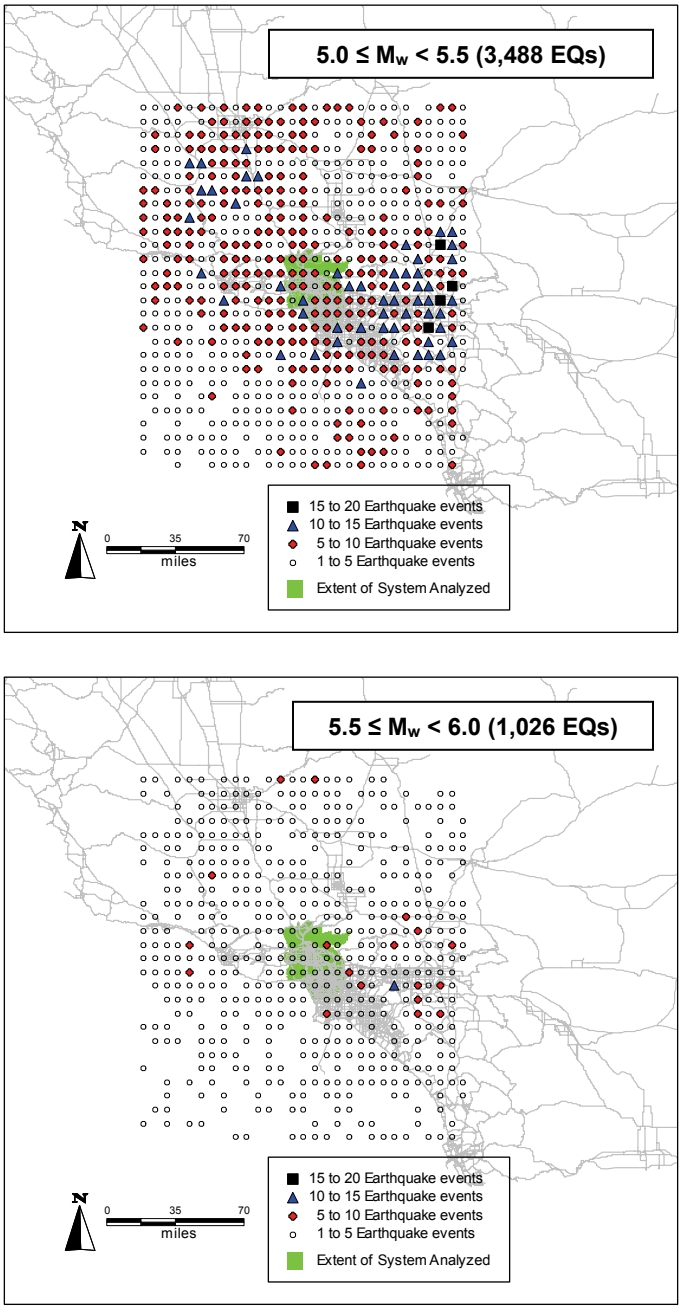

Figure 7-7. Epicenters of Earthquake Scenarios in 10,000-Year Walkthrough Table

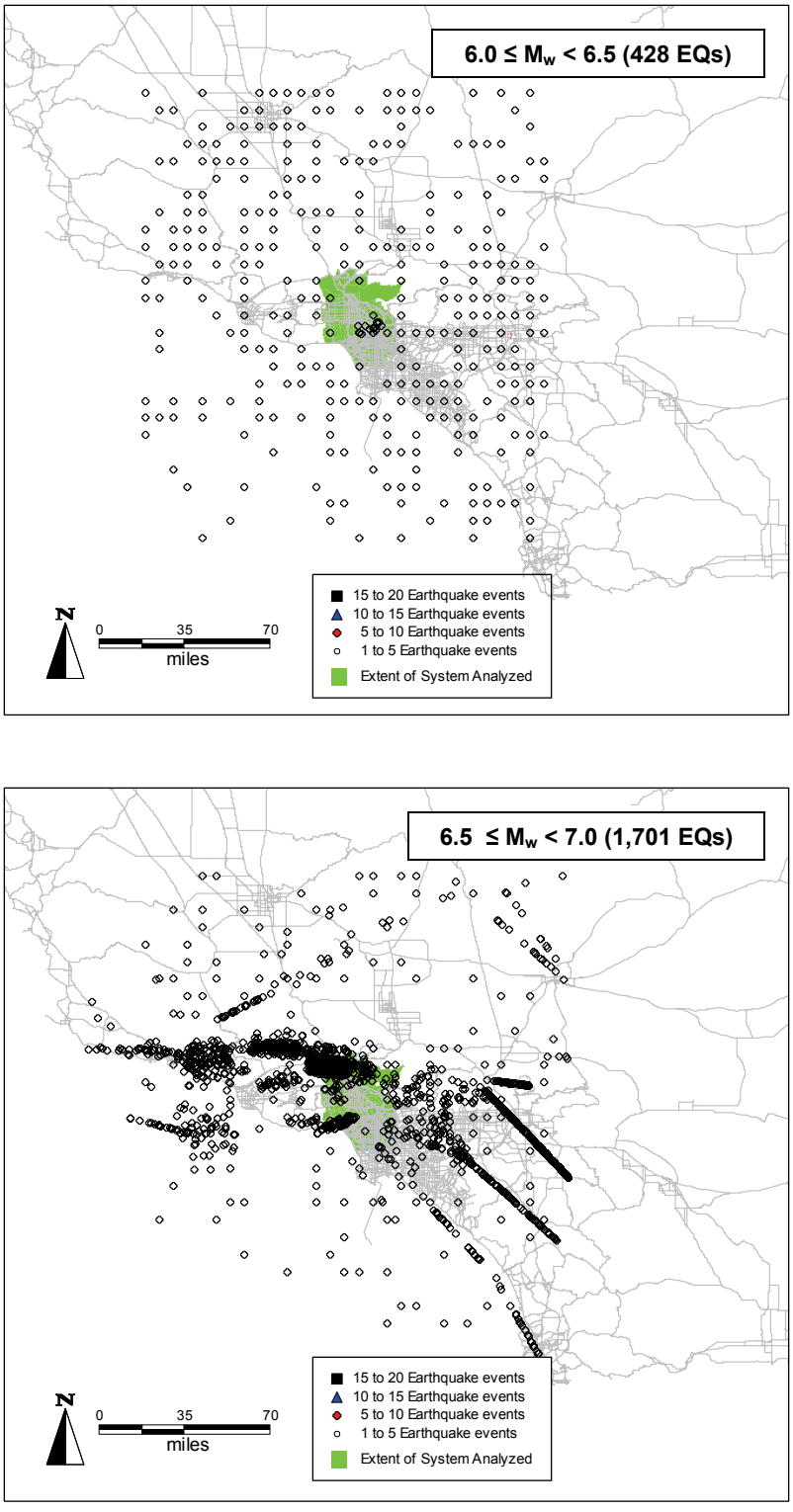

Figure 7-7. Epicenters of Earthquake Scenarios in 10,000-Year Walkthrough Table (continued)

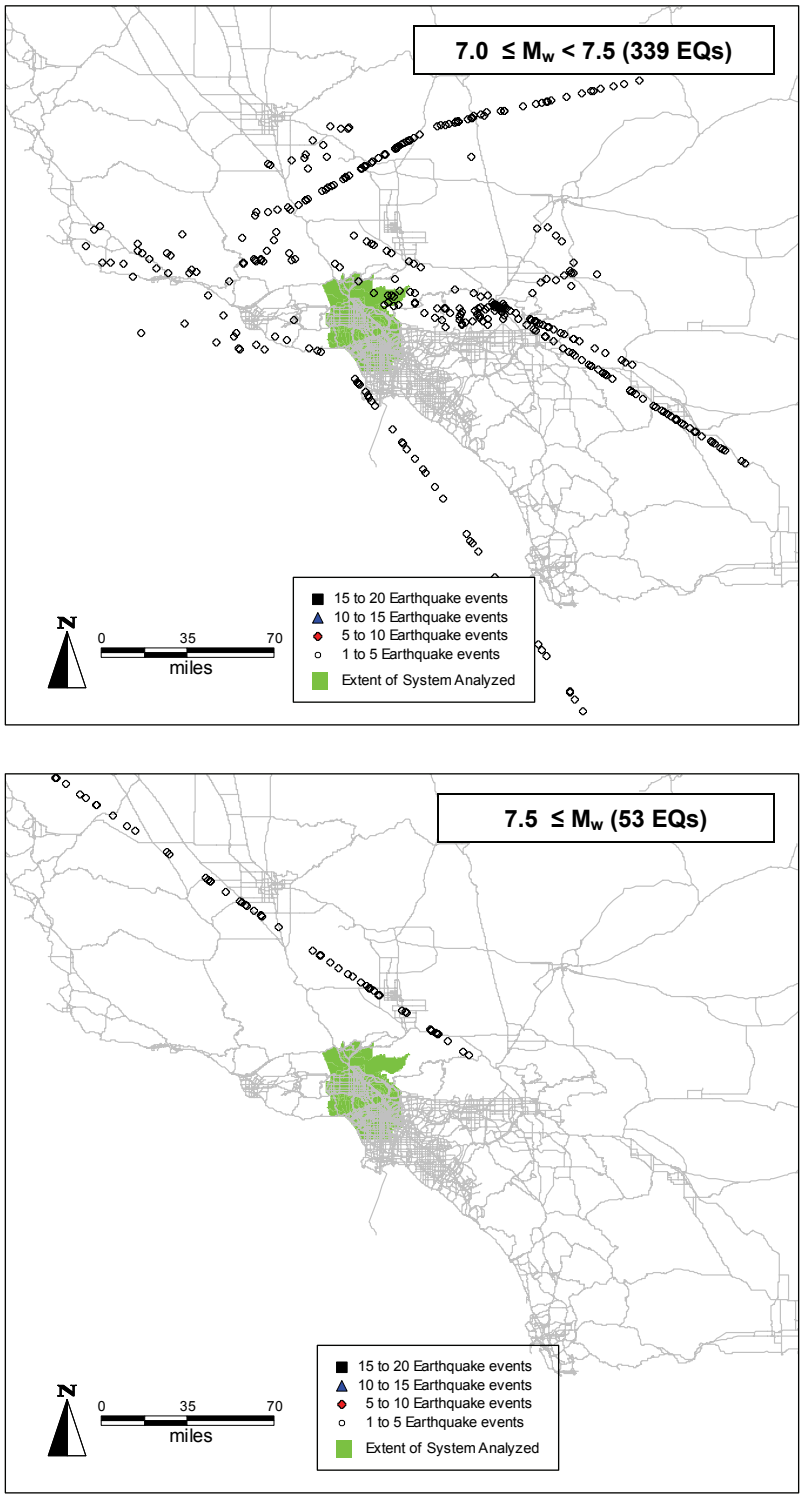

Figure 7-7. Epicenters of Earthquake Scenarios in 10,000-Year Walkthrough Table (concluded)

7.3 DETERMINISTIC ANALYSIS

The first part of this demonstration application consists of a deterministic analysis of the seismic performance of the LA-testbed highway system subjected to a single earthquake scenario. This analysis does not include effects of uncertainties; i.e., mean values of all uncertain parameters are used throughout the analysis. Its purpose is to illustrate the types of results that REDARS™ 2 can provide for such analyses, and how they can be interpreted.

7.3.1 EARTHQUAKE SCENARIO

The earthquake scenario used in this deterministic analysis has a moment magnitude of 6.6 and is caused by rupture along the Santa Monica Fault. This scenario occurs during Year 3,076 in the walkthrough table used in the probabilistic analyses of this LA-testbed system (see Secs. 7.4 and 7.5). The epicenter of this earthquake is located within the Pacific-Palisades/Santa-Monica area, about 2.5 km inland from the Pacific-Ocean coastline (e.g., Fig. 7-8).

The Santa Monica Fault is a reverse fault with a dip angle of 75 deg. The surface expression of the fault rupture for the above earthquake scenario is about 28-km. long and about 9.7 km wide[5]. It extends in a northeast direction from its origin in the Pacific Ocean along a path that parallels Sunset Boulevard to its terminus that is about five km beyond the San Diego Freeway (e.g., Fig. 7-8a). The hypocentral depth of this earthquake is about 8.2 km. Because of this depth and the dip angle of this reverse fault, the following figures show that earthquake's epicenter is slightly offset from its surface expression of fault rupture.

7.3.2 SEISMIC HAZARDS

7.3.2.1 Ground Shaking

Figure 7-8 shows the distribution and intensity of ground motions throughout this highway system that are caused by this earthquake scenario. These ground-motion results are provided as spectral accelerations at a period of 1.0 sec., since this is the ground-motion parameter that is used by the REDARS™ 2 default models for estimating bridge damage due to ground shaking (see App. G). However, REDARS™ 2 can also provide ground-motion results in terms of spectral acceleration at a period of 0.3 sec. (which is used by this bridge damage model for a few situations) and also as peak ground acceleration (which is often used in the calculation of liquefaction hazards).

These figures show that the intensity of the ground motions due to this earthquake scenario is largest at bridge sites along I-405 that are close to the fault rupture. At these sites, the spectral accelerations are as high as 0.83 g. However, significant ground shaking (on the order of 0.6 g to 0.8 g) also occurs along some segments of I-10 that are west of I-405.

[5] As described in Appendix B, the lengths and widths of the fault rupture for each earthquake scenario are estimated from Wells and Coppersmith (1994), including uncertainties. Uniform random variates are used to estimate the location of the epicenter within the projection of the fault plane onto the ground surface.

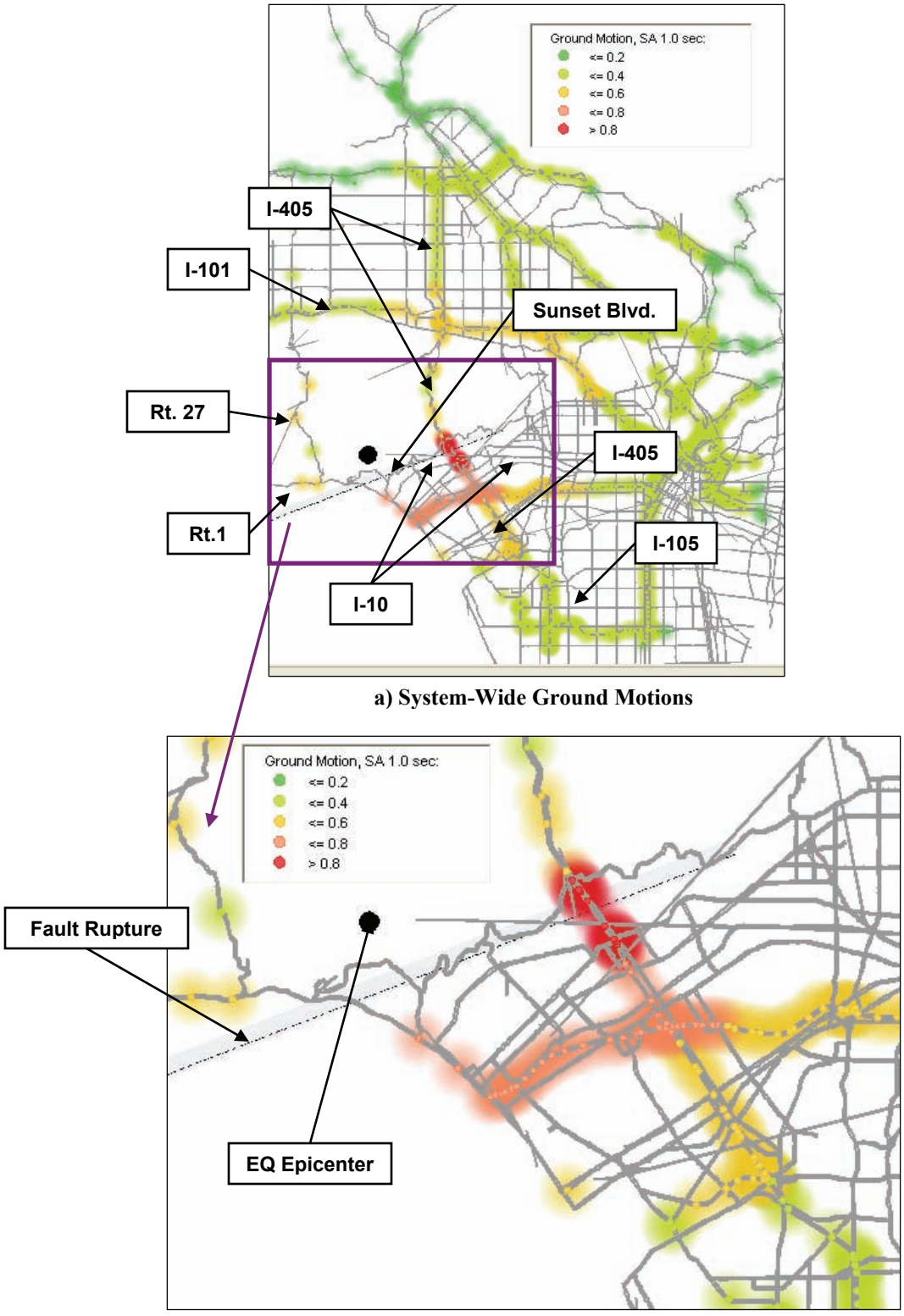

a) System-Wide Ground Motions

b) Area with Most Severe Ground Motion

Figure 7-8. Ground Motions (Spectral Acceleration at Period of 1.0 sec., in units of g)

7.3.2.2 Surface Fault Rupture

In addition to ground shaking, this earthquake scenario causes significant surface-fault-rupture hazards, with estimated permanent ground displacements of up to 26 in. Figure 7-9 shows that these hazards occur over an extended length of Sunset Boulevard, which seems plausible in view of the close proximity of this major roadway to the Santa Monica Fault.

This figure also shows significant fault-rupture displacements along a length of the Pacific Coast Highway (Route 1) that extends from Sunset Boulevard to Route 27. However, only the small segment of Route 1 that is actually within the zone of deformation of the Santa Monica fault rupture could undergo large displacements. This result is attributed to the modeling of this entire roadway segment by a single link (only a small part of which is actually in the fault-rupture zone) and also by the REDARS™ assumption that the ground displacement of any link in the network is governed by the largest displacement occurring anywhere along that link.

Figure 7-9 also shows large ground displacements along a long segment of Route 27 north of Route 1 (also modeled by a single link) and at the sites of two bridges along Route 1 just west of Route 27. Later sections of this chapter show that these displacements cause failure of these two bridges and along Route 27, leading to extended roadway closures in this localized area of the LA-testbed system. However, these results are somewhat counterintuitive, since the locations of the failures are not immediately adjacent to the ruptured fault segment. Thus, possible causes of these results will be further assessed by the REDARS™ development team. It is interesting to note that estimated fault-rupture displacements outside of this localized area and throughout the remainder of the LA-testbed highway system are much more consistent with intuition.

7.3.2.3 Approach Fill Settlement

Figure 7-9 also displays permanent ground displacements from approach-fill settlement. These small-to-moderate displacements are generally on the order of just a few inches.

7.3.3 COMPONENT PERFORMANCE

The seismic performance of the various components is this highway system is summarized in Table 7-1. This table shows that 20 of the 944 bridges in the system are estimated to suffer complete damage (i.e., collapse) and 31 additional bridges are estimated to experience extensive damage. The table also indicates complete damage to 54 of the system's 9,008 pavement links, and extensive damage to 10 of these links. The various tunnels in the system were not damaged, and the approach fills experienced only slight damage.

Figure 7-10 provides a map of the LA-testbed highway system that shows the locations of the various damaged components within this system. This figure shows that most of the collapsed bridges are located along the segment of I-405 between Sunset Boulevard and I-10, and also along I-10 between its western terminus and its interchange with I-405. The roadway-pavement segments that experience extensive or complete damage correspond to those segments that experience large ground displacements due to surface fault rupture, and are located within the estimated width of the fault-rupture zone.

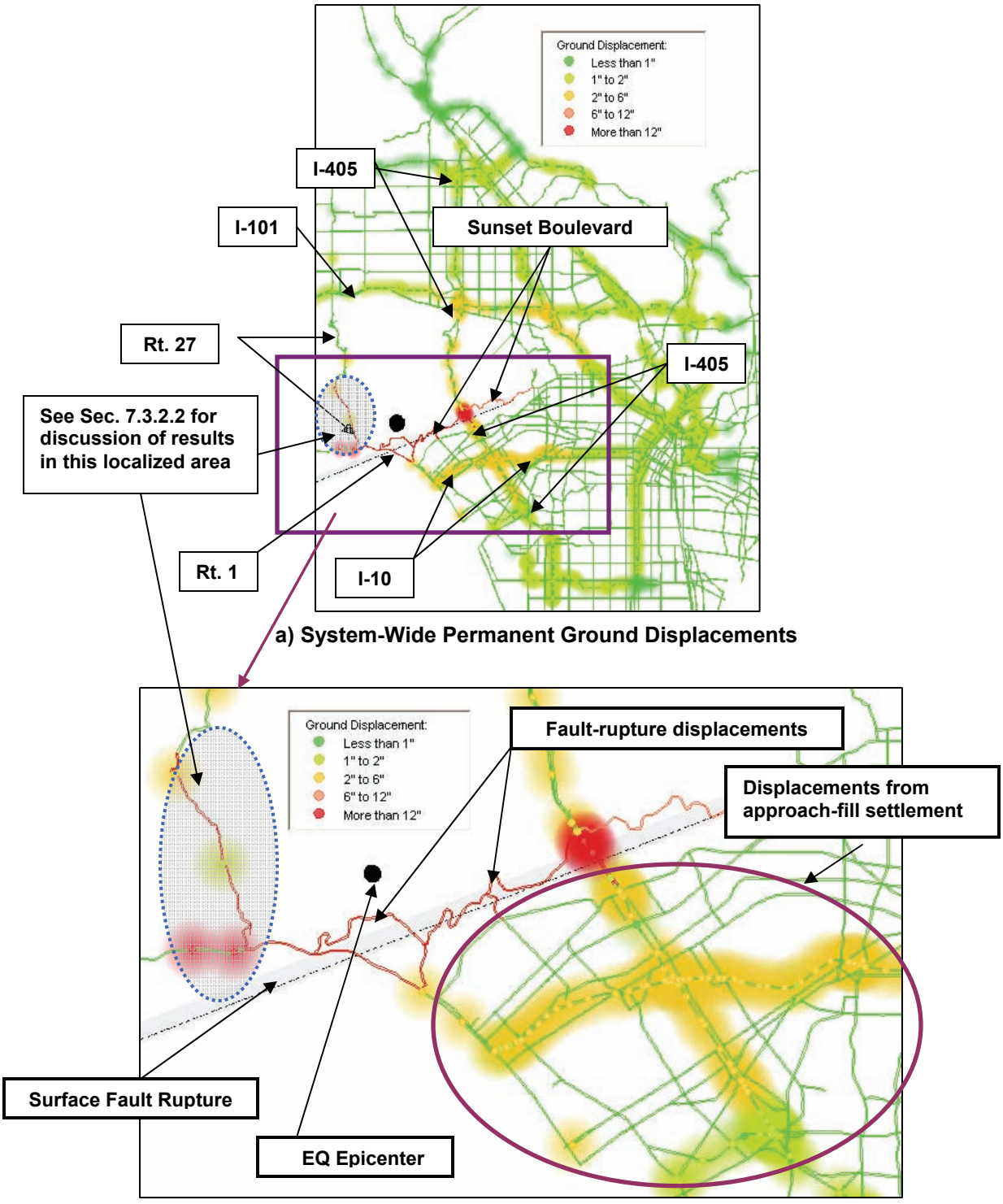

Figure 7-9. Permanent Ground Displacement from Surface Fault Rupture and Approach-Fill Settlement

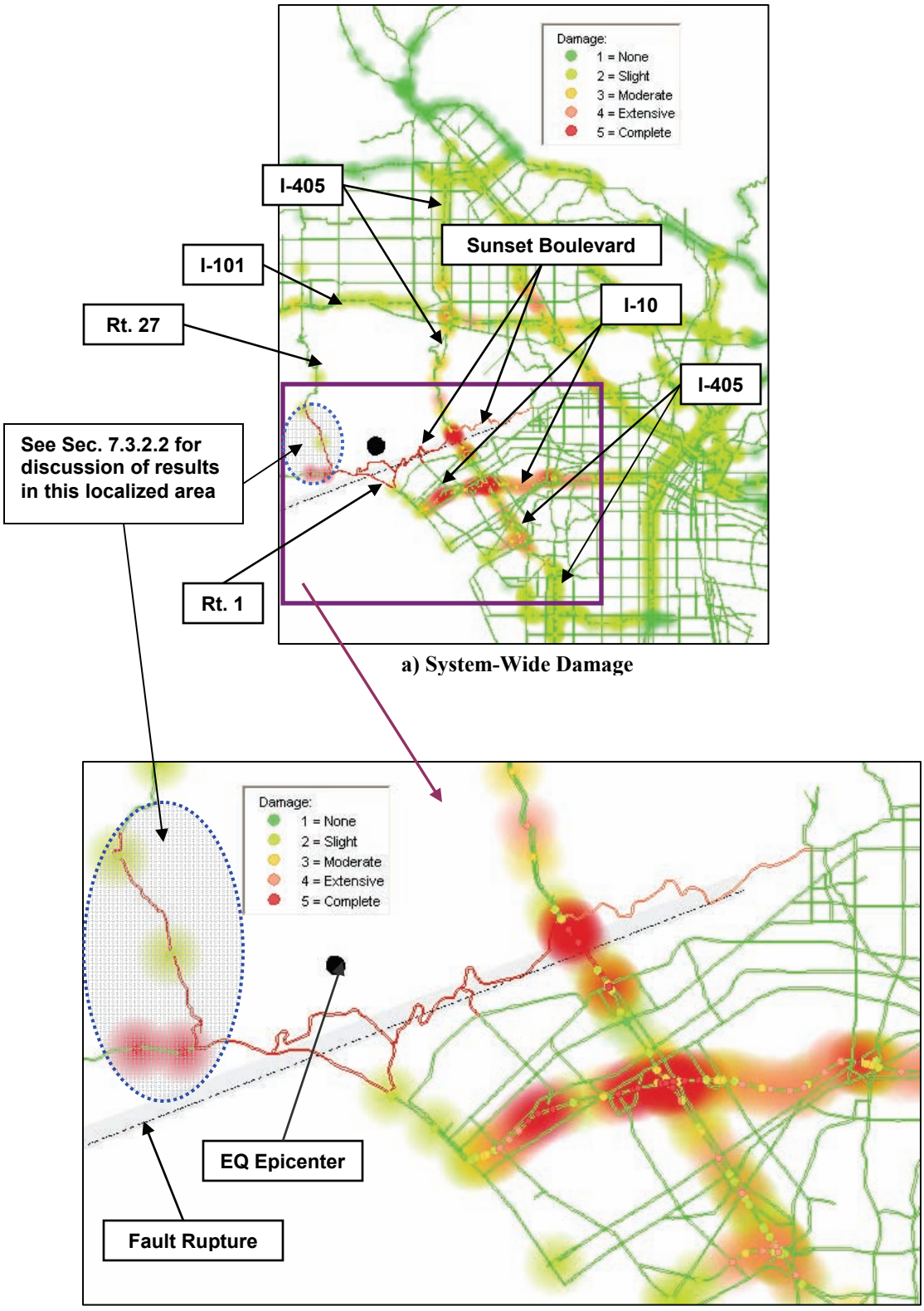

a) System-Wide Damage

b) Area with Greatest Damage to Components

Figure 7-10. Component Damage States

Table 7-1. Component Damage Summary

Damage State	Bridges	Approach Fills	Tunnels	Pavement Links
1. None	744	400	5	8,944
2. Slight	93	1,309	0	0
3. Moderate	56	0	0	0
4. Extensive	31	0	0	10
5. Complete	20	0	0	54
Totals	944	1,709	5	9,008

Examination of the data contained in Table 7-2 clarifies why this large number of bridge collapses has occurred. This table lists seismic-design, seismic-retrofit, and structural-attribute data for the 20 collapsed bridges and five nearby bridges that did not collapse, as well as each bridge's seismic hazards and damage state. The following trends are noted from this list:

- Five of the bridges (those highlighted with light blue shaking in Table 7-2) are estimated to have collapsed due to excessive fault-rupture displacement. Three of these collapsed bridges are located on I-405 near Sunset Boulevard, near the crossing of I-405 by the fault rupture crosses I-405. The two remaining collapsed bridges are located along Route 1 just west of Route 27, and are attributed to the fault-displacement issues discussed in Section 7.3.2.2.
- The remaining 15 bridges (highlighted with light grey shading in Table 7-2) are estimated to have collapsed due to strong ground shaking. Table 7-2 shows that all of these bridges are multi-span structures that were neither seismically designed (i.e., constructed prior to 1975) nor column jacketed. That is, no seismically-designed or column-jacketed bridge is estimated to have collapsed due to ground shaking from this earthquake scenario.
- Table 7-2 lists five un-collapsed bridges that are adjacent to the above 15 collapsed bridges. Two of these bridges (which are numbered 231 and 264 in Table 7-2 and are highlighted with turquoise shading) are neither seismically designed nor retrofitted, but are single-span structures. The REDARS™ 2 default bridge model indicates that such bridges have very robust seismic-performance characteristics.
- The three remaining non-collapsed bridges are numbered 211, 224, and 244 and are shown by orange shading. These are multi-span bridges that have either been seismically designed or retrofitted with column jacketing. They are near multi-span collapsed bridges that were neither seismically designed nor retrofitted (see Table 7-2 footnote).

Of course, the above trends should be interpreted with due regard to the various approximations that are inherent in the current REDARS™ 2 default bridge model, and in the use of mean values of all uncertain input parameters in this analysis (Chap. 4). Nevertheless, they do provide some indication of the possible effectiveness of modern seismic design and retrofit procedures in reducing the level of bridge damage due to strong ground shaking.

Table 7-2. Collapsed Bridges and Nearby Uncollapsed Bridges from Scenario Earthquake along Santa Monica Fault

ID No.	Bridge Number	Approximate Location	EQ Design (Year. Built)	Column Jacket Retrofit	Ground Motion (Spectral Acceleration at T = 1 sec) (GM)	Fault-Rupture Displacement (FRD)	Damage State	
							GM	FRD
285	53 036S	On Hwy 1, 1.68 km west of Rt. 27	No (1940)	No	0.54 g	22.9 in.	1	**5**
283	53 003S	On Hwy 1, just west of Rt. 27 (single-span)	No (1933)	No	0.54 g	24.2 in.	1	**5**
392	53 10425	On I-405 0.35 km south of Sunset Blvd OC	No (1956)	No	0.83 g	16.8 in.	2	**5**
390	53 10415	On I-405 0.40 km south of Sunset Blvd OC	No (1956)	No	0.83 g	16.8 in.	3	**5**
388	53 2390	On I-405 0.45 km south of Sunset Blvd OC	Yes (1975)	No	0.83 g	16.8 in.	4	**5**
339	53 0710	At interchange between I-405 and I-10???	**No (1957)**	**No**	0.81 g	0.0 in.	**5**	1
161	53 1597	On I-10 1.95 km NE of Highway 1	**No (1965)**	**No**	0.65 g	0.0 in.	**5**	1
163	53 1598	On I-10 2.40 km NE of Highway 1	**No (1965)**	**No**	0.66 g	0.0 in.	**5**	1
168	53 1599	On I-10 2.8 km NE of Highway 1	**No (1963)**	**No**	0.66 g	None	**5**	1
182	53 1604	On I-10 1.6 km SW of I-405	**No (1963)**	**No**	0.64 g	None	**5**	1
205	53 1605	On I-10 1.0 km SW of I-405	**No (1963)**	**No**	0.64 g	None	**5**	1
207	53 1620	On I-10 1.0 km SW of I-405	**No (1963)**	**No**	0.64 g	None	**5**	1
219	53 0939	On I-10 just SW of I-405	**No (1963)**	**No**	0.63 g	None	**5**	1
220	53 1628	On I-10 just SW of I-405	**No (1963)**	**No**	0.63 g	None	**5**	1
209	53 1638G	On I-405 just south of I-10	**No (1963)**	**No**	0.62 g	None	**5**	1
211*	53 1630G	On I-405 just south of I-10	No (1963)	**Yes**	0.62 g	None	**3**	1
223	53 1623	On I-405 just south of I-10	**No (1963)**	**No**	0.63 g	None	**5**	1
220	53 1628	On I-405 just south of I-10	**No (1963)**	**No**	0.63 g	None	**5**	1
226	53 1640	On I-10 just east of I-405	**No 1964)**	**No**	0.62 g	None	**5**	1
224*	53 1637F	On I-10 just east of I-405	No (1964)	**Yes**	0.63 g	None	**3**	1
229	53 1634	On I-10 about 0.9 km east of I-405	No (1964)	No	0.62 g	None	5	1
231	53 1617	On I-10 about 1 km east of I-405 **(single span)**	No (1963)	No	0.61 g	None	**1**	1
245	53 2791S	On I-10 about 5.3 km east of I-405	**No (1964)**	**No**	0.50 g	None	**5**	1
244*	53 2791	On I-10 about 5.3 km east of I-405	**Yes (1994)**	No	0.50 g	None	**2**	1
264	53 1611S	On I-10 about 5.3 km east of I-405 **(single span)**	No (1964)	No	0.50 g	None	**1**	1

* Note: Retrofitted and un-collapsed Bridge 211 is near collapsed Bridges 209, 223, and 220; retrofitted and un-collapsed Bridge 224 is next to collapsed Bridge 226, and un-collapsed and seismically designed Bridge 244 is near collapsed Bridge 245.

7.3.4 SYSTEM STATES

After the component damage states are estimated, the REDARS™ 2 component-repair model is used to estimate corresponding repair costs, downtimes, and the ability of the damaged component to accommodate traffic at various times after the earthquake while the repairs are proceeding. As described elsewhere in this Technical Manual, the default component-repair models that are now included in REDARS™ 2 were developed from close consultation with members of Caltrans' senior engineering and maintenance staff, in order to reflect Caltrans' experience, construction methods, and repair resources. Of course, these repair models should be modified when applying REDARS™ 2 to highway systems in other parts of the country, where experience levels, construction practices, and repair resources will usually differ from those of Caltrans.

For the levels and types of component damage summarized in Section 7.3.3, these repair models result in the estimated system states shown in Figure 7-11 for four different times after the earthquake (7-, 60-, 150-, and 221-days). In this assessment, the post-earthquake time of 7-days was chosen to typify an early time after the earthquake, when repair resources are first being mobilized to begin the repairs. The post-earthquake time of 221-days is the "system recovery time" for this particular roadway system and earthquake, which is the estimated time after the earthquake when all repairs are completed and the highway system first returns to its pre-earthquake condition (according to the default component repair models described in Appendices G and H). The post-earthquake times of 60-days and 150-days represent intermediate times after the initiation of the system repairs and before the repairs are completed.

The system state at 7-days after the earthquake contains the largest number closed roadway network links along which the more severely damaged components are located. Figure 7-11 shows that the most significant closures are located: (a) along I-405 between Sunset Boulevard and I-10 and also at a few other locations; and (b) along a larger segment of I-10 that extends from its western terminus to a location that is approximately midway between its I-405 interchange and downtown Los Angeles.

At subsequent days after the earthquake, Figure 7-11 shows that the number of closed roadway network links decreases as the repairs proceed in accordance with the REDARS™ component-repair models. These system states at successively increasing intermediate post-earthquake times will tend to converge toward the fully-open system state at the system recovery time of 221 days after the earthquake.

7.3.5 TRAFFIC AND TRIP-DEMAND IMPACTS

The next step in this deterministic analysis of this LA-testbed highway system consisted of application of the network analysis models described in Chapter 5 and Appendix I to each of the system states shown in Figure 7-11. These models estimate how earthquake-induced highway-system damage and associated traffic congestion affect post-earthquake travel times, traffic impacts, and trip demands on the system.

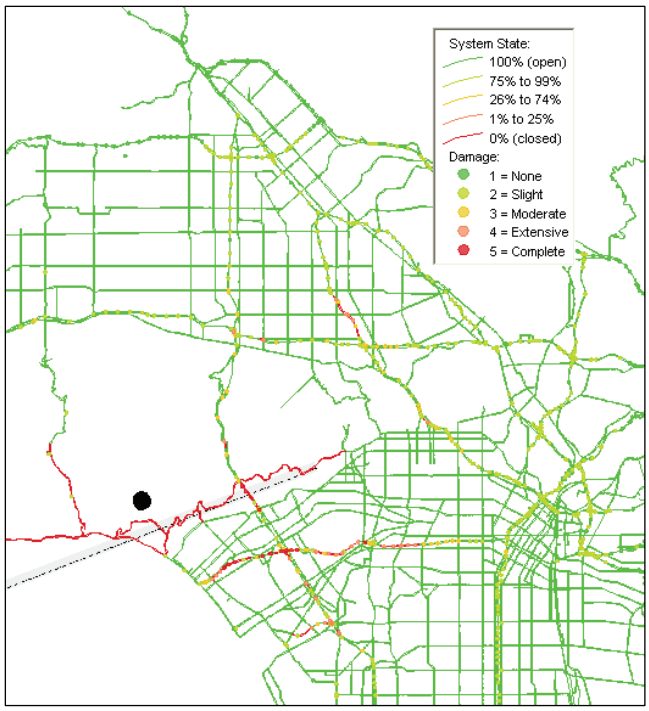

a) 7-Days after Earthquake

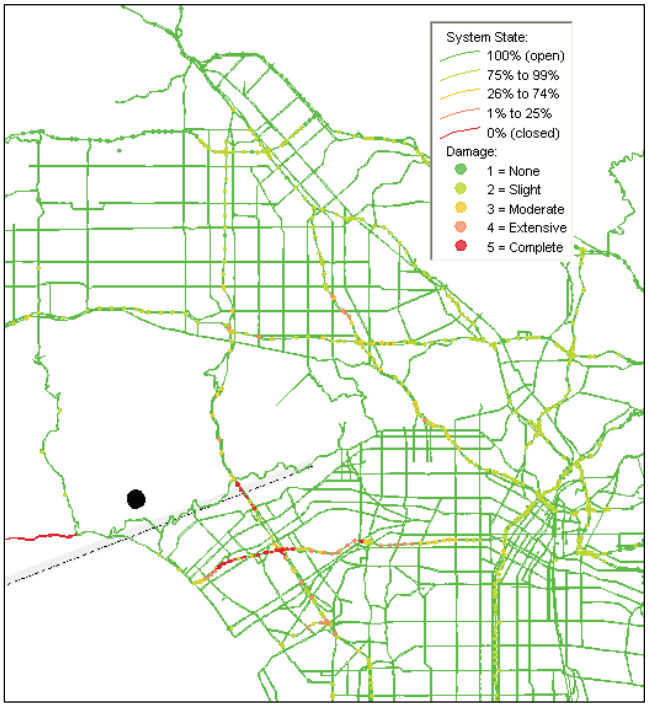

b) 60-Days after Earthquake

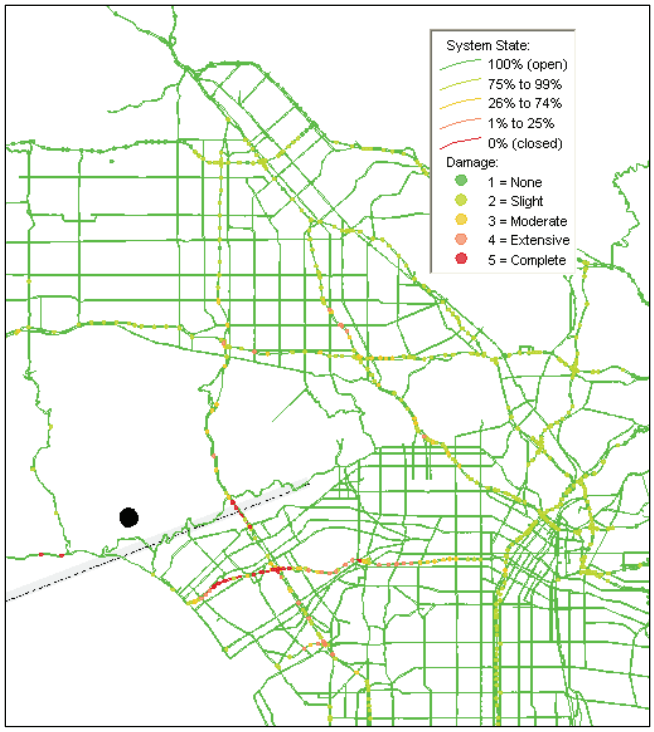

c) 150-Days after Earthquake

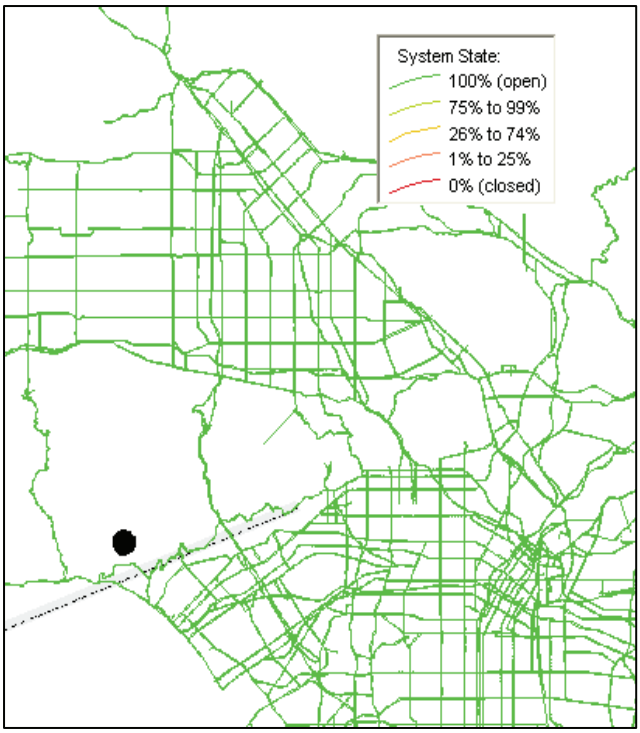

d) 221-Days after Earthquake

Figure 7-11. Post-Earthquake System States

Table 7-3 summarizes the estimated impacts of this earthquake scenario on available lane-miles and trip-demands at various times after the earthquake. It shows that, at 7-days after the earthquake, the total number of available lane-miles in the system is reduced by about 4-percent due to the damage experienced by the highway system, and that the trip demands on the system are reduced by about 8-percent. Table 7-3 also shows how these impacts decrease over time after the earthquake, as the repairs to the damaged components proceed.

Table 7-3. Summary of Estimated Earthquake Impacts on System-Wide Traffic

Days after the Earthquake	Traffic Impactions (reductions relative to pre-earthquake)	
	Lane-Miles	Trip Demands
7 days	4%	8%
60 days	1%	3%
150 days	0%	2%
221 days (system recovery time)	0%	0%

REDARS™ 2 provides several types of graphical system-wide maps and tabular data to show various traffic impacts from earthquake damage to the highway system. Graphical system-wide maps provided by REDARS™ 2 for this purpose are summarized below:

- ***System-Wide Post-Earthquake Traffic Volumes (Fig. 7-12).*** These system-wide maps show that, at 7-days after the earthquake, major sections of the I-405 and I-10 freeways in the western part of the city are estimated to be fully closed to traffic, as will sections of I-101 at the I-405 interchange, Route 1 near its crossing of the Santa Monica Fault rupture zone, and the western part of Sunset Boulevard. At 60-days after the earthquake, the freeway segments along I-405 and I-10 remain closed, but the other previously-closed highway segments can now accommodate partial pre-earthquake traffic volumes. At 150-days after the earthquake, the system-wide traffic volumes continue to improve, and only sections of I-10 remain closed. The travel volumes are restored to their full pre-earthquake levels at the system recovery time of 221-days after the earthquake.

- ***System-Wide Post-Earthquake Travel Times (Fig. 7-13).*** This set of maps shows how access and egress times to/from all of the TAZs in the region are affected by earthquake damage to this highway system. Output from this analysis provides these results for both automobile and freight traffic. Figure 7-13 shows results for automobile traffic only. At 7-days after the earthquake, this figure shows that automobile travel times are affected throughout much of the western and central part of LA and also in the southern part of the San Fernando Valley. At subsequent post-earthquake times, these travel time effects diminish as the system's traffic-carrying capacity is being restored.

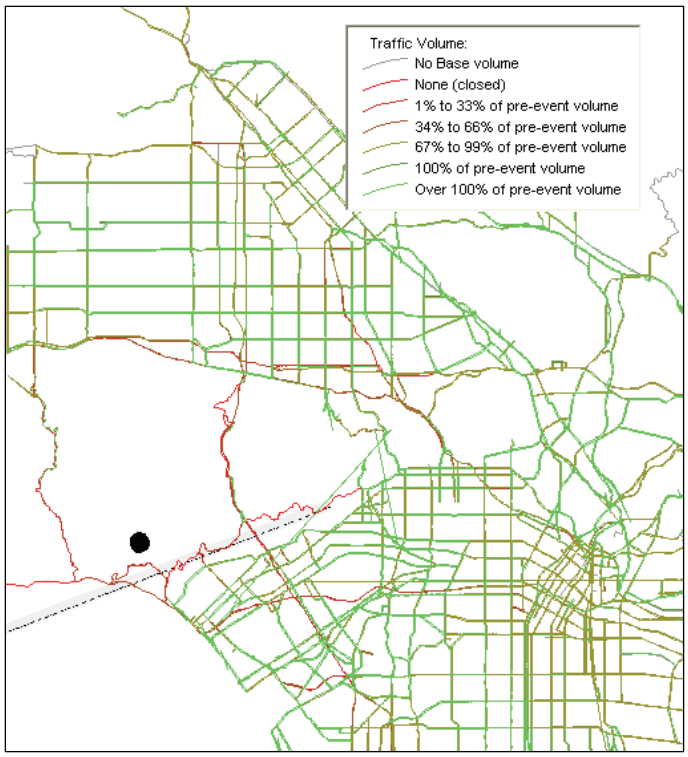

a) 7-Days after Earthquake

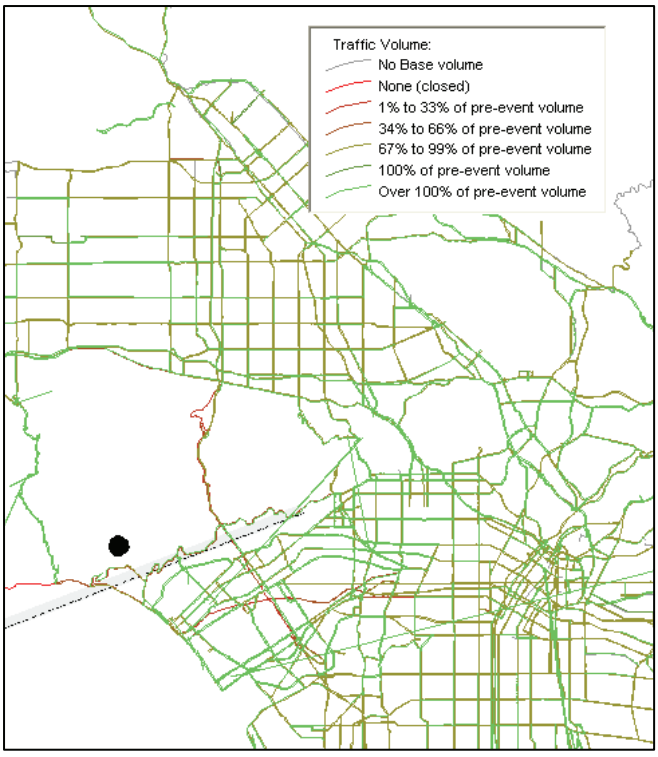

b) 60-Days after Earthquake

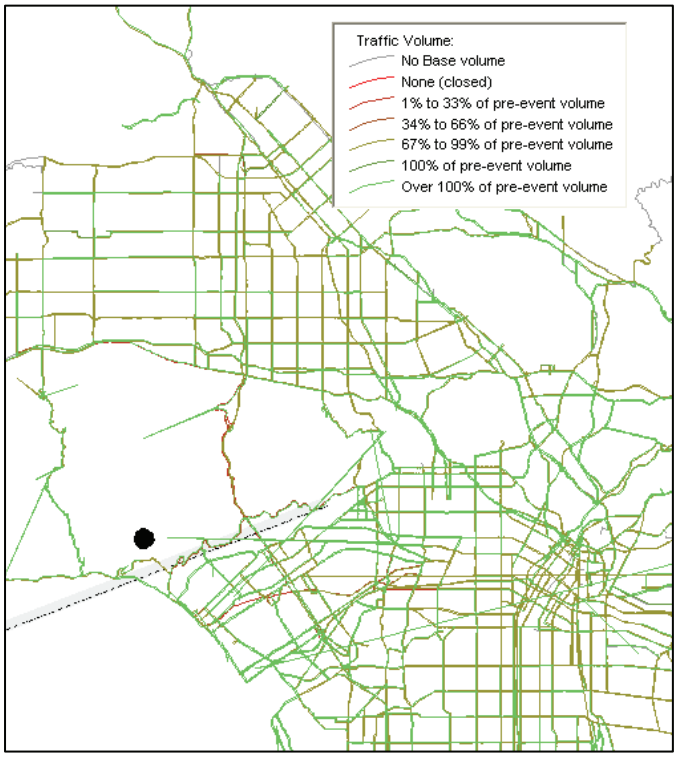

c) 150-Days after Earthquake

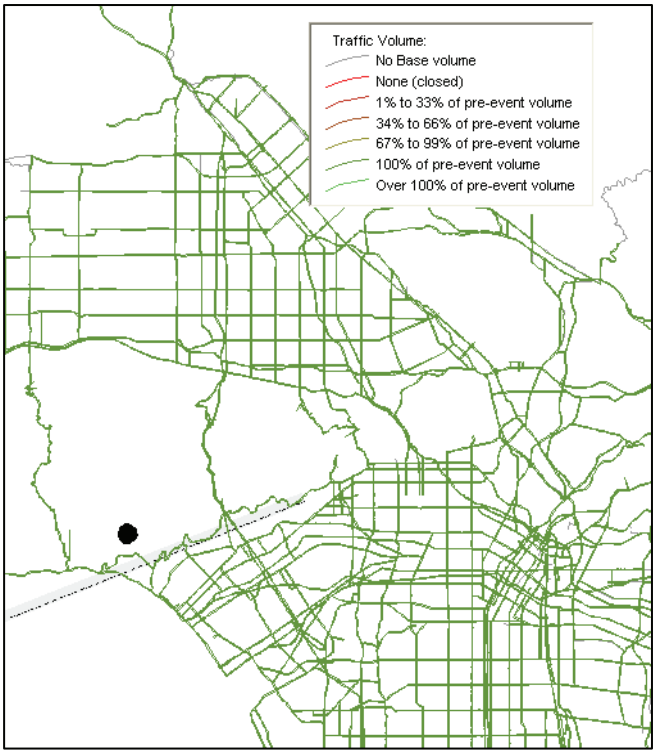

d) 221-Days after Earthquake

Figure 7-12. Post-Earthquake Traffic Volumes (as percentage of Pre-Earthquake Volumes)

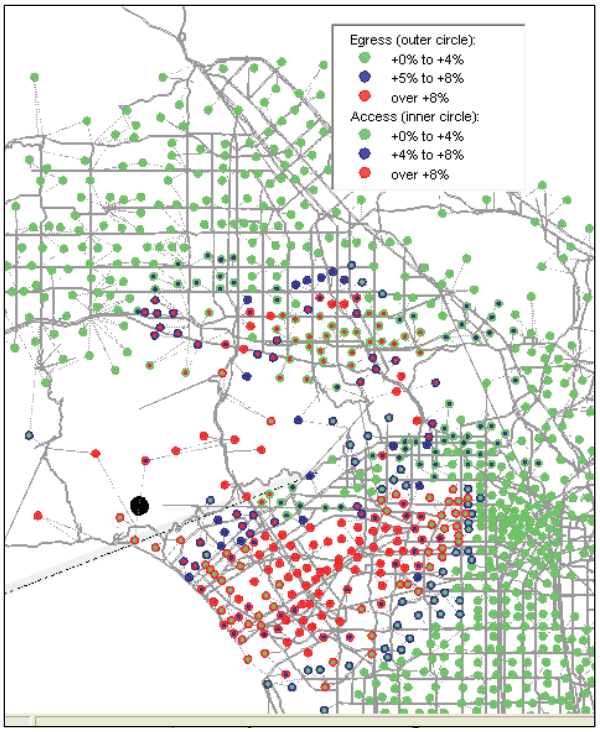

a) 7-Days after Earthquake

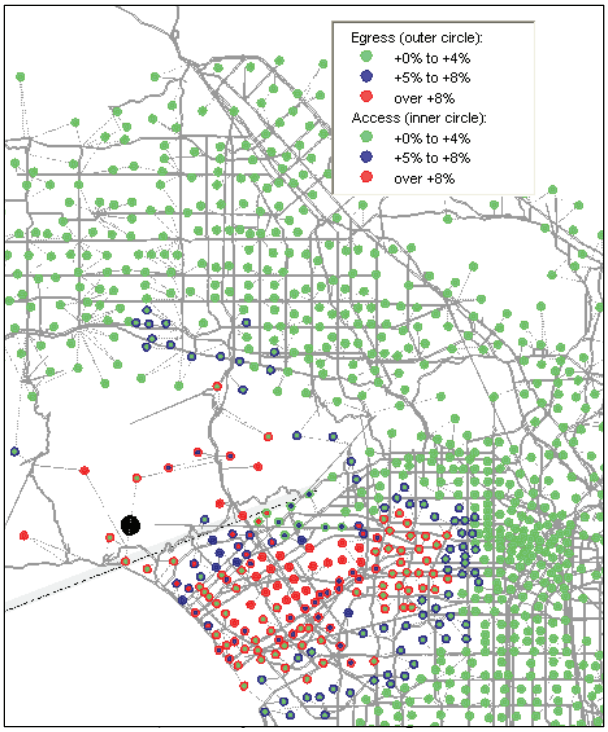

b) 60-Days after Earthquake

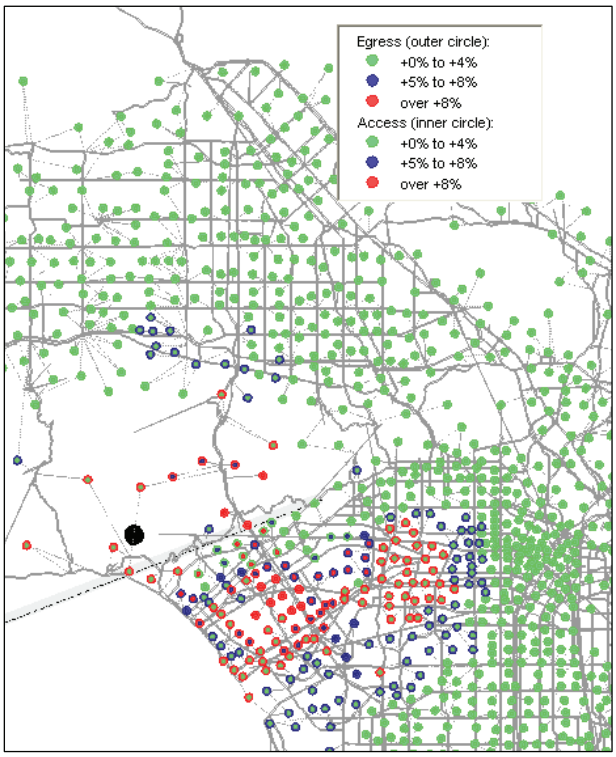

c) 150-Days after Earthquake

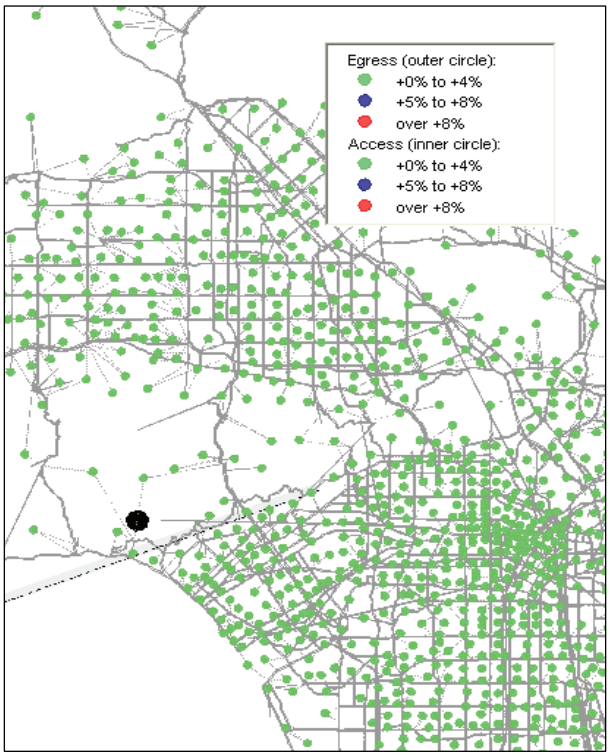

d) 221-Days after Earthquake

Figure 7-13. Post-Earthquake Travel-Time Increases for Automobile Trips (as percentage of Pre-Earthquake Travel Times)

- ***System-Wide Post-Earthquake Trip Demands (Fig. 7-14).*** This set of maps shows how automobile- and freight-trip demands on the LA-testbed highway system are affected by earthquake damage to the system. Figure 7-14 provides such results for automobile trips. At 7-days after the earthquake, the figure shows that the greatest reductions in automobile trip demands occur in the Santa-Monica and the western- and central-LA areas, and also in the southern part of the San Fernando Valley. At subsequent post-earthquake times, these trip demands steadily increase until, at 221-days after the earthquake, they reach their pre-earthquake levels.

In addition to the above maps of system-wide traffic impacts, REDARS™ 2 provides additional detailed data on travel times and trip demands to/from user-designated key locations and along user-designated key routes. Tables 7-4, 7-5, and 7-6 show how the earthquake damage affects travel times and trips to/from the various locations shown in Figure 7-5, as well as travel times along the particular routes shown in Figure 7-6. Such data can be helpful for emergency-response planning. These tables also show the spatial distribution and extents of the traffic impacts throughout the highway system and, in this way, supplement the information provided in Figures 7-12 through 7-14. The following paragraphs provide an example of how these data can be interpreted in order to gain insights into post-earthquake traffic-impact patterns.

- Tables 7-4 and 7-5 show that this scenario earthquake has the greatest impacts on travel times and trips to/from the Santa Monica, UCLA-Westwood, Encino, and North Hollywood TAZs. These large traffic impacts for the Santa Monica and UCLA-Westwood TAZs would be anticipated, since these are the designated TAZs from Figure 7-5 that are closest to the most severely damaged segments of the I-10 and I-405 freeways.

- However, the rather large travel-time and trip impacts for the Encino and North Hollywood TAZs are less intuitive in view of their greater distance from the severely damaged sections of the highway system. Therefore, it is necessary to further examine the data from Tables 7-4 to 7-6 in order to better understand the possible causes of these large impacts.

- For example, Table 7-6 contains earthquake-induced travel-time impacts for user-designated routes in the system. These data show major travel-time increases, not only for the damaged segments of the I-10 and I-405 freeways that are closest to the Santa Monica and UCLA-Westwood TAZs, but also for the I-101 freeway.

- From this, the following rationale for the above traffic impacts for the Encino and North Hollywood TAZs can be hypothesized: (a) the I-101 freeway parallels the I-10 freeway as a major route into the downtown-LA commercial center, and both of these freeways are heavily traveled; (b) thus, because of the severe damage along the I-10 freeway, many travelers that would ordinarily use that freeway as a route to downtown LA would instead use the I-101 freeway as an alternative route; and (c) because the I-101 freeway was already congested before the earthquake, the additional travelers now taking that route will cause all of the users of I-101 to experience markedly increased travel time delays; and (d) because of this increased congestion along I-101, travelers who previously used that freeway might instead opt to use major arterials or other alternative routes to downtown LA, resulting in a net decrease in the number of trips along I-101 after the earthquake.

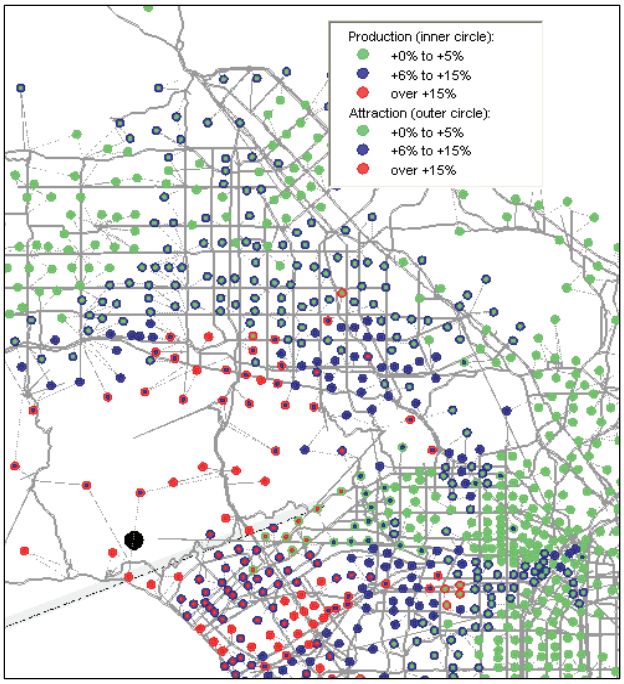

a) 7-Days after Earthquake

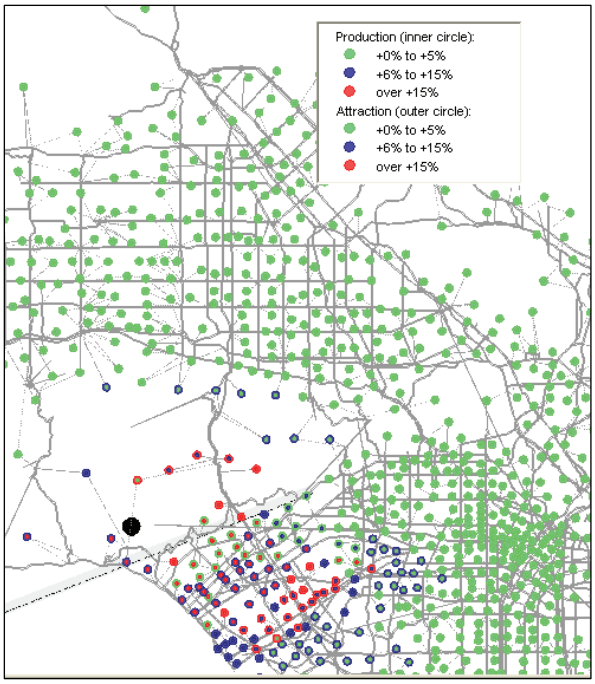

b) 60-Days after Earthquake

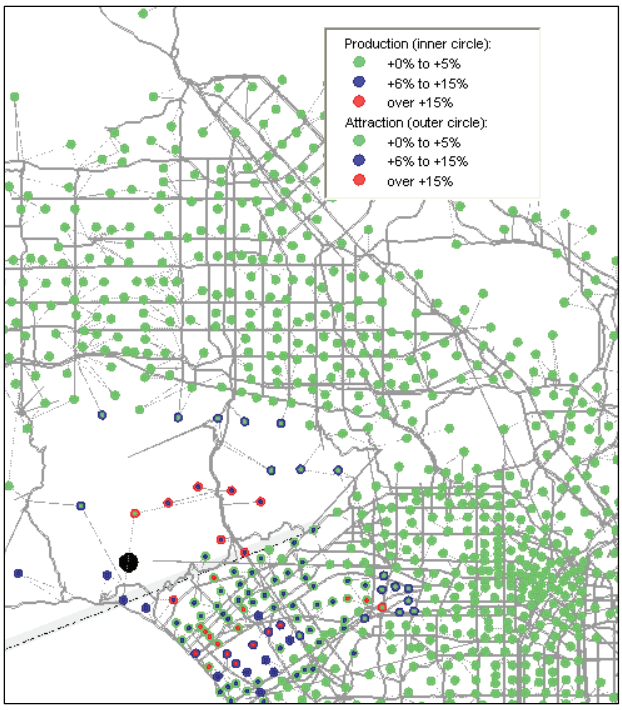

c) 150-Days after Earthquake

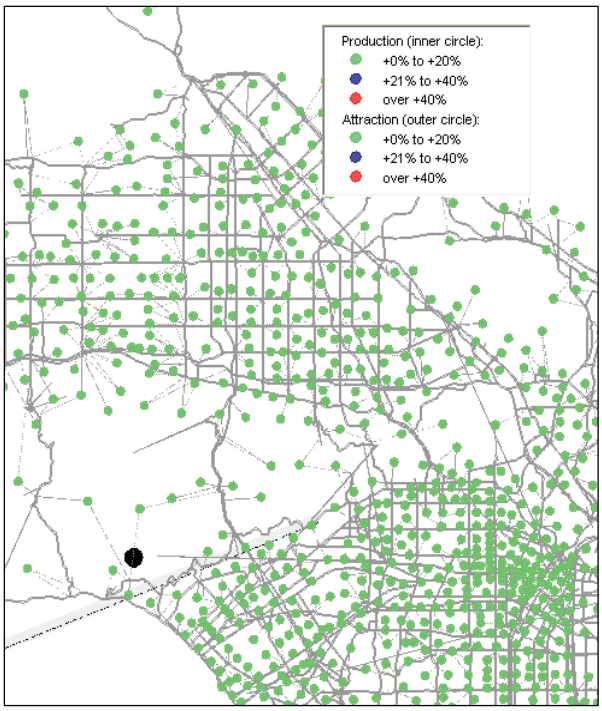

d) 221-Days after Earthquake

Figure 7-14. Post-Earthquake Reductions in Automobile Trips (as percentage of Pre-Earthquake Automobile Trips)

Table 7-4. Post-Earthquake Travels Time Increases for Traffic Analysis Zones shown in Figure 7-5

Traffic Analysis Zone	Post-Earthquake Travel-Time Increases (as percentage of pre-earthquake travel times) *(Note that 0.00% means no change in post-EQ travel time relative to pre-EQ time)*							
	7-Days after EQ		60-Days after EQ		150-Days after EQ		221-Days after EQ	
	Access Time	Egress Time	Access Time	Egress Time	Access Time	Egress Time	Access Time	Egress Time
San Fernando	0.17%	0.00%	0.13%	0.00%	0.13%	0.00%	0.00%	0.00%
Granada Hills	0.24%	0.00%	0.05%	0.00%	0.05%	0.00%	0.00%	0.00%
Chatsworth	1.52%	0.00%	0.51%	0.00%	0.42%	0.00%	0.00%	0.00%
Northridge	1.62%	2.15%	0.25%	0.66%	0.22%	0.66%	0.00%	0.00%
Van Nuys Airport	3.61%	0.00%	0.33%	0.00%	0.33%	0.00%	0.00%	0.00%
Panorama City	0.75%	0.00%	0.05%	0.00%	0.05%	0.00%	0.00%	0.00%
Burbank Airport	4.47%	3.55%	0.18%	0.00%	0.17%	0.00%	0.00%	0.00%
North Hollywood	17.45%	6.88%	0.31%	1.62%	0.31%	1.05%	0.00%	0.00%
Glendale	4.51%	0.00%	1.06%	0.00%	0.90%	0.00%	0.00%	0.00%
Woodland Hills	1.14%	1.37%	1.14%	1.37%	1.14%	1.37%	0.00%	0.00%
Reseda	2.47%	0.91%	0.99%	0.91%	0.93%	0.91%	0.00%	0.00%
Encino	20.12%	4.13%	0.48%	4.13%	0.48%	4.13%	0.00%	0.00%
Santa Monica	0.50%	13.22%	0.50%	8.56%	0.50%	7.27%	0.00%	0.00%
UCLA-Westwood	9.30%	3.56%	9.30%	2.66%	6.38%	2.00%	0.00%	0.00%
Beverly Hills – Wilshire Boulevard	1.47%	4.62%	1.47%	2.23%	1.47%	0.00%	0.00%	0.00%
Downtown LA	0.30%	1.06%	0.30%	1.06%	0.30%	1.06%	0.00%	0.00%
University of Southern CA	0.00%	2.47%	0.00%	2.47%	0.00%	2.47%	0.00%	0.00%
Inglewood	0.10%	3.09%	0.10%	3.09%	0.10%	3.09%	0.00%	0.00%
Los Angeles Airport	1.66%	5.21%	1.66%	5.00%	1.66%	5.00%	0.00%	0.00%

Table 7-5. Post-Earthquake Trips to/from Traffic Analysis Zones shown in Figure 7-5

Traffic Analysis Zone	Post-Earthquake Changes in Trips (as percentage of pre-earthquake trips) *(Note that 0.00% means no change in post-EQ trips relative to pre-EQ trips)*							
	7-Days after EQ		60-Days after EQ		150-Days after EQ		221-Days after EQ	
	From TAZ	To TAZ	From TAZ	To TAZ	From TAZ	To TAZ	From TAZ	To TAZ
San Fernando	-6.10%	-1.58%	-1.63%	0.00%	-1.63%	0.00%	0.00%	0.00%
Granada Hills	-4.87%	-0.84%	-1.07%	0.00%	-1.07%	0.00%	0.00%	0.00%
Chatsworth	-2.95%	-0.82%	-0.67%	0.00%	-0.67%	0.00%	0.00%	0.00%
Northridge	0.00%	0.00%	0.00%	0.00%	0.00%	0.00%	0.00%	0.00%
Van Nuys Airport	-7.94%	-1.25%	-1.86%	0.00%	-1.86%	0.00%	0.00%	0.00%
Panorama City	-6.00%	-1.40%	-0.97%	0.00%	-0.86%	0.00%	0.00%	0.00%
Burbank Airport	-7.88%	-2.76%	-0.95%	0.00%	-0.95%	0.00%	0.00%	0.00%
North Hollywood	-15.76%	-13.23%	-0.70%	-0.10%	-0.70%	-0.06%	0.00%	0.00%
Glendale	-6.46%	-6.48%	-0.62%	-0.44%	-0.62%	-0.31%	0.00%	0.00%
Woodland Hills	-7.63%	-8.50%	-0.46%	0.00%	-0.24%	0.00%	0.00%	0.00%
Reseda	-9.82%	-5.83%	-0.97%	0.00%	-0.74%	0.00%	0.00%	0.00%
Encino	-32.60%	-21.34%	-2.40%	-0.17%	-2.18%	-0.03%	0.00%	0.00%
Santa Monica	-11.02%	-37.96%	-5.39%	-26.08%	-2.90%	-18.44%	0.00%	0.00%
UCLA-Westwood	-6.71%	-30.63%	-5.49%	-12.54%	-0.25%	-4.66%	0.00%	0.00%
Beverly Hills – Wilshire Boulevard	-3.48%	-9.69%	-1.69%	-3.30%	-1.50%	-1.35%	0.00%	0.00%
Downtown LA	-6.69%	-5.80%	-2.11%	-0.77%	-1.14%	-0.56%	0.00%	0.00%
University of Southern CA	-3.50%	-2.61%	-1.00%	-0.49%	-0.17%	-0.33%	0.00%	0.00%
Inglewood	-3.28%	-3.03%	-0.47%	-1.53%	0.00%	-1.04%	0.00%	0.00%
Los Angeles Airport	-6.72%	-1.97%	-1.03%	-1.72%	-1.03%	-1.72%	0.00%	0.00%

Table 7-6. Post-Earthquake Travel Times along Key Routes shown in Figure 7-6

Key Route	Post-Earthquake Travel-Time Increases (as percentage of pre-earthquake travel times)			
	7-Days after EQ	60-Days after EQ	150-Days after EQ	221-Days after EQ
(a) I-5 (Golden State Freeway) from San Fernando to Burbank (pre-EQ travel time = 13.1 minutes)	16.30%	1.41%	0.88%	0.00%
(b) I-5 (Golden State Freeway) from Burbank to downtown LA (pre-EQ travel time = 13.9 minutes)	2.31%	1.67%	1.96%	0.00%
(c) I-405 (San Diego Freeway) from I-5 to I-10 Interchange (pre-EQ travel time = 37.0 minutes)	125.60%	34.61%	34.38%	0.00%
(d) I-405 (San Diego Freeway) from I-10 Interchange to LA Airport (pre-EQ travel time = 19.0 minutes)	134.00%	63.56%	3.04%	0.00%
(e) I-10 (Santa Monica Freeway) from Santa Monica to downtown LA (pre-EQ travel time = 18.1 minutes)	209.73%	91.37%	37.57%	0.00%
(f) I-110 (Harbor Freeway) from I-105 to downtown LA (pre-EQ travel time = 9.7 minutes)	-0.38%	-1.59%	-2.56%	0.00%
(g) I-101 (Ventura/Hollywood Freeway) from I-405 to downtown LA (pre-EQ travel time = 30.5 minutes)	108.35%	1.18%	0.89%	0.00%

7.3.6 ECONOMIC LOSSES

The REDARS™ 2 estimates of economic losses due to the earthquake damage to the LA-testbed highway system include repair costs, and losses due to travel-time delays and trips foregone. The repair costs are estimated by applying the default bridge, approach-fill, pavement, and tunnel models that are described in Appendices G and H of this report.

The losses due to travel-time delays and trips foregone will depend on the post-earthquake traffic impacts estimated by the REDARS™ 2 network analysis procedure that is described in Chapter 5 and Appendix I. These traffic impacts are computed for each of the four post-earthquake times that are input by the user. Therefore, the losses due to travel-time delays and trips foregone are estimated as dollar losses per day at each post-earthquake time. For this analysis, these losses as estimated at times of 7-, 60-, 150-, and 221-days after the earthquake are shown in Table 7-7.

Table 7-7. Economic Losses due to Travel-Time Delays and Trips Foregone

Time after the Earthquake	Loss per Day, Millions of Dollars
0-7 days	$4.90
60 days	$2.89
150 days	$2.11
221 days (system recovery time)	$0.00

a) Loss per day

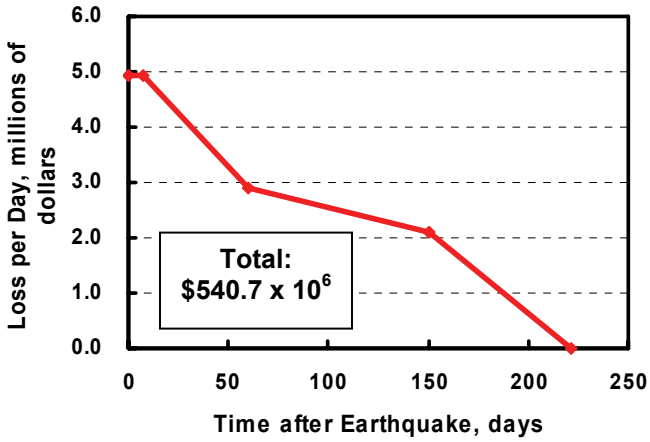

b) Computation of Total Loss from Travel-Time Delays and Trips Foregone

After these losses per day are estimated, they are plotted vs. time after the earthquake, as shown above. Then, the total economic loss due to travel-time delays and trips foregone is computed as the area under the resulting curve of loss/day vs. post-earthquake time. As shown in Table 7-7, this turns out to be $540.7 million-dollars. Finally, this loss is added to the damage repair costs in order to estimate the total economic loss due to this scenario earthquake. These results are shown in Table 7-8. This table shows that the economic loss due to travel-time delays and trips foregone are over twice as large as the repair costs.

Table 7-8. Estimated Total Economic Loss due to this Scenario Earthquake

Type	Loss, Millions of Dollars
Repair Cost	$255.4
Total Loss from Travel-Time Delays and Trips Foregone	$540.7
Total	$796.1

7.4 PROBABILISTIC ANALYSIS

A key feature of the REDARS™ 2 methodology is its ability to carry out probabilistic as well as deterministic analysis of a highway system. These probabilistic analyses can be: (a) conditionally probabilistic (e.g., an analysis for a single fixed earthquake event in which uncertainties in estimating seismic hazards and component damage states are considered); or (b) fully probabilistic (in which uncertainties in earthquake occurrence as well as seismic-hazard and component damage estimates are considered). Appendix K of this report provides an example of a conditional probabilistic application of REDARS™ 2 that was used to calibrate the REDARS™ 2 default bridge model against bridge-damage observations from the Northridge Earthquake.

The remainder of this section focuses on fully probabilistic applications of REDARS™ 2. It contains two parts. The first part describes the various types of probabilistic output that REDARS™ 2 can provide. The last part of this section describes convergence checks that have been built into REDARS™ 2 to enable the user to assess when, at some intermediate number of walkthrough years, the confidence intervals for the results are sufficient to justify termination the probabilistic analysis at that point.

7.4.1 PROBABILISTIC OUTPUT

REDARS 2 provides various types of probabilistic that can be used to characterize the seismic performance of the highway system, the seismic performance of individual components within the system, and seismic hazards at specified locations within the system.

7.4.1.1 Characterization of Seismic Performance of Overall Highway System

REDARS™ 2 provides the following four types of output for use in characterizing the seismic performance of a highway system:

- ***Economic Losses.*** REDARS™ 2 computes economic losses as the sum of the costs/losses due to the following effects of earthquake-induced damage to the highway system: (a) costs to repair the damaged highway-roadway infrastructure (e.g., App. C and D); (b) consequences of system-wide travel-time delays caused be earthquake damage to the system (Chap. 6); and (c) effects of trips foregone due to increased congestion caused this earthquake damage. Figure 7-15 shows probabilistic estimates of economic losses developed during this LA-area demonstration application. Subsection 7.4.2 illustrates how these probabilistic results can be used in benefit-cost assessments of alternative seismic-risk-reduction strategies.

- ***Travel Times to Key Locations.*** In addition to economic losses, other measures of the seismic performance of the highway system may be relevant. One such measure is how travel times to key locations (such as medical centers, airports, etc.) may be affected by earthquake damage to the system. For example, Figure 7-16 provides probabilistic estimates of travel times to the UCLA-Westwood area of LA, where a major medical center is located, and in addition, is the site of a large university and a center of commerce.

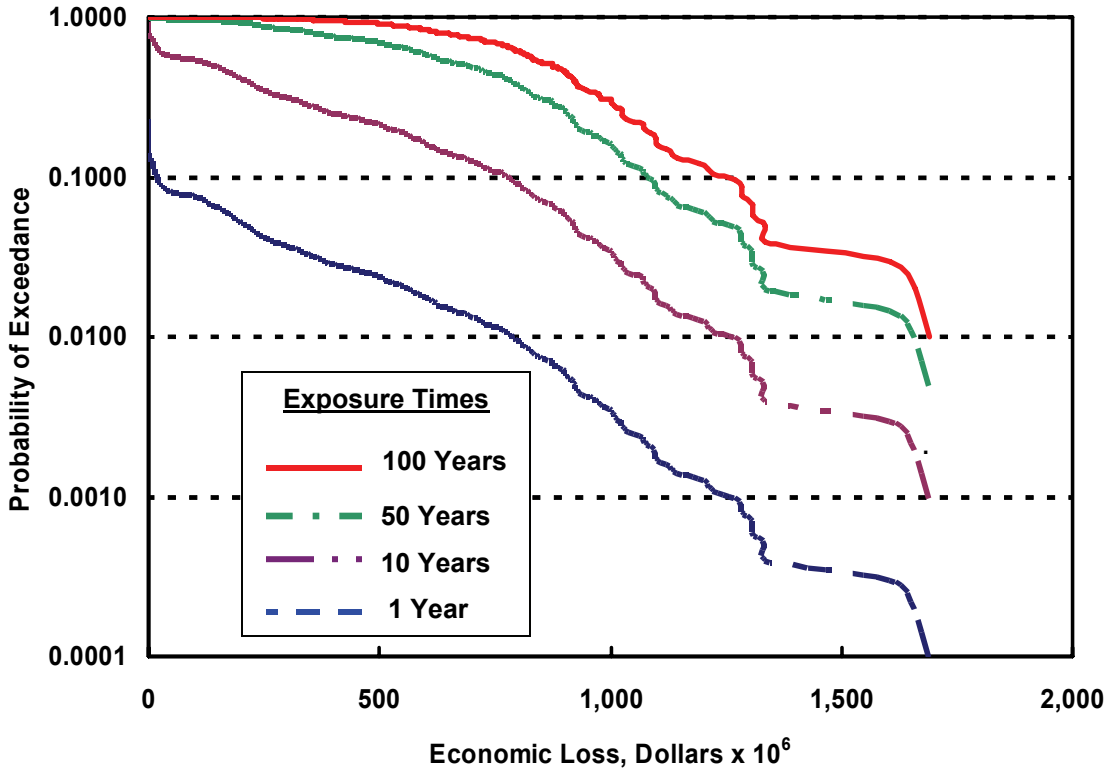

Figure 7-15. Economic Losses

- ***Travel Times along Key Routes.*** Certain routes in an earthquake-prone region may be designated as "lifeline routes", which means they must remain functional to carry emergency traffic after an earthquake. In addition, certain routes will be important for travel to/from a key location after an earthquake. Figure 7-17 displays probabilistic estimates of travel time delays along I-405 between I-10 and I-105 (route (d) in Fig. 7-6), which is an important link to/from the LA International Airport.[6]

- ***Trips to/from Key Locations***. Another possible impact of earthquake damage to a highway system is its effect on trips to/from key locations in a region. For example, if trips to a major center of commerce are substantially reduced, this could be an indicator of possible losses of customers (and revenues) to merchants in that area. Also, if trips from a center of manufacturing that provides machinery or equipment to businesses in the region (or beyond the region), this could represent losses of revenue not only to the manufacturers, but also to the businesses that depend on shipments from these manufacturers. Figure 7-18 displays probabilistic estimates of reductions in trips to downtown LA.

[6] Figure 7-17 shows that, in some cases, there may a slightly negative increase in travel times along these routes (which is actually a travel-time decrease). This can occur when effects of reductions in trips along the route exceed the effects of travel-time increases due to actual damage to the segment. For example, reductions in these trip demands along I-405 to the south of I-10 could be related to the damage to I-405 to the north (Sunset Boulevard and I-10 area).

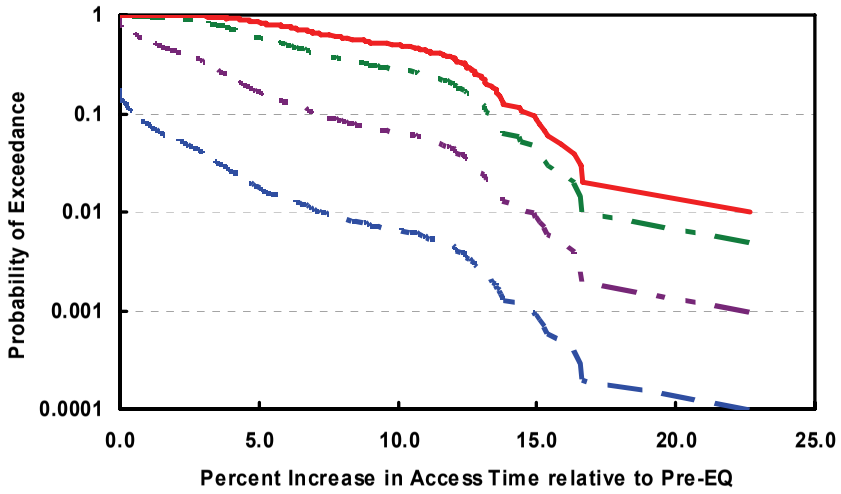

a) Time after EQ = 7-Days

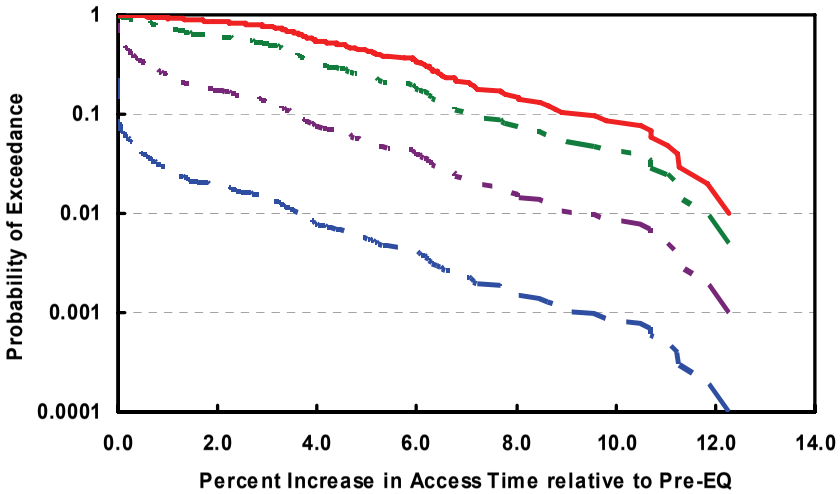

b) Time after EQ = 60-Days

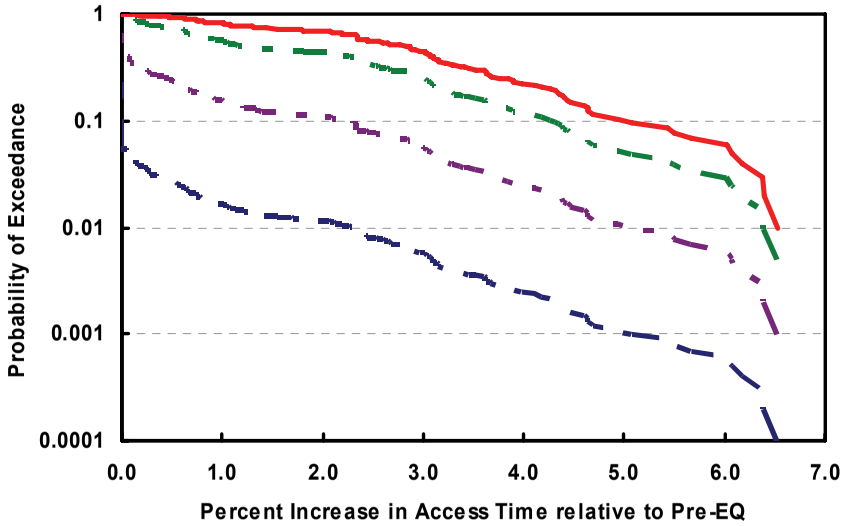

c) Time after EQ = 150-Days

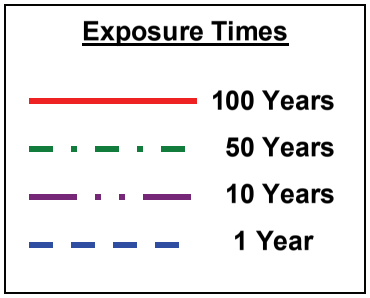

Note: At 221-days after EQ, system returns to pre-EQ state (percent increase in travel time = 0.0)

Figure 7-16. Percent Increase in Access Times to UCLA Medical Center

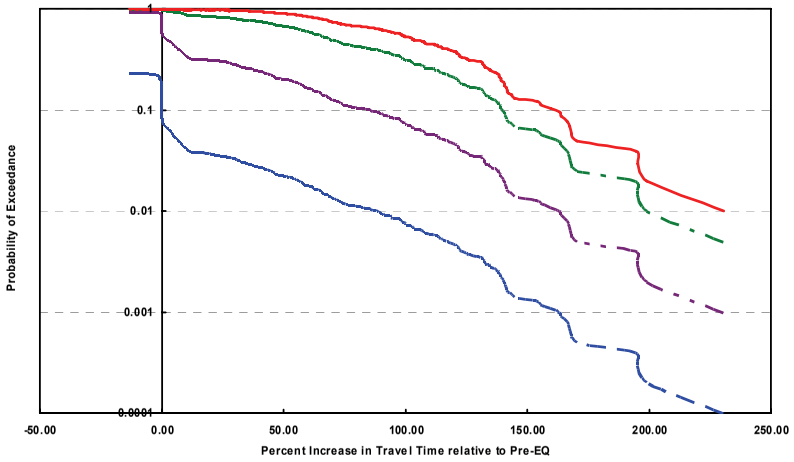

a) Time after EQ = 7-Days

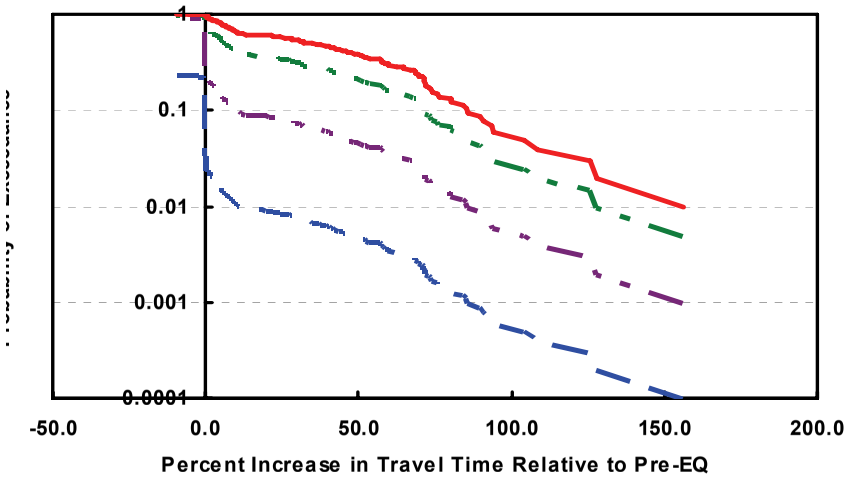

b) Time after EQ = 60-Days

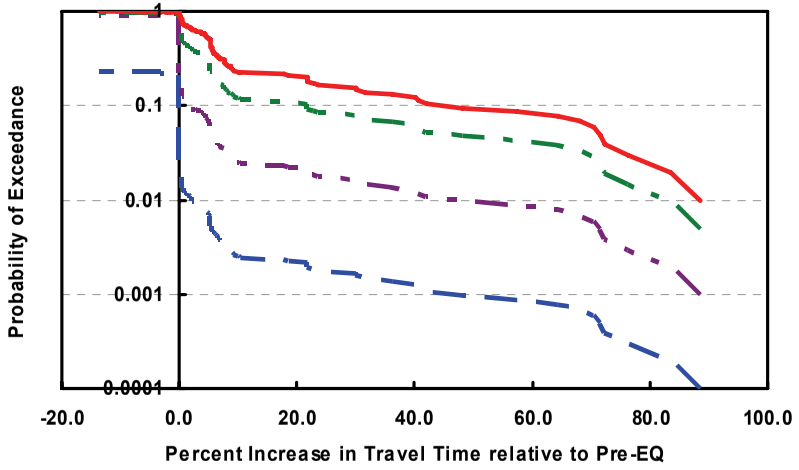

c) Time after EQ = 150-Days

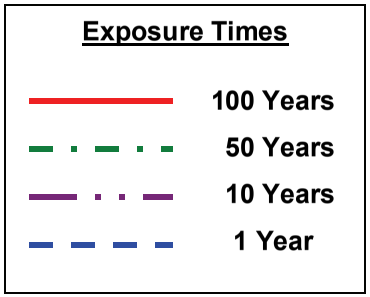

Note: At 221-days after EQ, system returns to pre-EQ state (percent increase in travel time = 0.0)

Figure 7-17. Percent Increase in Travel Time along I-405 between I-10 and I-105 (Key Route to LA International Airport)

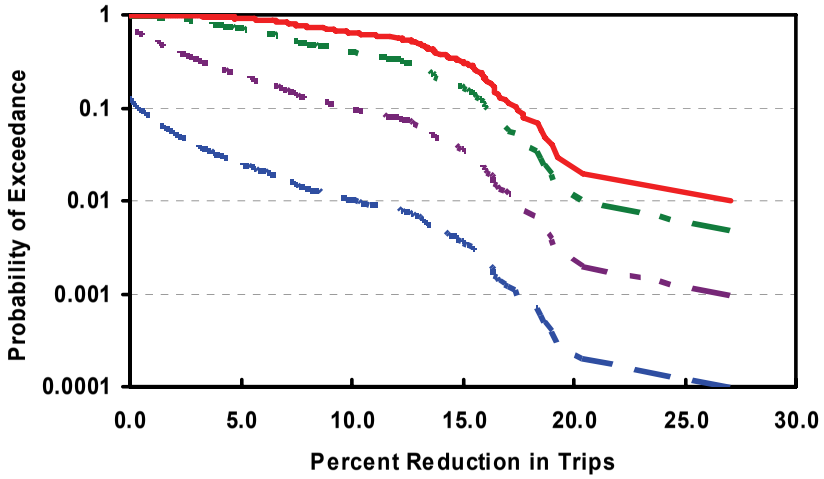

a) Time after EQ = 7-Days

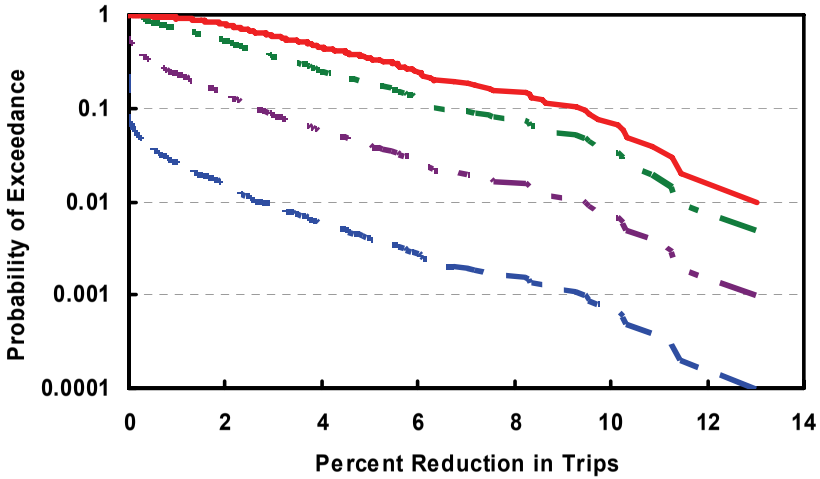

b) Time after EQ = 60-Days

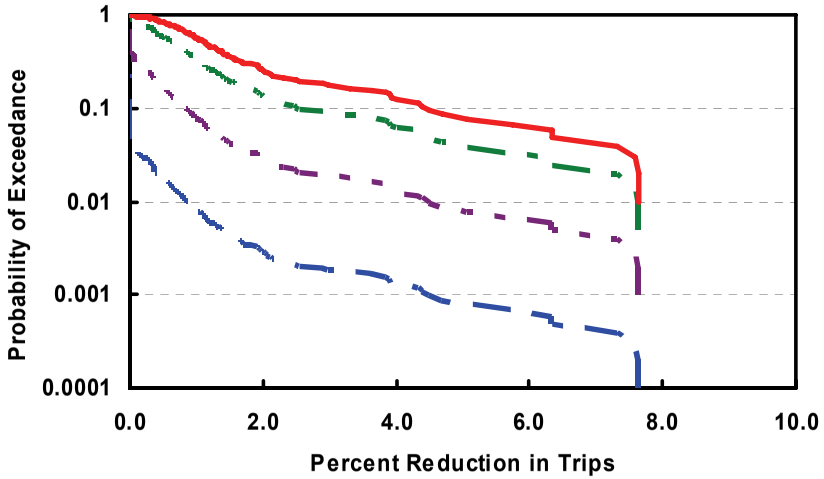

c) Time after EQ = 150-Days

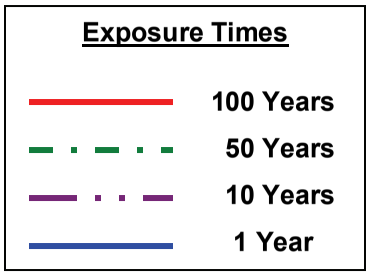

Note: At 221-days after EQ, system returns to pre-EQ state (percent reduction in trips = 0.0)

Figure 7-18. Percent Reduction in Trips to Downtown LA

In closing, the preceding figures illustrate that REDARS™ 2 results can to enable users to more directly consider a broad range of highway-system performance measures that could relate to economic losses to the surrounding region. For example, such considerations could be an impetus for the future development of region-specific criteria for performance-based design of new components along a highway system (e.g., Buckle 2003). They could also be important for assessing various options for seismic-risk reduction of existing components (e.g., see Sec. 7.5). Further development of such methods to consider system-performance measures in seismic-risk-reduction planning and criteria will be addressed in future projects that focus on the continued upgrading and development of the REDARS™ SRA methodology and software.

7.4.1.2 Characterization of Seismic Performance of Individual Components of Highway System

For highway system components, REDARS™ 2 can provide probabilities that a given component will be in the minor, moderate, extensive, and collapse damage states, as defined in Chapter 4. These probabilistic representations of component damageability incorporate effects of uncertainties in earthquake occurrence, and in the estimation of site-specific seismic hazards and component damage states. Therefore, this provides a much more complete picture of the vulnerability of a component than do more conventional component vulnerability representations in which effects of these uncertainties are not considered.

Figure 7-19 illustrates one type of display of system-wide component-damage probabilities -- which is in the form of a map of the LA-testbed highway system that shows the each bridge's probability of collapse. This display of bridge-collapse probabilities can be useful during overall planning of bridge seismic-upgrade programs, by identifying those bridges within the highway system that are most vulnerable. Use of this information, along with REDARS™ SRA results that indicate each bridge's importance to overall system-wide traffic flows, provides an improved basis for establishing bridge-retrofit priorities.[7]

Figures 7-20 and 7-21 show how REDARS™ 2 can also display bridge-damage probabilities for a single bridge in the system. Both figures contain bar charts that show probabilities that a given bridge will be in each of the discrete damage states that is currently considered in REDARS™ 2 (i.e., the minor, moderate, major, and collapse damage states). Figure 7-20 provides side-by-side bar charts for two different bridges in the LA-testbed system with differing levels of vulnerability. Such side-by-side comparisons of bar charts for different bridges clearly show at a glance the relative vulnerabilities of various bridges in the highway system.

These bar charts can also be used to assess effects of seismic retrofit of a given bridge. Figure 7-21 provide such results for a single bridge in the LA-area highway system that has been retrofitted, which clearly show the benefit of this retrofit in substantially reducing the probability of collapse.

[7] REDARS™ 2 is not yet able to provide system-wide bridge-collapse probability maps of the type shown in Figure 7-19. However, this inclusion of such maps will be a high priority task in the next set of future enhancements of REDARS™ that are now being planned.

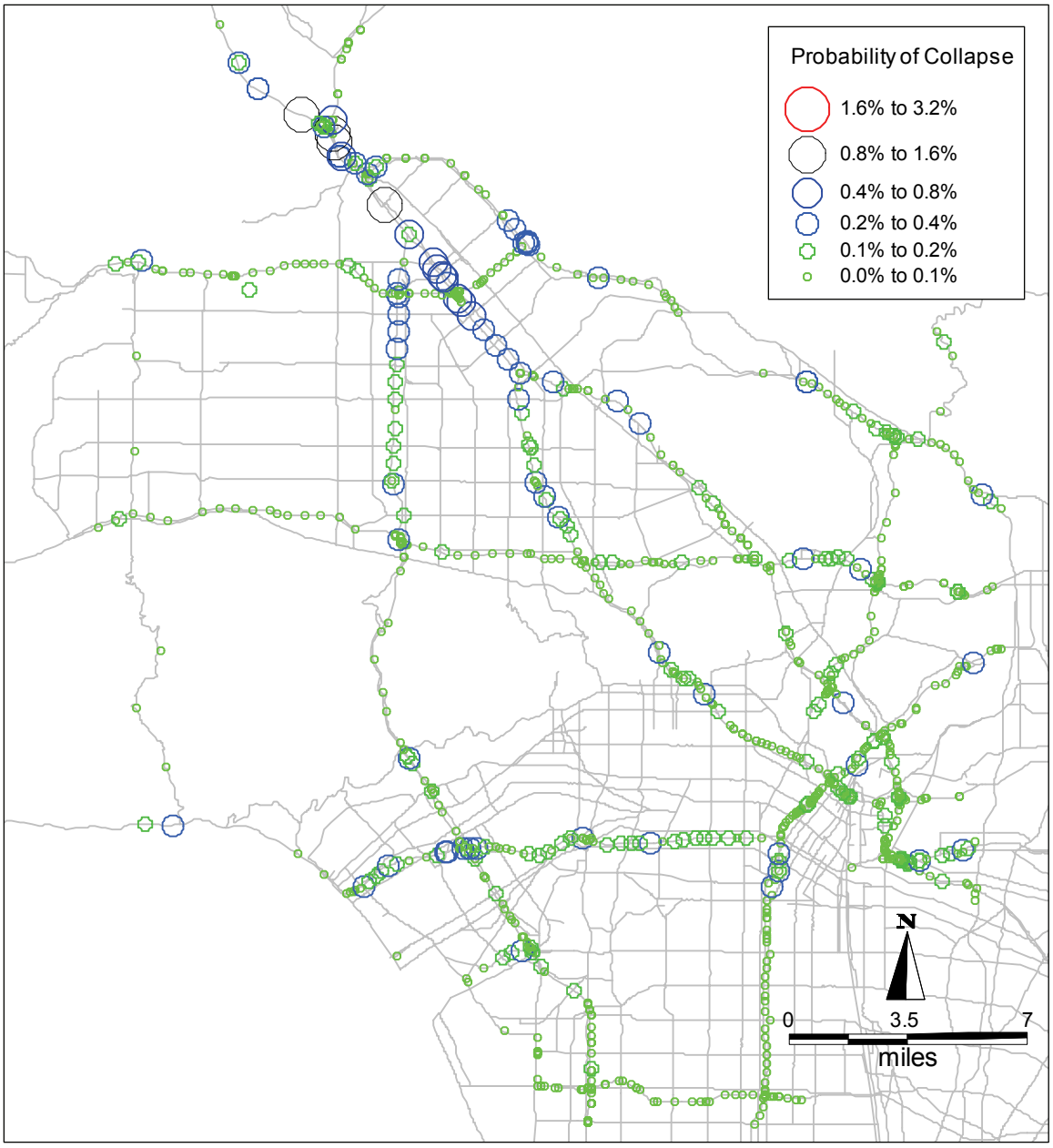

Figure 7-19. LA-Area Highway System Map showing Those Bridges with the Highest Probability of Collapse

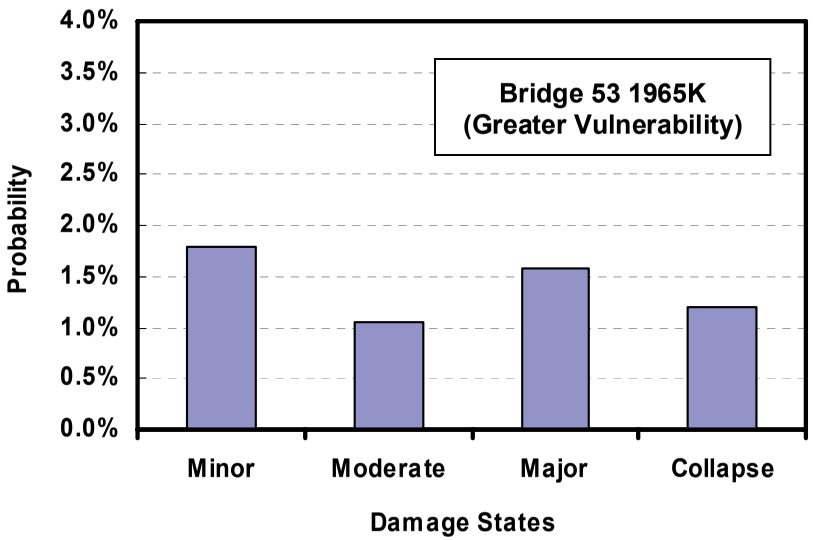

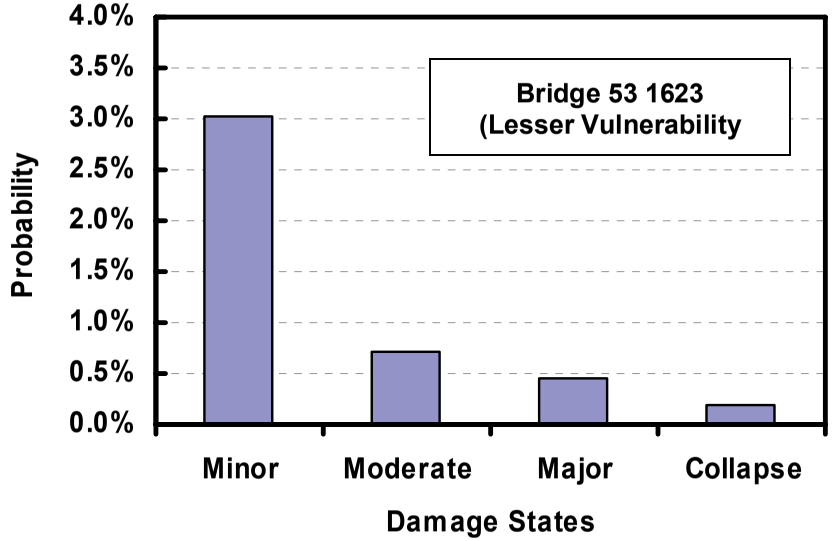

Figure 7-20. Probability Bar Charts for Bridges with Different Degrees of Vulnerability

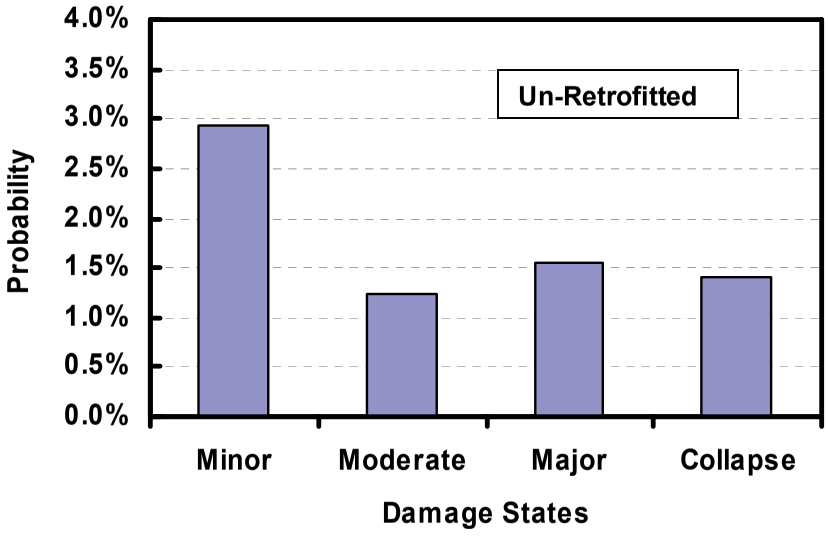

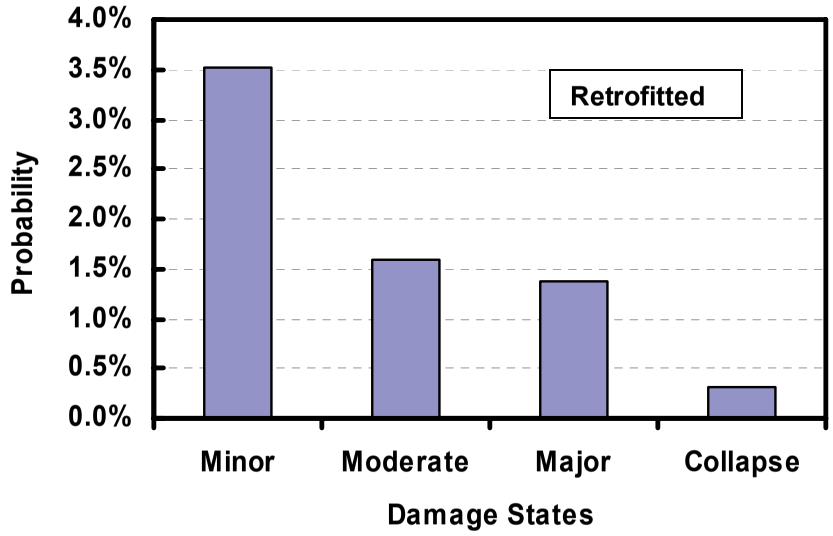

Figure 7-21. Probability Bar Charts for Unretrofitted and Retrofitted Bridge 53 1984L

7.4.1.3 Characterization of Uncertainties in Ground Motions

REDARS™ 2 can develop probabilistic estimates of the intensity of the ground motions at any site in the system, where ground motions are characterized in terms of peak ground acceleration or spectral accelerations at periods of 0.3 sec. or 1.0 sec. These estimates are provided as plots of probability of exceedance vs. ground-motion level at four different user-specified exposure times. Figure 7-22 provides an example set of probability estimates for spectral accelerations at a period of 1.0 sec. at Bridge 53-1318 in this testbed roadway system.

As the number of simulations increases, these probabilistic ground-motion estimates from REDARS™ 2 will tend to converge to estimates developed from conventional seismic-hazard-analysis methods that use the same ground-motion attenuation model and earthquake model as in the REDARS™ 2 analysis. Thus, a user can check any set of REDARS™ 2 probabilistic ground-motions estimates by performing an independent seismic-hazard-analysis with the same models.

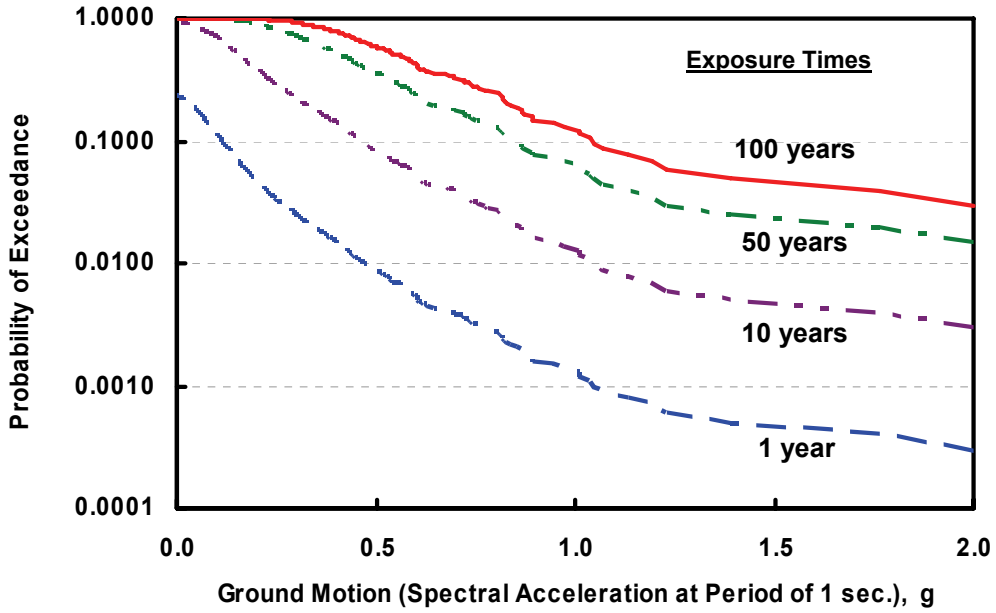

Figure 7-22. REDARS™ 2 Probabilistic Ground Motion Estimates at Bridge 53 1318 in LA-Testbed Highway System

7.4.2 CONVERGENCE CHECKS

7.4.2.1 Background

As described in Chapter 2, the REDARS™ 2 SRA methodology and software use a Monte Carlo process to develop statistically sound probabilistic SRA results. REDARS™ also includes a check of statistical confidence intervals in the AAL results as the analysis proceeds through successive damaging earthquake scenarios contained in the walkthrough table. If the REDARS™ 2 user judges that an acceptable confidence interval has been achieved after some intermediate

number of damaging earthquake scenarios has been considered, he/she can terminate the SRA at that stage of the analysis. This could result in significant reductions in the computer time needed to carry out the SRA, relative to the time that would be needed if SRA results were developed for all of the damaging earthquakes contained in the walkthrough table. To facilitate this check of convergence intervals, an advanced and efficient statistical analysis procedure – named the variance-reduction method – has been developed under this project and programmed into REDARS™ 2. This method is described in Appendix J.

The probabilistic SRA of the LA-testbed highway system that is described in Section 7.4 was carried out for all of the 2,645 damaging earthquakes that occurred throughout the overall 10,000-year duration of the earthquake walkthrough table (see Section 7.2.6). When the analysis was completed for each successive earthquake, updated confidence intervals were computed and stored. Section 7.4.2.2 shows how these confidence intervals converged as the analysis proceeded through each year of the walkthrough table.

7.4.2.2 Results

This convergence check estimated 95-percent confidence intervals. That is, these confidence intervals are represented by the term X, in the following statement: "there is a 95-percent confidence that the computed value of the AAL is within ±X-percent of the true value."

Two forms of results were developed in this convergence check. The first, which is shown in Figure 7-23a, is in the form of a "funnel test" which visually shows how the confidence interval about the computed and "true" values of the AAL improve as the number of walkthrough years increases. In this, the "true" value of the AAL was assumed to correspond to the value that resulted when the entire 10,000 year walkthrough was completed.

The second set of results, which are provided in Figure 7-23b, show the actual value of the 95-percent confidence interval, as a function of the number of walkthrough years processed. These results show that, if only about 2,500 of the 10,000 walkthrough years is considered, the 95-percent confidence interval is less than 10 percent. For most situations, this would be acceptable, and if the AAL is to be the basis for checking the confidence intervals in the REDARS™ 2 results, the SRA could be terminated at that time. This would result in a substantial reduction in the computer time needed to carry out this SRA.

However, it is noted that parameters other than or in addition to the AAL may be relevant to the user and, if so, confidence intervals in these results will differ from those developed here for the AAL. For example, if fractile values of the economic losses are relevant, a larger number of walkthrough years would need to be considered in order to obtain a given confidence interval. The development of confidence intervals for such other parameters will be addressed under future projects that further develop and upgrade the REDARS™ SRA methodology and software (see Chapter 8)

.

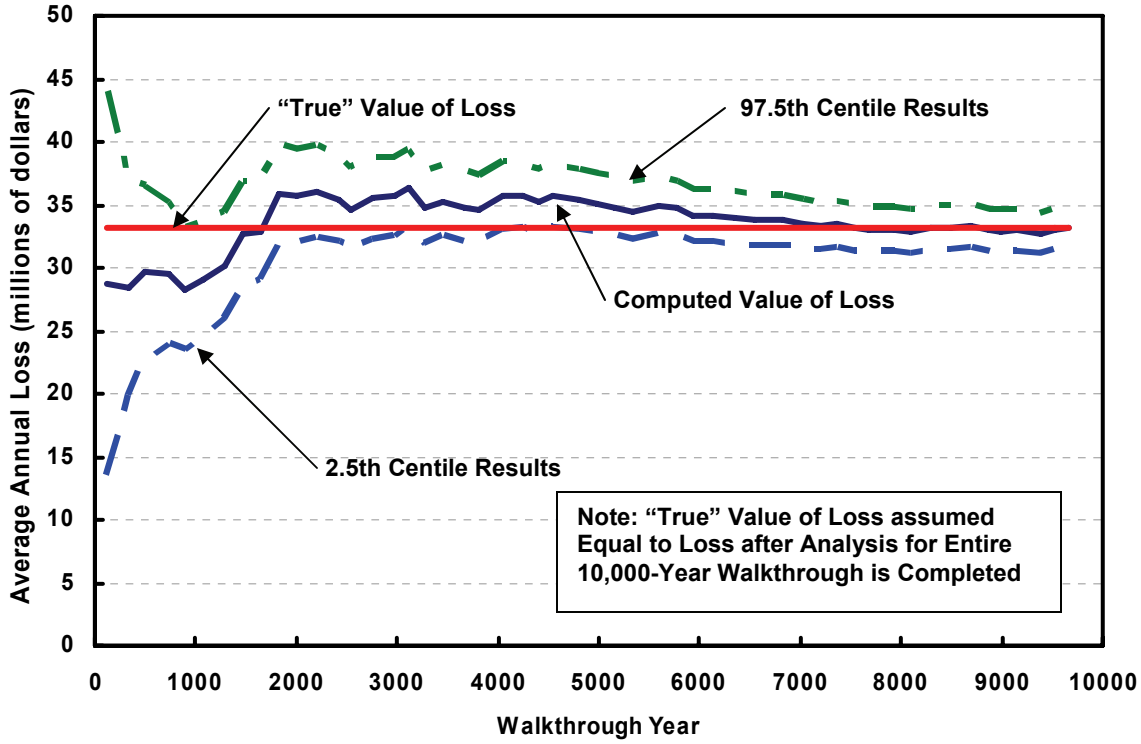

a) Funnel Test

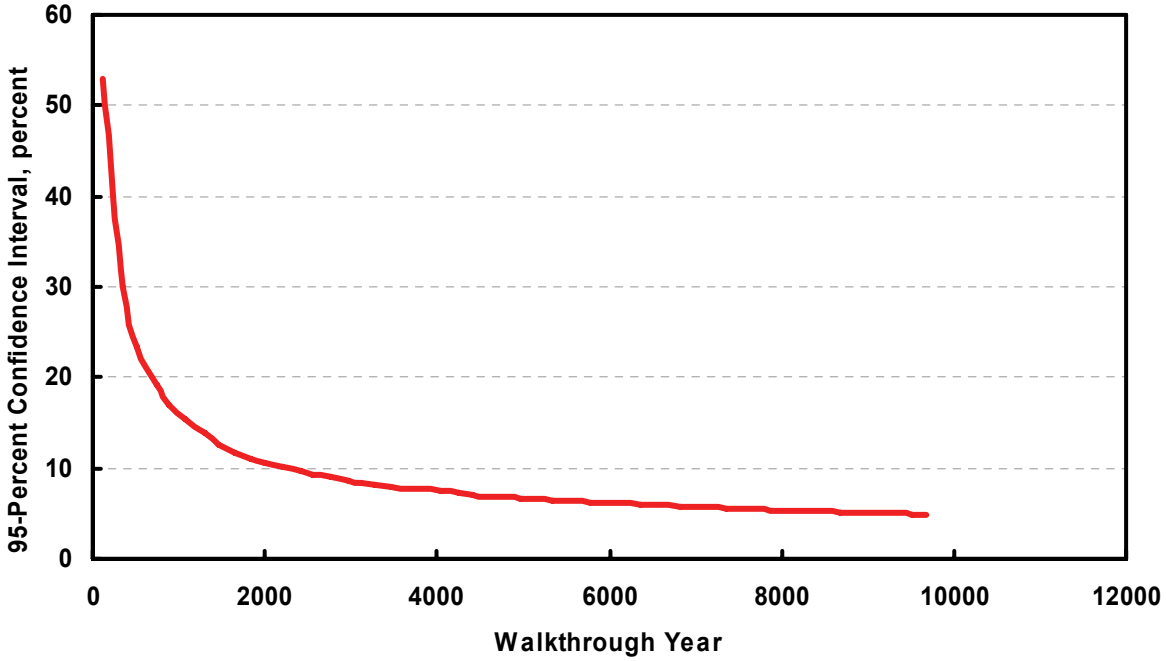

b) 95-Percent Confidence Interval vs. Number of Walkthrough Years Considered

Figure 7-23. Confidence Intervals for Results of Probabilistic SRA of LA-Testbed System

7.5 EXAMPLE ECONOMIC ANALYSIS OF A BRIDGE RETROFIT PROGRAM

7.5.1 BACKGROUND

This section provides an example application of REDARS™ 2 that shows how its probabilistic estimates of economic losses (Sec. 7.4.1.1) can facilitate seismic-risk-reduction decision making. In this example, these probabilistic loss estimates are used in an evaluation of the economic viability of a series of actual bridge seismic retrofits in the grater LA area that have been completed, as part of a major bridge-retrofit program that has been carried out throughout much of the state of California.

This economic analysis considers only those bridges that are located in the LA-testbed highway system and, in addition, only those bridge retrofits that have been carried out within this system since the 1994 Northridge Earthquake and up to the end of 2004. Within this system, 57 bridges had been column jacketed prior to this earthquake. After the Northridge Earthquake, and through the end of 2004, an additional 231 bridges within the testbed system were column jacketed -- resulting in a total of 288 column-jacketed bridges in the system as of the end of 2004 (Yashinsky 2005). Figure 7-24 shows the locations of the retrofitted bridges throughout the LA-testbed system, before and after these additional 231 bridge retrofits were completed, and Figure 7-25 provides probabilistic estimates of bridge collapses throughout the highway system with and without the additional bridge retrofits. This figure shows how these retrofits have reduced the estimated probabilities of bridge collapse throughout this system

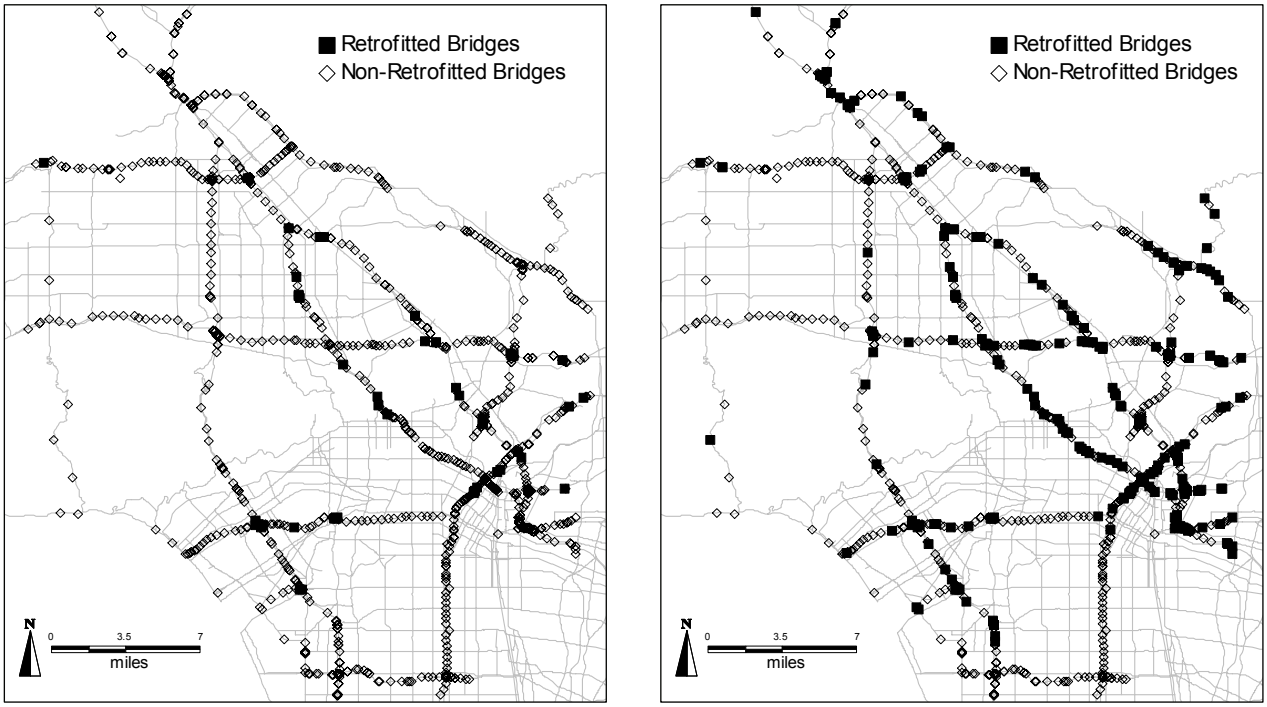

a) System Prior to Northridge Earthquake (early 1994)

b) System as of End of 2004

Figure 7-24. Column-Jacketed Bridges in LA Testbed Highway System

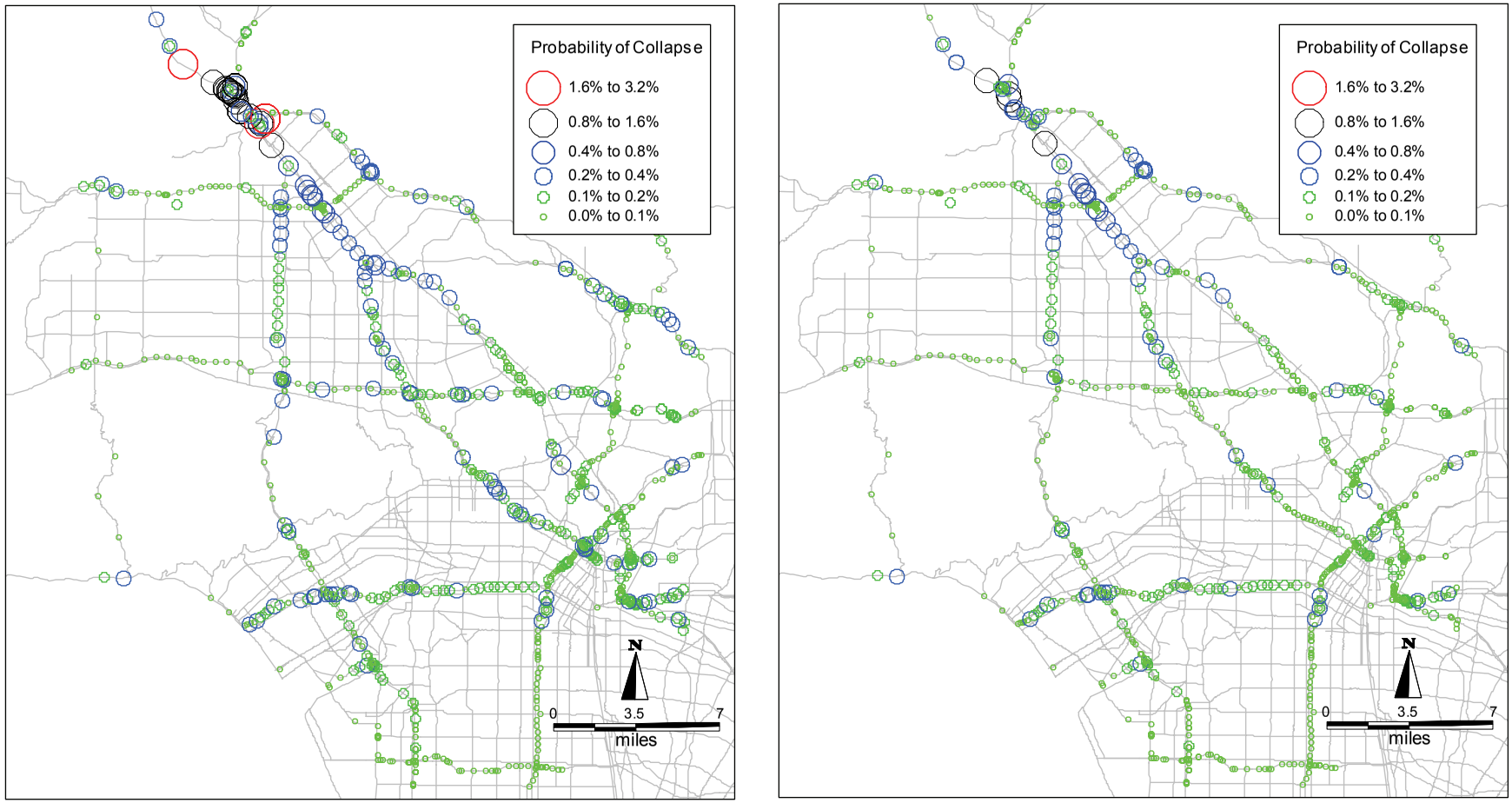

a) As of Early 1994, shortly after Northridge Earthquake

b) As of end of 2004

Figure 7-25. Maps showing Probabilities of Collapse of Bridges throughout LA Testbed Highway System

7.5.2 SUPPOSITIONS

This example analysis examines the economic viability of carrying out these additional 231 bridge retrofits. It is based on the following suppositions.

- It is the year 1994 just after the Northridge Earthquake, when only 57 of the bridges in the testbed system had been column-jacketed. Following this earthquake, a program to column-jacket an additional 231 bridges in the LA-testbed system has been proposed.
- Members of Caltrans' staff have been asked to assess the economic viability of this proposal, and specifically how much these 231 bridge retrofits might reduce economic losses due to earthquake-induced damage and resulting losses due to increased traffic congestion of this testbed system.
- REDARS™ 2 was available at that time, and was to be used to support this assessment.
- The staff used the economic analysis procedure described in the remainder of this section.

7.5.3 ANALYSIS APPROACH

This economic analysis consisted of: (a) estimation of the costs to carry out the column-jacketing retrofit of these 231 bridges; (b) estimation of the benefits of these retrofits, in reducing losses due to earthquake damage to the testbed highway system, with and without the 231 bridge retrofits; and (c) estimation of the standard deviation of these losses, also with and without the 231 retrofits. These steps are described below.

7.5.3.1 Estimation of Retrofit Costs

The costs of these retrofits were estimated from data provided by Caltrans (Bailey 2005; Yashinsky 2005), according to the following steps:

- The Caltrans bridge–retrofit program has led to the column jacketing of 625 of the 2,267 bridges in the LA area. The total cost of these retrofits was on the order of $300,000,000. This results in an average retrofit cost per bridge of $300,000,000/625 = $480,000.
- From this, the cost to retrofit the 231 bridges under consideration here is estimated to be $480,000. x 231 = $110,880,000. In this analysis, this was rounded off to $111,000,000.

7.5.3.2 Estimation of Reduction of Losses due to Bridge Retrofits

This step involved computation of the present value of the economic losses, over an appropriate exposure time. A range of different discount rates were used in these calculations (where the discount rate is defined as the difference between the rate charged to borrow money and the inflation rate). The following calculations comprised this step:

- Use REDARS™ 2 to perform a probabilistic SRA of the LA-testbed system as of early 1994, when none of the 231 bridge retrofits had yet been carried out (Fig. 7-25a). From the results of this analysis, obtain the average annualized loss (AAL_{1994}) and the standard deviation of the losses (σ_{1994}) from this SRA.

- Use REDARS™ 2 to perform a probabilistic SRA of the upgraded LA-testbed system as of late 2004, when the 231 bridge retrofits are in place (Fig. 7-25b). From the SRA results, obtain the AAL and the standard deviation of the losses (AAL_{2004} and σ_{2004}.respectively).

- Compute the difference between the AALs for these two cases as $\Delta_{AAL} = AAL_{1994} - AAL_{2004}$.

Use Equation 7-1 to compute the present value of this loss difference *PVL* for an exposure time *T* and a discount rate *j*. This value of PVL represents the assumed benefit of the retrofit of these 231 bridges in this demonstration application. As described below, this example includes computations of *PVL* for a range of plausible exposure times and discount rates.

$$PVL = \left[\frac{1-(1+j)^{-T}}{j}\right] * \Delta_{AAL} \qquad (7\text{-}1)$$

7.5.3.3 Computation of Benefit-Cost Ratio

Caltrans' costs to carry out these 231 bridge retrofits between 1994 and 2004 can be viewed as an investment in seismic-risk reduction. To decide whether this investment is sound, one would first assess its potential for providing a good equivalent financial yield. In this example, this measure of the investment's financial-yield potential was represented by the ratio of the potential benefits of the investment (assumed here to correspond to the parameter *PVL* as computed above) to the cost of the investment (which, in this example, is represented by the retrofit cost of $111,000,000 as computed in Section 7.5.3.1).

7.5.3.4 Computation of Standard Deviation of Losses

When evaluating whether to proceed with an investment, a prudent investor would also evaluate its potential volatility; i.e., whether the investment is overly risky. In this example, the volatility of Caltrans' investment in the retrofit of these 231 bridges is represented by the standard deviation of the losses for each simulation of the 10,000 year walkthrough; i.e., as the standard deviation decreases, the volatility/riskiness of an investment in the retrofit of these bridges can also be assumed to decrease.

7.5.4 RESULTS

7.5.4.1 Benefit-Cost Ratio

The exposure times used in these benefit-cost calculations were based on estimated bridge design lives. Since this analysis is for a California highway system, we considered estimated design lives for California, bridges, which Caltrans typically assumes to be about 75 years (Yashinsky, 2005). To bracket this estimate, exposure times of 50-, 75-, and 100-years were used in this analysis. In this, it is assumed that the trip demands provided by SCAG for use in this demonstration analysis will be valid throughout all of these various exposure times, which will not be the case. However, it is expected that trip demands on the LA-testbed highway system will actually during these extended exposure times, and will be larger than these SCAG trip

demands. This will actually increase the benefit of the seismic retrofit of the additional 231 bridges over and above the values shown below. Hence, these computed benefit-cost ratios are expected to be conservative (i.e., lower bound estimates) of the ratios that would be computed if actual trip demands for these extended exposure times could be provided.

Discount rates of 2.5, 4, and 7 percent are used in this analysis. Discount rates on the order of 2.5 and 4 percent have been common in recent years and are probably most representative of current values. Previously, discount rates of about 7 percent have been most representative.

Table 7-9 shows the benefit-cost ratios that have been computed on this basis. This table shows benefit-cost ratios of about 2.4 for the older discount rate of 7 percent, and much higher benefit-cost ratios (ranging from about 3.2 to 4.7) when the more current discount rates of 2.5 and 4 percent are used. These results indicate that the retrofit of these 231 bridges was a cost-effective investment in seismic risk reduction.

.

Table 7-9. Benefit-Cost Ratios for Evaluation of Economic Viability of Program to Retrofit 231 Bridges in LA-Testbed System between 1994 and 2004

Exposure Time	50 Years			75 Years			100 Years		
Discount Rate	2.5%	4%	7%	2.5%	4%	7%	2.5%	4%	7%
Benefit-Cost Ratio	3.90	3.19	2.41	4.45	3.42	2.45	4.74	3.51	2.46

7.5.4.2 Standard Deviation of Losses

Table 7-10 compares the standard deviations of the estimated losses for the LA testbed systems with and without the 231 bridge retrofits that occurred between 1994 and 2004.

Table 7-10. Standard Deviations of Losses for use in Evaluation of Economic Viability of Program to Retrofit 231 Bridges in LA-Testbed System between 1994 and 2004

LA-Testbed System	Standard Deviation of Losses	Ratio of Standard Deviation of 2004 System to that of 1994 System
As of Early 1994 (prior to additional 231 bridge retrofits)	$218,634,766	0.616
As of End if 2004 (after completing additional 231 bridge retrofits)	134,718,179	

This table shows that the standard deviation of the losses is reduced by over 38 percent when the additional 231 bridge retrofits are in place. Therefore, when the seismic retrofits of the additional 231 bridges are in place, the volatility (i.e., riskiness) of Caltrans' seismic-retrofit investment is substantially reduced.

7.6 CLOSING COMMENTS

This demonstration application of REDARS™ 2 to SRA of a large highway system in the greater LA area has demonstrated: (a) the range of results that can be obtained from deterministic or probabilistic application of the software; (b) how such results may be interpreted to facilitate pre-earthquake planning and post-earthquake emergency response; (c) how REDARS™ 2 results can facilitate evaluations of the economic feasibility of various seismic improvement options; and (d) how computed confidence-intervals for probabilistic SRA results may be used to assess whether a sufficient number of simulations has been developed. These and other aspects of the use of REDARS™ 2 are further discussed in Chapters 2 and 9.

CHAPTER 8: CONCLUSIONS

8.1 SUMMARY

This Technical Manual describes results from six-years of work to: (a) upgrade the SRA methodology that had previously been developed under the first FHWA-MCEER highway research project; (b) program this methodology into a public-domain software package named REDARS™ 2; and (c) test and document this software.

The eight earlier chapters and 11 appendices that comprise this Manual describe how these objectives were met. In addition to describing the many upgrades of the SRA methodology, that were completed, these chapters and appendices describe how REDARS™ 2 software can be used to enable a transportation agency to consider relative effects on post-earthquake traffic flows when evaluating various seismic improvement options under consideration. This, in turn, will enable the agency to make a more informed selection of a preferred seismic improvement option. Chapter 7 of this Manual illustrates this through a demonstration application of REDARS™ 2 to a major segment of the Los Angeles CA highway system.

The overall SRA methodology from the first FHWA-MCEER project was the starting point for ;the development of REDARS™ 2. That methodology had the following benefits: (a) it is structured to be modular, thereby facilitating the inclusion of improved models and procedures as they are developed from future research; (b) it is a multidisciplinary tool that is based on a synthesis of models developed by earth scientists, earthquake engineers, transportation system analysts, and risk analysts; and (c) it was designed to provide a variety to deterministic and probabilistic SRA results to meet the varied needs of potential users nationwide. The various upgrades of this SRA methodology that have subsequently been programmed into REDARS™ 2 are summarized below: (see Chap. 2):

- ***Probabilistic Framework.*** The framework for carrying out probabilistic SRA has been significantly extended through development of a variance-reduction procedure. This procedure uses advanced statistical analysis techniques to substantially reduce the number of simulations needed to achieve acceptable confidence intervals for probabilistic estimates of average annual losses from earthquake damage to a roadway system (see App. A and J).

- ***Seismic Hazard Module.*** New enhancements of this module for estimating system-wide site-specific ground-shaking and ground-displacement hazards have included: (a) the development of new earthquake walkthrough tables for Coastal California and the Central United States (see Chap. 3 and App. B); (b) the ability to calculate a wide range of different source-site distance measures, that will facilitate REDARS™ inclusion of a larger library of ground-motion models that may use different distance definitions (see Chap. 3 and App. D); (c) the inclusion of well-recognized models for estimating ground shaking from earthquakes in Coastal California and the Central United States (see Chap. 3 and App. D); and (d) the programming of established models for estimating hazards from liquefaction and surface fault rupture (see Chap. 3 and App. E and F).

- ***Component Module.*** New improvements to this module include: (a) modification of the HAZUS99-SR2 model that is the REDARS™ 2 default model for estimating bridge damage from ground shaking, by calibrating the model against bridge damage observations from the Northridge Earthquake (see Chap.4 and App. G and K); and (b) development of new default models for estimating earthquake damage and repair requirements for approach fills and roadway pavements (see Chap. 4 and App. H).

- ***Network Module.*** The REDARS™ 2 network analysis procedure has been improved to include: (a) a capability for assessing how trip demands as well as travel times are affected by earthquake-induced increases in traffic congestion (b) adaptation of a Duel-Simplex searching algorithm that substantially reduces network analysis run times; and (c) development of an ability to account for different types of trips (i.e., auto vs. various types of freight trips) by including separate O-D trip tables and unit economic-loss parameters for each trip type (see Chap. 5 and App. I).

- ***Economic Losses.*** The REDARS™ 2 economic loss estimation procedure has been extended to include: (a) component repair costs (see. Chap. 5 and 6 and App. G and H); and (b) increased travel times and reduced trip demands caused by increases in traffic congestion due to earthquake damage to the roadway system (see Chap. 5 and 6 and App. I).

- ***Input Data.*** Experience has shown that the effort needed to develop input data for SRA of an actual highway system can be formidable and time-consuming. Therefore, significant effort under this project was directed toward developing user interfaces with REDARS™ 2 that facilitate: (a) location of publicly available databases within the Wizard; (b) definition of study-region boundaries; (c) establishment of the various network, soil, and bridge input databases within REDARS™ 2; (d) definition of boundary conditions in the form of external trip demands from outside of the study-region's highway-roadway network; and (d) checking of network-model connectivity and continuity of O-D zones (see App. C and the companion Import Wizard technical report and user manual by Cho et al. (2006)).

- ***Software Development.*** All of the above features have been programmed into a REDARS™ 2 software package for application on personal computers. This Windows-based software includes an internal GIS capability and an extensive graphical user interface (Geodesy 2004).

8.2 COMMENTS

The following paragraphs provide comments regarding current accomplishments and future directions for further development of the REDARS™ 2 methodology and software:

- REDARS™ 2 is a technically-advanced and user-friendly software package that focuses on SRA of highway systems nationwide. This basic REDARS™ 2 framework can be extended to also address other non-earthquake natural hazards and man-made hazards.

- REDARS™ 2 is intended to provide an improved basis for guiding user assessment of various pre-earthquake seismic-improvement options and post-earthquake emergency-

response options that may be under consideration. For pre-earthquake applications, the software can be used with various acceptable-risk procedures to guide the selection of a seismic-improvement option that best meets transportation-agency and community needs (see Chap. 2). As a post-earthquake tool, REDARS™ 2 can be used in real time to estimate potential locations of earthquake-induced traffic bottlenecks and to assess various options for addressing these bottlenecks.

- Much has been accomplished over the years in bringing the REDARS™ 2 SRA methodology and software to its current level of development. However, the further development of additional software improvements and upgraded engineering and scientific models for future inclusion into this software must be an ongoing process. Vital to this development will be the application of this software by transportation agencies and consultants nationwide, and the suggestions and feedback that these users would provide.

- The REDARS™ 2 software has been extensively alpha tested by the REDARS™ development team and has also undergone external beta testing. However, continued application of REDARS™ 2 by future users nationwide will undoubtedly uncover bugs to be corrected as well as areas where the REDARS™ technology and software can be further improved. The REDARS™ development team looks forward to working with future users in addressing these issues as they arise.

8.3 FUTURE DIRECTIONS

In the course of this work, specific recommendations for further development of the REDARS™ 2 SRA methodology and software have been identified. These recommendations are summarized below:

- ***Maintenance and Support.*** There is a need to establish a process for continued maintenance and support of the REDARS™ software. This will be essential for enabling the REDARS™ development team to address bugs that may be uncovered, to address user questions and concerns that may arise, and to keep the software current with operating-system changes that will inevitably occur.

- ***Additional Testing and Application of REDARS 2 Nationwide.*** Thus far, there has been one beta tester of REDARS™ 2 -- the California Department of Transportation (Caltrans) in Sacramento CA. The feedback and beta-testing results received from Caltrans during this process have been immensely helpful to the development and final release of the REDARS™ 2 software. However, additional beta testing and applications of REDARS™ 2 by other transportation agencies and potential users nationwide will be necessary to identify other software issues that may arise, and to be sure that the varied needs of a multitude of future users of the REDARS™ software are being met.

- ***Improved Bridge Fragility Models; Ground Shaking Hazards.*** Work under this project and discussions during past Tri-Center workshops have demonstrated the need to develop improved fragility models for estimating bridge damage due to ground-shaking hazards (TCW 2003 and 2005),. This work should also consider the bridge-attribute data that would

be needed as input to the improved models that are developed, and how current publicly-available bridge databases can be extended to include these new data. This will be needed to facilitate the use of these models in future REDARS™ applications to highway systems with many bridges.

- ***Improved Bridge Fragility Models; Ground Displacement Hazards.*** There is also a need to develop improved models for bridges subjected to ground displacement hazards due to liquefaction, landslide, and surface fault rupture. As noted above, input-data needs of the improved models that are developed should also be considered as part of this task.

- ***Improved Seismic Hazard Models.*** The current REDARS™ 2 seismic-hazard module should be extended to include: (a) a landslide-hazards model; (b) upgrade of the current fault-rupture-hazard model to consider multiple fault-rupture segments instead of only a single segment; and (c) augmentation of the current REDARS™ 2 library of ground-motion models with additional established models for estimating ground-shaking hazards nationwide.

- ***Development of Additional Earthquake Walkthrough Tables.*** Thus far, earthquake walkthrough models for Coastal California and the Central United States region have been developed for use in future probabilistic SRA applications of REDARS™ 2 in these regions. Additional walkthrough tables should be developed for use in REDARS™ 2 SRA applications to highway systems in other regions of the country where seismic risks to these systems may be important (e.g., the Pacific Northwest, Utah, South Carolina, New York City and regions of New England nearby and north of Boston).

- ***Network Analysis.*** Further enhancements of the REDARS™ 2 network analysis procedure should include: (a) development of a stochastic route-choice model that accounts for uncertainties in the user's choice of a route within a congested highway system; and (b) development of improved trip-demand calibration tools for use in baseline (pre-earthquake) analyses of system-wide traffic flows and travel times.

- ***Future Software Development.*** To supplement current REDARS™ 2 software-usability features, various upgrades of the software have been recommended by REDARS™ 2 beta testers. These very helpful recommendations have been prioritized for implementation under future REDARS™ 2 software-enhancement activities. A prioritized list of these recommendations can be provided upon request.

- ***Input Data.*** To enhance the development of input data for REDARS™, the formation of a single master database for highway systems nationwide that includes relevant data from the NHPN, HPMS, and NBI databases should be considered.

CHAPTER 9: REFERENCES

Abrahamson, N.A. and Silva, W.L. (1997). "Empirical Response Spectral Attenuation Relations for Shallow Crustal Earthquakes," *Seismological Research Letters*, Vol. 68, No. 1, January/February, pp 94-127.

Ang, A.H.-S. and Tang, W.H. (1975). *Probability Concepts in Engineering Planning and Design, Volume I, Basic Principles*, New York: John Wiley & Sons.

Atkinson, G.M. and Boore, D.M. (1995). "New Ground Motion Relations for Eastern North America" *Bulletin of Seismological Society of America*, Vol. 85, No. 1, January, pp 17-30.

Bailey, M. (2005). Personal Communication with Stuart D. Werner.

Baker, J.W. and Cornell, C.A. (2006). "Which Spectral Acceleration Are You Using?," *Earthquake Spectra*, Vol. 22, No. 2, May, pp 293-312.

Bardet, J-P. Tobita, T. Mace, N., and Hu, J. (2002). "Regional Modeling of Liquefaction-Induced Ground Deformation," *Earthquake Spectra*, Vol. 18, No.1, February, pp 19-46.

Bartlett, S.F. and Youd, T.L. (1992). *Empirical Analysis of Horizontal Ground Displacement Generated by Liquefaction-Induced Lateral Spreads*, Report NCEER-92-0021, Buffalo NY: National Center for Earthquake Engineering Research.

Basoz, N. and Kiremidjian, A.S. (1996). *Risk Assessment for Highway Systems*, Technical Report 118, John A. Blume Earthquake Engineering Center, Department of Civil Engineering, Palo Alto CA: Stanford University.

Basőz, N. and Kiremidjian, A. S. (1998), *Evaluation of Bridge Damage Data from the Loma Prieta and Northridge, California Earthquakes*, Technical Report MCEER-98-0004, Buffalo NY: Multidisciplinary Center for Earthquake Engineering Research.

Basőz, N. and Mander, J.B. (1999). *Enhancement of the Highway Transportation Module in HAZUS*, Final Pre-Publication Draft (#7), Washington D.C.: National Institute of Building Sciences, March 31.

Beckmann, M.J., McGuire, C.B., and Winston, C.C. (1956). *Studies in the Economics of Transportation*, Yale University Press, New Haven CT.

Bolt, B. A. (1993). *Earthquakes*, New York: W. H. Freeman and Company.

Buckle, I.G. (2003). "Application of Seismic Risk Analysis Procedures to the Performance-Based Design of Highway Systems," *Advancing Mitigation Technologies and Disaster Response for Lifeline Systems, Proceedings of Sixth U.S. Conference and Workshop on Lifeline Earthquake Engineering* (J.E.Beavers, editor), ASCE Technical Council on Lifeline Earthquake Engineering Monograph No. 25, August 10-13, pp 886-895.

California Department of Transportation (Caltrans) (1995). *Northridge Earthquake Recovery, Final Comprehensive Transportation Analysis*, Caltrans District 7, Division of Operations, Los Angeles CA, prepared by Barton-Aschman Associates Inc., Pasadena and Irvine CA, August.

California Geological Survey (CGS) (2005). *Alquist-Priolo Earthquake Fault Zones*., http://www.conserv.ca.gov/CGS/rghm/psha/fault-parameters/htm/faultdata1.htm.

Campbell, K.W. (2003). "Engineering Models of Strong Ground Motions," *Earthquake Engineering Handbook* (edited by W-F Chen and C. Scawthorn), CRC Press, New York NY, pp 5-1 to 5-76.

Center for Earthquake Research and Information (CERI) (2005). *New Madrid Catalog*, http://folkworm.ceri.memmphis.edu/catalogs/html/cat_nm_help.html.

Chiou, B. (2005). Personal Communication with Stuart D. Werner, Craig E. Taylor, and Sungbin Cho.

Cho, S., Gordon, P., Moore, J.E. II, Richardson, H.W., Shinozuka, M., and Chang, S. (2001). "Integrating Transportation Network and Regional Economic Models to Estimate the Costs of a Large Urban Earthquake", *Journal of Regional Science*, Vol. 41, No. 1, pp. 39-65.

Cho, S., Huyck, C.K., Ghosh, S., and Eguchi, R.T. (2006a). *REDARS Validation Report*, Technical Report 06-0007, Buffalo NY: Multidisciplinary Center for Earthquake Engineering Research, August.

Cho, S., Ghosh, S., Huyck, C.J., and Werner, S.D. (2006b). *User Manual and Technical Documentation for the REDARS™ Import Wizard*, Technical Report 06-0015, Buffalo, NY Multidisciplinary Center for Earthquake Engineering Research, November.

Davison, A.C. and Hinkley, D. V (1998). *Bootstrap Methods and their Application*, Cambridge, U.K.: Cambridge University Press.

Daykin, C. D., T. Pentikainen, and M. Pesonen (1994). *Practical Risk Theory for Actuaries*, London: Chapman & Hall.

Dial, R., Glover, F., Karney, D., and Klingman, D. (1979). "A Computational Analysis of Alternative Algorithm and Labeling Techniques for Finding Shortest Path Tree", *Networks*, No. 9, pp 215-248.

Dutta, A. and Mander, J.B. (1998). "Seismic Fragility Analysis of Highway Bridges," *Earthquake Engineering Frontiers in Transportation Systems, Proceedings of the Center-to-Center Project Workshop* (H. Kameda and I. Friedland, editors), INCEDE Report 1999-05, Tokyo Japan, pp 1-36.

Efron, B. and Tibshirani, R.J. (1993). *Introduction to the Bootstrap*, New York: Chapman-Hall.

Evans, S.P. (1976). "Derivation and Analysis of Some Models for Combining Trip Distributions and Assignment," *Transportation Research*, Vol. 10, No.1, pp 37-57.

Federal Emergency Management Agency (FEMA) (2002). *HAZUS®99 Service Release 2 (SR2) Technical Manual*, developed by FEMA through agreements with National Institute for Building Sciences, Washington D.C.

Federal Highway Administration (FHWA) (2003). *Recording and Coding Guide for the Structure Inventory and Appraisal of the Nation's Bridges*, Available via compact disk from FHWA Office of Engineering, Bridge Division, Bridge Management Branch, Washington D.C..

Ferritto, J., Priestley, M.J.N., Werner, S.S., and Taylor, C.E. (1999). *Seismic Criteria for Marine Oil Terminals*, Vol. I, Technical Report TR-2103-SHR, Naval Facilities Engineering Center, Port Hueneme CA, July.

Florian, M. and Nguyen, S. (1976). "On Application and Validation of Equilibrium Trip Assignment Method," *Transportation Science*, Vol. 10, No. 4, pp 374-390.

Florian, M., Nguyen, S. and Pallottino, S. (1981) "A Dual Simplex Algorithm for Finding all Shortest Paths," *Networks,* Vol. 11, pp 367-378.

Frank, M. and Wolfe, P. (1956). "An Algorithm for Quadratic Programming," *Naval Research Logistics Quarterly,* Vol. 3*,* pp 95-110.

Frankel, A. D, Mueller, C., Barnhard, T., Perkins, D., Leyendecker, E.V., Dickman, N., Hanson, S., and Hopper, M. (1996). *National Seismic-Hazard Maps, June 1996 Documentation.* Denver, CO: U. S. Department of the Interior, U. S. Geological Survey, Open-File Report 96-532.

Frankel, A.D., Petersen, M.D., Mueller, C.S., Haller, K.M., Wheeler, R.L., Leyendecker, E.V., Wesson, R.L., Harmsen, S.C., Cramer, C.H., Perkins, D.M., and Rekstales, K.S. (2002). *Documentation for the 2002 Update of the National Seismic Hazard Maps*, Denver, CO: U. S. Department of the Interior, U. S. Geological Survey, Open-File Report 02-420.

Geodesy (2004). *REDARS™ 2 Software Specification Development Plan*, San Francisco CA, September 13.

Hanks, T.C. and Kanamori, H (1979). "A Moment Magnitude Scale," *Journal of Geophysical Research*, Vol. 84, pp 2348-2350.

Hastings, N. A. J. and Peacock, J.B. (1974). *Statistical Distributions*, London: Butterworth & Co (Publishers) Ltd.

Housner, G.W. and Jennings, P.C. (1982). *Earthquake Design Criteria*, Earthquake Engineering Research Institute, Berkeley CA, September.

Jernigan, J.B. (1998). *Evaluation of Seismic Damage to Bridges and Highway Systems in Shelby County, Tennessee*, Ph.D. Dissertation, University of Memphis, Memphis TN, December.

Kramer, S.L. (1996). *Geotechnical Earthquake Engineering*, Prentice-Hall, Inc., 653 pp.

Law, A.M. and Kelton, W.D. (1991). *Simulation Modeling and Analysis*, New York: McGraw-Hill, Inc.

Lemaire, J., Taylor, C.E., and Tillman, C. (1993). "Models for Earthquake Insurance and Reinsurance Evaluations," in *Proceedings of the Second International Symposium on Uncertainty Modeling and Analysis*, Los Alamitos, CA: IEEE Computer Society Press, April.

Mai, P. M. and Beroza, G.C. (2000). "Source Scaling Properties from Finite-Fault-Rupture Models," *Bulletin of the Seismological Society of America*, Vol. 90, No. 3, June, pp. 604-615.

Mander, J.B. (1999). Personal Communication to Stuart D. Werner.

Mander, J.B. and Basoz, N. (1999). "Seismic Fragility Curves for Highway Bridges" *Optimizing Post-Earthquake Lifeline System Reliability, Proceedings of the 5th U.S. National Conference on Lifeline Earthquake Engineering* (W.M. Elliott and P. McDonough, editors), Technical Council on Lifeline Earthquake Engineering Monograph No. 16, August, pp 31-40.

Meyer, Paul L., 1970, *Introductory Probability and Statistical Applications*, Reading, MA: Addison-Wesley Publishing Company.

Moore, E. (1957). "The Shortest Path through a Maze," *Proceedings of International Symposium on the Theory of Switching*. Harvard University Press, Cambridge, Mass, pp. 285-292.

Northern California Earthquake Data center (NCEDC) (2005). *Northern California Earthquake Catalogue Search*, http://quake.geo.berkeley.edu.

Panjer, Harry H. And Gordon E. Willmot, 1992, *Insurance Risk Models,* Schaumburg, Il: Society of Actuaries.

Pape, U. (1974) "Implementation and Efficiency of Moore-Algorithms for the Shortest Route Problem," *Mathematical Programming* 7 (2), pp. 212-222.

Priestley, M.J.N., Seible, F., and Calvi, G.M. (1996). *Seismic Design and Retrofit of Bridges*, John Wiley & Sons, New York NY, 686 pp.

Sadigh, K., Chang, C.Y., Egan, J.A., Makdisi, F., and Youngs, R.R. (1997). "Attenuation Relations for Shallow Crustal Earthquakes based on California Strong Motion Data," *Seismological Research Letters*, Vol. 68, No. 1, January/February, pp 180-189.

Seed, H. B. and Idriss, I. M. (1982). *Ground Motions and Soil Liquefaction during Earthquakes*, Earthquake Engineering Research Institute, Berkeley CA.

Sheffi, Y. (1985), *Urban Transportation Networks*, Prentice-Hall, Inc., Englewood Cliffs, New Jersey, pp. 125-129.

Shinozuka, M., Moore, J.E. II, Gordon, P., Richardson, H.W., Chang, S., and Cho, S.B. (1999). "An Integrated Model of Highway Networks and the Spatial Metropolitan Economy," *Earthquake Engineering Frontiers in Transportation Systems, Proceedings of the Center-to-Center Project Workshop* (H. Kameda and I. Friedland, editors), INCEDE Report 1999-05, Tokyo Japan, pp 1-36.

Shinozuka, M. (2004). *Report on Socio-Economic Effect of Seismic Retrofit Implemented on Bridges in Los Angeles Highway Network,* Report prepared for California Department of Transportation, Office of Earthquake Engineering and Structural Design, Irvine CA: University of California, June.

Silva, W., Gregor, N., and Darragh, R. (2002). *Development of Regional Hard-Rock Attenuation Relations for Central and Eastern North America*, Pacific Engineering and Analysis, El Cerritto CA.

Silva, W., Gregor, N., and Darragh, R. (2003). *Development of Regional Hard-Rock Attenuation Relations for Central and Eastern North America, Mid-Continent, and Gulf Coast Areas*, Pacific Engineering and Analysis, El Cerritto CA.

Small, E.P. (1997). "Alternatives for the Integration of Seismic Vulnerability Assessment within the Pontis Bridge Management System," *Proceedings of the National Seismic Conference on Bridges and Highways, Sacramento CA*, Federal Highway Administration and California Department of Transportation, pp 53-64, July 8-11.

Small, E.P. (1999). "Examination of Alternative Strategies for Integration of Seismic Risk in Bridge Management Systems," *Proceedings of the International Bridge Management Conference*, Transportation Research Board, Washington D.C., April,

Southern California Earthquake Center (SCEC) (2005). *Catalog of "A" Quality Earthquake Depths*, derived from http://www.data.scec.org/catalog-search/date-mag_loc.php.

Taylor, C. E., Lemaire, J., and Tillman, C. (1994). "A New Earthquake Insurance and Reinsurance Index: Uncertainties and Future Developments," *Uncertainty Modeling and Analysis: Theory and Applications*, B. M. Ayyub and M. M. Gupta, eds., Elsevier Science BV., pp. 497-514.

Taylor, C.E., Eguchi, R.T., and Chang, S. (1998). "Updating Real-Time Earthquake Loss Estimates: Methods, Problems, and Insights," *Proceedings of the Sixth U.S. National Conference on Earthquake Engineering, Seattle WA*, Oakland CA: Earthquake Engineering Research Institute, May 31- June 4, 484pdf, CD-ROM,

Taylor, C.E., Werner, S.D., and Jakubowski, S. (2001). "The Walkthrough Method for Catastrophe Decision Making," *Natural Hazards Review*, Vol. 2, No. 4, American Society of Civil Engineers, November, pp 193-202.

Taylor, C.E., Perkins, D.M., and Werner, S.D. (2004a). *Post-Sampling Variance Reduction for Seismic Risk Analysis of Spatially Distributed Lifeline Networks*, Technical Report for the Multidisciplinary Center for Earthquake Engineering Research under research contract FHWA Contract DTFH61-98-C-00094, July.

Taylor, C.E., Werner, S.D., Silva, W., Aschheim, M., and Scheibel, L. (2004b). *Exogenous Uncertainties in Earthquake Risk Modeling for Infrastructure Systems: A Demonstration Evaluation in Northern California*, Torrance, CA: Natural Hazards Management Inc. for the United States Geological Survey, Award No. 03HIGR0022, August.

Tri-Center Workshops (TCW) (2003 and 2005). Collaborative Workshop of Researchers in Bridge Earthquake Engineering, Seismic Risk Analysis of Highway Systems, and Transportation Network Analysis, Multidisciplinary Center for Earthquake Engineering Research (MCEER), Mid-America Center for Earthquake Engineering Research (MAE), and Pacific Earthquake Engineering Research Center (PEER), June 2003 (San Pedro CA), December 2003 (Las Vegas NV) and October 2005 (Las Vegas NV).

Tokimatsu, K. and Seed, H B, (1987). "Evaluation of Settlements in Sands due to Earthquake Shaking," *Journal of the Geotechnical Engineering Division, ASCE*, Vol. 113, No. 8, August, pp 861-878.

Toro, G.R. Abrahamson, N.A., and Schneider, J.F. (1997). "Model of Strong Motions from Earthquakes in Central and Eastern North America: Best Estimates and Uncertainties', *Seismological Research Letters*, Vol. 68, No. 1, January/February, pp 41-57.

Wardrop, J.G. (1952). "Some Theoretical Aspects of Road Traffic Research," *Proceedings, Institution of Civil Engineers*, Vol. II, No.1, pp 325-378.

Wakabashi, H. (1999). "Highway Network Reliability Assessment and Importance Analysis: Lessons Learned from the 1995 Kobe Earthquake," *Earthquake Engineering Frontiers in Transportation Systems, Proceedings of the Center-to-Center Project Workshop*, (H. Kameda and I. Friedland, editors), INCEDE Report 1999-05, Tokyo Japan, pp 151-166.

Wells, D.L. and Coppersmith, K.J. (1994). "New Empirical Relationships among Magnitude, Rupture Length, Rupture Area, and Surface Displacement," *Bulletin of Seismological Society of America*, Vol. 84, No. 4. August, pp 974-1002.

Werner, S.D. and Taylor, C.E. (2002). "Component Vulnerability Modeling Issues for Analysis of Seismic Risks to Transportation Lifeline Systems," *Acceptable Risk Processes: Lifelines and Natural Hazards* (edited by Craig Taylor and Erik VanMarcke), Monograph No. 21, Reston VA: American Society of Civil Engineers Council on Disaster Reduction and Technical Council on Lifeline Earthquake Engineering, March, pp 78-104.

Werner, S. D., Dickenson, S.E., and Taylor, C.E. (1997). "Seismic Risk Reduction at Ports: Case Study and Acceptable Risk Evaluation," *Journal of Waterway, Port, and Coastal Engineering, American Society of Civil Engineers*, Vol. 123, November-December, pp 337-346.

Werner, S.D., Taylor, C.E., and Ferritto, J.M. (1999). "Seismic Risk Reduction Planning for Ports Lifelines", Optimizing Post-Earthquake Lifeline System Reliability, *Proceedings of the Fifth U.S. Conference on Lifeline Earthquake Engineering,* Seattle WA, Technical Council on Lifeline Earthquake Engineering Monograph 16 (Edited by W. M. Elliot and P. McDonough), American Society of Civil Engineers, Reston VA, pp 503-512, August.

Werner, S.D., Taylor, C.E., Moore, J.E. III, Walton, J.S., and Cho, S. (2000). *A Risk-Based Methodology for Assessing the Seismic Performance of Highway Systems*, Buffalo, NY: Multidisciplinary Center for Earthquake Engineering Research, Technical Report MCEER-00-0014, FHWA Contract Number DTFH61-92-C-00016., December.

Werner, S.D., Taylor, C.E., Dahlgren, T., Lobedan, F., LaBasco, T.R., and Ogunfunmi, K. (2002). "Seismic Risk Analysis of Port of Oakland Container Berths," *Proceedings of Seventh U.S. Conference on Earthquake Engineering*, Boston MA, July 21-25, CD-ROM.

Werner, S.D., Lavoie, J-P, Eitzel, C., Cho, S., Huyck, C., Ghosh, S., Eguchi, R.T., Taylor, C.E., and Moore, J.E. II (2003). "REDARS™ 1 Demonstration Software for Seismic Risk Analysis of Highway Systems," *Research Progress and Accomplishments 2001-2003*, Report MCEER-03-SP01, Buffalo NY: Multidisciplinary Center for Earthquake Engineering Research, May, pp 17-34.

Werner, S.D., Taylor, C.E., Cho, S., Lavoie, J-P, Huyck, C.K., Eitzel, C., Eguchi, R.T., and Moore III, J.E. (2004). "New Developments in Seismic Risk Analysis of Highway Systems," *Proceedings of 13th World Conference on Lifeline Earthquake Engineering, Vancouver B.C., Canada*, Paper No. 2189, August 1-6.

Yashinsky, M. (2005). Personal Communication with Stuart D. Werner.

Youd, T. L. (1998). *Screening Guide for Rapid Assessment of Liquefaction Hazard at Highway Bridge Sites,* Provo, Utah: Brigham Young University for National Center for Earthquake Engineering Research, Buffalo NY under NCEER Task 106 E-3.1(B), FHWA Contract DTFH61-92-C-00106.

Youd, T.L. (2002). "Pavements," Chapter 6 of *Seismic Retrofitting Manual for Highway Structures: Retaining Structures, Slopes, Tunnels, Culverts, and Pavements*, Buffalo NY: Multidisciplinary Center for Earthquake Engineering Research, January.

Youd, T. L. and Perkins, D. L. (1978). "Mapping of Liquefaction Induced Ground Failure Potential," *Journal of the Geotechnical Engineering Division, ASCE*, Vol. 104, No. GT4, April, pp 433-446.

Youngs, R.R., Abrahamson, N.A., Makdisi, F., and Sadigh, K. (1995). "Magnitude-Dependent Dispersions in Peak Ground Acceleration', *Bulletin of the Seismological Society of America*, Vol. 85, pp 1161-1176.

Youngs, R.R., Arabascz, W.J., Anderson, R.E., Ramelli, A.R., Ake, J.P., Slemmons, D.J., McCalprin, J.P., Doser, D.I., Fridrich, C.J., Swan III, F.H., Rogers, A.M., Yount, J.C., Anderson, L.W., Smith, K.D., Brahn, R.L., Knuepfer, P.L.K., Smith, R.B., dePolo, C.M., O'Leary, D.W., Coppersmith, K.J., Pezzopane, S.K., Schwartz, D.P., Whitney, J.M., Olig, S.S., and Toro, G.R. (2003)."A Methodology for Probabilistic Fault Displacement Hazard Analysis (PFDHA)," *Earthquake Spectra*, Vol. 19, No. 1, February, pp 191-219.

Table of Contents

REDARS2 Methodology and Software for Seismic Risk Analysis of Highway Systems

Appendices A - K

MCEER-06-SP08
August 31, 2006

CONTENTS

APPENDIX/SECTION	PAGE
A PROBABILISTIC FRAMEWORK	A-1
A.1 Objective and Scope	A-1
A.2 Walkthrough Procedure: Overview	A-1
A.2.1 Scenario Earthquakes	A-2
A.2.2 Simulation Development Process	A-2
A.2.3 Nominal Confidence Intervals	A-3
A.3 Walkthrough Procedure: Underlying Concepts	A-3
A.3.1 Random Sampling	A-3
A.3.2 Bernoulli Trials	A-4
A.3.3 Planning Horizon	A-4
A.4 Development of Loss Distribution	A-5
A.4.1 Total-Loss Distribution	A-5
A.4.2 Conditional-Loss Distribution	A-6
B EARTHQUAKE SCENARIOS AND WALKTHROUGH FILES	B-1
B.1 Background	B-1
B.2 Selection of Earthquake Locations, Magnitudes, and Walkthrough Year Numbers	B-4
B.2.1 Step 1: Define Basic Information Needed to Characterize Scenario Earthquakes	B-4
B.2.2 Step 2: Define Duration (Number of Walkthrough Years) of Walkthrough File and Planning Horizon (Exposure Time) to be Considered	B-7
B.2.3 Step 3: Determine Number of Potentially Damaging Earthquakes during Each Year in Walkthrough Table	B-7
B.2.4 Step 4: Determine Source for Each Earthquake Scenario	B-10
B.2.5 Step 5: Determine Magnitude for Each Earthquake Scenario	B-12
B.3 Physical Specification of Earthquake Scenarios	B-14
B.3.1 Background	B-14
B.3.2 Models for Random Estimation of Earthquake Scenarios	B-15
B.4 Walkthrough Files Developed to Date	B-18
B.4.1 Walkthrough File Data	B-18
B.4.2 Comparisons of Walkthrough Files for Coastal California and Central United States	B-20
C IMPORT WIZARD	C-1
C.1 Background	C-1
C.2 Role of Import Wizard and its Graphical User Interface	C-1
C.3 Limitations of Import Wizard	C-2
C.4 Data Sources	C-3
C.4.1 Roadway Transportation Network	C-3
C.4.2 Bridges	C-4

CONTENTS

APPENDIX/SECTION	PAGE
C.4.3 Soils	C-4
C.4.4 Transportation Analysis Zones (TAZs)	C-5
C.4.5 Origin-Destination (O-D) Trip Tables	C-5
C.5 Implementation Steps	C-5
C.5.1 Step 1: Create Blank Database Files Set	C-5
C.5.2 Step 2: Populate HPMS Tables	C-6
C.5.3 Step 3: Populate NBI Tables	C-6
C.5.4 Step 4: Create and Populate NHPN Tables	C-6
C.5.5 Step 5: Establish Relationships between Tables and Create LINK Table	C-6
C.5.6 Step 6: Locate Bridges and Tunnels from NBI Database onto Links in Links Table	C-7
C.5.7 Step 7: Update Soil Type for Selected Highway Components	C-7
C.5.8 Step 8: Subset TAZs and Calibrate Demand Functions	C-7
C.5.9 Step 9: Populate Database with Data for Study Area	C-8
C.5.10 Step 10: Bridge/TAZ/VARS Tables/Clean-Up	C-8
C.5.11 Step 11: Baseline Analysis	C-8
C.6 Screens	C-8
D SOURCE-SITE DISTANCES AND GROUND-MOTION HAZARDS	D-1
D.1Objective and Scope	D-1
D.2 Source-Site Distances	D-1
D.2.1 Quantities Computed	D-1
D.2.2 Assumptions	D-1
D.2.3 Input Data	D-3
D.3 Adaptation of Abrahamson-Silva (1997) Ground-Motion Model	D-6
D.3.1 Overview	D-6
D.3.2 Implementation of Model in REDARS 2	D-7
D.4 Adaptation of Silva et al. (2002 and 2003) Ground-Motion Model	D-12
D.4.1 Step 1. Compute Earthquake Motions in Hard Rock	D-12
D.4.2 Step 2. Obtain Equivalent Firm-Rock (NEHRP Type B) Motions	D-14
D.4.3 Step 3. Develop Soil Amplification Factors	D-15
D.4.4 Step 4. Compute Site-Specific Ground Motions including Effects of Local Soil Conditions	D-15
E LIQUEFACTION HAZARDS	E-1
E.1 Introduction	E-1
E.2 Evaluation Procedure Overview	E-1
E.3 Screening for Liquefaction Potential	E-1
E.3.1 Input Data Requirements	E-1
E.3.2 Initial Screening based on Assessment of Local Geology and Soil Conditions	E-2
E.3.3 Review of Prior Liquefaction Evaluations by Others	E-2

CONTENTS

APPENDIX/SECTION	PAGE
E.4 Assessment of Liquefaction-Induced Lateral-Spread Displacement	E-4
E.4.1 Input Data	E-4
E,4,2 Median Value of Lateral-Spread Displacement	E-6
E.4.3 Treatment of Uncertainty	E-6
E.4.4 Discussion of Bardet et al. (2002) Model	E-7
E.5 Assessment of Liquefaction-Induced Vertical Settlement	E-8
E.5.1 Input Data	E-8
E.5.2 Basic Calculations	E-8
F SURFACE FAULT RUPTURE HAZARDS	F-1
F.1 Overview	F-1
F.2 Input Data	F-1
F.3 Check if Site can Undergo Displacement from Fault Rupture	F-2
F.3.1 General Procedure	F-2
F.3.2 Seed for Random-Number Generation	F-2
F.3.3 Maximum Fault Displacement	F-2
F.3.4 Parameters from REDARS 2 Source-Site Distance Calculation Procedure	F-3
F.3.5 Step 1. User-Specified Zone of Deformation	F-3
F.3.6 Step 2. Check Distance from Site to Fault Rupture	F-4
F.3.7 Step 3. Check Distance from Site to Hanging Wall of Dipping Fault Rupture	F-5
F.3.8 Step 4. Check Probability of Slippage	F-5
F.4 Calculation of Site-Specific Fault Displacement	F-6
F.4.1 Background	F-6
F.4.2 Development of Beta Distributions and Simulations	F-6
F.4.3 Probabilistic Estimates	F-9
F.4.4 Deterministic Estimates	F-9
G DEFAULT BRIDGE MODELING PROCEDURES	G-1
G.1Background	G-1
G.2 Estimation of Bridge Damage States from Ground Shaking	G-2
G.2.1 Overview of Modeling Procedure	G-2
G.2.2 Application Procedure	G-7
G.3 Estimation of Bridge Damage States from Ground Displacement	G-19
G.3.1 Step 1. Establish Median PGD Capacity for Each Bridge	G-19
G.3.2 Step 2. Estimate PGD Capacity including Effects of Uncertainties	G-21
G.3.3 Step 3. Determine if Bridge is in Damage State 5	G-21
G.3.4 Step 4. Determine if Bridge is in Damage State 4	G-21
G.4 Bridge Repair Model	G-21
G.4.1 Background	G-21
G.4.2 Assumptions	G-22
G.4.3 Repair Model Implementation	G-24

CONTENTS

APPENDIX/SECTION		PAGE
H	**DEFAULT MODELS FOR APPROACH FILLS AND ROADWAY PAVEMENTS**	H-1
	H.1 Approach Fills	H-1
	H.1.1 Estimation of Approach-Fill Settlement	H-1
	H.1.2 Damage States, Repair Costs, and Traffic States	H-2
	H.2 Roadway Pavements	H-6
	H.2.1 Model Basis and Assumptions	H-6
	H.2.2 Use of Model in REDARS 2	H-6
I	**POST-EARTHQUAKE TRIP REDUCTION AND UPDATED MINIMUM PATH ALGORITHM IN NETWORK ANALYSIS PROCEDURE**	I-1
	I.1 User-Equilibrium Model with Fixed Trip Demands	I-1
	I.2 Formulation and Solution Steps for Variable-Demand Model	I-2
	I.3 Economic Loss due to Earthquake Damage to Highway System	I-4
	I.4 Sample Calibration of Demand Function	I-5
	I.5 Numerical Example of Variable-Demand Model	I-6
	I.5.1 Base Data for Variable-Demand Model	I-6
	I.5.2 Solution Steps for the Variable-Demand Model	I-8
	I.6 Updating the Minimum-Path Algorithm	I-14
	I.6.1 Background	I-14
	I.6.2 Previously Implemented Minimum-Path Algorithm	I-14
	I.6.3 Dual-Simplex Algorithm	I-20
	I.6.4 Run-Time Comparisons	I-22
	I.7 Validation of Variable-Demand Model	I-26
	I.7.1 Data Used for Validation	I-26
	I.7.2 Traffic Volume Comparisons	I-28
J	**CONFIDENCE LIMITS FOR PROBABILISTIC SEISMIC RISK ANALYSIS RESULTS**	J-1
	J.1 Introduction	J-1
	J.2 Classical Statistical-Analysis Methods	J-1
	J.2.1 Estimation of CIs for Average Annualized Loss	J-2
	J.2.2 Estimation of CIs for Fractile Loss Estimates	J-3
	J.3 Variance-Reduction Approach	J-5
	J.3.1 Parametric Bootstrapping	J-5
	J.3.2 Summary of Method	J-6
	J.4 Sample Results and Comparisons	J-9
	J.5 Caveats	J-11
	J.6 Confidence Limits for Very Few Simulations	J-11
	J.6.1 Overview	J-11
	J.6.2 Square Root Rule-of-Thumb	J-11

CONTENTS

APPENDIX/SECTION	PAGE
K CALIBRATION OF DEFAULT BRIDGE-DAMAGE MODEL	K-1
K.1 Introduction	K-1
K.1.1 Statement of the Problem	K-1
K.1.2 Organization of this Appendix	K-2
K.2 Bridge System and Earthquake Characteristics	K-2
K.2.1 System Extent	K-2
K.2.2 Northridge Earthquake and its Bridge Damage	K-3
K.3 Calibration Procedure and Results	K-5
K.3.1 Overview	K-5
K.3.2 Starting Points	K-5
K.3.3 Analysis Steps and Results	K-8
K.4 Concluding Comments	K-14

Post-Sampling Variance Reduction for Seismic Risk Analysis of Spatially Distributed Lifeline Networks

APPENDIX A
PROBABILISTIC FRAMEWORK

A.1 OBJECTIVE AND SCOPE

The basic probabilistic framework for the REDARS™ 2 SRA methodology is a walkthrough procedure, which is a Monte Carlo time-series method (buttressed by a new bootstrap post-sampling method). Through use of random methods, this procedure avoids statistical biases present in other procedures in which scenario earthquakes (with specified magnitudes and locations) and simulations (the random estimation of losses due to these specific scenarios) are not picked randomly. At the same time, as a time-series method, the walkthrough method permits the evaluation of decisions in which time-considerations are critical.

This appendix updates previous accounts of the probabilistic framework for the REDARS™ walkthrough procedure, as found in Werner et al. (2000) and Taylor et al. (2001). It is organized into three remaining sections that: (a) provide an overview of the walkthrough procedure (Section A.2); (b) discuss basic concepts behind this procedure (Section A.3); and (c) show how loss distributions are developed from the loss results for each scenario earthquake and simulation (Section A.4).

Two major new developments in this probabilistic framework are covered in other appendices. One new development that is described in Appendix B consists of a more detailed specification of earthquake scenarios, so that various "distance" calculations (for alternative attenuation functions and for various other modules such as those estimating liquefaction displacements) can be accommodated. A second new development that is described in Appendix J uses a new bootstrap (sampling with replacement) "variance-reduction" procedure to develop loss estimates and their nominal confidence intervals much more efficiently than the earlier method based on classical statistics that is described in Werner et al. (2000). Improvements in the hazards, component-vulnerability, and network-analysis models as described in other appendices of this report also constitute important updates of the REDARS™ probabilistic framework.

A.2 WALKTHROUGH PROCEDURE: OVERVIEW

The walkthrough procedure is carried out for a user-specified duration (in years) that is established in accordance with basic principles summarized below. The procedure randomly selects values of the various uncertain parameters contained in the models that comprise the REDARS™ 2 SRA procedure, and then carries out a SRA using this set of parameters in order to develop one simulation of potential losses due to earthquake damage to the highway system (Sections A.2.1 and A.2.2.) This process is then repeated in order to develop additional simulations, and probabilistic loss distributions, and statistics are developed from the SRA results for each simulation developed so far. These results include the estimation of confidence intervals for the loss results from all of the simulations developed thus far, in order to guide the user's assessment of whether or not a sufficient number of simulations has been considered (Section A.2.4).

A.2.1 Scenario Earthquakes

A set of independent uniform random numbers is generated and used with regional seismicity and tectonics models to establish whether any potentially damaging earthquakes[1] occur in the surrounding region during each year of the walkthrough (i.e., for years 1, 2, etc.) For many simulated years, no damaging earthquakes will be found to occur, particularly for moderately seismic regions. For other years, it will be determined that one or more potentially damaging earthquakes occur. Additional series of uniform random numbers are then used with these models to establish the magnitude, location, rupture center, and rupture length of each of these earthquakes. This is provided in tabular form (for each year of the walkthrough) as input data for the subsequent SRA calculations. Appendix B describes how this procedure has been used to develop scenario earthquakes for two regions of the United States -- Coastal California and the region within the Central United States that could be affected by the New Madrid seismic zone.

A.2.2 Simulation Development Process

The REDARS™ 2 SRA procedure accounts for uncertainties in: (a) earthquake occurrence, magnitude and location; (b) ground-motion attenuation rates and soil amplification effects; (c) liquefaction-induced lateral-spread displacements; (d) surface fault rupture displacements; and (e) bridge, tunnel and approach-fill damage states due to ground shaking and permanent ground displacement. These uncertainties are considered by developing multiple "simulations" of earthquake-induced losses for successive years in the walkthrough table, as summarized below:

- Step 1. Scenario Earthquakes. Randomly sample an appropriate earthquake model for the region, in order to establish, for each year of the walkthrough, whether or not one or more earthquakes occur during that year and, if so, their magnitudes and locations.

- Step 2. Seismic Hazards. For each scenario earthquake, randomly sample the probability distributions from the ground motion, liquefaction, and fault rupture models to develop a random value of each of these hazards at each component site within the highway system.

- Step 3. Component Performance. For the above set of seismic hazards at each site, randomly sample the fragility curves for the various components in the highway system, in order to estimate each component's damage state. Then, using appropriate repair models, estimate each component's corresponding repair costs, repair time, and traffic state (i.e., whether the component is fully closed, partially open, or fully open to traffic at various post-earthquake times.) Note that these traffic states will vary with time after the earthquake, in order to reflect the rate of repair of the damage to the component (as estimated by the repair model.)

- Step 4. System States. Using the above traffic states for each component at each post-earthquake time, develop a series of system states -- one for each post-earthquake time. As noted in Section 2.0, each system state is essentially a "snapshot" of the entire highway system at that post-earthquake time, which shows which links throughout the system are fully closed, partially closed, and fully open to traffic at that time.

[1] Potentially-damaging earthquakes are defined as those events whose moment magnitude ≥ 5.0.

- Step 5. Network Analysis. Apply the REDARS™ 2 network analysis procedure to each system state, in order to estimate corresponding travel time delays, traffic flow disruptions, and reductions in trip demands at that post-earthquake time.

- Step 6. Losses. Estimate the losses due to earthquake damage to the highway system. In this, the term "loss" can represent economic loss, increase in travel time to/from any key location in the region, increase in travel times along key "lifeline" routes within the system, or any other adverse consequence of earthquake damage to the highway system.

The results of the above steps as applied for each scenario earthquake in the walkthrough is termed a "simulation". However, since "years" are a basic constituent in key loss statistics, one may speak of year-trials or year-samples. Year-trials for which no scenarios are postulated will have no losses. For year-trials for which there is more than one scenario postulated, the losses during that year (for the year-trial) are computed as the combination of losses for each scenario.

After simulations are developed for a sufficient number of years of the walkthrough (see Sec. A.2.3), REDARS™ 2 analyzes the loss results from these simulations developed so far, and develops probabilistic estimates of system-wide losses. REDARS™ 2 uses similar procedures to develop probabilistic estimates of seismic hazards (ground motions and permanent ground displacements) at any user-specified component site in the highway system, as well as probabilistic estimates of damage states for any user-specified component.

A.2.3 Nominal Confidence Intervals

The steps outlined in Section A.2.2 do not necessarily need to be carried out for all years of the walkthrough table. Rather, REDARS™ 2 uses procedures described in Appendix J, in order to estimate nominal confidence intervals (CIs) for the loss results from the walkthrough years considered so far. If the user determines that these nominal CIs are inadequate, additional walkthrough years are considered and new simulations are developed for each of these additional years. Revised loss distributions are then obtained from all of the walkthrough years and simulations considered so far, and new nominal CIs are estimated from this now-expanded number of simulations. This process is repeated until the user determines that the nominal CIs are acceptable. At that time, the walkthrough analysis can be terminated.

A.3 WALKTHROUGH PROCEDURE: UNDERLYING CONCEPTS

Key to the above walkthrough procedure are the concepts of random sampling, Bernoulli trials, and the planning horizon (exposure times) that is used to assess the probabilistic-loss results. These concepts are summarized below.

A.3.1 Random Sampling

As noted in Section A.2, random sampling is used to establish the value of each uncertain parameter used in the SRA for each simulation that is developed. Modern statistical theory has shown that this use of random-sampling methods for a relatively small number of samples will

greatly increase statistical soundness (e.g., the lack of statistical bias, the ability to estimate CIs) relative to that for non-random sampling for a much larger number of samples[2]).

A.3.2 Bernoulli Trials

The notion of Bernoulli trials fits well with the above random sampling process and the establishment of CIs for the SRA results. A Bernoulli trial is a statistical sampling process in which: (a) each sample is independent of all other samples; and (b) the probability remains constant for each sample. It is assumed here -- with some caveats as discussed below -- that the ensemble of SRA results developed from the above walkthrough process can be treated as Bernoulli trials. Appendix J describes how this assumption facilitates the establishment of nominal CIs which, in turn, serve to guide the user's assessment of whether a sufficient number of walkthrough years and corresponding simulations has been considered.

To illustrate the Bernoulli trial concept, suppose that 10,000 years are simulated as described in Section A.2.1, in order to estimate earthquake losses. Assuming that each year leads to an independent statistical sample, each of these estimated losses will have an equal probability of occurrence (of 1/10,000). The number of non-zero losses from these 10,000 years of simulations will depend on the regional seismicity and tectonics and on the seismic response characteristics of the highway-system components. For example, for the Los Angeles area highway system analyzed in Chapter 7, approximately 2,600 of these 10,000 simulated losses will be non-zero (even though the earthquake sources for these losses will have widely varying probabilities.)

There are certain caveats in the use of this Bernoulli trial assumption in this methodology for estimating risks and losses due to earthquake damage to a highway system. Minor caveats pertain to how diverse earthquake faults may be modeled in a non-Poissonian fashion. Selected faults can be modeled as having very slightly varying probabilities from year except after an event on the fault, when probabilities drop precipitously. Major caveats primarily pertain to downstream modeled changes in traffic and traffic patterns, the highway system itself, and seismic modifications to pertinent components and soils. To anticipate the next section, the basic "independent unit" of time will be a planning horizon whose duration can be the basis for each Bernoulli trial.

A.3.3 Planning Horizon

As used basically to develop statistics such as average annualized losses, the walkthrough process can be conceived of as consisting of a large number of Bernoulli trials (10,000 trials for a 10,000 year walkthrough). Models of earthquake faults in which probabilities change from year to year do not impact this case, because one can merely use the probability for the "next year."

[2] For example, in the 1936 presidential election, a straw poll of 3,000,000 respondents (without random sampling) predicted that Alf Landon would be a clear winner over Franklin Roosevelt. Modern random sampling methods would require polling of only about of about 1,000 (rather than 3,000,000) respondents, and are deemed to be much more accurate than a straw poll of a biased sample of respondents (Taylor et. al., 1998).

However, the walkthrough method is designed as a time-series method principally because it can also be used to consider modifications over different planning horizons, e.g., with durations of say 5-years, 10-years, 25-years, or 50-years. Significant modifications over time can be expected in traffic patterns and trip demands. Likewise, there may be projected changes in roadway components and links, and in their seismic resistance (through seismic upgrade, etc.).

REDARS™ 2 cannot now consider effects of such projected changes over time. However, to the extent that reliable projections can be made over various planning horizons, REDARS™ 2 can be readily extended to evaluate effects of projected changes and various alternative changes as well. For instance, one may project changes in traffic demands from year to year and projected new links in some specific years. If, for example, a five-year planning horizon is used for a 10,000-year walkthrough, then 2,000 simulations or Bernoulli trials of this five-year planning horizon can be developed.

Within this notion of a planning horizon, a non-Poissonian evaluation of the rate of occurrence on a specific fault system can be readily accommodated. Probabilities can be developed, say, for each of the next five years and, if an event is randomly picked on this fault system for any of the first four years, then the probabilities of occurrence of an event on this fault for subsequent years can be suitably reduced.

Very long planning horizons such as 50-years and 100-years are less suitable for the time-series evaluation of travel-time losses in REDARS™ 2. In particular, projections can be very unreliable for such long planning horizons. In these cases, one may use REDARS™ 2 merely to develop pertinent statistics as described in the opening paragraph of this section. These longer-term exposures are more suitably applied to the evaluation of downtimes and probabilities of various levels of damage for individual components within a highway system because such components often have long exposure periods.

A.4 DEVELOPMENT OF LOSS DISTRIBUTIONS

Once the probabilistic SRA results are obtained from the walkthrough analysis process summarized in Section A.2, they can be used to develop either total-loss distributions or conditional loss distributions, as described below.

A.4.1 Total-Loss Distribution

A total-loss distribution is a plot of loss value vs. the probability that this value will be exceeded during a designated exposure time. The process for establishing a total-loss distribution from the SRA walkthrough results is summarized below, for the general case of Y' simulations (i.e., Y' Bernoulli Trials).

- The results of the walkthrough analysis are given as an output matrix with Y' rows and two columns. In each row, the first column contains the trial number, and the second column contains the value of the total loss for that trial. In this matrix, most of the Y' rows will have no potentially damaging earthquake occurrence.

- Each of these Y' loss-severity estimates is treated as a statistical sample of the loss due to earthquake damage to the highway system. Each sample is assumed to be equally probable, with a frequency of occurrence of $1/Y'$.

- The Y' loss values are arranged in decreasing order with the highest value first, the next highest value second, and so on. Then, the i^{th} loss value L_i in this sequence is considered to have a frequency of exceedance of X_i, which is the number of occurrences of loss values equal to or greater than L_i. For example, the frequency of exceedance of the first (highest) loss value is $1/Y'$ and the frequencies of exceedance of subsequent loss values in the sequence are $2/Y'$, $3/Y'$, and so on.

- For an exposure time of T years, the probability P_i that the loss L will equal or exceed the i^{th} loss value, L_i is computed from the following Poisson equation:

$$P_i = P(L \geq L_i) = i = \exp(-TX_i) \qquad \text{(A-1)}$$

- The results of the walkthrough analysis are given as an output matrix with Y' rows and two columns. In each row, the first column contains the trial number, and the second column contains the value of the total loss for that trial.

A.4.2 Conditional-Loss Distribution

A similar procedure can be used to develop conditional loss distributions. For example, suppose that it is desired to develop loss distributions that are conditional on the occurrence of a particular earthquake event with a designated magnitude and location. Also suppose that S simulations (that account for uncertainties in estimation of seismic hazards and component damage states) are to be used to develop this conditional-loss distribution. Then, the user carries out the SRA and loss estimation for these S simulations and the fixed earthquake event. Finally, for this set of results, the user repeats the above procedure for development of a total loss distribution. This involves: (a) forming a loss matrix with S rows and two columns; (b) assuming all of the loss values have an equal probability of $1/S$; (c) ordering the loss results for each simulation in decreasing order; and (d) adapting Equation A-1 to estimate the probability of exceedance for each loss value.

-

APPENDIX B
EARTHQUAKE SCENARIOS AND WALKTHROUGH FILES

B.1 BACKGROUND

As explained in Appendix A, a key element in the walkthrough procedure is the earthquake walkthrough file. This file consists of a tabulation of randomly selected regional earthquake scenarios over time that is developed from and is consistent with established earthquake models for the region. Individual earthquake scenarios within this file can be considered in deterministic or conditional probabilistic estimates of seismic risks to the highway system, and large numbers of earthquakes within this file are used in fully probabilistic estimates of these risks.

This appendix describes the development and application of a significantly updated version of the procedure previously used to develop earthquake walkthrough files for analysis of seismic risks to the highway system in Shelby County, Tennessee (see Appendix C in Werner et al, 2000). These updates include:

- Application of more recent regional earthquake source models that were used by the United States Geological Survey (USGS) in their national probabilistic hazard mapping program (see Frankel et al, 2002 as an update on Frankel et al., 1996), along with: (a) new data for the CUS that were contributed by the Center for Earthquake Research and Information (CERI) in Memphis, Tennessee; and (b) new data for California that were provided by the California Geological Survey (CGS, the Northern California Earthquake Data Center (NCEDC) and the Southern California Earthquake Center (SCEC) in California; and

- Use of these more recent models to develop new earthquake walkthrough files for a region of the Central United States (CUS) whose seismic risks could be affected by the New Madrid seismic zone (Fig. B-1), and for Coastal California (Fig. B-2). In the future, methods similar to those described in this appendix will be used to develop walkthrough files for other regions of the United States with moderate to substantial earthquake hazards.

- Significantly more detailed specification of earthquake scenarios in order to facilitate the current and future use of a wide variety of seismic-hazard models within REDARS™ 2 for estimating site-specific ground motion, liquefaction, and surface fault rupture hazards.

- Random-areal earthquakes in each region that: (a) are assumed to occur along faults whose orientation and attributes are estimated from regional seismologic and tectonic data (see Sec. B.3.2); and (b) have epicenters that are assumed to be located at the centroid of one of the many microzones that comprise the region's total area. (In the earlier CUS walkthrough files described in Werner et al., 2000, random-areal earthquakes were assumed to have a single point source located at the center of one of these microzones.)

These three updates, especially the third, have not only required substantially more data and new assumptions, but have also raised several new scientific and statistical issues pertaining to what constitutes an appropriate level of detail of the modeling of the faults relative to potential hypocenter depths and centers of energy release. Such issues include:

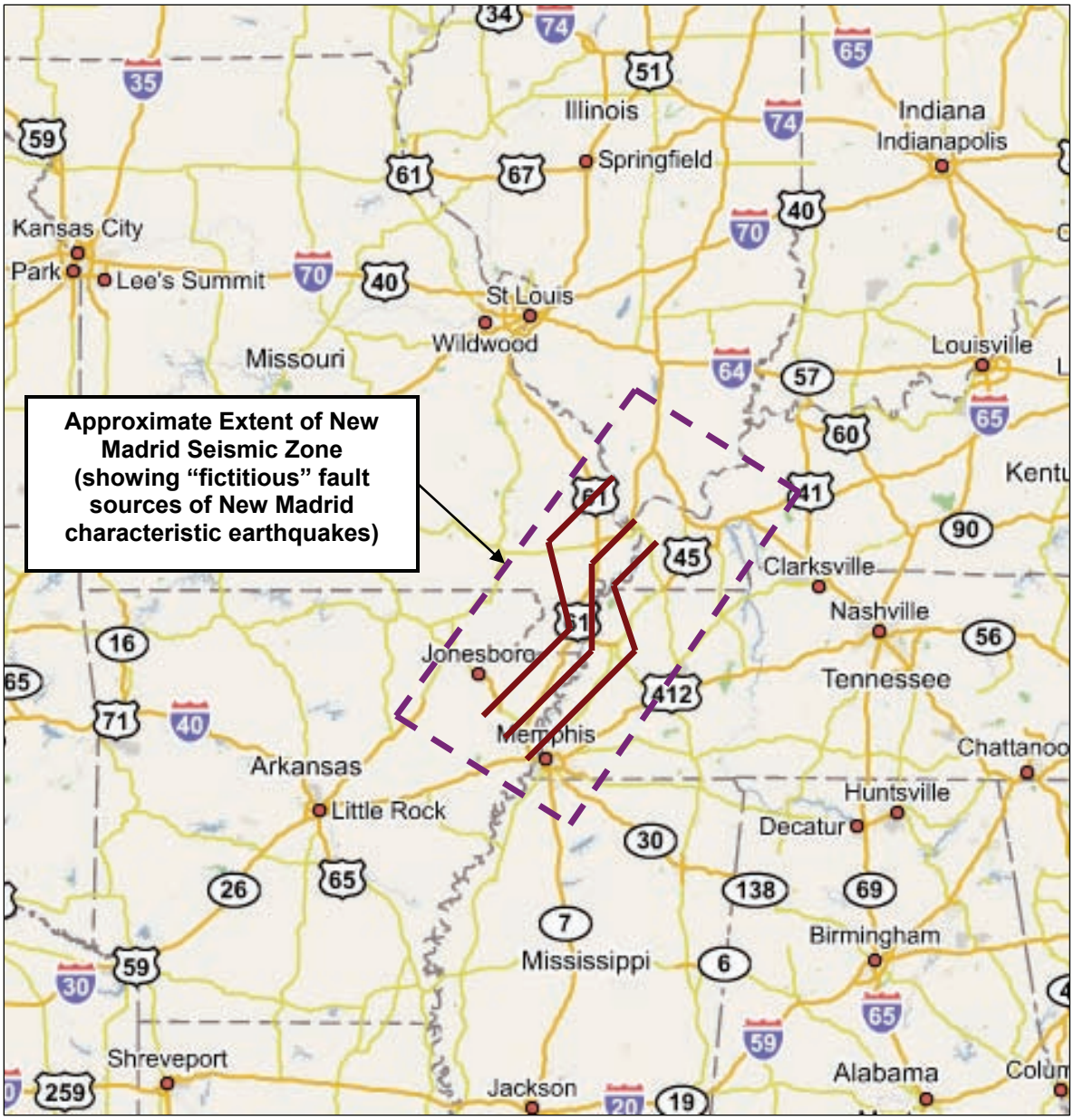

Source: http:///maps.google.com

Figure B-1.
Region covered in this Earthquake Walkthrough File for Central United States

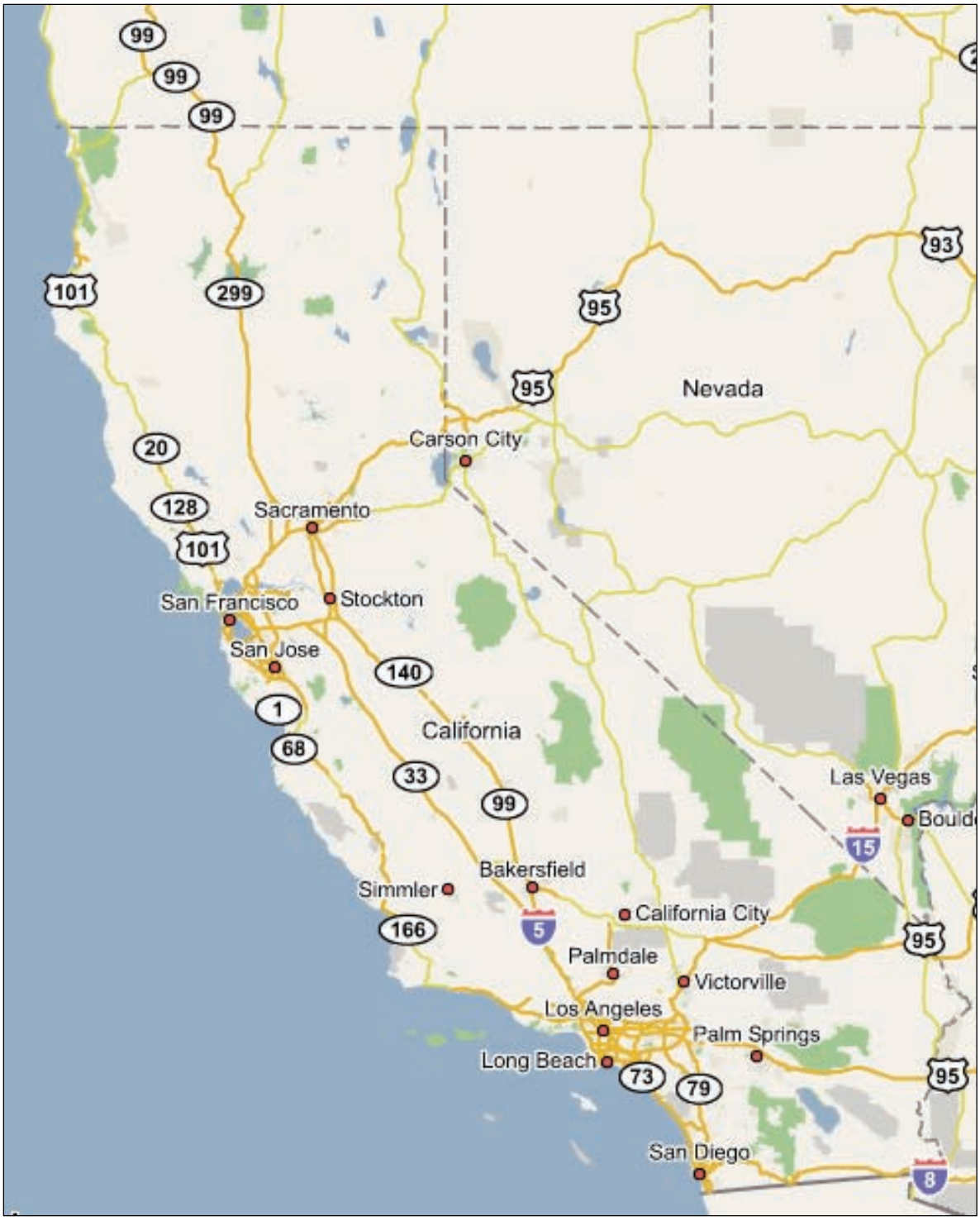

Source: http:///maps.google.com

Figure B-2.
Region Covered in this Earthquake Walkthrough File for Coastal California

- Are the rectangular models of fault planes that are used in this current development to achieve these updates too complex (given past earthquake data) or too simple (given more detailed modeling of specific earthquakes that is currently available)?

- Can strike-slip faults in California generate major earthquakes yet not create significant surface ruptures owing to hypocenters that exceed fault plane widths?

- What are predominant strike angles and/or azimuths for random earthquake sources? And

- How many fault segments are required for a sufficiently accurate representation of specific major faults?

These outstanding issues should be addressed in future development of further improvements to the earthquake walkthrough modeling procedure described in this appendix.

The remainder of this appendix contains three main sections. Section B.2 describes how general locations, moment magnitudes, and year numbers are specified for earthquakes in the CUS and Coastal California regions. Next, Section B-3 summarizes how a rectangular model of the real or hypothetical causative fault is defined in terms of that fault's rupture length, rupture zone, and dip angle are specified for the causative fault for each fault-based scenario earthquake, along with the earthquake's epicenter, hypocenter, seismogenic depth, and center-of-energy release. Finally, Section B-4 illustrates the end results of this walkthrough-file development process in terms of: (a) displays of walkthrough data for a few years of actual walkthrough files; (b) comparisons of earthquake-occurrence rates from the earthquakes included in the walkthrough files for the coastal California and CUS region; and (c) figures that show the spatial distribution of the earthquakes that were generated for the two regions.

B.2 SELECTION OF EARTHQUAKE LOCATIONS, MAGNITUDES, AND WALKTHROUGH YEAR NUMBERS

The procedure that has been used in this project to develop earthquake locations, magnitudes and year numbers for the CUS and coastal California regions consists of the five steps that are summarized in the following subsections.

B.2.1 Step 1: Define Basic Information needed for Characterizing Scenario Earthquakes

Step 1 defines the basic data that are needed to characterize scenario earthquakes in the walkthrough file that are associated either with known active fault systems having a specific number of fault segments or with random sources. These data include, hypocenter depths, azimuths, strike angles, minimum and maximum moment magnitudes, and coefficients used to estimate frequencies of occurrence of various earthquake magnitude levels. The major source of these data is updated files developed by the USGS and used in the Frankel et al. (2002) national seismic hazards mapping. As noted earlier, these USGS data are supplemented by seismic information from CGS; NCEDC, and SCEC in California, and from CERI in Memphis, Tennessee (see Sections B.2.1.1 and B.2.1.2).

B.2.1.1 Coastal California Earthquakes

The USGS earthquake models for Coastal California include 171 known active faults that are each modeled as a single segment with a fixed dip angle. Some of these faults are modeled as being "characteristic", i.e., with a surface fault rupture that is identical to the fault trace, a highly constrained earthquake magnitude level, and specified rates of earthquake occurrence. Other faults are modeled as being characteristic some of the time and random (or non-characteristic) on other occasions, i.e., with a surface fault rupture whose location and length along the fault trace is variable, and with a less constrained earthquake magnitude level. For those faults treated as being random, "a" values are provided in accordance with the following Gutenberg-Richter equation

$$\log_{10} M_w = a - bM_w \tag{B-1}$$

where N is the frequency of earthquake occurrence, M_w is the moment magnitude, and "a" and "b" are coefficients to be determined. In this, USGS specifies a "b" value of 0.8 for all active faults in California. The USGS also provides maximum magnitudes for those faults treated as being random, and specifies a minimum magnitude of 6.5 for these randomly-selected faults.

To supplement these USGS data, additional data on fault "azimuths" have been gathered from CGS (2005) in order to aid in the estimation of the predominant direction of dipping faults. In addition, a sample of hypocenter depths have been developed by combining curated data from NCEDC (2005) and SCEC (2005). In this, slight differences in hypocenters depths between northern and southern California have been ignored. Finally, the earthquake model constrains the locations of the centers-of-energy-release to lie within the bottom half of the fault rupture plane.

For random areal faults, USGS data subdivide the coastal California regions into a series of square microzones with a side dimension of 11.1 km, and provide earthquake-occurrence data for these regions. These data include separate "a" values for various groupings of the microzones, along with a fixed "b" value of 0.8 in Equation B-1 for all microzones. The maximum magnitude is given as 7.0, and this project assumes a minimum magnitude of 5.0. As noted previously, and in accordance with Frankel et al. (2002), the earthquake scenarios from random areal sources are considered to have a randomly estimated fault rupture length, which, of course, will be short for smaller magnitude earthquakes. Moreover, the fault plane is modeled as rectangular, in accordance with Section B.1.

B.2.1.2 Central United States Earthquakes

The updated USGS model for the Central United States (CUS) that is described in Frankel et al. (2002) includes changes in the mean recurrence time, characteristic magnitude, and spatial distribution of New Madrid sources of large earthquakes. These changes are summarized below:

- The mean recurrence time for the characteristic earthquakes in New Madrid is now estimated to be 500 years, as opposed to the 1,000-year recurrence time for magnitude 8.0 earthquakes that was used in the 1996 model.

- The characteristic magnitude for the large earthquakes in the New Madrid seismic zone is now represented by a logic tree with the following weights: $M_w = 7.3$ (0.15 weight), $M_w = 7.5$ (0.2 weight), $M_w = 7.7$ (0.5 weight), and $M_w = 8.0$ (0.15 weight). These weights are meant to characterize the current range of expert opinion regarding the magnitude of the largest events of the 1811-1812 earthquake sequence. The 1996 USGS model assumed that these earthquakes had a characteristic magnitude of 8.0.

- In both the 1996 and 2002 models, the source of the New Madrid characteristic earthquakes is represented by three "fictitious sources" that consist of a fault trace that matches recent micro-earthquake activity and two adjacent sources that are located near the borders of the Reelfoot Rift (see Fig. B-1). In the 1996 model, these three sources were equally weighted whereas, in the 2002 model, the center fault is given twice the weight of the two side faults. The effective recurrence rate for these faults after weighting (1.0×10^{-3} per year for the center fault and 0.5×10^{-3} per year for the side faults) sum to a total recurrence rate of 1/500 per year.

In this adaptation of the USGS model for use with REDARS™ 2, the above three fictitious sources within the New Madrid seismic zone are the only faults that are included. The Wabash Valley Fault, which was previously modeled specifically, is now represented as a small random areal source zone.

In addition to the fictitious faults within the New Madrid seismic zone, the model includes random-areal sources over a very large rectangular area that covers portions of the CUS up through the most northern latitudes in the USGS files (see Fig. B-1). This area is subdivided into 11.1 km square microzones which are used to define the locations of all of the random-areal earthquakes in the USGS files that are within at least 400 km of either St. Louis, Missouri or Memphis, Tennessee. Also, the magnitudes and recurrence rates for these earthquakes depend on where their epicenter is located relative to two large macrozones that are contained in the USGS model for the CUS. These macrozones intersect the general New Madrid seismic zone (see Fig. B-1) and have diverse maximum-magnitudes and "b" values in Equation B-1. Thus, it has been necessary to retain these different values in the microzones used in this project. The USGS files also contain "a" values for the various 11.1 km squared microzones.

Supplementing this information are hypocentral-depth data from the CERI (2005), catalogue of magnitude 3+ earthquakes that have occurred in the CUS between 1974 and 2005. These data are used in the designation of random causative faults for each areal earthquake. In the absence of causative-fault data for CUS earthquakes, fault dip-angles and azimuths for these earthquakes were estimated from USGS data for California faults. These areal earthquakes are assumed to have a lower-bound magnitude of 5.0, although it is arguable that such an earthquake magnitude can damage vulnerable highway structures over a large region of the CUS area that is shown in Figure B-1.

B.2.2 Step 2: Define Duration (Number of Walkthrough Years) and Planning Horizon (Exposure Time) to be Considered.

The earthquake walkthrough file developed for Coastal California, has a duration of 10,000 years whereas, for the region of the CUS that is shown in Figure B-1, a walkthrough duration of 50,000 years is used. This difference results from the greater overall seismicity in the Coastal California region, and the need for the walkthrough file for each region to include a sufficient number of potentially-damaging earthquake scenarios (which are scenarios that damage the region's highway systems, and are assumed here to correspond to earthquakes with a moment magnitude (M_w) of 5.0 or greater). For this reason, the 10,000-year walkthrough file for coastal California contains over 28,000 potentially damaging earthquakes, whereas the 50,000-year walkthrough file for the CUS contains a much smaller number (more than 17,00) of potentially damaging earthquakes (see Section B.4.2).

The large number of so-called "potentially-damaging" earthquake scenarios in the walkthrough file for each region should not be construed as implying that all of these earthquakes will actually damage the highway system being analyzed. This is because these earthquakes can occur throughout a very large region and, as a result, many of the earthquakes will not be sufficiently close to any single highway system to actually damage that system. In addition, the structural resistances/capacities of the bridges and other components in a typical highway system are expected to withstand smaller and more distant earthquakes without damage.

B.2.3 Step 3. Determine Number of Potentially Damaging Earthquakes during Each Year-in Walkthrough Table

When a walkthrough table is developed for a large region, such a region will typically contain several sets of active-fault and areal-zone earthquake sources for known active faults and for random areal events respectively. Each of these sets will have its own overall mean rate of occurrence of potentially damaging earthquakes (again, assumed here to correspond to an earthquake with M_w of 5.0 or greater). Therefore, the following procedure for estimating the total number of earthquake occurrences during each year of the walkthrough is applied separately for each of these fault/areal-source zone sets. The total number of earthquake scenarios for each specific year is then computed as the sum of the earthquake scenarios developed from each of these fault/areal-source sets.

In the procedure used here, the rate of occurrence of potentially damaging earthquakes along a given active fault or areal zones is assumed to follow a Poisson process as represented by the following equation:

$$P(i) = \frac{\lambda^i \exp(-\lambda)}{i!} \tag{B-2}$$

where i is the number of earthquakes occurrences during a given year with $M_w \geq 5.0$, $P(i)$ is the probability of occurrence of i such earthquakes during a given year, and λ is the overall rate of occurrence of earthquakes with $(M_w) \geq 5.0$. Therefore, the probability of occurrence of zero or

one damaging earthquakes during each year -- denoted as *P(0)* and *P(1)* respectively -- is obtained by setting $i = 0$ or 1 in Equation B-2, which results in the following expressions:

$$P(0) = \exp(\lambda) \quad \text{and} \quad P(1) = \lambda \exp(-\lambda) \tag{B-3}$$

From this, the probability of occurrence of one or more earthquakes and two or more earthquakes during a given year -- denoted as $P(i \geq 1)$ and $P(i \geq 2)$ respectively -- is calculated as

$$\begin{aligned} P(i \geq 1) &= 1 - P(0) = 1 - \exp(-\lambda) \\ P(i \geq 2) &= 1 - P(0) - P(1) = 1 - (1 + \lambda)\exp(-\lambda) \end{aligned} \tag{B-4}$$

where P(0) > P(1) > P(2) etc. In addition, it is, of course, possible to use Equation B-2 to compute the probability of occurrence of 3 or more earthquakes, 4 or more earthquakes etc. during a given year. The REDARS™ 2 walkthrough files for coastal California and the CUS can accommodate the occurrence of larger number of earthquakes during a year although, even though the areas of these regions are very large, occurrences of more than one earthquake in a single year is extremely rare.

The calculation of $P(i \geq 1)$ and $P(i \geq 2)$ is illustrated by considering the earthquake model for the very large CUS region that is shown in Figure B-1. For this region, it turns out that $\lambda = 0.344$ for areal sources and $\lambda = 0.002$ for the virtual line sources used to represent the New Madrid faulting events. The resulting values of $P(i \geq 1)$ and $P(i \geq 2)$ are given in Table B-1.

Table B-1. Probabilities of Earthquake Occurrence in Random Areal Source and along Linear Source for CUS Region Considered Here

Probability	Earthquakes in Areal Source ($\lambda = 0.3441$)	Earthquakes along Linear Source ($\lambda = 0.002$)
$P(i \geq 1)$	0.291	0.002
$P(i \geq 2)$	0.047	negligible

Next, a uniform random number between 0 and 1 is generated and with the above probabilities to determine the number of earthquakes that occur along an areal source anywhere in the CUS region during a given year. For example, if this uniform random number is greater than 0.291, then no earthquake occurs in any of the random areal zones during the given year. If the random number is between 0.0291 and 0.047, then one earthquake is considered to occur in one of the random areal zones during the year. Finally, if the number is less than 0.047, two earthquakes are assumed to occur in the one of the areal zones during the year. Equation B-2 is

applied so that one can estimate even a very large number of earthquakes in a specific year, until the likelihood of that number becomes negligible.

This process is then repeated to determine the number of earthquakes that occur along one of the virtual linear sources for New Madrid faulting events during the same year. In this, another uniform random number between 0 and 1 is generated. If this random number exceeds 0.002 (referring to Table B-1), no earthquake is considered to occur along any of the linear sources during the given year. If the number is equal to or less than 0.002, then one earthquake is assumed to occur along one of the linear sources during the year.

Table B-2 shows how the walkthrough procedure can be used to determine whether a potentially damaging earthquake has occurred during a given year relative to either an areal zone or a linear source.. The procedure begins with Year 1. Suppose that, for this year, the uniform random number that is selected for the random areal zone is 0.136. Then, since this number is between 0.047 and 0.291, one earthquake occurs in an areal zone within the region during Year 1, since this random number is between 0.047 and 0.291. Suppose further that the random number selected for the New Madrid faulting event is 0.138. Then, since 0.138 > 0.002, no New Madrid fault event occurs during the year. As illustrated in Table B-2, this process is repeated for each year of the walkthrough.

Table B-2. Determination of Number of Potentially Damaging Earthquakes During Given Year

Year	Areal Zone		Linear Source (New Madrid Faults)	
Year	Random Number	Number of Earthquakes	Random Number	Number of Earthquakes
1	0.136	1	0.138	0
2-12	> 0.291	0	0.835	0
13	0.032	2	--	0
14	0.457	0	0.083	0
15	0.083	1	0.482	0
16-17	> 0.291	0	0.857	0
18	0.089	1	0.078	0
19-20	> 0.291	0	0.621	0
21	0.178	1	0.711	0
22-28	> 0.291	0	0.183	0
etc.	etc	etc	etc.	etc.
388	0.428	0	0.0018	1

Now, assume that similar results occur for Years 3 through 12. Then, in Year 13, suppose the first random number that is generated has a value of 0.032, and the second random number has a value of 0.162. Since the value of the first random number is less than 0.047 and the second random number exceeds 0.002, two potentially damaging earthquakes occur in an areal source and no earthquakes occur along a line source during Year 13.

As this process proceeds for each subsequent year of the walkthrough, Table B-2 shows that during Year 388, the second random number has a value of 0.0018. Since this number is less than 0.002, a potentially damaging earthquake is considered to have occurred during that year, along one of the virtual line sources used to model the New Madrid fault zone.

B.2.4 Step 4. Determine Source for Each Earthquake Scenario

For both coastal California and the CUS regions, Step 3 implies that USGS files permit the development of rates of occurrence for specific magnitudes (say, $M_w = 5.0$ and above) for all microzones and faults modeled.

For all such zones and faults, one can develop for each of these regions a cumulative conditional probability distribution. This is a cumulative probability distributions (ranging from 0 to 1.0) dependent on the occurrence of some earthquake. For instance, if the rate of occurrence in one zone (or fault) is 0.004 events equaling or exceeding 5.0 per year and the rate of occurrence in another zone (or fault) is 0.002 events per year, then the former will be twice as likely to occur as the latter. For each earthquake scenario identified in Step 3, a uniform random generator is then applied to such a cumulative conditional probability distribution in order to derive which fault or random areal zone is the source of the scenario.

To illustrate the procedure for identifying the areal zone associated with a potentially damaging earthquake, Table B-3 shows, for a hypothetical set of 20 zones, probabilities of occurrence of an earthquake within one specific zone, given that one earthquake occurs within the 20 zones. This table indicates that the probability of occurrence of a potentially damaging earthquake (i.e., an earthquake with $M_w \geq 5.0$) is 0.045 in Zone 1. This table also shows that the cumulative conditional probability of occurrence of a postulated earthquake in Zones 1 or 2 is 0.098, in Zones 1, 2, or 3 is 0.137, and so on.

To use these cumulative probabilities to assign the earthquake to a specific areal zone, a uniform random number between 0 and 1 is generated. Then, in order to establish the zone where the earthquake occurs, this random number is compared to the range of cumulative conditional probabilities that are shown for each zone in Table B-3. For example, suppose that a uniform random number with a value of 0.43 is generated. Then, Table B-3 shows that this corresponds to a potentially damaging earthquake that is located in Areal Zone 10.

A similar approach is used to identify the location of the fault-based earthquake in the New Madrid seismic zone that occurs during Year 388. As shown in Figure B-1, that zone is represented by three fictitious fault traces, and it is desired to determine which trace is the source of the fault-based earthquake that occurred during Year 388. This is determined by assigning cumulative conditional probabilities of earthquake occurrence along each fault trace, in

accordance with the relative earthquake occurrence rate for each trace. As noted in Section B.2.1.2, UGSG has assumed that earthquakes are twice as likely to occur along the central fault trace (Trace 2) than along the two outer traces (Traces 1 and 3). The resulting cumulative-conditional probabilities for each trace are listed in Table B-4.

Table B-3. Illustrative Cumulative Conditional Probabilities of Occurrence of Potentially Damaging Earthquake in Hypothetical Set of 20 Areal Zones

Zone	Cumulative Conditional Probability	Zone	Cumulative Conditional Probability
1	0.000 – 0.045	2	0.046 – 0.098
3	0.099 – 0.137	4	0.138 – 0.167
5	0.168 – 0.212	6	0.213 – 0.267
7	0.268 – 0.313	8	0.314 – 0.360
9	0.361 – 0.404	10	0.405 – 0.446
11	0.447 – 0.491	12	0.492 – 0.540
13	0.541 – 0.593	14	0.594 – 0.645
15	0.646 – 0.699	16	0.700 – 0.753
17	0.754 – 0.811	18	0.812 – 0.877
19	0.878 – 0.933	20	0.934 – 1.000

Table B-4. Cumulative-Conditional Probabilities of Earthquake Occurrence along Virtual Fault Traces used to Model New Madrid Fault Zone

Virtual Fault Trace	Cumulative Conditional Probability of Earthquake Occurrence
1 (outer trace)	0.000 – 0.249
2 (central trace)	0.250 – 0.750
3 (outer trace)	0.751 – 1.000

To use Table B-4 to establish which virtual fault trace is the source for this particular earthquake, a uniform random number with a value between 0 and 1 is generated. This number is then compared to the cumulative conditional probabilities in Table B-4. For example, if the random number has a value of 0.45, then the earthquake is centered along Trace 2. In Step 3, the location of the rupture zone along this trace is established concurrently with the estimation of the moment magnitude of the earthquake (see section A.3.3).

This approach is also used to identify the causative fault for a fault-based earthquake in Coastal California. In this, each fault in the region is weighted according to its earthquake occurrence rate relative to the rate for each of the other faults in the region. A cumulative probability distribution is developed from these weights, and this distribution can be displayed in

a table whose format is very similar in that shown in Table B-4. Then, as before, a random number between 0 and 1 is generated and compared to the cumulative probabilities for each fault, in order to identify the causative fault for any postulated fault-based earthquake.

B.2.5 Step 5. Determine Magnitude for Each Earthquake Scenario

Once earthquake occurrences and their locations are identified for each year of the walkthrough, the moment magnitude of each of these earthquakes is then estimated. This estimation will depend on whether a given earthquake is associated with a characteristic fault, non-characteristic fault, or random-areal earthquake source, as summarized below.

B.2.5.1 Treating a Known Active Fault Characteristically

A known active fault that is treated characteristically generates earthquakes whose best-estimate of the moment magnitude (say, from 6.5 to 7.9 along coastal California) has a highly constrained uncertainty (± 0.2) with an upper-bound magnitude of 8.0. In addition, the surface fault rupture length is assumed to extend over the entire length of the fault trace.

B.2.5.2 Treating a Known Active Fault Non-Characteristically

A known active fault that is treated non-characteristically generates earthquakes whose magnitudes are less constrained and whose fault-rupture length extends over only a portion of the fault trace. In their Coastal California earthquake model, USGS uses a lower-bound magnitude of 6.5 for earthquakes along known active fault that is treated non-characteristically, and specifies a separate upper-bound magnitude for each fault. The earthquake-occurrence rate for each fault is estimated from the previous Gutenberg-Richter equation

$$\log_{10} N = a - bM_w \tag{B-5}$$

where N is the number of earthquakes per year whose moment magnitude $\geq M_w$, "b" is assumed by USGS to be 0.8 for all non-characteristic faults in the coastal California region, and USGS files provide a separate value of "a" for each non-characteristic fault in the region.

From these assumptions, one can construct a cumulative conditional probability distribution for the occurrence of earthquakes whose moment magnitude is between a specified lower-bound and upper-bound moment magnitude for a known active fault treated non-characteristically. This probability, or relative frequency, is computed as:

$$P(M_i < M_w \leq M_{i+1}) = \frac{N_{i,i+1}}{N_{tot}} \tag{B-6}$$

where $N_{i,i+1}$ is the total number of earthquakes between moment magnitudes M_i and M_{i+1} along the fault, and N_{tot} is the total number of earthquakes between the fault's specified lower-bound and upper-bound moment magnitudes.

Table B-5 shows the conditional probabilities established for 12 moment-magnitude increments (with magnitude increments of 0.1) for earthquakes along a hypothetical fault that is treated non-characteristically. The lower-bound and upper-bound magnitudes for this fault are assumed to be 6.5 and 7.5 respectively, and the "*b*" value in Equation B-5 is assumed to be 0.8.

Table B-5. Cumulative-Conditional Probabilities for Earthquake Magnitudes along Hypothetical Fault Treated Non-Characteristically*

Moment Magnitude, M_i	Cumulative-Conditional Probability of Occurrence of Earthquake with Magnitude ≥ M_i	Moment Magnitude, M_i	Cumulative-Conditional Probability of Occurrence of Earthquake with Magnitude ≥ M_i
6.5	[1.000 – 0.806)**	6.6	[0.805 – 0.644)
6.7	[0.644 – 0.510)	6.8	[0.510 – 0.398)
6.9	[0.398 – 0.306)	7.0	[0.306 – 0.229)
7.1	[0.229 – 0.164)	7.2	[0.164 – 0.111)
7.3	[0.111 – 0.067)	7.4	[0.067 – 0.030)
7.5	[0.030 – 0.000]		

* ,These results assume b = 0.8 and lower-bound and upper-bound moment magnitudes of 6.5 and 7.5 respectively.

** "[" denotes a closed interval and ")" denotes an open interval.

In general, to obtain the moment magnitude for a scenario earthquake along a fault treated non-characteristically, one can use a uniform random number along with a table like Table B-5.

In the USGS model for the New Madrid virtual faults, Frankel et al. (2002) have assumed weights of 0.15 for M_w = 7.3, 0.2 for M_w = 7.5, 0.5 for M_w = 7.7, and 0.15 for M_w = 8.0. From these assumptions, one can use a uniform random number along with the development of a cumulative conditional probability distribution (Table B-6) in order to obtain the moment magnitude for a scenario earthquake occurring in the New Madrid seismic zone.

Table B-6. Probabilities for Magnitudes of Earthquakes along New-Madrid Virtual Faults

Moment Magnitude	Cumulative Conditional Probability of Earthquake Occurrence
7.3	(0.000 – 0.150]*
7.5	(0.150 – 0.350]
7.7	(0.350 – 0.850]
8.0	(0.850 – 1.000]

* "]" denotes a closed interval and "(" denotes an open interval

B.2.5.3 Random-Areal Sources

For earthquakes generated in a particular microzone that has been generated under Step 4 of this procedure (see Section B.2.4), Equation B-1 can be used to develop a conditional cumulative probability distribution for moment magnitudes between the specified lower-bound and upper-bound values for that microzone. In the USGS model, earthquakes generated by a random-areal source within a given microzone are: (a) universally assumed to have a lower-bound moment magnitude of 5.0; and (b) are characterized by a "b" value and an upper-bound moment magnitude that depends on the general tectonic zone within which the microzone is located. It is noted that there are two separate tectonic zones that intersect the general New Madrid region, and a different conditional cumulative probability distributions is generated for each of these zones. Only one tectonic zone is modeled in the coastal California region.

Once this probability distribution for each tectonic zone is developed, a uniform random number is generated and used with the cumulative distribution for earthquake locations within the relevant region. From this, a moment magnitude for the earthquake scenario is identified.

B.3 PHYSICAL SPECIFICATION OF EARTHQUAKE SCENARIOS

B.3.1 Background

An important difference between the updated walkthrough files described in this appendix and the previous walkthrough files described in Werner et al. (2000) is that the scenario earthquakes in the updated files are specified in greater detail. Reasons for this include:

- The requirement in more recent USGS developments that earthquake sources in the CUS be represented as minimum-length fault ruptures rather than , say, a single-point epicenter.

- Future upgrades of the REDARS™ 2 software will include a library of established ground-motion models for each region of the country. These upgrades will enable users to select a preferred model for their particular REDARS™ application, and will also facilitate sensitivity evaluations of the effects of alternative ground-motion models on the results of the REDARS™ 2 application. However, the various ground motion models use different definitions of the "distance" from a site to the earthquake source. These include distance to the epicenter, hypocenter, center-of-energy release, or surface rupture and also distance to a projection of the fault plane or to the fault plane itself. In addition, some ground-motion models require a distinction between footwall and hanging wall, and more recent models directly incorporate a directivity effects that require the determination of additional earthquake attributes. To enable REDARS™ to accommodate this range of ground-motion models in the future, calculations of these various distance measures have been programmed into the software (see Section D.2 of Appendix D). Therefore, more earthquake specifications are required now than in previous REDARS™ 2 developments.

- REDARS™ 2 includes state-of-practice models to estimate permanent ground displacements due to liquefaction and surface fault-rupture hazards. Such models require greater specificity in the earthquake modeling than was previously used.

Figure B-3 provides a perspective of the earthquake-scenario dimensions developed in the current work (along with directivity parameters discussed in Appendix D). These additional dimensions enable a user to select from a library of ground-shaking and ground-displacement models that will be built into REDARS™ in the future. To minimize arbitrariness in the development of such detailed scenario models -- i.e., arbitrariness that would arise if deterministic dimensions were used and uncertainties were ignored -- as much randomness has been included into these models as possible. This is described in the following section.

B.3.2 Models for Random Estimation of Earthquake Scenarios

B.3.2.1 General Approach

In order to develop the level of specificity required for current REDARS™ 2 applications, various models and data are needed. In cases in which models are not well-developed, data are in the current work typically bootstrapped; i.e., they are sampled randomly with replacement from data-sets that include only higher quality data (e.g., many estimates of earthquake depths are of poor quality). (See Efron and Tibshirani, 1993 and Davison and Hinkley, 1998 for descriptions of bootstrap methods.)

B.3.2.2 Fault Rupture Length

The Wells and Coppersmith (1994) model is used to estimate fault rupture length as a function of moment magnitude, including effects of uncertainties:

$$\log_{10} RUP = -3.22 + 0.69 M_w + \varepsilon_1 \qquad \text{(B-7)}$$

where RUP is the surface fault rupture length (km), M_w is the moment magnitude, and ε_1 is an uncertainty factor that is normally distributed with an assumed standard deviation of 0.22.

B.3.2.3 Fault Rupture Width

The fault rupture width is computed as a function of the rupture displacement, seismic moment and moment magnitude, and material shear modulus, according to the following steps:

- Compute the surface fault displacement, D (in meters) including effects of uncertainties by using the following equation from Wells and Coppersmith (1994):

$$\log_{10} D = -5.46 + 0.82 M_w + \varepsilon_2 \qquad \text{(B-8)}$$

  in which ε_2 is a normally-distributed uncertainty factor with a standard deviation of 0.22..

- Compute the seismic moment M_o (in newton-meters) as a function of the moment magnitude M_w by using the following expression from Hanks and Kanamori (1979) and Bolt (1993):

$$\log_{10} M_o = 1.5(M_w + 6.0) \qquad \text{(B-9)}$$

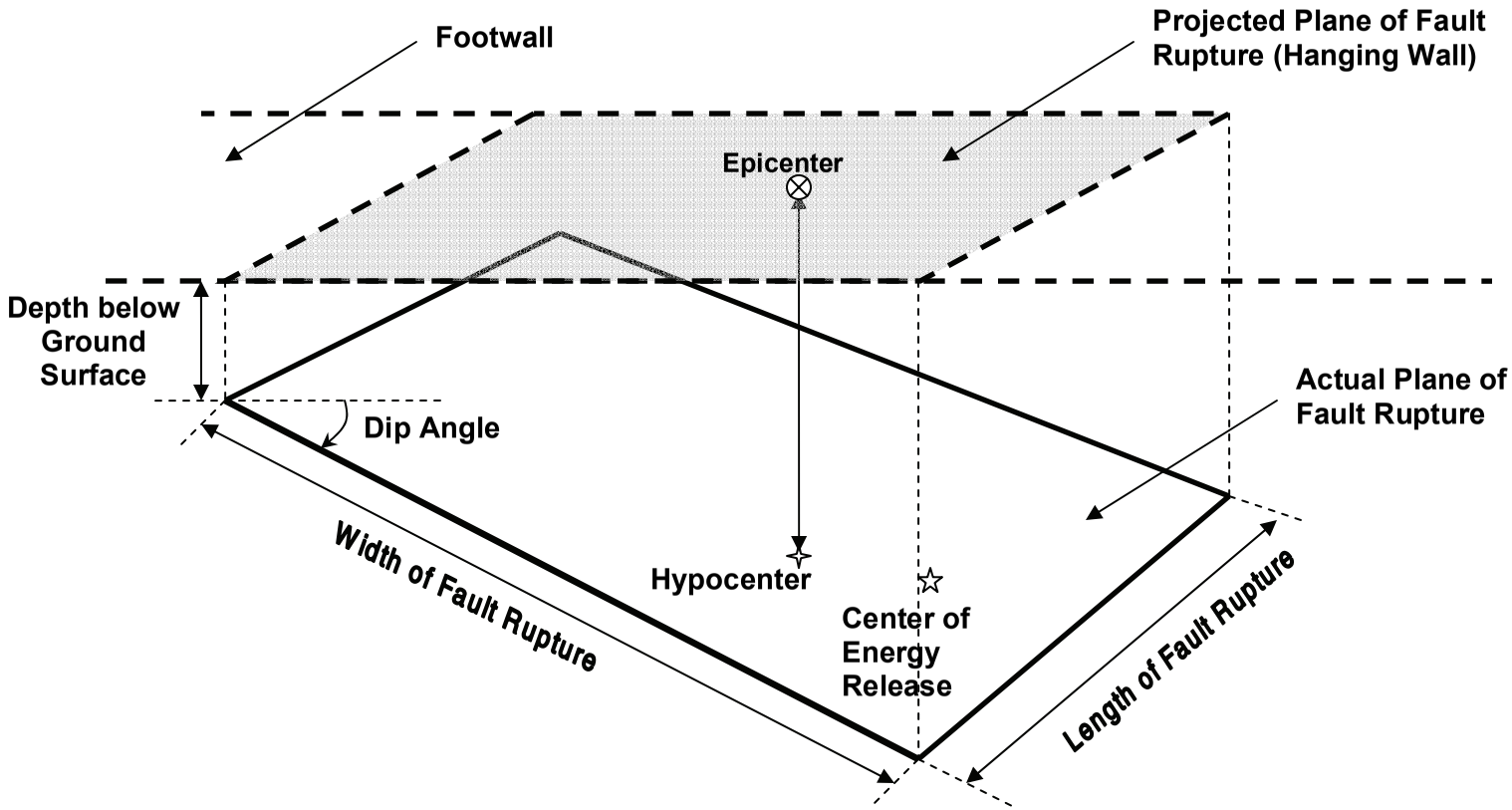

Figure B-3.
Detailed Earthquake Characterizations in REDARS™ 2 Walkthrough Files

- Compute the seismogenic rupture area A (in square kilometers) as a function of the seismic moment Mo, the shear modulus of rock μ (in dyne-centimeters), and the surface fault displacement D (in meters).

$$A = \frac{10^{-5} * M_o}{\mu * D} \tag{B-10}$$

where the rock shear modulus μ is estimated to be on the order of 3 x 10^{11}, and the fault rupture displacement *D* corresponds to the relative displacement between the two sides of the fault (here construed, without adjustment, as the average displacement derived from Equation B-7 when uncertainty is properly taken into account).

- Compute the fault width of the seismogenic rupture plane, *W* (in meters), from the above seismogenic rupture area *A* and the fault rupture length *RUP* as computed by Equation B-6.

$$W = \frac{A}{RUP} \tag{B-11}$$

In practice, the above relationships among the rupture length, moment magnitude, seismic moment, rupture area, and fault width will need to be constrained,, because the uncertainties in the rupture length as determined from Equation B-7 may yield unreasonable estimates of the fault width. In general, constraints on these relationships require further scientific evaluation. For example, such constraints are needed if, for a given moment magnitude, the fault rupture length is estimated to be very long. Based on the foregoing equations, this very long fault rupture length would result in a very small fault width, given the area of the fault plane consistent with the moment magnitude. (For more progress on these matters, see Mai and Benoza, 2000.)

B.3.2.4 Dip Angles, Azimuths, Strike Angles, Hypocenter Depths, and Directivity

In the Coastal California and CUS walkthrough files developed for use with REDARS™ 2 random techniques based on current knowledge and judgment have been used to estimate required causative-fault and earthquake-location attributes: (a) for those fault-based earthquakes for which these attributes were not included in the USGS files; and (b) for all earthquakes associated with random-areal sources. These random techniques are summarized as follows:

- *Dip Angles*. For random-areal sources in the coastal California region, dip angles were bootstrapped from dip-angle data for the 171 California faults that are included in the USGS database. In the absence of additional information, these data were also bootstrapped to estimate dip angles for random-areal sources in the CUS region.

- *Strike Angles*. For random-areal sources, strike angles were derived from the use of uniform random variates. No predominant directions of strike were assumed.

- *Fault Azimuths for Dipping Faults.* For faults with dip angles other than 90 degrees, nominal azimuths for known faults in the coastal California region were derived from California Geologic Survey data (CGS, 2005). For random-areal sources in Coastal California, nominal azimuths were bootstrapped from these CGS data. For random-areal sources in the CUS, nominal azimuths were developed by use of uniform random variates. .

- *Earthquake Hypocenter Depths.* For random-areal earthquake scenarios in the Coastal California region, hypocenter depths were bootstrapped from "Quality A" data from the Southern California Earthquake Center (SCEC, 2005) and the Northern California Earthquake Data Center (NCEDC, 2005). Slight differences between hypocenter depths for earthquakes in Northern and Southern California were ignored. For the CUS, hypocenter depths were bootstrapped from data provided by the Center for Earthquake Research and Information (CERI, 2005).

- *Earthquake Epicenter Locations.* Uniform random variates were used to determine epicenter locations relative to the surface fault rupture line. For dipping faults, the hypocenter depth and trigonometry procedures were used to determine the location of the epicenter on the projection of the fault plane on the earth's surface. For random areal sources, epicenters along with corresponding fault planes were re-oriented trigonometrically so that these epicenters were at the centers of their microzone.

- *Earthquake Center-of-Energy-Release Locations.* Uniform random variates along with calculations that emphasize lower-than-median depths were used to locate the center-of-energy release. Further development of procedures to develop more definitive estimates of the center-of-energy release is recommended.

- *Predominant Seismic-Wave-Propagation Directions.* The predominant direction of seismic waves is assumed to be "upwards" (towards the footwall) for dipping faults and to be toward the fault segment end farthest from the epicenter for strike-slip faults.

In the future, the uncertainties implied by the above random techniques can be reduced as improved scientific data and models for overall regions and for specific faults are developed (e.g., improved definitions of fault systems, expanded earthquake-catalogue data, improved methods to relate data to specific earthquake scenarios.).

B.4 WALKTHROUGH FILES DEVELOPED TO DATE

B.4.1 Walkthrough File Data

Table B-7 provides a portion of the walkthrough file (from Years 73 through 77) that has been developed for a REDARS™ 2 seismic risk analysis of the northern and central Los Angeles area within the overall Coastal California region. This file lists all of the source and earthquake data that are contained in the walkthrough file for each earthquake occurring during each year of the walkthrough. All earthquake scenarios developed for Coastal California are assumed at this time to be generated by one single fault-rupture segment. Multi-segment fault modeling is developed only for the New Madrid faults within the CUS walkthrough file.

Table B-7. Data Contained in Walkthrough Files as shown by Portion of File developed for REDARS™ 2 Analysis of Northern Los Angeles Roadway System

Fault/ Earthquake Data		Walkthrough Year			
Type	Description/Units	73	75	76	77
EQ Number during Year	Can be 0, 1, 2 or more.	1	1	1	1
Moment Magnitude	--	5.2	7.4	7.2	6.8
Fault Style	Integer from 1-4 (1 = strike-slip fault, 2 = reverse fault, 3 = normal fault, 4 = other (e.g., reverse oblique)	1	1	2	2
Fault Number	Random sources are numbered "0".	0	137	156	108
Fault Name	--	random	San Andreas	Sierra Madre	Oak-Ridge
No. of End-End Segments defining Fault Rupture	One segment now used for coastal CA faults. Multi-segment model for New-Madrid fault in CUS.	1	1	1	1
Fault-Rupture Plane End-Point Latitudes, Longitudes	End Point 1 along Top of Fault Plane, deg.	34.795, -119.515	34.310, -117.530	34.280, -118.290	34.170, -119.656
	End Point 2 along Top of Fault Plane, deg.	34.805, -119.484	33.350 -115.710	34.197 -117.707	34.140, -119.357
	End Point A along Base of Fault Plane, deg.	34.795, -119.515	34.310, -117.530	34.357, -118.257	34.092, -119.656
	End Point B along Base of Fault Plane, deg.	34.805, -119.484	33.350 -115.710	34.197 -117.707	34.092, -119.357
Fault Plane Orientation	Dip Angle, deg.	90	90	45	30
	Azimuth of Dipping Plane of Fault, deg.	0	0	0	180
EQ Hypocenter Depth	km.	14.72	8.99	9.04	4.99
Total Width of Fault Plane	m.	9.96	4.73	9.40	7.90
EQ Epicenter Coordinates	Latitude and Longitude, deg.	34.800, -119.500	33.792, -116.549	34.295, -118.045	34.092, -119.509
EQ Seismogenic Zone	Depth to Rupture Plane, km. (assumed to be 3 km)	4.757	4.256	3.0	3.0
EQ Center-of-Energy-Release	Depth from ground surface, km	11.017	6.507	8.78	4.96
	Latitude and Longitude, deg.	34.801, -119.496	33.754, -116.477	34.245, -117.967	34.131, -119.646
Fault Plane Widths on Either Side of Fault Plane	Integer named ZD (=1 if user-specified input fault widths are provided; =2 if default values are used)	0	0	0	0
Zone of Deformation Widths (to left and to right of main trace of fault rupture)	Units of m; Ignored if ZD = 0	--	--	--	--

B.4.2 Comparisons of Walkthrough Files for Coastal California and Central United States

Figures B-4 and B-5 show the magnitudes and locations of all earthquakes contained in the walkthrough files for the Coastal California and CUS regions. The Coastal California file has a total walkthrough duration of 10,000 years and covers an area that consists of 9,436 square microzones with a side dimension of 11.1 km. This walkthrough file contains 28,576 earthquakes with a moment magnitude of 5.0 or greater.

Because the CUS region is much less seismically active than Coastal California, its walkthrough duration is much longer (50,000 years), in order to enable the walkthrough file to contain a statistically significant number of earthquakes. Also, the area of the CUS region, which contains 16,296 microzones, is much larger than the area of the coastal California region (9,436 microzones). However, even with its longer walkthrough duration and larger area, the CUS walkthrough file contains fewer earthquakes of moment magnitude 5.0 or greater (17,281 earthquakes) than does the coastal California file (28,576 earthquakes).

The rate of occurrence of such earthquakes in the Coastal California and CUS regions is compared in Table B-8. This earthquake occurrence rate is provided in units of earthquakes per year per microzone-area. On this basis, Table B-8 shows that the Coastal California region has an earthquake occurrence rate that is about 15 times larger than the rate for the CUS region.

Table B-8. Comparison of Earthquake Occurrence Rates indicated by Walkthrough Files for Coastal California and Central United States Regions.

Data	Coastal California Region (as shown in Fig. B-2)	Central U.S. Region (as shown in Fig. B-1)
1. Walkthrough Duration (years)	10,000	50,000
2. Total Area of Region (in terms of number of micozones)	9,436	16,926
3. Number of Earthquakes with $M_w \geq 5.0$ contained in Walkthrough File	28,576	17,281
4. Earthquake Occurrence Rate (number-of-EQs/area-of-region/year) = (Row 3)/(Row 2)/(Row 1)	3.03×10^{-4}	2.04×10^{-5}

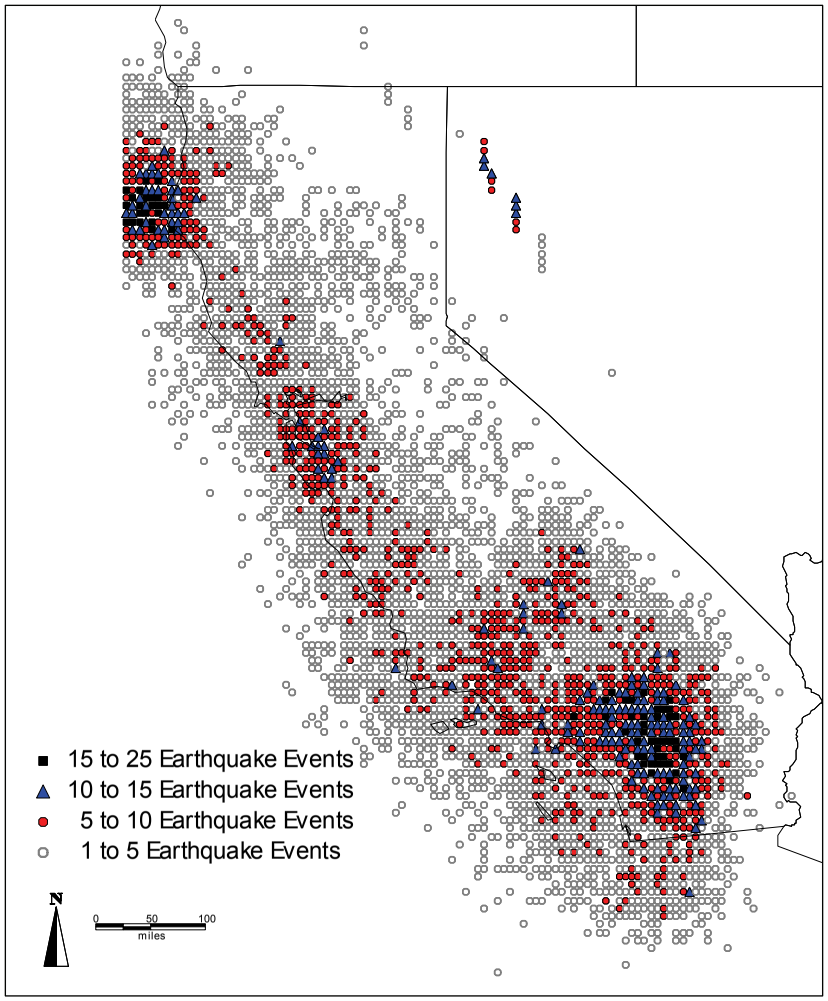

a) 5.0 ≤M_w < 5.5 (14,704 Earthquakes)

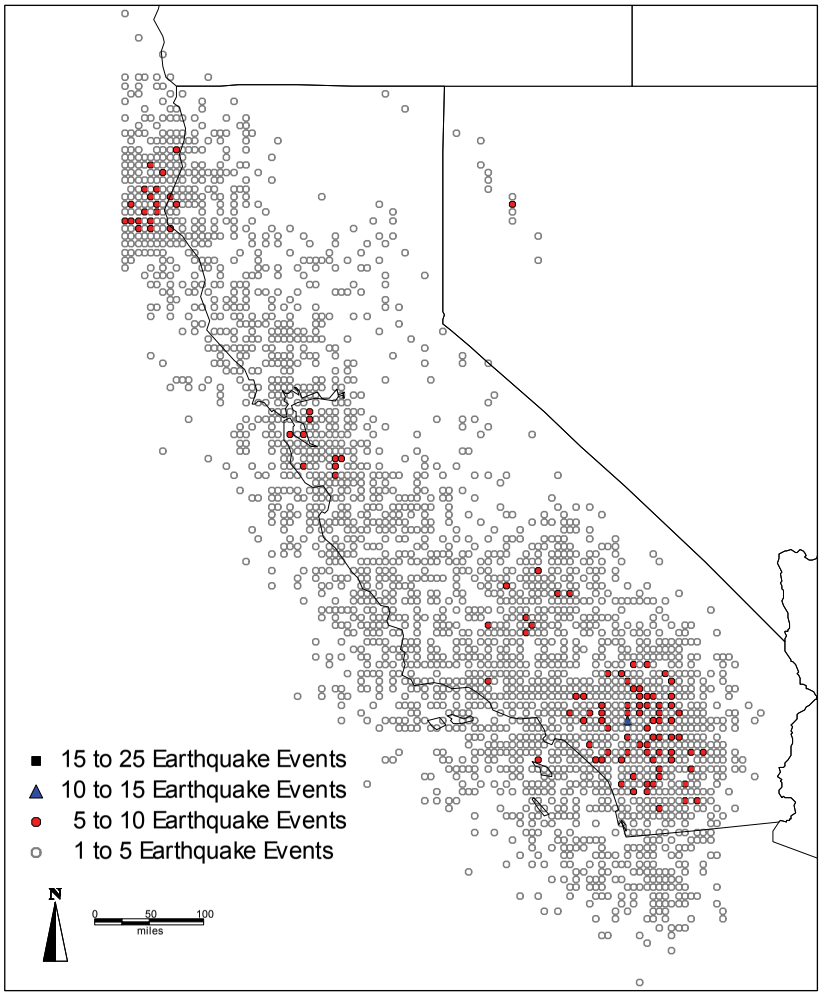

b) 5.5 ≤M_w < 6.0 (4,371 Earthquakes)

Figure B-4. Magnitudes and Epicenter Locations for Earthquakes in Coastal California Walkthrough Table (page 1 of 3)

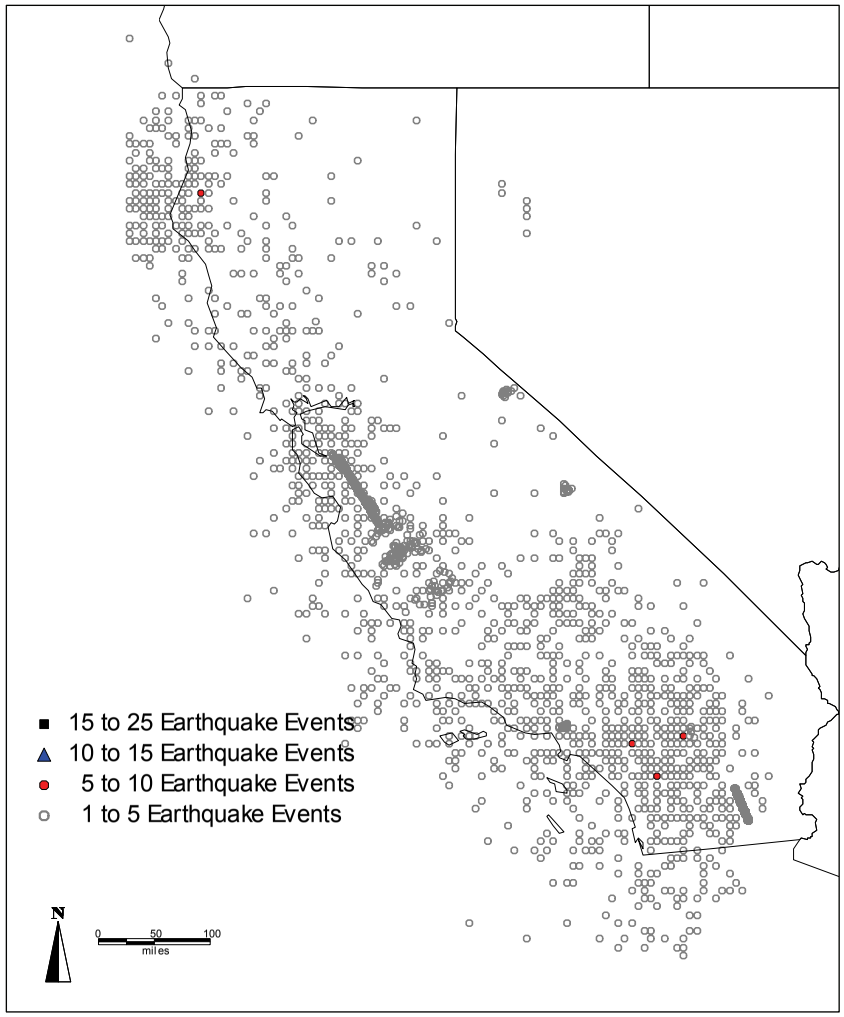

c) 6.0 ≤M_w < 6.5 (2,691 Earthquakes)

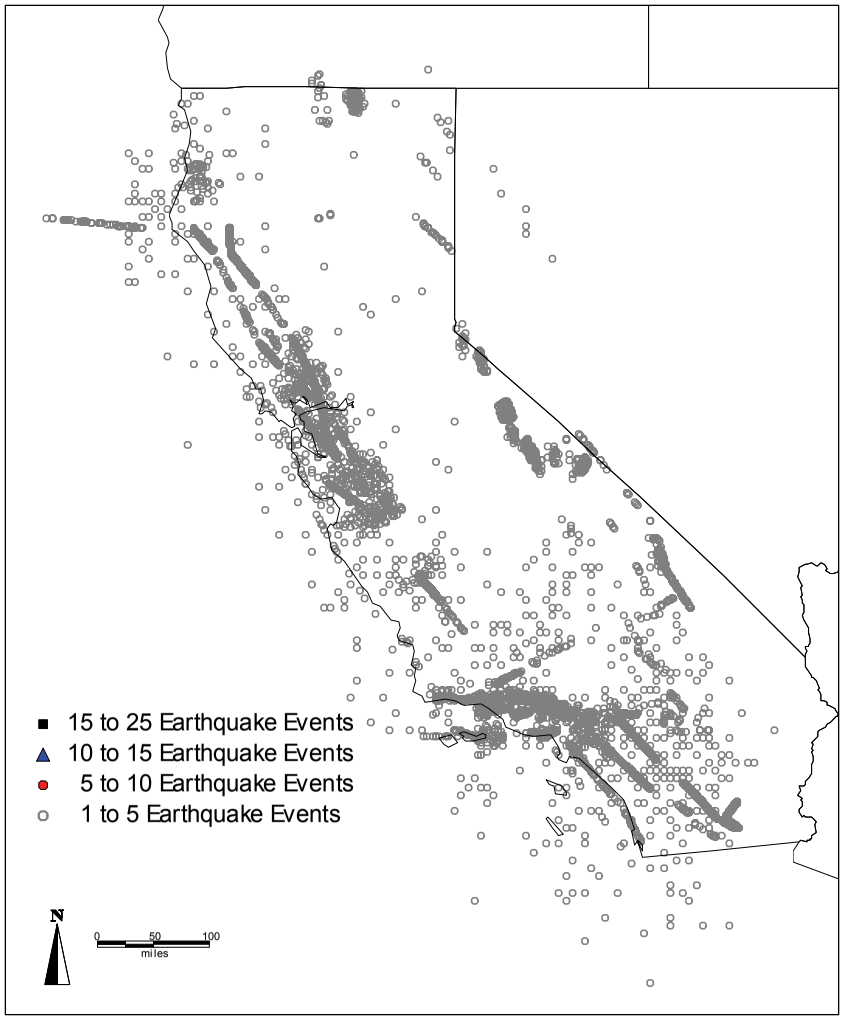

d) 6.5 ≤M_w < 7.0 (5,408 Earthquakes)

Figure B-4. Magnitudes and Epicenter Locations for Earthquakes in Coastal California Walkthrough Table (page 2 of 3)

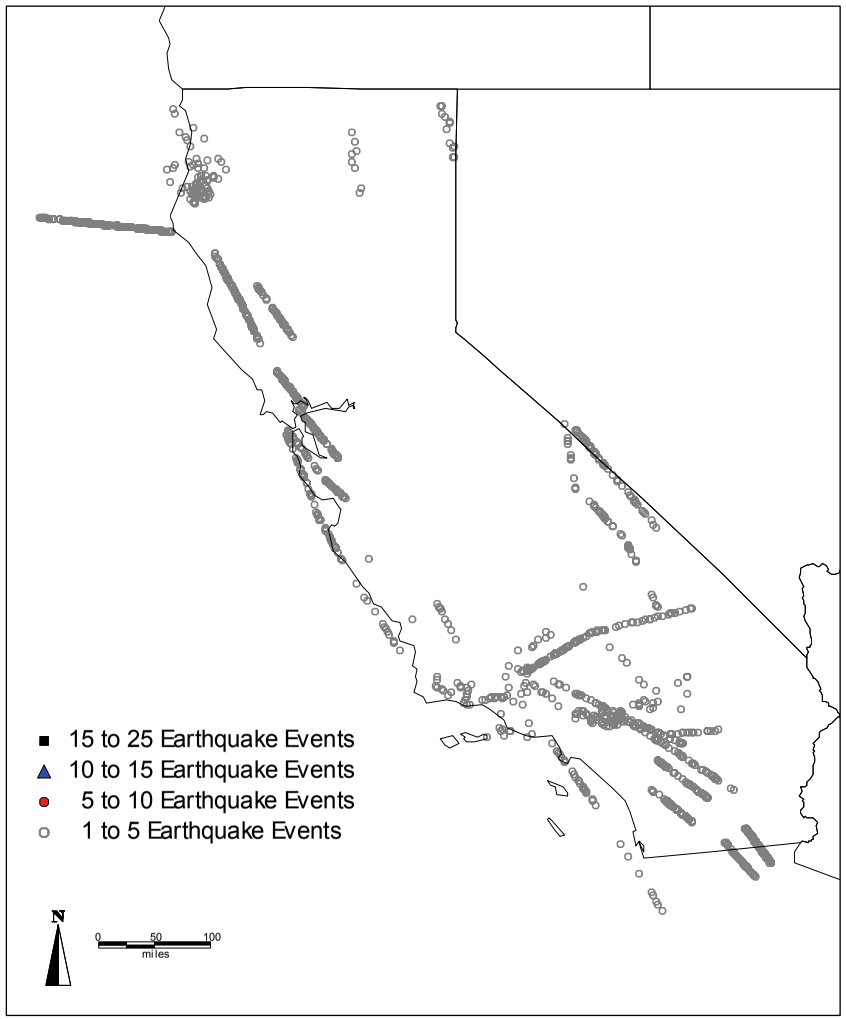

c) 7.0 ≤M_w < 7.5 (1,371 Earthquakes)

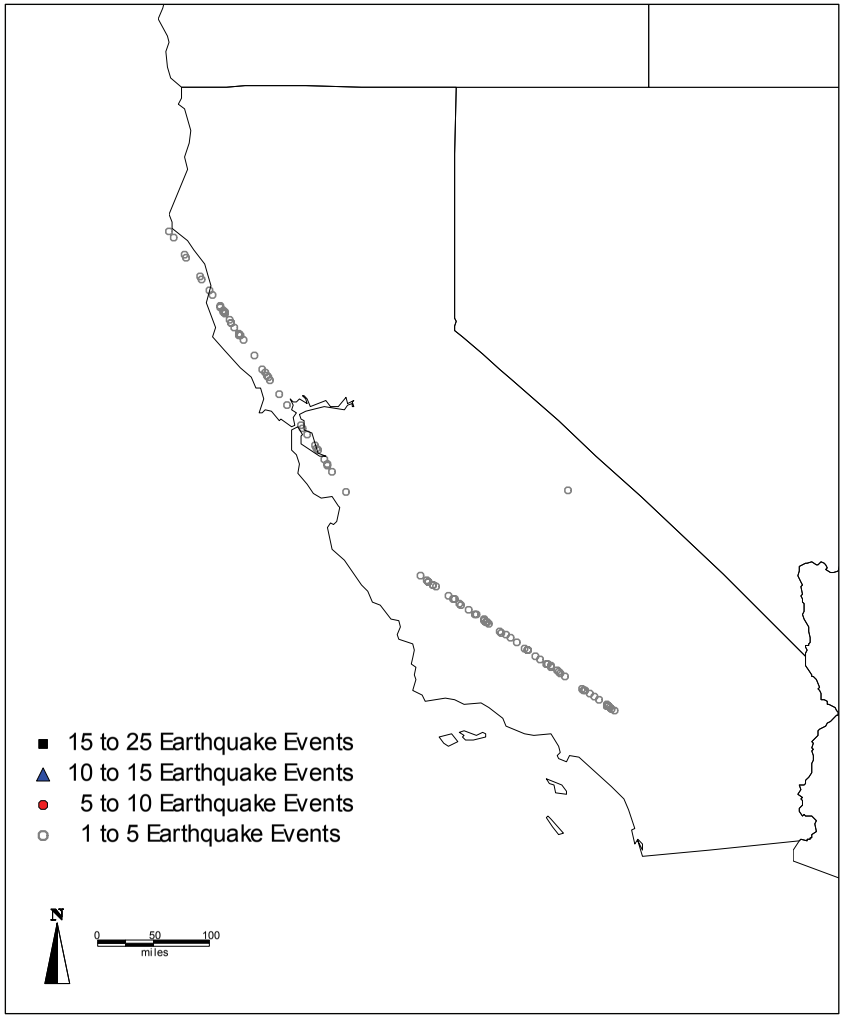

d) 7.5 ≤M_w < 7.0 (95 Earthquakes)

Figure B-4. Magnitudes and Epicenter Locations for Earthquakes in Coastal California Walkthrough Table (page 3 of 3)

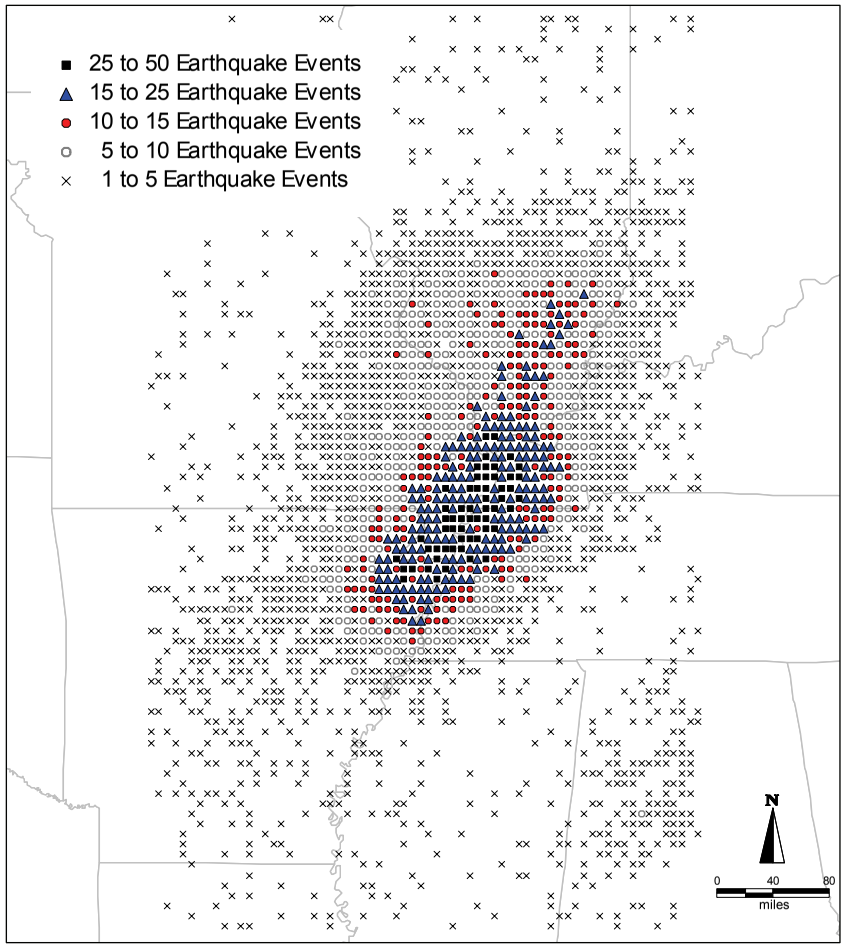

a) 5.0 ≤M_w < 5.5 (12,639 Earthquakes)

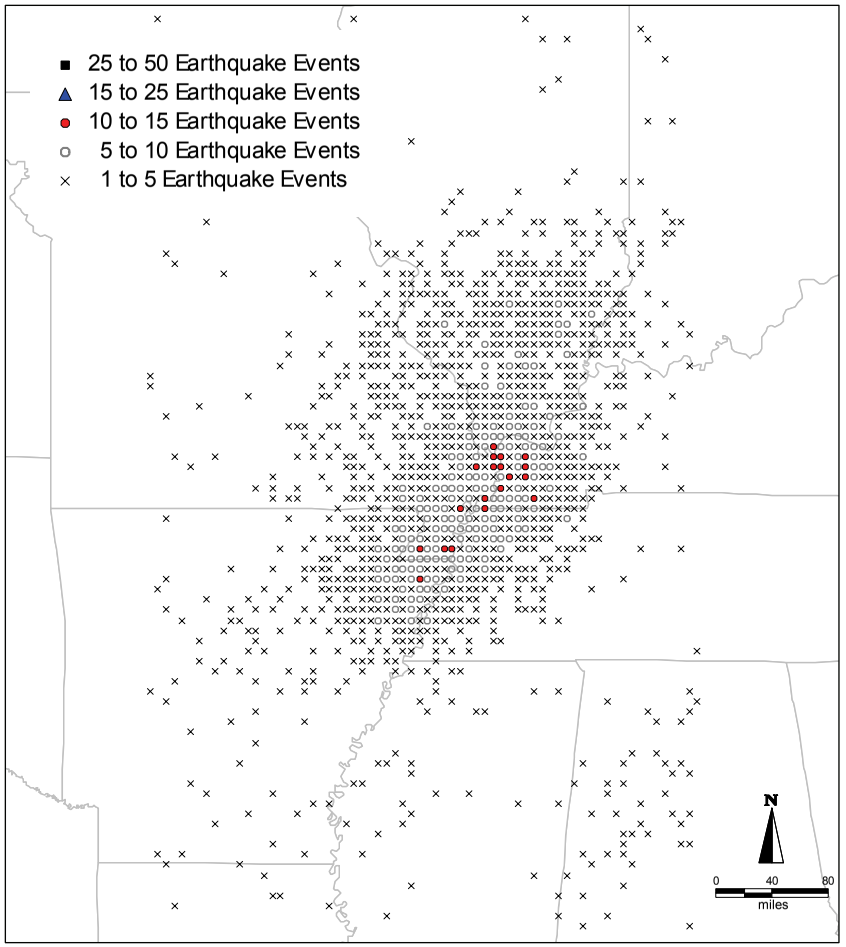

b) 5.5 ≤M_w < 6.0 (3,086 Earthquakes)

Figure B-5. Magnitudes and Epicenter Locations for Earthquakes in Central-United-States Walkthrough Table (page 1 of 3)

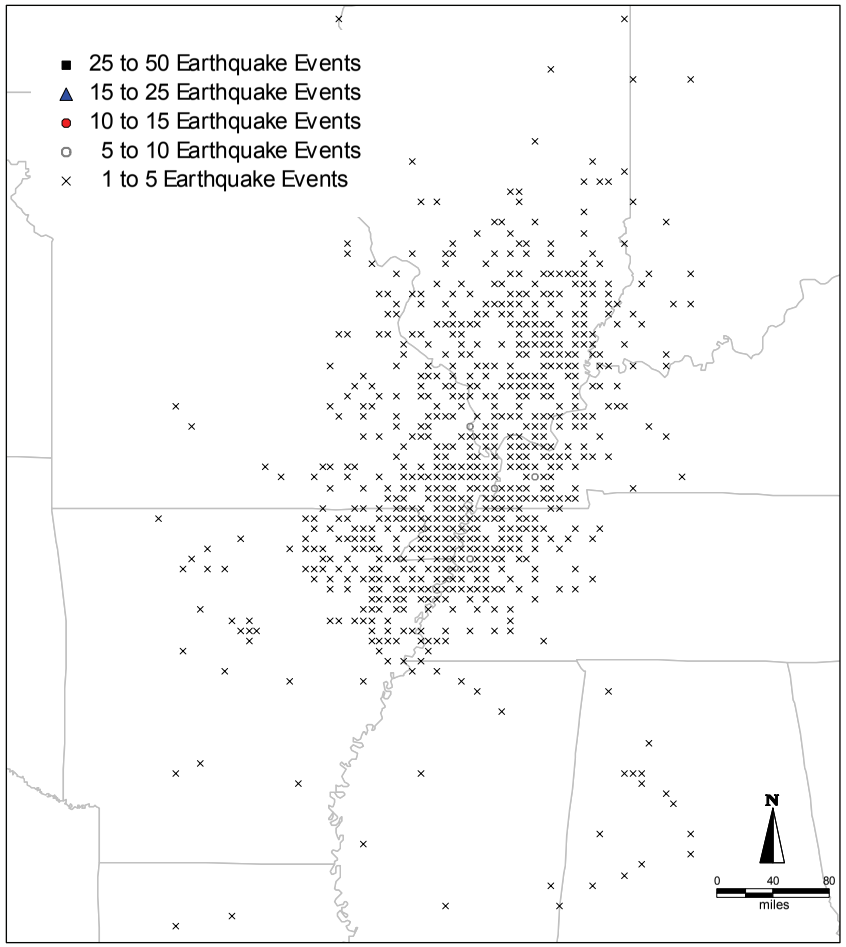

c) 6.0 ≤M_w < 6.5 (1,044 Earthquakes)

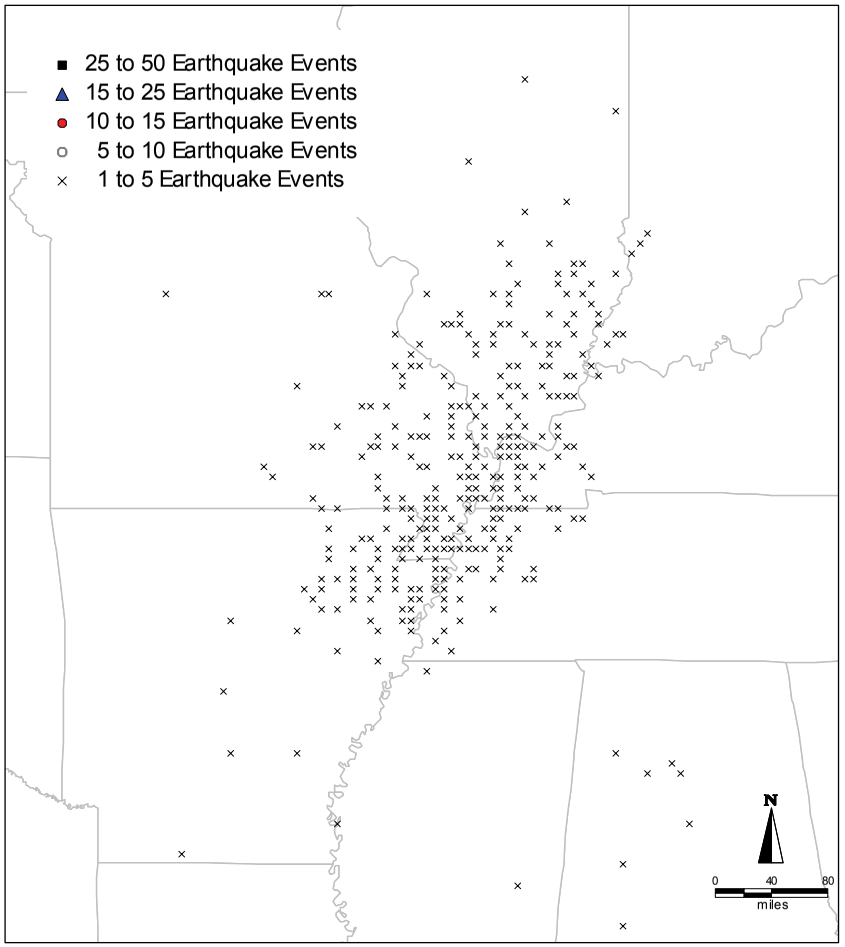

d) 6.5 ≤M_w < 7.0 (366 Earthquakes)

Figure B-5. Magnitudes and Epicenter Locations for Earthquakes in Central-United-States Walkthrough Table (page 2 of 3)

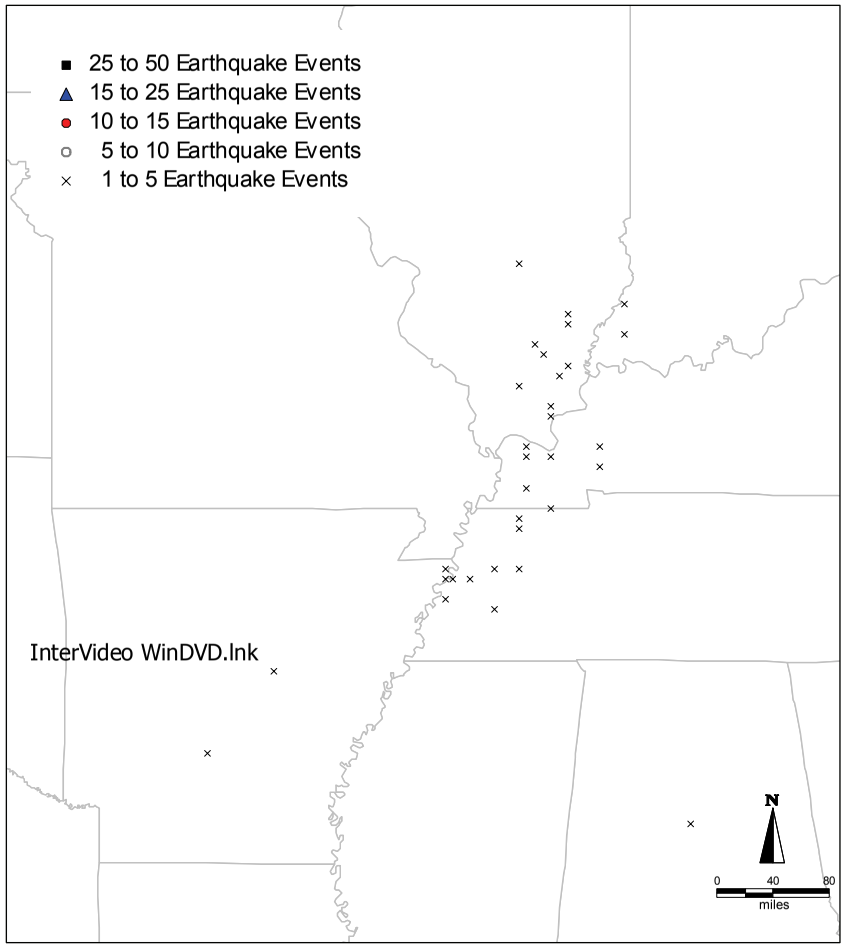

e) 7.0 ≤M_w < 7.5 (35 Earthquakes)

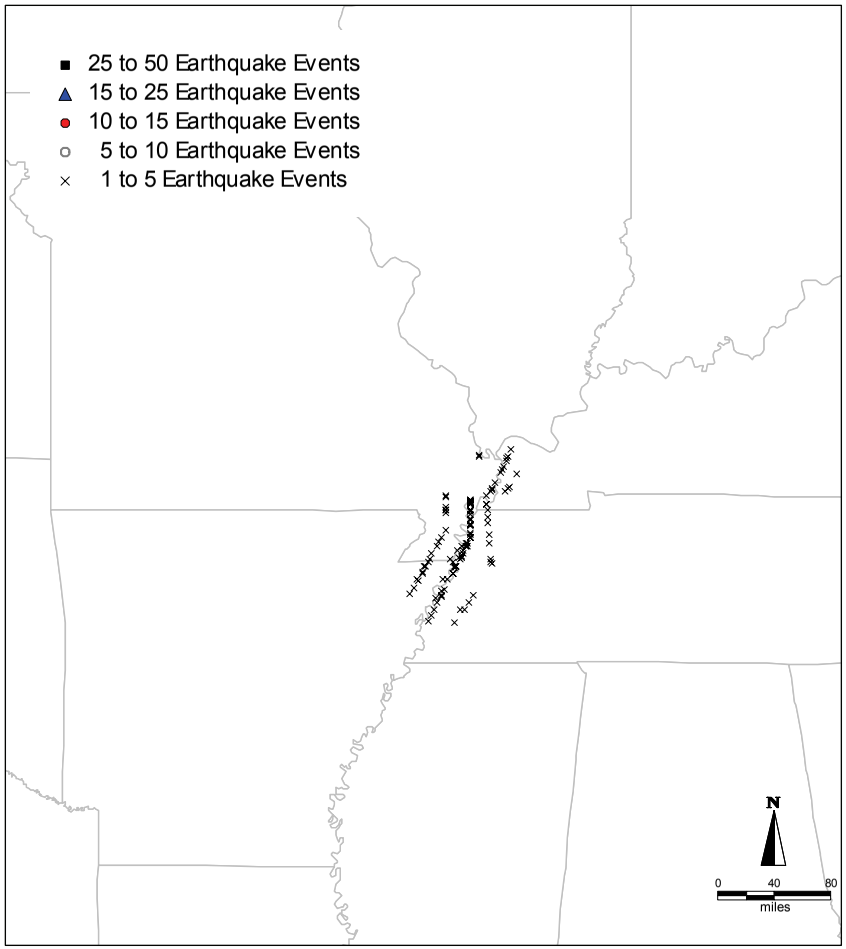

f) 7.5 ≤M_w (111 Earthquakes)

Figure B-5. Magnitudes and Epicenter Locations for Earthquakes in Central-United-States Walkthrough Table (page 3 of 3)

APPENDIX C
IMPORT WIZARD

C.1 BACKGROUND

REDARS™ 2 requires the integration of several data sets from various federal, state, and local government agencies that characterize the highway system, its seismic hazards, bridges and other components. Previously, users of this software had to manipulate the raw data into a transportation network format that is suitable for a REDARS™ 2 traffic-flow analysis. However, this is a significant and time-consuming effort. Therefore, the Import Wizard was developed to automate most of this data manipulation, and to thereby significantly reduce input preparation time and to also reduce the potential for incorrect input data in REDARS™ 2.

This appendix summarizes the Import Wizard and how it imports data into REDARS™ 2. In this, an effort has been made to include as much publicly available and federally distributed data as possible. This minimizes the user's tasks associated with collecting the data. The Import Wizard also guides the user through the process of identifying databases on the hard drive, and integrates the various default or user-specified data sets into the required REDARS™ 2 format. An additional more detailed description of the Import Wizard is provided in Cho et al., (2006b).

C.2 ROLE OF IMPORT WIZARD AND ITS GRAPHICAL USER INTERFACE

The role of the Import Wizard is to assign the paths to the input-data files and to define the study region (see Figure C-1.) The input data files are either default national databases or databases that the user specifies in a predefined format. The Import Wizard locates these files and defines the study area, based on the extent of the analysis that the user specifies. Its final product is a database that defines the study area's highway system, bridges, soils, and origin-destination trip tables, and can be directly input into the REDARS™ 2 core program.

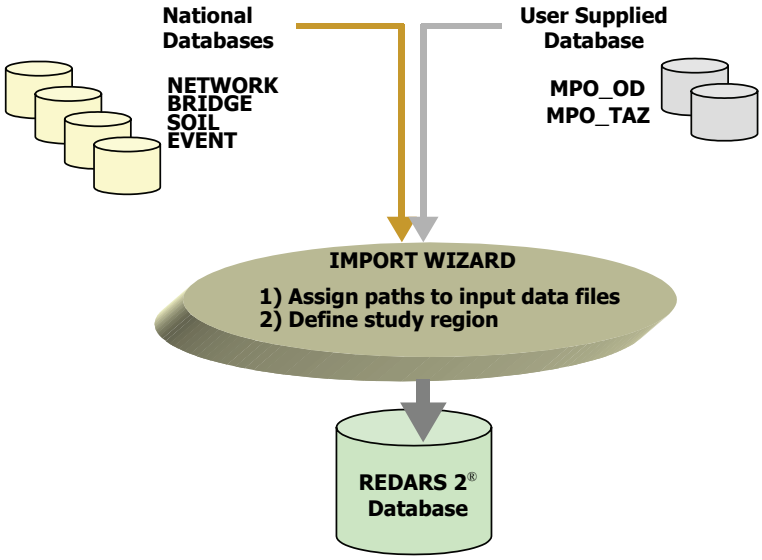

Figure C-1. Role of the Import Wizard

The Graphical User Interface (GUI) for the Import Wizard guides the user through a series of simple steps for identifying the data sources needed to create the REDARS™ 2 input database. It provides brief explanations of the steps involved, the data sources, default and optional data that the user might want to use, and the format of data to be used. When geographic data sources are to be identified, the GUI describes the required file formats, coordinate system, datum etc for geographic file, and also provides file formats required for other file types. In addition, the GUI provides simple geographic information system (GIS) tools that enable the REDARS™ 2 user to select a study region for analysis by a series of simple clicks on a map.

C.3 LIMITATIONS OF IMPORT WIZARD

The REDARS™ 2 Import Wizard uses nationally available FHWA datasets to enable prompt creation of highway-roadway network study regions. Although the program depends on FHWA data, the actual datasets are provided by the states themselves. They may vary in accuracy and completeness, depending on the original developer's interpretation of data requirements and the completeness of the base data. These factors, in turn, will affect the usability of the databases for a given area. The following paragraphs identify such difficulties that may arise due to problems with a region's base data and, where possible, recommends solutions to these difficulties.

- In the roadway network study region, bridges may be missing or misplaced. This is often due to problems in the Linear Referencing System (LRS) of the base data. For example, some state transportation agencies do not track subroute ID, or do so in a manor that is inconsistent with National Bridge Inventory (NBI) data. Milepost markers are often incorrect, reversed, or in the wrong units, which results in misplaced or omitted bridges. Possible solutions include correcting the LRS in a GIS system, or editing the original-data fields to be consistent with the NBI data.
- The NBI, the National Highway Planning Network (NHPN) and the Highway Performance Monitoring System (HPMS) do not contain sufficient information for locating bridges on ramps. A freeform field in the NBI data does accommodate entering the information, but this is rarely entered consistently enough to parse bridge location. At this time, REDARS™ 2 conservatively assumes that damaged ramps impact traffic in both directions of the freeway.
- The attribute data may contain incorrect or no information regarding number of lanes, link type, rural or urban designation, and route attributes. Such base-data issues must be resolved by the REDARS™ 2 user, after which the Import Wizard can be rerun.
- The NBI only tracks state and federal bridges which are located primarily on freeways and highways. If desired by the REDARS™ 2 user, more detailed network data can be obtained from the cognizant Metropolitan Planning Organization (MPO) for the region, and more detailed bridge data can be obtained from local jurisdictions. These data will vary by region and are not supported by the Import Wizard. Users can create a roadway network study region outside of the Import Wizard using the REDARS™ 2 open database format.
- Public transit is currently not supported within REDARS™ 2. One-way routes are not distinguished in the NHPN data. Users can represent one-way routes by deleting the extra directional link record in the final REDARS™ 2 input data for the study region.

C.4 DATA SOURCES

In order to model the effects of a seismic event on the transportation network, the Import Wizard integrates different types of nationally available geospatial databases and creates a REDARS™ 2 study region through database queries and software code. Underlying the REDARS™ 2 study region is a database containing link, node, bridge, and OD tables for transportation analysis. The sources of data that populate these underlying tables include NHPN and HPMS databases for the transportation network, the NBI database for bridges, National Earthquake Hazards Reduction Program (NEHRP) soils data, and regional-MPO trip data in the form of Traffic-Analysis-Zone (TAZ) and Origin-Destination (OD) databases. The Import Wizard extracts information from these data sources and populates key fields of the link, node, bridge, and OD data tables. Detailed descriptions of the data sources are provided in this section.

The Import Wizard uses various data types to create a network study region. REDARS™ 2 requires an integrated network for analyzing post-earthquake traffic route and travel costs. Network data refers to the spatial data that replicates the real highway and street system (highway, arterials, and local streets) using a set of links and nodes. Nodes are points where traffic flow originates, terminates, or transmits, and links are the conduits for the flow between nodes. Such a node-link network model uses a linearly referenced data structure and maintains both connectivity and real-world properties (location, capacity, free flow speed, etc). The following discussion describes the data elements of the network and examines their sources.

C.4.1 Roadway Transportation Network

The Import Wizard uses the NHPN and HPMS national highway databases to model the spatial configuration and attributes of the highways and roadways in the study area.

C.4.1.1 National Highway Planning Network (NHPN) Database

The NHPN is a spatial network database for highways and major arterials. The data in this database are collected by the states and maintained by FHWA, and are in files that are in a zipped ARC/INFO© Interchange (.e00) format. REDARS™ 2 requires spatial network data for the roadway system to be in this format. NHPN Metadata are available from the following website: http://www.fhwa.dot.gov/planning/nhpn/docs/metadata.html. Further information on the NHPN database is provided in Cho et al. (2006b).

C.4.1.2 Highway Performance Monitoring System (HPMS) Database

The HPMS is a FHWA database of highway network attribute data that reflects the extent, condition, performance, use, and operating characteristics of the highways. HPMS files are delimitated text file with a metadata in a schema file (a text file). This database also contains Linear Referencing System (LRS) that can be used to associate attributes with the spatial elements of the NHPN database. HPMS data and documentation can be obtained from the following website: http://www.transtats.bts.gov/DataIndex.asp.

C.4.2 Bridges

REDARS™ 2 requires input data for all bridges in the roadway system. These data define each bridge's location, geometry, structural attributes, age, lanes, etc., in order to estimate bridge damage states, and associated repair costs, repair times, and traffic states during repairs (see Appendix G for further description of the input data needed for the REDARS™ 2 default bridge model.) In the REDARS™ 2 Import Wizard, a linearly referenced data structure makes it possible to integrate the bridge locations into the street network. Bridge placement along the roadway links is achieved through dynamic segmentation.

The FHWA National Bridge Inventory (NBI) database is the source of bridge data for the REDARS™ 2 Import Wizard (FHWA, 2002). This database contains data supplied by the states, in order to form a complete inventory of the number and condition of the nation's bridges on public roads that can be periodically reported to the Congress. It is intended for use by State, Federal and local agencies, and is maintained in a format prescribed by the "Recording and Coding Guide" for the Structure Inventory and Appraisal of the Nation's Bridges. The NBI database is made available to the public, usually in a delimited text file format, through the FHWA Office of Bridge Technology.

The NBI database is intended to facilitate assessment of the need for replacement and rehabilitation of the Nation's bridges. It was not developed to provide structural attribute information that would ordinarily be required to assess the seismic performance of these bridges. However, because the NBI database is currently the only electronic database of bridges nationwide, it is necessary to use this database in REDARS™ 2 in order to approximately deduce information needed for bridge seismic performance evaluation. Appendix G describes just what NBI data are used for this purpose, and how they are applied in the default bridge models currently included in REDARS™ 2. Further extensions of the current NBI database to provide more complete information needed for seismic analysis of bridges have been proposed and are currently under consideration. (Small, 1997; Yashinsky, 2005).

C.4.3 Soils

In order to assess effects of local soil conditions on site-specific ground motions at each roadway component site, the ground-motion models that are currently included in REDARS™ 2 require soils data based on the National Earthquake Hazard Reduction Program (NEHRP) soil-type classification. The Import Wizard accommodates such data if: (a) the digital data are based on local geology and shear wave velocity, and are provided in ESRI Shapefile format; (b) the data are in a geographic coordinate system; and (c) the datum matches the NHPN base data, which are currently in NAD 1927.

In addition to the above soils data for estimating ground motion hazards, REDARS™ 2 requires data for estimation of site-specific liquefaction hazards. These data are not readily available in a national electronic database. Rather they must be developed separately by the REDARS™ 2 user through: (a) geologic screening of the soil conditions throughout the roadway network being analyzed, in order to identify those component sites that may be prone to liquefaction during an earthquake; and (b) for those sites, estimation of soil-layer properties that

are needed as input to the liquefaction-hazard model currently included in REDARS™ 2. Appendix E provides more information on these particular input data requirements.

C.4.4 Transportation Analysis Zones (TAZs)

In order to enable local and state governments to monitor user trip demands on the highway-roadway system (particularly in terms of journey-to-work and place-of-work statistics), the region surrounding the system is subdivided into a set of subregions named Traffic Analysis Zones (TAZs). TAZ files are usually available from the local Metropolitan Organizations (MPOs). The REDARS™ 2 Import Wizard requires that the TAZ file be provided in ESRI Shapefile format within a geographic coordinate system. The datum must match the NHPN base data, which is currently in NAD 1927.

C.4.5 Origin-Destination (O-D) Trip Tables

An origin-destination (O-D) trip table (or O-D matrix) is a two-dimensional table that defines the number of trips from each TAZ in the surrounding region to all other TAZs in the region. O-D trip tables are input as a matrix of trips, and the Import Wizard requires the O-D file to be a tab, comma or space delineated TXT file that consists of the following columns:

- Column 1: Zone number for the TAZ that is the origin of this set of trips.
- Column 2: Zone number for the TAZ that is the destination for this set of trips.
- Columns 3, 4, 5…n: Number of trips between the zone-pair, grouped by trip types. That is, column 3 would include the number of automobile trips between the zones, and columns 4, 5, etc. would include the number of Freight Type 1, 2, etc. trips between the zones.

These O-D trip-table data are typically available through the MPO for the region.

C.5 IMPLEMENTATION STEPS

The following data importing steps are implemented when a user creates a study region using the Import Wizard:

C.5.1 Step 1: Create Blank Database Files Set

In Step 1 of the database creation process, the Import Wizard creates five Microsoft Access Database (MDB) files. These consist of the three distinctive MDB files contained in the REDARS™ 2 core program -- which are named RDF (REDARS™ Data File), RVB (REDARS™ Visual Basic for Application), and RPR (REDARS™ PRobabilistic Analysis) -- plus two additional temporal MDB files generated by the Import Wizard. Instead of relying on ADOX (Active Data Object Extension) for manipulating MDB file structure (including creation of the files), the individual files are created by "melting" binary files that contain all of the required data structure. This "melting" method is convenient since it does not require changing the program code to accommodate changes in data or database structure during development of REDARS™ 2.

C.5.2 Step 2: Populate HPMS Tables

The HPMS (Highway Performance Monitoring System) files are comma delimitated text file with a metadata in a schema file (a text file). The Import Wizard reads the metadata file to capture the data structure, including data field name and field length. A text parser in the Import Wizard reads the required data and populates tables in the temporary Import Wizard file.

C.5.3 Step 3: Populate NBI Tables

The bridge data from the NBI (Nation Bridge Inventory) database is also delivered in a column-based text file without delimiting characters. A text parser in the Import Wizard reads the file according to a pre-defined structure.

C.5.4 Step 4: Create and Populate NHPN Tables

The roadway system spatial data from the NHPN (National Highway Planning Network) are delivered in an uncompressed ArcInfo export file, e00. The Import Wizard reads the state-wide NHPN file, and populates the temporal Import Wizard tables for arc geometry, arc attributes, node attributes, route information, and linear referencing system.

C.5.5 Step 5: Establish Relationships between Tables and Create LINK Table

The Import Wizard creates two separate link tables -- one is for a region-wide network analysis that is carried out under Step 11, and the other is for the study area that is specified by the user. The region-wide link table is created by the following series of queries:

- Identify nodes within the Transportation Analysis Zone Map (TAZ).
- Identify links, of which any end-node is included in the node-set identified in the previous step.
- Identify "outside" nodes which are not within the TAZs, but are end-nodes of the selected links.
- Update the attributes of the selected links using HPMS attribute data.
- Add virtual links to connect the TAZ centroids to the selected nodes.

The link table for the selected study area is created from the HPMS-updated region-wide link table as follows:

- Identify nodes within the user-drawn boundary.
- In addition, identify nodes in the selected TAZs from the user-drawn boundary.
- Identify links, for which any end-node is included in the node set that was identified in the two previous steps.
- Identify "outside" nodes, which are nodes that are not within the user-drawn boundary, or within selected TAZs, but are instead end-nodes of the selected links.

- Add new virtual links to connect the centroids of the selected TAZs to the nodes in the study area.
- Create virtual links to connect adjacent "outside" nodes.
- Update the external virtual links between adjacent "outside" nodes to represent boundary conditions.

C.5.6 Step 6: Locate Bridges and Tunnels from NBI Database onto Links in LINK Table

Under Step 6, the data records in the NBI database are scrutinized to identify bridges and tunnels that are in the study area. The location of each bridge or tunnel in the study area is calculated through dynamic segmentation using a linear referencing system.

C.5.7 Step 7: Update Soil Type for Selected Highway Components

If NEHRP soils data are not available, REDARS™ 2 assumes that the soils at each component site correspond to NEHRP Type C default soil conditions (which can be overridden by the REDARS™ 2 user). These conditions are automatically stored in the Bridge, Tunnel, and Link tables in the RDF file. However, if NEHRP soils data for each component site are provided in the format described in Section C.4.1.3, Step 7 of this Import Wizard implementation procedure updates the Bridge, Tunnel, and Link tables by using a point-to-polygon relationship to replace the default soil conditions with the site-specific NEHRP site conditions.

C.5.8 Step 8: Subset TAZs and Calibrate Demand Functions

Under Step 8, the following calculations are carried out:

- ***Region-Wide Travel Times and Trip Demands.*** Apply the user-equilibrium network analysis procedure (App. J) to the region-wide network and O-D trip tables (Sec. C.4.1.5), assuming that the trip demands are fixed at their baseline (pre-earthquake) levels. Note that the region analyzed in this calculation extend beyond the study area whose seismic risks are to be analyzed using REDARS™ 2. Use this analysis to develop zone-to-zone travel time and partial trip-demand matrices[1] between the TAZs in this model that are beyond the study area. This step is time consuming because it involves very large network and OD trip-table matrices, and traces all routes throughout this network in order to count partial demand.
- ***Outside-Zone Travel Times and Trip Demands.*** Assuming that the travel times along the links between the outside-zones and the study area are infinite, and using the above partial trip demands for the outside zone only, compute the travel times for these trips. This gives the travel times on virtual links between "outside" nodes.

[1] This is termed a "partial trip-demand matrix", since it includes only those trips originating from the outside TAZs that also have destinations within these TAZs. The remaining trips from these outside TAZs (which are trips that end in TAZs within the interior study area rather than within the surrounding outside TAZs) are excluded from the partial trip demand matrices.

- ***Decay Function***. Develop parameters for estimation of how trip rates vary with travel time by regressing the pre-earthquake O-D trip-table data against the travel-time matrix, using an exponential function.
- ***Calibrated Demand Function Parameters.*** Apply the Deming-Stephan-Furness algorithm for balancing the gravity model that includes the above decay function, in order to calibrate the parameters needed to estimate how post-earthquake trip demands are affected by travel-time delays.

C.5.9 Step 9: Populate Database with Data for Study Area

All processes up to this current step are done using the temporal MDB file. The current step populates the Link, Node, and Shape-Points tables considering the virtual links, new node IDs, new link IDs, and geographic objects.

C.5.10 Step 10: Bridge / TAZ / VARS Tables / Clean Up

The remaining tables are populated by importing selected data from the temporal MDB file. Actual updating of link attributes is done through data transaction. Scratch tables, and files are cleaned up. TAZ tables are created according to the OD file.

C.5.11 Step 11: Baseline Analysis

During the creation of the RDF file, the Import Wizard performs a network analysis of a larger baseline (pre-earthquake) regional network roadway system that includes the study area to be analyzed REDARS™ 2. In this, analysis all links in the network are 100% functional. The link and TAZ tables are then populated with the calibrated demand function parameters. Once everything is arranged in the RDF file, Import Wizard performs the baseline analysis. This analysis provides pre-earthquake travel-times and traffic volumes for the selected study area, which will be compared to the post-earthquake values of these quantities as obtained from the subsequent REDARS™ 2 SRA of the study area.

The Import Wizard's overall running time will depend on the size of the region-wide TAZ, since this size defines the time needed to: (a) calibrate the demand function; and to also (b) subset the OD data for the REDARS™ 2 SRA study area from the larger regional network considered in the above baseline analysis. The size of the study area (number of TAZs selected and geographic area) is also important because the number of highway-roadway components (roadway links and nodes, bridges, and tunnels) is also related to the study area. The Import Wizard takes about 45-to-55 minutes to process 3,217 Southern California TAZs, and about 10 minutes to process TAZs for a small section of the northern San Francisco Bay Area that was considered in the beta testing of REDARS™ 2.

C.6 SCREENS

The following pages provide Import Wizard screen displays and brief descriptions of each of the steps required by the user to develop REDARS™ 2 input data.

When the REDARS™ 2 Import Wizard is first opened, the "Introduction" screen (Fig. C-2) provides a brief description of the steps required to create a REDARS™ 2 study region.

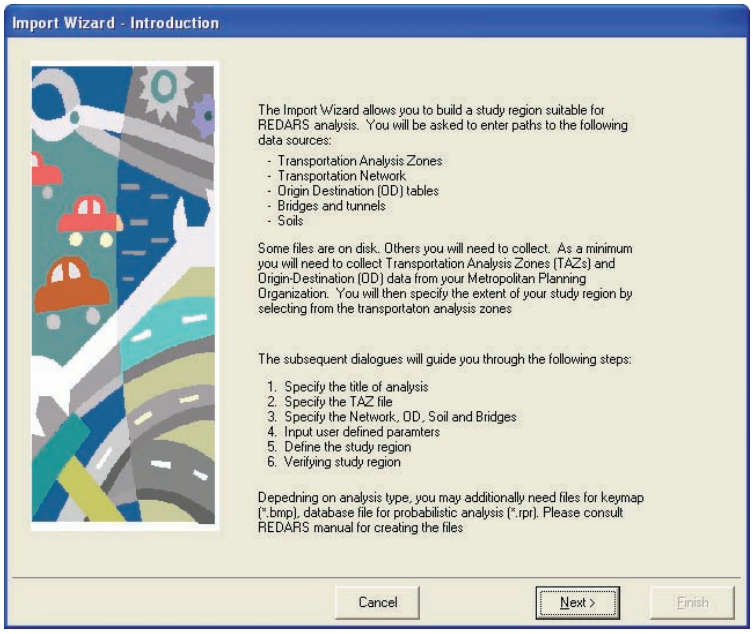

Figure C-2. Introduction Screen for REDARS™ 2 Import Wizard

This screen (Fig. C-3) allows the user to specify a name for the study region and a name for the REDARS™ 2 database file.

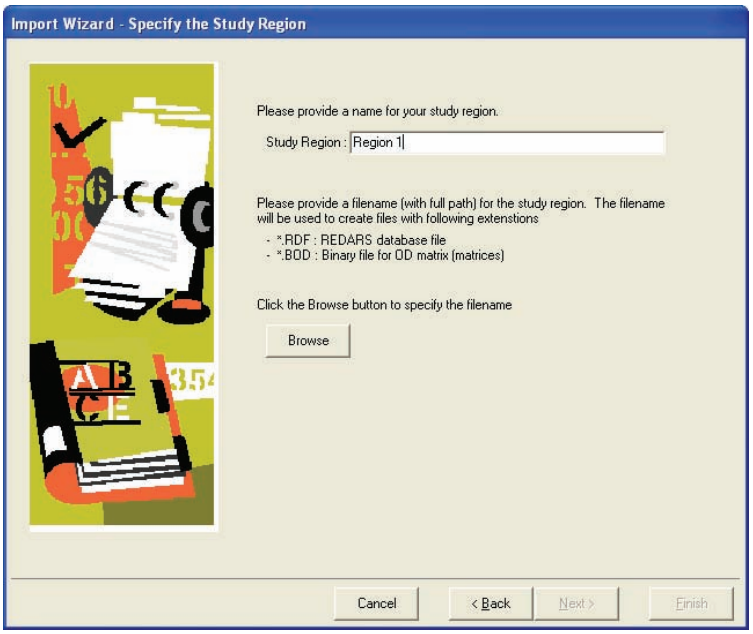

Figure C-3. Screen to Specify Study Region Name and REDARS™ 2® Database Filename

This screen (Fig C-4) allows the user to specify the location of NHPN and HPMS data files on disk. The Import Wizard reads and converts NHPN and HPMS data files to create a transportation network for use with REDARS™ 2.

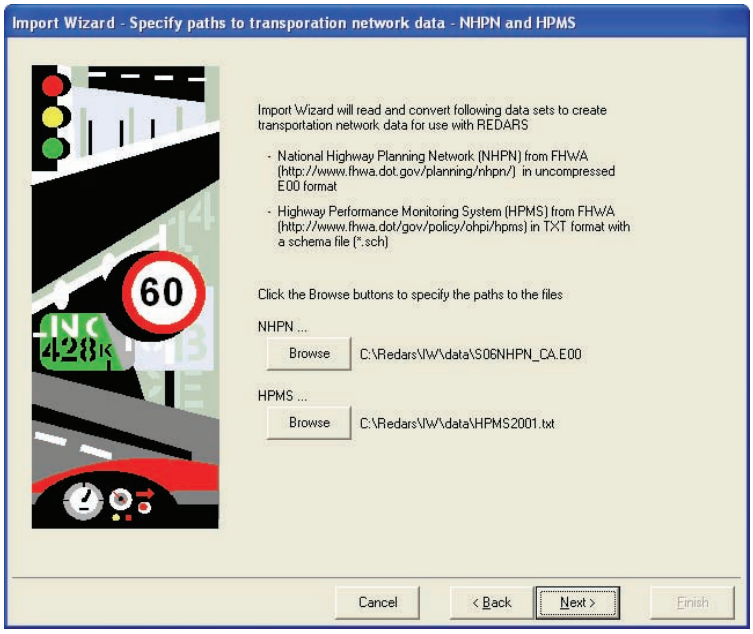

Figure C-4. Screen to Specify Paths to Network Data: NHPN and HPMS

This screen (Fig C-5) allows the user to specify the paths to the NBI bridge data files and the NEHRP soil data files on disk. The Import Wizard reads the NBI bridge data file and locates the bridges on the transportation network for use with REDARS™ 2.

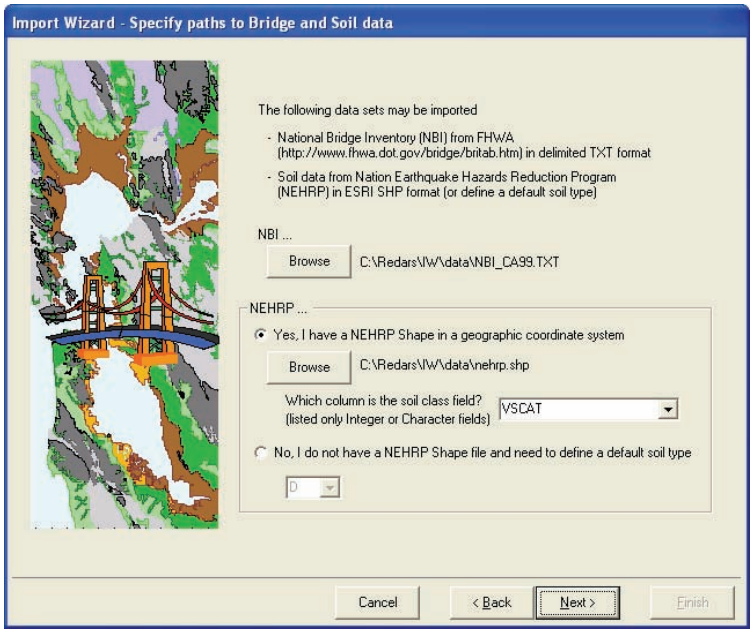

Figure C-5. Screen to Specify Paths to Bridge and Soil Data

This screen (Fig C-6) allows the user to specify the path to the Traffic Analysis Zone (TAZ) data file on disk. Traffic Analysis Zone (TAZ) files are usually available from the local Metropolitan Organizations (MPO).

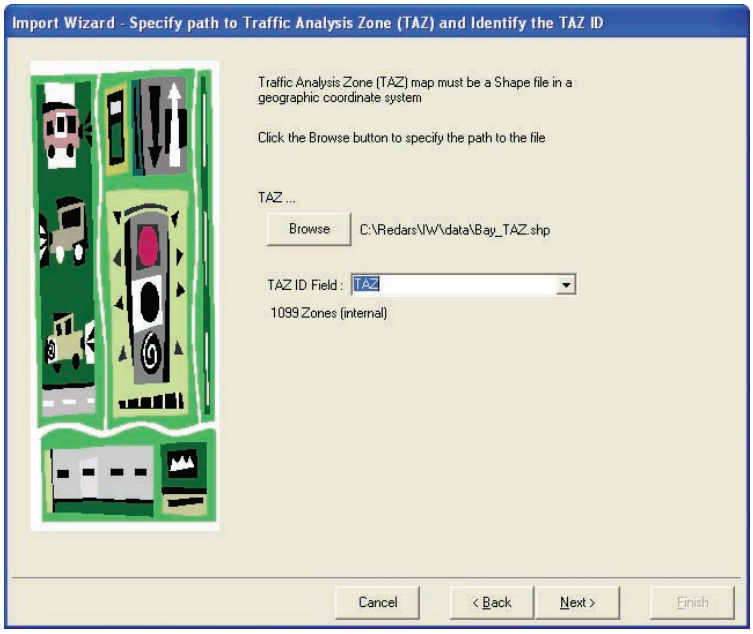

Figure C-6. Screen to specify path to TAZ data and identify TAZ ID field

This screen (Fig C-7) allows the user to specify the Origin Destination (OD) file on disk. OD files are usually available from the local Metropolitan Organizations (MPO).

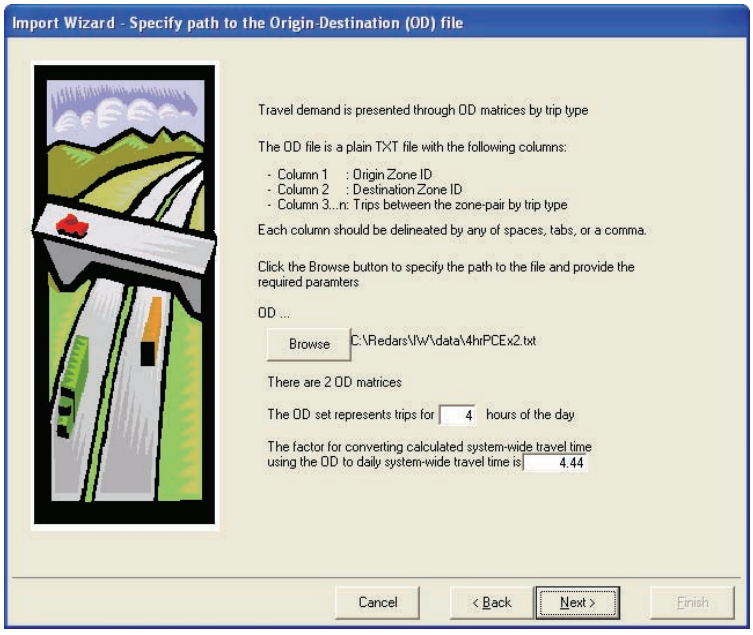

Figure C-7. Screen to Specify Path to OD Data

This screen (Fig C-8) allows the user to enter information on the Origin Destination (OD) parameters.

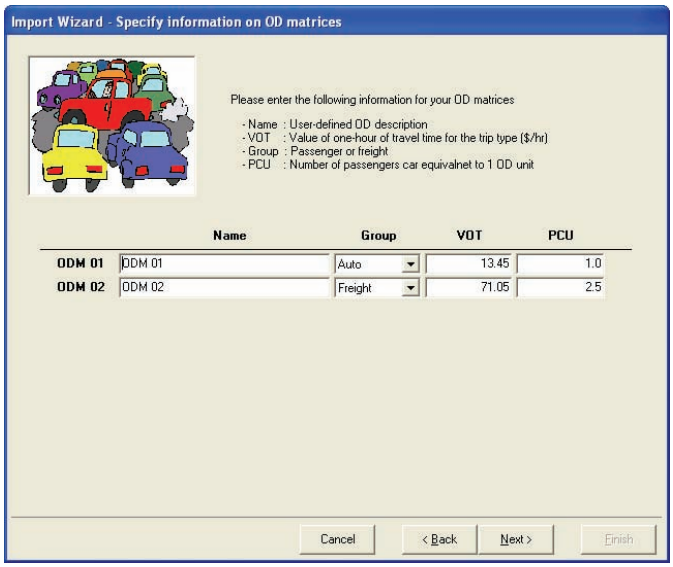

Figure C-8. Screen to Specify Information on OD Matrices

This screen (Fig C-9) is used to select the study region. It displays the transportation network overlaid on the TAZ map. A toolbar with standard GIS tools (zoom, pan, select) is available to the user to navigate the map and select the study region interactively. The TAZs are selected by drawing a polygon on the interactive map using the "Select TAZ" tool (see Fig.C-5). After drawing the study region, the user clicks the "Finish" button to start the data import process.

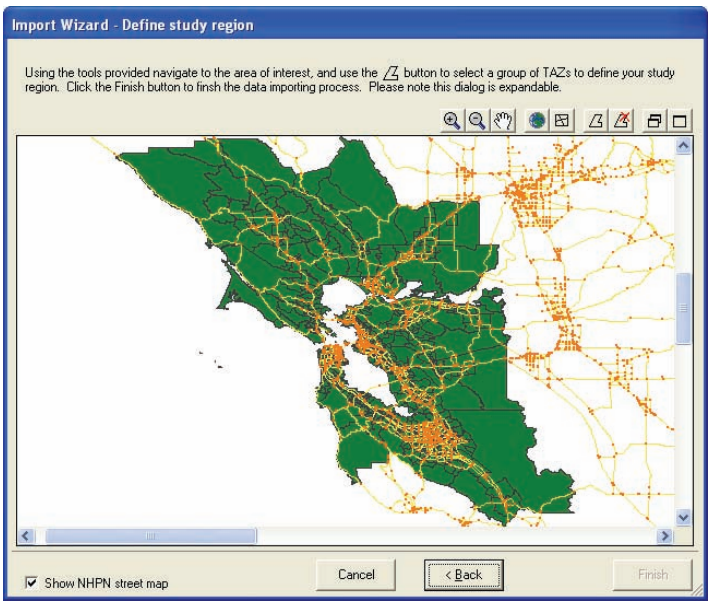

Figure C-9. Screen to Define Study Region Boundary

APPENDIX D
SOURCE-SITE DISTANCES AND GROUND-MOTION HAZARDS

D.1 OBJECTIVE AND SCOPE

As noted earlier, a key feature of the REDARS™ 2 software is modularity -- which enables the software to readily accommodate a variety of existing models for estimating seismic hazards and component performance, as well as new models that are developed in the future. However, with regard to seismic hazards, many of the ground-motion models, as well as models for estimating hazards from liquefaction and surface fault rupture, use different definitions of distances from the earthquake source to the site under consideration. Therefore, to enable REDARS™ 2 to readily accommodate a wide variety of different hazard models, algorithms have been developed and included in a Visual Basic Application (VBA) software package named *SourceSiteDist* to compute distance definitions that are used in many of these models. In addition, this VBA software computes several parameters needed for estimation of site-specific surface fault rupture displacement hazards. Section D.2 summarizes this software.

In accordance with the above modularity feature, REDARS™ 2 now includes two ground-motion models -- the Abrahamson-Silva (1997) model for shallow crustal earthquakes in the Western United States, and the Silva et al. (2002 and 2003) model for earthquakes in the Central United States. The REDARS™ 2 adaptation of these models is summarized in Sections D.3 and D.4. Future versions of REDARS™ will include a library of ground-motion models for various regions of the United States, so that users can select whatever model from this library that they prefer for use in the particular region where the REDARS™ analysis is to be carried out. This library will include appropriate models from each region that are now available, as well as new models that are developed from future research.

D.2 SOURCE-SITE DISTANCES

D.2.1 Quantities Computed

The source-site distance measures and other quantities that are computed in REDARS™ 2 are shown in Figure D-1 and Table D-1. Two sets of quantities are calculated -- one for ground motions and the other for permanent ground displacements due to surface fault rupture. These computations account for the fault's orientation (azimuth) and direction of dip relative to the location of the site of each component in the highway system being analyzed by REDARS™ 2. Parameters needed for ground-motion models that include directivity effects are also obtained.

D.2.2 Assumptions

The REDARS™ 2 source-site distance calculations assume rupture along a single rectangular fault plane (i.e., rupture along multiple segments and trapezoidal fault planes are excluded). The computed distances will also depend on: (b) whether a normal can be drawn from the site to the ruptured fault; and (c) if a such a normal can be drawn, and if the fault plane is dipping, whether the site is along the hanging wall or foot wall of the ruptured fault. Ground-motion models with directivity parameters also require data on the predominant direction of the fault rupture.

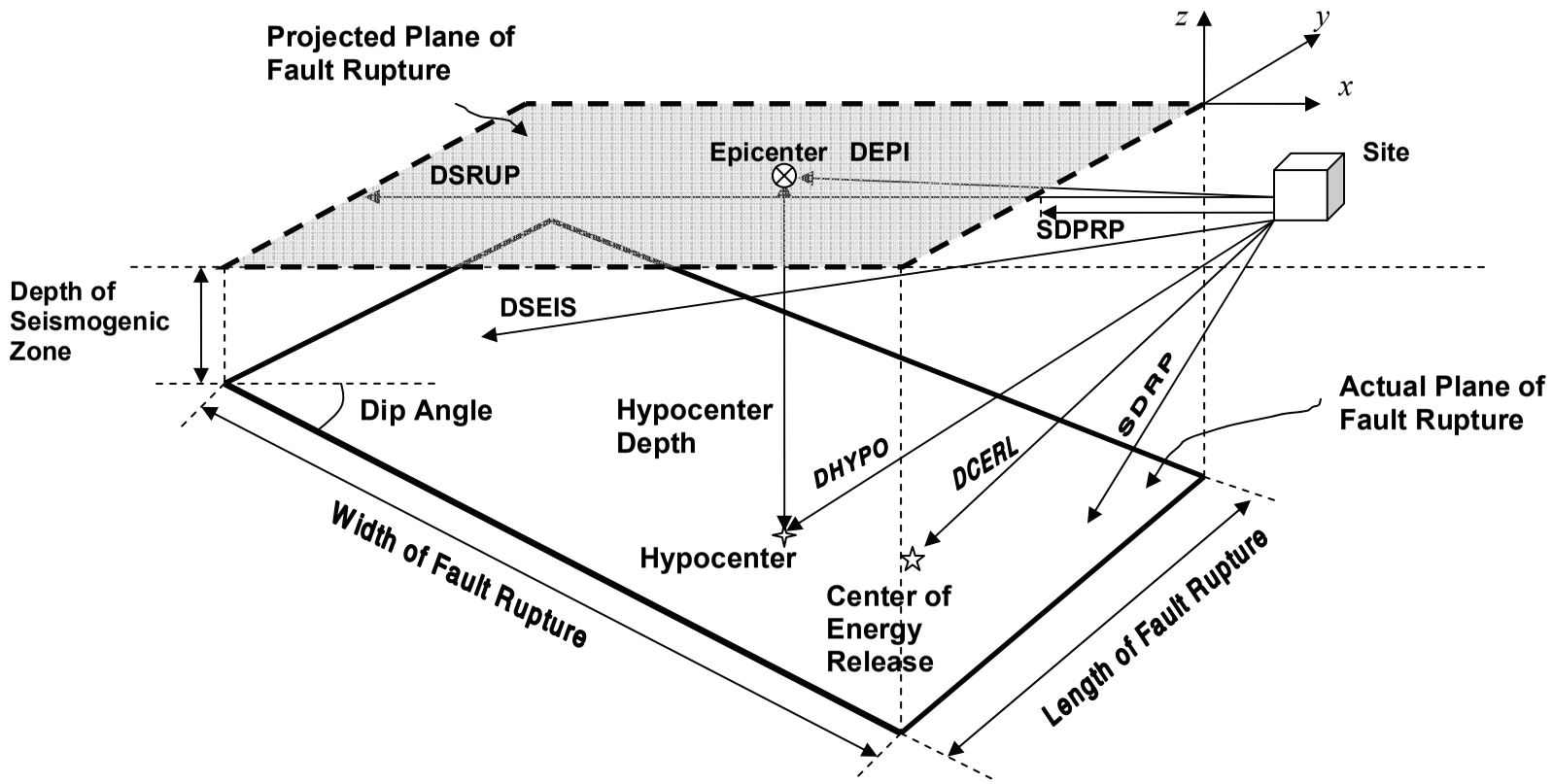

Figure D-1. Distance Measures Obtained from REDARS™ 2 Source-Site Distance Calculations

Table D-1.
Parameters Obtained from Source-Site Distance Calculations (see Figs. D-1 to D-6)

Use in REDARS™ 2	Parameter
Site-Specific Ground Motions (Fig. D-1)	Epicentral Distance (DEPI)
	Hypocentral Distance (DHYPO)
	Distance to Center of Energy Release (DCERL)
	Minimum Distance to Seismogenic Zone (DSEIS)
	Minimum Distance to Fault Rupture (SDRP)
	Minimum Distance to Surface Projection of Fault Rupture Plane (SDPRP)
	Minimum Distance from Site to Ruptured Fault Segment at Ground Surface. (DSRUP)
Other Parameters for Ground-motion Models that Consider Directivity Effects	For Strike-Slip Faults: (a) Predominant Direction of Strong Ground Motions Relative to Site (Fig. D-2); and (b) Angle THETA (Fig. D-3).
	For Dipping Faults: (a) Predominant Direction of Strong Ground Motions relative to Footwall and Hanging Wall and to Site (Fig. D-4); (b) Angle PHI (Fig. D-5) and (c) Whether Site is Subjected to Directivity Adjustments (Fig. D-6).
	Predominant Direction of Ground Motions: Estimated from Location of Epicenter along Ruptured Fault. Assumed to be toward Fault End furthest from Epicenter.
Site-Specific Ground Motions or Fault Rupture Displacement	Whether Site is on Hanging Wall or Footwall of Normal or Reverse Fault. Computed only if NORMAL = 1.
Fault Rupture Displacement	Whether Line can be Drawn from Site that is Normal to Ruptured Fault. If so, NORMAL = 1; otherwise NORMAL = 0
	Ratio of Minimum Distance of Intersection of NORMAL with Fault Line to Length of Fault Plane. Computed only if NORMAL =1.

D.2.3 Input Data

To compute the parameters listed in Table D-1, the walkthough table must include the following quantities for each fault-based earthquake: (a) the azimuth (clockwise angle measured from true north) of .the main trace of the ruptured fault; (b) the latitude, longitude, and depth below the ground surface of the earthquake's center of energy release; (c) the dip angle of the fault rupture; (d) the latitude and longitude of the earthquake epicenter; (d) the type of fault -- i.e., whether it is strike-slip, reverse, normal, etc.; (e) the depth of the earthquake's hypocenter below the ground surface; (f) the latitudes and longitudes of each of the four corners of the fault rupture plane; and (g) the length and width of the fault rupture. Appendix B describes how these quantities are determined for inclusion in the REDARS™ 2 walkthrough tables.

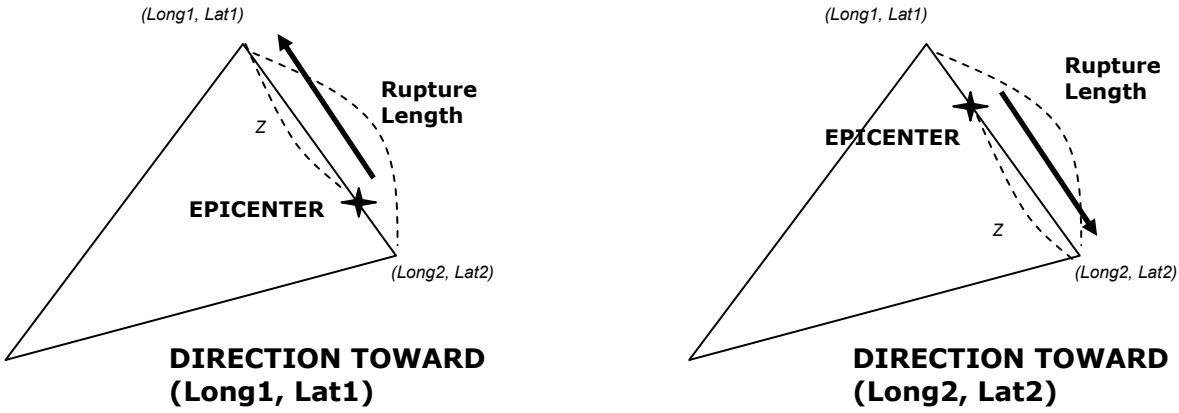

Figure D-2. Direction of Rupture Propagation for Strike-Slip Faults

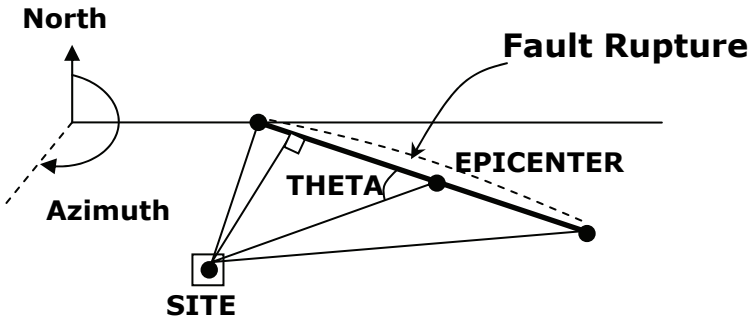

Figure D-3. Plan View of Any Fault Illustrating "Theta"

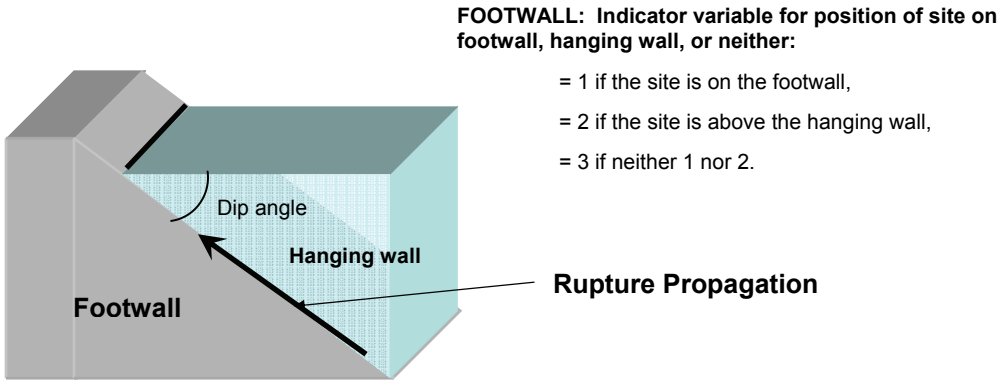

Figure D-4. Assumed Direction of Rupture Propagation for Dipping Faults (Reverse, Reverse/Oblique)

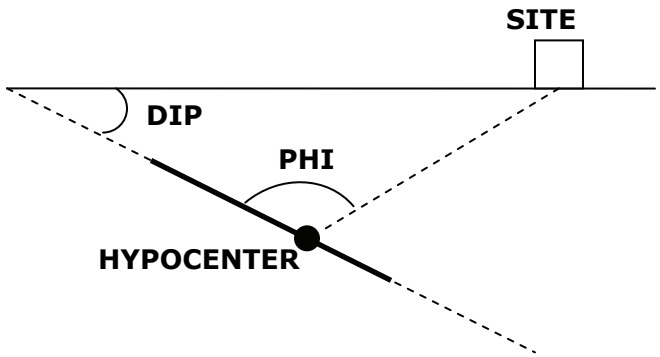

Figure D-5. Section View of Dipping Fault Illustrating Phi

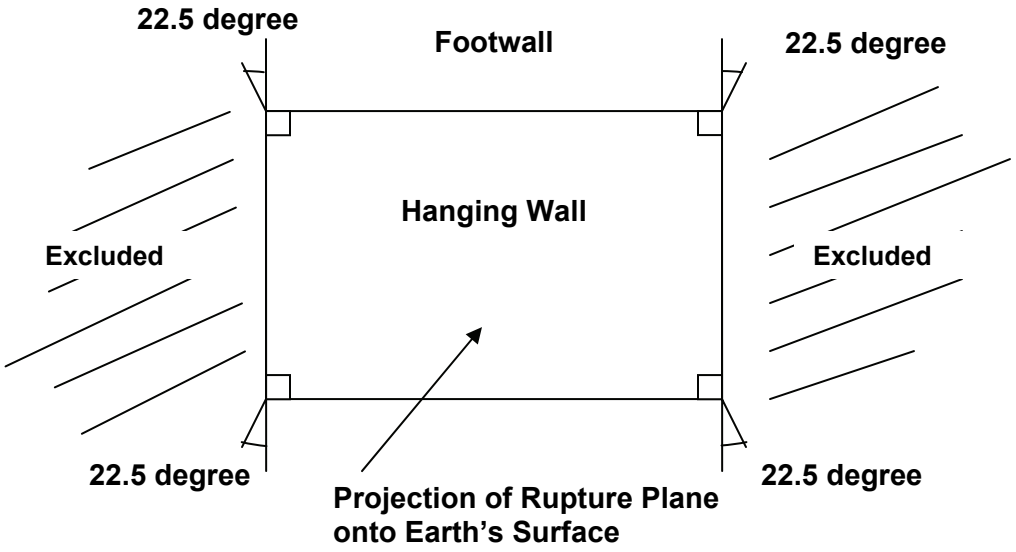

Figure D-6. Plan View of Projection of Fault Plane and Regions Excluded from Directivity Effects

D.3 ADAPTATION OF ABRAHAMSON-SILVA (1997) GROUND-MOTION MODEL

D.3.1 Overview

The Abrahamson-Silva (1997) ground-motion model as adapted into REDARS™ 2 has the following main features:

- It estimates spectral accelerations caused by shallow crustal earthquakes in active tectonic regions of the Western United States, excluding subduction earthquakes.

- It is in the form of a mathematical equation that expresses the natural logarithm of the ground motion as a function of the earthquake magnitude, source-site distance, local soil conditions, type of faulting, whether the site is along the hanging wall or footwall of the ruptured fault plane, and inter-event and intra-event uncertainties. This functionality is represented through a series of numerical coefficients that are used to compute each term in this equation.

- The numerical coefficients that are used to express this functionality enable the model to calculate both horizontal and vertical components of spectral acceleration. However, since the current component damage-state models in REDARS™ 2 use horizontal ground motions only, the coefficients for computing vertical accelerations are excluded from this adaptation of the Abrahamson-Silva (1997) model. However, if future component models are added into REDARS™ that require vertical as well as horizontal input ground motions, the Abrahamson-Silva coefficients for computing vertical motions can be readily added.

- The Abrahamson-Silva model actually provides these coefficients for 28 periods ranging from 0.01 sec. to 5.0 sec. However, since the current bridge models in REDARS™ 2 only consider periods of 0.3 sec. and 1.0 sec., and since current REDARS™ 2 liquefaction models consider peak ground acceleration only (i.e., spectral accelerations for a period = 0.0 sec.), this REDARS™ 2 adaptation of the Abrahamson-Silva model includes coefficients for those periods only. However, if future component or liquefaction models in REDARS™ consider other periods, coefficients for these periods can be readily added.

- This model uses moment magnitude (M_w) to represent earthquake magnitude, and defines the source-site distance (r_{rup}) as the closest distance from the site to the rupture plane. In this, if the fault plane is vertical or is dipping away from the site, r_{rup} will be the distance from the site to the fault-rupture location on the ground surface (and will be straightforward to calculate.) However, if the fault plane is dipping toward the site, r_{rup} depends on the dip angle and is more complicated to compute.

- This ground-motion model considers two site classifications: a rock site (with a soil thickness < 20m that overlies rock) and a deep soil site (with soils whose thickness exceeds 20 m).

- The model also includes: (a) a "style-of-faulting" factor that accounts for whether the causative fault is reverse or strike-slip; and (b) a "hanging-wall" factor that models differences in ground motion on the hanging wall vs. the foot wall of a dipping fault.

- Abrahamson and Silva define the horizontal spectral acceleration as representing the average (and not the upper bound) of the two components of horizontal motion recorded during the various earthquake events cited in their paper.

D.3.2 Implementation of Model in REDARS™ 2

The Abrahamson-Silva (1997) model for estimating site-specific ground motions at the i^{th} site in the highway system has the following form:

$$\ln S_a(g)_i = f_1(M_w, r_{rup})_i + Ff_3(M_w) + HWf_4(M_w, r_{rup})_i + Sf_5(\overline{pga}_{rock})_i + \varepsilon_{\text{int}er}(M_w) + (\varepsilon_{\text{int}ra})_i \quad \text{(D-1)}$$

In this equation, the subscript *i* denotes those terms that, for each earthquake, are computed separately for each component site (where *i* is the component number). Those quantities without the subscript *i* are computed once for each earthquake only. The term $f_1(M_w, r_{rup})_i$ is the basic functional form of the attenuation model for rock sites and strike-slip faulting. The terms $Ff_3(M_w)$, $HWf_4(M_w, r_{rup})_i$, and $Sf_5(\overline{pga}_{rock})_i$ represent modifications to this basic form to account for effects of other types of faulting, hanging-wall effects, and local soil conditions. The quantities $\varepsilon_{\text{int}er}(M_w)$ and $(\varepsilon_{\text{int}ra})_i$ represent effects of inter-event uncertainties (earthquake-dependent only) and intra-event uncertainties (earthquake- and component-dependent).

The remainder of this section describes the input data and the steps for developing each of the above terms in Equation D-1. The first two steps describe the determination of those terms in Equation D-1 that depend only on the scenario earthquake -- the style-of-faulting term $Ff_3(M_w)$ and the inter-event uncertainty term $\varepsilon_{\text{int}er}(M_w)$. Therefore, these terms are determined only once for each earthquake. The remaining steps describe the determination of those terms in Equation D-1 that must be computed separately for each component's site in the highway system.

D.3.2.1 Input Data

In addition to the data already included in the walkthrough table for REDARS™ 2, additional data that are needed in order to apply the Abrahamson-Silva model to each component site in the highway network are the site's soil classification *S,* and hanging-wall factor, HW.

D.3.2.2 Step 1 (For Each Earthquake Only): Compute Style of Faulting Factor, $Ff_3(M_w)$

The REDARS™ 2 earthquake walkthrough table (Appendix B) will define the style of the causative fault for each scenario earthquake in the table (i.e., whether it is a strike-slip, reverse, or reverse/oblique fault.) From this, the style-of-faulting factor in the Abrahamson-Silva model is obtained by defining the quantity F to represent the fault type (1 for reverse faulting, 0.5 for reverse/oblique faulting, and 0 otherwise), and

$$
\begin{aligned}
f_3(M_w) &= 0 && \text{for } M_w \le 5.5, \\
&= M_w - 5.5 && \text{for } 5.5 < M_w < 6.5 \\
&= 1 && \text{for } M_w \ge 6.5
\end{aligned}
\tag{D-2}
$$

As noted previously, this style-of-faulting factor is independent of site location and is therefore computed only once for each scenario earthquake.

D.3.2.3 Step 2 For Each Earthquake: Calculate Inter-Event Uncertainty Factor, $\varepsilon_{inter}(M_w)$

For each earthquake scenario, the inter-event uncertainty factors for PGA, $S_a(0.3)$, and $S_a(1.0)$ are computed only once, as described below:

- Compute the quantity τ (for PGA, $S_a(0.3)$, and $S_a(1.0)$) according to the following procedure (Youngs et al., 1995):

  For $5.0 \le M_w < 7.0$:

$$X_1 = \frac{-0.373 * (M_w - 5.0) + 0.938}{-0.122 * (M_w - 5.0) + 1.096} \tag{D-3}$$

$$C = \sqrt{\frac{1}{X_1^{\,2} + 1}} \tag{D-4}$$

$$\tau = X_1 * C * \left[b_5 - b_6 * (M_w - 5)\right] \tag{D-5}$$

  For $M_w \ge 7.0$:

$$\tau = 0.222\left[b_5 - 2b_6\right] \tag{D-6}$$

  where the parameters b_5 and b_6 are obtained from Table D-2.

- Generate a uniform random number X from a normal distribution with a mean of 0 and a standard deviation of 1. Then, compute the inter-event uncertainty factor as

$$\varepsilon_{inter}(M_w) = \tau * X \tag{D-7}$$

  where it is again noted that the above calculations leading to $\varepsilon_{inter}(M_w)$ (Eqs. D-3 to D-7) are carried out separately for each earthquake scenario.

Table D-2. Parameters for Estimating Inter-Event Uncertainty Factor

Ground Motion	b_5	b_6
Spectral acceleration at 1.0 sec. ($S_a(1.0)$)	0.83	0.118
Spectral acceleration at 0.3 sec. ($S_a(0.3)$)	0.78	0.135
Spectral acceleration at 0.0 sec., or peak ground acceleration (PGA)	0.70	0.135

D.3.2.4 Step 3: For Each Earthquake and Each Component Site: Compute Intra-Event Uncertainty Factor (ε_{intra})$_i$

The intra-event uncertainty factor is computed for each earthquake and each component site as described below:

- Compute the quantity σ (for PGA, $S_a(0.3)$, and $S_a(1.0)$) according to the following procedure (Youngs et al., 1995):

$$\text{For } 5.0 \le M_w < 7.0: \qquad \sigma = C * [b_5 - b_6 * (M_w - 5)] \tag{D-8}$$

$$\text{`For } M_w \ge 7.0: \qquad \sigma = 0.975[b_5 - 2b_6] \tag{D-9}$$

  where C is obtained for each earthquake from Equation D-4, and the parameters b_5 and b_6 are obtained from Table D-1.

- For the i^{th} component site in the highway system (where i = 1, 2, ….total number of sites), generate a uniform random number X_i from a normal distribution with a mean of 0 and a standard deviation of 1. Then, compute the intra-event uncertainty factor for that site as

$$(\varepsilon_{i\,intra})_i = \sigma * X_i \tag{D-10}$$

  This generation of the random number X_i and the computation of the intra-event uncertainty factor $(\varepsilon_{intra})_i$ are carried out separately for each component site.

D.3.2.5 Step 4 (For Each Earthquake and Each Component Site): Obtain Minimum Distance from Site to Rupture Plane, r_{rup}

The minimum distance from the site to the rupture plane (r_{rup}) will depend on the fault's orientation (strike), dip angle, and proximity to the site. In REDARS™ 2, r_{rup} .is obtained from the source-site distance calculation process that is summarized in Section D.2.

D.3.2.6 Step 5 For Each Earthquake and Each Component Site: Establish Basic Ground-motion Attenuation Form, $f_1(M_w, r_{rup})$

As noted earlier, the starting point for the Abrahamson-Silva model is a basic attenuation form for rock sites and strike-slip faulting that is termed $f_1(M_w, r_{rup})$ and is computed as follows:

For $M_w \le 6.4$:

$$f_1(M_w, r_{rup}) = a_1 + 0.512(M_w - 6.4) + a_{12}(8.5 - M_w)^2 + \left[a_3 + 0.17(M_w - 6.4)\right]\ln R \tag{D-11}$$

For $M_w > 6.4$:

$$f_1(M_w, r_{rup}) = a_1 - 0.144(M_w - 6.4) + a_{12}(8.5 - M_w)^2 + \left[a_3 + 0.17(M_w - 6.4)\right]\ln R \tag{D-12}$$

where

$$R = \sqrt{r_{rup}{}^2 + c_4{}^2} \tag{D-13}$$

and the constants a_1, a_2, a_{12}, a_3 and c_4 are given in Table D-3.

Table D-3
Coefficients in Equations D-11 thru D-13

Period, sec.	c_4	a_1	a_3	a_5	a_6	a_9	a_{10}	a_{11}	a_{12}
1.0	3.70	0.828	-0.8383	0.490	0.013	0.281	0.423	0.000	-0.1020
0.3	4.80	2.114	-1.0350	0.610	0.198	0.370	-0.219	-0.195	-0.0360
0.0	5.60	1.640	-1.1450	0.610	0.260	0.370	-0.417	-0.230	0.0000

D.3.2.7 Step 6 (For Each Earthquake and Each Component Site): Compute Hanging-Wall Effect, $HWf_4(M_w, r_{rup})$

This factor accounts for whether the site is on the hanging-wall side of the rupture and within the edge of the rupture. In this, HW is a dummy variable for hanging-wall sites (= 1 for sites over the hanging wall, 0 otherwise) and

$$f_4(M_w, r_{rup}) = f_{HW}(M_w) f_{HW}(r_{rup}) \tag{D-14}$$

where the various terms in Equation D-14 are defined as follows:

$$\begin{aligned} f_{HW}(M_w) &= 0 && \text{for } M_w \le 5.5, \\ &= M_w - 5.5 && \text{for } 5.5 < M_w < 6.5 \\ &= 1 && \text{for } M_w \ge 6.5 \end{aligned} \tag{D-15}$$

and

$$\begin{aligned} f_{HW}(r_{rup}) &= 0 && \text{for } r_{rup} < 4 \\ &= a_9 \frac{r_{rup} - 4}{4} && \text{for } 4 < r_{rup} < 8 \\ &= a_9 && \text{for } 8 < r_{rup} < 18 \\ &= a_9 \left(1 - \frac{r_{rup} - 18}{7}\right) && \text{for } 18 < r_{rup} < 24 \\ &= 0 && \text{for } r_{rup} > 25 \end{aligned} \tag{D-16}$$

and the constant a_9 is given in Table D-2. This cannot be called out in the walkthrough table, since it will vary from site to site.

D.3.2.8 Step 7 (For Each Earthquake and Each Component Site): Develop Site-Response Factor, $Sf_5(PGA_{rock})$

The Abrahamson-Silva model uses a variable S to characterize site soil conditions (= 0 for rock or shallow soil, 1 otherwise), and

$$f_5(\overline{PGA}_{rock}) = a_{10} + a_{11} \ln(\overline{PGA}_{rock} + 0.03) \tag{D-17}$$

where $\overline{PGA}_{rock}$ = expected peak acceleration (in g's) on rock (as predicted by the median attenuation relationship, Equation D-1, with $S = 0$) and the constants a_{10} and a_{11} are given in Table D-2. In this, it is assumed that the Abrahamson-Silva rock sites correspond to NEHRP site classifications A, B, and C, and that Abrahamson-Silva soil sites correspond to NEHRP site classifications D and E.

D.3.2.9 Step 8 (For Each Earthquake and Each Component Site): Calculate Resultant Site-Specific Ground Motions

In Step 8, the terms computed in Sections D.3.1 through D.3.8 are substituted into Equation D-1 in order to obtain the resulting spectral acceleration for each site in the highway network.

D.4 ADAPTATION OF SILVA ET AL. (2002 and 2003) GROUND-MOTION MODEL

This section describes the site-specific ground-motion models by Silva et al. that are currently used in REDARS™ 2 applications to highway systems in the Central United States (CUS) region that is shown in Figure B-1 of Appendix B. This model contains the following steps: (1) computation of earthquake motions in hard rock (NEHRP Type A sites) as a function of earthquake magnitude and source-site distance; (2) conversion of these hard-rock motions to corresponding motions in firm rock (NEHRP Type B sites); (3) development of a soil amplification factor relative to firm-rock; and (4) use of this factor with the firm-rock motions from Step 2 to estimate site-specific ground motions including local site effects and uncertainties. These steps are summarized below.

In accordance with the bridge models now being used in REDARS™ 2, the ground motions estimated by this model at this time are spectral accelerations at periods of 0.0 sec. (peak ground acceleration), 0.3 sec., and 1.0 sec. Future versions of REDARS™ with updated fragility models may use spectral accelerations at other periods, which can be readily estimated by this model.

D.4.1 Step 1: Compute Earthquake Motions in Hard Rock

D.4.1.1 General Equation for Hard-Rock Motions

In Step 1, the following equation (Silva et al., 2003) is used to estimate hard-rock motion:

$$\ln S_{aA}'(T) = \ln \overline{S}_{aA}(T) + \varepsilon \qquad \text{(D-18)}$$

where $S_{aA}'(T)$ is the hard-rock motion (spectral acceleration at period T for NEHRP Type A site conditions) including uncertainties, $\overline{S}_{aA}(T)$ is the median value of $S_{aA}'(T)$ (computed using Equation D-19), and ε is the uncertainty in $S_{aA}'(T)$ (computed using Equation D-20).

$$\ln \overline{S}_{aA}(T) = C_1 + C_2 * M_w + (C_6 + C_7 M_w) * \ln(R + \exp^{C_4}) + C_{10} * (M_w - 6.0)^2 \qquad \text{(D-19)}$$

$$\varepsilon = X\sigma_{S_{aA}(T)} \qquad \text{(D-20)}$$

In Equation D-19, M_w is the moment magnitude of the earthquake, R is the closest distance from the site to the surface projection of the rupture surface (as computed using the REDARS™ 2 source-site distance calculation summarized in Section D.2), C_1, C_2, C_4, C_6, C_7, and C_{10} are period-dependent regression coefficients that depend on whether a single-corner model or double-corner model is to be applied (see Tables D-3 and D-4). In Equation D-20, $\sigma_{S_{aA}(T)}$ is the

period-dependent standard deviation of $S_{aA}'(T)$ that also depends on whether a single-corner or double-corner model is applied (Tables D-4 and D-5), and X is a normally distributed random number with a mean of 0 and a standard deviation of 1.

Table D-4. CEUS Regression Coefficients for Single-Corner Model with Variable Stress Drop as a Function of M_w (from Table D-5 with parametric σ from Silva et al., 2002)

Period, sec.	C_1	C_2	C_4	C_6	C_7	C_{10}	σ
0.0 (PGA)	4.19301	0.07506	2.70	-3.00408	0.20195	-0.08927	0.6912
0.3	1.27630	0.43069	2.60	-2.56373	0.15989	-0.14085	0.6231
1.0	-4.35940	1.10344	2.60	-2.19556	0.12077	-0.29213	0.5697

Table D-5. CEUS Regression Coefficients for Double-Corner Model with Saturation (from Table 7 with Parametric σ from Silva et al., 2002)

Period, sec.	C_1	C_2	C_4	C_6	C_7	C_{10}	σ
0.0 (PGA)	5.91196	-0.15727	2.90	-3.42401	0.26564	-0.07004	0.6912
0.3	2.27626	0.27031	2.80	-2.95623	0.22193	-0.11697	0.6231
1.0	-3.10841	0.79561	2.80	-2.58562	0.18195	-0.15020	0.5697

D.4.1.2 Model Application

The application of the above model to estimate hard-rock motions for a given site and earthquake event will consist of the following steps:

1. *Estimate Median Value of Hard-Rock Motion using Single-Corner Model,* $\overline{S}_{aASC}(T)$. This involves application of Equation D-19 with the regression coefficients from Table D-4.

2. *Estimate Standard Deviation of Hard-Rock Motion,* σ_{SC}*, using Single-Corner Model.* This involves use of the value of σ from in Table D-4.

3. *Estimate Median Value of Hard-Rock Motion using Double-Corner Model,* $\overline{S}_{aA\,DC}(T)$. This involves application of Equation D-19 with the regression coefficients from Table D-5.

4. *Estimate Standard Deviation of Hard-Rock Motion,* σ_{DC}*, using Double-Corner Model.* This involves use of the value of σ from Table D-5.

5. *Obtain Weighted Median Value of Hard-Rock Motion,* $\overline{S}_{aAW}(T)$. This uses the following weighting of the single-corner and double-corner estimates of the median hard-rock motion:

$$\overline{S}_{aAW}(T) = 0.6\overline{S}_{aASC}(T) + 0.4\overline{S}_{aADC}(T) \qquad \text{(D-20)}$$

6. *Obtain Weighted Standard Deviation of Hard-Rock Motion,* $\sigma_{WSaA(T)}$. This involves the following assumed weighting between the single-corner and double-corner estimates of the standard deviation of the hard-rock motion:

$$\sigma_{WSaA(T)} = \sqrt{0.6\sigma_{SC}{}^2 + 0.4\sigma_{DC}{}^2} \tag{D-21}$$

7. Generate a normally distributed random number, *X*, with a mean of 0 and a standard deviation of 1. Then, use Equation D-22 to obtain the uncertainty term ε_W as:

$$\varepsilon_W = X * \sigma_{WSaA(T)} \tag{D-22}$$

8. Evaluate the site's hard-rock motion for this simulation by substituting Equations D-20 and D-22 into Equation D-18, and taking the exponent.

$$\ln S_{aA}'(T) = \ln \overline{S}_{aAW}(T) + \varepsilon_W \tag{D-23}$$

D.4.2 Step 2: Obtain Equivalent Firm-Rock (NEHRP Type B) Motions

For a given site, Equation D-24 is used to convert the ground motions from Step 1 from NEHRP Type A to Type B site conditions for this simulation

$$S'_{aB}(T) = \overline{C}_{A-B}(T) * S_{aA}'(T) \tag{D-24}$$

where, for this simulation, $S'_{aB}(T)$ is the site's spectral acceleration (including uncertainties) for NEHRP Type B site conditions at T = 0.0 sec., 0.3 sec., and 1.0 sec., $\overline{C}_{A-B}(T)$ -- the median value of the conversion factor -- is obtained from Table D-6, and $S'_{aA}(T)$ -- the site's spectral accelerations for Type A rock conditions – has been computed under Step 1.

Table D-6. Conversion Factors, $\overline{C}_{A-B}(T)$

Period T, sec.	Median, $\overline{C}_{A-B}(T)$
0.0	0.950301
0.3	1.505817
1.0	1.100014

.

D.4.3 Step 3: Develop Soil Amplification Factors

The development of the site's soil amplification factor (SAF) for this scenario earthquake and simulation will require the following substeps.

D.4.3.1 Substep 3-1: Compute Mean Values and Standard Deviations of SAFs

Using the site's peak acceleration for Type B site conditions (from Step 2) and the site's NEHRP classification, go to the appropriate table in Tables D-7 through D-12 to obtain the median values of the site amplification factors ($\overline{SAF}_S(T=0)$, $\overline{SAF}_S(T=0.3)$, and $\overline{SAF}_S(T=1.0)$) and the standard deviations of these factors ($\sigma_{SAF_S(T=0)}$, $\sigma_{SAF_S(T=0.3)}$, and $\sigma_{SAF_S(T=1.0)}$).

D.4.3.2 Substep 3-2: Obtain Uniform Random Number from Distribution *N(0,1)*

Generate a uniform normally-distributed random number X with a mean of 0 and a standard deviation of 1.

D.4.3.3 Substep 3-3: Compute SAFs for this Earthquake and Simulation

For this given site, use Equations D-25a through D-25c to compute the SAFs (including uncertainties) to be used for this scenario earthquake and simulation.

$$SAF'_S(T=0) = \overline{SAF}_S(T=0) * \exp(X * \sigma_{SAF_S(T=0)}) \quad \text{(D-25a)}$$

$$SAF'_S(T=0.3) = \overline{SAF}_S(T=0.3) * \exp(X * \sigma_{SAF_S(T=0.3)}) \quad \text{(D-25b)}$$

$$SAF'_S(T=1.0) = \overline{SAF}_S(T=1.0) * \exp(X * \sigma_{SAF_S(T=1.0)}) \quad \text{(D-25c)}$$

D.4.4 Step 4: Compute Site-Specific Ground Motions including Effects of Local Soil Conditions

For this scenario earthquake and simulation, use Equations D-26a through D-26c to compute the site-specific ground motions $S'_{aS}(T)$, including uncertainties and local site effects:

$$S'_{aS}(T=0.0) = S'_{aB}(T=0.0) * SAF'_S(T=0.0) \quad \text{(D-26a)}$$

$$S'_{aS}(T=0.3) = S'_{aB}(T=0.3) * SAF'_S(T=0.3) \quad \text{(D-26b)}$$

$$S'_{aS}(T=1.0) = S'_{aB}(T=1.0) * SAF'_S(T=1.0) \quad \text{(D-26c)}$$

where $S'_{aB}(T)$ is the Type B rock motion as obtained from Step 2; and $SAF'_S(T)$ is the site amplification factor from Step 3.

Table D-7. NEHRP Type A Site Conditions in CEUS (Silva et al., 2002)

Period, sec.	PGA_B = 0.05 g	PGA_B = 0.10 g	PGA_B = 0.20 g	PGA_B = 0.30 g	PGA_B = 0.40 g	PGA_B = 0.50 g	PGA_B = 0.75 g
1.0	0.9118966	0.9098705	0.9093926	0.9090797	0.9087743	0.9085138	0.9078581
0.3	0.6634737	0.6655601	0.6648104	0.6640913	0.6632008	0.6623759	0.6602756
0.0 (PGA)	1.015875	1.036374	1.046970	1.052298	1.056135	1.059185	1.065125

a) Median Soil Amplification Factor, $\overline{SAF}_A$ ($PGA_B = S_{aB}'(T=0)$ from Eq. D-24)

Period, sec.	PGA_B = 0.05 g	PGA_B = 0.10 g	PGA_B = 0.20 g	PGA_B = 0.30 g	PGA_B = 0.40 g	PGA_B = 0.50 g	PGA_B = 0.75 g
1.0	1.014607	1.015682	1.015808	1.015866	1.015889	1.015902	1.015922
0.3	1.088266	1.087953	1.088070	1.088102	1.088129	1.088150	1.088168
0.0 (PGA)	1.183159	1.190851	1.194395	1.195770	1.196554	1.197034	1.197602

b) Standard Deviation of Soil Amplification Factor, σ_{SAF_A} ($PGA_B = S_{aB}'(T=0)$ from Eq. D-24)

Table D-8. NEHRP Type B Site Conditions in CEUS (Silva et al., 2002)

Period, sec.	PGA_B = 0.05 g	PGA_B = 0.10 g	PGA_B = 0.20 g	PGA_B = 0.30 g	PGA_B = 0.40 g	PGA_B = 0.50 g	PGA_B = 0.75 g
1.0	1.0	1.0	1.0	1.0	1.0	1.0	1.0
0.3	1.0	1.0	1.0	1.0	1.0	1.0	1.0
0.0 (PGA)	1.0	1.0	1.0	1.0	1.0	1.0	1.0

a) Median Soil Amplification Factor, $\overline{SAF}_B$ ($PGA_B = S_{aB}'(T=0)$ from Eq. D-24)

Period, sec.	PGA_B = 0.05 g	PGA_B = 0.10 g	PGA_B = 0.20 g	PGA_B = 0.30 g	PGA_B = 0.40 g	PGA_B = 0.50 g	PGA_B = 0.75 g
1.0	0.00	0.00	0.00	0.00	0.00	0.00	0.00
0.3	0.00	0.00	0.00	0.00	0.00	0.00	0.00
0.0 (PGA)	0.00	0.00	0.00	0.00	0.00	0.00	0.00

b) Standard Deviation of Soil Amplification Factor, σ_{SAF_B} ($PGA_B = S_{aB}'(T=0)$ from Eq. D-24)

Table D-9. NEHRP Type B/C Site Conditions in CEUS (Silva et al., 2002)

Period, sec.	$PGA_B = 0.05$ g	$PGA_B = 0.10$ g	$PGA_B = 0.20$ g	$PGA_B = 0.30$ g	$PGA_B = 0.40$ g	$PGA_B = 0.50$ g	$PGA_B = 0.75$ g
1.0	1.206254	1.211956	1.215325	1.218209	1.221541	1.224887	1.231358
0.3	1.119031	1.126973	1.136433	1.144768	1.154395	1.164138	1.180151
0.0 (PGA)	1.350111	1.339832	1.325622	1.313639	1.301445	1.288230	1.265030

a) Median Soil Amplification Factor, $\overline{SAF}_{B-C}$ ($PGA_B = S_{aB}'(T=0)$ from Eq. D-24)

Period, sec.	$PGA_B = 0.05$ g	$PGA_B = 0.10$ g	$PGA_B = 0.20$ g	$PGA_B = 0.30$ g	$PGA_B = 0.40$ g	$PGA_B = 0.50$ g	$PGA_B = 0.75$ g
1.0	1.133111	1.130123	1.129682	1.129417	1.128835	1.128460	1.128097
0.3	1.351495	1.350228	1.355022	1.358535	1.362289	1.368374	1.375033
0.0 (PGA)	1.276182	1.275780	1.266794	1.257777	1.249880	1.239190	1.222640

b) Standard Deviation of Soil Amplification Factor, $\sigma_{SAF_{B-C}}$ ($PGA_B = S_{aB}'(T=0)$ from Eq. D-24)

Table D-10. NEHRP Type C Site Conditions in CEUS (Silva et al., 2002)

Period, sec.	$PGA_B = 0.05$ g	$PGA_B = 0.10$ g	$PGA_B = 0.20$ g	$PGA_B = 0.30$ g	$PGA_B = 0.40$ g	$PGA_B = 0.50$ g	$PGA_B = 0.75$ g
1.0	1.720109	1.717642	1.727490	1.734434	1.743202	1.745760	1.747499
0.3	1.474326	1.461003	1.437271	1.407859	1.369055	1.317687	1.231579
0.0 (PGA)	1.353303	1.306655	1.240078	1.185258	1.133129	1.083909	0.9994305

a) Median Soil Amplification Factor, $\overline{SAF}_{C}$ ($PGA_B = S_{aB}'(T=0)$ from Eq. D-24)

Period, sec.	$PGA_B = 0.05$ g	$PGA_B = 0.10$ g	$PGA_B = 0.20$ g	$PGA_B = 0.30$ g	$PGA_B = 0.40$ g	$PGA_B = 0.50$ g	$PGA_B = 0.75$ g
1.0	1.500996	1.482618	1.482200	1.479927	1.481994	1.477954	1.468075
0.3	1.404853	1.388789	1.375102	1.357686	1.345110	1.326261	1.332198
0.0 (PGA)	1.267915	1.266918	1.261484	1.258200	1.258520	1.259774	1.268029

b) Standard Deviation of Soil Amplification Factor, σ_{SAF_C} ($PGA_B = S_{aB}'(T=0)$ from Eq. D-24)

Table D-11. NEHRP Type D Site Conditions in CEUS (Silva et al., 2002)

Period, sec.	$PGA_B = 0.05$ g	$PGA_B = 0.10$ g	$PGA_B = 0.20$ g	$PGA_B = 0.30$ g	$PGA_B = 0.40$ g	$PGA_B = 0.50$ g	$PGA_B = 0.75$ g
1.0	2.363349	2.345327	2.310039	2.199857	2.094171	2.020892	1.929046
0.3	1.690411	1.629107	1.494538	1.380737	1.248931	1.113333	0.9020683
0.0 (PGA)	1.668142	1.459669	1.214897	1.062375	0.9437199	0.8524503	0.7259755

a) Median Soil Amplification Factor, $\overline{SAF}_D$ ($PGA_B = S_{aB}'(T = 0)$ from Eq. D-24)

Period, sec.	$PGA_B = 0.05$ g	$PGA_B = 0.10$ g	$PGA_B = 0.20$ g	$PGA_B = 0.30$ g	$PGA_B = 0.40$ g	$PGA_B = 0.50$ g	$PGA_B = 0.75$ g
1.0	1.573316	1.521139	1.469390	1.412737	1.400189	1.405819	1.461915
0.3	1.394965	1.395215	1.398624	1.452470	1.581125	1.644137	1.747778
0.0 (PGA)	1.320732	1.336129	1.375664	1.389553	1.428778	1.455471	1.507446

b) Standard Deviation of Soil Amplification Factor, σ_{SAF_D} ($PGA_B = S_{aB}'(T = 0)$ from Eq. D-24)

Table D-12. NEHRP Type E Site Conditions in CEUS (Silva et al., 2002)

Period, sec.	$PGA_B = 0.05$ g	$PGA_B = 0.10$ g	$PGA_B = 0.20$ g	$PGA_B = 0.30$ g	$PGA_B = 0.40$ g	$PGA_B = 0.50$ g	$PGA_B = 0.75$ g
1.0	3.468236	3.320492	2.667635	2.270436	2.031032	1.816679	1.434469
0.3	1.541128	1.145728	0.7539840	0.5771288	0.4600821	0.3789863	0.2894955
0.0 (PGA)	1.292572	0.9590081	0.6788728	0.5460030	0.4670651	0.4071466	0.3254445

a) Median Soil Amplification Factor, $\overline{SAF}_E$ ($PGA_B = S_{aB}'(T = 0)$ from Eq. D-24)

Period, sec.	$PGA_B = 0.05$ g	$PGA_B = 0.10$ g	$PGA_B = 0.20$ g	$PGA_B = 0.30$ g	$PGA_B = 0.40$ g	$PGA_B = 0.50$ g	$PGA_B = 0.75$ g
1.0	1.428695	1.405269	1.364846	1.428719	1.467666	1.528848	1.567584
0.3	1.377671	1.427722	1.562875	1.664149	1.716229	1.762579	1.844318
0.0 (PGA)	1.196678	1.254175	1.369497	1.437981	1.473763	1.504813	1.531796

b) Standard Deviation of Soil Amplification Factor, σ_{SAF_E} ($PGA_B = S_{aB}'(T = 0)$ from Eq. D-24)

APPENDIX E
LIQUEFACTION HAZARDS

E.1 INTRODUCTION

REDARS™ 2 uses adaptations of the models by Bardet et al. (2002) and Tokimatsu-Seed (1987) to estimate liquefaction-induced lateral-spread displacements and vertical settlements respectively. These adaptations are described in this appendix.

The remainder of this appendix contains four main sections. Section E.2 provides an overview of the methods used in REDARS™ 2 to estimate site-specific liquefaction hazards. Following this, Section E.3 summarizes how to identify potentially liquefiable soil sites within the highway system, and to then obtain the soils data at those sites that are needed as input to the REDARS™ 2 estimation of liquefaction-induced permanent ground displacements (PGD). Then, Sections E.4 and E.5 summarize the adaptations of the Bardet et al. (2002) and Tokimatsu-Seed (1987) models that are used in REDARS™ 2 to estimate these PGD hazards.

E.2 EVALUATION PROCEDURE OVERVIEW

Prior to the evaluation of liquefaction hazards in REDARS™ 2, the user must first screen the geologic and soils data at all component sites in the highway system, in order establish which of these sites have a low potential for liquefaction and can therefore be excluded from further analysis of liquefaction hazards in REDARS™ 2. Then, for those potentially liquefiable sites that are not excluded by this screening, REDARS™ 2 uses the following steps to compute site-specific liquefaction hazards for each earthquake scenario and simulation: (a) the Bardet et al. (2002) method is used to estimate liquefaction-induced lateral-spread displacements; (b) the Tokimatsu-Seed (1987) method is used to estimate liquefaction-induced vertical settlements; and (c) a resultant liquefaction-induced displacement is computed as the vector sum of these lateral-spread and vertical settlement values.

E.3 SCREENING FOR LIQUEFACTION POTENTIAL

As noted above, the purpose of the user's initial screening of the sites throughout the highway system is to identify those sites within the system whose liquefaction potential is judged to be sufficiently low to justify their elimination from further liquefaction hazard analysis in REDARS™ 2. Although the user can apply any appropriate screening procedure, one such procedure that has been recommended by Youd (1998) is summarized below.

E.3.1 Input Data Requirements

The input data for this screening consists of: (a) locations and properties of Quaternary geologic units in the area; (b) highest average or likely depth to unconfined ground water table, either permanent and perched; (c) soil boring log data consisting of penetration resistance, Atterberg limits, clay content, and natural moisture content; and (d) soil classifications, by either the AASHTO, Unified, or NEHRP classification systems.

E.3.2 Initial Screening based on Assessment of Local Geology and Soil Conditions

- ***Step 1. Geologic Analysis.*** Geologic units and depositional processes are evaluated in order to identify those sites along the highway system that can be classed as low-hazard sites. These sites are eliminated from further liquefaction analysis. This evaluation is based on comparisons of the geologic input data to geologic screening criteria that are shown in Table C-1 and are based on analysis of geologic conditions at sites of past liquefaction (Youd and Perkins, 1978).

- ***Step 2. Water-table Analysis.*** For those sites not eliminated by Step 1, water-table depths at these sites are evaluated. In Youd (1998), it is recommended that sites with water-table depths in excess of 15 m should be eliminated from further liquefaction analysis.

- ***Step 3. Evaluation for Extra-Sensitive Clays.*** A check is made for potential loss of strength in clays with large fractions of colloidal-sized particles in which loss of strength is usually caused be leaching of salts from interstitial water. These clays are found in only a few areas of the U.S. (Alaska, St. Lawrence River valley, and saline lakes of the Great Basin or in estuarine sediments along coastal rivers or bays). Clays are classed as extra-sensitive if all of the following conditions are met: (a) liquid limit < 40%; (b) moisture content > 0.9 times the liquid limit (liquidity index > 0.6); (c) a corrected penetration resistance $(N_1)_{60} < 5$, or a corrected and normalized cone penetration resistance < 1 MPa. Only UCS soil types CL or ML and AASHTO soil types A-4, A-2-4, A-6, and A-2-6 meet these criteria. If the soils at a site do not meet all of these conditions, they are classed as non-sensitive.

- ***Step 4. Soil Classification Evaluation.*** Fine-grained soils are classed as potentially liquefiable if they meet all of the following conditions: (a) clay fraction (percent finer than 0.005 mm) < 15%; (b) liquid limit (LL) > 35%; and (c) moisture content (MC) < 0.9LL. Fine-grained soils that do not meet all of these conditions are classed as non-liquefiable.

E.3.3 Review of Prior Liquefaction Evaluations by Others

In addition to screening based on geologic and subsurface soils data, the user should review any prior liquefaction evaluations by others that have been carried out in the region that includes the highway system. These may be: (a) prior liquefaction evaluations at sites near the highway system; (b) liquefaction hazard maps for the quadrangles or regions where the system is located; and (c) reports of liquefaction occurrences along or near the system during past earthquakes.

Table E-1. Estimated Susceptibility of Sedimentary Deposits to Liquefaction during Strong Seismic Shaking (Youd and Perkins, 1978)

Type of Deposit	General Distribution of Cohesionless Sediments in Deposits	Likelihood that Cohesionless Sediments when Saturated would be Susceptible to Liquefaction (by Age of Deposit)			
		<500 years	Holocene	Pleistocene	Pre-Pleistocene
(a) Continental Deposits					
River Channel	Locally Variable	Very High	High	Low	Very Low
Flood Plain	Locally Variable	High	Moderate	Low	Very Low
Alluvial Fan and Plain	Widespread	Moderate	Low	Low	Very Low
Marine Terraces and Plains	Widespread	--	Low	Very Low	Very Low
Delta and Fan Delta	Widespread	High	Moderate	Low	Very Low
Lacustrine and Playa	Widespread	High	Moderate	Low	Very Low
Colluvium	Variable	High	Moderate	Low	Very Low
Talus	Variable	High	Moderate	Low	Very Low
Dunes	Widespread	Low	Low	Very Low	Very Low
Loess	Widespread	High	Moderate	Low	Very Low
Glacial Till	Variable	High	High	High	Very Low
Tuff	Variable	Low	Low	Very Low	Very Low
Tephra	Rare	Low	Low	Very Low	Very Low
Residual Soils	Widespread	High	High	?	Very Low
Sebka	Rare	Low	Low	Very Low	Very Low
	Locally Variable	High	Moderate	Low	Very Low
(b) Coastal Zone					
Delta	Widespread	Very High	High	Low	Very Low
Esturine	Locally Variable	High	Moderate	Low	Very Low
Beach					
High Wave Energy	Widespread	Moderate	Low	Very Low	Very Low
Low Wave Energy	Widespread	High	Moderate	Low	Very Low
Lagoonal	Locally Variable	High	Moderate	Low	Very Low
Fore Shore	Locally Variable	High	Moderate	Low	Very Low
(c) Artificial					
Uncompacted Fill	Variable	Very High	--	--	--
Compacted Fill	Variable	Low	--	--	--

E.4 ASSESSMENT OF LIQUEFACTION-INDUCED LATERAL-SPREAD DISPLACMENT

As noted earlier, REDARS™ 2 uses the Bardet et al. (2002) four-parameter model to estimate lateral-spread displacements at each site in the highway system that was not eliminated by the earlier liquefaction screening process. An attractive feature of this model is that it is less input-data intensive than other models that could have been included in REDARS™ 2 at this time. This is important because, for most regions of the country, there is no electronic database of soils data that would be needed to assess liquefaction hazards. Therefore, such data must be obtained manually which, for highway systems with many potentially liquefiable sites, can be very time consuming. The use of a less data-intensive model, such as the Bardet et al. (2002) four-parameter model, will reduce the effort needed to develop these data.

E.4.1 Input Data

Three sets of input data are needed to implement the Bardet et al. (2002) four-parameter model. These consist of earthquake-dependent data, site topographic data, and site soils data.

E.4.1.1 Earthquake-Dependent Data

This set of input data depends on the particular earthquake scenario being used in the REDARS™ 2 analysis. They consist of: (a) the moment magnitude of the earthquake, M_w, and (b) the horizontal distance from the seismic energy source to the site, in kilometers, R. For sites west of the Rocky Mountains, the distance R can be taken as the actual distance from the earthquake scenario to each site along the highway system. For sites east of the Rocky Mountains, R is defined in terms of an equivalent distance R_{eq} that is estimated as described below (Bartlett and Youd, 1992).

- From the moment magnitude of the earthquake scenario (M_w) and the peak ground acceleration at a given site, (PGA), use Equation E-1 to compute the parameter b:

$$b = M_w - 12 * PGA \qquad \text{(E-1)}$$

- Use the computed value of b together with Table E-2 to estimate the value of R_{eq} for the given site and earthquake scenario. Where this computed value of b falls between two values of b_{eq} in Table E-2, use linear interpolation to obtain the value of R_{eq}.

- To illustrate this process, assume that M_w = 5.5 and PGA = 0.1 g. For this case, Equation E-1 leads to a value of b = 4.3, and Table E-2 shows that R_{eq} is about 28 km. It is noted that the limiting R_{eq} values given in Figure 5-2 of Youd (1998) range from 1 km to 200 km.

Table E-2. Determination of R_{eq} for Sites East of Rocky Mountains

R_{eq} (km)	1	5	10	20	30	40	50	60	80	100	150	200
b_{eq}	2.5	2.7	3.0	4.0	4.4	4.9	5.2	5.5	5.9	6.3	6.8	7.2

E.4.1.2 Site Topography Data

Input data describing the site topography consists of: (a) S = the ground slope, in percent; and (b) W = the ratio of the height (H) of the free face to the distance (L) from the base of the free face to the point in question, in percent (see Equation E-2 and Figure E-1)

$$S = \frac{1}{X} * 100{,}0 \qquad \text{and} \qquad W = \frac{H}{L} * 100.0 \tag{E-2}$$

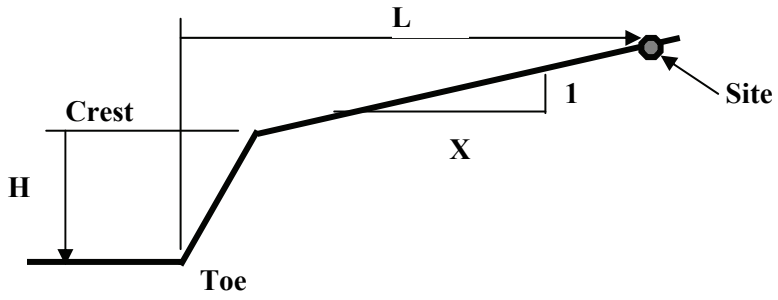

Figure E-1. Definition of Slope, S, and Free-Face Ratio, W

E.4.1.3 Site Soils Data

Use Equation E-3 to calculate the cumulative thickness of all saturated granular layers with corrected blowcounts $(N_1)_{60cs} < 15$, where $(N_1)_{60cs}$ is the layer's standard-penetration resistance after corrections for overburden pressure, hammer-energy ratio, borehole diameter, rod length, lined or unlined samplers, and fines content that are described in Youd (1998):

$$T_{15} = \sum_{i=1}^{L} T_i \tag{E-3}$$

In Equation E-3, T_i is the thickness of the i^{th} layer with $(N_1)_{60cs} < 15$, and L is the total number of such layers at the site.

E.4.2 Median Value of Lateral-Spread Displacement

The Bardet et al (2002) four-parameter model uses Equations E-4 and E-5 to estimate the deterministic (median) value of the liquefaction-induced lateral-spread displacement:

For ground-slope conditions:

$$\log_{10}(D_H + 0.01) = -6.815 + 1.017M_w - 0.278\log_{10} R - 0.026R + 0.454\log_{10} S + 0.558\log_{10} T_{15} \quad \text{(E-4)}$$

For free-face conditions:

$$\log_{10}(D_H + 0.01) = -7.280 + 1.017M_w - 0.278\log_{10} R - 0.026R + 0.497\log_{10} W + 0.558\log_{10} T_{15} \quad \text{(E-5)}$$

E.4.3 Treatment of Uncertainty

The Bardet et al (2002) uses the following approach to treat uncertainties in values of all of the independent parameters in Equations E-4 and E-5:

- *Step 1*: Use Equation E-4 or E-5 to calculate the median value of $\log_{10}(D_H + 0.01)$.

- *Step 2*: Generate a uniform random number Z from the distribution $N(0,1)$, which is a normal distribution with a mean of 0 and a standard deviation of 1.

- *Step 3*: Define the following two matrices:

$$(X_o)^T = (1, Q, M_w, R, \log_{10} R, \log_{10} W, \log_{10} S, \log_{10} T_{15}) \quad \text{(E-6)}$$

= 1 x 8 vector where Q = 0 or 1 for ground-slope or free-face conditions respectively.

(X_o) = transpose of vector $(X_o)^T$

- *Step 4*: Define the following 8 x 8 symmetric matrix $[C]$ (shown with symmetry implied):

$$[C] = \begin{bmatrix} 0.46 & 0.14 & 0.00 & 0.08 & -0.03 & -0.40 & 0.02 & 0.01 \\ & 46.52 & -0.77 & -0.25 & 0.13 & -39.92 & -11.30 & -5.13 \\ & & 0.60 & -2.25 & 0.00 & -0.39 & 0.63 & -1.19 \\ & & & 24.74 & -0.53 & 6.07 & -2.71 & -5.63 \\ & & & & 0.03 & -0.18 & 0.06 & 0.11 \\ & & & & & 46.84 & 0.04 & -0.16 \\ & & & & & & 44.29 & 10.62 \\ & & & & & & & 22.33 \end{bmatrix} \quad \text{(E-7)}$$

- *Step 5:* Use matrix multiplication to derive the variance of $A = \log_{10}(D_H + 0.01)$ as follows:

$$Var(A) = s^2 (X_o)^T [C](X_o) \quad \text{(E-8)}$$

where $s^2 = 0.084$, and Equation E-8 results in a single number (a scalar (s^2) times a 1 x 1 matrix) which corresponds to the variance of A. From this, the standard deviation of A is computed as

$$SD(A) = \sqrt{Var(A)} \quad \text{(E-9)}$$

- *Step 6:* Thus, for a given simulation, D_{est} = value of lateral-spread displacement including uncertainties can be expressed as:

$$\log_{10}(D_{est} + 0.01) = \log_{10}(D_H + 0.01) + \varepsilon \quad \text{(E-10)}$$

where $\log_{10}(D_H + 0.01)$ = median value of lateral-spread displacement (from Equation E-4 or E-5), and ε (lateral-spread displacement uncertainty term) is computed as:

$$\varepsilon = SD(A) * Z \quad \text{(E-11)}$$

In Equation E-11, Z is the random number obtained under Step 2 of this procedure.

E.4.4 Discussion of Bardet et al. (2002) Model

In addition to the four-parameter model, Bardet et al. (2002) describe a six-parameter model that besides the parameters shown in Equations E-4 and E-5, include the parameters F_{15} -- which is the average fines content (% finer than 75μm), of all layers included in T_{15}, and $(D_{50})_{15}$ -- which is the average D_{50} grain size (mm) of all layers included in T_{15}. Although this six-parameter model yields somewhat more reliable results than the four-parameter model (R^2 on the order of 0.8 vs. 0.6 for the four-parameter model), its additional parameters F_{15} and $(D_{50})_{15}$ can be time consuming to obtain, especially for the possibly large number of potentially liquefiable sites that may be included in a highway system. For this reason, the Bardet et al. four-parameter model has been selected for inclusion into REDARS™ 2.

It is also important to recognize the ranges of the various input parameter values used in the four-parameter model, which are: (a) a moment magnitude (M_w) range of 6.4 to 9.2; (b) a distance (R) range of 0.2 to 100 km; (c) a free-face ratio (W) range of 1.64 to 55.68 percent; (d) a slope (S) range of 0.05 to 5.9 percent; and (e) a range of thicknesses of saturated cohesionless soils with $(N_1)_{60cs} < 15$ (T_{15}) that extends from 0.2 to 19.7 km. Sensitivity evaluations over time could evaluate some of the consequences of these ranges and possible combinations of values, including values that could arise outside these ranges.

E.5 ASSESSMENT OF LIQUEFACTION-INDUCED VERTICAL SETTLEMENT

The Tokimatsu-Seed (1987) model is used in REDARS™ 2 to compute liquefaction-induced vertical ground settlement. This section describes the input data needed to apply this model, and the process followed by REDARS™ 2 to use the model to estimate site-specific settlement.

E.5.1 Input Data

Input data needed apply the Tokimatsu-Seed model are the peak ground acceleration, various soils data described below, and the identification of the site's potentially liquefiable layers.

E.5.1.1 Peak Ground Acceleration

The site-specific peak ground acceleration *PGA*, as computed using the ground motion models described in Appendix D for the particular earthquake scenario and simulation being considered must be provided.

E.5.2.2 Soils Data

The following soils data must be input for all layers in the site's soil profile: (a) the corrected standard penetration test blowcounts $(N_1)_{60cs}$ (as summarized in Section E.4.1.3); (b) the layer's depth below the ground surface, z, and thickness; and (c) the layer's total overburden pressure σ_{vo} and effective overburden pressure σ_{vo}'.

E.5.2.3 Identification of Those Layers that could Settle due to Liquefaction

In addition to the above input data, it is necessary to identify those layers within the site that are to be included in the settlement calculations. In this, it is noted that, because of dilatency, moderately dense sands do not easily deform in shear but can still densify somewhat. Therefore, it is reasonable that the criteria for including layers in the settlement calculations and the lateral-spread displacement calculations (Section E.2.4.1.(c)) should be different. Saturated granular soils with corrected blowcounts of $(N_1)_{60cs} \geq 15$ are too dense to significantly deform in shear, but may settle with volumetric strains up to 2 percent (Youd, personal communication, 1999). Accordingly, REDARS™ 2 includes all saturated granular layers in the ground-settlement calculations for the site, regardless of their corrected blowcount values.

E.5.2 Basic Calculations

Figure E-2 shows that the Tokimatsu-Seed model has the form of a series of curves that define those combinations of demand cyclic-stress-ratio (computed as subsequently described in Section E.5.2.1) and corrected blowcounts $(N_1)_{60cs}$ that lead to various fixed values of volumetric strain. In the REDARS™ 2 adaptation of the Tokimatsu-Seed model, best-fit equations are used to represent each of these curves (see Section E.2.5.2.2).

The REDARS™ 2 adaptation of this model at each potentially liquefiable site consists of the following steps: (a) compute each saturated sand layer's demand cyclic-stress-ratio caused by the earthquake scenario considered in each simulation; and (b) with this cyclic-stress-ratio and the layer's corrected blowcounts $(N_1)_{60cs}$, enter the REDARS™ 2 equations that represent the various Tokimatsu-Seed volumetric-strain curves in order to determine that layer's volumetric strain for this particular earthquake; (c) multiply the layer's volumetric strain by its thickness in order to obtain the change in thickness of that layer; and (d) repeat Steps (a) through (c) for each saturated sand layer in the site; and (e) sum each layer's change in thickness in order to obtain the total vertical settlement at the site. These steps are further described in the following subsections.

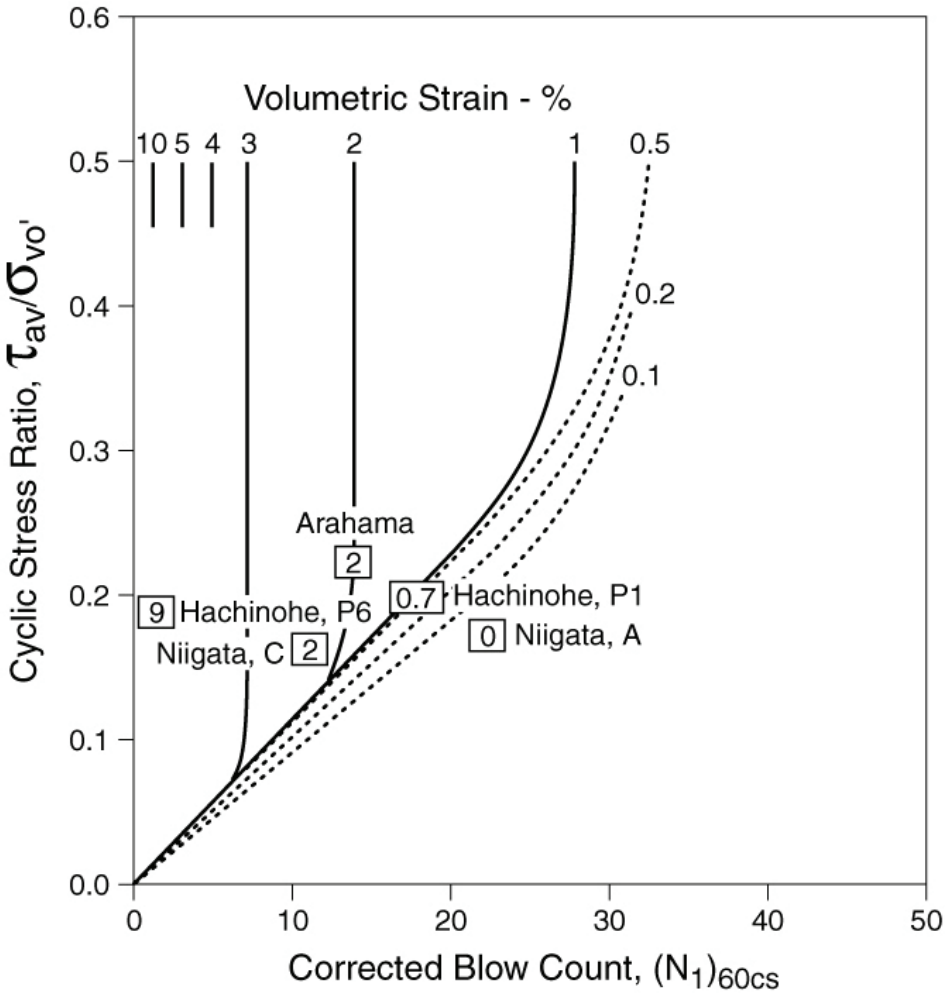

Figure E-2. Liquefaction-Induced Volumetric Strains for Each Saturated Sand Layer in Site (Tokimatsu-Seed, 1987)

E.5.2.1 Cyclic-Stress-Ratio

The demand cyclic-stress-ratio, CSR, is computed as:

$$CSR = 0.65\frac{PGA * \sigma_{vo}}{g * \sigma_{vo}'}\mathrm{r_d} \qquad \text{(E-12)}$$

where

PGA = peak ground acceleration at the ground surface which is obtained from the application of the REDARS™ 2 ground motion model for each earthquake scenario and simulation,

g = acceleration of gravity (981.5 cm/sec^2, or 32.2 ft/sec^2),

σ_{vo} = layer's total overburden pressure,

σ_{vo}' = layer's effective overburden pressure, and

r_d = depth-dependent stress reduction factor that is computed using one of the following equations, in which z is the depth to the mid-thickness of the layer, in meters.

$$r_d = 1.0 - 0.00765z \quad \text{for} \quad z \le 9.2m \qquad \text{(E-13)}$$
$$r_d = 1.174 - 0.0267z \quad \text{for} \quad 9.2m \le z < 23m \qquad \text{(E-14)}$$
$$r_d = 0.744 - 0.008z \quad \text{for} \quad 23m \le z \le 30m \qquad \text{(E-15)}$$
$$r_d = 0.50 \quad \text{for} \quad z > 30m \qquad \text{(E-16)}$$

E.5.2.2 Volumetric Strain in Each Layer

With the layer's CSR now computed and its effective blowcounts $(N_1)_{60cs}$ input, the layer's volumetric strain is computed from the following steps.

Step 1. Check potential for volumetric strain in the layer.

- If $(N_1)_{60cs} \ge 35$, $VS = 0.0\%$. Otherwise go to Step 2.

Step 2. Estimate VS for the layer (in units of percent strain) where CSR and $(N_1)_{60cs}$ fall within vertical line regime of Figure E-2 for VS of 2% - 10%.

Substep 2-1. Check to see if within above vertical line regime.

- If $(N_1)_{60cs} > 13$, go to Step 3 (i.e., not within vertical line regime of above VS curves).
- $(N_1)_{60cs} \le 13$. If $CSR \ge 0.01 * (N_1)_{60cs}$, go to Substep 2-2. Otherwise go to Step 3.

Substep 2-2. Now that we have established that we are in above vertical line regime, check to see if we are within vertical line regime where VS = 10%.

- If $(N_1)_{60cs} < 1$, $VS = 10\%$. Otherwise go to Substep 5-2-3.

Substep 2-3. Check whether we are in vertical line regime where VS is between 5 and 10 percent.

- If $(N_1)_{60cs} < 3$, compute VS from Equation E-17. Otherwise, go to Substep 2-4.

$$VS = 12.5 - 2.5 * (N_1)_{60cs} \quad \text{(E-17)}$$

where $1 \le (N_1)_{60cs} < 3$ and $10\% \ge VS > 5\%$.

Substep 2-4. Check whether we are in vertical line regime where VS is between 3 and 5 percent.

- If $(N_1)_{60cs} < 7$, compute VS from Equation E-18. Otherwise, go to Substep 2-5.

$$VS = 6.5 - 0.5 * (N_1)_{60cs} \quad \text{(E-18)}$$

where $3 \le (N_1)_{60cs} < 7$ and $5\% \ge VS > 3\%$.

Substep 2-5. Use Equation E-19 to compute VS for vertical line regime where VS is between 2 and 3 percent.

$$VS = 4.16667 - 0.16667 * (N_1)_{60cs} \quad \text{(E-19)}$$

where $7 \le (N_1)_{60cs} < 13$ and $3\% \ge VS > 2\%$.

Step 3. Estimate** VS **where** CSR **and** $(N_1)_{60cs}$ **fall within inclined or curved line regimes of Figure E-2. (From Step 2 above, this corresponds to condition where either** $(N_1)_{60cs} > 13$ **or where** $CSR < 0.01 * (N_1)_{60cs}$**.)

Substep 3-1. Check whether $2\% \ge VS > 1\%$

- Calculate $y = 0.000036 * [(N_1)_{60cs}]^3 - 0.00118 * [(N_1)_{60cs}]^2 + 0.0202 * (N_1)_{60cs}$ (E-20)
- If $CSR < y$, go to Substep 3-2. Otherwise, $VS(\%) = 1\% + 0.00067 * [28 - (N_1)_{60cs}]$ (E-21)

Substep 3-2. Check whether $1\% \ge VS > 0.05\%$

- Calculate $y = 0.000023 * [N_1)_{60cs}]^3 - 0.0075 * [N_1)_{60cs}]^2 + 0.016167 * (N_1)_{60cs}$ (E-22)
- If $CSR < y$, go to Substep 3-3. Otherwise, $VS = 0.5\% + 0.0005 * [30 - (N_1)_{60cs}]$ (E-23)

Substep 3-3. Check whether VS = 0.2%.

- Calculate $y = 0.0000153*[(N_1)_{60cs}]^3 - 0.00051*[(N_1)_{60cs}]^2 + 0.013567*(N_1)_{60cs}$ (E-24)
- If $CSR < y$, go to Substep 3-4. Otherwise, $VS = 0.2\%$.

Substep 3-4. Check whether VS = 0.1%.

- Calculate $y = 0.000018*[(N_1)_{60cs}]^3 - 0.00059*[(N_1)_{60cs}]^2 + 0.0131*(N_1)_{60cs}$ (E-25)
- If $CSR < y$, then $VS = 0.1\%$. Otherwise, $VS = 0.0\%$.

E.5.2.3 Incremental Change in Thickness of Each Layer

With the layer's volumetric strain computed as described above, the incremental change in thickness of the layer is obtained by assuming one-dimensional consolidation and carrying out the following computation.

$$(\Delta T)_i = \frac{(VS)_i T_i}{100} \tag{E-26}$$

where $(\Delta T)_i$ is the change in thickness of the i^{th} layer with volumetric strain $(VS)_i$ and thickness T_i, and the above division by 100 is because $(VS)_i$ has been computed in units of percent.

E.5.2.4 Total Settlement of Site

The total liquefaction-induced settlement of the site, Z is computed as the sum of the above incremental thickness changes for each of the site's L saturated sand layers, i.e,

$$Z = \sum_{i=1}^{L} (\Delta T)_i \tag{E-27}$$

APPENDIX F
SURFACE FAULT RUPTURE HAZARDS

F.1 OVERVIEW

For any earthquake scenario that is caused by rupture along a fault of finite length, REDARS™ 2 estimates surface fault rupture hazards for all sites in the highway system that are in the zone of deformation of the fault rupture. REDARS™ 2 adapts a probabilistic approach by Youngs et al. (2003) to estimate these hazards. This approach consists of:

- Fault-attribute and rupture data are input for each earthquake scenario in the walkthrough table that is caused by fault rupture (Sec. F.2).

- Initial calculations that are carried out for each component site, in order to establish whether that site might experience fault displacement during the earthquake scenario (Sec. F.3). For most of the component sites, this will rule out such a possibility.

- If these calculations show that a given site may experience fault rupture, the surface fault displacements at that site is estimated. This estimate is probabilistic in order to include effects of uncertainties (Secs. F.4 and F.5). However, this approach can be adapted to develop deterministic estimates of fault rupture hazards as well (Sec. F.6).

F.2 INPUT DATA

The input data for each earthquake occurring during year in which one or more earthquakes are generated are described in detail in Appendix B and are summarized below as consisting of:

- Moment magnitude.

- General fault parameters, including: (a) the causative fault type -- i.e., whether the fault is strike-slip, reverse, normal, or other; (b) the fault number which in the Coastal California walkthrough table will have a value of 1 - 171 for known California faults, and 0 for random faults; and (c) the fault name (e.g., Hayward Fault), which is often blank or “random”.

- The number of end-to-end segments that comprise the fault rupture. For each segment, a unique dip angle, and projection of the bottom of rupture along the fault plane onto the earth’s surface are provided. In the walkthrough tables described in Appendix B, fault rupture is currently assumed to consist of one rupture segment only. Future extensions of the REDARS™ will enable multiple rupture segments to be considered.

- Coordinates of earthquake’s epicenter and center of energy release.

- Depth of earthquake’s hypocenter, center of energy release, and seismogenic zone.

- Zone of deformation (ZOD) parameter for each fault segment. If this parameter = 0, a user-specified ZOD has not been provided, and default ZOD values are used (100 m on each side of a strike-slip fault and 500 m on the hanging wall side of a reverse or normal fault). If the parameter = 1, the user specifies the ZOD along each side of each fault rupture segment.

F.3 CHECK IF SITE CAN UNDERGO DISPLACEMENT FROM FAULT RUPTURE

F.3.1 General Procedure

The REDARS™ 2 surface fault rupture model and the REDARS™ 2 source-site distance calculations (see Sec. D.2) estimate which, if any, component site(s) in the highway system are prone to surface fault rupture hazards. This model assumes that a component site can experience fault-rupture hazards if any of the following four conditions hold:

- Condition 1: (a) The probability of some displacement at the site ≥ 0.004; and (b) There is a normal from the site to the ruptured fault zone.

- Condition 2: The component is within the fault zone of deformation for a user-specified fault zone and relative to the linear fault rupture zone as defined in the walkthrough table (by implication, there is a normal from the site to the fault rupture zone)

- Condition 3: The component has a normal to the fault and is within 100m of the fault.

- Condition 4: The component has a normal to the fault and is within 500m of the hanging wall of the fault.

If any of these conditions are met, surface fault displacements at the site are calculated as described in Sections F.4 and F.5. If none of these conditions is met, REDARS™ 2 assumes that the site will not experience fault displacement (i.e., $DISP_{i,j,k} = 0$ for the j^{th} earthquake occurring during the i^{th} year of walkthrough and for the k^{th} component), and then proceeds to the next site.

F.3.2 Seed for Random-Number Generation

A unique number (seed) is generated that is used to generate random numbers needed to calculate the fault displacement. For the j^{th} earthquake scenario occurring during the i^{th} year of the walkthrough, and for component k of the highway system, this seed $NS_{i,j,k}$ is computed as:

$$NS_{i,j,k} = 1000 * k + 10 * i + j \tag{F-1}$$

F.3.3 Maximum Fault Displacement

The maximum fault displacement from the j^{th} earthquake occurring during the i^{th} year of the walkthrough, $(D_{\max})_{i,j}$ in meters, is computed by Equation F-2 (Wells and Coppersmith, 1994):

$$\log(D_{\max})_{i,j} = -5.46 + 0.82 * (M_w)_{i,j} + 0.42 * X_{i,j} \tag{F-2}$$

where $(M_w)_{i,j}$ is the moment magnitude of the j^{th} earthquake occurring in the i^{th} year of the walkthrough, and $X_{i,j}$ is a normally distributed random variate. This uncertainty factor will apply to the maximum fault displacement throughout the earthquake scenario.

F.3.4 Parameters from REDARS™ 2 Source-Site Distance Calculation Procedure

This section describes the parameters needed to estimate fault-displacement hazards that are obtained or adapted from the procedure used in REDARS™ 2 to calculate source-site distances.

First and foremost, the procedure provides an indicator, $NORMAL_{i,j,k}$ that specifies whether there is a normal from the component site to the ruptured fault for the j^{th} earthquake that occurs during the i^{th} year of the walkthrough and for the site of the k^{th} component. If $NORMAL_{i,j,k} = 1$, a normal exists. If $NORMAL_{i,j,k} = 0$, no fault displacement occurs. The calculation then proceeds to the next component in the highway system.

If $NORMAL_{i,j,k} = 1$, the following results are provided by the source-site distance calculation procedure:

- $DSRUP_{i,j,k}$, which is the minimum distance from k^{th} component to the ruptured fault segment for the j^{th} earthquake in the i^{th} walkthrough year -- which is named the i-j^{th} earthquake.

- $DOVERL_{i,j,k}$, which is the minimum distance from the end of the ruptured fault segment to a point along the segment where a line from the k^{th} component that is normal to the segment intersects the segment, divided by the rupture length for the fault causing the i-j^{th} earthquake.

- $FOOTWALL_{i,j,k}$ which indicates whether k^{th} component site is located on hanging wall or foot wall of the i-j^{th} fault, where:

  $FOOTWALL_{i,j,k} = 1$: If the ruptured i-j^{th} fault is strike-slip, or if the k^{th} component site is located along the foot wall of a reverse fault that has ruptured or along the hanging wall of a normal fault that has ruptured.

  $FOOTWALL_{i,j,k} = 2$: If the k^{th} component site is located along the hanging wall of a reverse fault that has ruptured or along the foot wall of a normal fault that has ruptured.

  $FOOTWALL_{i,j,k} = 3$: Otherwise.

F.3.5 Step 1: User-Specified Zone of Deformation

After obtaining the above parameters and completing the above initial calculations, the procedure assesses whether a given component site can undergo fault-rupture displacement. This assessment involves the four steps that are summarized in this and the following three subsections. This first step (Step 1) checks whether a user-specified zone of deformation (ZOD)

is provided and, if so, checks whether any component in the highway system is located within this zone. This step makes use of a parameter named $FLT_{i,j}$ that is obtained from the walkthrough table and is defined as follows.

- $FLT_{i,j} = 0$ if no user-specified ZOD is provided for the *i-j*th fault (which is the causative fault for the *j*th earthquake occurring during the *i*th year of the walkthrough).

- $FLT_{i,j} = 1$ if a user-specified ZOD is provided for *i-j*th fault.

If $FLT_{i,j} = 0$, REDARS™ 2 sets $SLIP_{i,j,k} = 0$ and proceeds to Step 2, which is described in Section F.3.6. Otherwise, if $FLT_{i,j} = 1$, the dimensions of the user-specified ZOD for the *i-j*th fault are provided as follows:

- $NSIDE1_{i,j}$: Number of points along Side 1 of *i-j*th fault zone for which latitude-longitude coordinates defining extent of fault zone will be specified.

- $LAT1_{i,\ j}$, $LAT2_{i,\ j,}$ $i=1,2,....NSIDE1_{i,j}$: A total of $NSIDE1_{i,j}$ latitude-longitude pairs are specified to define the extent of the zone of deformation along Side 1 of the fault zone.

- $NSIDE2_{i,j}$: Number of points along Side 2 of *i-j*th fault zone for which latitude-longitude coordinates defining extent of fault zone will be specified.

- $LAT1_{i,\ j}$, $LAT2_{i,\ j,}$ $i=1,2,....NSIDE2_{i,j}$: A total of $NSIDE2_{i,j}$ latitude-longitude pairs are specified to define the extent of the zone of deformation along Side 2 of the fault zone.

From these inputs, REDARS™ 2 performs the following two calculations to determine whether any component falls within the fault's ZOD as so defined:

- The first calculation determines whether the linear fault rupture zone as specified in the walkthrough table is shorter than the fault trace.

- The second calculation determines whether each specific component site lies within the user-specified ZOD. If yes, REDARS™ 2 sets $SLIP(i, j, k) = 1$ for that site and proceeds to the calculation of the site's fault displacement, which is described in Section F.4. If the component site is not within the user-specified ZOD, REDARS™ 2 sets $SLIP(i, j, k) = 0$ for that site and proceeds to Step 4, which is described in Section F.3.8.

F.3.6 Step 2: Check Distance from Site to Fault Rupture

Steps 2 through 4 apply to the situation where no user-defined ZOD has been specified for the fault. Step 2 consists of the following checks:

- First, REDARS™ 2 checks whether there is a normal distance from the *k*th component to the ruptured segment of the *i-j*th fault (i.e., whether $NORMAL_{i,j,k} = 1$).

- If such a normal distance exists, REDARS™ 2 then checks whether the k^{th} component site is within 0.1 km of the fault trace, by checking the value of the parameter $DSRUP_{i,j,k}$ as defined in Section F.3.4. If $DSRUP_{i,j,k} \le 0.1\,\text{km}$, REDARS™ 2 sets $SLIP_{i,j,k} = 1$ and calculates the site's fault displacement as described in Section F.4. If $DSRUP_{i,j,k} > 0.1\,\text{km}$, REDARS™ 2 proceeds to Step 3, as described in Section F.3.7.

F.3.7 Step 3: Check Distance from Site to Hanging Wall of Dipping Fault Rupture

Under Step 3, REDARS™ 2 checks first whether the ruptured fault is either reverse or normal and therefore has a hanging wall and foot wall. If so, and if it has been determined that there is a normal distance from the k^{th} component site to the ruptured segment of the i-j^{th} fault, Step 3 then checks whether the k^{th} site is within 0.5 km of the ruptured fault segment (i.e., if $DSRUP_{i,j,k} \le 0.5$). If all of these conditions are met, then REDARS™ 2 sets $SLIP_{i,j,k} = 1$ and calculates the component site's surface fault displacement as described in Section F.4. Otherwise, REDARS™ 2 proceeds to Step 4, which is described in Section F.3.8.

F.3.8 Step 4: Check Probability of Slippage

Step 4 applies to the above instances where, so far, $SLIP_{i,j,k} = 0$ and $NORMAL_{i,j,k} = 1$. For this situation, the probability of slippage at the site of the k^{th} component is estimated from the following procedure:

- *Step 4a: Estimate $f(x)_{i,j,k}$ from Equation 8 of Youngs et al. (2003)*

$$f(x)_{i,j,k} = 3.27 + [-8.28 + 0.577(M_w)_{i,j} + 0.629 HANG_{i,j,k}] * \ln[DSRUP_{i,j,k} + 4.14] + 0.611 X_{i,j} \quad \text{(F-3)}$$

where

$(M_w)_{i,j}$ = moment magnitude for earthquake j in Year i

$HANG_{i,j,k}$ = 1, hanging wall indicator for component k, year i, and earthquake j

$DSRUP_{i,j,k}$ = shortest distance from component k to fault zone for earthquake j in year i

$X_{i,j}$ = normal variate with zero mean and unit variance for earthquake j during year i

- *Step 4b: Estimate probability of slippage for component k during earthquake j in year i*

$$P(slip)_{i,j,k} = \frac{\exp\lfloor f(x)_{i,j,k} \rfloor}{1 + \exp[f(x)_{i,j,k}]} \quad \text{(F-4)}$$

- *Step 4c. Check value of* $P(slip)_{i,j,k}$. If $P(slip)_{i,j,k} \geq 0.004$, set $SLIP_{i,j,k} = 0$ and proceed to Step 4d. If $P(slip)_{i,j,k} < 0.004$ then assume that slippage will not occur at component *k* during earthquake *j* in year *i*, and proceed to the next component site.

- *Step 4d. Generate random number and compare its value to* $P(slip)_{i,j,k}$. Generate a uniformly distributed random number *U*. If $U > P(slip)_{i,j,k}$, assume that slippage will not occur at the site of component *k* during earthquake *j* in year *i*, and proceed to the next component. If $U \leq P(slip)_{i,j,k}$, set $SLIP_{i,j,k} = 1$, and calculate the site's surface fault displacement as described in Section F.4.

F.4 CALCULATION OF SITE-SPECIFIC FAULT DISPLACEMENT

F.4.1 Background

Youngs et al. (2003) provides a methodology for performing a site-specific probabilistic analysis of fault-displacement hazards that has been adapted for use in REDARS™ 2. This methodology relates the occurrence of fault displacement at or near the ground surface to the occurrence of earthquakes (fault slip at depth) in the site region, in much the same manner as is done in a probabilistic seismic hazard analysis (PSHA) for ground shaking, in which the ground motion attenuation function in a PSHA is now replaced by a fault displacement attenuation function. The end result of the methodology is the spatial distribution and cumulative probability of exceedance of the ratio of the site-specific fault displacement to the maximum displacement, $DISP_{i,j,k}/(D_{max})_{i,j}$, where $(D_{max})_{i,j}$ is computed using Equation F-2. Section F.4.2 describes the procedure followed by Youngs et al. to compute this displacement ratio.

F.4.2 Development of Beta Distributions and Simulations

The Young et al. procedure represents $DISP_{i,j,k}/(D_{max})_{i,j}$ as a beta distribution that varies with *DOVERL*. The development of this distribution for REDARS™ 2 involved the following steps:

- For a selected value of *DOVERL* between 0 and 0.5, the following equations (reproduced from Page 216 of Youngs et al., 2003) were used to compute coefficients for obtaining the beta distributions. These equations are plotted in Figure F-1.

$$a = \exp\left[0.6064 + 21.83 * DOVERL - 108.0(DOVERL)^2 + 136.6(DOVERL)^3\right] \quad \text{(F-5)}$$

$$b = \exp\left[2.027 + 12.21 * DOVERL - 87.90(DOVERL)^2 + 115.5(DOVERL)^3\right] \quad \text{(F-6)}$$

- From this, the mean and variance of the beta distributed $DISP_{i,j,k}/(D_{max})_{i,j}$ for this particular *DOVERL* value was calculated as:

$$\left(\frac{DISP_{i,j,k}}{(D_{\max})_{i,j}}\right)_{mean} = \frac{a}{a+b} \quad \text{and} \quad \left(\frac{DISP_{i,j,k}}{(D_{\max})_{i,j}}\right)_{variance} = \frac{ab}{(a+b)^2 * (a+b+1)} \quad \text{(F-7)}$$

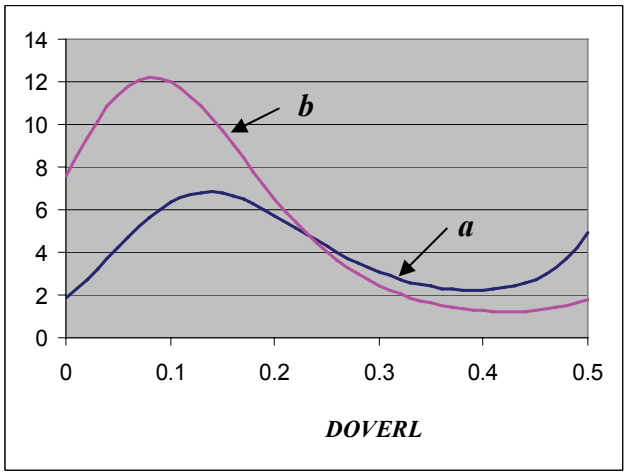

Figure F-1. Beta Distribution Coefficients "a" and "b" vs. *DOVERL*

- Next, the results from Equation F-7 were used to construct the curves displayed in Figure F-2, which show how various statistics for $DISP(i,j,k)/D_{max}(i,j)$ vary with *DOVERL*. In this, the standard deviation is seen to fluctuate slightly with *DOVERL*, but is on the order of 0.2.

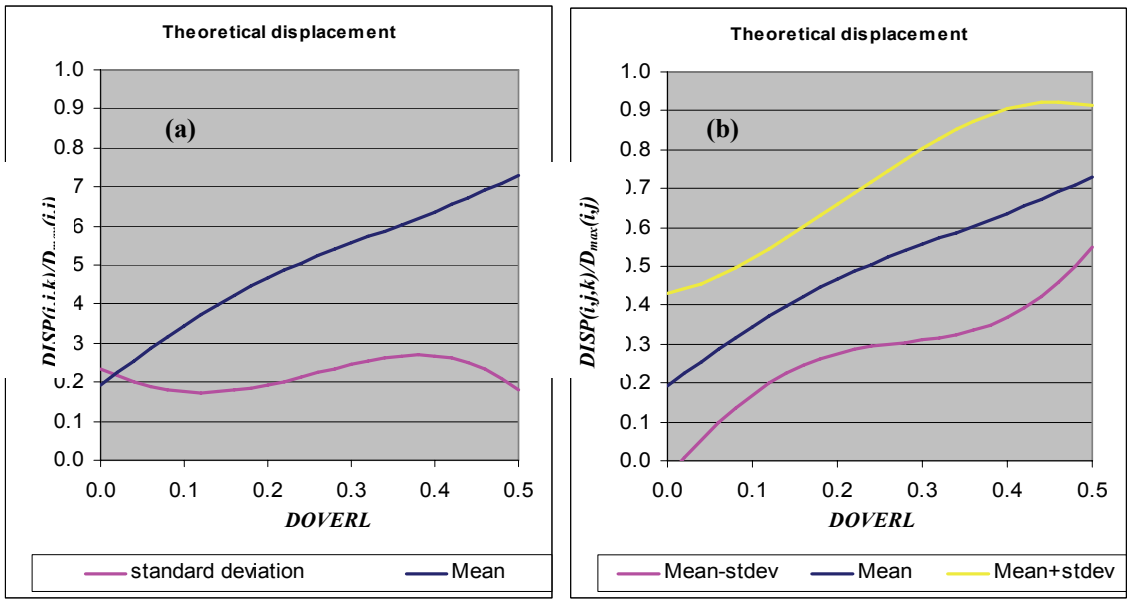

Figure F-2. Theoretical Displacement Ratio as a Function of *DOVERL*. (a) Shows Mean and Standard Deviation (b) shows Mean Plus/Minus One Sigma.

- Equation F-7 was also used to construct the curves provided in Figure F-3, which show cumulative probabilities for $DISP(i,j,k)/D_{max}(i,j)$ as a function of *DOVERL*.

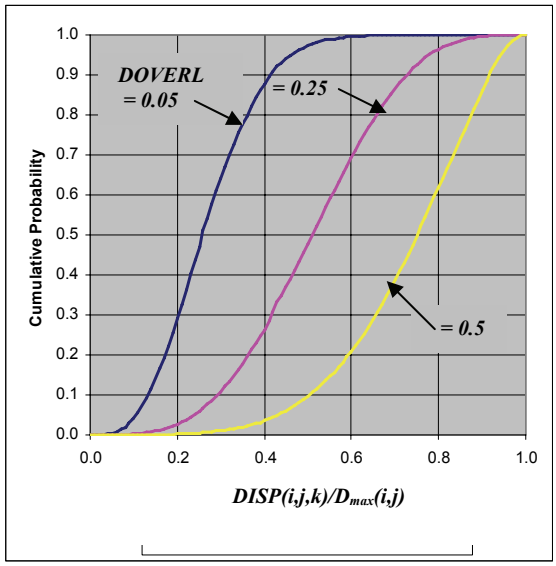

Figure F-3. Cumulative Probabilities for *DISP(i,j,k)/D_{max}(i,j)*

- Finally, 10,000 simulations for each value of *DOVERL* were used to test this procedure. In each simulation, a uniform random number was generated and used to enter the beta distribution for *DISP(i,j,k)/D_{max}(i,j)* to obtain a randomized value of this ratio. Figure F-4 shows the statistics on *DISP(i,j,k)/D_{max}(i,j)* that were developed from this simulation process.

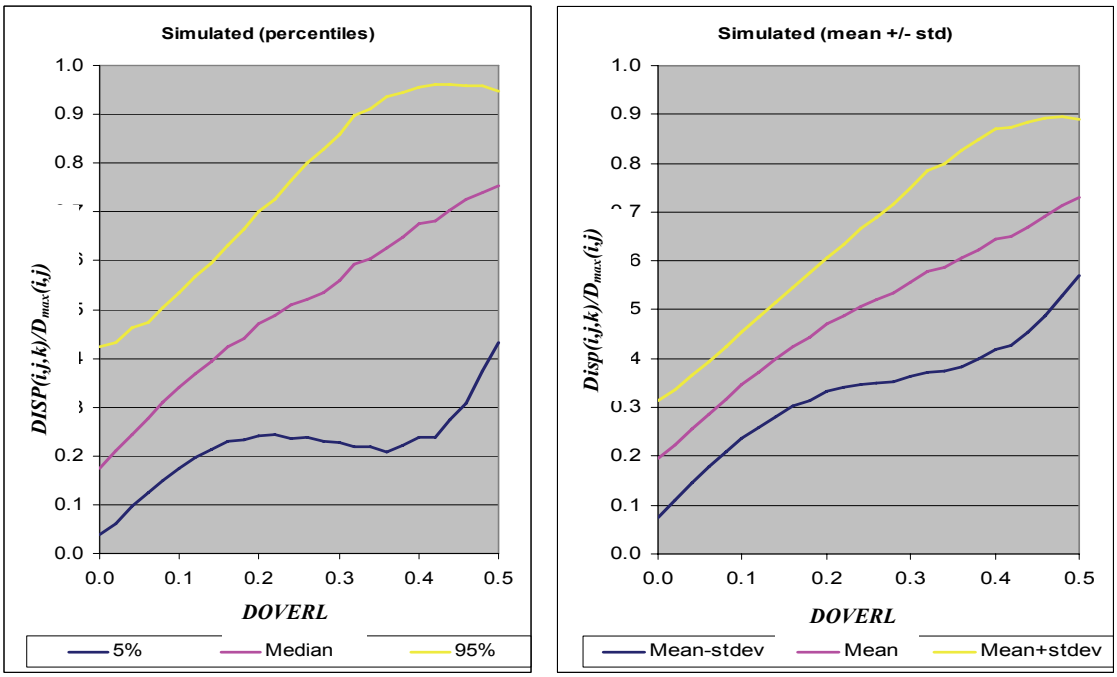

Figure F-4. Simulation Results

F.4.3 Probabilistic Estimates

For each earthquake scenario and simulation, the REDARS™ 2 estimate of surface fault displacement hazards consists of: (a) using the procedure outlined in Section F.3 to identify those component sites at which surface fault rupture will occur; and (b) using the simulation procedure summarized in Section F.4.2, develop a randomized value of the surface fault rupture displacement, *DISP(i,j,k)* for each of these sites.

F.4.4 Deterministic Estimates

Surface fault rupture hazards can also be estimated if the SRA is deterministic. The adaptation of the above procedure to develop deterministic estimates of surface fault displacement hazards is as follows:

- The maximum fault displacement $(D_{max})_{i,j}$ is computed using Equation F-2 with the uncertainty term deleted.

- As before, REDARS™ 2 checks if the site is within a user-specified zone of deformation (Sec. F.3.5) or, in the absence of this user specification, if the site is within 0.1 km of the ruptured fault (Sec. F.3.6) or within 0.5 km of the hanging wall of a dipping fault (Sec. F.3.7).

- If it is determined that the site location is within any of the above distances from the ruptured fault, the site's surface fault displacement is obtained as the median value (for a cumulative probability of 0.5) from Figure F-3.

APPENDIX G
DEFAULT BRIDGE MODELING PROCEDURES

G.1 BACKGROUND

As noted in Chapter 4, the REDARS™ 2 methodology for SRA of highway systems provides users with two options for estimating bridge damage states and associated repair costs and downtimes. One option consists of user-specified models, in which the user would carry out separate detailed analyses for any bridge in the system, in order to develop fragility curves for input into REDARS™ 2 that characterize the seismic performance of that bridge. However, although this process would provide the most complete seismic performance representation, the time requirements to implement the detailed analyses would render it impractical for application to all of the many bridges in a typical highway system. Therefore, in SRA of highway systems, this approach should be reserved for those bridges with unique configurations or whose seismic performance would have a particularly significant effect on the ability of the highway system to accommodate traffic demands after an earthquake.

For the remaining large number of more-or-less "typical" bridges within a highway system, practical SRA time and cost constraints require use of a more simplified modeling procedure that can be readily applied to many bridges subjected to many different earthquake scenarios. To meet this requirement, REDARS™ 2 provides a second bridge modeling option that serves as the default model for all bridges in the system, unless overridden by a user-specified model for various individual bridges. For bridges subjected to ground shaking hazards, this default model is a modified version of the model that is documented in the HAZUS99-SR2 technical manual (FEMA-NIBS, 2002). The remainder of this appendix describes this model and its application in REDARS™ 2. It also describes REDARS™ 2 default models for estimating bridge damage due to permanent ground displacement, and for estimating post-earthquake repair costs, downtimes, and traffic states as a function of the bridge's damage state.

The above HAZUS99-SR2 bridge models are used as the REDARS™ 2 default bridge modeling procedure because they are the only models now available that: (a) can be applied to bridges of various construction types nationwide; (b) are applicable to bridges subjected to both ground shaking and permanent ground displacement hazards; and (c) were readily available when the programming of REDARS™ 2 was initiated (in 2004). However, this procedure has the following limitations:

- The procedure addresses only some of the many facets of bridge seismic performance that may be important for assessing bridge damage states and repair requirements.
- SRA of highway systems requires input of structural-attribute data for each bridge in the system. Ideally, these data should be obtained from an electronic database that defines the structural attributes needed to characterize the bridge's seismic performance. However, the only such database for bridges nationwide is from the Federal Highway Administration's National Bridge Inventory (NBI) program (FHWA, 2003). This database, which provides the data used by the HAZUS99-SR2 model, was developed solely to provide information for bridge maintenance, and does not include the additional structural data needed for analysis of

seismic performance. Thus, the HAZUS99- SR2 models must deduce these additional data from the bridge attribute information provided in the existing FHWA-NBI database.

- The procedures use qualitative and somewhat subjective bridge damage-state descriptors (see Sec. G.2.1) that do not provide a complete basis for estimating bridge repair costs, downtimes, and post-earthquake traffic states.
- The primary structural-mechanics basis for the current HAZUS99-SR2 model for estimating damage state of bridges has been subjected to ground shaking hazards was developed by Mander and his associates and is well documented (e.g., Dutta and Mander, 1998; Basoz and Mander, 1999). However, no such documentation is now available for the HAZUS99-SR2 model for estimating damage states of bridges subjected to ground displacement hazards.

In closing, the development of improved bridge models that circumvent many of the above limitations is now area of active research (e.g., TCW, 1993 and 1995). As improved models are developed that are suitable for use in REDARS™, the modular structure of the REDARS™ software (see Chapter 2) will facilitate the inclusion of these models.

G.2 ESTIMATION OF BRIDGE DAMAGE STATES FROM GROUND SHAKING

G.2.1 Overview of Modeling Procedure

This overview section summarizes: (a) damage state and standard bridge definitions that are key to the HAZUS99-SR2 procedure; (b) how bridge capacities associated with each damage state are established; (c) how demand ground motions are defined and compared to the above bridge capacities; and (d) why the procedure's structural-capacity estimates have been modified under this REDARS™ 2 development project.

G.2.1.1 Damage State and Standard Bridge Definitions

The HAZUS99-SR2 bridge model defines bridge capacities in terms of spectral accelerations leading to the onset of each of the five damage states listed shown in Table G-1 for each of several "standard bridge" classifications. It starts with the estimation of these quantities for a "standard bridge", which is defined as a long bridge with no skew, and no three-dimensional (3D) effects from deck-arching membrane action. The standard bridge types that are considered are: (a) simply-supported bridges on multi-column bents; (b) discontinuous box-girder bridges on single-column bents (unique to California); (c) continuous reinforced- or prestressed-concrete bridges; (d) continuous steel bridges; (e) single-span bridges; and (f) major bridges, whose span length exceeds 150 m.

G.2.1.2 Characterization of Onset of Damage States for Standard Bridges

The steps that were used by Basoz and Mander (1999) to characterize each damage state from Table G-1 for each standard bridge classification are summarized below. In this summary, the five-percent damped spectral accelerations at periods of 1.0 sec. and 0.3 sec. are denoted as $S_a(1.0)$ and $S_a(0.3)$ respectively.

Table G-1. Damage States considered in HAZUS99-SR2 Bridge Model

Damage State Designation		Description
Number	Level	
1	None	First yield.
2	Slight	Minor cracking and spalling of the abutment, cracks in shear keys at abutment, minor spalling and cracking at hinges, minor spalling of column requiring no more than cosmetic repair, or minor cracking of deck.
3	Moderate	Any column experiencing moderate shear cracking and spalling (with columns still structurally sound), moderate movement of abutment (< 5.1 cm) (< 2 inches), extensive cracking and spalling of shear keys, connection with cracked shear keys or bent bolts, keeper bar failure without unseating, rocker bearing failure, or moderate settlement of approach.
4	Extensive	Any column degrading without collapse (e.g., shear failure) but with column structurally unsafe, significant residual movement of connections, major settlement of approach fills, vertical offset or shear key failure at abutments, or differential settlement.
5	Complete	Collapse of any column, or unseating of deck span leading to collapse of deck. Tilting of substructure due to foundation failure.

- ***Step 1: Development of Capacity Spectrum.*** A pushover-type capacity spectrum is developed for each standard bridge classification. This spectrum is represented as a plot of $S_a(1.0)$ vs. spectral displacement, which can be related to drift. Along this plot, the spectral displacement (drift) that leads to the onset of each damage state is identified.
- ***Step 2: Determination of Median Spectral Accelerations for Each Damage State and Standard Bridge Type.*** The starting point for Step 2 is a five-percent damped NEHRP spectrum shape for Soil Type B, which is the assumed site condition for a standard bridge. This spectrum shape is then scaled by different values of $S_a(1.0)$ until it first intersects the capacity spectrum from Step 1 at the spectral displacement (drift) that represents the onset of that damage state. The value of $S_a(1.0)$ at which this occurs for the i^{th} damage state at the m^{th} standard bridge type, is defined as the median spectral acceleration for that damage state and bridge type,. For each of the six standard bridge types, Tables G-2 and G-3 list the median spectral acceleration values for each damage state.
- ***Step 3: Short-Period Response Cases.*** If the spectral displacement for the i^{th} damage state falls within the short-period portion of the NEHRP spectrum, an equivalent median value of the spectral acceleration at a period of 0.3 sec is used to define the onset of that damage state. It is obtained by using a factor related to the NEHRP spectrum shape to scale the median value of $S_a(1.0.)$. If the spectral displacement (drift) for the i^{th} damage state occurs within the longer-period portion of the NEHRP spectrum, the median value of $S_a(1.0)$ is used to characterize the onset of the damage state for that standard bridge type.

Table G-2. Median Ground Motions Leading to Onset of Various Damage States for Conventionally Designed "Standard" Bridges

Bridge Type	NBI Class	Damage State	Median Spectral Acceleration, g, at Period = 1.0 sec. for Damage Functions due to Ground Shaking	
			Non-California	California
Single Span	All	2	0.80*	0.80*
		3	1.00	1.00
		4	1.20	1.20
		5	1.70	1.70
Major Bridges	All	2	0.40	0.40
		3	0.50	0.50
		4	0.70	0.60
		5	0.90	0.80
Multi-Column Bents and Simply-Supported Concrete Superstructure	101-106 501-506	2	0.25	0.30
		3	0.35	0.50
		4	0.45	0.60
		5	0.70	0.90
Single-Column Bents and Concrete Box-Girder Superstructure	205-206 605-606	2	Not applicable	0.35
		3		0.45
		4		0.55
		5		0.80
Continuous Reinforced-Concrete Superstructure	201-204	2	0.60*	0.90*
		3	0.90	0.90
		4	1.10	1.10
		5	1.50	1.50
Continuous Prestressed-Concrete Superstructure	601-604 607	2	0.60*	0.90*
		3	0.90	0.90
		4	1.10	1.10
		5	1.50	1.50
Simply-Supported Steel Superstructure	301-310	2	0.25	0.30
		3	0.35	0.50
		4	0.45	0.60
		5	0.70	0.90
Continuous Steel Superstructure	402-410	2	0.75*	0.75*
		3	0.75	0.75
		4	0.75	0.75
		5	1.10	1.10
All Other Non-Classified Bridges	All	2	0.80	0.80
		3	1.00	1.00
		4	1.20	1.20
		5	1.70	1.70

*Short period motions govern; therefore use demand and capacity at 0.3 sec. to assess damage state.

Table G-3. Median Ground Motions Leading to Onset of Various Damage States for Seismically Designed "Standard" Bridges

Bridge Type	NBI Class	Damage State	Median Spectral Acceleration, g, at Period = 1.0 sec. for Damage Functions due to Ground Shaking	
			Non-California	California
Single Span	All	2	0.80*	0.80*
		3	1.00	1.00
		4	1.20	1.20
		5	1.70	1.70
Major Bridges	All	2	0.60	0.60
		3	0.90	0.90
		4	1.10	1.10
		5	1.70	1.70
Multi-Column Bents and Simply-Supported Concrete Superstructure	101-106 501-506	2	0.50	0.50
		3	0.80	0.80
		4	1.10	1.10
		5	1.07	1.70
Single-Column Bents and Concrete Box-Girder Superstructure	205-206 605-606	2	Not applicable	0.60
		3		0.90
		4		1.30
		5		1.60
Continuous Reinforced-Concrete Superstructure	201-204	2	0.90*	0.90*
		3	0.90*	0.90*
		4	1.10	1.10
		5	1.50	1.50
Continuous Prestressed-Concrete Superstructure	601-604 607	2	0.90*	0.90*
		3	0.90*	0.90*
		4	1.10	1.10
		5	1.50	1.50
Simply-Supported Steel Superstructure	301-310	2	0.50	0.50
		3	0.80	0.80
		4	1.10	1.10
		5	1.07	1.70
Continuous Steel Superstructure	402-410	2	0.90*	0.90*
		3	0.90*	0.90*
		4	1.10	1.10
		5	1.50	1.50
All Other Non-Classified Bridges	All	2	0.80	0.80
		3	1.00	1.00
		4	1.20	1.20
		5	1.70	1.70

*Short period motions govern; therefore use demand and capacity at 0.3 sec. to assess damage state.

G.2.1.3 Characterization of Onset of Damage States for Actual Bridge Being Investigated

It now remains to modify the above median spectral acceleration at each damage state for the relevant standard bridge type, in order to obtain the median spectral acceleration at that damage state for the actual bridge being investigated. This is accomplished by using factors to correct the standard-bridge $S_a(1.0)$ value, in order to account of the skew and 3D effects for the actual bridge. This correction is summarized later in this appendix.

Table G-2 shows that, for conventionally designed continuous steel bridges, only Damage States 2 and 5 will occur. For these bridge types, Mander (1999) has indicated that: (a) Damage State 2 is caused by high forces where the pushover capacity spectrum intersects the flat-top portion of the demand spectrum; (b) there is no intermediate structural damage at Damage States 3 or 4; and (c) the next damage state represents incipient unseating (Damage State 5). This means that the probabilities of occurrence of Damage States 1, 2, and 5 sum to 1.0, and the probabilities of occurrence of Damage States 3 and 4 are zero. A similar situation is observed in Table G-3 for seismically designed continuous steel bridges, for which the probability of occurrence of Damage State 3 is zero, and the probabilities of occurrence of the remaining damage states sum to 1.0.

G.2.1.4 Estimation of Site-Specific Ground Motions for Each Earthquake Scenario

Once the spectral acceleration capacity for a given bridge is estimated as summarized above, the REDARS™ 2 ground-motion model is used to estimate the bridge's site-specific demand ground motions (in terms of $S_a(1.0)$ and $S_a(0.3)$) for each earthquake scenario. The ground-motion model also estimates the site-specific peak ground acceleration, which is needed for analysis of liquefaction hazards (App. E).. These site-specific ground motion estimates include effects of local soil conditions at the site, and are provided for each earthquake scenario. Estimation of these ground motions for different earthquake scenarios includes effects of uncertainties in earthquake magnitude and location, ground-motion attenuation characteristics, and soil amplification effects.

G.2.1.5 Estimation of Bridge Damage States for Each Earthquake Scenario

For a given earthquake scenario, each bridge's demand spectral acceleration as estimated above is compared to the bridge's spectral acceleration capacity that leads to the onset of each damage state (Sec.G.2.1.3. These comparisons are carried out, first for Damage State 5 and then for each successively lower damage state. The bridge's damage state is considered to correspond to that damage state for which the demand spectral acceleration first exceeds the bridge's spectral acceleration capacity.

G.2.1.6 Modification of HAZUS99-SR2 Procedure

During this research, the HAZUS99-SR2 bridge model was used to predict bridge damage states during the 1994 Northridge Earthquake, and these predictions were then compared to observed bridge damage from this earthquake. These comparisons showed that the model substantially overestimated the number of bridges that collapsed during the Northridge

Earthquake. This was particularly important for REDARS™ 2 applications, because the default bridge repair models included in REDARS™ 2 indicate that by far the most extensive bridge downtimes will when bridges collapse; i.e., the downtimes are estimated to be much shorter when a bridge undergoes lesser degrees of damage (Sec. G.5). Therefore, this over-prediction of bridge collapses will have a major effect on REDARS™ 2 estimates of earthquake-induced losses to a highway system.

To address this problem, new conditional probabilistic analyses were performed to identify the causes of the model's over-prediction of bridge collapses, and to develop strategies for modifying the HAZUS99-SR2 model so that its predictions of bridge collapses from the Northridge Earthquake compared more favorably with observed collapses. In these analyses, the earthquake model, location, and magnitude were fixed to represent those of the Northridge Earthquake, and multiple simulations were developed to include effects of uncertainties in bridge-specific ground-motion estimates and damage states. In addition, capacity modification factors from Shinozuka (2004) were used to model the increased structural capacities of those bridges in the system that had been column-jacketed at the time of the Northridge Earthquake.

These analyses led to numerical factors for modifying the HAZUS99-SR2 bridge structural capacities, such that the number and locations of the predicted bridge collapses during the Northridge Earthquake were, on the average, consistent with observed bridge collapses. These factors, which are provided in Section G.2.2.4, are incorporated into the REDARS™ 2 default model for estimation of bridge damage due to ground-motion hazards. Appendix K provides further details on the development of these factors.

As discussed in Appendix K, it is recognized that this set of structural-capacity modifications is based on calibrations for one California earthquake only. If similar analyses could be based on calibrations for other earthquakes and other regions of the country, it is expected that different capacity modification factors could occur. However, the difficulties in compiling system-wide structural-attribute data for actual bridges that were in place during prior California earthquakes, along with the lack of damaging earthquakes in other parts of the country, have precluded carrying out these additional analyses at this time.

G.2.2 Application Procedure

G.2.2.1 Capacity and Demand Characterization

The following steps are used to apply the above default bridge model in REDARS™ 2:

- ***Structural Capacity.*** Preceding the SRA for each earthquake scenario and simulation, the process outlined in Section G.2.1 is used to establish equivalent five-percent damped spectral accelerations for each bridge that represent the onset of each damage state for that bridge. In this, the estimation of bridge damage states assumes a lognormal distribution with a standard deviation of 0.35.

- ***Demand.*** For each earthquake scenario and simulation, the ground-motion model from the REDARS™ 2 Hazards Module estimates soil-amplified five-percent-damped demand spectral

accelerations at periods of 0.3 sec. and 1.0 sec. at each bridge site. These are denoted as $D(0.3)_{j,k,m}$ and $D(1.0)_{j,k,m}$ for the j^{th} earthquake scenario, the k^{th} simulation, and the site of the m^{th} bridge.

- ***Demand-Capacity Comparison.*** For the m^{th} bridge, the demand spectral acceleration (from the j^{th} earthquake scenario and the k^{th} simulation) is compared to the spectral acceleration leading to the onset of each damage state at that bridge (including uncertainties), in order to estimate the bridge's damage state for this particular earthquake and simulation. Depending on whether the short-period response or the long-period response governs for this bridge's damage state, the spectral accelerations at periods of either 0.3 sec or 1.0 sec are used in these comparisons.

G.2.2.2 Input Data

G.2.2.2.1 Bridge Location

An alphanumeric parameter named *STATE* is specified to delineate between California and non-California bridges. This is a two-digit parameter that denotes the state where the bridge is located. Bridges in California are identified by specifying *STATE = CA*.

G.2.2.2.2 Structural Attributes from National Bridge Inventory (NBI) Database

This subsection summarizes the various parameters from the NBI database that are used as input to this bridge modeling procedure. Table G.4 shows how several of these parameters are used in this procedure to deduce bridge damage-state fragilities.

- ***Bridge Type (ITYPE).*** The parameter, *ITYPE*, represents the general structure type for the main bridge being analyzed as represented in the National Bridge Inventory (NBI) database (FHWA, 2003). It is a three-digit number that corresponds to Item 43 in the NBI database. The first (single-digit) number denotes the material type, and the second (2-digit) number indicates the type of construction. The *ITYPE* parameter establishes the process followed by the HAZUS99-SR2 bridge model for computing the median $S_a(1.0)$ for the onset of each damage state for a "standard" bridge. This is applied for each bridge type described below.
  - *Simply Supported Bridges.* If the input value of *ITYPE* falls in any of the following ranges -- 101-106, 301-306, 501-506, or 701-706 -- the bridge is recognized as being simply supported. In this, the first (single-digit) number represents the material type and indicates that the bridge is simply supported (ss); i.e. 1 = reinforced concrete ss, 3 = steel ss, 5 = prestressed concrete ss, and 7 = wood or timber ss. The second (two-digit) number represents the type of bridge construction; i.e., 01 = slab, 02 = stringer/multi-beam or girder, 03 = girder and floor beam system, 04 = tee beam, 05 = multiple box beam or girders, and 06 = single or spread box beam or girders.

  -

- *California-Type Bridges with Single Column Bents and Box Girder Superstructure.* This bridge type denotes bridges from California that have a concrete box-girder superstructure and a substructure consisting of single-column bents. These bridges are continuous over the bents, but may have joints within the various spans. To represent such bridges in REDARS™ 2, it is necessary to first set the input parameter *STATE = CA*. Then, if *ITYPE* has a value of 205-206 or 605-606, the bridge is considered to fall in this category. In this, the first (single-digit) number represents the material type for the continuous spans, and will have a value of 2 for continuous reinforced concrete and a value of 6 for continuous prestressed concrete. The second (two-digit) number represents the type of bridge superstructure construction, and has values of either 05 for a multiple-box-beam superstructure or 06 for a single box-beam superstructure that typifies a California-type bridge.
- *Continuous Bridges*. This bridge type represents any non-California continuous bridge structure (to differentiate it from the California "continuous" bridges addressed in Section 2.3.2.2.2). Therefore, this bridge type would be identified as follows: (a) *STATE* $\neq$ *CA*; and (b) a value of the parameter *ITYPE* that is in the ranges of 201-207 or 601-607 (for continuous concrete superstructures) or 401-410 (for continuous steel superstructures.)

- ***Number of Spans (NSPAN).*** The parameter *NSPAN* defines the total number of spans in the main portion of the bridge plus the approach spans. It is a three-digit number that corresponds to the sum of Item 45 and 46 in the NBI database. If *NSPAN* = 1, then REDARS™ 2 recognizes that the bridge is a single-span structure.

- ***Total Length of Maximum Span (SPNMAX).*** The parameter *SPNMAX* is the length of the maximum span of the bridge. It is a five-digit number that corresponds to Item 48 of NBI database. If *SPNMAX* $\geq$ 150 meters, REDARS™ 2 assumes that the bridge is in the major bridge category. Such bridges can also be modeled by user-specified fragility curves.

- ***Year of Construction (YEAR).*** The parameter *YEAR* represents the bridge's year of construction. It is a four-digit number that corresponds to Item 27 of the NBI database. The HAZUS99-SR2 model uses this parameter to infer whether the bridge has been seismically designed.

- ***Skew Angle (ANGLE).*** The parameter *ANGLE* is the skew angle of the bridge, in degrees, between the centerline of a pier and a line normal to the roadway centerline. It is a two-digit number that corresponds to Item 34 of the NBI database. For a right bridge with no skew, *ANGLE* = 0 degrees. If the bridge is curved has a variable skew, the average skew is recorded. Sometimes the NBI database will show that *ANGLE* = 99 degrees, which signifies a major variation in skews of the substructure units across the length of the bridge.

- ***Deck Width (BDECK).*** The parameter *BDECK* is the width of the deck, in meters. It is a four-digit number that corresponds to Item 52 of the NBI database. This quantity is used in the computation of the replacement value of the bridge.

Table G-4. Use of Fields in NBI Database used by Mander et al. to Infer Bridge Fragility Curves (Mander and Basoz, 1999)

NBI Data Item	Definition	Skew Factor	3-D Response Factor	Use in Inferring Bridge Fragility
1	State *(STATE)*		X	To infer seismic design code used.
8	Structure Number			General ID Number.
27	Year Built *(YEAR)*		X	To Infer whether seismic or conventional design.
34	Skew *(ANGLE)*	X		To compute capacity modification factor that accounts for skew
42	Service Type			To select highway bridges (e.g., rather than rail or pedestrian bridges) from NBI database.
43	Structure Type *(ITYPE)*		X	To infer which type of "standard" bridge to use as basis for fragility curve development.
45	Number of Spans in Main Unit and Approach Spans *(NSPAN)*		X	To infer whether single- or multiple-span bridge.
48	Maximum Span Length *(SPNMAX)*		X	To also infer if bridge is a major bridge (as defined in FEMA, 2002).
49	Structure Length *(SLGTH)*		X	To infer average span length, and to compute replacement value.
52	Deck Width *(BDECK)*			To compute replacement value.
54	Minimum Vertical Underclearance *(MINVUC)*			To infer default value of approach-fill thickness (if accurately specified in FEMA, 2003).

- ***Structure Length (SLGTH).*** The parameter *SLGTH* is the total length of the roadway supported between the bridge abutments, and therefore corresponds to the total length of the main structure plus the approach spans. It is given as a six-digit number to the nearest tenth of a meter (i.e. 000355 = 35.5 m). *SLGTH* corresponds to Item 49 of the NBI database. It is used to: (a) compute bridge repair costs (Sec. G.5); (b) compute the parameter K_{3D} for steel bridges (Sec. G.2.2.2.4); and (c) compute the parameter f_i used in the estimation of bridge damage states due to permanent ground displacement hazards (Sec. G.3.1.1).

- ***Minimum Vertical Underclearance (MINVUC).*** The parameter *MINVUC* is the minimum vertical clearance from an underlying feature (e.g., an underlying roadway) to the bottom of the bridge deck. This quantity corresponds to Item 54 of the NBI database. As described in Appendix H, it is used in REDARS™ 2 as a default estimate of the bridge's approach-fill thickness.

G.2.2.2.3 Identification of Retrofitted Bridges

For each bridge in the highway system, REDARS™ 2 enables users to specify whether that bridge has been seismically retrofitted with column jacketing. This will affect the value of the structural capacity modification factor that is used in REDARS™ 2 to improve comparisons between predicted vs. observed damage states for unretrofitted and retrofitted bridges during the 1994 Northridge Earthquake (see Sections G.2.1.6 and G.2.2.4, and Appendix K).

G.2.2.2.4 Identification of Bridge Overpasses

If a bridge that overlies another roadway is severely damaged, this damage will affect traffic along the underlying roadway as well as the bridge itself. REDARS™ 2 enables users to identify such bridges, together with the link number for the part of the underlying roadway that passes beneath the bridge. Although not used for bridge damage estimation, this information is used in the default bridge repair model (Sec. G.4) to estimate post-earthquake traffic states.

G.2.2.2.5 Demand Ground Motion

The demand ground motions (spectral accelerations at periods of 0.3 sec. and 1.0 sec.) at each bridge site are obtained by applying the ground-motion model in the REDARS™ 2 Hazards Module for each simulation. These are termed $D(0.3)_{k,m}$ and $D(1.0)_{k,m}$ for the k^{th} simulation, and the site of the m^{th} bridge. These estimates include effects of local soil conditions in amplifying (or de-amplifying) the subsurface rock motions. To estimate potential liquefaction hazards at the m^{th} bridge site, the peak ground acceleration at the site, denoted as $D(0.0)_{k,m}$, is also obtained.

G.2.2.3 Median Spectral Acceleration Capacity for Onset of i^{th} Damage State at m^{th} Bridge

Once the above input data are provided, the following steps are used to compute the median spectral acceleration capacity for each bridge type. These steps are repeated for each damage state at each bridge.

G.2.2.3.1 Step 1: Bridge Type and Location

In Step 1, the input parameter *ITYPE* is used to define the bridge type for each bridge in the system, and the parameter *STATE* is used to indicate whether the bridge is located in California.

G.2.2.3.2 Step 2: Typical vs. Seismic Design

In Step 2, the input parameter *YEAR* is used to indicate whether the bridge was seismically designed. Seismically designed bridges are: (a) California bridges built in 1975 or later; or (b) bridges outside of California built in 1990 or later. Conventionally designed bridges are defined as California- or non-California-bridges whose year of construction precedes those given above.

G.2.2.3.3 Step 3: Median Spectral Acceleration at 1.0 Sec. for Standard Bridge

In Step 3, Tables G-2 or G-3 are used to obtain the median spectral acceleration at a period of 1.0 sec. for each damage state of the "standard bridge" type that corresponds to the m^{th} bridge and a NEHRP Type B site condition. Table G-2 is used for conventionally designed bridges, and Table G-3 is used for seismically designed bridges. This spectral acceleration is termed $S_a(1.0)_{i,m}$ for the i^{th} damage state at the m^{th} bridge.

G.2.2.3.4 Step 4: Capacity Modification Factors to Convert from Standard to Actual Bridge

To convert the median spectral acceleration for the standard bridge to the actual bridge, the following factors are computed to account for effects of skew and three-dimensional deck-arching membrane action. In this, skew effects are represented by the factor K_{skew} , computed as:

$$K_{skew} = \sqrt{\sin(90 - ANGLE)} \tag{G-1}$$

where *ANGLE* is the bridge's skew angle which, as defined in the NBI database, is the angle between a line normal to the centerline of the roadway to the centerline of the pier (e.g., *ANGLE* = 0 for an unskewed bridge). Effects of three dimensional deck-arching membrane action are represented by the parameter K_{3D} which, as shown in Table G-5, depends on the number of spans (*NSPAN)*, the bridge length (*L)* and type *(NBI Class)*, and if the bridge is seismically designed.

G.2.2.3.5 Median Structural Capacity of Actual Bridge for Damage States 3, 4, and 5

For Damage States 3, 4, and 5, which are always governed by long period response, the median spectral accelerations leading to the onset of the i^{th} damage state at the m^{th} bridge (termed $C'(1.0)_{i,m}$) are computed for rock (NEHRP Type B) site conditions

$$C'(1.0)_{i,m} = K_{skew} * K_{3D} * S_a(1.0)_{i,m} \tag{G-2}$$

G.2.2.3.6 Median Structural Capacity of Actual Bridge for Damage State 2

For those bridges from Tables G-2 and G-3 that are governed by short period response at Damage State 2, the median spectral acceleration at the onset of this damage state ($C'(0.3)_{2,m}$) is modified by first computing the factor K_{shape} according to Equation G-3:

$$K_{shape} = \frac{2.5 * S_a(1.0)}{S_a(0.3)} \tag{G-3}$$

where $S_a(1.0)$ and $S_a(0.3)$ are the demand spectral accelerations at periods of 1.0 sec. and 0.3 sec. respectively.

Table G-5. Computation of K_{3D}

Bridge Type	NBI Class	Conventionally Designed Bridges*	Seismically Designed Bridges (non-CA bridges built after 1990 or CA bridges built after 1975)*
Single Span	All	1.25**	1.25**
Major Bridge	All	1+0.25/(*NSPAN* – 1)	1+0.25/(*NSPAN* – 1)
Multi-Column Bents and Simply-Supported Concrete Superstructure	101-106 501-506	1 + 0.25/(*NSPAN* – 1)	1 + 0.25/(NSPAN – 1)
Single-Column Bents and Concrete Box-Girder Superstructure	205-206 605-606	1 + 0.33/*NSPAN*	1 + 0.33/(*NSPAN* – 1)
Continuous Reinforced-Concrete Superstructure	201-204	1 + 0.33/*NSPAN*	1 + 0.33/(*NSPAN* – 1)
Continuous Prestressed -Concrete Superstructure	601-604 607	1 + 0.33/*NSPAN*	1 + 0.33/(*NSPAN* – 1)
Simply-Supported Steel Superstructure	301-310	1 + 0.09/(*NSPAN* – 1); L ≥ 20 m 1+0.20/(*NSPAN* – 1); L < 20m	1 + 0.25/(*NSPAN* – 1)
Continuous Steel Superstructure	402-410	1 + 0.05/*NSPAN*; L ≥ 20 m 1+0.10/*NSPAN*; L < 20m	1 + 0.33/(*NSPAN* – 1)
All Other Unclassified Bridges***	All	1.0	1.0

* *NSPAN* > 1 for all bridge types except for "Single-Span" bridges, for which *NSPAN* = 1, and $K_{3D} = 1.0$.

** As per information provided by HAZUS99-SR2 technical staff on December 2, 2004.

*** Not included in HAZUS99-SR2 Manual.

Then, the median spectral accelerations for the standard bridges that are denoted by an asterisk (*) in Tables G-2 and G-3 are modified to be

$$C'(1.0)_{2S,m} = Minimum(1, K_{shape}) * C(1.0)_{2,m} \quad \text{(G-4)}$$

where $C(1.0)_{2,m}$ is the median spectral acceleration for the corresponding standard bridge type, as directly obtained from Tables G-2 or G-3.

For those bridges that Tables G-2 and G-3 show to be governed by long-period response at Damage State 2, the median spectral acceleration at the onset of this damage state ($C'(1.0)_{2,m}$) is equal to the median spectral acceleration for the corresponding standard bridge type, i.e.

$$C'(1.0)_{2.m} = C(1.0)_{2,m} \quad \text{(G-5)}$$

Equations G-4 and G-5 exclude correction factors for skew and 3D effects since, at Damage State 2, the structural displacements are too small for these corrections to be significant.

G.2.2.4 Structural Capacity Modifications based on Northridge Earthquake Calibrations

As noted in Section G.2.1.6, the HAZUS99-SR2 bridge structural capacities have been modified to enable the model's predicted bridge damage from the Northridge Earthquake to be consistent with observed damage. The capacity modification factors developed by the statistical analysis are shown in Table G-6. They are based on the following representation of the bridge's i^{th} damage state including effects of uncertainties, for the m^{th} bridge and the k^{th} simulation:

$$\ln C''(T)_{i,m,k} = \ln\left(\alpha_i * C'(T)_{i,m}\right) + \beta_i * X_k \quad \text{(G-6)}$$

where

$C''(T)_{i,m,k}$ = structural capacity including uncertainties (in terms of spectral acceleration at a period T of 1.0 sec. or 0.3 sec.),

α_i = scale factors for the median structural capacity for the i^{th} damage state as obtained from the statistical analysis described in Appendix K (as listed in Table G-6),

β_i = standard deviation of the structural capacity for the i^{th} damage state, as also obtained from the analysis described in Appendix K (as also listed in Table G-6), and

X_k = uniform random variate for the k^{th} simulation that is generated in REDARS™ 2.

G.2.2.5 Retrofit Enhancement Factors

Numerous test programs have demonstrated that the seismic performance of non-seismically-designed bridges will be substantially improved by encasing their columns in steel or composite-material jackets (Priestley et al., 1996). REDARS™ 2 represents these beneficial effects of column jacketing by enhancing the structural capacities of those bridges in the highway system

that the REDARS™ 2 user has identified as being jacketed. These enhancements are based on results from Shinozuka (2004), who used nonlinear analyses to assess the beneficial effects of column jacketing on fragility curves for a variety of different bridge configurations. The resulting enhanced structural capacity factors that are used REDARS™ 2 are listed in Table G-7.

Table G-6.
Structural Capacity Modification Factors for Bridges with No Column-Jacket Retrofit based on Northridge Earthquake Bridge Damage Observations (see Appendix K)

Damage State, *i*	Probabilistic		Deterministic
	α_i in Eq.G-6	β_i in Eq. G-6	α_i in Eq.G-6 (in which $\beta_i = 0$)
5	1.44 (1.3– 1.7)	0.35	0.7
4	1.12 (1.0-1.25)	0.35	1.0
3	1.0	0.35	1.0
2	1.0	0.35	1.0

Notes: Parentheses show range of permissible values of α_5 identified by analyses described in Appendix K.

Table G-7.
Structural Capacity Modification Factors for Column-Jacketed Bridges (Shinozuka, 2004) (assumed to be same for probabilistic or deterministic applications of REDARS™ 2

Damage State	α_i in Eq.G-6 (including median retrofit enhancement factor from Shinozuka (2004)
5	2.68
4	1.98
3	1.58
2	1.34

G.2.2.6 Estimation of Damage State for Actual Bridge

With the median spectral acceleration leading to the onset of each damage state now established, it remains to establish the bridge's actual damage state for the k^{th} simulation/earthquake. This is carried out as part of the SRA for each earthquake scenario and simulation by carrying out the following steps.

G.2.2.6.1 Step 1 – Input Demand Spectral Accelerations

Under Step 1, the site-specific demand ground motions at the m^{th} bridge site are obtained by applying an appropriate ground-motion model from the Hazards Module for the k^{th} simulation and earthquake. In this, uncertainties in ground-motion attenuation and soil amplification effects are considered. As noted earlier in Section G.2.2.2.5, these demand motions at are specified as spectral accelerations at periods of 0.0 sec., 0.3 sec., and 1.0 sec. For period p, they are referred to as $D(p)_{j,k,m}$, where p = 0.0, 0.3, and 1.0 sec.

G.2.2.6.2 Step 2 – Develop Random Variate X_k

Under this step, REDARS™ 2 generates a uniform random variate X_k. for the k^{th} simulation.

G.2.2.6.3 Step 3 – Evaluate whether Bridge is in Damage State 5

- *Substep 3-1. Compute Capacity including Effects of Uncertainties.* Under this substep, the spectral acceleration at the onset of Damage State 5 (including effects of uncertainties) is computed as the quantity $C''(1.0)_{5,m}$ in Equation G-7

$$C''(1.0)_{5,m,k} = \exp\left[\ln\left(\alpha_5 * C'(1.0)_{5,m}\right) + \beta_5 X_k\right] \quad \text{(G-7)}$$

  where α_5 and β_5 are obtained from Table G-6, $C'(1.0)_{5,m}$ is obtained from Equation G-2 for i = 5, X_k is the random variate for the k^{th} simulation that is obtained under Step 2, and the subscripts "5" and "m" represent Damage State 5 for the m^{th} bridge.

- *Substep 3-2. Compare Demand to Capacity for Damage State 5.* This substep checks whether $D(1.0)_{k,m}$ (which is the demand spectral acceleration at the m^{th} bridge site due to the k^{th} earthquake scenario and simulation) $\geq C''(1.0)_{5,m,k}$ (the capacity spectral acceleration for this bridge site, and kth simulation as obtained in Substep 3-1). If so, the bridge has a damage state of 5. Otherwise, the method proceeds to Step 4.

G.2.2.6.4 Step 4 – Evaluate whether Bridge is in Damage State 4

- *Substep 4-1. Compute Capacity including Effects of Uncertainties.* Under this substep, the spectral acceleration at the onset of Damage State 4 (including effects of uncertainties) is computed as the $C''(1.0)_{4,k,m}$ in Equation G-8

$$C''(1.0)_{4,m,k} = \exp\left[\ln\left(\alpha_4 * C'(1.0)_{4,m}\right) + \beta_4 X_k\right] \quad \text{(G-8)}$$

  where α_4 and β_4 are obtained from Table G-6 for i = 4, $C'(1.0)_{4,m}$ is obtained from Equation G-2 for i = 4, X_k is the random variate for the k^{th} simulation that is obtained under Step 2, and the subscripts 4 and m represent Damage State 4 for the m^{th} bridge.

- *Substep 4-2. Compare Demand to Capacity for Damage State 4.* This substep checks whether $D(1.0)_{k,m}$ (which is the demand spectral acceleration at the m^{th} bridge site due to the k^{th} earthquake scenario and simulation) $\geq C''(1.0)_{4,m,k}$ (the capacity spectral acceleration for this bridge site, and simulation/earthquake as obtained in Substep 4-1). If so, the bridge has a damage state of 4. Otherwise, the method proceeds to Step 5.

G.2.2.6.5 Step 5 – Evaluate whether Bridge is in Damage State 3

- *Substep 5-1. Compute Capacity including Effects of Uncertainties.* Under this substep, spectral acceleration at the onset of Damage State 3 (including effects of uncertainties) is computed as the quantity $C''(1.0)_{3,k,m}$ in Equation G-9

$$C''(1.0)_{3,m,k} = \exp\left[\ln\left(\alpha_3 * C'(1.0)_{3,m}\right) + \beta_3 X_k\right] \quad \text{(G-9)}$$

  where α_3 and β_3 are obtained from Table G-6 for $i = 3$, $C'(1.0)_{3,m}$ is obtained from Equation G-2 for $i = 3$, X_k is the random variate for the k^{th} simulation that is obtained under Step 2, and the subscripts 3 and m represent Damage State 3 for the m^{th} bridge.

- *Substep 5-2. Compare Demand to Capacity for Damage State 3.* This substep checks whether $D(1.0)_{k,m}$ (which is the demand spectral acceleration at the m^{th} bridge site due to the k^{th} earthquake scenario and simulation) $\geq C''(1.0)_{3,m,k}$ (the capacity spectral acceleration for this bridge site and simulation/earthquake as obtained in Substep 5-1). If so, the bridge has a damage state of 3. Otherwise, the method proceeds to Step 6.

G.2.2.6.6 Step 6 – Evaluate whether Bridge is in Damage State 2

If the bridge structure is not asterisked in Tables G-2 or G-3, its damage is governed by long-period response, and the damage estimation proceeds to Section G.2.2.4.6(a). Otherwise, the damage is governed by short-period response and is estimated using Section G.2.2.4.6(b).

G.2.2.6.6(a) Bridges where Long Period Response Governs

- *Substep 6a-1. Compute Capacity including Effects of Uncertainties.* Under this substep, the spectral acceleration at the onset of Damage State 2 when long-period response governs (including uncertainties) is computed as the quantity $C''(1.0)_{2L,m,k}$ in Equation G-10

$$C''(1.0)_{2L,m,k} = \exp\left[\ln\left(\alpha_2 * C'(1.0)_{2L,m}\right) + \beta_2 X_k\right] \quad \text{(G-10)}$$

  where α_2 and β_2 are obtained from Table G-6 for $i = 2$, $C'(1.0)_{2L,m}$ is obtained from Equation G-2 for $i = 2$ (since long period response governs), X_k is the random variate for the k^{th} simulation that is obtained under Step 2 (Sec. G.2.2.6.2), and the subscripts $2L$ and m represent long-period response for Damage State 2 at the m^{th} bridge.

- *.Substep 6a-2. Compare Demand to Capacity for Damage State 2.* This substep checks whether $D(1.0)_{k,m}$ (which is the demand spectral acceleration at the m^{th} bridge site due to the k^{th} earthquake scenario and simulation) $\geq C''(1.0)_{2L,m,k}$ (the capacity spectral acceleration for this bridge site, and simulation/earthquake as obtained in Substep 6a-1). If so, the bridge has a damage state of 2. Otherwise, the bridge has a damage state of 1.

G.2.2.6.6(b) Bridges where Short Period Response Governs (Asterisked in Tables G-2 or G-3)

- *Substep 6b-1. Compute Modified Median Spectral Acceleration for Short-Period Structure*. From Section G.2.2.3.6, an equivalent structural capacity (median spectral acceleration at a period of 1.0 sec.) is obtained by first using Equation G-3 (repeated below) to compute K_{shape}.

$$K_{shape} = \frac{2.5 * S_a(1.0)}{S_a(0.3)} \qquad \text{(G-3)}$$

  where S_a(1.0 and S_a(0.3) are the site-specific demand spectral accelerations at periods of 1.0 sec. and 0.3 sec. respectively. Then, Equation G-4 of Section G.2.2.3.6 (repeated below) is used to compute the median spectral acceleration as

$$C'(1.0)_{2S,m} = Minimum(1, K_{shape}) * C(1.0)_{2,m} \qquad \text{(G-4)}$$

  where the subscript *2S* refers to Damage State 2 when short-period response governs, and $C(1.0)_{2,m}$ is the structural capacity of the bridge for Damage State 2 in its "standard" configuration as given in Tables G-2 or G-3 (without corrections for skew and for 3D membrane effects that are considered for long period bridges).

- *Substep 6b-2. Compute Capacity including Effects of Structural Uncertainties.* Under this substep, spectral acceleration at the onset of Damage State 2 when short-period response governs (including structural uncertainties) is termed $C''(1.0)_{2S,m,k}$ and is computed as

$$C''(1.0)_{2S,m,k} = \exp\left[\ln\left(\alpha_2 * C'(1.0)_{2S,m}\right) + \beta_2 X_k\right] \qquad \text{(G-11)}$$

  where α_2 and β_2 are obtained from Table G-6 for $i = 2$, $C'(1.0)_{2,m}$ is obtained from Equation G-4 (since short-period response governs), X_k is the random variate for the k^{th} simulation from Step 2, (Sec. G.2.2.4.2., the subscript *2S* represents Damage State 2 governed by short-period response, and the subscript *m* refers to the m^{th} bridge. Note from Table G-6 and Equations G-10 and G-11 that the capacity modification factors based on the Northridge Earthquake calibrations -- α_2 and β_2 -- are assumed to be the same regardless of whether long-period bridge response or short-period bridge response governs for Damage State 2.

- *Substep 6b-3. Compare Demand to Capacity for Damage State 2.* This substep checks whether $D(1.0)_{k,m}$ (which is the demand spectral acceleration at the m^{th} bridge site due to the

k^{th} earthquake scenario and simulation) $\geq C''(1.0)_{2S,k,m}$ (the capacity spectral acceleration for this bridge site, and simulation/earthquake as obtained in Substep 7b-2). If so, the bridge has a damage state of 2. Otherwise, the bridge has a damage state of 1.

G.3 ESTIMATION OF BRIDGE DAMAGE STATES FROM PERMANENT GROUND DISPLACMENT

There has been a paucity of research to develop methods that estimate bridge damage states due to permanent ground displacement (PGD) from liquefaction or surface fault rupture. Therefore, REDARS™ 2 uses the HAZUS99-SR2 model for this purpose. In this model, the only types of bridge damage due to PGD that are considered are incipient unseating and collapse, which correspond to Damage States 4 and 5 respectively. In addition, initial damage to bearings (which would correspond to Damage States 2 or 3) is not considered. Therefore, in REDARS™ 2, these damage states are excluded from the model. The model also does not consider the possibly significant effects of PGD hazards on bridge foundations and abutments. In view of these shortcomings, there is clearly a need for further research that would include effects of PGD on the superstructure and well as the abutments and foundation during an earthquake.

For each simulation in the SRA of the highway system, REDARS™ 2 computes PGD hazards only at those sites that the user has identified beforehand as being susceptible to liquefaction or surface fault rupture. For each bridge located on such sites, the resulting demand value of the PGD is termed $(PGD_{dem})_{m,k}$ for the m^{th} bridge and the k^{th} simulation. The following steps are carried out to estimate that bridge's damage state due to this demand ground displacement.

G.3.1 Step 1. Establish Median PGD Capacity for Each Bridge

G.3.1.1 Median PGD Capacity including Bridge Geometry Modification Factors

The median PGD capacity for the i^{th} damage state at the m^{th} bridge, termed $(PGD_{cap})_{i,m}$, is obtained from the values provided in Table G-8 for the appropriate standard bridge type.

G.3.1.2 Median PGD Capacity to Account for Possible Unseating

Next, to account for potential PGD-induced unseating, this displacement capacity is modified as shown in Equation G-13:

$$(PGD_{cap})'_{i,m} = (PGD_{cap})_{i,m} * f_i \tag{G-14}$$

where f_i is a PGD modification factor given in Table G-7. In this table, the following equation is used to compute the PGD modification factor for bridges with either: (a) multi-column bents and a simply-supported concrete or steel superstructure; or (b) a continuous concrete superstructure.

$$f_i = \frac{0.5 * L}{N * W * \sin\gamma} \tag{G-15}$$

In Equation G-15, L and W are the length and width of the bridge, N is the number of spans, and γ is the skew angle as defined in Section G.2.2.2.2.

Table G-8. Permanent Ground Displacement Capacities for Various Bridge Damage States

Bridge Type	NBI Class	Damage State	Median Permanent Ground Displacement (PGD), inches,	PGD Modification Factor shown in Equation G-14, f_1, f_2, f_3, f_4
Multi-Column Bents and Simply Supported Concrete or Steel Superstructure	101-106 301-310 501-506	2 3 4 5	3.9 3.9 3.9 13.8	Equation G-15 Equation G-15 Equation G-15 Equation G-15
Single Column Bents and Box Girder Concrete Superstructure	205-206 605-606	2 3 4 5	3.9 3.9 3.9 13.8	1 1 1 $\sin \alpha$
Continuous Concrete Superstructure	201-206	2 3 4 5	3.9 3.9 3.9 13.8	1 1 1 $\sin \alpha$
Continuous Concrete Superstructure	601-607	2 3 4 5	3.9 3.9 3.9 13.8	Equation G-15 Equation G-15 Equation G-15 Equation G-15
Continuous Steel Superstructure	402-410	2 3 4 5	3.9 3.9 3.9 13.8	1 1 1 $\sin \alpha$
Single Span	All	2 3 4 5	3.9 3.9 3.9 13.8	1 1 1 1
Major Bridges and all other Non-Classified Bridges	All	2 3 4 5	3.9 3.9 3.9 13.8	1 1 1 1
All Other Non-Classified Bridges	All	2 3 4 5	3.9 3.9 3.9 13.8	1 1 1 1

G.3.2 Step 2. Estimate PGD Capacity including Effects of Uncertainties

The m^{th} bridge's PGD capacity for the i^{th} damage state, including effects of uncertainties, is termed $(PGD_{cap})''_{i,m,k}$ for the k^{th} simulation. This bridge capacity is expressed as:

$$(PGD_{cap})''_{i,m,k} = \exp\left[\ln\left(PGD\right)'_{i,m} + 0.20X_k\right] \quad \text{(G-16)}$$

where, according to HAZUS99-SR2, 0,20 = the log of the standard deviation of the bridge capacity for all damage states. The quantity X_k is a random variate for the k^{th} simulation that is generated in REDARS™ 2 under this step.

G.3.3 Step 3. Determine if Bridge is in Damage State 5

To determine if the bridge is in Damage State 5, Equation G-16 is used to compute the bridge's ground-displacement capacity for that damage state, termed $(PGD_{cap})''_{5,m,k}$. Then, if the demand value of the ground displacement $(PGD_{dem})_{m,k} > (PGD_{cap})''_{5,m,k}$, the bridge is in Damage State 5. Otherwise, the process goes to Section G.3.4.

G.3.4 Step 4. Determine if Bridge is in Damage State 4

Next, the process summarized in Section G.3.1.3 is repeated in order to estimate the bridge's ground-displacement capacity for Damage State 4, $(PGD_{cap})''_{4,m,k}$, and to check whether $(PGD_{dem})_{m,k} > (PGD_{cap})''_{4,m,k}$. If so, the bridge is in Damage State 4. Otherwise, the bridge is undamaged due to the permanent ground displacement hazard from the k^{th} simulation.

G.4 BRIDGE REPAIR MODEL

G.4.1 Background

REDARS™ 2 uses the repair model described in this section as defaults for use with the default damage-state models for bridges subjected to ground shaking and PGD hazards that are summarized in Sections G.2 through G.4. For each of these damage states, this default repair model provides first-order estimates of corresponding bridge repair costs, durations, and traffic states as the repairs are proceeding. As noted earlier in this report, these first-order repair models can be overridden by the user, either: (a) for individual bridges within the highway system being analyzed, (e.g., for major bridges along non-redundant roadways where more refined damage and repair estimates are appropriate); or (b) for all bridges throughout the highway system (e.g., to account for bridge construction and repair practices and resources in the region being analyzed that differ from those represented by these models).

G.4.2 Assumptions

The default bridge repair models described in this appendix are based on several assumptions that are listed below.

G.4.2.1 California-Based Model

This default repair model was developed in collaboration with senior bridge engineering and maintenance personnel at the California Department of Transportation (Caltrans) in Sacramento CA, and is based on their judgment and experience.. Therefore, the model is applicable to California bridges and to the construction types, maintenance practices, and post-earthquake repair resources and strategies that Caltrans has developed. REDARS™ 2 users from outside of California should modify this default model as appropriate to best represent the construction, maintenance, and repair procedures/resources for their particular highway transportation system.

A benefit of this default repair model is that it incorporates Caltrans' extensive experience in post-earthquake bridge damage assessment and repair that is unmatched elsewhere in the United States. Hopefully, this experience can benefit REDARS™ 2 users from outside of California in their planning of their own post-earthquake repair strategies. Therefore, these users should view this default model as an experience-based starting point that can and should be modified as appropriate to represent their particular practices and resources. The REDARS™ 2 software has been structured to facilitate such repair-model modifications.

G.4.2.2 Qualitative Damage State Descriptions

This default model is based on the HAZUS99-SR2 damage state descriptors listed in Table G-1. However, these qualitative damage descriptors do not provide information on the types, extents, and locations of earthquake damage throughout the bridge system with a level of detail that would ordinarily be needed to estimate bridge-system repair requirements. There is a well-recognized need for research to develop next-generation bridge-damage models that include improved bridge-system damage descriptions for estimation of repair procedures, costs, times, and traffic states. (TCW, 2003 and 2005).

As noted earlier, the HAZUS99-SR2 model assumes that PGD can only cause incipient unseating and collapse of a bridge (corresponding to Damage States 4 and 5). Therefore, in this repair model, it is assumed that if Damage States 4 or 5 do occur, the repair strategies, costs, time, and effects on bridge traffic states during the repairs will be the same regardless of whether this damage was caused primarily by ground motions or PGD. It is also assumed that the occurrence of Damage States 2 or 3 due to PGD hazards at bridges is excluded from this model. Nevertheless to provide users with the option to consider the possible occurrence of Damage States 2 and 3 due to PGD, or to consider different repair strategies for Damage State 4 if it is caused primarily by PGD instead of ground shaking, the model includes separate tables for defining post-earthquake traffic states for Damage State 4 due to PGD vs. ground shaking.

G.4.2.3 Damage States and Associated Repair Consequences and Strategies

Table G-9 describes the general repair consequences and strategies that are assumed for each of the HAZUS99-SR2 damage states.

Table G-9. Assumed Repair Consequences and Strategies for Each Bridge Damage State

Damage State (Table G-1)	Repair Consequences and Strategies
1 (None)	No repair costs or interruption of traffic.
2 (Slight)	Minor repair costs but no shoring is needed. No interruption of traffic.
3 (Moderate)	Bridge damage is repairable, but shoring will be needed before repairs proceed. Shoring must be sufficient to totally support all dead loads and full traffic loads during repairs. Any jacking/ramping needed at locations of moderate settlement and offset will be done while shoring is proceeding. Bridge will be fully closed to traffic during shoring, and then fully reopened to traffic while repairs proceed. Moderate repair costs will be incurred.
4 (Extensive)	Some bridge elements are irreparably damaged and must be replaced. However, replacement of these elements can occur without replacing entire bridge. Bridge will first be extensively shored so that all dead loads and full pre-earthquake traffic loads are completely supported during replacement of damaged elements. Any jacking or ramping needed at locations of significant offset or settlement will be done while shoring is proceeding. Bridge will be fully closed to traffic during shoring, and then fully reopened to traffic during replacement of damaged elements. Major costs for replacement of damaged elements will be incurred. The shoring requirements for extensively damaged bridges will be more extensive than the shoring for moderately damaged bridges.
5 (Complete)	Irreparable damage is sufficiently extensive to require replacement of entire bridge.

G.4.2.4 Repair Resources

If an earthquake causes major damage to many elements of the region's infrastructure (e.g., to its buildings, power systems, and other lifelines), there could be competition for repair resources, particularly if such resources are scarce. However, this bridge repair model assumes that the responsible transportation agency will have rapid access to sufficient equipment, labor, and material resources so that shoring and repair of all damaged bridges can proceed without delays. These resources may be available within the agency itself, and/or through outside on-call contractors who can be rapidly mobilized to initiate the repairs of the damaged bridges. If such resources are not available, the REDARS™ 2 user should adjust this default repair model.

G.4.2.5 Accessibility of Bridge Damage

It is assumed that all elements of the damaged bridges will be readily accessible for repairs. For any bridges that cross major rivers or have other accessibility constraints, the repair costs, durations, and traffic states provided in this default model could underestimate actual repair requirements. For such bridges, this default repair model should be overridden by the user.

G.4.2.6 Underlying Roadways

If a damaged bridge crosses over an underlying roadway, this default bridge repair model accounts for possible effects of this damage on traffic along that roadway. In this model, it is assumed that there is sufficient clearance along and between the underlying roadways so that

shoring of the overlying damaged bridge will not extend into the lanes of these roadways. As a result, once the overlying bridge is shored, the traffic along the underlying roadways will be fully open to traffic.

G.4.2.7 Non-Roadway Infrastructure

Experience from past earthquakes has shown that traffic along bridges can be affected by damage to adjacent buildings and to co-located power, water, wastewater, natural gas, and communications pipelines or conduits. Effects of such damage on post-earthquake traffic states along the bridges are neglected in this default repair model.

G.4.2.8 Emergency Repairs

After the Northridge Earthquake, Caltrans implemented a special emergency strategy for rapid replacement of certain collapsed bridges along freeways that were essential to the recovery of the Los Angeles area. This strategy included a bonus-incentive program for the construction contractors that increased replacement costs but substantially reduced the repair durations (thereby accelerating the time for restoration of normal traffic operations along these freeways).

The repair costs and durations provided in this default model are assumed to apply for non-emergency repairs only. If it is decided to carry out the above emergency strategy for any bridge, the user can assume that the bridge replacement costs are doubled relative to those estimated in this default repair model, and the repair durations are cut in half.

G.4.3 Repair Model Implementation

The implementation of the default bridge repair model that is based on the above assumptions allows the user to carry out different estimates of traffic states due to damage from ground shaking and PGD, and then use the most severe of these estimates as the governing traffic state for the bridge. At this time, REDARS™ 2 does not provide separate estimates of repair costs from damage due to ground shaking and PGD. Such upgrades will be considered as a possible future improvement to the REDARS™ 2 software, along with the parallel development of improved models for estimating bridge damage states due to PGD.

G.4.3.1 Step 1: Estimate Traffic States during Repair of Damage from Ground Shaking and Ground Displacement

After the bridge's damage state due to ground shaking hazards is estimated as described in Section G.2, Table G-10 is used to estimate the traffic state of the bridge and its underlying roadway (if any) while the initial inspection, shoring, mobilization and repairs are proceeding..

`In addition, after the bridge's damage state due to PGD is estimated as described in Section G.3, Table G-11 is used to estimate the traffic state of the bridge and its underlying roadway (if any) at various times after the earthquake. If the bridge's estimated traffic state due to damage from ground shaking and PGD are different at any post-earthquake time, REDARS™ 2 assumes that the most severe of these traffic states will govern.

Table G-10. Default Traffic States during Repair of Bridge Damage from Ground Motions

Bridge Damage State (Table G-1)	Number of Bridge Spans	Post-Earthquake Traffic State: Bridge		Post-Earthquake (EQ) Traffic State: Underlying Roadway	
		Time after EQ, days	Percent of Pre-EQ Traffic-Carrying Capacity	Time after EQ, days	Percent of Pre-EQ Traffic-Carrying Capacity
None or Slight	--	0 days	100%	0 days	100%
Moderate	--	0-4 days	0%	0-4 days	0%
		> 4 days	100%	> 4 days	100%
Extensive	--	0-12 days	0%	0-12 days	0%
		> 12 days	100%	> 12 days	100%
Collapse:	3 spans	0-140 days	0%	0-30 days	0%
		> 140 days	100%	> 30 days	100%
	4 spans	0-180 days	0%	0-30 days	0%
		> 180 days	100%	> 30 days	100%
	≥ 5 spans	0-220 days	0%	0-30 days	0%
		> 220 days	100%	> 30 days	100%

Table G-11. Default Traffic States during Repair of Bridge Damage from PGD

Bridge Damage State (Table G-1)	Number of Bridge Spans	Post-Earthquake Traffic State: Bridge		Post-Earthquake (EQ) Traffic State: Underlying Roadway	
		Time after EQ, days	Percent of Pre-EQ Traffic-Carrying Capacity	Time after EQ, days	Percent of Pre-EQ Traffic-Carrying Capacity
None or Slight	--	--	--	--	--
Moderate	--	--	--	--	--
		--	--	--	--
Extensive	--	0-12 days	0%	0-12 days	0%
		> 12 days	100%	> 12 days	100%
Collapse:	3 spans	0-140 days	0%	0-30 days	0%
		> 140 days	100%	> 30 days	100%
	4 spans	0-180 days	0%	0-30 days	0%
		> 180 days	100%	> 30 days	100%
	≥ 5 spans	0-220 days	0%	0-30 days	0%
		> 220 days	100%	> 30 days	100%

It is noted that the default traffic state estimates provided in Tables G-10 and G-11 do not consider partial bridge traffic-carrying capacity. That is, a bridge is assumed to be either fully open to traffic or fully closed to traffic at all times, from the time of the occurrence of the

earthquake to the time when the bridge is 100% repaired. However, these estimates can be overridden by the user, during which the possibility of the bridge being reopened to partial traffic at any time during the repairs can be considered. For this situation, Table G-12 represents a default definition of a partially reopened bridge as a function of the number of bridge spans. This reopened bridge definition can also be modified by the user if desired.

G.4.3.2 Step 2: Estimate Bridge Repair Cost

In this repair model, the repair cost is computed as the product of a repair cost ratio (*RCR*) which depends on the bridge's damage state, and the replacement cost, which depends on the bridge's surface area. Table G-13 provides default values for the *RCR*s and the bridge's unit replacement costs, which can be overridden by the user. The most severe of the damage states estimated for this bridge due to ground shaking and PGD is used as the damage state in this table.

Table G-12. Default Definition of "Partially Opened" Bridge

Bridge Damage State (Table G-1)	Number of Lanes Each Way Open to Traffic after Earthquake					
	Pre-EQ Lanes = 1	Pre-EQ Lanes = 2	Pre-EQ Lanes = 3	Pre-EQ Lanes = 4	Pre-EQ Lanes = 5	Pre-EQ Lanes = 6
None	1	2	3	4	5	6
Slight	1	2	3	4	5	6
Moderate	0	1	2	3	4	5
Extensive	0	1	1	2	2	2
Collapse	0	0	0	0	0	0

Table G-13. Default Bridge Repair Costs

Damage State Designation	Best Estimate Repair-Cost Ratio (*RCR*)[1, 2]
None	*RCR* = 0.0
Slight	*RCR* = 0.03
Moderate	*RCR* = 0.25
Extensive	*RCR* = 0.75
Collapse	*RCR* = 1.0

1 Repair-Cost Ratio (*RCR*) is defined as the ratio of the repair cost for each damage state to the replacement cost.

2 Bridge replacement cost *(REP)* is computed as the product of a unit replacement costs (in dollars/ft^2) and the surface area of the bridge in ft^2 (defined as the product of the total bridge's length and its width.) The default replacement cost in this repair model is assumed to be \$150/ft^2, which corresponds to data provided by Caltrans for a typical cast-in-place prestressed-concrete box-girder bridge in Northern California. However, since this replacement cost may differ for other materials of construction and for other regions of the country, REDARS™ 2 is structured to enable users to override this default replacement cost for any bridge in the system. The above default *RCR* values can be readily overridden for any bridge.

APPENDIX H
DEFAULT MODELS FOR APPROACH FILLS AND HIGHWAY PAVEMENTS

REDARS™ 2 contains default models for estimating post-earthquake repair costs, downtimes, and traffic states for bridge approach fills subjected to earthquake-induced ground settlement (assuming dry soils) and for highway pavements subjected to earthquake-induced permanent ground displacements (PGD) due to liquefaction or surface fault rupture. These models are summarized in this appendix.

H.1 APPROACH FILLS

If approach fills alongside bridge abutments have not been adequately compacted during construction, they are vulnerable to damage from earthquake-induced differential settlement. These differential settlements are often localized due to the rigidity of the abutment wall, and the difficulty in manipulating large compactors near walls.

Although approach-fill settlement does not typically result in extensive repair costs and durations, it has been the most commonly occurring type of highway-system damage during recent earthquakes in the United States. Therefore, default models for estimating approach-fill settlements and corresponding damage states, traffic states, and repair costs have been included in REDARS™ 2.

H.1.1 Estimation of Approach-Fill Settlement

This procedure for modeling earthquake-induced settlement of bridge approach fills is based on the Youd (2002) model for dry soils. This settlement is computed separately for each earthquake scenario and simulation, once the magnitude and location of the earthquake are specified and the level of ground shaking is estimated throughout the system.

H.1.1.1 Input Data

Two sets of input data are required to estimate approach-fill settlement. These consist of bridge-dependent data and earthquake- and simulation-dependent data.

H.1.1.1.1 Bridge-Dependent Data

The bridge-dependent data needed to estimate approach-fill settlement consist of: (a) the bridge number and location within the highway system; (b) the relative compaction of the approach fill soils (standard Procter density) (RC); and (c) the maximum thickness of the approach fill (T_{AF}).

The bridge number and location are specified as part of the input provided by the Import Wizard (see Chapter 5 and Appendix C). Also, in the absence of actual RC and T_{AF} data at a bridge site, the following default values of these parameters are included in REDARS™ 2: (a) RC = 95%; and (b) T_{AF} = 12 ft. (see Figure H-1). These default values for any bridge in the system can be overridden by REDARS™ 2 users.

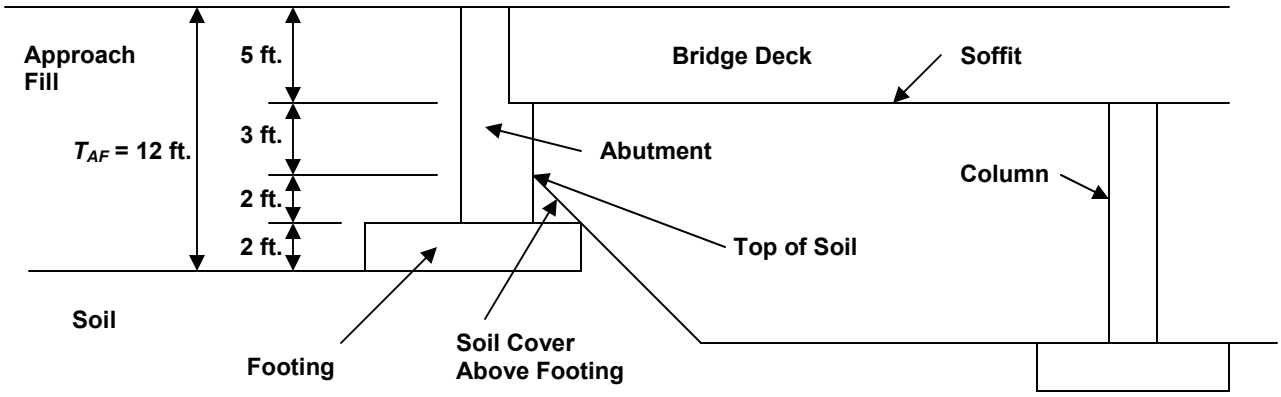

Figure H-1. Estimation of Default Value of Approach-Fill Thickness

H.1.1.1.2 Earthquake- and Simulation-Dependent Data

The earthquake- and simulation-dependent data needed to compute approach-fill settlement are: (a) the moment magnitude of the earthquake scenario (M_w); and (b) the peak ground acceleration at the bridge site (PGA). The moment magnitude is obtained from the earthquake-scenario designation, and the PGA is computed for each earthquake scenario and simulation, using the REDARS™ 2 ground motion model that the user had selected for this analysis (see Appendix D).

H.1.1.2 Evaluation Procedure

The evaluation of approach-fill settlement for each bridge, earthquake scenario, and simulation consists of the following steps:

- For the M_w of the earthquake scenario, the site-specific PGA for the earthquake and simulation, and the RC of the approach fills, use Table H-1 to estimate the volumetric strain of the approach fill materials (ε_{AF}) .

- Compute the total settlement of the approach fill (S_{AF}) as:

$$S_{AF} = \varepsilon_{AF} T_{AF} \qquad \text{(H-1)}$$

H.1.2 Damage States, Repair Costs, and Traffic States

This section describes the REDARS™ 2 default model for estimation of repair costs and downtimes due to earthquake-induced approach-fill settlement. This default model was developed from collaboration with and recommendations by senior members of the Caltrans engineering staff. Therefore, the model is applicable to approach-fill construction and repair practices in California only. Since these practices may differ in other regions of the country where REDARS™ 2 may be applied, this default model may require modification by users from these other regions to reflect any differences in these practices.

Table H-1. Best-Estimate Value of Maximum Volumetric Strain in Dry Soil due to Seismic Shaking (Youd, 2002)

Earthquake scenario and Simulation Data		Volumetric Strain (%)		
Earthquake Magnitude (M_w)	Peak Ground Acceleration (PGA), (g)*	Loose Fill (RC < 90%)	Moderately Dense Fill (90% ≤ RC < 95%)	Dense Fill (RC ≥ 95%)
$M_w \geq 7.0$	PGA ≥ 0.4 g	10%	5%	1%
	0.2 g < PGA < 0.4 g	5%	2%	0.5%
	0.1 g < PGA ≤ 0.2 g	2%	0.5%	0.1%
$5.0 < M_w < 7.0$	PGA ≥ 0.4 g	6%	3%	0.5%
	0.2 g < PGA < 0.4 g	2%	1%	0.2%
	0.1 g < PGA ≤ 0.2 g	1%	0.2%	0.05%
Mw ≤ 5.0	PGA ≥ 0.4 g	3%	1%	0.2%
	0.2 g < PGA < 0.4 g	1%	0.2%	0.05%
	0.1 g < PGA ≤ 0.2 g	0.5%	0.1%	0.01%

* In REDARS™ 2, it is assumed that no approach-fill settlement will occur if PGA < 0.1 g.

H.1.2.1 Approach Slab Configuration and Design

California approach slabs consist of a 30-ft. long by 1-ft. thick reinforced concrete slab that is underlain by a 6-inch thick permeable base. Soils beneath the concrete slab and permeable base consist of granular fills that are compacted to 95% Procter density.

In California, the reinforced concrete approach slab is designed to function as a simply-supported bridge. Therefore, if part of the underlying soil settles away from the slab and creates a void, the slab will still be able to function structurally and support traffic loads. Because of this, all bridges along lifeline routes in California have approach slabs.

H.1.2.2 Replacement Costs

In REDARS™ 2, all component repair costs are specified as multiples of the replacement cost. For approach fills, this replacement cost is estimated from the following assumptions:

- The cost to replace an approach slab in California is about $13,000/lane (where a lane is typically 12 ft. wide.) This would involve removing the existing slab, constructing a paving notch (if needed), leveling the subgrade with aggregate base, constructing the new slab, and replacing the joint seal. Since this work would be carried out under an emergency contract rather than a formal bid, these costs include appropriate markups for CCO. Costs for mobilization (usually about 10 percent) or contingencies are excluded from this estimate.

- If an approach slab were sufficiently damaged to require replacement, it is probable that the underlying fills will require some compaction and new fills would need to be added. Unit costs for this fill compaction/addition are estimated to be about $\$100/m^3$. If it is conservatively assumed that the total volume of fill to be compacted/added for each highway lane will be equal to the total slab length (30-ft.) x the lane width (12-ft) x the approach-fill settlement, this cost is about $1,000/lane/(ft. of approach-fill settlement). For a bridge that has settled 1.5-ft. (which is an upper-bound settlement for soils with a 95% compaction), this works out to be about $1,500/lane. Thus, the total cost to replace the approach slab and to add/compact the underlying fill is assumed to be $14,500/lane. For a 30-ft approach slab and a 12-ft. lane, this turns out to be about $\$434/m^2$.

H.1.2.3 Repair Costs

In this model, repairs are defined for three different levels of approach-fill settlement: (a) more than 0.5 ft. (6 in.); (b) between 0.083 ft. (1 in.) and 0.5 ft. (6 in.), and (c) less than 0.083 ft. (1 in.). It is noted that none of these levels of settlement are considered to lead to replacement of the approach slab. This is because, as noted above, the approach slabs are designed to bridge over settled fills and continue to accommodate traffic loads.

- If an approach slab has settled more than 0.5 ft., temporary repairs would involve building up an asphalt-concrete (AC) ramp. Under emergency conditions, this will require total closure of the bridge for about 4 days, after which full traffic can be accommodated. The total unit cost to repair the 1-ft. thick structural slab and the underlying 0.5-ft. thick permeable base will be $\$600/m^3$ and $\$350/m^3$ respectively. This works out to be $6,117/lane for repair of the structural slab and $1,784/lane for repair of the underlying base, which amounts to a total cost of about $7,900/lane, or about 0.55 x the above unit replacement cost,

- If an approach slab has settled less than about 0.5-ft. but more than about 0.083 ft., repairs will consist of mud jacking (coring holes and pumping in grout) and then ramping up with AC. Repair costs for this process will be about $\$50/m^2$ which, for a 30-ft long approach slab and a 12-ft. lane width, works out to be about $1,700/lane, or about 0.12 x the above unit replacement cost.

- REDARS™ 2 uses the following algorithm to estimate a default number of approach fills for any given bridge, as a function of the number of bridge elements and highway elements immediately adjacent to the bridge in the highway system model:
  - If the elements on both sides of the bridge are highways, the bridge is assumed to have two approach fills -- one at each end of the bridge.
  - In REDARS™ 2, an elevated viaduct of extended length will be modeled as a series of bridges connected end to end. For a bridge in this series that is connected to a highway element on one side and to a bridge element on the other side, the bridge is assumed to have one approach fill only. For a bridge in this series that is connected to a bridge element on both sides, the bridge is assumed to have no approach fills.

H.1.2.4 Default Repair Model

Based on the above assumptions, the REDARS™ 2 default repair model for approach fills is shown in Table H-2. This table provides repair procedures, post-earthquake traffic states, and repair costs as a function of approach-fill settlement.

Table H-2. Post-Earthquake Traffic States and Repair Costs due to Approach-Fill settlement

Damage State		Repair Procedure	Traffic State		Repair Cost (fraction of replacement cost)*
REDARS™ Designation	Approach-Fill Settlement, in.		Day after EQ	Traffic Capacity (fraction of Pre-EQ Capacity)	
1	≤ 0.083 ft. (1.0 in.)	No repairs needed.	0	1.00	0.00
2	between 0.083 ft. (1.0 in.) and 0.5 ft. (6.0 in.)	Closed for 1 day for during inspection and mobilization. Repair consists of mud jacking (coring holes and pumping in grout) and then ramping up with A/C. Repairs during off hours.	0-1 days > 1 day	0.00 1.00	0.12
3	≥ 0.5 ft. (6.0 in.)	Closed for one day for inspection and mobilization. Temporary repairs involve building up an A/C ramp, and will require closure of bridge for additional three days. Subsequent permanent repairs done during off hours. (Assuming only small-moderate settlement and no fault rupture.)	0-4 days ≥ 5 days	0.00 1.00	0.55

*Replacement Cost assumed to be $14,500/lane which, for an approach that is 30 ft. long and has lanes that are 12 ft. wide, works out to be about $434/m^2.

H.2 HIGHWAY PAVEMENTS

H.2.1 Model Basis and Assumptions

The REDARS™ 2 default model for highway pavements is based on the judgment and recommendations of senior Caltrans staff members who are familiar with pavement construction, maintenance, and repair practice in California. This should be regarded as a first-order model that may be upgraded in the future, as further experience and data regarding the seismic performance of pavements are developed. The model does not differentiate between concrete and asphalt pavements.

This default model will characterize the seismic performance and associated repair costs and post-earthquake traffic states for pavements. Since it is a default model, it can be readily modified by REDARS™ 2 users. In particular, since this model is based on pavement construction and repair practices in California, it may not apply to pavements in other regions of the country where construction and repair procedures and resources may differ from those in California. REDARS™ 2 users from these other regions should modify this default model as needed to best reflect their particular construction and repair practices.

H.2.2 Use of Model in REDARS™ 2

For a given earthquake scenario and simulation being analyzed, REDARS™ 2 will estimate the PGD along each highway link within the highway system that is located in potentially liquefiable soils or in the zone of deformation of the causative fault. Then, for each of these links, the model described in this appendix will be used to estimate the level of damage due to this PGD, and the link's associated repair cost, duration, and traffic state (ability of the link to accommodate partial or full traffic as the repairs are proceeding). If a highway pavement is not located within the rupture zone for the causative fault and is not sited on potentially liquefiable soils, REDARS™ 2 will not compute PGD hazards or estimate PGD-induced pavement damage states and repair requirements.

With this as background, this default highway-pavement repair model is shown in Table H-3. The assumed highway-pavement damage states on which this repair model is based are further illustrated in Figures H-2 through H-5.

Table H-3. Default Earthquake Repair Model for Highway Pavements and Subsurface Materials

Damage State				Traffic State		Repair Costs (per lane-mile)
REDARS™ Designation	Perm. Ground Displacement, inches.	Description (see Figures 1 through 4)	Repair Procedure	Days after EQ (incl. mobilization time)	Lanes Available (% of Pre-EQ lanes)	
1 (None)	< 1 in.	No repairs needed	None	0	100%	$0
2 (Slight)	≤ 1 in and <3 in.	Slight cracking/ movement. No interruption of traffic.	Horizontal Displacement: crack/seal. Vertical Displace: mill and patch.	0	100%	$50,000 (=0.083*RC)
3 (Moderate)	≤ 3 in and <6 in.	Localized moderate cracking/ movement. Reduced structural integrity of pavement surface.	No repair needed for subbase. If asphalt pavement, or if damage to concrete pavement extends over long length, use AC overlay. If damage to concrete pavement is localized, replace concrete slab.	0-3 days ≥ 4 days	0% 100%	$100,000 (=0.167*RC)
4 (Extensive)	≤ 6 in and <12 in.	Failure of pavement structure, requiring replacement. Movement but not failure of subsurface soils.	Rebuild pavement structure and subbase. Provide soil improvement for subsurface materials.	0-7 days ≥8 days	0% 100%	$300,000 (=0.500*RC)
5 (Irreparable)	≥ 12 in.	Failure of pavement structure and subsurface soils.	Remove and replace existing pavement structure and subsurface materials.	0 – 49 days ≥ 50 days	0% 100%	$600,000 (=RC)

Figure H-2. Examples of Highway Pavement Damage State 2
(Description: No closure to traffic. Minor repairs can be carried out during off hours)

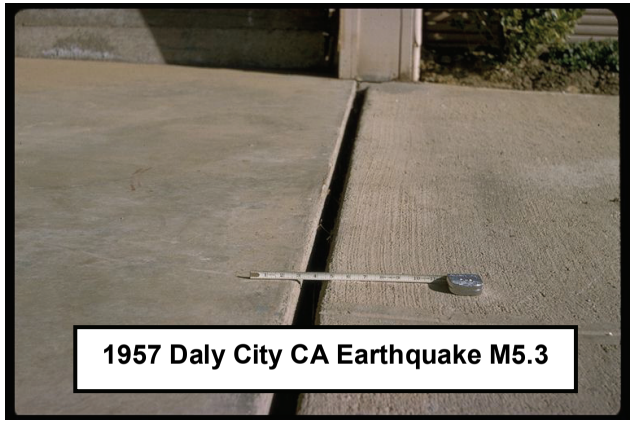

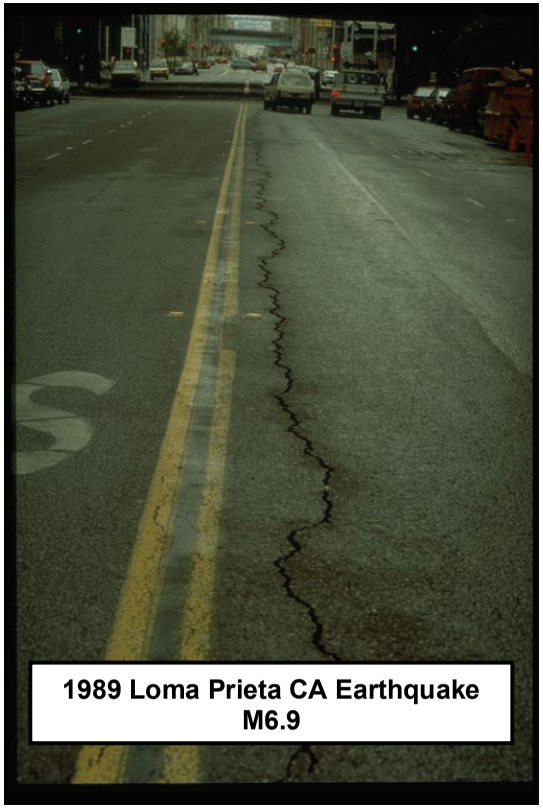

All photographs courtesy of Earthquake Engineering Research Center Library, University of California at Berkeley, Richmond CA.

Figure H-3. Examples of Highway Pavement Damage State 3
(Description: Closure to Traffic for 2-3 Days for Repair of Moderate Pavement Damage. No Subbase Damage)

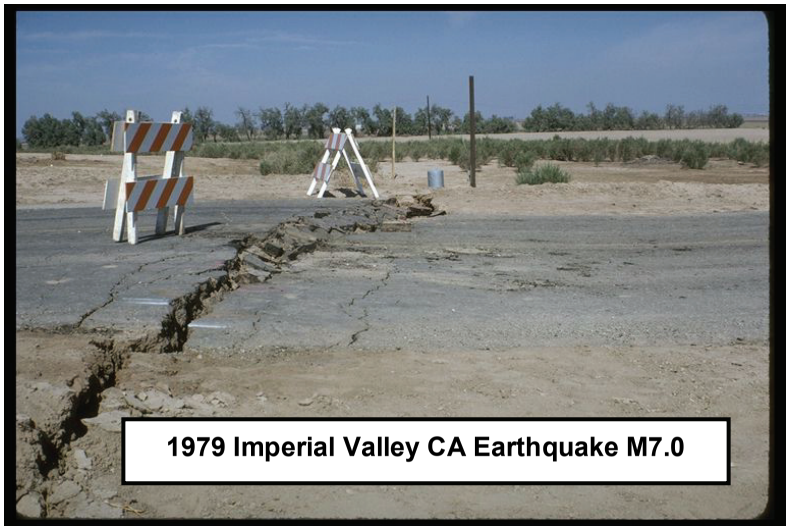

All photographs courtesy of Earthquake Engineering Research Center Library, University of California at Berkeley, Richmond CA.

Figure H-4. Examples of Highway Pavement Damage State 4
(Description: Pavement Structure has Failed (must be Rebuilt) and Soils have Deformed (Closure for 7 Days)

All photographs courtesy of Earthquake Engineering Research Center Library, University of California at Berkeley, Richmond CA.

Figure H-5. Examples of Highway Pavement Damage State 5
(Description: Total Failure Requiring Reconstruction of Pavement and Underlying Soils (Closure for 7 Weeks)

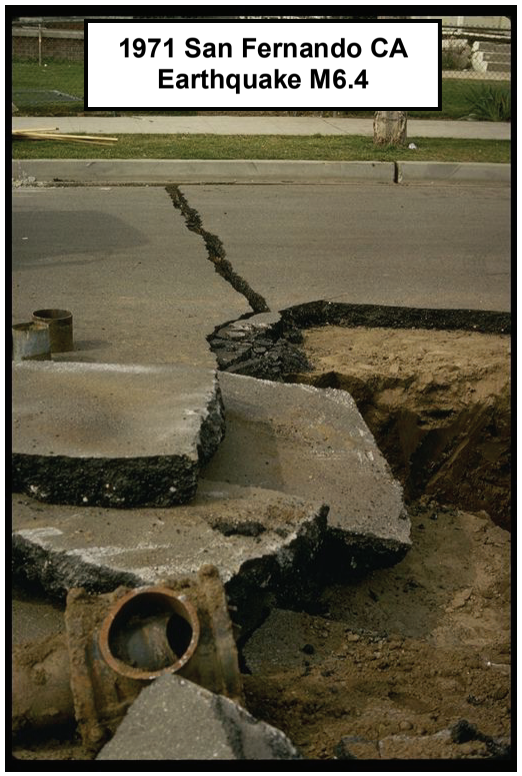

All photographs courtesy of Earthquake Engineering Research Center Library, University of California at Berkeley, Richmond CA.

APPENDIX I
IMPLEMENTATION OF POST-EARTHQUAKE TRIP REDUCTION AND UPDATED MINIMUM-PATH ALGORITHM IN NETWORK-ANALYSIS PROCEDURE

1.1 USER-EQUILIBRIUM MODEL WITH FIXED TRIP DEMANDS

Modern transportation network models are based on the Wardrop's rules of network equilibrium (Wardrop, 1952, recited from Sheffi 1985). According to these rules, the travel times along the *used* paths in a network are shorter than the travel times along the *unused* path and, in addition, individual drivers can not improve their driving time by altering their route. Thus, "user-equilibrium models" are models that estimate travel time and link volumes according to these Wardrop's rules. Based on the conceptual developments of Beckmann, et al. (1956), Frank-Wolfe (1956) developed an efficient user-equilibrium solution algorithm that could be applied to a large-scale transportation network.

To illustrate, a simple transportation network is used here to derive the mathematical formulation of network equilibrium. In this, a total of T drivers will travel from Zone 1 to Zone 2 along Paths 1 and 2, as shown in Figure I-1a. In Figure I-1b, x_i, and t_i represent the traffic volume and travel time respectively along Path i.

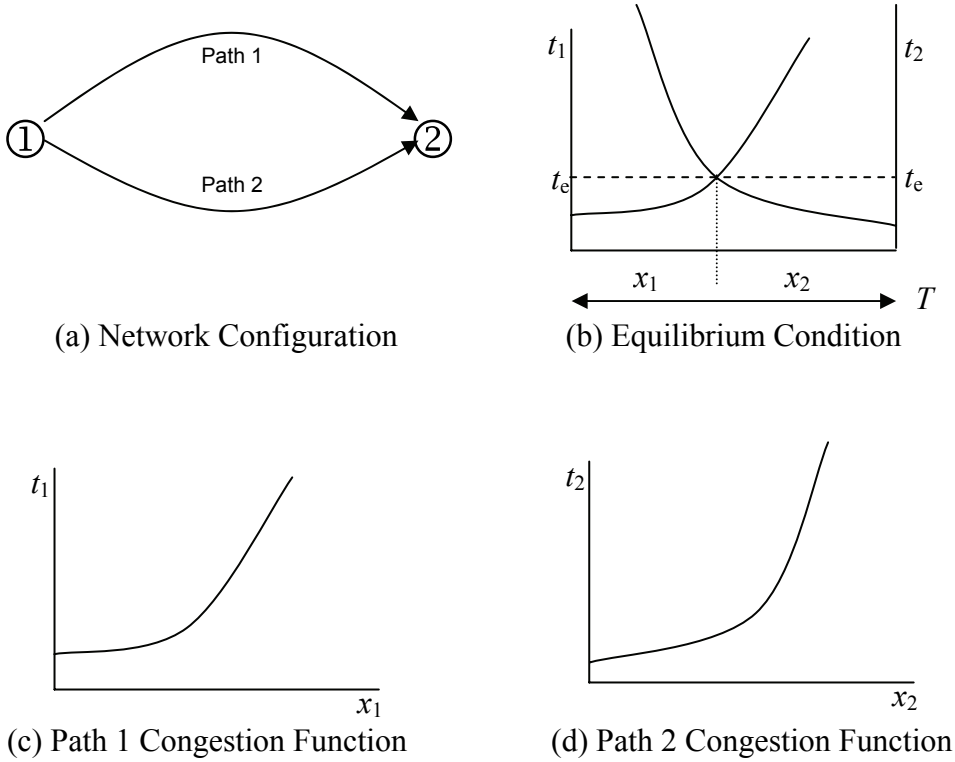

(a) Network Configuration (b) Equilibrium Condition

(c) Path 1 Congestion Function (d) Path 2 Congestion Function

Figure I-1. Simple Network for Demonstration of User-Equilibrium Condition

To represent congestion, the travel time t_i is represented as a convex function of traffic volume. The resulting congestion functions for Path 1 and 2 are shown graphically in Figures I-1c and I-1d. At equilibrium, the travel time along both paths should be identical. This is shown in Figure I-1b, in which the total number of drivers, T is divided into traffic volumes, x_1 and x_2, according to the equilibrium travel time, t_e. Many researchers have proven that the area beneath these two congestion functions is minimized for a given travel demand T, when the trips are divided in such a way that the travel times on Path 1 and 2 are identical. From this, the user-equilibrium network model has following mathematical form:

$$\max\ z(\mathbf{x}) = \sum_a \int_0^{x_a} t_a(w)\ \ dw \tag{I-1}$$

subject to

$$\sum_k f_k^{rs} = q_{rs} \qquad \forall r,s \tag{I-2}$$

$$f_k^{rs} \geq 0 \qquad \forall k, r, s \tag{I-3}$$

$$q_{rs} \geq 0 \qquad \forall r,s \tag{I-4}$$

$$x_a = \sum_{rs}\sum_k f_k^{rs} \cdot \delta_{a,k}^{rs} \quad \forall a \tag{I-5}$$

where

t_a : link performance function of link a.

f_k^{rs} flow on path k connecting OD pair r-s.

q_{rs}: travel demand between OD pair r-s.

x_a : flow on link a.

$\delta_{a,k}^{rs}$ 1 if link a is on path k between OD pair r-s, otherwise 0.

I.2 FORMULATION AND SOLUTION STEPS FOR VARIABLE-DEMAND MODEL

Going beyond the user-equilibrium model with fixed trip demands, the variable-demand model was developed to estimate link volumes, link travel times, and travel demands that satisfy the equilibrium condition. At equilibrium, the travel time on all used paths between any origin-destination zone pair are equal, and are less than the travel times on any unused paths. In addition, trip rates between an origin and destination are consistent with travel time, as calculated by a given demand function. These conditions define the user-equilibrium model with variable demand, whose mathematical form is as follows:

$$\max\ z(\mathbf{x},\mathbf{q}) = \sum_a \int_0^{x_a} t_a(w)\ \ dw - \sum_{rs} \int_0^{q_{rs}} D_{rs}^{-1}(w)\ \ dw \tag{I-7}$$

subject to

$$\sum_k f_k^{rs} = q_{rs} \qquad \forall r,s \qquad \text{(I-8)}$$

$$f_k^{rs} \geq 0 \qquad \forall k, r, s \qquad \text{(I-9)}$$

$$q_{rs} \geq 0 \qquad \forall r,s \qquad \text{(I-10)}$$

$$q_{rs} = D_{rs}(u_{rs}) \qquad \forall r,s \qquad \text{(I-11)}$$

$$x_a = \sum_{rs}\sum_k f_k^{rs} \cdot \delta_{a,k}^{rs} \qquad \forall a \qquad \text{(I-12)}$$

where

t_a : link performance function of link *a*.

D : demand function.

D^{-1}: inverse of demand function.

f_k^{rs} : flow on path *k* connecting OD pair *r*-*s*.

q_{rs}: trip rate between OD pair *r*-*s*.

u_{rs}: travel time between OD pair *r*-*s*.

x_a : flow on link *a*.

$\delta_{a,k}^{rs}$: 1 if link a is on path *k* between OD pair *r*-*s*, otherwise 0.

The first term on right-hand side of Equation I-7 represents link volumes and travel times that satisfy the user-equilibrium model. The second term adjusts the travel-demand rates between zone-pairs such that the loaded travel demand on the network is consistent with its travel time.

Evans (1976) and Florian et al (1976) separately used the secant method to develop the algorithm to solve the above system of equations. This algorithm is basically identical to the algorithm used to represent the conditions of the user-equilibrium model for fixed travel demands, except that it includes the additional step of finding an auxiliary trip rate in Step 2.

Step 0: Initialization.

Find an initial feasible flow pattern $\{x_a^n\}$, $\{q_{rs}^n\}$. Set *n*:=1.

Step 1: Update Link Travel Time and Time Associated with Trip Making

Set $t_a^n = t_a(x_a^n) \; \forall a$; compute $D_{rs}^{-1}(q_{rs}^n) \; \forall r,s$.

Step 2: Find Auxiliary Link Volume and Trip Rate

Compute the shortest path, *m*, between each O-D pair *r*-*s* based on link travel time $\{t_a^n\}$, $c_m^{rs^n} = \min_{\forall k}\{c_k^{rs^n}(t_a^n)\}$

Find auxiliary trip rate

If $c_m^{rs^n} < D_{rs}^{-1}(q_{rs}^n)$, set $g_m^{rs^n} = \overline{q_{rs}}$ where *m* is shortest path, and $\overline{q_{rs}}$ is upper bound of trip rate

If $c_m^{rs^n} > D_{rs}^{-1}\left(q_{rs}^n\right)$, set $g_k^{rs^n} = 0 \ \forall k$

If $\left| c_m^{rs^n} - D_{rs}^{-1}\left(q_{rs}^n\right)\right| < \varepsilon$, set $g_m^{rs^n} = g_m^{rs^{n-1}}$

Auxiliary link volume $y_a^n = \sum_{rs}\sum_k g_k^{rs^n} \cdot \delta_{a,k}^{rs} \ \forall a$

Auxiliary trip rate $v_{rs}^n = \sum_k g_k^{rs^n} \ \forall r,s$

Step 3: Find Best Moving Step

Solve following system for α.

$$\min z(\alpha) \sum_a \int_0^{x_a^n + \alpha\left(y_a^n - x_a^n\right)} t_a(w)dw \ - \sum_{rs} \int_0^{q_{rs}^n + \alpha\left(v_{rs}^n - q_{rs}^n\right)} D_{rs}^{-1}(w)dw$$

subject to $0 \le \alpha \le 1$

Step 4: Flow Update

$$x_a^{n+1} = x_a^n + \alpha_n\left(y_a^n - x_a^n\right)$$

$$q_{rs}^{n+1} = q_{rs}^n + \alpha_n\left(v_{rs}^n - q_{rs}^n\right)$$

Step 5: Convergence Test

If following inequality holds for very small κ, terminate. Otherwise, set n:=n+1 and go to Step 1.

$$\sum_{rs} \frac{\left| D_{rs}^{-1}\left(q_{rs}^n\right) - u_{rs}^n \right|}{u_{rs}^n} + \sum_{rs} \frac{\left| u_{rs}^n - u_{rs}^{n-1} \right|}{u_{rs}^n} \le \kappa$$

I.3 ECONOMIC LOSS DUE TO EARTHQUAKE DAMAGE TO HIGHWAY SYSTEM

Earthquake damaged transportation systems experience increased congestion and reduced trips. To represent the effects of increasing congestion, the difference between total travel times spent by drivers under pre- and post earthquake conditions, λ is calculated from Equation (I-13). In this, computation of the total travel time in the congested system is based on links (Equation I-13 a) as well as zone-pairs (Equation I-13b). The zone-to-zone travel time, c_{ij}, is computed as the sum of link travel times along the route between the zone pair. Again, under conditions of equilibrium, all routes between a zone-pair should have an identical travel time.

$$\lambda = \sum_a x'_a \, t'_a(x'_a) - \sum_a x_a t_a(x_a) \qquad \text{(I-13a)}$$

$$= \sum_i \sum_j \left(q_{ij} \cdot c_{ij} - q'_{ij} \cdot c'_{ij}\right) \qquad \text{(I-13b)}$$

where

x_a : volume on link a in intact network (pre-earthquake)

t_a : travel time on link *a* in intact network (pre-earthquake)

x'_a : volume on link *a* in damaged network (post-earthquake)

t'_a : travel time on link *a* in damaged network (post-earthquake)

q_{ij} : trips from zone *i* to zone *j* in intact network (pre-earthquake)

c_{ij} : travel time zone *i* to zone *j* in intact network (pre-earthquake)

q'_{ij} : trips from zone *i* to zone *j* in damaged network (post-earthquake)

c'_{ij} : travel time zone *i* to zone *j* in damaged network (post-earthquake)

The calculation of economic loss due to forgone trips, φ is

$$\varphi = \sum_i \sum_i \left(\int_{c_{ij}}^{c'_{ij}} D(w)\, dw \right) - \lambda \tag{I-14}$$

where

c_{ij} : travel time zone i to zone j in intact network (pre-earthquake)

c'_{ij} : travel time zone i to zone j in damaged network (post-earthquake)

D : the demand function, $q_{ij} = D(c_{ij})$, $q'_{ij} = D(c'_{ij})$

I.4 SAMPLE CALIBRATION OF DEMAND FUNCTION

Travel demand is endogenous in the VDM, and modeled by demand functions. In the following exercise, the demand function is based on Equation I-15. The number of trips between two zones is proportional to the total trips generated from the origin O_r, and total trips reaching the destination D_s. On the other hand, the trips are inversely related to the travel time, c_{rs}. This logic is similar to the gravity model, in which the interaction between two objects is proportional to the mass and inverse to the distance squared. Because of this similarity, the demand function is also called the gravity model.

$$q_{rs} = \frac{O_r \cdot D_s \cdot A_r \cdot B_s}{1 + \exp(\alpha + \beta \cdot c_{rs})} \tag{I-15}$$

where

q_{rs}: trip rate between OD pair *r*-*s*.

c_{rs}: travel time between OD pair *r*-*s*.

O_r: trip production from origin zone *r*.

D_s: trip attraction to destination zone *s*.

A_r: coefficient to be estimated associated with origin zone *r*.

B_s: coefficient to be estimated associated with destination zone *s*.

α, β: model parameters to be estimated.

In the VDM, the demand function is bounded by a maximum value of $O_r \cdot D_s \cdot A_r \cdot B_s$. Even in cases where the travel time is close to zero, the trips estimated by the function is limited to this value.

Since the parameters α and β in Equation I-15 were not given, they were estimated by devising an iterative process. With an origin-destination (O-D) trip requirement matrix (q_{rs}) the user-equilibrium model estimated zone-to-zone travel time (u_{rs}), and an econometric model estimated α and β from O-D trip requirements and zone-to-zone travel times. For these travel times and estimated parameters α and β, the gravity model was used to estimate zonal coefficients (A_r, B_s). Once all unknowns were estimated, a new O-D trip requirement matrix (q_{rs}) was re-generated. These steps were repeated until the estimated parameters α and β were unchanged over successive iterations. Table I-1 shows α, β values at the end of each iteration, in which the last set of values was applied in the analysis.

Table I-1: Calibration of the Demand Function Parameters

Iteration	α	β	R^2 to MTC OD
1	2.452310	0.088682	0.71769
2	2.543508	0.081813	0.69403
3	2.537076	0.082275	0.69594
4	2.538349	0.082190	0.69564
5	2.538382	0.082190	0.69564
6	2.538378	0.082191	0.69564
7	2.538379	0.082193	0.69565
8	2.538371	0.082192	0.69565

I.5: NUMERICAL EXAMPLE OF VARIABLE-DEMAND MODEL

This section describes an application of the variable-demand model to a small synthetic transportation system. Its small size on this system enables display of calculation results in every step and for all variables. Results from this example are used to estimate social cost.

I.5.1 Base Data for Variable-Demand Model

The transportation system in this example (Figure I-1) includes five links, labeled by L_a, and four traffic zones, Z_r. In this, the link L_2 is used by all three zone pairs in the system. Travel between zones Z_1 and Z_4 can occur along routes through L_1, and L_4+ L_2. For travel between zones Z_2 and Z_4, only link L_4 is used. $t_i(x)$ represents the congestion function for Link, L_a, which defines travel time for given traffic volumes along each link. The following function is used for this purpose, along with assumed traffic capacities and free-flow travel times.

$$t_1(x) = 10 \cdot \left(1 + 0.15 \cdot \left[\frac{x}{8}\right]^4\right), \quad t_2(x) = 7 \cdot \left(1 + 0.15 \cdot \left[\frac{x}{12}\right]^4\right), \quad t_3(x) = 9 \cdot \left(1 + 0.15 \cdot \left[\frac{x}{6}\right]^4\right),$$

$$t_4(x) = 4 \cdot \left(1 + 0.15 \cdot \left[\frac{x}{3}\right]^4\right), \quad t_5(x) = 4 \cdot \left(1 + 0.15 \cdot \left[\frac{x}{3}\right]^4\right)$$

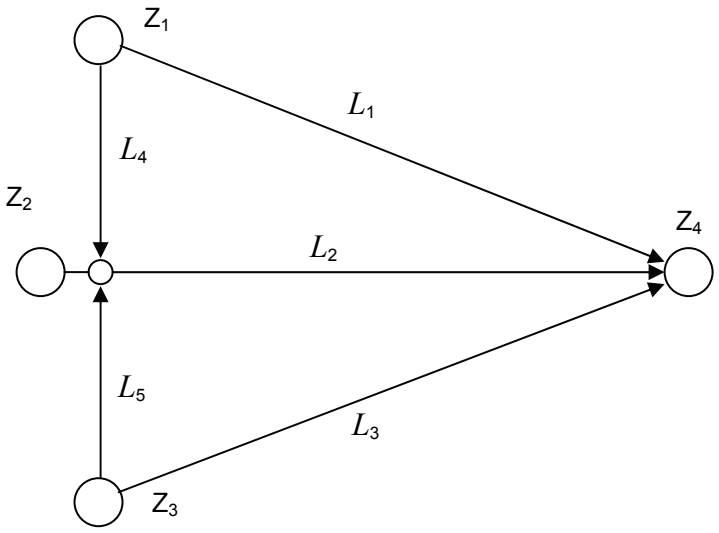

Figure I.2. Network Configuration for Numerical Example

Two types of travel demands originate from Zones Z_1, Z_2, and Z_3 and have zone Z_4 as their destination. Travel demand is modeled by the following demand functions D_{pq}^k, for each zone-pair. These functions are a simplified form of the demand function shown by Equation I-15. In REDARS™ 2, the parameters are calibrated by the Import Wizard, while this example assumes that the negative exponential function characterizes the decreasing demand over increasing travel time.

$$D_{14}^1 = 36.0 \cdot \exp(0.3 - 0.1 \cdot t_{14}) \qquad D_{14}^2 = 9.8 \cdot \exp(0.002 - 0.05 \cdot t_{14})$$
$$D_{24}^1 = 14.4 \cdot \exp(0.3 - 0.1 \cdot t_{24}) \qquad D_{24}^2 = 6.0 \cdot \exp(0.002 - 0.05 \cdot t_{24})$$
$$D_{34}^1 = 18.0 \cdot \exp(0.3 - 0.1 \cdot t_{34}) \qquad D_{34}^2 = 14.0 \cdot \exp(0.002 - 0.05 \cdot t_{34})$$

Note that the coefficients in the exponent are unique by trip types because those are usually calibrated for each OD matrix against travel time.

Maximum demand, $\bar{q}_{rs}$ is required in to calculate auxiliary demand, and is assumed as follows:

$$\bar{q}_{14}^1 = 20, \quad \bar{q}_{24}^1 = 9, \quad \bar{q}_{34}^1 = 12$$
$$\bar{q}_{14}^2 = 7, \quad \bar{q}_{24}^2 = 4, \quad \bar{q}_{34}^1 = 10$$

I.5.2 Solution Steps for the Variable-Demand Model

Based on this input data, detailed calculation steps from the first three iterations (0 to 2) are provided as follows.

Iteration 0

Step 0: Initialization

In the initial stage, all the link volumes and demands are assumed to be zero

	L_1	L_2	L_3	L_4	L_5
Volume, x_a	0.00	0.00	0.00	0.00	0.00

		Z_{14}	Z_{24}	Z_{34}
Demand, q_{rs}	Trip Type1	0.00	0.00	0.00
	Trip Type2	0.00	0.00	0.00

Step 1: Update Link Travel Time

This step applies the assumed link traffic volume (0 in Iteration 0) to the congestion function, in order to calculate link travel times (which in this case is the free-flow travel time)

	L_1	L_2	L_3	L_4	L_5
Time, $t_a^n = t_a\left(x_a^n\right)$	10.00	7.00	9.00	4.00	4.00

Step 2: Auxiliary Demand

The auxiliary demand is calculated by comparing the travel time along the shortest path, to the inverse of demand function, D^{-1}, which estimates corresponding travel time to the demand estimated from previous iteration. If the shortest travel time is less than the time from the inverse of the demand function, the auxiliary demand is set equal to the maximum demand, $\overline{q}_{rs}$. Otherwise it will be zero.

In Iteration 0, the demand is 0 and, as a result, the inverse of demand function results in an infinite time unit. Therefore, all auxiliary demands are equal to the maximum demand.

		Z_{14}	Z_{24}	Z_{34}
Time on shortest path $c_m^{rs^n} = \min_{\forall k}\left\{c_k^{rs^n}\left(t_a^n\right)\right\}$		10.00	7.00	9.00
D^{-1}	Trip Type1	∞	∞	∞
	Trip Type2	∞	∞	∞
Auxiliary Demand, v_{rs}	Trip Type1	20.00	9.00	12.00
	Trip Type2	7.00	4.00	10.00

Step 3: Auxiliary Link Volume

Auxiliary link volume is obtained by loading the auxiliary demand on to the current shortest path.

	L_1	L_2	L_3	L_4	L_5
Auxiliary volume, y_a	27.00	13.00	22.00	0.00	0.00

Step 4: Best Moving Step

The best moving step is calculated by solving the following one-dimensional optimization problem with respect to α.

$$\min z(\alpha) = \sum_a \int_0^{x_a^n + \alpha\left(y_a^n - x_a^n\right)} t_a(w)dw \; - \sum_{rs} \int_0^{q_{rs}^n + \alpha\left(v_{rs}^n - q_{rs}^n\right)} D_{rs}^{-1}(w)dw$$

However, for Iteration 0, α=1 is used to replace the assumed 0 demand, and 0 link volumes with the auxiliary demand and volumes.

Step 5: Update Flow

Since α=1 in Iteration 0, the updating is actually replacing the 0 demand, and 0 link volumes with the auxiliary demand and volumes.

		Z_{14}	Z_{24}	Z_{34}
Demand, q_{rs}	Trip Type1	20.00	9.00	12.00
	Trip Type2	7.00	4.00	10.00

	L_1	L_2	L_3	L_4	L_5
Link Volume, x_a	27.00	13.00	22.00	0.00	0.00

Iteration 1

Step 1: Update Link Travel Time

As non-zero link volumes are estimated from Iteration 0, travel times through the used links are very high.

	L_1	L_2	L_3	L_4	L_5
Time, $t_a^n = t_a\left(x_a^n\right)$	204.62	8.45	253.02	4.00	4.00

Step 2: Auxiliary demand

At the end of the prior iteration, the demand is set equal to the auxiliary demand, which is the same as the maximum demand, $\overline{q}_{rs}$. Thus, the inverse of the demand function, D^{-1}, provides possible lowest time units. On the other hand, some part of network is already congested. In this case, no travel times along shortest paths are less than D^{-1}, so all of the auxiliary demand is zero.

		Z_{14}	Z_{24}	Z_{34}
Time on shortest path $c_m^{rs^n} = \min_{\forall k}\left\{c_k^{rs^n}\left(t_a^n\right)\right\}$		12.45	8.45	12.45
D^{-1}	Trip Type1	8.88	7.70	7.05
	Trip Type2	6.77	8.15	6.77
Auxiliary Demand, v_{rs}	Trip Type1	0.00	0.00	0.00
	Trip Type2	0.00	0.00	0.00

Step 3: Auxiliary link Volume

Loading the zero auxiliary demand onto the shortest path yields zero auxiliary link volumes.

	L_1	L_2	L_3	L_4	L_5
Auxiliary volume, y_a	0.00	0.00	0.00	0.00	0.00

Step 4: Best Moving Step

Solving the following optimization problem with respect to α yields α=0.5256.

$$\min z(\alpha) = \sum_a \int_0^{x_a^n + \alpha\left(y_a^n - x_a^n\right)} t_a(w)dw - \sum_{rs} \int_0^{q_{rs}^n + \alpha\left(v_{rs}^n - q_{rs}^n\right)} D_{rs}^{-1}(w)dw$$

Step 5: Update Flow

Linearly combining the previous demand and volume with the auxiliary estimations for which α=0.5256 yields the following results. Up to this iteration, some links are not yet used, since their free flow travel times are longer than the congested travel times along other routes.

		Z_{14}	Z_{24}	Z_{34}
Demand, q_{rs}	Trip Type1	9.49	4.27	5.69
	Trip Type2	3.32	1.90	4.74

	L_1	L_2	L_3	L_4	L_5
Link Volume, x_a	12.81	6.17	10.44	0	0

<u>Iteration 2</u>

Step 1: Update Link travel time

The high link travel time estimated at the beginning of Iteration 1 dissipates as demand and volume are adjusted

	L_1	L_2	L_3	L_4	L_5
Time, $t_a^n = t_a\left(x_a^n\right)$	19.86	7.07	21.36	4.00	4.00

Step 2: Auxiliary Demand

As the path time reaches equalization, the travel time along the shortest path is less than D^{-1}. So, once again, the maximum demand, $\overline{q}_{rs}$ corresponds to the auxiliary demand.

		Z_{14}	Z_{24}	Z_{34}
Time on shortest path $c_m^{rs^n} = \min_{\forall k}\left\{c_k^{rs^n}\left(t_a^n\right)\right\}$		11.07	7.07	11.07
D^{-1}	Trip Type1	16.33	15.16	14.51
	Trip Type2	21.68	23.06	21.68
Auxiliary Demand, v_{rs}	Trip Type1	20.00	9.00	12.00
	Trip Type2	7.00	4.00	10.00

Step 3: Auxiliary Link Volume

	L_1	L_2	L_3	L_4	L_5
Auxiliary volume, y_a	0.00	62.00	0.00	27.00	22.00

Step 4: Best Moving Step

Solving the following optimization problem with respect to α, yields α=0.1647.

$$\min z(\alpha) = \sum_a \int_0^{x_a^n + \alpha\left(y_a^n - x_a^n\right)} t_a(w)dw - \sum_{rs} \int_0^{q_{rs}^n + \alpha\left(v_{rs}^n - q_{rs}^n\right)} D_{rs}^{-1}(w)dw$$

Step 5: Update Flow

Eventually, all of the five links are used by the demand. However, comparisons of the alternative path travel times show that the model has not yet converged. For example, for zone-pair Z_1-Z_4, the travel time on path L_4+L_2 is about twice (19.81 minutes) the travel time along Link L_1 (10.70 minutes).

		Z_{14}	Z_{24}	Z_{34}
Demand, q_{rs}	Trip Type1	11.22	5.05	6.73
	Trip Type2	3.92	2.24	5.60

	L_1	L_2	L_3	L_4	L_5
Link Volume, x_a	10.70	15.36	8.72	4.45	3.62

Table I-2 and I-3 summarize the zone-to-zone trip rates (travel demand), and travel time on shortest path resulted at the end of each iteration respectively.

Table I-2. Trip Rates Estimated by Variable-Demand Model for the Numerical Example

Iteration	Demand, q_{rs}, Type 1			Demand, q_{rs}, Type 2			Travel Time on Shortest Path			Moving step
	Z_{14}	Z_{24}	Z_{34}	Z_{14}	Z_{24}	Z_{34}	Z_{14}	Z_{24}	Z_{34}	
1	9.49	4.27	5.69	3.32	1.90	4.74	12.45	8.45	12.45	0.5256
2	11.22	5.05	6.73	3.93	2.24	5.61	11.07	7.07	11.07	0.1647
3	9.15	5.78	5.49	4.49	2.57	6.42	14.80	9.82	15.02	0.1845
4	9.68	5.94	5.81	4.62	2.64	6.60	13.69	9.51	14.08	0.0489
5	10.10	6.06	5.57	4.71	2.69	6.73	15.07	10.24	14.48	0.0404
6	10.33	6.13	5.72	4.60	2.72	6.81	15.04	10.15	14.64	0.0234
7	9.99	6.22	5.54	4.45	2.77	6.58	15.83	10.48	15.51	0.0329
8	10.18	6.28	5.66	4.50	2.79	6.65	15.10	10.39	14.69	0.0192
9	10.28	6.30	5.60	4.52	2.80	6.58	15.47	10.34	15.40	0.0101
10	10.41	6.34	5.53	4.56	2.82	6.50	15.48	10.55	15.15	0.0131
11	10.08	6.42	5.36	4.41	2.85	6.61	15.90	10.51	14.84	0.0313
12	10.22	6.46	5.45	4.45	2.87	6.65	15.19	10.43	14.95	0.0140
13	10.29	6.48	5.41	4.47	2.88	6.61	15.54	10.39	15.19	0.0070
14	10.39	6.50	5.35	4.50	2.89	6.54	15.48	10.53	15.30	0.0107
15	10.27	6.53	5.43	4.44	2.90	6.58	15.83	10.50	15.03	0.0114
16	10.09	6.57	5.33	4.49	2.92	6.46	15.56	10.47	15.18	0.0174
17	10.19	6.60	5.40	4.51	2.93	6.50	15.42	10.42	15.03	0.0094
18	10.22	6.61	5.42	4.52	2.94	6.51	15.53	10.40	15.04	0.0035
19	10.12	6.63	5.37	4.48	2.95	6.54	15.64	10.54	15.23	0.0097
20	10.20	6.65	5.42	4.50	2.96	6.57	15.43	10.59	15.05	0.0084
30	10.23	6.71	5.33	4.50	3.03	6.57	15.62	10.64	15.18	0.0066

Table I-3. Link Volume and Time Estimated by Variable-Demand Model for the Numerical Example

Iteration	Link Travel Time					Link Volume				
	L_1	L_2	L_3	L_4	L_5	L_1	L_2	L_3	L_4	L_5
1	204.62	8.45	253.02	4.00	4.00	12.81	6.17	10.44	0.00	0.00
2	19.86	7.07	21.36	4.00	4.00	10.70	15.36	8.72	4.45	3.62
3	14.80	9.82	15.02	6.89	5.28	10.02	14.92	8.96	3.63	2.95
4	13.69	9.51	15.70	5.28	4.56	10.85	15.91	8.52	3.45	3.89
5	15.07	10.24	14.48	5.05	5.69	11.50	15.79	8.58	3.31	3.73
6	16.41	10.15	14.64	4.89	5.43	11.23	16.19	8.89	3.70	3.64
7	15.83	10.48	15.51	5.39	5.30	10.86	16.09	8.60	3.58	3.52
8	15.10	10.39	14.69	5.21	5.14	11.17	16.03	8.86	3.51	3.45
9	15.70	10.34	15.41	5.12	5.05	11.06	16.27	8.77	3.75	3.42
10	15.48	10.55	15.15	5.46	5.01	11.27	16.23	8.65	3.70	3.37
11	15.90	10.51	14.84	5.38	4.96	10.91	16.13	8.69	3.58	3.27
12	15.19	10.43	14.95	5.22	4.85	11.14	16.08	8.88	3.53	3.22
13	15.64	10.39	15.48	5.15	4.80	11.06	16.25	8.82	3.70	3.20
14	15.48	10.53	15.30	5.38	4.78	11.23	16.22	8.72	3.66	3.17
15	15.83	10.50	15.03	5.32	4.74	11.10	16.18	8.88	3.61	3.13
16	15.56	10.47	15.47	5.26	4.71	11.03	16.12	8.72	3.55	3.08
17	15.42	10.42	15.03	5.18	4.66	11.18	16.09	8.85	3.52	3.05
18	15.72	10.40	15.38	5.14	4.64	11.14	16.26	8.81	3.60	3.11
19	15.64	10.54	15.29	5.25	4.70	11.03	16.32	8.73	3.57	3.18
20	15.43	10.59	15.05	5.20	4.76	11.17	16.29	8.84	3.54	3.15
30	15.62	10.64	15.18	5.14	4.71	11.24	16.35	8.78	3.50	3.11

I.6 UPDATING THE MINIMUM-PATH ALGORITHM

I.6.1 Background

In transportation network analysis, the vector of traffic volume on each link is unknown, and thus, the algorithm keeps improving link-volume estimates, as described in Section I.2. In Step 2 of the algorithm, the model searches paths from each zone to all other zones.. The path-search algorithm is optimized by using "one-to-all tree building", instead of searching zone combinations one-by-one, in which the algorithm searches one path that connects one "root" zone to all other zones, as a pattern like the branches of a tree. The path-search algorithm is repeated for as many iterations as there are zones multiplied by the number of time intervals analyzed. Sheffi (1985) measured the running time of transportation analysis model, and concluded about 95% of the running time is involved in the path search.

I.6.2 Previously Implemented Minimum-Path Algorithm

The pseudo code of the previously implemented algorithm is presented in Figure I-3. Given the root, r, the algorithm identifies an set of nodes ordered ascending by travel time. In this set, a given node, b_i, is the node that precedes the node *i* on the path from the root, so that trips from the root always traverse node *bi*, to reach node *i*. Therefore, b_i is the "From-Node" link, while *i* is the "To-Node" of the link. For this relationship, b_i is called *back-node* of node *i*. Unless isolated from the network, all nodes should have only one *back-node* after the algorithm is terminated. Also, a node has only one *back-node*, otherwise a node can be reached from the root node via more than one path.

The algorithm consists of four major steps – (1) initialization , (2) identifying a set of nodes accessible from a hub node (called forward-star. see Figure I-4 and the description below), (3) examination of the travel time to the forward-star nodes, and (4) maintaining the set of hub node S.

In this algorithm, node *i* in Figure I-4 is a selected as the hub node. From the hub node, travel time from the root to the "To-Nodes" of links, *j* are examined to see if the hub is the *back node*. . If the sum of travel time to the hub node (from root, c_{ri}) and link travel time (t_{ij}) is less than the current travel cost to *j*, the hub is the *back node* of the "To-Node" (Figure I-5, left). However, if the "To-Node" *j* has a lower travel time, (via another hub) the *back-node* remains unchanged, as illustrated in the right hand side of Figure I-5. This process is presented in Step 3 of the algorithm.

Initialize:

$S = \emptyset$

$b_i = \infty \quad \forall i \in N$

$c_i = \infty \; \forall i \in N$

r = Origin node (root of the tree)

$i = r$

$b_i = 0$

$c_{ri} = 0$

InsertTail i into S

(1)

Start_Algorithm:

Pop i from S

$R_i = \{ j \in N \mid l_{ij} \in A \}$ (2)

Do loop for each node j in R

If $c_{rj} < c_{ri} + t_{ij}$ then

$c_{rj} = c_{ri} + t_{ij}$

$b_j = i$

(3)

If j has ever been in S but not in S now

InsertHead j into S

Else if j has never been in S

InsertTail j into S

End if

(4)

End if

End Loop

If S is empty, terminate algorithm

Else go to *Start_Algorithm*:

Figure I-3: Pseudo-Code of Moore-Pape Minimum-Path Algorithm

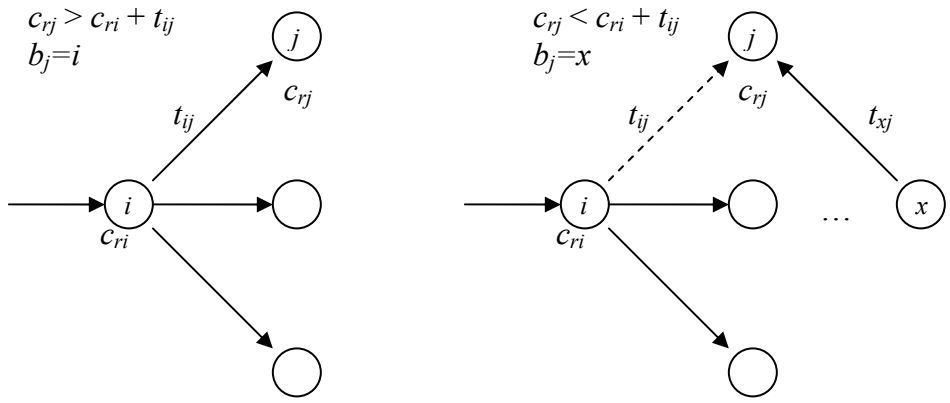

Figure I-4. Examination of Forward Star

R in Step 2 of the algorithm, is the set of node j, which consists of all the To-Nodes of the collection of links where the From-Node is the hub, as illustrated in Figure I-4. Sheffi (1985) refers to the set as a *forward-star* because of the shape of the subsystem and the directionality from the root to each destination. A typical transportation network contains less nodes than links, and finding a path by comparing travel time to nodes is more efficient than comparing link travel times from the root node. Therefore the algorithm performs repeated comparisons for each node in R until every node in the network system is examined.

Once examination from a hub node is completed, the algorithm requires specification of the next node that is to be used as the hub of examination. Whenever a lower travel cost for a node is identified (a new *back-node*), the node can be a hub in the next iteration because every node on the path can possibly be *back-node*. Therefore, one way to supply hub nodes in consecutive examinations is to have a temporary memory storage populated whenever the *back-node* of a node is updated. The set *S* in Step 4 of the algorithm is stored in this memory. In the Moore-Pape algorithm, *S* has special characteristics as discussed below that make the algorithm more efficient.

S is temporary data storage (or an array), generally referred to as the "queue". A queue is a unidirectional data storage model that is similar to a line in front of a teller window which is served under a first-in-first-out policy. Customers come into the queue through the tail and go out through the head. However, S is a special queue that has two entrances on both sides, and one exit from the side. Since it is a two-sided queue, data (candidates for the hub) are inserted into *S* through the head and tail, and data (the hub node for the next examination) pops out from the head of the queue. Elements in *S* are connected to adjacent elements. The head and tail of S are maintained by other complementary pointers in computer memory. Figure I-5 shows how to implement the structure of *S* in a computer, and the process of entering the queue (i.e., insertion) and exiting the queue (pop) that is used during examination of the hub.

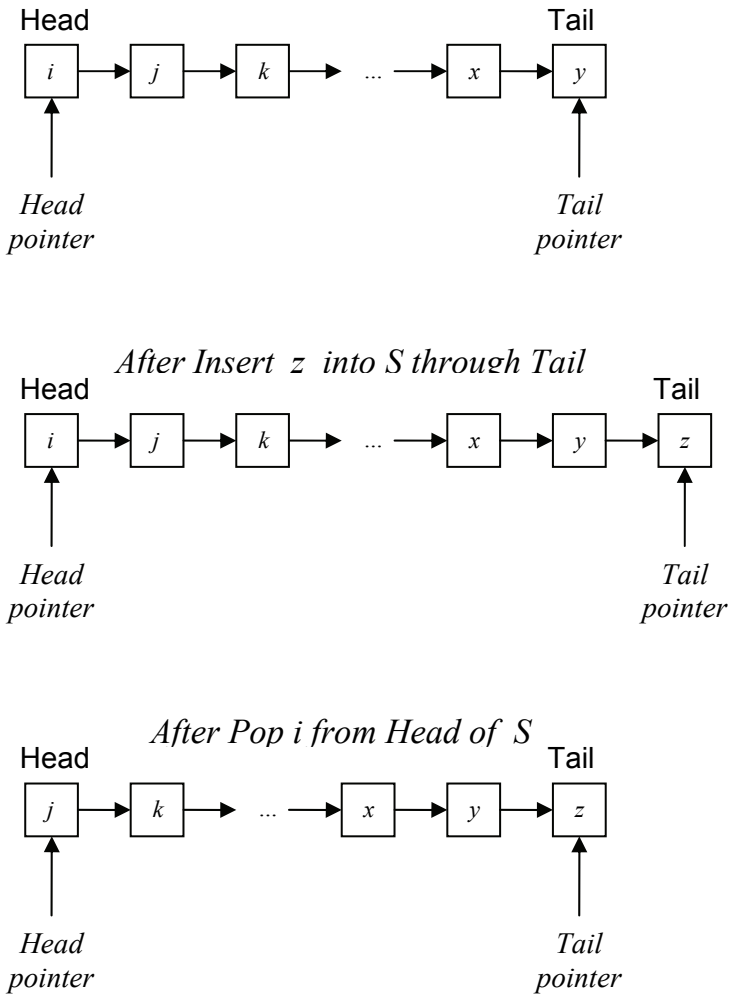

Figure I-5. Structure of S after Performing Insertion and Pop

To illustrate this process, a numerical example is provided. This example considers the network shown in Figure I-6 that has 6 nodes and 18 links. Node 1 is the root in this example. Each line presents bi-directional links.

Note that, from examination from hub node 5, nodes 2, 3, and 4 are reinserted into *S* because their new travel costs are lower than previous ones respectively. In the next examination, node is taken as hub. It is not because elements in *S* are sorted with respect to node ID, but because node 2 has been in S, and reinserted. Examination from hub 2 updates travel cost to node 3 again, and its *back-node*.

(a) Sample Network

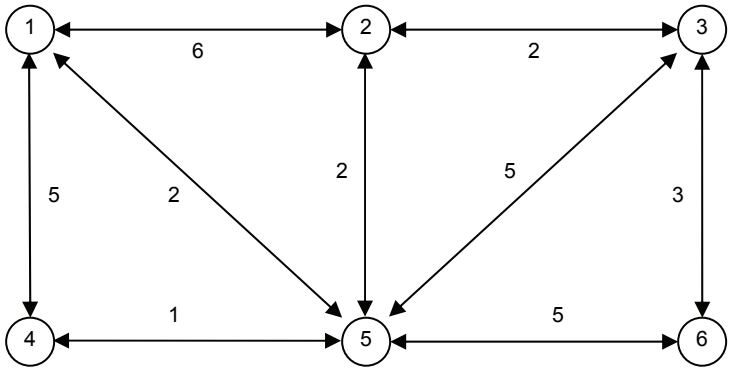

(b) Minimum Path Searching Steps

Initialization
Root = 1

Node	Cost to reach from node 1	Back-node
1	0	0
2	∞	∞
3	∞	∞
4	∞	∞
5	∞	∞
6	∞	∞

S={1}
Hub = 1 (cost to hub from root = 0)
R= {2, 4, 5}

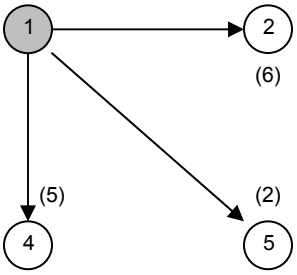

Node	Cost to reach from node 1	Back-node
1	0	0
2	6	1
3	∞	∞
4	5	1
5	2	1
6	∞	∞

Figure I-6. Numerical Example of Moore-Pape's Minimum-Path Algorithm (Part 1 of 3)

S = {2, 4, 5}
Hub =2 (cost to hub from root = 6)
R= {1, 3, 5}

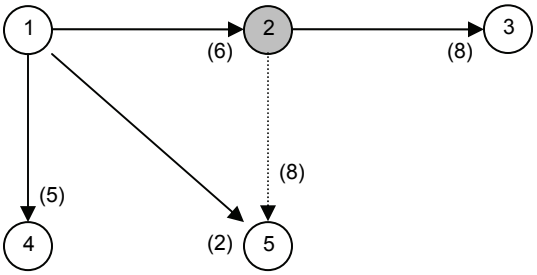

Node	Cost to reach from node 1	Back-node
1	0	0
2	6	1
3	8	2
4	5	1
5	2	1
6	∞	∞

S = {4, 5, 3}
Hub = 4 (cost to hub from root = 5)
R = {1, 5}

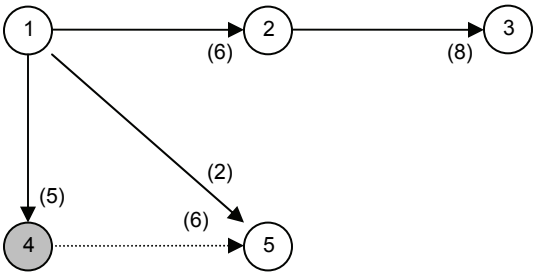

Node	Cost to reach from node 1	Back-node
1	0	0
2	6	1
3	8	2
4	5	1
5	2	1
6	∞	∞

S = {5, 3}
Hub = 5 (cost to hub from root = 2)
R = {1, 2, 3, 4, 6}

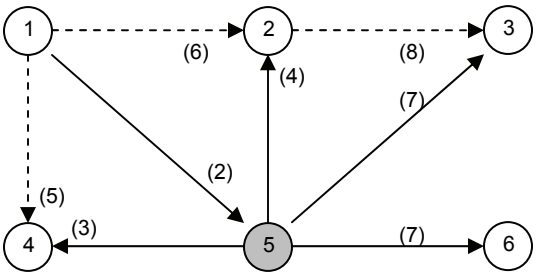

Node	Cost to reach from node 1	Back-node
1	0	0
2	4	5
3	7	5
4	3	5
5	2	1
6	7	5

Figure I-6. Numerical Example of Moore-Pape Minimum-Path Algorithm (Part 2 of 3)

S = {2, 3, 4, 6} (nodes 2, 3, 4 are reinserted into S through head because those were used once as hub node)
Hub = 2 (cost to hub from root = 4)
R = {1, 3, 5}

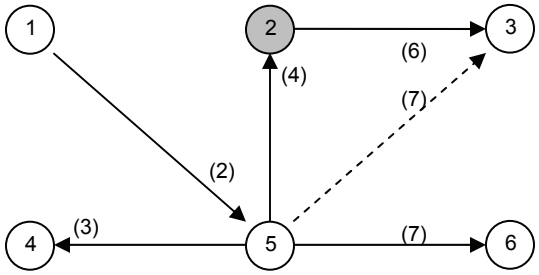

Node	Cost to reach from node 1	Back-node
1	0	0
2	4	5
3	6	2
4	3	5
5	2	1
6	7	5

S = {3, 4, 6}
Examinations from hub 3, 4, and 6 do not update any travel cost, or *back-node*

(c) Resulting minimum path rooted from node 1

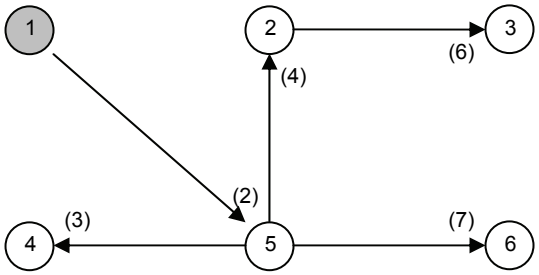

Figure I-6. Numerical Example of Moore-Pape Minimum-Path Algorithm (Part 3 of 3)

I.6.3 Dual-Simplex Algorithm

The Dual-Simplex method is a solution technique of linear programming. Linear programming is an optimization problem that consists of a linear objective function, linear constraints, and non negativity constraints, such as

$$\max \sum_i c_i \cdot x_i \qquad \text{(I-16)}$$
$$s.t.\ a_i \cdot x_i \le b_i\ ,\ x_i \ge 0$$

In the solution process, the Dual-Simplex algorithm improves the objective function in two ways: a) from an optimization solution, it replaces an infeasible variable to improve feasibility; and b) from a feasibility solution, it replaces a variable to improve optimality.

Let us assume that Nodes *i* and *j* are adjacent zone centroids, as shown in Figure I-7. Once a path from Node *i* is established, the process goes to Node *j*. Node *i* is connected via links grouped in *a*. From Node *i*, Node *j* is connected via links grouped in *a*' to the main body of the path tree. Establishment of a path from Node *j* actually consists of the following steps:

- Step 1: Remove links that connect the prior root node to the main body of the tree (link group a).
- Step 2: Add links that connect the main body of the tree to the prior root node (link group b)
- Step 3: Remove the links that connect the main body of the tree to the new root node (link group a')
- Step 4: Add links that connect the new root node to the main body of tree (link group b')

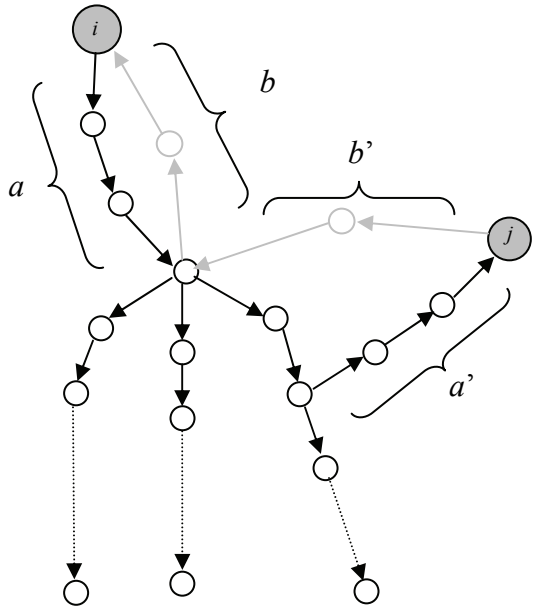

Figure I-7. Establishing Path from a New Root by Dual-Simplex Algorithm

Steps 1 and 3 are removing links to achieve feasibility, while Steps 2 and 4 increase optimality. Actually, the links in Group *a* and *a*' are examined one-by-one. Also, links in Group b and b' are identified simultaneously while identifying the so-called "main body" of the tree.

Identification of the main body of the tree should not be more costly than examination of all nodes and links according to the Moore-Pape algorithm. Faster identification of the main body of the tree is accomplished by 1) the tree-branch topology of the previous path; and 2) nodes connecting links in group *b* that are used to connect the previous root to the common path, and *b*' that connects the adjacent root to the common part of path.

The topology of the previous path is stored in a special data structure that is specified by Dial et al. (1979).

I.6.4 Run-Time Comparisons

Both the Moore-Pape and Dual-Simplex algorithms are implemented in an OCX, and the CPU running time for the search paths are compared. Five different sets of transportation network data are used in this comparison.

- SCAG-1534 is a simplified version of the base network for a 1990 transportation survey of the five-county Southern California region. Consecutive links with similar attributes are merged..
- SCAG-3217 is the original form of the base transportation network for the 1996 supplement survey.
- SCAG-1470 is a simplified version of SCAG-3217. Instead of merging links, zones are merged in this case. The centroids of the merged zones are connected to nodes that were zone centroids in SCAG-3217 system. Thus, 1470 nodes and 6434 (2*3217) links were added.
- LA-480 is developed from the SCAG-1534 and NHPN databases. It covers the area that was affected by the 1994 Northridge Earthquake, including downtown Los Angeles. Its zone system follows SCAG-1534.
- Bay-1120 is the base transportation network database (as of 1998) for the San Francisco Bay area, posted on the website of the Metropolitan Planning Commission, who is the Metropolitan Planning Organization (MPO) for the region

Table I-4 summarizes the size of each network, and Figure I-8 shows parts of each network. In particular, Figures I-8a, b, and c show the identical area of the network data used in this test.

Table I-4: Size of Networks used for Running-Time Comparison

Network	Number of Zones	Number of Nodes	Number of Links
SCAG-1534	1,534	7,478	22,244
SCAG-3217	3,217	28,467	88,649
SCAG-1470	1,470	29,937	95,083
LA-480	480	1,970	6,230
Bay-1120	1,120	9,405	26,904

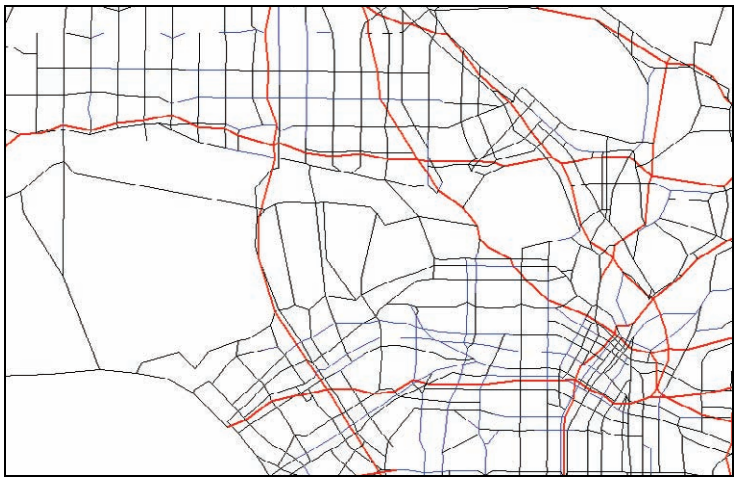

(a) SCAG-1534

(b) SCAG-3217

(c) LA-480

Figure I-8. Network Data used for Comparison (Part 1 of 2)

(d) Bay-1120

Figure I-8. Network Data used for Comparison (Part 2 of 2)

Computation times for 30 all-to-all paths are compared. In the transportation network analysis, 15-to-30 extreme feasible solutions are used to improve the global solution (as explained above). This means that 15-to-30 sets of all-to-all paths are required. In the actual network analysis model, the paths keep changing according to the network configurations (and, in turn, the travel time). In this comparison, the algorithms are used to repeatedly establish the all-to-all path (30 different times).

Table I-5 demonstrates the efficiency of the dual-simplex algorithm. In all cases, the Dual-Simplex algorithm is faster than the Moore-Pape algorithm for the all-to-all minimum path search, by factors ranging from 24-percent to 57-percent.

As one might expect, the running time is closely related to the size of the network, as shown in Figure I-10. However, the efficiency of new algorithm seems to be related to the redundancy of the network, as indicated by the following examples:

- Since the SCAG-3217 and SCAG-1470 databases are very detailed, they provide more paths between zone-pairs. The Dual-Simplex algorithm does not need to examine all possible paths as does the Moore-Pape algorithm, the benefits from implementing the Dual-Simplex algorithm are high in this case (see Figure I-11).
- The Bay-1120 database contains very detailed network data but the configuration of this network is relatively simple. Only a few of the bridges cross over the San Francisco Bay, so the paths between some zone-pairs are limited. Therefore, the reductions in run time afforded by the Dual-Simplex algorithm relative to the Moore-Pape algorithm (about 28-percent) are not as great as for the SCAG databases.

Table I-5. Computer Run Times for Searching All-To-All Paths (30 times) by Networks and Algorithms (in seconds)

Network	Computer Run Time, seconds		Percent Reduction in Run Time when Dual-Simplex Algorithm is Used
	Moore-Pape Algorithm	Dual-Simplex Algorithm	
SCAG-1534	9.63	7.30	24.2 %
SCAG-3217	194.62	88.04	54.8 %
SCAG-1470	131.64	56.47	57.1 %
LA-480	0.69	0.53	24.0 %
Bay-1120	9.83	7.09	27.9 %

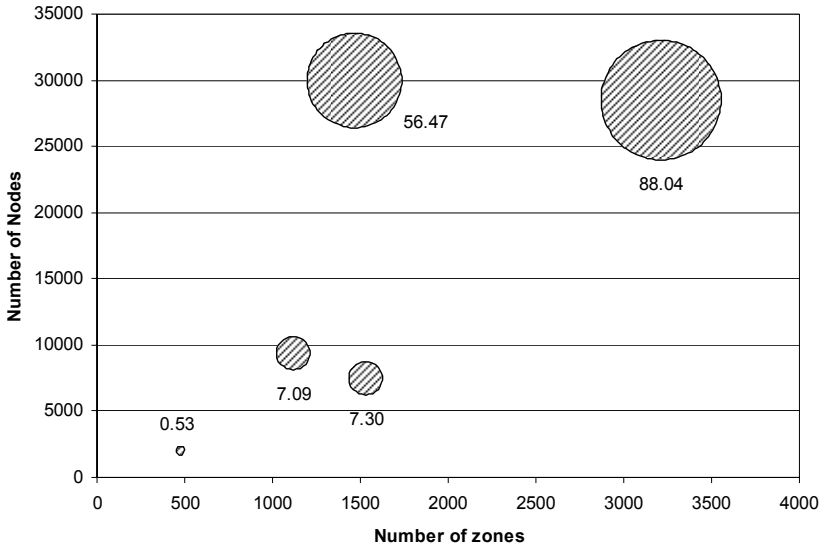

Figure I-9. Computer Run-Times of Dual-Simplex Algorithm as a Function of Network Size

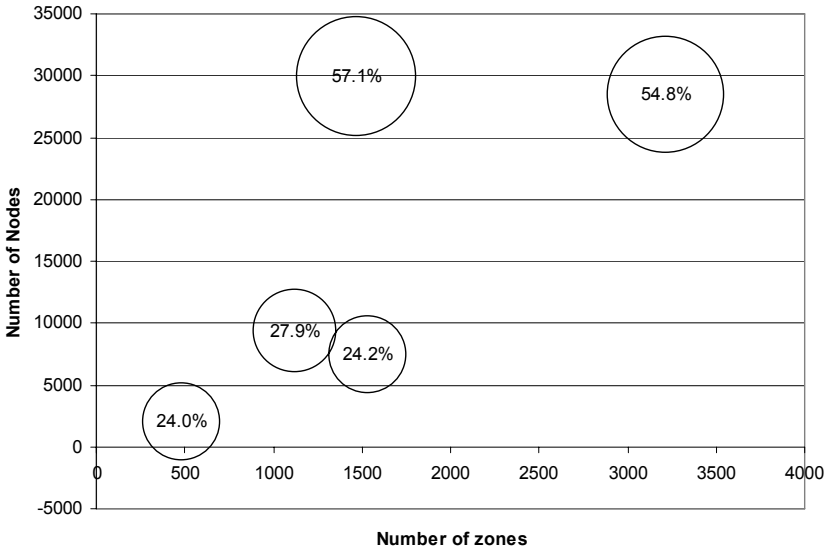

Figure I-10. Percent Reduction in Computer Run Time when Dual-Simplex Algorithm is Used, as a Function of Network Size

I.7 VALIDATION OF VARIABLE-DEMAND MODEL

In this section, the VDM is validated by comparing estimated traffic volume after the 1994 Northridge Earthquake to: (a) observed traffic volume after the earthquake; and (b) traffic volumes estimated by the fixed-demand user-equilibrium model that was implemented in prior versions of REDARS™. The section begins with a brief description of the data used in these comparisons. Then, these comparisons involving the VDM are presented in the form of a series of regression analysis results. Finally, overall economic losses due to Northridge-Earthquake-damage as obtained from the VDM results are compared to prior economic loss estimates by Caltrans.

I.7.1 Data used for Validation

According to the Northridge Earthquake Recovery Report (Caltrans,1995), traffic passing 10 locations was counted for 24 hours for the next day of the earthquake. In this validation, 1993 AADT data for the corresponding 10 locations are used for pre-earthquake traffic volumes. Local traffic counts occurred for 12-hours on a day in October 1993 (exact date unknown) to represent pre-earthquake traffic volumes, as well as on January 18, 1994, yielding the post-earthquake traffic volumes. These data covered 35 streets segments in the west-central Los Angeles area that is centered about the intersection of I-10 and La Cienega Boulevard, and is bounded by Jefferson Boulevard to the South, Wilshire Boulevard to the North, Crenshaw Boulevard to the East, and Robertson Boulevard to the West. This area is shown in Figure I-11.

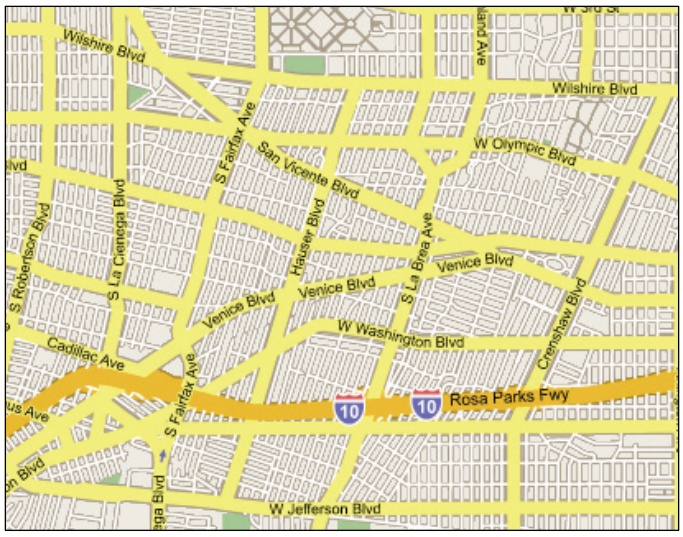

Source: maps.google.com

Figure I-11. Region Covered in Validation of Variable-Demand Model

Two sets of network data were created to estimate traffic volume corresponding to the Caltrans surveys: one network for freeways, and one network for local streets. A subset of the NHPN network was created for freeway traffic estimation, as well as the economic loss calculation, extending from I-105 to the south, just north of the I-5 /SR-14 intersection to the north, I-710 to the east, and the Ventura-County / LA-County boarder to the west. This network consists of 1,036 TAZs, including 58 external zones. 3-hr daily average traffic demand was created from the 1996 SCAG planning OD. The Import Wizard was used to subset the OD into corresponding TAZs. Figure I-12 shows the resulting network.

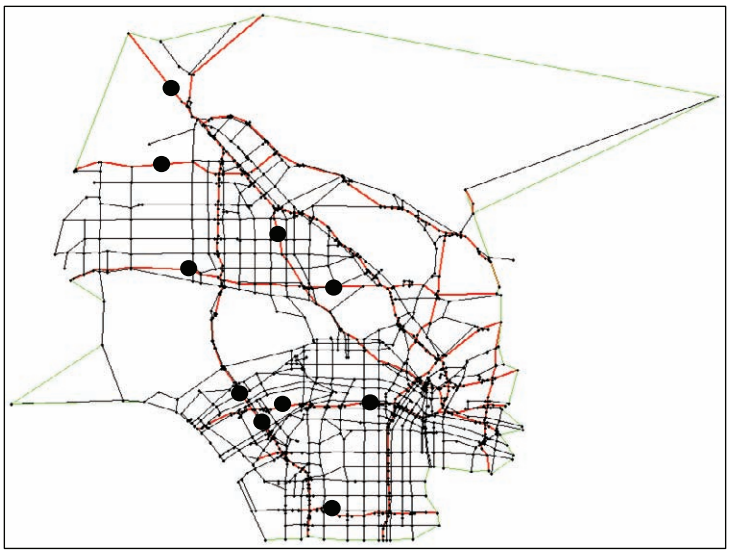

Figure I-12. The Regional REDARS™ Network used for Freeway Traffic Comparison (points are where volumes are counted)

Additionally, a detailed local network data was created to represent the local streets around I-10 / La Cienega Boulevard, as shown in Figure I-11, based on 1996 SCAG planning network, and 2000 Tiger maps. This network data consists of 52 TAZs, including 31 external zones. Figure I-13 shows the resulting network. The demand-function coefficients are initially estimated using the demand-function calibration module, as described in Chapter 5.2.5, and implemented in the Import Wizard.

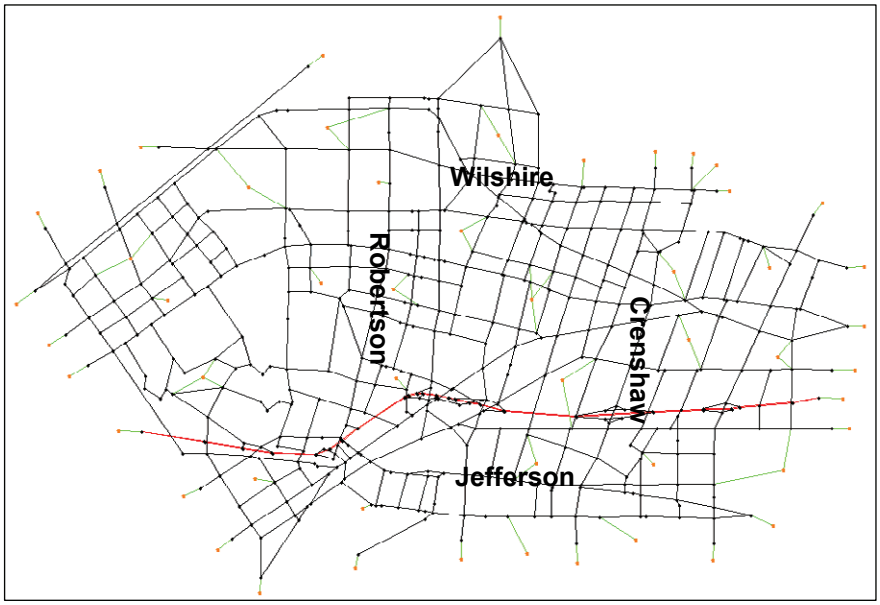

Figure I-13. The Regional REDARS™ Network Used for Local Traffic Comparison near Intersection of I-10 and La Cienega Boulevard

I.7.2 Traffic-Volume Comparisons

The traffic volumes in all the eight cases were analyzed by using the traffic modeling components of REDARS™ 2. As Table I-6 summarizes, the eight individual cases involve pre- and post-earthquake traffic volumes for both freeways and local streets, each analyzed using the fixed demand UE and VDM. The fixed demand UE model was temporarily programmed in the Import Wizard as a part of the baseline demand function calibration procedure; for purposes of this validation.

The volume estimated by the VDM is nearly always less than the volume estimated from the fixed demand UE model, in all of the cases listed in Table I-5, except for one data point that is explained below. In the VDM, trips and travel times are inversely related, so that any positive travel time increase will cause the trip demands to be reduced relative to the baseline (pre-earthquake) trip demands However, the fixed-demand UE, assumes that the post-earthquake trip demands are the same as the pre-earthquake demands, regardless of how the network's travel times and congestion are affected by earthquake damage. Because of this difference, the VDM traffic-volume estimates should not be greater than the volumes estimated by the fixed demand model.

Table I-5. Traffic Volumes Analyzed for Validation

Case No.	Network Configuration	Network Model	Network Data
1	Pre-Earthquake	VDM	Freeway
2	Pre-Earthquake	VDM	Local
3	Pre-Earthquake	Inelastic	Freeway
4	Pre-Earthquake	Inelastic	Local
5	Post-Earthquake	VDM	Freeway
6	Post-Earthquake	VDM	Local
7	Post-Earthquake	Inelastic	Freeway
8	Post-Earthquake	Inelastic	Local

In some case the VDM algorithm *as implemented* might not adjust trip demands relative to travel-time changes precisely as stated above.. For example, the VDM estimates a small positive volume on I-5, north of its interchange with SR-14. This is because of how the so-called "residual capacities" are handled in the VDM vs. how they are handled in the fixed-demand UE model. That is, to account for travel along smaller capacity roadways that are impractical to include into what is already a very large network model, REDARS™ 2 allows the user to account for this additional travel by specifying a residual traffic-carrying capacity for links that are disconnected. In this validation, 0.1% of each link's pre-earthquake capacity was used as the link's residual capacity when it is disconnected.

When the fixed-demand UE model is used, this small residual capacity results in extremely long travel times, because this incremental capacity increase tends to overload what may be an already near-capacity highway; i.e., because of this, the model shows that there no traffic volume is estimated north of I-5. By comparison, the VDM allocates some traffic to the link initially, because when the model starts analyzing the network, as demonstrated in Appendix I.5.2, the algorithm assumes that there is no volume on any of the links at the first iteration. The residual capacity does not effect the free-flow travel time on I-5. In subsequent iterations, although the traffic is getting smaller on the link as the algorithm of VDM proceeds, the algorithm actually does not reduce the volume to zero within a practical number of iterations. Despite this idiosyncrasy, using the residual capacity option is more appropriate for the VDM than for the fixed demand UE version, since the VDM maintains a small amount of traffic on links with minimal residual capacity.

The regression analysis reveals strong linear relationships between observed and estimated data from both the fixed-demand UE model, and the VDM. The statistics from the simple regressions summarized in Table I-6 indicate highly significant results for F-statistics, the confidence level, and a meaningful *t*-statistic on the estimated slope (β). There is no significant difference in the fit of the two models, since their calculated r^2 values have similar ranges when compared to the estimated traffic volumes. However, with regard to the pre-and-post-volume ratio, r^2 based on VDM estimations are much higher than for the fixed-demand UE model. Figures I-14 and I-15 show the data used for the series of regression analyses.

Because the difference between pre and post earthquake conditions is the basis for analyzing losses, traffic volumes estimated under pre earthquake conditions is as important as the volumes under post-earthquake conditions. As Figure I-16 shows, the actual increment of post-earthquake traffic volume was observed by Caltrans to be as much as twice the pre-earthquake link volume. Note that the post-earthquake network configuration includes the closed bridges on I-10, and only the local streets are used to accommodate the travel demand. Even though the VDM reduces the number of trips, the remaining trips increase link traffic volume. The VDM estimates a similar change ratio of 2.1 whereas the fixed demand UE model results in as much as 5.7 times the post-earthquake volumes on local streets. This simple test shows that the VDM adequately maintains the traffic volumes on pre and post earthquake network configurations.

In closing, the above results show that the VDM is a more appropriate for SRA than fixed demand model because of the manner in which residual traffic is accounted for when modeling detours, and the pre- to post earthquake traffic volume change ratio.

Table I-6. Regression Statistics for Variable-Demand and Fixed Demand Models

a) Traffic Volume on Freeways

Dependent Variable	α	β	r^2	F
Pre-Earthquake, Fixed Demand	23437.2 (t=2.816, p=0.023)	0.2212 (t=6.832, p=0.000)	0.8537	46.671 (p=0.000)
Pre-Earthquake, VDM	23122.4 (t=3.921, p=0.004)	0.1639 (t=7.142, p=0.000)	0.8644	51.010 (p=0.000)
Post-Earthquake, Fixed Demand	23608.3 (t=2.781, p =0.024)	0.2726 (t=6.255, p=0.000)	0.8303	39.128 (p=0.000)
Post-Earthquake, VDM	14299.5 (t=2.425, p=0.042)	0.2126 (t=7.024, p=0.000)	0.8605	49.337 (p=0.000)
Change Ratio, Fixed Demand	0.3468 (t=2.869, p=0.021)	0.7875 (t=4.876, p=0.001)	0.7483	23.779 (p=0.001)
Change Ratio, VDM	0.2453 (t=3.381, p=0.010)	0.7893 (t=8.143, p=0.000)	0.8923	66.311 (p=0.000)

b) On Local Street near Intersection of I-10 and La Cienega Boulevard

Dependent Variable	α	β	r^2	F
Pre-Earthquake, Fixed Demand	-7162.5 (t=-0.971, p=0.338)	2.5869 (t=9.234, p=0.000)	0.7149	85.274 (p=0.000)
Pre-Earthquake, VDM	-1775.6 (t=-1.046, p=0.303)	0.6252 (t=9.695, p=0.000)	0.7344	93.991 (p=0.000)
Post-Earthquake, Fixed Demand	11161.1 (t=0.646, p=0.523)	3.6831 (t=5.667, p=0.000)	0.4858	32.119 (p=0.000)
Post-Earthquake, VDM	-2346.8 (t=-1.032, p=0.310)	0.6484 (t=7.584, p=0.000)	0.6484	57.522 (p=0.000)
Change Ratio, Fixed Demand	-1.5888 (t=-4.332, p=0.000)	3.4309 (t=10.124, p=0.00)	0.7509	102.503 (p=0.000)
Change Ratio, VDM	-0.1464 (t=-1.561, p=0.128)	1.1344 (t=13.088, p=0.00)	0.8344	171.309 (p=0.000)

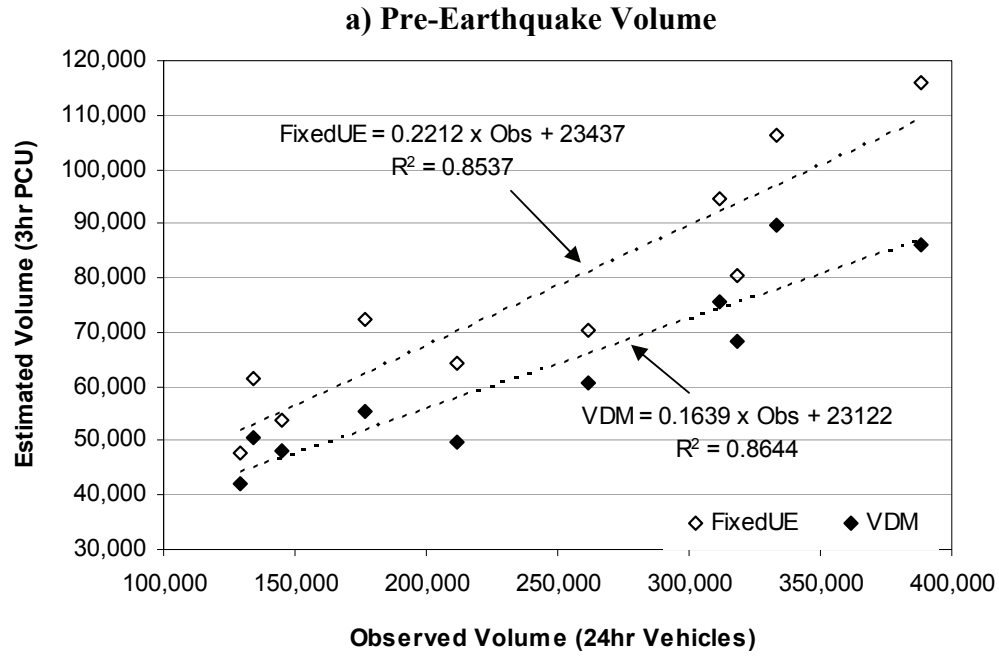

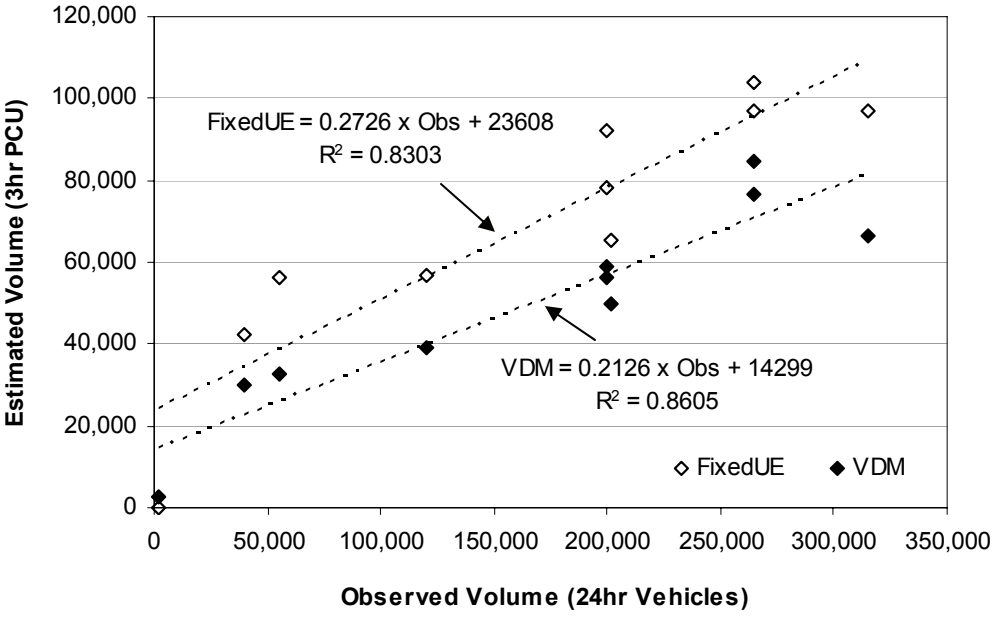

Figure I-14. Comparisons of Pre-Earthquake and Post-Earthquake Traffic Volumes: Freeways

(a) Pre-Earthquake Volume

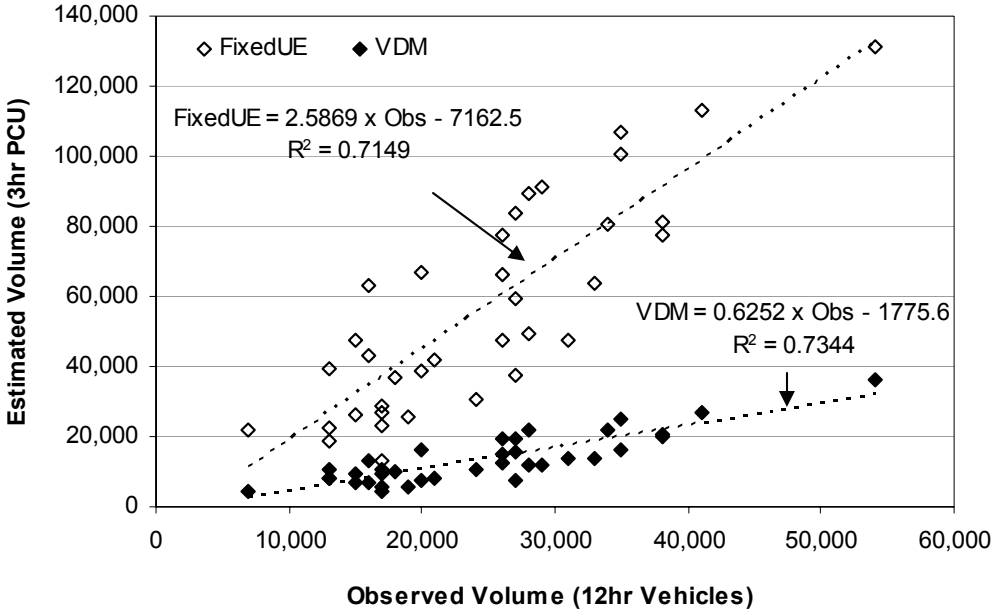

(b) Post-Earthquake Volume

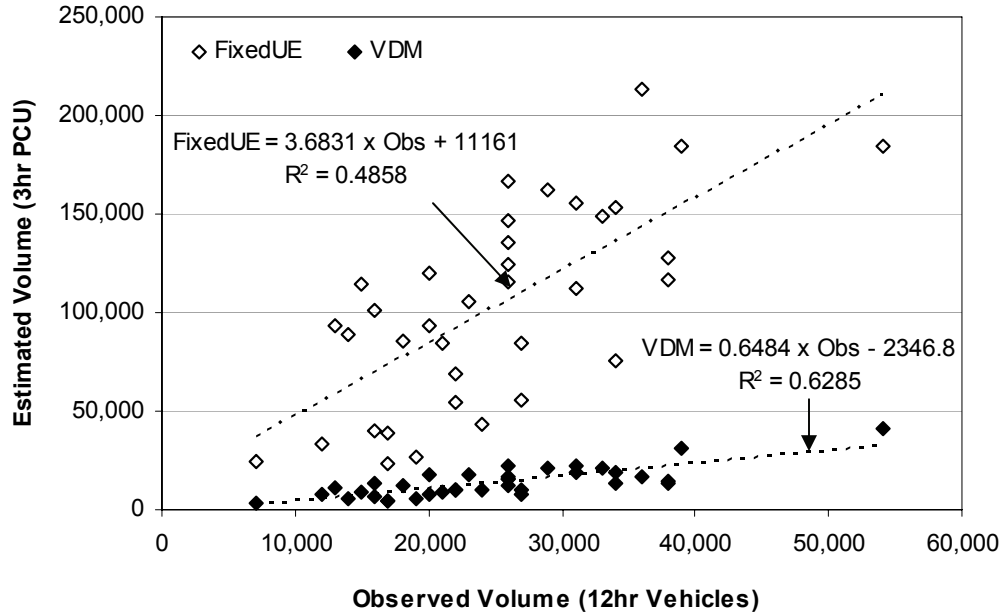

Figure I-15. Comparisons of Pre-Earthquake and Post-Earthquake Traffic Volumes: Local Roads

(a) Volume Changes on Freeway due to the earthquake

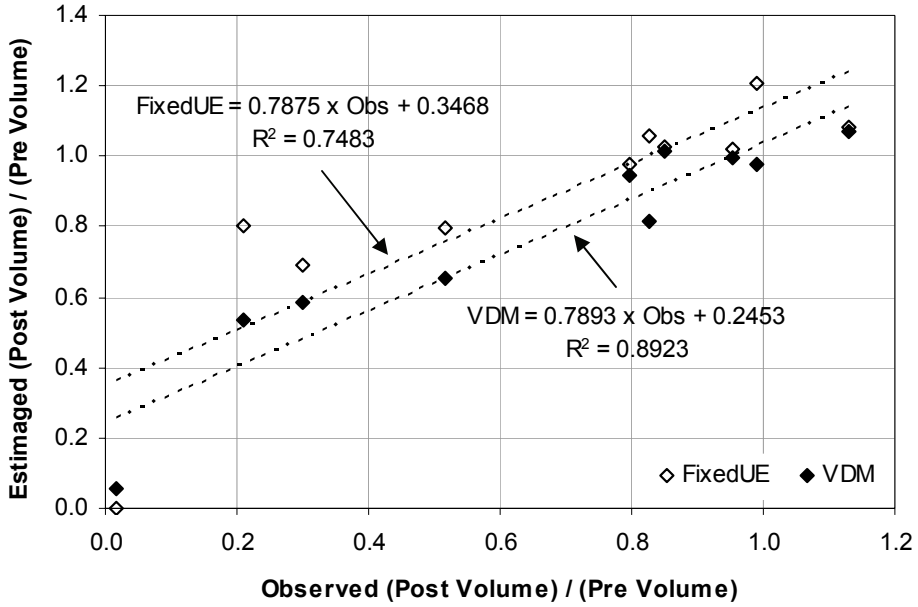

(b) Volume Changes on Local Streets due to the earthquake

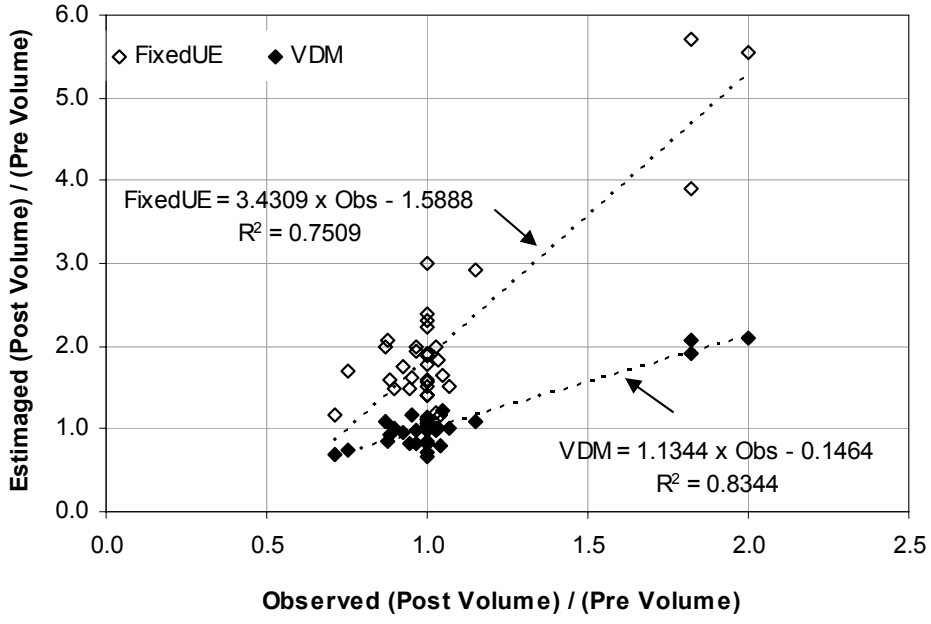

Figure I-16. Ratio of Pre-Earthquake to Post-Earthquake Traffic Volumes

I.7.3 Economic-Loss Estimation

Caltrans estimates a $217 million loss from transportation disruption near collapsed bridges following the Northridge earthquake. Table I-7 presents the economic loss estimated using REDARS™ 2, the result is very comparable at $213million.

Table I-7. Economic Losses Estimated Using REDARS™ 2

Days [3] from EQ.	Passenger [1]		Freight [2]		Daily Loss ($ 1,000)	Total Loss over the days ($1,000)
	Forgone Trips (PCU*Hr)	Congestion (PCU*Hr)	Forgone Trips (PCU*Hr)	Congestion (PCU*Hr)		
11	1,460	78,650	301	5,875	2,661	29,268
12	1,373	76,887	299	5,666	2,593	2,627
15	1,244	69,609	276	5,131	2,348	7,413
81	375	25,745	242	1,723	863	105,989
123	89	23,034	8	920	695	32,726
174	72	10,470	1	642	336	26,283
228	0	0	0	0	0	9,062
					Sum	213,367

1) $6 / PCU·Hr to convert daily loss
2) $19.2 / PCU·Hr to convert daily loss
3) Recovery schedule from Northridge Earthquake Recovery Report – Final Comprehensive Transportation Analysis, Caltrans District 7, 1995.

Note that this promising economic loss estimation is obtained by using only the transportation model in REDARS™ 2 outside of the standard software package. In this calculation, the networks are analyzed for 7 time periods, while REDARS™ 2 can accept 4 time periods after earthquake. Furthermore, the system states at each time period were entered, instead using REDARS™ to estimate.

Although the difference is small, it is less than the Caltrans estimation. For a deterministic analysis, the model may not be conservative, as is required for planning models. This may be related to the low estimation of pre-earthquake traffic volume. The validation found VDM volumes are consistently lower than the fixed demand model, even in the pre-earthquake conditions. This is by design, the input OD is used by the VDM as an upper bound for demand which is reduced according to travel time. Since the MPO OD was developed for normal network conditions, any network model should use all of the OD without any reduction for pre-earthquake condition. Once the pre-earthquake trips are estimated, the VDM further reduces trips to adjust for post-earthquake network capacity. Further improvement of the VDM should address the elasticity of pre-earthquake demand.

APPENDIX J
CONFIDENCE INTERVALS FOR PROBABILISTIC ANALYSIS RESULTS

J.1 INTRODUCTION

REDARS™ 2 uses a Monte Carlo process to develop statistically sound probabilistic SRA loss results for each year in a multi-year walkthrough table in which it has been determined that a potentially damaging earthquake has occurred. However, if such SRA results are developed for all damaging earthquakes in the full walkthrough table, the analysis can be very time consuming.

To address this potential problem, REDARS™ 2 uses statistical-analysis methods to develop running displays of confidence intervals (CIs) in SRA loss results, as a function of the number of simulations (year samples) analyzed thus far in the probabilistic SRA. Since these CIs will improve as the number of analyzed simulations increases, their display in REDARS™ 2 will guide the user's assessment of whether a sufficient number of simulations has been considered. In particular, these CI displays enable the user to either:: (a) continue with the SRA without interruption if the CIs attained thus far are judged to be unacceptable; (b) terminate the probabilistic SRA if he/she determines that the CIs are acceptable; or (c) stop the SRA, review the CIs and other results obtained thus far, and then restart the SRA from where it was terminated, if further improvements in the CIs are desired.

Appendix J describes the various methods used in REDARS™ 2 to estimate CIs. The remainder of the appendix contains five main sections. Section J.2 describes classical statistical methods that have been used in earlier versions of REDARS™ to estimate CIs, and have been found to work in all test cases. Section J.3 describes parametric-bootstrap procedures -- named variance-reduction methods -- that are adapted into REDARS™ 2 and have been experimentally designed to reduce the number of simulations needed to achieve given CI values. As will be indicated, the procedures have been tested successfully in all but one case. Section J.4 provides comparisons of results from classical statistics and the variance-reduction method. Caveats in the method are summarized in Section J.5. Finally, Section J.6 summarizes how CIs may be estimated when very few simulations are desired.

Given the levels of modeling and analysis procedures used in REDARS™ 2, we believe that 95th percent CIs of about ± 10 percent in the average annualized loss (AAL) should be reasonable for most uses. This CI is now generally attainable, given the developments described in this appendix.

J.2 CLASSICAL STATISTICAL-ANALYSIS METHODS

This section summarizes two classical statistical-analysis methods that have been used in prior versions of REDARS™ to estimate CIs in loss results developed from the REDARS™ Monte Carlo simulations (Werner et al., 2000, Taylor et al., 2001.) These consist of methods previously used to estimate CIs in average annualized loss results (Section J.2.1) and in fractile loss estimates, such as losses with a 500-year return period (Section J.2.2).

J.2.1 Estimation of CIs for Average Annualized Loss

Earlier REDARS™ procedures for estimating CIs for average annualized loss (AAL) were based on the assumption that the sampling distribution of the mean is normal, in accordance with the Central Limit Theorem. With this assumption, the nominal CI for an AAL (average annualized loss) estimate is defined from the following formula:

$$AAL \pm \frac{t_\alpha s_A}{\sqrt{N}} \tag{J-1}$$

where

N = number of Bernoulli trials (years simulated);
t_α = value of Student's t-distribution corresponding to any designated nominal confidence level and value of n (where, for a 95th-centile confidence level, $t_\alpha = 1.96$); and
s_A = standard deviation of the estimated loss distribution.

Note that Equation J-1 indicates that the CI for the *AAL* estimate is proportional to the standard deviation of the sampled loss distribution, and is inversely related to the number of Bernoulli trials. This equation is often used to show the number of trials needed to obtain a sufficiently narrow CI. However, it also shows that, if the standard deviation of the estimate of the mean loss is reduced, then the number of trials needed to achieve a desired CI is also reduced. This is the basic motivation for the investigation of variance-reduction techniques described later in this appendix.

To illustrate the application of Equation J-1, results are presented here from the previously noted application of the REDARS™ methodology for SRA of highway systems to the highway system in Shelby County, Tennessee (Werner et al., 2000). This application used 50,000 walkthrough years which, because of the moderate overall seismicity of the region, resulted in only 768 years with non-zero losses to the Shelby County highway system. For these years, the REDARS™ SRA results showed- an average annualized loss (*AAL*) of \$2.11M due to earthquake-induced travel time delays, and a standard deviation of these losses (s_A) of \$29.88M. Substituting these values into Equation J-1, and using t_α = 1.96 for a 95th-centile confidence level, resulted in the following equal-tailed 95th-centile confidence intervals:

$$(\$2.11 \pm \$0.262) \times 10^6$$

These results show that, for this application, there is a 95th-centile nominal confidence that the true value of the *AAL* is within ±12.4 percent of the computed value. This CI was judged to represent acceptable precision of the computed *AAL*. However, it turned out that the computer run time needed to perform the SRA for these 50,000 Bernoulli trials was excessive. This underscored the need to investigate whether alternative statistical-analysis procedures can be used that require fewer simulations (and hence reduced run times) to achieve a given target CI.

J.2.2 Estimation of CIs for Fractile Loss Estimates

REDARS™ 2 includes a classical statistical-analysis procedure for evaluation of CIs for various fractile estimates of losses. In particular, for a fractile loss L_p (which has a frequency of occurrence *p* and a corresponding return period of *1/p*), this procedure determines the range of values of L_p about its best-estimate value within which there is some nominal confidence level (say, the 95th-centile level) where the true value of L_p resides.

The starting point for this procedure is a series of REDARS™ 2 loss estimates for *N* simulations (year-samples). In this, it is assumed that these loss values have been rank-ordered from the highest to the lowest values (i.e., $l_1 > l_2 > l_3 ..... > l_j > l_i .....l_N$, where l_i is the i^{th} highest value of loss from the various simulations.) Then, from Hogg and Klugman (1984), it can be shown that the probability that L_p is between loss values l_i and l_j is computed exactly as

$$P(l_i < L_p < l_j) = \sum_{k=i}^{j-1} \frac{N!\, p^k (1-p)^{N-k}}{k!(N-k)!} \qquad \text{(J-2)}$$

According to Meyer (1970), the Poisson distribution can be used to approximate the above probability calculation for binomially distributed data and when *N* is large and *p* is small. For example, if *p* = 0.01 (which corresponds to losses with a 100-year return period) and *N* is large, the following Poisson approximation is useful for computing the probability that the fractile loss L_p is equal to the j^{th} loss value in the ordered sequence of loss results being analyzed:.

$$P(L_p = l_j) = \frac{\alpha^j \exp^{-\alpha}}{j!} \qquad \text{(J-3)}$$

where $\alpha \to N * p$. This approximation is used in accordance with the following steps to estimate confidence intervals about the best estimate value of L_p:

- Assume that loss results are provided from a 10,000-year walkthrough ($N = 10{,}000$) and it is desired to develop 95th-centile CIs for fractile losses with a 500-year return period ($p = 0.002$).

- The "best estimate" value of this 500-year loss is the $(n * P)^{th}$ value in the ordered sequence of 10,000 losses which, in this example, is value number *j* = 0.002*10,000 = 20. For this case, Equation J-3 is used to compute probability levels, first for the 20th loss value, and then for the 19th and 21st value, the 18th and 22nd value, and so on until the sum of the probabilities computed from all of the loss values that are included reaches 0.95. For this example, it turns out that the total probability is 0.944 that the losses will be between the 12th and 28th values, and is 0.967 that the losses will be between the 11th and 29th values (Table J-1).

Table J-1.
Losses to Include in Estimation of 95th-Centile Confidence Intervals for 500-Year Losses and 10,000 Year Walkthrough Duration

Term in Equation J-3			
j	α^j	$j!$	$P(L_p=l_j)$
1	20	1	4.12231E-08
2	400	2	4.12231E-07
3	8000	6	2.7482E-06
4	160000	24	1.3741E-05
5	3200000	120	5.49641E-05
6	64000000	720	0.000183214
7	1280000000	5040	0.000523468
8	25600000000	40320	0.001308669
9	5.12E+11	362880	0.002908153
10	1.024E+13	3628800	0.005816307
11	2.048E+14	39916800	0.010575103
12	4.096E+15	4.79E+08	0.017625171
13	8.192E+16	6.23E+09	0.027115648
14	1.6384E+18	8.72E+10	0.03873664
15	3.2768E+19	1.31E+12	0.051648854
16	6.5536E+20	2.09E+13	0.064561067
17	1.31072E+22	3.56E+14	0.075954196
18	2.62144E+23	6.4E+15	0.084393552
19	5.24288E+24	1.22E+17	0.088835317
20	1.04858E+26	2.43E+18	0.088835317
21	2.09715E+27	5.11E+19	0.084605064
22	4.1943E+28	1.12E+21	0.076913695
23	8.38861E+29	2.59E+22	0.066881474
24	1.67772E+31	6.2E+23	0.055734561
25	3.35544E+32	1.55E+25	0.044587649
26	6.71089E+33	4.03E+26	0.034298192
27	1.34218E+35	1.09E+28	0.025406068
28	2.68435E+36	3.05E+29	0.018147191
29	5.36871E+37	8.84E+30	0.012515304
30	1.07374E+39	2.65E+32	0.008343536

Sequence Number for Best Estimate Loss →

For $12 \le j \le 28$: $\Sigma P = 0.94428$

For $11 \le j \le 29$: $\Sigma P = 0.96737$

J.3 VARIANCE-REDUCTION APPROACH

As noted earlier, Equation J-1 shows that, as the standard deviation (or variance) of the estimate of the mean loss is reduced, the number of trials (simulations, year-samples, etc.), the CIs in the loss results will improve. This, in turn, could justify terminating the REDARS™ 2 probabilistic analysis at some intermediate stage when the user decides that the CIs in the loss results are acceptable.

Of course, one way to estimate CIs is through the classical statistical-analysis procedures summarized in Section J.2. This section summarizes yet another approach, which is a variance-reduction procedure based on a parametric bootstrap analysis technique. Research results provided in Taylor et al. (2004a) show that the variance-reduction procedure can reduce the number of simulations needed to attain acceptable CIs by factors exceeding three or more. The advantage of this variance-reduction procedure (over the classical statistical-analysis approaches) is that, for reasons given later in this section, it provides more refined and lower estimates of variances for a given number of trials. This, in turn, will enable users of REDARS™ 2 to terminate the probabilistic SRA sooner than would be the case if classical statistical-analysis procedures are used to estimate CIs.

The remainder of this section is organized into three main parts. The first part describes the parametric-bootstrap approach that is the basis for the variance-reduction method. The second part summarizes the variance-reduction method, which is described in more detail in Taylor et al. (2004). The final part provides some results from the method, and also discusses caveats.

J.3.1 Parametric Bootstrapping

The parametric-bootstrap approach for estimating mean (average annual) losses is often referred to as a "sampling with replacement" procedure. It consists of the following steps:

1. As a starting point, obtain the N non-zero loss results from the REDARS™ probabilistic SRA.

2. Rank-order these losses from largest values to smallest values, and obtain the cumulative-probability distribution. Compute the mean loss from these loss results.

3. Pick a random number between 0.0 and 1.0, enter the above cumulative-probability distribution, and select a loss value from the existing array of values.

4. Carry out Step 3 N times, rank-order this new array of loss values, obtain their cumulative-probability distribution, and compute the mean loss.

5. Repeat Steps 3 and 4 multiple times to obtain successive revisions to the cumulative-probability distribution and mean loss from the array of loss values. This process of repeated sampling with replacement operations leads to successively improved estimates of the cumulative-probability distribution and the mean losses.

J.3.2 Summary of Method

The report by Taylor et al.(2004a) provides a detailed description of the variance-reduction method, and recounts the extensive testing of this method to achieve statistically sound efficiencies in estimating CIs. This section outlines the basic formulation of the method (ignoring additional complexities) that is currently programmed into REDARS™ 2.

J.3.2.1 Compound Poisson Distribution

This formulation begins with the prior assumption that an earthquake loss distribution for a highway system can be analyzed as a Compound Poisson distribution, with an exponential loss distribution adequately describing the conditional loss distribution -- the distribution of losses given that some loss has occurred. The Compound Poisson process in general is a method of analyzing an absolute or unconditional loss distribution into (a) a distribution for the probability of some loss (here called lambda) and (b) a distribution for the severity of that loss. This process assumes that the probability of some loss can be treated as a Poisson process (using the Poisson distribution). (This approach is common in the actuarial literature; see Daykin et al., 1994; Panjer and Willmot , 1992; Lemaire et al., 1993; Taylor et al., 1994) In Section J.5, it will be indicated that this assumption fits well enough all but one loss distribution tested to date. (These include test cases from Taylor et al., 2004b.)

The Poisson probability for number of events in time, t, is expressed as follows (see Panjer and Willmot, 1992; Ang and Tang, 1975, pp. 114ff.; Law and Kelton, 1991, pp. 349ff.):

$$P(E = J) = (\lambda t)^J \frac{e^{-\lambda t}}{J!} \qquad \text{(J-4)}$$

where

E = a variable for the number of events in time interval t
λ = the mean rate of occurrence for each time unit
J = 0, 1, 2, ...

REDARS™ 2 includes a pre-processor that first estimates lambda (λ) for the entire distribution of losses. The primary purpose of this estimate is to reduce to a very small level the uncertainty in this parameter, so that the primary focus is on uncertainties in the conditional loss distribution—the distribution of network losses given that some loss occurs (Taylor et al., 2004a). For any specific highway system, lambda (λ) depends on such factors as:

- Seismicity affecting the lifeline network;

- Site-specific seismic hazards, including strong ground motion patterns in the region of the network, local-soil-amplification and de-amplification effects on ground motions, and earthquake-induced ground-deformation effects;

- The vulnerability of key lifeline facilities to strong ground motion and permanent ground deformation effects (in which, key facilities are those whose damage -- alone or in combination -- can lead to some degree of network loss); and

- The areal extent of the network (larger networks have higher probabilities of some loss, everything else being equal)

In addition, we have found through extensive testing that the reduced computer time (number of simulations) for a specific network is directly related to lambda (λ).

J.3.2.2 Starting Point: Rank-Ordered Losses from Probabilistic SRA Thus Far

The starting point for the variance-reduction method is an array of loss results from *N* years during which non-zero losses due to earthquake damage to the highway system have been computed by REDARS™ 2. In this, *N* represents only a part of the total number of years for which damaging earthquakes are estimated to have occurred in the walkthrough table. These loss results are rank ordered from highest to lowest.

J.3.2.3 Bootstrapping

Carry out 1,000 bootstraps from these initial loss results (Sec. J.3.1.) For each bootstrapped sample, the mean loss is computed and a conditional-probability distribution is developed.

J.3.2.4 Parametric Control Function

Next, for each of the 1,000 bootstraps, a parametric control function is used as a first-order estimate of the actual conditional-probability distribution. In REDARS™ 2, this control function is considered to be in the form of an exponential distribution (Law and Kelton, 1991; Hastings and Peacock, 1974), whose density function $f(x)$ and cumulative density function $F(x)$ are:

$$f(x) = \left(\frac{1}{b}\right) e^{-\frac{x}{b}} \quad \text{and} \quad F(x) = 1 - e^{-\frac{x}{b}} \tag{J-5}$$

with mean value *b*, variance b^2, and coefficient of skewness 2. For each bootstrap, this fitted exponential function is established by setting *b* = mean of the losses computed for that bootstrap.

J.3.2.5 Sample Differences

For the i^{th} bootstrap, compute the difference $\Delta(j)$ between the conditional-probability distribution for the control function $P_{CF}(j)$ and the bootstrapped data $P_{ACT}(j)$ at each of the N non-zero loss values, as computed below and illustrated in Figure J-1:

$$\Delta_i(j) = P_{CF,i}(j) - P_{ACT,i}(j) \quad j = 1,2,.....N \tag{J-6}$$

Also compute the i^{th} bootstrap's average difference for all *N* non-zero loss values, $\Delta_{avg}{}^{(i)}$ as:

$$\Delta_{avg}{}^{(i)} = \frac{\sum_{j=1}^{N} \Delta_i(j)}{N} \tag{J-7}$$

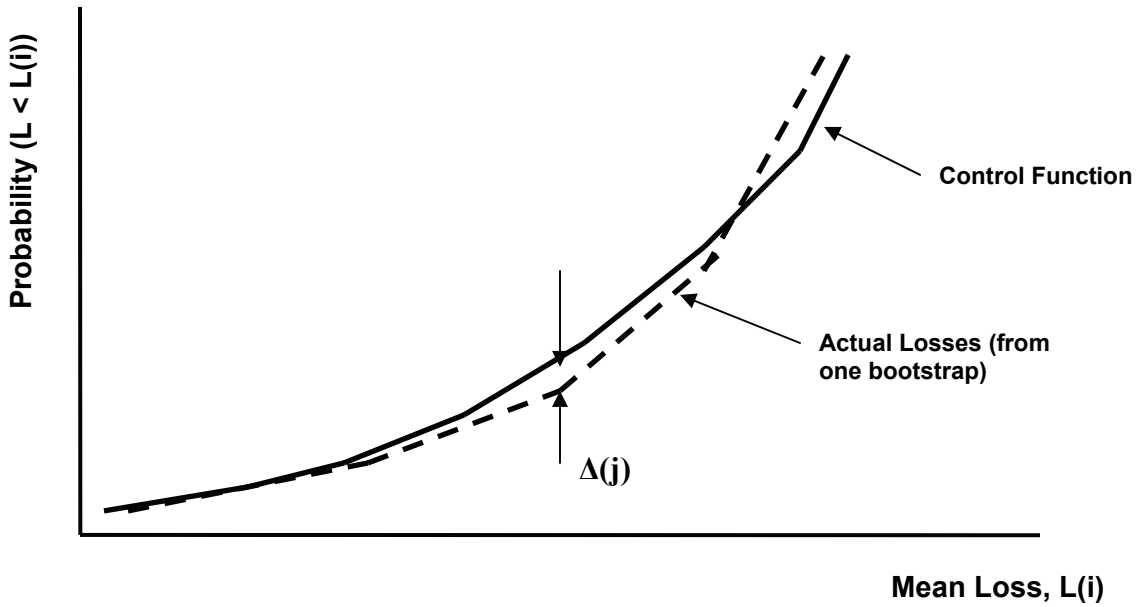

Figure J-1. Difference between Probabilities from Control Function and from Actual; Losses

J.3.2.6 Additional Calculation Steps

The REDARS™ 2 variance-reduction procedure carries out the above calculations for each of the 1,000 bootstraps. Then, the following calculations are carried out:

- Average difference between the control function and actual distribution from all bootstraps:

$$D_{avg} = \frac{\sum_{i=1}^{1,000} \Delta_{avg}^{(i)}}{1{,}000} \tag{J-8}$$

- Mean difference for each bootstrap:

$$DIF^{(i)} = \Delta_{avg}^{(i)} - D_{avg} \tag{J-9}$$

- Equivalent standard deviation (standard error) , s_A, from all bootstraps:

$$s_A = \sqrt{\frac{\sum_{i=1}^{1,000} DIF^{(i)}}{1{,}000 - 1}} \tag{J-10}$$

J.3.27 Confidence Intervals

Finally, the above equivalent standard deviation s_A along with the number of years with nonzero losses, N, considered in computing s_A is substituted into Equation (J-1) in order to compute the CIs for the mean losses at this stage of the probabilistic SRA

$$AAL \pm \frac{t_\alpha s_A}{\sqrt{n}} \tag{J-1}$$

where, as before

n = number of Bernoulli trials (years simulated thus far);

t_α = value of Student's t-distribution corresponding to any designated nominal confidence level and value of n (where for a 95th-centile confidence level, $t_\alpha = 1.96$); and

s_A = standard deviation of the estimated loss distribution.

J.4 SAMPLE RESULTS AND COMPARISONS

Section J.3.2 shows that the standard deviation, s_A, as obtained through this variance-reduction method (Equation J-10) is based on differences between the actual losses and losses estimated through the control function. Standard deviations computed in this way will be lower than those computed from classical statistics (which are based on differences between actual losses and the overall mean loss). For this reason, CIs computed for a given sample size by the variance-reduction method will be more favorable than those estimated by classical statistics.

This result has been verified from application of the variance-reduction and classical statistics methods to losses estimated from SRA of a number of highway systems as well as other lifeline infrastructure systems. One such highway system is the system in Shelby County, Tennessee that has been analyzed using an earlier version of REDARS™ (Werner et al., 2000). In that analysis, a walkthrough with a total duration of 50,000 years was considered. From this total walkthrough duration, only 768 of the years resulted in non-zero losses.

Tables J-1 and J-2 show results of this application to the conditional-loss distribution from the Shelby County SRA -- which is the distribution given some loss, and from the unconditional-loss distribution respectively. Each set of results is for 10,000- 20,000- 30,000- 40,000- and 50,000-years of simulations. For each of these years of simulations, first a classical approach and then the variance-reduction approach (with an exponential control function) is used to estimate the standard deviation of the losses.

Tables J-1 and J-2 also show major reductions in the number of simulations when variance-reduction is used. However, when the unconditional loss distribution is considered, the large number of years in which no losses occur limits these reductions. Taylor et al. (2004a) shows that these efficiencies increase with increasing as lambda (λ) and why this is the case.

Table J-1
Standard Deviations of Losses from SRA of Shelby County Highway System: Applications to Conditional Loss Distribution (in $M)

Parameter	Results as Function of Number of Years Simulated				
	10,000 Years	20,000 Years	30,000 Years	40,000 Years	50,000 Years
Mean of Losses: Classical Statistics	$137.67M	$141.94M	$144.55M	$137.58M	136.41
Standard Deviation of Losses: Classical Statistics	$199.92M	$204.63M	$209.23M	$202.19M	$203.38M
Mean of Losses: Variance-Reduction	$135.49M	$141.22M	$144.16M	$137.56M	$136.51M
Standard Deviation of Losses: Variance-Reduction	$10.42M	$7.80M	$6.46M	$5.23M	$4.64M
Percent Reduction in Standard Deviations when Variance-Reduction Method is Used	**95%**	**96%**	**97%**	**97%**	**97%**

Table J-2
Standard Deviations of Losses from SRA of Shelby County Highway System: Applications to Unconditional Loss Distribution

Parameter	Results as Function of Number of Years Simulated				
	10,000 Years	20,000 Years	30,000 Years	40,000 Years	50,000 Years
Mean of Losses: Classical Statistics	$2.11M	$2.18M	$2.22M	$2.11M	$2.10M
Standard Deviation of Losses: Classical Statistics	$29.88M	$30.74M	$31.39M	$30.21M	$30.44M
Mean of Losses: Variance-reduction	$2.08M	$2.17M	$2.21M	$2.11M	$2.11M
Standard Deviation of Losses: Variance- Reduction	$16.68M	$17.39M	$17.73M	$16.92M	$17.11M
Percent Reduction in Standard Deviations when Variance-Reduction Method is Used	**44%**	**43%**	**44%**	**44%**	**44%**

J.5 CAVEATS

Two caveats with the use of the variance-reduction method developed so far have been identified during the development and testing of this method. First, Taylor et al. (2004a) show that, given the high skewness of earthquake network loss distributions, variance-reduction methods for estimating confidence intervals for mean (average annualized) losses may perform poorly if there are fewer than about 40 non-zero losses.

In addition to this problem, testing by Taylor et al. (2004a and 2004b) has indicated one other problem with these variance-reduction methods -- a problem that has become more pronounced in 2005 with a more recent test case distribution. In particular, for earthquake scenarios generated from a single fault system, the loss distribution could be multi-modal. Multi-modalism occurs when there is a recognizable gap between two loss levels. For an earthquake evaluation of a highway system, this multi-modalism can arise from a combination of the non-linearity of highway-system performance subjected to varying levels of trip demands and the high degree of uncertainties in the component-vulnerability and especially the seismic-hazard models. This multi-modalism is also currently associated with a situation in which one or two known faults tend to dominate the loss statistics. For example, should one simulation contain a large strong ground motion for a very critical component and another simulation contain a significantly smaller strong ground motion for this component, the resulting travel-time losses for the two simulations may be widely different.

The use of an exponential distribution as a control function assumes that the loss distribution is uni-modal. To rectify this problem, it is very possible that one or more complex (i.e., two- or more- parameter) distributions should be used -- at least in special cases. Until this problem is resolved for potential multi-modal cases, the user can resort to the more classical (and broader) estimates of confidence intervals as indicated in Section J.2 -- especially for instances in which one fault appears to dominate loss statistics.

J.6 CONFIDENCE INTERVALS FOR VERY FEW SIMULATIONS

J.6.1 Overview

A main reason for considering variance-reduction techniques is to reduce the number of simulations needed. Under some circumstances, very few simulations may be desired. Serious time constraints or initially very coarse models or sub-models may discourage application of many simulations. This section, which has been extracted from Taylor et al. (2004a), spells out how confidence intervals increase as the number of simulations decrease.

J.6.2 Square Root Rule-of-Thumb

A helpful rule for evaluating increased limits is the square root rule. This states that as the number of simulations decrease by a multiplicative factor of Q then the confidence intervals increase by the square root of Q. This rule is a statistical approximation to the limits for the average annualized loss (AAL) as stated previously by Equation J-1:

$$AAL \pm \frac{t_\alpha s_A}{\sqrt{N}} \qquad \text{(J-1)}$$

This rule applies to Bernoulli trials, without the advantages of variance-reduction techniques. For a constant t_o and a constant σ_A, the confidence intervals will increase by almost the square root of Q as the number of trials, n, decreases by a multiplicative factor of Q. The application of this rule to confidence intervals as estimated by variance-reduction techniques is rather more problematic, as will be indicated in more detail below.

To illustrate the square root rule for the Shelby County highway system previously analyzed by a prior version of REDARS™, we first take the results of the raw Monte Carlo evaluation without variance-reduction. These yielded 95th-centile confidence intervals of +/-0.274 (or ±12.6 percent of the computed *AAL*) for a 50,000 year simulation with 768 non-zero losses. Reducing the simulations by a factor of 4 (e.g., from 50,000 to 12,500 year-samples), one multiplies confidence intervals by a factor of two (2) (e.g., +/-0.548). Reducing the original simulations by a factor of 16 (e.g., 781 year-samples), one multiplies the confidence intervals by a factor of four (4) (e.g., to 2.192). In general, if one desires confidence intervals that are +/-2.0, one reduces the number of simulations by a multiplicative factor of $(2/0.274)^2$, or 53.28, to 938 year-samples. This rule yields 15 non-zero losses (16 based on actual trials).

Similar results based on variance-reduction techniques are summarized in Table J-3. Note that in this table, the square root rule is best conceived of as a rule-of-thumb. Variance-reduction techniques imply in Table J-3 that only about 7 or 8 non-zero losses are required to achieve 95th-centile confidence intervals of +/-2. Some actual results for multiple samples of size 8 show that even smaller bootstrap confidence intervals can be calculated. However, for samples this small, the calculated means are frequently biased by amounts far larger than the bootstrap standard deviation. For the exponential distribution, for samples this small, the 95th-centile confidence intervals calculated according to Equation J-1 do not include the "true" mean up to 50-percent of the time! (This may not be as severe a problem for distributions which have central modes, but such distributions are less likely to represent loss distributions of the sort we are studying).

Table J-3
Illustrative Effects of Reducing Number of Simulations on
Confidence intervals Estimated by Variance-Reduction Techniques

Total Years Simulated	Total Years with Non-Zero Losses	Average Annualized Loss AAL ($M)	95th-Centile Confidence Intervals
50,000	768	2.10	+/-0.15
12,500	192	2.21	+/-0.31
3,125	48	2.36	+/-0.67
781	12	2.62	+/-1.53
500	7	2.41	+/-2.01

Brief studies suggest that somewhat better performance can be achieved by scaling the sample mean to provide better centering for symmetric confidence intervals, increasing the symmetric range to provide proper cover, or using unsymmetric semivariances. Transforming the sample data may also help (Small samples appear to be square-root normal.).

The gains achieved by variance-reduction technique have to be balanced by the increase of the likelihood of bias. Continuing research is being devoted to specification of minimal sample sizes to avoid bias. For developing more accurate results, our current guess is that at least 100 non-zero losses should be employed.

APPENDIX K
CALIBRATION OF DEFAULT BRIDGE-DAMAGE MODEL

K.1 INTRODUCTION

K.1.1 Statement of the Problem

The REDARS™ 2 Component Module contains a default model of the vulnerability of bridge structures subjected to earthquake ground motions. The bridge model described in HAZUS99-SR2 is currently being used for this purpose (NIBS, 2002).

During the initial phases of the development of REDARS™ 2, the various models that comprise the REDARS™ seismic risk analysis (SRA) methodology were independently checked (Cho et al., 2006a). Evaluation of the HAZUS99-SR2 bridge model was based on using the HAZUS99-SR2 model to predict bridge damage states during the 1994 Northridge Earthquake, for 944 bridges within the most affected segments of the overall Los Angeles (LA) area highway system. Then, the predicted damage states for these various bridges were compared to their observed damage states, and these comparisons were used to gauge the acceptability of the HAZUS99-SR2 model for inclusion into REDARS™ 2 as a default bridge model.

These comparisons showed that the HAZUS99-SR2 model significantly overestimated the number of observed bridge collapses due to the Northridge Earthquake. This will cause REDARS™ 2 to substantially overestimate the effects of earthquake damage to the highway system on post-earthquake traffic flows, since the program's default bridge repair model shows that by far the longest post-earthquake downtimes occur when the bridge is in a collapse damage state (see Sec. G.4 of Appendix G).

Therefore, it became clear that some adjustment of this model was needed before it could be included in REDARS™ 2 as a default model for estimating bridge damage due to ground shaking hazards. To meet this objective, refined statistical testing procedures were used to base this adjustment on a calibration against bridge damage observations from the Northridge Earthquake. This was accomplished by adjusting the model's structural capacity so that its predicted number of collapsed bridges and extensively-damaged bridges during the Northridge Earthquake were more consistent with observations. In this, differences in seismic performance of bridges with and without column jacketing were considered. This appendix describes this calibration effort.

It is noted that additional calibrations of this and other bridge models against damage observations from other major California earthquakes (e.g., the 1971 San Fernando and 1989 Loma Prieta Earthquakes) is clearly a worthwhile future study for further improving the current models. However, many of the bridges that are now in the areas affected by these earthquakes have attributes that differ substantially from the attributes of the bridges that were in place when these earthquakes occurred. In addition, data that define these prior attributes are not readily available. For these reasons, compilation of attribute data from bridges affected by these past earthquakes could not be attempted under this project.

K.1.2 Organization of this Appendix

The remainder of this appendix is organized into three main sections. Section K.2 describes the system of bridges considered in this calibration task, and the Northridge-Earthquake's characteristics and bridge damage. The calibration procedure and results are provided in Section K.3, and Section K.4 contains concluding comments.

K.2 BRIDGE SYSTEM AND EARTHQUAKE CHARACTERISTICS

K.2.1 System Extent

Figure K-1 shows the highway system within the greater LA area whose bridges have been considered in this bridge-model calibration. This system extends from the town of Santa Clarita to the north to just beyond the Century Freeway (I-105) to the south, and from the Pacific coast east to just beyond downtown LA.

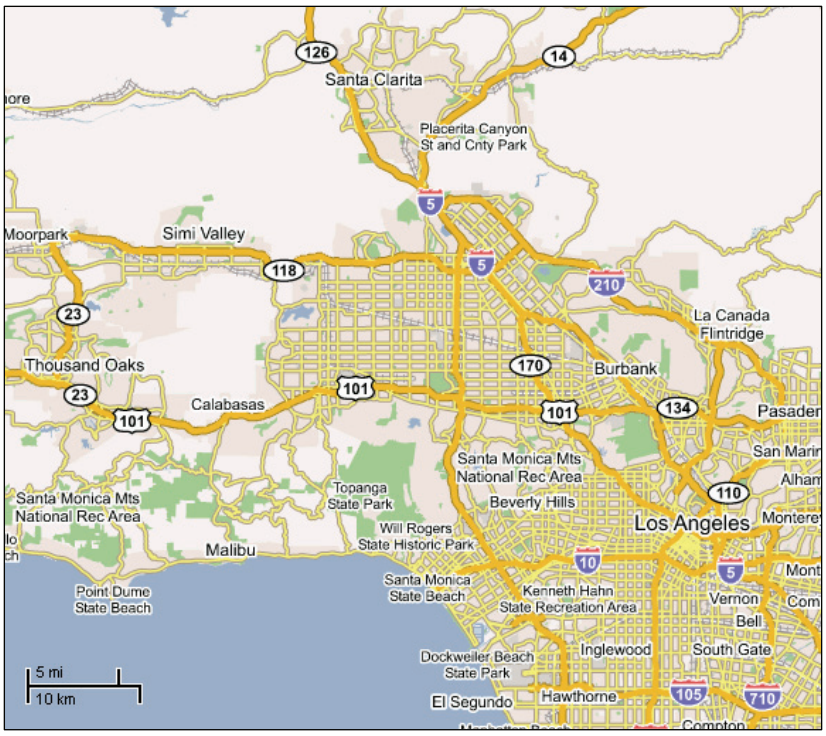

Source: maps.google.com

Figure K-1. Extent of System of Bridges considered in this Calibration

The system contains the 944 bridges that were in place at the time of the Northridge Earthquake (see Figure K-2). A total of 53 of these bridges had been column jacketed at the time of the earthquake. The structural attributes of these bridges that were input to this REDARS™ 2 analysis correspond to those of the in-place bridges at the time of the earthquake. This system is identical to the LA-testbed highway system used in the REDARS™ 2 demonstration application that is described in Chapter 7.

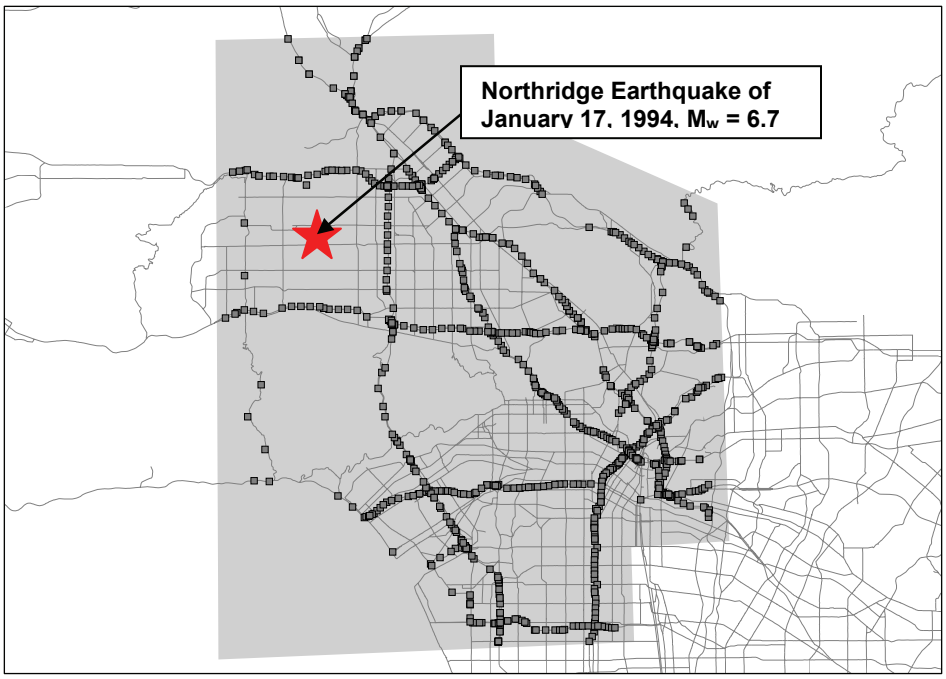

Figure K-2. Earthquake and Bridge Locations (944 Bridges)

K.2.2 Northridge Earthquake and its Bridge Damage

The Northridge Earthquake occurred on January 17, 1994. It had a moment magnitude of 6.7, and was centered in the northern part of the San Fernando Valley in the LA area (Fig. K-2). This earthquake disrupted traffic flows throughout this region and in west-central LA as well.

Table K-1 and Figure K-3 provide a breakdown of the bridge damage due to the Northridge Earthquake. They show that 10 of the bridges collapsed during the earthquake and another 36 were extensively damaged. None of the bridges that had been column jacketed collapsed during the earthquake.

Table K-1. Breakdown of Bridges by Damage State and Level of Retrofit

Damage State (see Table 4-3 of Chapter 4)	Bridges with No Column Jacketing	Bridges with Column Jacketing	Total
5 (Collapse)	10	0	10
4 (Extensive)	34	2	36
3 (Moderate)	69	9	78
2 (Minor)	64	6	70
1 (None)	714	36	750
TOTAL	891	53	944

Route	Bridge		
	Name	State Bridge Number	
		Before 1994	After 1994
Interstate-5	Gavin Canyon Undercrossing (2 bridges)	53-1797 R/L	53-2790 R/L
Interstate-5 and State-Route-14 Interchange	North-Connector Overcrossing	53-1964F	53-2796F
	South-Connector Overcrossing	53-1960F	53-2795F
	North-Separator Overcrossing	53-1963F	53-2797F
	South-Separator Overcrossing	53-1960G	53-2795G
State Route 118	Mission-Gothic Undercrossing	53-2205	53-2793
	Bull Creek Canyon Channel Undercrossing	53-2206	53-2794
Interstate 10	Fairfax-Washington Blvd. Undercrossing	53-1580	53-2792
	La Cienega Blvd. Undercrossing	53-1609	53-2791

a) Collapsed Bridges (Basoz and Kiremidjian, 1998)

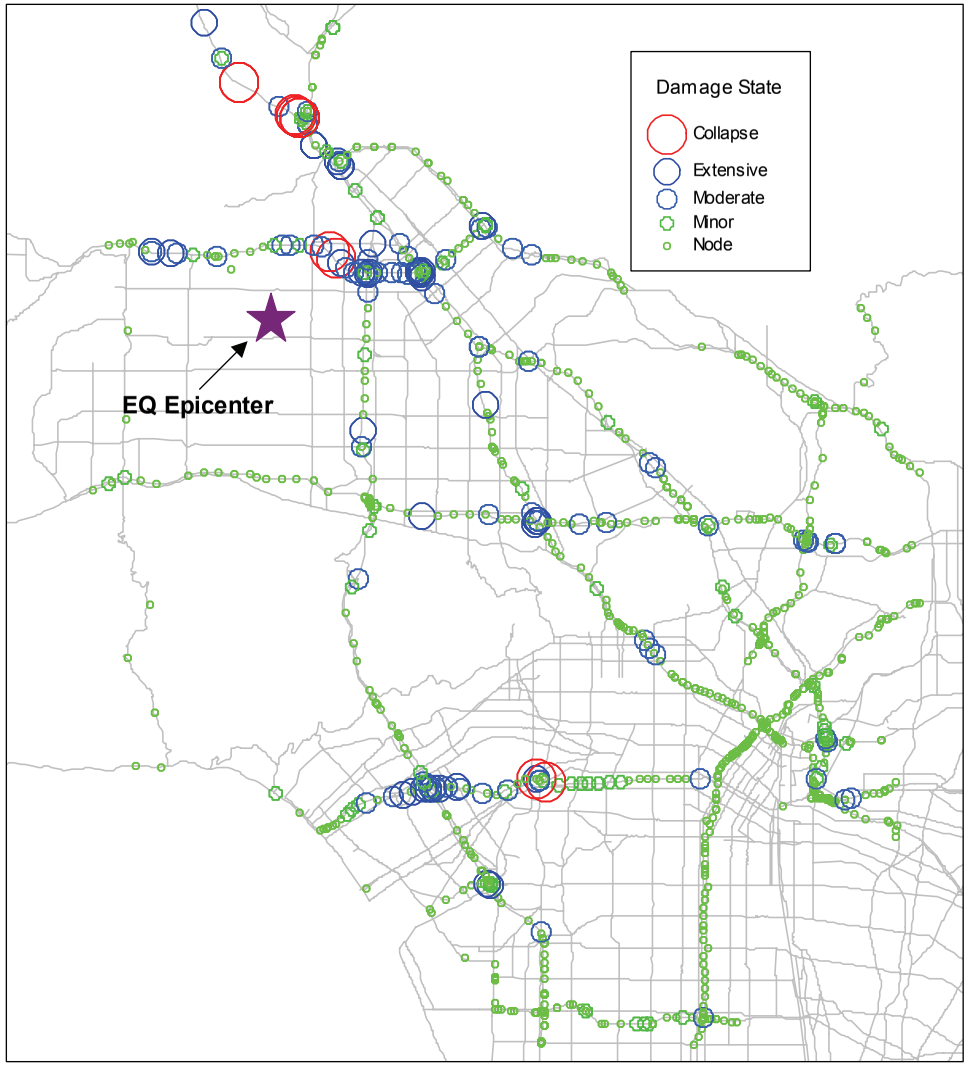

b) Locations of Damaged Bridges

Figure K-3. Bridge Damage due to 1994 Northridge Earthquake

K.3 CALIBRATION PROCEDURE AND RESULTS

K.3.1 Overview

This calibration of the HAZUS99-SR2 model to Northridge Earthquake bridge-damage observations involved the use of REDARS™ 2 to carry out a series of conditional-probabilistic analysis of the highway system that is shown in Figure K-1. In this analysis, the earthquake event was fixed (as the Northridge Earthquake), and uncertainties in the estimation of site-specific ground motions and bridge damage states were considered. In these conditional probabilistic analyses, the bridge damage-capacity term in the HAZUS99-SR2 model was systematically incremented, and the joint probability of achieving 10 collapsed bridges and 36 extensively-damaged bridges within the system was computed. The incremented values of the structural capacities that led to the largest joint probability of occurrence of 10 collapsed bridges and 36 extensively-damaged bridges was selected to represent the calibrated capacities in the HAZUS99-SR2 bridge model. In addition, the locations of the bridges with the largest joint probabilities of occurrence of these major levels of damage were compared to the actual locations of this bridge damage (see Fig. K-3b) to be sure that they compared reasonably well. This process is further described in the following subsections.

K.3.2 Starting Points

K.3.2.1 HAZUS99-SR2 Structural Capacity Representation

The HAZUS99-SR2 model represents structural capacities for unretrofitted bridges as the value of the spectral acceleration at a period of 1.0 sec. ($S_a(1.0)$) that leads to the onset of each of the five damage states listed in Table K-1. This spectral acceleration capacity for each damage state is expressed by the following equation that is consistent with the lognormal probability distribution assumed by the HAZUS99-SR2 bridge model.

$$\ln C_{i,j}'' = \ln(\alpha_i C_i') + \beta_i X_j \qquad \text{(K-1)}$$

In Equation K-1, C_i'' is the spectral-acceleration capacity leading to the onset of the i^{th} damage state for the j^{th} simulation including effects of uncertainties, C_i' is the median value of this spectral-acceleration, X_j is a uniform random variate for the j^{th} simulation and α_i and β_i are the mean value and standard deviation respectively of the uncertain structural capacity for the i^{th} damage state.

The goal of this calibration was to obtain modified values of α_i and β_i for Damage States 5 (collapse) and 4 (extensive damage) that result in the largest joint probability of occurrence of 10 collapsed bridges and 36 extensively-damaged bridges (as per the Northridge Earthquake bridge-damage observations). In this, estimation of the number of bridge collapses is particularly important, since the REDARS™ 2 default repair model that is described in Appendix G indicates that by far the most extensive downtimes will occur if a bridge has collapsed; i.e., the downtimes associated with the lesser damage states will be much shorter.

K.3.2.2 Analysis Parameters and Uncertainties

K.3.2.2.1 Ground Motion Uncertainties

As noted earlier, uncertainties in ground-motion estimates as well as damage-state estimates are considered in this calibration procedure. This is because median values of ground motions -- represented here as peak values of spectral acceleration at periods of 1.0 sec. and 0.3 sec.-- which are denoted as $S_a(1.0\,\text{sec})$ and $S_a(0.3\,\text{sec})$ respectively) -- may not represent the actual levels of ground shaking that affected the seismic performance of the various bridges during the Northridge Earthquake. Since these actual levels of ground shaking will never be known (without strong-motion accelerometers to actually record the motions), it is essential to consider uncertainties in their estimates so as to represent the broad scatter of possible ground-shaking levels at a particular bridge site. This scatter can be important for explaining why some bridges have performed well during an earthquake, whereas others have not.

K.3.2.2.2 Ground Motion Models

Experience has shown that different ground-motion models will not always provide similar estimates of site-specific ground motions, particularly for earthquake magnitude and distance combinations for which little or no strong-motion recordings are available. Therefore, under this task, special care has been taken to use well-regarded ground-motion models that were developed by respected geoscientists. Two ground-motion models that meet these criteria have been used here -- the Abrahamson-Silva (1997) and the Sadigh et al. (1997) models. In this, the Abrahamson-Silva model was used in most of the calibration analyses, but results were also developed using the Sadigh et al. model so that the sensitivity of the calibration results to these different models could be assessed. For each of these models, "intra-event" uncertainty factors were established in collaboration with Chiou (2005) and are shown in Table K-2.

Table K-2. Assumed Lognormal Standard Deviations for Representing Intra-Event Uncertainties (Chiou, 2005)

Ground-Motion Model	Lognormal Standard Deviation for Representing Intra-Event Uncertainties	
	$S_a(1.0\,\text{sec.})$	$S_a(0.3\,\text{sec.})$
Abrahamson-Silva (1997)	0.56	0.50
Sadigh et al. (1997)	0.54	0.50

K.3.2.2.3 Shape of Fault-Rupture Plane

Yet another parameter of interest is the assumed shape of the fault-rupture plane for the Northridge Earthquake. Both rectangular and non-rectangular shapes have been considered in this analysis. Owing to the complexity of modeling multiple earthquake scenarios as having non-rectangular fault-rupture planes, REDARS™ 2 currently uses rectangular rupture planes.

However, in this calibration analysis, some calculations were also carried out using non-rectangular rupture planes in order to assess the sensitivity of the calibration results to this parameter.

K.3.2.2.4 Calibration Philosophy

If large ranges of α_i and β_i values are considered in this calibration process, the number of possible combinations of α_i and β_i to be considered could become so large as to be impractical. To avoid this possible situation, it was decided to constrain the number of solutions to be considered by assuming that β_i for the modified model will have a fixed value of 0.35, which is approximately the so-called "aleatory" component of the uncertainties in the original development of the HAZUS99-SR2 bridge model (see Dutta and Mander, 1998). Note that the current HAZUS99-SR2 bridge model as documented in NIBS (2002) is based on $\beta_i = 0.6$, which also includes the epistemic component of the uncertainties. However, we have found that this current model (with $\beta_i = 0.6$) already significantly overestimates the number of bridge collapses during the Northridge Earthquake. To modify this result and provide more favorable comparisons with the observed number of bridge collapses, one would not increase this uncertainty factor β_i ; i.e., this uncertainty factor would only be increased if the HAZUS99-SR2 model significantly underestimated the bridge collapses.

Therefore, all calibrations described in this appendix involved adjustments of α_i only. This means that the modified values of α_i and β_i that were developed from this calibration would not represent optimum comparisons with Northridge Earthquake bridge-damage observations. Rather, it was intended that the calibrations should lead to a range of plausible and statistically-acceptable values, particularly since the number of bridge collapses from the Northridge Earthquake represents experience from only one earthquake.

Finally, as noted below, calibrations of α_i against Northridge Earthquake bridge-damage observations were based on a series of conditional-probabilistic analyses that considers a fixed earthquake event corresponding to the Northridge Earthquake and uncertainties in the ground-motion and structural-capacity estimates. In this, α_i values for Damage States 5 and 4 were incremented, and the joint probability of occurrence of 10 bridge collapses and 36 extensively damaged bridges was estimated for each incremented value. Those values of α_i for these damage states that led to the highest joint probability of occurrence of the above number of collapsed and extensively damaged bridges was selected for the subsequent REDARS™ 2 applications under this project. Each of these conditional probabilistic analyses included 4,000 simulations, which was considered to be sufficient to capture most of the extremely low probabilities that the model accounts for the number of collapses and extensively damaged bridges. For situations in which even 4,000 simulations are insufficient to capture some of the extremely low probabilities, a normal distribution was simulated as a proxy to estimate these low probabilities.

K.3.3 Analysis Steps and Results

K.3.3.1 Step 1: Develop REDARS™ 2 Model of Highway System

In Step 1, a REDARS™ 2 model of the highway system shown in Figures K-1 was developed. This model is identical to that used in the demonstration analysis of the LA highway system that is described in Chapter 7; however, now, the model was used only to estimate bridge damage states. The following model characteristics are relevant to this application:

- The model includes all of the system's freeways and major arterials. It contains 1,694 nodes and 5,100 links, whose locations and traffic capacities were obtained from the Highway Performance Monitoring System (HPMS) and the National Highway Planning Network (NHPN), as accessed by the REDARS™ 2 Import Wizard (Cho et al., 2006).
- The basic structural attributes of the 944 bridges in this system were obtained from the National Bridge Inventory (NBI) database, as also accessed through the REDARS™ 2 Import Wizard. Data from Caltrans' statewide bridge database were used to update some of these attributes, and to also identify the 53 bridges in the system that had been column-jacketed when the Northridge Earthquake occurred. The improved seismic performance of the column-jacketed bridges was represented by applying retrofit enhancement factors for Damage States 5 and 4 that were developed by Shinozuka (2004) (see Sec. G.2.2.5).
- The soil conditions within the system are identical to those described in Chapter 7, and are shown in Figure K-4.

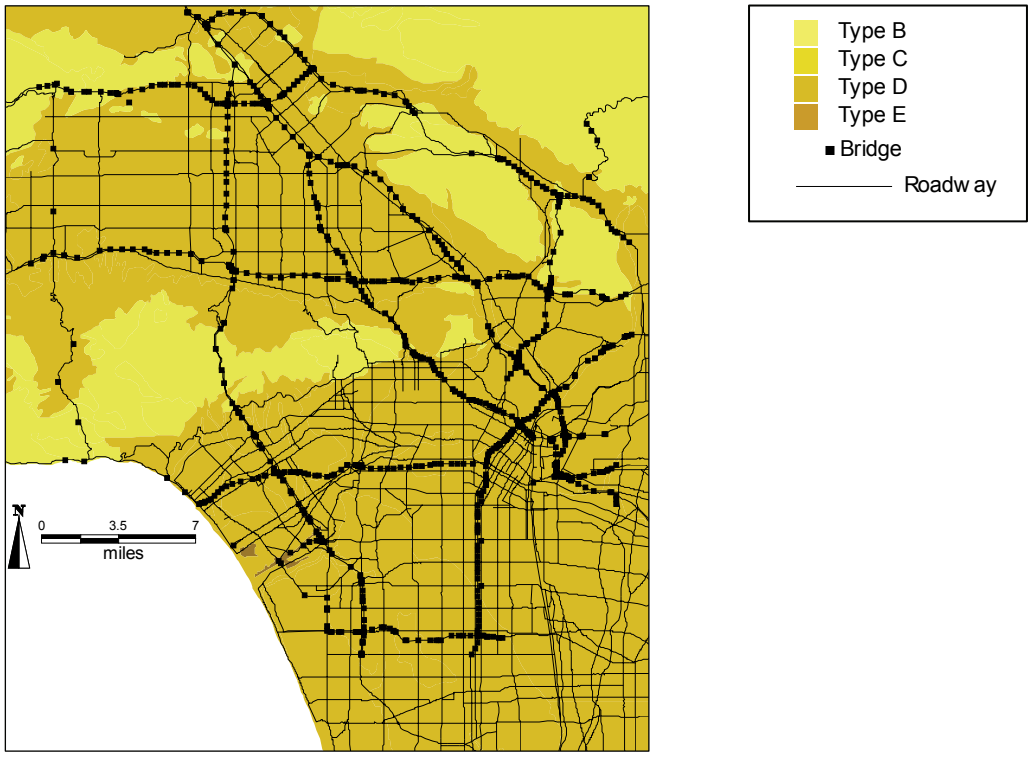

Figure K-4 Soil Conditions at Bridge Sites

K.3.3.2 Step 2: Estimate Probability of Collapse using α_i and β_i Factors used in Current HAZUS99-SR2 Model

The HAZUS99-SR2 model currently uses αi and β_i factors of 1.0 and 0.35 respectively for all damage states. Under Step 2, these factors were used in a REDARS™ 2 conditional-probabilistic analysis in order to estimate the probability of occurrence of 10 bridge collapses. If this probability turned out to be very small, as anticipated, development of modified values of α_i for damage states 5 and 4 under the previously-described strategy was undertaken.

This analysis involved 4,000 simulations in which, for a fixed earthquake event corresponding to the Northridge Earthquake, uncertainties in ground motion and damage state estimates were included. Its results, which are displayed in Figure K-5, showed that this computed probability of occurrence of 10 collapses was indeed very small. It also yielded a median estimate of 39 bridge collapses, which is 3.9 times larger than the observed number of collapses. Thus, the HAZUS99-SR2 bridge model in its current form was shown to substantially overestimate the observed number of bridge collapses during the Northridge Earthquake.

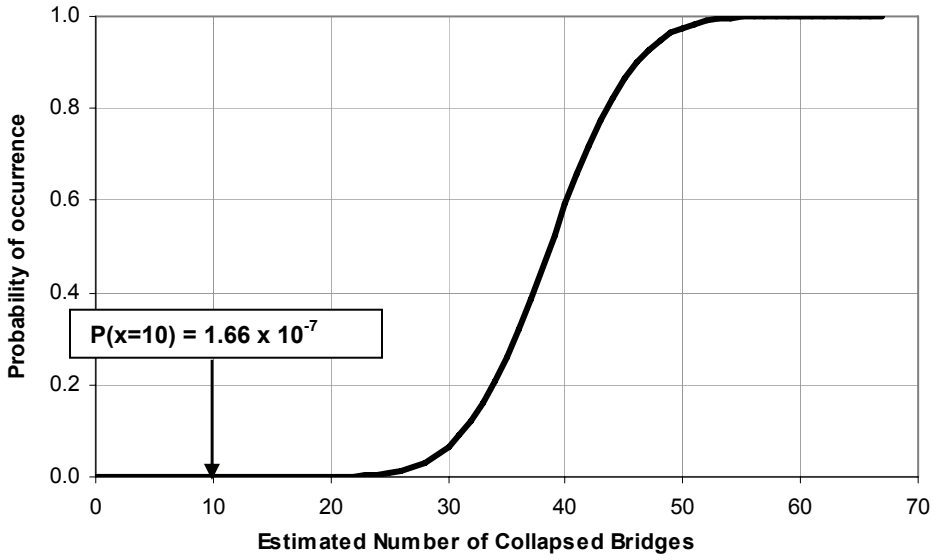

Figure K-5. Number of Bridge Collapses Estimated to have Collapsed using Current HAZUS99-SR2 Bridge Model (α_5 = 1.0 and β_5 = 0.35) using Abrahamson-Silva (1997) Ground-Motion Model and Rectangular Fault-Rupture Model

K.3.3.3 Step 3: Develop Modified Model that Maximizes Probability of 10 Collapses

Under this step, a modification to the HAZUS99-SR2 model (i.e., to the models current values of α_5 and β_5 was developed that maximizes the probability of 10 bridge collapses. This modification was based on the following procedures:

- As previously noted, the parameter β_5, which is the standard deviation of lognormal distribution represented by Equation K-1, was assumed to have a fixed value of 0.35 (which is the same as the value of β_5 that is used in the current HAZUS99-SR2 model).
- For this fixed value of β_5 = 0.35, the parameter α_5 was incremented between values of 0.8 and 2.2 and, for each α_5 value, the probability of occurrence of 10 collapses was computed. In this, 141 different values of α_5 were considered (in which α_5 was incremented by 0.01 within the above limits) and, for each discrete value of α_5, 4,000 simulations (i.e., repeated applications of the Northridge Earthquake) were developed according to Equation K-2, in which x_5 is the number of collapsed bridges.

$$P(x_5 = 10|\alpha_5) = P(x_5 \le 10|\alpha_5) - P(x_5 \le 9|\alpha_5) \quad \text{(K-2)}$$

- From this, the value of α_5 that led to the largest value of the probability of 10 collapses was identified, and normalized to 1. Figure K-6 shows that when α_5 = 1.43, the largest probability of occurrence of 10 collapses was obtained.
- The final operation under this step involved identifying all values of α_5 that are within 80-percent of the above value. This range of α_5 values was used in the joint-probability calculations that were carried out under Step 4.

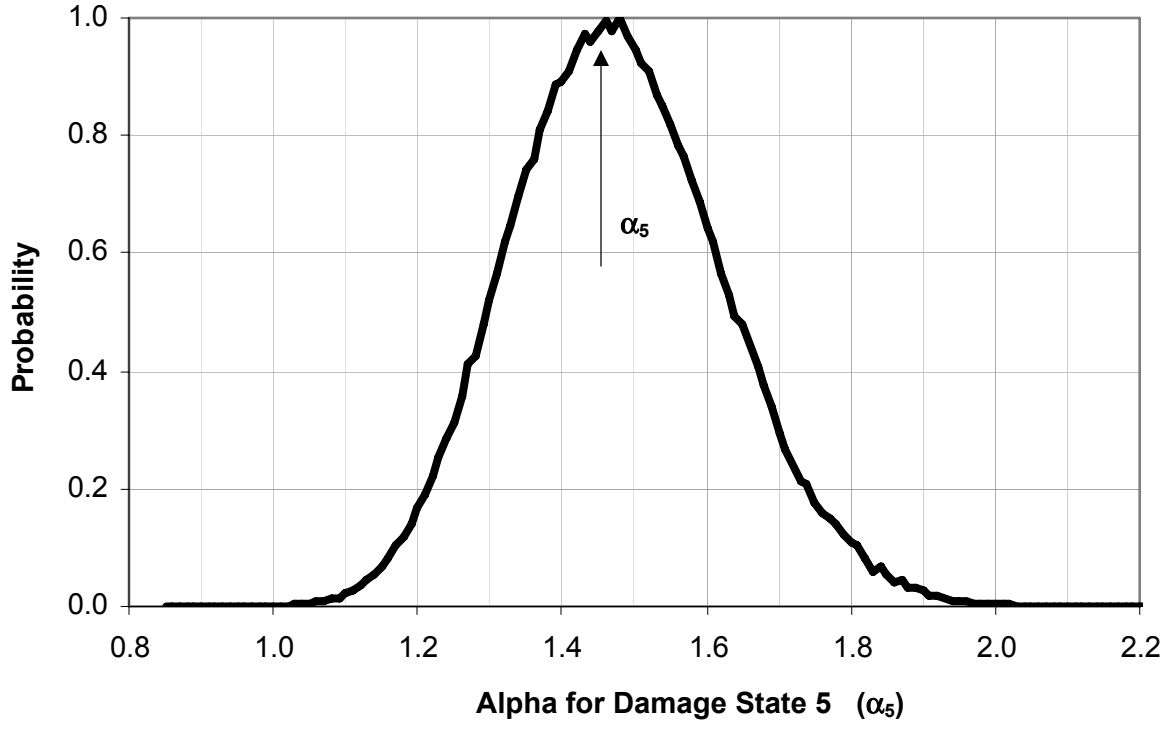

Figure K-6. Normalized Probability of Occurrence of 10 Collapses, as a Function of α_5 (for β_5 = 0.35) using Abrahamson-Silva (1997) Ground-Motion Model and Rectangular Fault-Rupture Model

K.3.3.4 Step 4. Develop Modified Model that Results in the Maximum Joint Probability of Occurrence of 10 Collapsed Bridges and 35 Extensively-Damaged Bridges

Under this step, combinations of parameters α_5 and α_4 were identified that, together with $\beta_5 = \beta_4 = 0.35$, resulted in the highest joint probability of occurrence of 10 collapsed bridges and 36 extensively-damaged bridges according to Equation K-3.

$$P(x_5 = 10, x_4 = 34 | \alpha_5, \alpha_4) = P(x_5 = 10 | \alpha_5) \cdot \{P(x_4 \le 34 | \alpha_5, \alpha_4) - P(x_4 \le 33 | \alpha_5, \alpha_4)\} \quad \text{-- (K-3)}$$

where x_5 is the number of collapsed bridges and x_4 is the number of extensively damage bridges. As noted above, values of α_5 were used here that were within ± 80-percent of the value that led to the largest probability of 10 bridge collapses in Step 3.

The results of this step were provided in terms of the joint density function that is shown in Figure K-7. From this, α_i and β_i values for Damage States 5 and 4 that represent the modifications of the HAZUS99-SR2 model were developed (using the Abrahamson-Silva (1997) and a rectangular fault-rupture model). These α_i and β_i values are shown in Table K-3.

Table K-3. Summary of Modifications to HAZUS99-SR2 Model (based on use of Abraham-Silva (1997) Ground Motion Model and Rectangular Fault-Rupture Model

Damage State	α_i	β_i
5 (Collapse)	1.50	0.35
4 (Extensive)	1.12	0.35
3 (Moderate)	1.0	0.35
2 (Minor)	1.0	0.35

K.3.3.5 Step 5: Perform Sensitivity Evaluations

The calculations under each of the above steps used the Abrahamson-Silva (1997) ground-motion model and a rectangular model of the fault-rupture plane. Under Step 5, revised calculations were carried out that instead used the Sadigh et al. (1997) ground-motion model and a non-rectangular representation of the fault-rupture plane (Fig. K-8). The purpose of these revised calculations was to evaluate the sensitivity of the results to the differences between these ground-motion and fault-source models. Results from these analyses (which are shown in Table K-4) show that the values of α_5 and α_4 values increase by at most 15-percent and typically less than 10-percent due to these model changes.

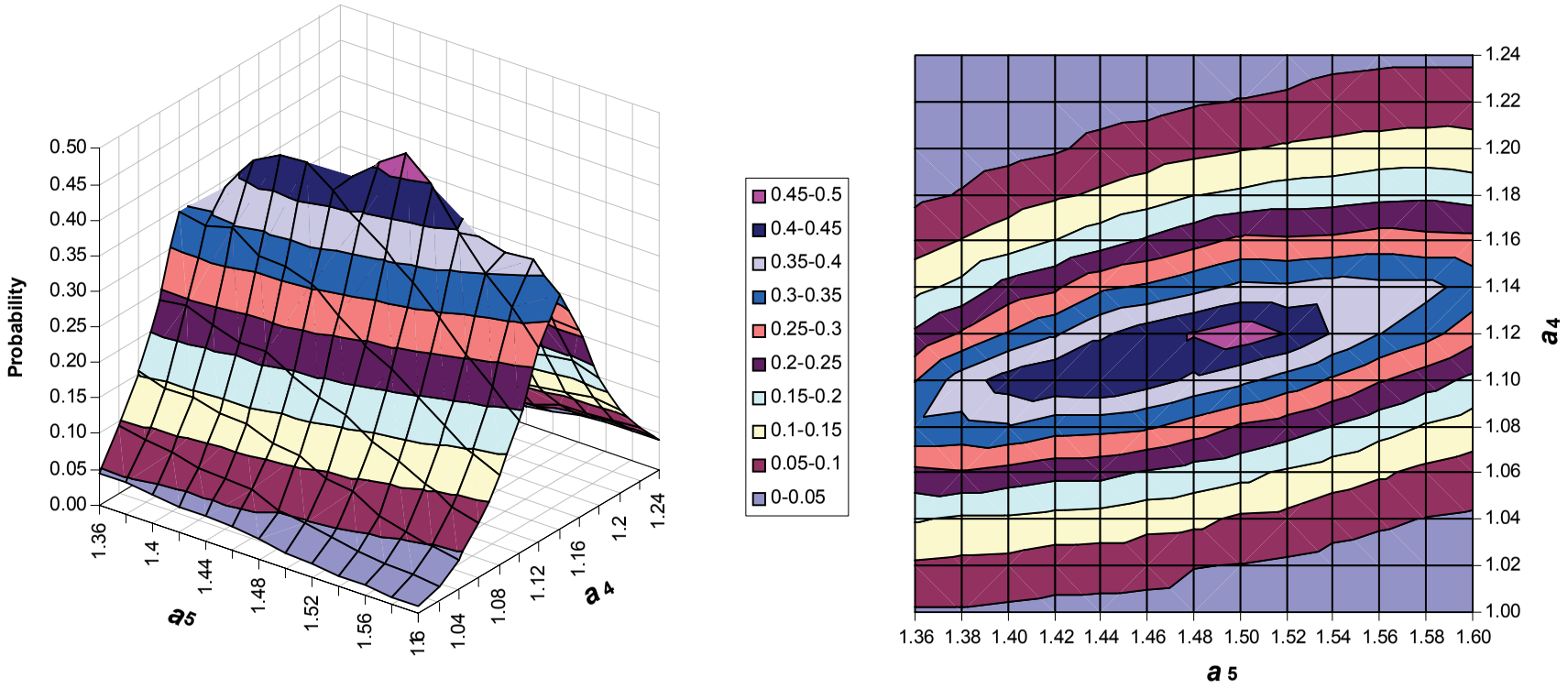

a) Three-Dimensional View

b) Plan View

Figure K-7. Combined Density Function showing Combinations of α_5 and α_4 Values that Result in Largest Joint Probability of Occurrence of 10 Collapsed Bridges and 36 Extensively-Damaged Bridges (using Abrahamson-Silva (1997) Ground-Motion Model and Rectangular Fault-Rupture Model)

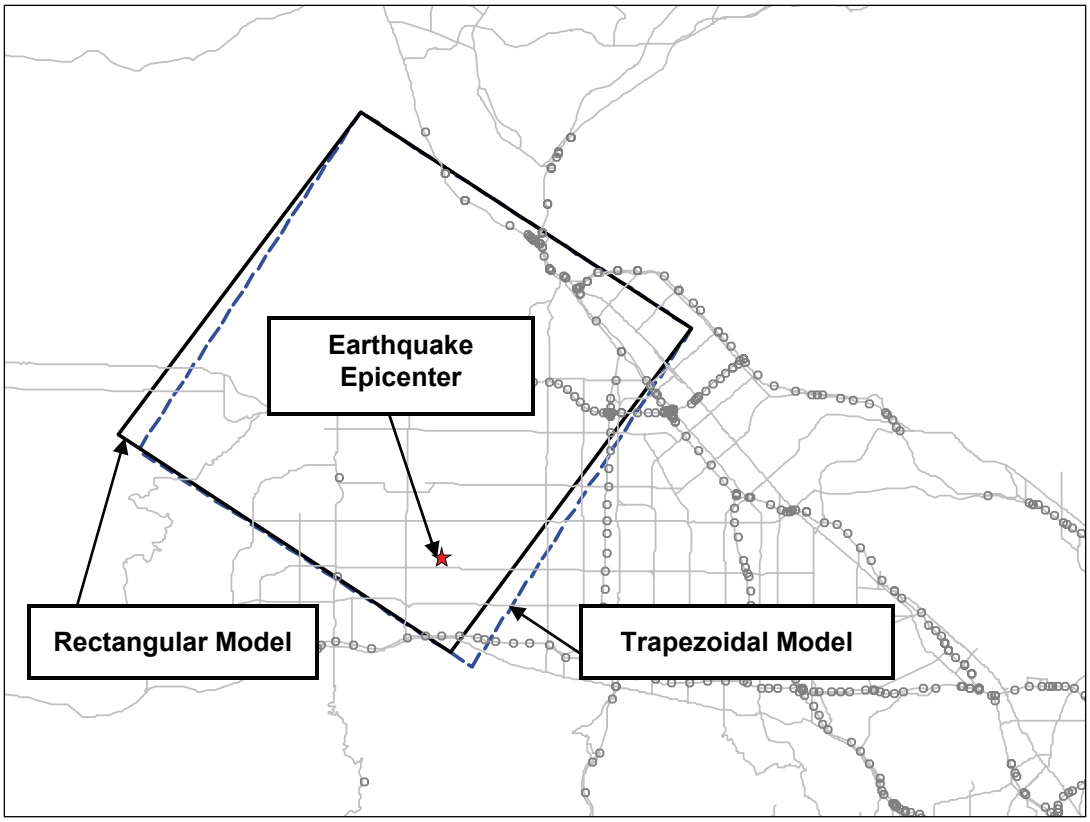

Figure K-8. Rectangular and Trapezoidal Models of Fault-Rupture Plane for Northridge Earthquake (Chiou, 2005)

Table K-4. Sensitivity of Calibrated Bridge Model Parameters to Changes in Ground Motion Models and Models of Fault Rupture Plane (Chiou, 2005)

Damage State	Values of α_i (for fixed $\beta_i = 0.35$)			
	Abrahamson-Silva (1997) Ground-Motion Model		Sadigh et al. (1997) Ground-Motion Model	
	Rectangular Model of Fault-Rupture Plane	Trapezoidal Model of Fault-Rupture Plane	Rectangular Model of Fault-Rupture Plane	Trapezoidal Model of Fault-Rupture Plane
5 (Collapse)	1.50	1.65	1.61	1.72
4 (Extensive)	1.12	1.20	1.14	1.22
3 (Moderate)	1.00	1.00	1.00	1.00
2 (Minor)	1.00	1.00	1.00	1.00

K.4 CONCLUDING COMMENTS

This appendix has shown how refined probabilistic-analysis procedures can be used to calibrate a bridge model's damage predictions against observed bridge damage from an actual earthquake. This analysis was motivated by early assessments of the HAZUS99-SR2 bridge model that showed the model to substantially overestimate the observed number of bridge collapsed due to the Northridge Earthquake. Because this HAZUS model is currently the REDARS™ 2 default model for estimating damage to bridges from ground shaking, it was clear that the above overestimates could have significant effects of the losses due to earthquake damage to a highway system that would be estimated by REDARS™ 2. Therefore some adjustment to the model was needed.

The results from this appendix show that adjustments to the HAZUS99-SR2 bridge model to reduce these overestimates of bridge collapses were successfully carried out. However, it is important to recognize that these model calibrations and adjustments have been based on damage observations from only one earthquake. Clearly, if such calibrations were to be made against bridge-damage observations from other earthquakes or for other highway systems in different regions of the United States, the adjustments to the HAZUS99-SR2 model would most probably differ from those developed here from calibrations against Northridge Earthquake bridge damage observations. However, these additional calibrations would require complete (electronic) databases that define the attributes of the bridges, highway system, and trip demands at the times of these past earthquakes.

An initial attempt under this project to look into this for the 1989 Loma Prieta, California Earthquake showed that such databases are not readily available. Furthermore, the potential for performing additional calibrations with observed bridge damage from other earthquake-prone regions of the country is complicated by the lower seismic activity (relative to California) in most of these other regions, as well as differing bridge construction, maintenance, and repair practice in these regions (also relative to California).

Nevertheless, this situation is expected to improve in the future, as computerized databases of bridge attributes become more common, and the compilation of earthquake-damage data becomes more sophisticated. When such calibrations become possible and feasible, they are highly recommended as a way to use actual earthquake data to its fullest advantage to improve the safety of highway systems located in an earthquake-prone region.

Technical Paper

POST-SAMPLING VARIANCE REDUCTION FOR SEISMIC RISK ANALYSIS OF SPATIALLY DISTRIBUTED LIFELINE NETWORKS

by

Craig E. Taylor[1], David M. Perkins[2], and Stuart D. Werner[3]

Prepared under Task B1-2 of Research Project entitled

Seismic Vulnerability of the Highway System (FHWA Contract DTFH61-98-C-00094)

for

Multidisciplinary Center for Earthquake Engineering Research Buffalo, New York

July 2004

[1] Natural Hazards Management Inc., Torrance California

[2] United States Geological Survey, Golden Colorado

[3] Seismic Systems & Engineering Consultants, Oakland, California

PREFACE

The development of the variance reduction methodology that is described in this report was motivated by the need to introduce certain efficiencies in the REDARS™ 2 probabilistic seismic risk analysis methodology. It was anticipated that these efficiencies would result by showing that the variance in modeled losses estimated from random models can be decreased by the use of special techniques, notably importance sampling and control functions. For the 700-odd modeled losses we used, the variance of the estimated mean loss and mean conditional loss could be notably reduced. From this, we anticipated that, for a given level of variance, the number of modeled losses (and corresponding computer run times) needed to achieve target confidence intervals in the loss results could be notably decreased. Applications of REDARS™ 2 that incorporate the variance reduction methodology have shown that the methodology will meet this objective in most cases.

This report was prepared in 2004 and, at that time, represented the state-of-the-art for incorporation of the above efficiencies into REDARS™ 2. However, the technology for addressing this important issue will continue to evolve over time, and this has led to new insights at this time (2006) and since this report was prepared. From this, new directions have been identified for further improvement of the technology and for addressing certain issues that were not readily apparent in 2004. For example, for several exponential or at least heavily tailed loss distributions that we have studied, we have found that there is a real possibility that decreasing the number of modeled losses by, say, more than a factor of 3, begins to introduce bias in the samples. That is to say, if very large losses which can influence the mean are rare, and hence can be expected to be sparse in a sample of a given size, the variance can appear to be decreased, but the bias can be significant compared to the reduced variance. Therefore, under such conditions, this renders variance reduction as a tradeoff between bias and efficiency, where the bias can on some occasions be large.

This underscores the need to improve current procedures in order to enable them to better estimate the size of the largest modeled losses, their relative frequency of being sampled, and their capacity to influence the mean. In many applications these can be accomplished either by use of prior knowledge or by pilot studies in which some distribution parameters can be suppressed, so that a quick large sample can be obtained by which to make this determination. Once these estimates have been made, it should be relatively easy to determine a minimum size of sample for a given variance and bias.

FOREWARD

Procedures for seismic risk analysis (SRA) of spatially distributed lifeline networks (e.g., the REDARS methodology for SRA of highway-roadway systems being developed under FHWA-MCEER Project 094) typically use random (Monte Carlo) selection of multiple independent simulations, in order to develop probabilistic estimates of losses due to earthquake damage to the network. In this, the number of random simulations is a function of the desired numerical precision of the loss results, expressed in terms of target confidence levels and limits (CLLs). The CLLs, in turn, depend on the variance (or standard deviation) of the estimate in question (e.g., mean loss, 500-year loss) from the loss distribution; i.e., if the variance of the estimate is reduced, then the number of simulations needed to achieve target CLLs will also decrease. In view of the computational needs associated with SRA of moderate to large lifeline networks, reduction in the required number of simulations is desirable in order to reduce the time required for these SRAs.

This report addresses this issue through statistical analysis procedures in the literature called "variance reduction" techniques. The goal of this research is to evaluate the effectiveness of such techniques in reducing the computation time required for SRA of spatially distributed lifeline networks. Results of this research show that post-sampling variance reduction techniques can reduce the number of simulations required for SRA of a spatially distributed lifeline network by a multiplicative factor exceeding three and sometimes more. This factor varies with the annual probability of some network loss which, in turn, depends on such factors as the seismicity of the region, the spatial distribution and intensity of the seismic hazards, the vulnerability of the lifeline system to these hazards, and the areal extent of the network.

ACKNOWLEDGEMENTS

The contributions of Craig E. Taylor and Stuart D. Werner to this research were carried out under Task B1-2 of the project entitled *Seismic Vulnerability of the Highway System.* This project is being conducted by the Multidisciplinary Center for Earthquake Engineering Research (MCEER) of Buffalo NY, and is being sponsored by the Federal Highway Administration of Washington D.C under Contract No. DTFH61-98-C-00094. David M. Perkins was supported in this research by the United States Geological Survey of Golden CO. The support/sponsorship of each of these agencies is gratefully acknowledged.

CONTENTS

Section	Page
1.0 INTRODUCTION	1
1.1 Overview	1
1.2 Outline of Remaining Sections	2
2.0 LEXICON	3
3.0 BACKGROUND	7
3.1 Previous Efforts	7
3.2 Basic Goal Restated	8
4.0 BASIC STEPS IN TESTING OF VARIANCE REDUCTION TECHNIQUES	9
4.1 Step 1. Develop Prototype Network Loss Distribution(s)	9
4.2 Step 2. Develop Basic Statistics for Prototype Loss Distribution	9
4.3 Step 3. Develop Control Function or Distribution for Conditional Loss Distribution	10
4.4 Step 4. Rank-Order Original Conditional Loss Distribution and Control Function	10
4.5 Step 5. Develop Bootstrap Samples from Original-Loss, Conditional-Loss, and Control Distribution	10
4.6 Step 6. Develop Bootstrap Statistics from Bootstrap Samples	10
4.7 Step 7. Develop Bias Corrections	11
4.8 Step 8. Determine Impact of Techniques on CLLs and Simulations Needed to Meet Target CLLs	11
5.0 BASIC COMPOUND POISSON APPROACH	12
5.1 Background	12
5.2 Poisson Distribution	12
5.3 Conditional Loss Distribution Modeled by Exponential Distribution as Control Function	13
5.4 Combining Conditional Distribution and Lambda into Compound Poisson Distribution	13
5.5 Uncertainties in Compound Poisson Distribution	15
6.0 SIZABLE VARIANCE REDUCTIONS FOR CONDITIONAL LOSS DISTRIBUTION	17
6.1 Overview	17
6.2 Use of Exponential Distribution as Control Function for Conditional Loss Distribution	17
6.3 Summary of Variance Reduction for Conditional Loss Distribution	19
7.0 SMALLER BUT SIGNIFICANT REDUCTIONS IN VARIANCE OF ESTIMATE OF MEAN LOSS FOR UNCONDITIONAL LOSS DISTRIBUTION	21
7.1 Overview	21
7.2 Summary of Findings for Unconditional Loss Distribution	21

CONTENTS (continued)

Section	Page
7.3 Sample Calculations for Illustrate How Variance Reductions for Unconditional Mean Loss Reach Asymptotic Limits	22
7.4 Maximum Reductions in Estimate of Variance of Unconditional Mean as Function Of Lambda	23
8.0 CONFIDENCE LIMITS FOR VERY FEW SIMULATIONS	25
8.1 Overview	25
8.2 Square Root Rule-of-Thumb	25
REFERENCES	27
APPENDIX A. ALGEBRAIC DERIVATION OF EQUATION 9 FROM EQUATION 8	28

SECTION 1
INTRODUCTION

1.1 OVERVIEW

Procedures for seismic risk analysis (SRA) of spatially distributed lifeline networks (e.g., the REDARS methodology for SRA of highway-roadway systems being developed under FHWA-MCEER Project 094) typically use random (Monte Carlo) selection of multiple independent simulations, in order to develop probabilistic estimates of losses due to earthquake damage to the network. In this, the number of random simulations is a function of the desired numerical precision of the loss results, expressed in terms of target confidence levels and limits (CLLs). The CLLs, in turn, depend on the variance (or standard deviation) of the estimate in question (e.g., mean loss, 500-year loss) from the loss distribution; i.e., if the variance of the estimate is reduced, then the number of simulations needed to achieve target CLLs will also decrease. In view of the computational needs associated with SRA of moderate to large lifeline networks, reduction in the required number of simulations is desirable in order to reduce the time required for these SRAs.

This report addresses this issue through statistical analysis procedures in the literature called "variance reduction" techniques (see the lexicon in Section 2.0 for this and other technical terms used). The goal of this research is to evaluate the effectiveness of such techniques in reducing the computation time required for SRA of spatially distributed lifeline networks.

The remainder of this report will describe procedures and results leading to the basic finding of this research: ***post-sampling variance reduction techniques can reduce the number of simulations required for SRA of a spatially distributed lifeline network by a multiplicative factor exceeding three and sometimes more***. This factor varies with the annual probability of some network loss which, in turn, is dependent on many factors, including

- Seismicity affecting the lifeline network
- Strong ground motion patterns in the region of the network
- Local soil strong ground motion amplification and de-amplification effects
- Local soil earthquake-induced ground deformation effects
- The vulnerability of key lifeline facilities to strong ground motion and permanent ground deformation effects (in which, key facilities are those whose damage -- alone or in combination -- can lead to some degree of network loss)
- Areal extent of the network (larger networks have higher probabilities of some loss, everything else being equal)

The reduction in the required number of simulations needed to achieve a target CLL will depend on the frequency of occurrence of earthquakes that produce some loss within a given region or for a specific roadway network. For example, in a recent application of REDARS to SRA of the highway-roadway system in Shelby County, Tennessee, it turned out that the annualized probability of loss was only about 0.016 and therefore, as further discussed in Section 3.0, the number of simulations required to achieve acceptable CLLs was large. Indeed, when applied only to the conditional loss distribution (i.e., considering the loss distribution produced

for non-zero losses only), variance reduction techniques evaluated here reduce the estimate of variance by very large multiplicative factors. This report will explain why this result does not translate into much greater reductions in the number of simulations needed for the unconditional loss distribution where the annualized probability of loss is small.

This report does not cover many pertinent topics. Of special note is that this report does not cover pre-sampling variance reduction techniques. These would consist of the development of weighting or other methods in order to select earthquake scenarios. The report also does not cover how the confidence limits may have unequal tails, e.g., the estimate may be safer on the upside (or downside). In addition, this report focuses on estimates of the mean loss, and de-emphasizes fractile estimates of loss.

1.2 OUTLINE OF REMAINING SECTIONS

The remainder of this report is organized into seven main sections and one appendix. The remaining main sections of the report consist of:

- A lexicon of relevant terminology used throughout the report (Section 2.0).
- A summary of previous related efforts and a restatement of the goals of this investigation (Section 3.0).
- An outline of basic major steps in testing various variance reduction techniques (Section 4.0)
- An outline of the basic compound-Poisson approach (Section 5.0). In this, basic formulae are provided which demonstrate an asymptotic limit on how much one can reduce the number of simulations required through post-sampling techniques using this approach.
- An outline of sizeable variance reductions achieved for the conditional loss distribution through combining the use of an exponential control function, normalized, with Latin squares sampling and with fractile-sampling for the exponential control function (Section 6.0)
- An explanation why these sizeable variance reductions for the mean conditional loss have resulted in more modest reductions in confidence limits for the mean annual loss at a pre-specified confidence level (here, 95 centile) (Section 7.0)
- An illustration of the power of these techniques with respect to small numbers of samples or simulations; few simulations are needed to yield mean loss estimates with a CLL of a factor of two for a 95^{th} centile confidence level (Section 8.0)

Following this, Appendix A provides supplementary algebraic derivations in support of the material presented in Sections 5.0 through 8.0.

This report emphasizes both successes and failures in the attempt to apply variance reduction techniques. The report also emphasizes the exploratory nature of findings to date. Not only are further tests applied to other catastrophe loss distributions still very desirable, but also further questions arise in the course of the findings in this document.

SECTION 2
LEXICON

Inasmuch as this topic is unfamiliar to many people, this section provides very brief characterizations of various terms used in this working report. These definitions of the terms used should not be regarded as being complete; rather, they instead are intended to serve as initial summary definitions only. Here, it is assumed that the reader have some background in some statistical terminology such as "mean," "variance," and "Poisson distribution."

AAL (average annualized loss). Mean annualized loss.

Absolute or unconditional loss distribution. A probability distribution in which losses comprise the X-(horizontal) axis and discrete probabilities comprise the Y-(vertical) axis. This unconditional distribution does not depend on any special parameter or condition (see "conditional loss distribution").

Antithetic variates. When one selects a uniform random generator U between 0 and 1, one next selects the uniform random generator 1-U. This technique permits the selection of "balanced" uniform random variates and is especially helpful if one desires to simulate such central values as the median and the mean.

Asymmetry of Confidence Limits. Asymmetry of confidence limits is when the limits exclude different amounts of the distribution. This is most often employed when the distribution is asymmetric and one desires to exclude more of the distribution on the long-tailed side. (See equal-tailed confidence limits.)

Bias. Deviation of an estimated population parameter from the true population value. Bias correction generally consists in employing a technique that estimates directly or indirectly the best estimate as a basis to correct the bias.

Bootstrap sampling methods. For purposes here, chiefly methods which consist of developing statistics based on repeated sampling with replacement from an original set of data. (See Efron and Tibshirani, 1993; Davison et al., 1998)

Compound Poisson process. A method of analyzing an absolute or unconditional loss distribution into (a) a distribution for the probability of some loss (see "lambda") and (b) a distribution for the severity of that loss. This process assumes that the probability of some loss can be treated as a Poisson process (using the Poisson distribution). (This approach is common in the actuarial literature; see Daykin et al., 1994; Panjer and Willmot , 1992; Lemaire et al., 1993; Taylor et al., 1994)

Conditional loss distribution. A probability distribution in which losses comprise the X-axis and probabilities comprise the Y-axis, and which depends on some pre-specified condition/parameter. In this report, the condition of interest is "Should a network loss occur." Thus, the conditional loss distribution of interest in this report is one in which the values on the

X-axis always exceed zero. For purposes here, the conditional loss distribution is the severity distribution of a Compound Poisson Process.

Control functions. These are functions or, in this report, parametric distributions that are used as a first-order estimate of the actual distribution. [This first-order estimate is not a "fitting" process so much as a procedure for implementing importance sampling or decreasing the amplitude of bootstrapped quantities.) Typical uses are those of subtraction (utilizing the differences between the control function and the actual distribution) and division (providing weights to insure more frequent sampling of the more important parts of the data). In either use, the variance of the result is less than the variance of simple resampling.

Equal-Tailed Confidence Limits. These are confidence limits that are evenly divided between the upper bound and the lower bound, most often used when in which the estimate in question lies in the middle (is the mean and median) of these confidence limits. (See asymmetry of confidence limits)

Fractile-Based Sampling. A method as applied to a parametric distribution that results in equally spaced fractiles. For instance, if 50 samples are selected, then samples are drawn at the 1^{st} centile, 3^{rd} centile, 5^{th} centile,...,97^{th} centile, and 99^{th} centile levels.

Lambda. For this working report, "lambda" refers to the annualized probability of some network loss from earthquakes.

Latin Squares (in this report, also called Balanced Sampling, Permutation Sampling and Latin Hypercube sampling). If one begins with a data set such that for any value x_i which occurs, Y_i% in the data set, then this sampling technique assures that after the planned number of bootstrap samples, the overall percent of the occurrences of the value x_i in all such samples taken collectively is assured to be Y_i%. (Latin squares sampling for multiple distributions replaces exhaustive combinations with exclusive sampling of fractiles for each distribution, i.e., for a given sample, if a fractile is sampled for distribution *i*, that fractile is not used for distribution *j*.)

Monte Carlo methods. These methods basically use random values of the distributions of input parameters along with models and assumptions in order to develop a result, here, an estimate of a network loss. For purposes here, without variance reduction techniques, the use of repeated Monte-Carlo samples to obtain some level of accuracy can be very computer- and time-intensive.

Nominal confidence levels and limits. These are confidence levels and limits as determined from the input models, parameters, and assumptions. Roughly speaking, these estimates of confidence levels and limits are no better than the input models, parameters, and assumptions.

Parametric procedures. These procedures basically "fit" the data to some simplified mathematical formula or formulas. Parametric procedures bring information with them and so permit greater generalization with sparse data. For large data sets, fitting may oversimplify, with some loss of information.

Post-sampling variance reduction techniques. These techniques simulate additional network loss data samples by bootstrapping an existing sample in such a manner as to reduce the variance in the estimate in question. (See pre-sampling variance reduction techniques.)

Pre-sampling variance reduction techniques. These variance reduction techniques stress the selection of the more consequential or more representative earthquake scenarios in advance of any sampling of losses in order to reduce the variance compared to that obtained by simple random sampling. Such techniques as importance sampling and Latin Squares (or balanced) sampling in magnitudes and distances can be used as pre-sampling variance reduction techniques.

Purposive sampling. Sampling that is not random, and that may introduce biases for specific types of results, but that may be helpful in developing other types of results. For instance, Latin Squares or Balanced pre-sampling may assist in estimating the annualized mean loss, but may not produce realistic simulations of losses and their variabilities over specific time-frames (e.g., over 50-year exposure periods). For another instance, an historic earthquake may be simulated in order to evaluate how a roadway system responds to an event that is familiar.

Risk evaluations. Evaluations that require the development of a probability distribution of adverse consequences (of seismic hazards), such as dollar losses. Results may be displayed in terms of key statistics (e.g., the mean annualized loss and its variance) or in terms of a loss distribution (with loss severity as one axis and probability of occurrence as another axis.)

Scenarios. Used in this report to describe hypothetical or actual earthquake events defined in terms of earthquake magnitude and location of fault rupture. These hypothetical or actual earthquake events are not confined to known fault zones. (See "simulations.") A Monte-Carlo method is often used to generate a suite of scenarios.

Semi-Standard Deviation. The square root of the semi-variance (see semi-variance).

Semi-Variance. The variance that only considers loss values either above or below the mean.

Simulations. Used in this report to describe the development of a sample loss from a scenario. Given uncertainty distributions in the resulting strong ground motions, component vulnerabilities for a given ground motion, and system response to damage to all component damages, a random value is obtained for each distribution and a sample loss developed. (Since the process can be repeated for the scenario, using other random values, one scenario may have many simulations and hence yield many estimates of network losses. However, in this report only one simulation is used for each scenario.)

Stratification techniques. These basically consist of the use of mutually exclusive groups of losses to characterize the (loss) data. Strata are often chosen to have similar means, similar variances, or proportionate numbers in each group, in such a manner as to optimize information gain and reduce uncertainty.

Variance reduction techniques. In Monte Carlo sampling, a suite of data is developed from which some statistical parameter can be derived. This derived parameter will have a variance that represents its uncertainty. Variance reduction techniques use bootstrapping, importance sampling, control variates and other procedures to reduce the variance *in the estimate* of a specific parameter. (e.g., Lui, 2001; Davison et al., 1998; Efron and Tibshirani, 1993.)

SECTION 3
BACKGROUND

3.1 PREVIOUS EFFORTS

In the development of the REDARS methodology for SRA of highway-roadway networks (Taylor et al., 2001; Werner et al., 2000), a simulation method was formulated that:

- is open, straightforward, and tractable
- randomly selects earthquake scenarios so that a loss distribution can be produced
- yields a time-series of simulated losses
- permits intermediate outputs that are completely consistent with results of a probabilistic seismic hazard analysis (PHSA), given the same input earthquake hazard models and assumptions, and
- permits the incorporation of known uncertainties in exposure, hazard, component vulnerability, and system vulnerability models

A key factor in the REDARS development effort has been the *random* (e.g., Monte Carlo) selection of earthquake scenarios, defined as specific events with an earthquake magnitude and rupture location (or epicentral location for smaller magnitude events). This random selection has provided trials (time-units such as years or else exposure times for systems that change over time) that are independent. This independence has permitted the application of a binomial distribution for the estimation of nominal confidence levels and limits for specific loss values.

In particular, it was assumed that the sampling distribution of the mean is normal, in accordance with the Central Limit Theorem. Thus, the nominal confidence limit interval for an AAL (average annualized loss) estimate is defined from the following formula:

$$AAL \pm \frac{t_\alpha s_A}{\sqrt{n}} \tag{1}$$

in which

n = number of Bernoulli trials (years simulated);
t_α = value of Student's t-distribution corresponding to any designated nominal confidence level and value of n; and
s_A = standard deviation of the estimated loss distribution.

Note that Equation (1) indicates that the confidence limit interval for the *AAL* estimate is proportional to the standard deviation of the sampled loss distribution, and is inversely related to the number of Bernoulli trials. The equation is often used to show the number of trials needed to obtain a sufficiently narrow confidence limit interval. However, it is also clear from this equation that, if the standard deviation of the estimate of the mean loss is reduced, then the number of trials needed to achieve a desired confidence limit interval is also reduced. This is the basic motivation for the investigation of variance reduction techniques described in this report.

To illustrate the application of Equation (1), results are presented here from the previously noted application of the REDARS methodology for SRA of highway systems to the highway-roadway network in Shelby County, Tennessee. This application used 50,000 Bernoulli trails, of which as reconstructed in this project only 768 trials resulted in non-zero losses to the Shelby County roadway system (owing to the moderate overall seismicity of the region). For these trials, the REDARS SRA (without the use of the variance reduction methods described subsequently in this report) led to the following estimates of economic losses caused by travel time delays due to earthquake damage to the Shelby County system:

AAL = \$2.11M
t_α = 1.96 for a 95th centile confidence level, and
s_A = \$29.88M

Based on Equation (1), the following equal-tailed 95th centile confidence limits are derived:

$$(\$2.11 \pm \$0.262) \times 10^6$$

which indicates that, for this application, there is a 95th-centile nominal confidence that the true value of the AAL is within ±12.4 percent of the computed value. This CLL was judged to represent acceptable numerical precision of the computed AAL. However, it turned out that the computer run time needed to perform the SRA for these 50,000 Bernoulli trials was excessive. This underscored the need to investigate whether alternative statistical analysis procedures can be used that require fewer simulations (and hence reduced run times) to achieve a given target CLL.

3.2 BASIC GOAL RESTATED

The basic goal of this report is to reduce the number of simulations needed to achieve the confidence levels attained by the employment of Monte Carlo methods. The reduction of the variance of the estimate that is obtained from a specific number of simulations is but a means to achieve this basic goal. In effect, this report will first show that very significant reductions in variance can be achieved for the conditional loss distribution. Secondly, the report will show that these significant reductions result in reduced but nevertheless still important reductions in the number of simulations needed for the unconditional loss distribution.

For this report, as with above-mentioned previous efforts, the simulation estimate of special interest is the estimate of the mean (annualized) loss (AAL). A more extended treatment would be required to demonstrate the reduction of the variance of other fractile estimates of special interest (e.g., the loss with a return interval of 500 years).

This presentation relies heavily on the use of the single sample earthquake loss distribution derived from previously noted application of REDARS to the SRA of the Shelby County, Tennessee highway-roadway system. However, this prototype loss distribution has many of the same features as over forty earthquake loss distributions previously surveyed (see Lemaire et al., 1993; Taylor et al., 1994).

SECTION 4
BASIC STEPS IN TESTING VARIANCE REDUCTION TECHNIQUES

This section presents basic steps in testing variance reduction techniques. These steps summarize what might otherwise be much more extended and detailed computer programs.

4.1 STEP 1. DEVELOP PROTOTYPE NETWORK LOSS DISTRIBUTION(S)

The first step of this procedure is to develop a prototype network loss distribution or distributions for evaluation. In previous work, many earthquake loss distributions had been evaluated and determined to more or less fit a compound Poisson distribution, with either an exponential or a gamma distribution as a good fit to the conditional loss distribution (See Lemaire et al., 1993; Taylor et al., 1994). This research begins with the loss distribution resulting from the REDARS SRA of the Shelby County highway-roadway system that was referred to earlier in this report (see Werner et al., 2000). As previously noted, this distribution has 768 non-zero simulations (years in which losses exceed zero) with the remainder of the 50,000 simulations (years) having no loss. This research has confirmed that this loss distribution is a compound Poisson distribution whose intensity distribution can be fitted. However, "fitting" or parametric distributions are not the goal of this research. Instead, the goal is to reduce variance largely through non-parametric (bootstrap) procedures. Other conditional loss distributions (e.g., Weibull) should respond in a similar manner to the subsequent steps in this procedure.

This overall sample annual-loss distribution can also be broken down into smaller distributions covering fewer simulations (years sampled). Based on the walkthrough method (a time-series evaluation), one can truncate the overall distribution (and its corresponding conditional loss distribution) at any specified number of years (simulations), e.g., 5,000 years, 10,000 years, and so on. (See Taylor et al., 2001 and Werner et al., 2000 for a description of the walkthrough method.)

4.2 STEP 2. DEVELOP BASIC STATISTICS FOR PROTOTYPE LOSS DISTRIBUTION

Step 2 of this procedure develops basic statistics for this sample prototype network loss distribution and for the conditional loss distribution which contains all non-zero losses. Basic statistics here for this loss distribution are the arithmetic mean and standard deviation. Lambda can also be readily calculated, along with the arithmetic mean and standard deviation of the conditional loss distribution. Coefficients of skewness are also of considerable interest in simulation studies of such extreme distributions, but are not emphasized in this report. For the mean of the overall (unconditional) loss distribution, it is also necessary to calculate the confidence limits for some specified confidence level. For this presentation, the confidence level specified is the 95^{th} centile confidence level.

This procedure is applied in this research not only to the overall distribution containing 50,000 years simulated but also to 5,000 year samples, 10,000 year samples, and so on.

4.3 STEP 3. DEVELOP CONTROL FUNCTION OR DISTRIBUTION FOR CONDITIONAL LOSS DISTRIBUTION

This third step applies for all cases except those using antithetic variates alone, Latin square sampling alone, or the unconditional distribution alone (or some combination thereof). Most variance reduction techniques examined use a control function or distribution. This research has evaluated in some detail the application of the exponential and gamma distributions, and has also found that a Weibull distribution should also work. For most purposes, use of an exponential distribution as a control function for the conditional loss distribution suffices to illustrate methods evaluated.

4.4 STEP 4. RANK-ORDER ORIGINAL CONDITIONAL LOSS DISTRIBUTION AND CONTROL FUNCTION

For these purposes, the control function or distribution must be simulated to approximate the original distribution. This control distribution sample may be re-weighted to yield a control distribution that has a mean equal to the mean of the original conditional loss distribution. Rank ordering is required in order to compare the control distribution and the conditional loss distribution. This comparison may be done in terms of residuals (differences between corresponding elements in the control function and the original distribution) or weights (ratios of corresponding values in the control function and the original distribution). Thus, subtraction and division are the two independent methods used in major variance reduction techniques.

4.5 STEP 5. DEVELOP BOOTSTRAP SAMPLES FROM ORIGINAL-LOSS, CONDITIONAL-LOSS, AND CONTROL DISTRIBUTION

In this fifth step of the procedure, bootstrap samples are developed from the original loss distribution, the conditional loss distribution, or the control distribution. How bootstrap samples are performed will depend on the specific variance reduction technique (or combination of techniques) that are employed.

4.6 STEP 6. DEVELOP BOOTSTRAP STATISTICS FROM BOOTSTRAP SAMPLES

Following Ephron and Tibshirani (1993, p. 12ff), the bootstrap standard error of a statistic, s, is calculated as

$$\mathrm{SE(bootstrap)} = \sqrt{\frac{\sum_{b=1}^{B}\left[s(x^b) - s(\cdot)\right]^2}{B-1}} \qquad (2)$$

If s is the mean of a data set, x, then

B is the number of Bootstrap samples
$s(x^b)$ is the mean of the b^{th} bootstrap sample, and
$s(\cdot)$ is the mean of all B bootstrap samples.

(In addition, N is the size of the data set. For instance, a 5000-year sample of random walks would be a data set of size 5000.)

Equation (2) can be modified to also estimate the (upper or lower) semi-standard error (square root of the semi-variance) which is of interest in evaluating the degree to which the standard error is asymmetric. Procedures developed in Taylor et al., 2001 and Werner et al., 2000 and embodied in Equation (1) relied chiefly on what is called "normal" or "Gaussian" theory. That is, in particular, use of the "*t*" values assumes that the sampling distribution of the mean is normal (Law and Kelton, 1991). Given that we are dealing with very extreme loss distributions, this assumption may prove to be non-conservative. So, the "precision" of the methods previously used, based on *t*-values, can be called into question.

These above remarks are corroborated in Efron and Tibshirani (1993, pp 66-67) who state that pre-computer statistics were based on a limited number of distributions and so the "*t*" values used were based on asymptotic normal distribution theory, or on assessing the asymptotic behavior of this small class of distributions. In this project, asymmetries have been noted in the confidence level tails, but have not been the focus of efforts.

4.7 STEP 7. DEVELOP BIAS CORRECTIONS

The seventh step of this procedure develops corrections for any biases that may appear in the bootstrap samples. The techniques used in this report yield unbiased estimates of the mean loss.

4.8 STEP 8. DETERMINE IMPACT OF TECHNIQUES ON CLL'S AND SIMULATIONS NEEDED TO MEET TARGET CLL'S

The eighth and final step of this procedure is to determine from this bootstrap sampling procedure how much the variance reduction technique has reduced the estimate of the variance (for the conditional and/or unconditional loss distribution) and especially the confidence limits for the specified confidence level.

SECTION 5
BASIC COMPOUND POISSON APPROACH

5.1 BACKGROUND

From the actuarial literature, many investigators have disaggregated the basic loss distribution into a distribution for the number or frequency of claims and a distribution for the claim size. Analogously, this report distinguishes between the frequency of earthquakes having some network loss and the distribution for the network loss given some non-zero loss event.

5.2 Poisson Distribution

In this approach, the Poisson distribution is used to model the frequency of occurrence of some network loss. For a roadway network, this may be approximated through an estimation of how frequently there is some damage that causes downtime (e.g., closed lanes) in the network system. As stated earlier, the probability of some network loss (lambda) is a function of many parameters, such as

- The seismicity of the region encompassing the network
- The areal extent of the network
- Pertinent strong ground motion attenuation patterns
- Site amplification or de-amplification factors
- Soil deformation potential at roadway sites
- The operational vulnerability of key roadway structures and facilities

The application of a Poisson distribution for this evaluation assumes that the occurrence of earthquake-damage-producing events is independent of time. This assumption is consistent with methods used in the National Earthquake Probabilistic Hazard Mapping Program, as well as by methods used by many other practitioners. Not explored in this presentation are modifications to this approach that would account for dependencies of earthquake occurrence in space and time.

The Poisson probability for number of events in time, t, is expressed as follows (See Panjer and Willmot, 1992; Ang and Tang, 1975, pp. 114ff.; Law and Kelton, pp. 349ff.):

$$P(E = J) = (\lambda t)^J \frac{e^{-\lambda t}}{J!} \tag{3}$$

in which

E = a variable for the number of events in time interval t
λ = the mean rate of occurrence for each time unit
J = 0, 1, 2, ...

5.3 CONDITIONAL LOSS DISTRIBUTION MODELED BY EXPONENTIAL DISTRIBUTION AS CONTROL FUNCTION

Following Lemaire et al. (1993), both the exponential and the gamma distributions are evaluated as control functions. To repeat, control functions are functions or distributions used to provide a first-order estimation for the data to be sampled. In this evaluation, the exponential distribution has been found to fare as well as the gamma distribution as a control function (see section 6.0).

For the exponential distribution (see Law and Kelton, 1991; Hastings and Peacock, 1974), the density function is

$$f(x) = \left(\frac{1}{b}\right) e^{-\frac{x}{b}} \tag{4}$$

and the cumulative distribution function (cdf) is

$$F(x) = 1 - e^{-\frac{x}{b}} \tag{5}$$

with mean value b, variance b^2, and coefficient of skewness 2.

5.4 COMBINING CONDITIONAL DISTIBUTIONS AND LAMBDA INTO COMPOUND POISSON DISTRIBUTION

For combining the two distributions, the following density function applies (see Panjer and Willmot, 1992, pp. 166ff.):

$$g(l) = \sum_{k=0}^{\infty} f(l \mid J = k) P(J = k) \tag{6}$$

in which

$f(l \mid J = k)$ is the conditional loss distribution, or the loss distribution given that k non-zero loss events occur within a time period t, and

$P(J = k)$ is the probability that exactly k non-zero loss events occur.

For this combined distribution, it turns out (see Daykin et al., 1994, pp. 59ff.; Panjer and Wilmot, 1992, pp. 167ff.) that the mean annual loss is given by

$$\bar{l} = \lambda\mu \tag{7}$$

in which μ is the mean of the conditional loss distribution. (For instance, if the exponential distribution with parameter b exactly fits the conditional loss distribution, then $\mu = b$.)

In this report, special attention is devoted to the derivation of the variance of the estimate of the unconditional mean loss or AAL inasmuch as this variance directly leads to estimates of CLLs. In this derivation, which is expounded more fully in Appendix A, the estimated variance of the unconditional mean loss is by definition

$$V = \left[\sum_{i=1}^{N} (l_i - \lambda\mu)^2\right] / N \tag{8}$$

in which

l_i is the network loss for the ith simulation (year),
n is the number of simulations (years) in which network losses exceed zero
N is the total number of simulations (years)
$\lambda = n/N$ is the annual probability of some network loss
μ is the mean loss of the conditional loss distribution
$\mu\lambda$ is the mean loss of the unconditional loss distribution (Equation (7))

For simplification purposes, it is useful to define

$$Z^2 = \left[\sum_{i=1}^{N} (l_i)^2\right] / N$$

Appendix A provides the algebraic reasoning whereby Equation (8) yields the following equation for estimating V, the variance of the annual loss:

$$V = Z^2 - n^2\mu^2 / N^2 = Z^2 - \lambda^2\mu^2 \tag{9}$$

This elegant little equation shows part of the role of λ in the variance of the annual loss. As λ approaches 1, V becomes the usual equation for variance—the average of the square of the variable less the square of the average of the variable. The role as λ decreases is not so clear, however, because Z^2 decreases as well. In Appendix A, we also find that

$$Z^2 = \lambda\left(V_1 + \mu^2\right) \tag{10}$$

where V_1 is the *conditional* variance around the *conditional* mean. We see that Z^2 decreases at the same rate as λ!

To see the role of λ, we restate the equation for the variance of the unconditional annual loss,

$$V = \lambda\left(V_1 + \mu^2(1-\lambda)\right)$$

Note, now, that as $\lambda \to 1,\ V \to V_1$, as expected. However, what we did not see before is that as $\lambda \to 0,\ V \to 0$!

Most importantly, see what happens for ordinary values of λ, when we attempt to decrease the variance in the conditional loss distribution. As

$$V_1 \to 0,\ V \to \mu^2 \lambda(1-\lambda)$$

Thus it is not possible to reduce the variance of the unconditional mean below some limiting value governed by λ and μ.

This research has confirmed that one may reduce the estimate of the conditional variance by very significant multipliers without reducing the estimate of the overall variance to anywhere near the same extent. (For practical examples of this, see Section 6.3.)

5.5 UNCERTAINTIES IN COMPOUND POISSON DISTRIBUTION

For developing a compound Poisson approach, estimates must be made of λ and b, respectively. Evaluations made in this project have shown that to estimate both values in the same computer evaluation is somewhat time-consuming. For this reason, uncertainties in the estimation of λ have been examined in greater detail. In particular, to estimate these uncertainties, the standard error of the estimate of the mean λ of the Poisson distribution (see Efron, 1993) may be calculated as:

$$SE(\lambda) = \sqrt{\frac{\lambda}{N}} \tag{11}$$

in which N is the number of sampled time units (in this case, years).

For this presentation, N is assumed to be at least 10,000 years. Table 1 illustrates how the standard error increases for the lower seismic risk regions (combinations of lesser seismicity, smaller areas covered, and/or higher seismic resistance of the network). Therefore, this table along with separate bootstrap calculations, suggests that

- More trials (years sampled) are desirable in lower seismic zones (chiefly, but not exclusively, regions of lower seismicity) and
- A strategy for reducing computational time consists in using a rapid pre-processor which identifies only those years/scenarios having some network damage as a means to develop λ with a high degree of nominal confidence; afterwards, the user can determine how many of the resulting scenarios to evaluate in order to focus on the more computationally intensive conditional loss distribution.

Table 1. Variation of the Standard Error of the Mean for the Poisson Distribution with this Mean (10,000 trials or years sampled)

Seismicity (depending also on area covered and network vulnerability)	Estimate of Poisson Parameter λ (mean frequency of loss occurrences per year)	Standard Error of the Estimate (see Equation (11))	Ratio of Standard Error of the Estimate to the Mean (λ)
Low-to-moderate	0.005	0.0007	0.141
Test Case—Memphis roadway system	0.0156	0.0012	0.080
Moderate-to-high	0.05	0.0022	0.045
Very high (and large and/or very vulnerable)	0.5	0.0071	0.014

SECTION 6
SIZEABLE VARIANCE REDUCTIONS FOR CONDITIONAL LOSS DISTRIBUTION

6.1 OVERVIEW

The main purpose of Section 6.0 is to outline some of the major features of a method that yields sizeable reductions in the variance of the estimate for the mean of the conditional loss distribution. This method employs the exponential distribution as a control function for the conditional loss distribution. Fractile-based Latin squares sampling is also used to assure a representative distribution of elements in the resampling of the original data set.

As this section will show, this combination of variance reduction techniques results in sizeable reductions in variance (i.e., for a sufficient number of years sampled, variance reductions exceeding a factor of 100). As a result of other efforts in this investigation, it is believed that the use of importance sampling (the use of weights rather than residuals), the use of a Weibull distribution, and/or other techniques might further improve these results. (Early results with the application of a gamma distribution showed no improvement over the use of an exponential distribution perhaps because the exponential distribution is a special case of a gamma distribution.) However, Section 7.0 will indicate why these marginal increases were not pursued in detail: there is an asymptotic limit on how effectively one can reduce the number of simulations needed for producing the same CLLs in the unconditional mean loss (given a specific confidence level) for low-probability events such as earthquakes affecting localized roadway networks.

6.2 USE OF EXPONENTIAL DISTRIBUTION AS CONTROL FUNCTION FOR CONDITIONAL LOSS DISTRIBUTION

On page 340 of Efron and Tibshirani (1993), a numerical integration method is outlined that uses control functions. In this, suppose we are attempting to measure some e, such as AAL, as an integral of the function with respect to measure G,

$$e = \int f(z)\,dG \tag{12}$$

The goal is to find a function $g(z)$ that approximates $f(z)$, but for which the integral can be determined without error, analytically. If such a function is found, then it follows from equation (11) that

$$e = \int g(z)dG + \int [f(z) - g(z)]dG \tag{13}$$

To modify Efron and Tibshirani slightly, let us define

$$A_1 = \int g(z)dG \tag{14a}$$

and

$$A_2 = \frac{1}{B}\sum_{1}^{B}[f(z_i) - g(z_i)] \text{ which is approximate to } \int [f(z) - g(z)]dG \quad (14b)$$

Then, an approximation to "*e*" is

$$\hat{e} = A_1 + A_2 \quad (14c)$$

The uncertainty is A_1 is zero. The uncertainty in A_2 is defined as follows:

$$\text{var}(\hat{e}) = \frac{1}{B}\text{var}[f(z) - g(z)] \quad (14d)$$

which will be much smaller than $\text{var}[f(z)]/B$ if the function *g(z)* is a good approximation to *f(z)*.

To illustrate, three different "control functions" were selected in order to compare and contrast how much variance was reduced through such methods. The first was simply to let g(z) = 0. In effect, this first "control function" provides the basis for estimating what happens if no control function is selected. The second was to use a straight-line control function, letting *g(z)* = z_i for z_i ranging from 1 to *N*. Then each z_i was multiplied by the ratio of the mean conditional loss divided by the mean of the numbers from 1 to *N*. The third was the exponential distribution.

This exponential distribution is simulated as follows:

- Obtain from the data the mean conditional loss. This mean loss is the estimate of the exponential parameter estimate of "*b*" in Equation (4).
- Variates $U_1,...,U_m$ are produced which have a uniform distribution over the interval (0, 1). For every *i*, the quantity $-b\log U_i$ is exponentially distributed.

Using the exponential distribution as a control function proceeds as follows. First, the original loss data are taken as an empirical distribution function. Then, fractile values can be determined from the ordered data. For example, one method is to assign the value $(n - i + 0.5)/n$ to the i^{th} largest value on the list, calling it f_i. To develop corresponding values of the exponential control function, one can use Equation (5) to find the value, x_i, for the corresponding fractile value of the cdf, and set $g_i = x_i$. For any given bootstrap set of conditional losses, the bootstrap estimate of the conditional mean loss is given by

$$\hat{e}_i = A_1 + \frac{1}{768}\sum_{j=1}^{768}(f_j - g_j)$$

and for B = 1,000 bootstrap samples of conditional losses,

$$\hat{e}_{boot} = A_1 + \frac{1}{1000}\sum_{i=1}^{1000}\hat{e}_i$$

6.3 SUMMARY OF VARIANCE REDUCTIONS FOR CONDITIONAL LOSS DISTRIBUTION

Table 2 summarizes how variance (or, in this case, standard deviation) is reduced through the application of this bootstrap sampling combined with the use of an exponential control function, Latin squares sampling, and fractile-based sampling for the exponential control function.

Table 2
Results for the Application of the Exponential Distribution as a Control Function

Control Function	Sampled Value	NUMBER OF YEARS SIMULATED				
		10,000	20,000	30,000	40,000	50,000
Original sample	Initial Mean	137.67	141.94	144.55	137.58	136.41
	Initial Standard Deviation	199.92	204.63	209.23	202.19	203.38
Fractile-based Control Function (No bootstrap samples)	Average Standard Deviation	68.95	69.70	70.86	71.81	71.83
	Reduction in Standard Deviation	**66%**	**66%**	**66%**	**64%**	**65%**
Bootstrap method in which *g(z)* is an exponential distribution, with fractile-based sampling. Results shown for 1,000 samples with Latin squares sampling.	Initial Mean	137.67	141.94	144.55	137.58	136.41
	Resulting Mean	135.49	141.22	144.16	137.56	136.51
	Mean of Differences	-2.18	-0.72	0.39	-0.02	0.10
	Average Standard Deviation	10.42	7.80	6.46	5.23	4.64
	Reduction in Standard Deviation	**95%**	**96%**	**97%**	**97%**	**97%**

Table 2 has three parts. The first part provides mean conditional losses and their standard deviations (square root of the variance) for the original sample, for walkthrough durations ranging from 10,000 years to 50,000 years.

The second part of Table 2 provides results from the use of a control function without bootstrap sampling. In effect, the technique employed used fractile-based sampling for the exponential function and then evaluated differences between the original distribution and the

fractile-based control function sample. The standard deviation of this procedure was based on the standard deviation for the differences between the control function sample and the original sample. In effect, This part of Table 2 demonstrates that the standard deviation of the estimate can be reduced by about 60% through the application of the control function alone, and without the use of bootstrap methods.

The third and final part of Table 2 provides results from the use of the bootstrap method with Latin squares sampling, along with a fractile-based exponential control function. These results show that the differences between the bootstrap sampled mean (for 1,000 samples) and the actual mean are very small. Reductions in the standard deviation through the use of this method (relative to those of the original sample) are about a factor of 20 or more. This indicates that variance reduction methods are extremely effective in dealing with the conditional loss distribution (which has no zero loss values).

However, results that are this extreme have been viewed with suspicion throughout this project. Since the focus in the project is ultimately on the unconditional loss distribution, these interim results have not been evaluated further for the conditional loss distribution. One should not be led to believe that this report supports the view that one can reduce the number of simulations for the conditional loss distribution by a multiplicative factor of 20 in order to achieve the same CLLs. At some point, reduction in number of simulations may increase the likelihood of missing an important part of the loss distribution, leading to increased bias. The actual reduction in the number of simulations needed for the conditional loss distribution would require further investigations in each specific case.

SECTION 7
SMALLER BUT SIGNIFICANT REDUCTIONS IN VARIANCE OF ESTIMATE OF MEAN LOSS FOR UNCONDITIONAL LOSS DISTRIBUTION

7.1 OVERVIEW

Section 7.2 summarizes the reductions in the variance of the estimate of the mean loss from the unconditional loss distribution. This section also provides sample calculations that show how the first term in Equation (9) dominates the estimate of the variance in the estimate of the mean loss. As a result, as in section 7.3, one can determine in advance the asymptotic limit for variance reduction depending on the lambda (probability of some network loss) given that the conditional distribution is similar to the one that has been tested in this project. Finally, Section 7.4 illustrates the maximum amount of reduction of the variance relative to lambda, given that the conditional distribution is similar to the one that has been tested in this investigation.

7.2 SUMMARY OF FINDINGS FOR UNCONDITIONAL LOSS DISTRIBUTION

Table 3 provides results in which the reductions in standard deviation (SD) of the estimate of the mean conditional loss in Table 2 are used to estimate corresponding reductions in the SD of the estimate of the mean unconditional loss. In this table, the resulting estimates of the mean unconditional loss are derived from Equation (7) and the estimates of the mean conditional loss given in Table 2. Estimates of the SD are derived from Equation (9). Table 3 shows that, although reductions of the SD for the conditional mean loss are very sizeable, resulting SD reductions of the unconditional mean loss are by comparison modest.

Table 3
Derived Results from Table 2 for Unconditional Distribution

Control Function	Sampled Value	NUMBER OF YEARS SIMULATED				
		10,000	20,000	30,000	40,000	50,000
Original sample	Initial Mean	2.11	2.18	2.22	2.11	2.10
	Initial Standard Deviation	29.88	30.74	31.39	30.21	30.44
Bootstrap method in which *g(z)* is an exponential distribution, with fractile-based sampling. Results shown for 1,000 samples with Latin squares sampling	Resulting Mean	2.08	2.17	2.21	2.11	2.11
	Resulting Standard Deviation	16.68	17.39	17.73	16.92	17.11
	Reduction in Standard Deviation	**44%**	**43%**	**44%**	**44%**	**44%**
	Reduction in Variance/ Needed Simulations	**69%**	**68%**	**68%**	**69%**	**69%**

7.3 SAMPLE CALCULATIONS TO ILLUSTRATE HOW VARIANCE REDUCTIONS FOR UNCONDITIONAL MEAN LOSS REACH ASYMTOTIC LIMITS

Given the values shown in Table 2, one can derive the basic findings in Table 3. In addition, one can derive the upper bound reduction in variance of the estimate of the unconditional mean loss. These calculations require the use of Equations 9 and 10 (see below) as applied to the conditional loss distribution,:

$$V = Z^2 - \lambda^2 \mu^2 \tag{9}$$

$$Z^2 = \lambda\left(V_1 + \mu^2\right) \tag{10}$$

The use of these equations to derive the unconditional variance for the mean loss, is summarized below.

For the non-bootstrap or original estimate for a 50,000 year walkthrough (N=50,000), the conditional standard deviation is 203.378 and the conditional mean is 136.413. The value of n is 768. From these values, one uses Equation (10) to obtain

$$Z^2 = \frac{768}{50{,}000}\left(203.378^2 + 136.413^2\right) = 921.156$$

From Equation (9) we compute the unconditional variance as follows,

$$V = 921.156 - \left(\frac{768}{50{,}000}\right)^2 (136.413)^2 = 916.766$$

The corresponding standard deviation, which is the square root of V, is 30.2781.

For the bootstrap (variance reduction) estimate for a 50,000 year walkthrough (N=50,000), the conditional standard deviation is 4.64, and the conditional mean is 136.413. The value of n remains at 768. For this, Equations (10) and (9) lead to:

$$Z^2 = \frac{768}{50000}\left(4.64^2 + 136.413^2\right) = 286.157$$

$$V = 286.157 - \left(\frac{768}{50{,}000}\right)^2 (136.413)^2 = 281.767$$

This variance corresponds to a standard deviation of 16.7859.

Here we see that a substantial reduction of the standard deviation of the conditional mean resulted in a reduction of only about a factor of 2 in the standard deviation of the unconditional

mean. Suppose that the variance reduction methods had reduced the variance of the conditional mean to zero. Assuming the same conditional mean, then the least Z^2 can be is

$$Z^2 = \frac{768}{50000}\left(0^2 + 136.413^2\right) = 285.827$$

Recall that for the bootstrap (variance reduction) version, the Z^2 value was 290.36, and that for the original version the Z^2 value was 934.70. Thus, the bootstrap version is very close to the minimum value of Z^2. and, hence, the same must be true for the variance of the unconditional mean

7.4 MAXIMUM REDUCTIONS IN ESTIMATE OF VARIANCE OF UNCONDITIONAL MEAN AS FUNCTION OF LAMBDA

As stated previously, there is one main factor in this asymptotic limit on the number of simulations for the unconditional loss distribution that can be reduced through variance reductions on the conditional mean loss. This factor is lambda, or the probability of some loss. This section uses the prototype distribution that has been used throughout the process in order to evaluate these basic limits. A second factor, not considered in this report, is the shape of the conditional loss distribution insofar as this affects the conditional mean loss. For this report, it is assumed for heuristic purposes that one can scale this mean loss relative to lambda.

Based on the foregoing line of reasoning, one can derive the minimum value of the variance based on the following equation:

$$Z^2_{\min} = \lambda\mu^2 \tag{17}$$

in which the minimum value of Z is achieved when V_1, the variance of the estimate of the conditional loss, is reduced to zero.

Under these circumstances, $V_{\min}$, the minimum variance for the estimate of the mean loss attainable as derived from Equation (9), is as follows:

$$V_{\min} = \lambda\mu^2 - \lambda^2\mu^2 \tag{18}$$

If one assumes that the conditional mean loss is 136.413 for a sample of 768 (as obtained from Table 2 for the original sample, when N=50,000) , and scales this value for higher values of lambda (= n/N), then one can derive the results shown in Table 4, which show how values of lambda affect the multiplicative factor for loss reductions. This table shows that the maximum value of the multiplicative factor is fairly constant for very low probabilities, but finally ascends considerably as lambda approaches unity. Values of the multiplicative factor shown at the very end of Table 4 would need to be checked, inasmuch as there are prima facie a minimum number of non-zero simulations required for sound statistics.

Table 4
Multiplicative Factor for Reduced Simulations (Reduction in Variance for Estimate of Unconditional Mean Loss) as Function of Lambda

Lambda *(=n/N)*	Multiplicative Factor for Reduced Simulations
0.000154	3.22
0.000768	3.22
0.001536	3.23
0.003072	3.23
0.006144	3.24
0.009216	3.24
0.012288	3.25
0.01568 (test case)	3.26
0.018432	3.26
0.019968	3.27
0.024576	3.28
0.029184	3.29
0.04608	3.33
0.06144	3.37
0.07680	3.41
0.10752	3.49
0.13824	3.58
0.15360	3.63
0.30720	4.20
0.46080	5.12
0.61440	6.76
0.76800	10.58
0.84480	15.32
0.92160	29.35
0.96768	69.77

SECTION 8
CONFIDENCE LIMITS FOR VERY FEW SIMULATIONS

8.1 OVERVIEW

A main reason for considering variance reduction techniques is to reduce the number of simulations needed. Under some circumstances, very few simulations may be desired. Serious time constraints or initially very coarse models or sub-models may discourage application of many simulations. This section spells out how confidence limits increase as the number of simulations decrease.

8.2 SQUARE ROOT RULE-OF-THUMB

A helpful rule for evaluating increased limits is the square root rule. This states that as the number of simulations decrease by a multiplicative factor of Q then the confidence limits increase by the square root of Q. This rule is a statistical approximation to the limits for the average annualized loss (AAL) as stated previously by Equation (1):

$$AAL \pm \frac{t_o s_A}{\sqrt{n}} \tag{1}$$

This rule applies to Bernoulli trials, without the advantages of variance reduction techniques. Given a constant t_o and a constant σ_A, then the confidence limits increase by almost the square root of Q as the number of trials, n, decreases by a multiplicative factor of Q. The application of this rule to confidence limits as estimated by variance reduction techniques is rather more problematic, as will be indicated in more detail below.

To illustrate the square root rule for the Shelby County TN roadway system previously analyzed by REDARS, we first take the results of the raw Monte Carlo evaluation without variance reduction. These yielded 95th centile confidence limits of +/-0.274 (or ±12.6 percent of the computed *AAL*) for a 50,000 year simulation with 768 non-zero losses. Reducing the simulations by a factor of four (4) (e.g., from 50,000 to 12,500 year-samples), one multiplies confidence limits by a factor of two (2) (e.g., +/-0.548). Reducing the original simulations by a factor of 16 (e.g., 781 year-samples), one multiplies the confidence limits by a factor of four (4) (e.g., to 2.192). In general, if one desires confidence limits that are +/-2.0, one reduces the number of simulations by a multiplicative factor of (2/0.274)**2, or 53.28, to 938 year-samples. This rule yields 15 non-zero losses (16 based on actual trials).

Similar results based on variance reduction techniques are summarized in Table 5. Note that in this table, the square root rule is best conceived of as a rule-of-thumb. Variance reduction techniques imply in Table 5 that only about 7 or 8 non-zero losses are required to achieve 95th centile confidence limits of +/-2. Some actual results for multiple samples of size 8 show that even smaller bootstrap confidence limits can be calculated. However, for samples this small, the calculated means are frequently biased by amounts far larger than the bootstrap standard deviation. For the exponential distribution, for samples this small, the 95th centile confidence limits calculated according to equation (1) do not include the "true" mean up to 50 percent of the

time! (This may not be as severe a problem for distributions which have central modes, but such distributions are less likely to represent loss distributions of the sort we are studying.)

Table 5
Illustrative Effects of Reducing Number of Simulations on
Confidence Limits Estimated by Variance Reduction Techniques

Total Years Simulated	Total Years with Non-Zero Losses	Average Annualized Loss AAL ($M)	95th Centile Confidence Limits
50,000	768	2.10	+/-0.15
12,500	192	2.21	+/-0.31
3,125	48	2.36	+/-0.67
781	12	2.62	+/-1.53
500	7	2.41	+/-2.01

Brief studies suggest that somewhat better performance can be achieved by scaling the sample mean to provide better centering for symmetric confidence limits, increasing the symmetric range to provide proper cover, or using unsymmetric semivariances. Transforming the sample data may also help (Small samples appear to be square-root normal.).

The gains achieved by variance reduction technique have to be balanced by the increase of the likelihood of bias. Continuing research is being devoted to specification of minimal sample sizes to avoid bias. For developing more accurate results, our current guess is that at least 100 non-zero losses should be employed.

REFERENCES

Ang, Alfredo H.-S. and Wilson H. Tang, 1975, *Probability Concepts in Engineering Planning and Design, Volume I, Basic Principles*, New York: John Wiley & Sons.

Davison, A.C. and D. V. Hinkley, 1998, *Bootstrap Methods and their Application*, Cambridge, U.K.: Cambridge University Press.

Daykin, C. D., T. Pentikainen, and M. Pesonen, 1994, *Practical Risk Theory for Actuaries*, London: Chapman & Hall.

Efron, Bradley and Robert J. Tibshirani, 1993, *An Introduction to the Bootstrap*, New York: Chapman & Hall.

Hastings, N. A. J. And J. B. Peacock, 1974, *Statistical Distributions*, London: Butterworth & Co (Publishers) Ltd.

Hogg, R. V. And S. A. Klugman, 1984, *Loss Distributions*, New York: John Wiley & Sons.

Law, A. M. And W. D. Kelton, 1991, *Simulation Modeling and Analysis*, New York: McGraw-Hill.

Lemaire, J., C. Taylor, and C. Tillman, 1993, "Models for Earthquake Insurance and Reinsurance Evaluations," in *Proceedings of the Second International Symposium on Uncertainty Modeling and Analysis*, Los Alamitos, CA: IEEE Computer Society Press, April.

Liu, Jun S., 2001, *Monte Carlo Strategies in Scientific Computing*, New York: Springer-Verlag.

Panjer, Harry H. And Gordon E. Willmot, 1992, *Insurance Risk Models,* Schaumburg, Il: Society of Actuaries.

Taylor, Craig E., Stuart D. Werner, and Steve Jakubowski, 2001, "Walkthrough Method for Catastrophe Decision Making," *Natural Hazards Review*, November, pp. 193-202.

Taylor, C. E., J. Lemaire, and C. Tillman, 1994, "A New Earthquake Insurance and Reinsurance Index: Uncertainties and Future Developments," *Uncertainty Modeling and Analysis: Theory and Applications*, B. M. Ayyub and M. M. Gupta, eds., Elsevier Science BV., pp. 497-514.

Werner, Stuart D., Craig E. Taylor, James E. Moore III, Jon S. Walton, and Sungbin Cho, 2000, *A Risk-Based Methodology for Assessing the Seismic Performance of Highway Systems*, Buffalo, NY: Multidisciplinary Center for Earthquake Engineering Research, Technical Report MCEER-00-0014, FHWA Contract Number DTFH61-92-C-00016.

APPENDIX A
ALGEBRAIC DERIVATION OF EQUATION 9 FROM EQUATION 8

The estimated unconditional variance of the annual loss, V, is defined in Equation (8) is as follows:

$$V = \left\lceil \sum_{i=1}^{N} (l_i - \lambda\mu)^2 \right\rceil / N$$

in which

l_i is the network loss for the i^{th} simulation (year),
n is the number of simulations (years) in which network losses exceed zero
N is the total number of simulations (years)
$\lambda = n/N$, is the probability of some network loss
μ is the mean loss of the conditional loss distribution
$\mu\lambda$ is the mean loss of the unconditional loss distribution.

For simplification purposes, it is useful to define

$$Z^2 = \left\lceil \sum_{i=1}^{N} (l_i)^2 \right\rceil / N$$

From this, Equation (9) is derived as follows, in which the estimated variance = $Z^2 - \lambda^2\mu^2$. The goal of this derivation is to show, then, how Equation (9) follows from Equation (8). To develop this result, reorder the losses such that all non-zero losses constitute the first n terms of the sequence. The remaining terms of the loss sequence (from n+1 to N) are zero dollars loss.

For simplification purposes, we will multiply Equation 8 by V and work with NV. With these definitions and goals in mind, the proof proceeds as follows:

$$NV = \left\lceil \sum_{i=1}^{n} (l_i - \lambda\mu)^2 \right\rceil + \left\lceil \sum_{i=n+1}^{N} (0 - \lambda\mu)^2 \right\rceil \qquad \text{(A-1)}$$

Thus,

$$\begin{aligned} NV &= \sum_{i=1}^{n} (l_i)^2 - 2\sum_{i=1}^{n} l_i \lambda\mu + \sum_{i=1}^{n} (\lambda\mu)^2 + \sum_{i=n+1}^{N} (\lambda\mu)^2 \\ &= \sum_{i=1}^{n} (l_i)^2 - 2\lambda\mu \sum_{i=1}^{n} l_i + \sum_{i=1}^{N} (\lambda\mu)^2 \end{aligned} \qquad \text{(A-2)}$$

and hence, by the definition of the mean loss μ for the conditional loss distribution:

$$NV = \sum_{i=1}^{n} (l_i)^2 - 2n\lambda\mu^2 + N\lambda^2\mu^2 \tag{A-3}$$

Note that

$$NZ^2 = \sum_{i=1}^{N} (l_i)^2 = \sum_{i=1}^{n} (l_i)^2 + \sum_{i=n+1}^{N} (l_i)^2 = \sum_{i=1}^{n} (l_i)^2 \tag{A-4}$$

by the definition of Z^2 and the reordering such that the first n terms alone are nonzero.

Hence, it follows directly that

$$NV = NZ^2 - 2n\lambda\mu^2 + N\lambda^2\mu^2 \tag{A-5}$$

Dividing by N and substituting $\lambda = n/N$, we arrive at

$$V = Z^2 - 2\lambda^2\mu^2 + \lambda^2\mu^2 = Z^2 - \lambda^2\mu^2 \tag{A-6}$$

which was to be proved.

Let us now restate this equation in terms of V_1, the variance of the conditional mean,

$$V_1 = \frac{1}{n}\sum_{i=1}^{n} (l_i - \mu)^2 = \frac{1}{n}\sum_{i=1}^{n} (l_i)^2 - \mu^2$$

Solving this equation for the sum and substituting the result in the equation for Z^2

$$Z^2 = \frac{1}{N}\left[n\left(V_1 + \mu^2\right)\right] = \lambda\left(V_1 + \mu^2\right)$$

So,

$$V = \lambda\left(V_1 + \mu^2\right) - \lambda^2\mu^2 = \lambda\left[V_1 + \mu^2(1-\lambda)\right]$$

DISCLAIMER

❖ This document has been reproduced from the best copy furnished by the sponsoring agency.

This report was prepared by MCEER through a contract from the Federal Highway Administration. Neither MCEER, associates of MCEER, its sponsors, nor any person acting on their behalf makes any warranty, express or implied, with respect to the use of any information, apparatus, method, or process disclosed in this report or that such use may not infringe upon privately owned rights; or assumes any liabilities of whatsoever kind with respect to the use of, or the damage resulting from the use of, any information, apparatus, method, or process disclosed in this report.

The material herein is based upon work supported in whole or in part by the Federal Highway Administration, New York State and other sponsors. Opinions, findings, conclusions or recommendations expressed in this publication do not necessarily reflect the views of these sponsors or the Research Foundation of the State of New York.

University at Buffalo, The State University of New York
Red Jacket Quadrangle Buffalo, New York 14261
Phone: (716) 645-3391 Fax: (716) 645-3399
E-mail: *mceer@buffalo.edu* WWW Site *http://mceer.buffalo.edu*

University at Buffalo *The State University of New York*